# THE SUSCEPTIBILITY OF VARIOUS UK AGGREGATES TO ALKALI SILICA REACTION.

RICHARD GRANTLEY SIBBICK

DOCTOR OF PHILOSOPHY

THE UNIVERSITY OF ASTON IN BIRMINGHAM

OCTOBER 1993

THE UNIVERSITY OF ASTON IN BIRMINGHAM

# THE SUSCEPTIBILITY OF VARIOUS UK AGGREGATES TO ALKALI SILICA REACTION.

RICHARD GRANTLEY SIBBICK DOCTOR OF PHILOSOPHY 1993

## SUMMARY

A group of lithologically varied UK aggregates have been incorporated into concrete prisms of variable alkali content to ascertain the alkali levels at which significant ASR first occurs at 38°C and 100 % RH. Petrographical analysis was used to establish the source of reactivity. The results of these expansion tests showed that significant ASR can develop with certain aggregates at initial alkali levels as low as 3.5 kg/m$^3$ $Na_2O_e$.

Similar prisms were made at initial alkali levels, well above, on and just below the alkali thresholds for each aggregate. These prisms were placed in salt solution to establish the effects on ASR. The results showed that an external source of NaCl does accentuate ASR in high alkali mixes. However, in low alkali mixes the ASR initiated was even greater than that developed by the high alkali mixes. It was proposed that an 'initial alkali pessimum' existed for each aggregate type for specimens placed in salt solution.

Electron microprobe analysis of the ASR gels from concretes immersed in salt solution, showed that two compositionally varied gel suites develop. The first suite was derived from ASR caused by the initial alkalis in a concrete mix and was identical to ASR gels derived from the various concretes when immersed in distilled water. The second suite was developed by alkalis derived from a reaction between NaCl and the $C_3A$ component of the cement paste. It was demonstrated that the 'initial alkali pessimum' was probably due to a combination of these two ASR types at the alkali threshold point where both suites of ASR gel can develop.

Equivalent mixes were made with a 25 % replacement of the cement by pulverised fuel ash (pfa) to establish whether alkalis released from the pfa could initiate ASR in otherwise non-reactive low alkali mixes. The addition of air entrainment to reactive concrete mixes was also examined as a method of suppressing ASR.

**KEY WORDS.** Lithologically varied reactive aggregates, Deicing salt, ASR gel compositions, alkali thresholds, pfa.

This work is dedicated to my son Geode Samuel.

## ACKNOWLEDGEMENTS

I wish to thank Prof. C.L. Page for the guidance and discussions he has provided throughout the duration of this project.

I would also like to thank Dr. P.J. Nixon, Dr. W.J. French, Dr. D.W. Hobbs, Dr. G. Sergi, Dr. T. Miyagawa, Mr K. Pettifer, Mr B.Q. Blackwell, Mr A.S. Smith and Mr. P. Livesey for the useful discussions and suggestions provided during the undertaking of this project.

Grateful thanks are also extended to Mr. M. Lyons for his help in producing the large numbers of petrographical thin sections required and Mr C.J. Thompson for his invaluable technical experience and assistance with the experimental work.

Thanks are also due to the various companies and organisations who provided the materials used.

Finally, I would like to thank Miss Helen Gilles for her considerable patient encouragement and support during the long and tiring course of producing this thesis.

# LIST OF CONTENTS

## LIST OF FIGURES

## LIST OF PLATES

## LIST OF TABLES

## GLOSSARY OF ABBREVIATIONS

| | | |
|---|---|---|
| (A) | - | Aggregate analysis |
| AAR | - | Alkali aggregate reaction |
| AE | - | Air entrainment |
| AEA | - | Air entrainment agent |
| AEL | - | Air entrainment level |
| ASR | - | Alkali silica reaction |
| ASR (SS) | - | ASR induced by salt solution |
| ASR (IA) | - | ASR induced by internal alkalis |
| pfa | - | Pulverised fuel ash |
| $Na_2O_e$ | - | Sodium oxide equivalent = {$Na_2O$ % + 0.658 ($K_2O$ %)} |
| CA gel | - | ASR gel from within the reactive coarse aggregate |
| CP gel | - | ASR gel from within the cement paste |
| (CP) | - | Cement paste |
| $C_3S$ | - | Tricalcium silicate 3CaO $SiO_2$ |
| $C_2S$ | - | Dicalcium silicate 2CaO $SiO_2$ |
| $C_3A$ | - | Tricalcium aluminate 3CaO $Al_2O_3$ |
| $C_4AF$ | - | Tetracalcium aluminoferrite 4CaO $Al_2O_3$ $Fe_2O_3$ |
| DW | - | Distilled water |
| S S | - | salt solution |
| W / D | - | Wet / dry cycled in salt solution |
| PC | - | Portland cement |
| DR | - | Dry Rigg siltstone |
| HL | - | Horrocksford limestone |
| MD | - | Maentwrog greywacke |
| VQ | - | Venn Quarry siltstone |
| RP | - | Trent Valley gravel |
| TV | - | Thames Valley gravel |
| AG | - | Anglesey strained granite |
| CL | - | Cheddar limestone (inert) |
| FF | - | Fiddler's Ferry pfa |
| WB | - | West Burton pfa |
| EMP | - | Electron microprobe |
| PU | - | Paste undefined analysis |
| OPC | - | Ordinary Portland cement |
| IN / OUT | - | Sample half immersed in salt solution and half dry |
| ETT | - | Ettringite analysis |

# THE SUSCEPTIBILITY OF VARIOUS UK AGGREGATES TO ALKALI SILICA REACTION.

# CHAPTER 1

## Introduction

### 1.1 Statement of the problem

Alkali aggregate reaction (AAR) is a collective term for a group of deleterious expansive reactions which affect some hardened concretes. These reactions are caused by an interaction between certain aggregates and alkaline pore solutions derived from the cement paste. Alkali aggregate reactions can be subdivided into the forms known as alkali silica reaction (ASR), alkali carbonate reaction (ACR) and alkali silicate reaction. The majority of cases worldwide are in the form of alkali silica reaction and to date in the UK only ASR has ever been reported and confirmed. The research to be described in this thesis is solely concerned with the alkali silica reaction.

In comparison with the total volume of concrete structures produced worldwide, the number of reported cases of AAR is small and represents only a minor part of the overall problem of concrete deterioration. Thus it was found in a French survey (Paterson, 1984) that design, maintenance and construction faults accounted for some 94% of building defects and of the remaining materials-related defects most were as a result of other problems such as reinforcement corrosion and sulphate attack.

A main cause of concern presently however, is the progressive increase in the number of structures affected by ASR and this is probably a major reason for the growth in research into the subject. Worldwide the number of aggregate and cement related problems encountered is expected to increase further as the demands on finite resources become stretched, due to economical and environmental constraints. For example during the 1970's attempts by the cement industry to comply with new environmental legislation on air pollution and also to reduce the costs of production resulted in increased alkali content (Parkinson, 1981). However, the rationalisation of the cement industry in the 1980's has led to the closure of a number of high alkali cement works. This combined with changes of raw materials used has led to the present situation, where the fewer remaining cement works all produce moderate to low alkali cements. Since 1982, no UK cement works has produced cement with an annual average $Na_2O_e$ content of greater than 1.0 % by mass (Hobbs, 1988).

The use of new untried aggregate sources and poorer quality materials also gives cause for concern that an increasing number of ASR occurrences may appear in the future. With this in mind a lot of research has been directed towards developing reproducible rapid test methods to establish a material's ASR reactivity potential prior to its use in new structures. Less research is carried out into methods of avoidance of ASR and also into better understanding of the detailed mechanisms of the reactions and their associated expansions.

## 1.2 Historical background

Alkali silica reaction was first recognised in the USA in the mid 1930's. A number of relatively new concrete structures developed a random cracking from which a gel was seen to exude. T.E.Stanton (1940) determined that this cracking was due to an expansive gel formed by a reaction between siliceous aggregate and cement with a high alkali content. Research continued in the USA during the 1940's and 50's as the number of affected structures increased. The ASR was soon to become recognised as a problem throughout the world, first in Denmark in the early 1950's, in West Germany in the early 1960's, in the UK in the early 1970's and Japan in the early 1980's. Many other countries have reported a significant numbers of affected structures including South Africa, Canada, Iceland, New Zealand and China. Since 1974 nine international conferences have been devoted to the alkali aggregate reaction.

### 1.2.1 Historical review of ASR in the UK

The first work published in connection with ASR in the UK dates back to the late 1940's. The work reported the findings of a national survey of aggregates (Jones and Tarleton, 1952 / 58). Although many potentially reactive siliceous aggregates were used in the UK at that time, none of those tested was shown to be particularly reactive and therefore ASR was considered unlikely to be a problem in the UK. In part due to this work and in part because no cracking due to ASR had been encountered in the UK, ASR continued to not be considered a problem here until the late 1970's. For example, in the BRE Digest 126 published in 1971 the following comment was made:

The first recorded occurrence of ASR in the UK was the Val de Mare dam on Jersey. In 1971 a detailed study began which established ASR to be the primary cause of failure in this dam (Coombes, 1976 and Cole, 1988). In this case the ASR observed was due to 'opaline' material from dykes and veins occurring in the diorite igneous host rock which made up the bulk of the aggregate. However, this highly reactive constituent, has not to date been found in significant quantities on the UK mainland.

Following this initial discovery of ASR a series of other structures were soon found on the UK mainland that were also affected. It has now been established that well over 200 structures built between 1931 and 1975 have cracked to some extent due to ASR. A number of the more well documented cases include the CEGB sub station concrete foundation blocks (Palmer, 1978), Charles Cross car park, Plymouth (Winney, 1980), Maentwrog Dam, North Wales (Blackwell et al, 1992), Royal Devon and Exeter Hospital, Exeter (Byrd, 1985), Marsh Mills viaduct, Exeter (Dumbleton, 1986), Midlands Link motorway bridges (NCE, 1985) and the M40 in Oxfordshire (Sibbick and West, 1989).

In 1976 a group of structures located in the South West of England were found to be suffering ASR and all had the same fine aggregate used in them. This was a marine-dredged aggregate from the English Channel and when it was combined with a high alkali cement (1.05 to 1.4 % $Na_2O_e$, Plymstock average 1969 -71) extreme cases of ASR developed (Fookes et al. 1982 / 83). By 1976 the ASR found in a number of structures in the English Midlands had been attributed to Trent Valley gravels which were the first land-based aggregate to be considered significantly ASR reactive. Initially the occurrence of ASR was felt to be geographically specific, as almost all the early cases were confined to the south west of England and the Midlands. However, with the further discoveries since the late 1970's, it is now fairly widely accepted that ASR can potentially occur almost anywhere in the UK. Known reactive aggregate sources and the location of a few ASR affected structures are shown in Figure 1.1 (page 194).

To date, of the structures affected by ASR in the UK, only two have been demolished with extensive repairs and strengthening being carried out on a number of others, (Marsh Mills viaduct) *. The affected structures have received extensive attention in the national press and British trade journals (Byrd, 1985, 87, Webb, 1988, and Anon, 1980, 84).

The British cement and concrete industry recognised ASR as being a potentially

very serious and expensive problem of which little was known by the many members of that industry. With this in mind in the early 1980's a working party of the industry, government and academic researchers was set up. The findings of that working party were published in 1983 (Hawkins Committee, Working Party Report, 1983) and revised in 1985 (Concrete Society) and 1987 (Concrete Society). The findings were presented as guidance notes for engineers and contractors on how to minimise the risk of ASR occurring in new structures. The report discussed the present state of knowledge on the subject and suggested a number of methods to avoid ASR by altering the mix constituents, so reducing the initial alkali content or by the addition of other ASR retarding materials (see section 1.4).



(NSL, 1993).

## 1.3 Mechanism of the alkali silica reaction

The alkali silica reaction is a deleterious expansive chemical reaction that develops in hardened concretes. The reaction usually occurs between hydroxyl ions in the pore solution of a concrete and certain forms of silica which occur in some aggregates (Diamond, 1975). ASR is not a reaction between the sodium and potassium ions and reactive silica. The ASR process can be divided into two separate phases; firstly the reaction forming the gel and secondly the expansion process.

### 1.3.1 Formation of ASR gel

The hydration of normal OPC cement results in the formation of a pore solution which is found in the cement paste and contains calcium, potassium and sodium hydroxides. Most of the calcium hydroxide produced during hydration is present as a sparingly soluble crystalline hydroxide (Portlandite), but alkali metal hydroxides derived from the readily soluble sodium and potassium sulphates in cement phase minerals remain in the pore solution. When water is added to the cement these alkali sulphates take part in complex reactions with the $C_3A$, $C_4AF$ and $Ca(OH)_2$ phases present in the cement. Calcium sulpho-aluminate (Ettringite) is precipitated into the paste and the aqueous pore solution is further enriched in Na+, K+ and OH- ions. By this time the pore solution consists almost entirely of sodium and

potassium hydroxides (Lawrence, 1966 Longuet, 1973) which can produce a pore solution pH value well in excess of 13. It is only in concretes with these high hydroxyl concentrations that significant attack of reactive silica particles can occur, (Hobbs, 1988, page 6). A high alkali content cement can have a hydroxyl concentration in the pore solution, ten times that of a low alkali cement; therefore it is usually with the high alkali content cements that ASR develops.

This highly alkaline pore solution then 'attacks' the reactive silica. The surface of any silica particle displays a weak acid characteristic which increases with increasing surface area or crystalline disorder. Common crystalline vein quartz is strongly ordered into bonded silicon oxygen tetrahedra, ($3[SiO]_2$) and is apparently stable in all alkaline conditions. At the other extreme of potential reactivity is opal. Opal is made up of a random network of tetrahedra with spaces in between the groups of molecules which in normal environmental conditions are filled by water. In the highly alkaline conditions found in a concrete these spaces are quickly filled by the alkaline pore solutions. At the reactive silica / pore solution interface an acid / alkali reaction occurs and a hydrous silicate is formed. Hydroxyl ions are imbibed into the silica particle and some of the silicon to oxygen linkages are attacked weakening the bonds locally. Sodium and potassium cations then diffuse in to maintain the electrical neutrality and attract more water to form a gelatinous alkali-metal-ion hydrous silicate. Once the Si-O-Si linkages are disrupted more water and further hydroxyl ions are able to enter the system, being imbibed and forming more gel which again results in further pressure. Whilst the hydroxyl ion concentration remains high and the source of silica is still available the expansive gel forming processes are self perpetuating. In saturated concrete, the gel product imbibes water and alkalis, at a rate which is dependent on the hydroxyl concentration (Hobbs 1988, page 8). The loss of hydroxyl ion into the ASR gel results in a progressive loss of this material from the pore solution, until a point is reached at which no further gel formation is possible, due to the pore solution alkali level now being depleted below the alkali threshold for significant ASR with that particular reactive aggregate mix. The chemical reaction can be shown simply by the equation shown below:

$SiO_2$ + 2NaOH or KOH + $H_2O$ --------> $(Na / K)_2.SiO_2.^* H_2O$

SILICA + ALKALI METAL HYDROXIDE + WATER ALKALI SILICA GEL

* - Totally variable number of water molecules. (ASR gel is an 'alkali-metal-ion hydrous silicate' (Hobbs, 1988).

N.B All reactive / expansive ASR gels appear to also contain a proportion of calcium (see chapter 7).

### 1.3.2 Mechanism of expansion

The process by which the gel absorbs the water and expands has been debated since ASR research began back in the 1940's. Two main theories existed to explain the mechanism of expansion caused by ASR. In the first, the stresses that induce the cracking in the concrete are attributed to the growth of gel caused by absorption of pore fluids (Vivian, 1950) whilst the second, which is termed the osmotic cell theory, involves the development of internal stresses due to an hydraulic pressure developed across a semi-permeable membrane (Hansen, 1944).

In the absorption theory, the expansion induced is dependent on the total gel volume, localised concentration, the rate of gel formation and physical properties such as viscosity. If gel growth is slow, then the internal stresses may be dissipated by migration of the gel into the concrete. If the gel formation occurs relatively rapidly, the internal stresses can build up within the aggregate particle initially, to a high enough level to cause cracking and expansion in the concrete. If the gel produced has a low viscosity, then it will dissipate before exerting any internal pressure.

In the case of the osmotic cell theory (Hansen, 1944) it is suggested that the cement paste acts as an impermeable membrane towards the silicate ions.The membrane allows hydroxyl ions, water and the alkali metal ions to enter the reactive aggregate but does not allow the silicate ions out. Under these conditions any reacting site would exert pressure on the cement paste eventually cracking it. Therefore the diffusion of pore solution through the membrane should accelerate the reaction. Vivian (1950) criticised this theory on the grounds that extensive cracking has been seen to occur after the initial reaction has started, therefore creating cracks in the reactive aggregate, which means the impermeable membrane would be unable to function.

In summary, at the present time the mechanism of water uptake by the gel is considered to be by direct sorption or imbibition from the pore solution or other external water source (Gillot, 1975; Pike, 1955 and Dent Glasser, 1979). The reaction between these two components forms a hygroscopic alkali silica gel. This alkali silica gel which forms and initially is located in or around the reactive aggregate particle absorbs / imbibes any free water and swells. This rapid swelling of the gel exerts an internal pressure within the aggregate particle which may, in the

more reactive cases, cause the aggregate and eventually the surrounding cement paste to crack.

### 1.3.3 ASR cracking

ASR is a long term phenomemen and it may be that only after 4 to 5 years will a network of cracks be found on the surface of affected structures. However, structures monitored in Denmark, USA and South Africa have shown microcracking within 1 to 3.5 years (Hobbs, 1988 page 15). In an unreinforced structure these cracks will take on the form described as 'map cracking' (see Plates 1.1 to 1.2, page 253). This cracking appears to be a random divergent form often developing at single points from which three separate cracks will separate. In constrained or reinforced concretes this pattern of 'map cracking is usually modified with larger cracks running parallel to the reinforcement bars. In the case of a concrete pavement (Sibbick and West, 1992) constrained in all directions but upwards the major cracks develop in the concrete-subparallel to the top surface (direction of least compression).

Other deleterious activities that affect concretes in similar environmental situations can also produce expansive crack patterns. These features can be caused by frost attack, sulphate attack, severe plastic shrinkage, and shrinking aggregates. All these various deleterious activities can usually be separated by petrographical analysis. In extreme cases the ASR gel is also exuded on to the outer surfaces of the concrete and is often associated with damp 'sweaty' patches (see Plate 1.3). As confirmed by petrographical analysis the texture and colour of the ASR gel is variable, dependent on other factors such as aggregate type, iron staining and the pick up of fine rock debris by the gel (see 1.4.2).

It has been stated by some workers (Hobbs,1990) that only microcracking observed petrographically to exhibit the typical divergent cracking seen in chert-rich aggregate can be regarded as being representative of concrete affected primarily by ASR. The less well documented microcracking observed in greywackes, siltstones and silicified limestones (see section 3.5), however, is just as typical for those specific aggregate types (Pettifer, 1986). Variations in the lithology, texture, chemistry and crystal / particle size of these aggregates clearly should have a great bearing on the form of ASR microcracking these aggregates exhibit.

### 1.3.4 Alkali silica gel

The chemical composition of the alkali silica gel has been studied frequently, the first data being published by Stanton in 1942. The gel compositions are observed to vary greatly (Poole, 1992a page 17). Most present day analyses are carried out using an electron microprobe (EMP) which requires the sample to be completely desiccated prior to analysis. It is worth pointing out, first that elements with atomic number less than 11 such as carbon are not detected, so reliable analyses of gel carbonation ($CaCO_3$) as opposed to $Ca(OH)_2$ take from the cement paste maybe questioned, without backing up these results with localised alkalinity testing. Secondly that most modern analyses are computer-corrected determinations normalised to 100 %. So with the full compositional analyses shown it should always remembered that factors such as the variable water content in establishing the degree of gel expansivity at a particular location. Problems of excessive carbonation of the prepared samples can also lead to poor chemical analysis results.

Alkali silica gel is composed of variable proportions of sodium, potassium, silicon, calcium, magnesium, oxygen and water ($H_2O$) which is lost from the analyses. The role of these chemical constituents of the gel, particularly the calcium in determination of the overall expansion is still unclear. Knudsen and Thaulow (1975) noted that the amount of calcium in the gel varied as it passed from aggregate to cement paste. The gel in the aggregate was high in alkalis, whilst that found in the paste was higher in calcium. Verbeck and Gramlich (1955) suggested that if calcium hydroxide was present, then the ASR gel formed was calcium rich and the fluidity was reduced. Diamond et al. (1981) working with synthetic gels, also confirmed that calcium rich gel has reduced fluidity, but could find no relationship between gel composition and swelling. Recently Chatterji et al. (1986a / 89) have also suggested that calcium hydroxide is a requirement of ASR, a view endorsed by Diamond (1989).

It is clear that when an alkali silica gel first forms in the reactive aggregate particle it will be very viscous, (pressures of up to 11 MPa have been recorded), but as it absorbs more water from the pore solutions it will swell and become less viscous becoming fluid enough to flow along the microcracks formed during the initial ASR induced expansion and flowing into air voids and micropores in the cement paste. Much research has been undertaken to establish a composition to expansive behaviour relationship (Diamond et al. 1981 and Moore, 1978). It seems clear now

however, that the behaviour of the gel within a concrete undergoing ASR is most complex and not as dependent on chemical composition as was originally thought (Poole, 1992a page 19). Petrographical inspection of ASR reactive concretes often reveal a series of different looking gels, as generations or pulses, carbonated gel material and even gel that has apparently recrystallised into an alkali silica 'mineral'. The cause of these differences are still not fully understood.

Most recently Laing et al. (1992) carrying out gel composition analysis on synthetic and real structural concrete, observed a compositional progression and possible phase boundary between high alkali, low calcium gel in the aggregate and low alkali, high calcium gel in the cement paste. Both gels appeared petrographically identical. This work was carried out on Thames Valley gravel mixes. No work has as yet been carried out on the gel composition of different ASR reactive aggregates comparing the results to the established theories and degree of observed expansion taking factors such as initial alkali content and mix design as constant.

## 1.4 Reducing the risk of ASR development.

It is considered by some workers, (French, 1990a and Hobbs, 1990) that ASR occurs to a limited extent in all concretes regardless of aggregate type and there is some support for this view. The deleterious affects of the reaction never visibly develop in most cases as, either the microcracking is on too fine a scale to be seen or the internal alkali supply in the concrete runs out leaving a few microcracks and a little ASR gel. These microcracks become resealed by secondary ettringite and / or portlandite and the gel becomes carbonated resealing the microcracks still further.

Therefore in summary three components are required to develop ASR:

1. a reactive silica constituent to the aggregate,
2. a sufficient supply of alkali usually derived from the cement paste pore solution,
3. moisture freely available and able to be imbibed by the gel causing expansion.

If any one of these three reactants is missing or in insufficient quantities then the reaction is not going to take place and / or develop. Thus if measures can be taken to obtain this requirement, then ASR should be avoided (see 1.5). The discussion of methods used to avoid ASR at present is given below.

### 1.4.1 Methods employed in reducing risks of ASR

The following different methods are used at present to avoid the occurrence of ASR.

1. Use of non-reactive aggregates, (section 1.4.2).
2. Use of a low alkali content cement or even a lower cement content, if the structural circumstances allow it, (section 1.4.3).
3. Sealing concrete structures to avoid moisture ingress and detailing constructions in such a way as to avoid producing locations of high relative humidity and temperature, (section 1.4.4).
4. Addition of cement replacement materials such as, pulverised fuel ash, (pfa's), microsilica and ground granulated blast furnace slag, (ggbfs), (section 1.4.5).
5. Addition of air entrainment, (section 1.4.6).
6. Addition of lithium compounds (Diamond,1992).

A number of these methods are discussed in some detail below.

### 1.4.2 Aggregates

In the UK a number of lithologically varied aggregates have been identified that are potentially ASR reactive. These reactive aggregates are dominated by flint and chert bearing gravels and natural sands, mainly derived from fluvial, river terrace, and glacial gravel source materials. There are also a number of reactive sea-dredged aggregates, in which the reactive constituent is dominantly chert (French, 1990a). The large number of structures affected by ASR in the South west of England can now be attributed to the use of a sea-dredged sand from the English Channel, combined with an exceptionally high alkali cement manufactured at that time. Both the cement and aggregate concerned are no longer in use.

In the past lists have been produced of potentially reactive and non-reactive aggregates (The Concrete Society, 1987). This classification method now seems to be rather fallible. The cause of ASR in a concrete is the occurrence in the aggregate of one or more of the forms of reactive silica discussed in section 1.4.2.2. As such, if one of those forms is identified petrographically in any aggregate in sufficient quantities, then it should be considered potentially reactive, regardless of the aggregate's lithology. As more UK rock sources are studied for ASR potential the list of non-reactive aggregates types is becoming smaller and smaller. Having stated this, some rock types are more likely than others to be ASR susceptible, based on their normal constituent minerals. These rock types include; siltstone, quartzite, silicified limestone, greywacke, phylite, and chert.

In recent years a number of crushed rock aggregates have been identified that exhibit extreme reaction in comparison to the river gravels. The reactivity of an aggregate appears to be dependent on a number of variables including : silica content, form / phase of quartz (see section 1.4.2.2) crystal structure / size, porosity, water absorption, dispersion of reactive particles in the aggregate and finally possibly strain and defects to the quartz crystal lattice (Zhang et al.1990) all of which are discussed here.

The size of the reactive aggregate particles in a mix has a significant affect on the rate and degree of expansion recorded. French has stated (1990b) that though expansion results are often quick using a small size reactive material and therefore useful for rapid testing (Hobbs and Gutteridge, 1979), the use of larger reactive aggregate particles gives greater expansion results over a longer time periods which are more in line with the expansion recorded from field structures.

In one particular case of ASR affecting a concrete pavement containing 100 % Thames Valley gravel (Sibbick and West, 1989) the ASR was seen to only affect the highly porous and water absorbent white flint material also known as 'patina', the rest of the aggregate remaining apparently inert. This white flint material had a water absorption value of up to 9.76 % and a relative density of down to 2.08 (RDODB)* compared to the black flint material which had a water absorption value of 0.78% and a relative density of up to 2.54 (RDODB)* (Sibbick, 1988). The observation made in this work on flint reactivity has been recently confirmed by a detailed study of flint reactivity (Rayment, 1992). The smaller the aggregate particle, the higher was the observed water absorption value and, as expected, the greater the amount of white patina material observed. This condition left the aggregate highly susceptible to frost damage as well as ASR. A recent clause to the Department of Transport (UK) specification for highway works has now limited the water absorption of flint aggregates, which should exclude most frost susceptible and therefore, potentially ASR reactive aggregates (Department of Transport, 1988). The conclusion that can be drawn from this is that highly water absorbent and porous chert aggregates are more potentially reactive than dense material of equivalent chemical composition.

* RDODB = Relative density on oven dried basis.

A full explanation of aggregate reactivity that is still considered to have some authority can be found in Building Research Digest 330, March 1988, page 5.

### 1.4.2.1 Reaction pessimum

The cherts and flints, which were the first mainland aggregates to show the effects of ASR, exhibit the interesting feature of a 'reaction pessimum'. With flint and chert based aggregates there is a certain proportion of reactive material which gives a maximum expansion. All reactive aggregates will display a pessimum value, but in most cases this is 100 %. However, opaline material, for example, displays a pessimum of approximately 5 %. This means that to obtain the maximum expansion for that particular aggregate 5 % must be present in the concrete. With flint and chert materials, concrete containing approximately 20 % chert material and 80 % inert material will give the greatest expansion, whilst a concrete with 100 % chert will give little, if any recorded expansion. The pessimum effect is best shown by Figure 1.2. The 'pessimum' is the proportion of reactive aggregate that gives the most adverse effects. Assuming that the alkali threshold to initiate reaction with that aggregate has been obtained, mixes made up at the same alkali level but different reactive aggregate contents will show the 'pessimum' effect. The reasons for the occurrence of a pessimum are not totally understood, but it is thought it may relate to the rates of alkali silica gel formation, compared to the availability of the alkali and water to produce it (Nixon et al. 1983). Alternatively it may be that the rate of gel production is varied for the different amounts of reactive aggregate and the ability of this gel volume to disperse into the cement paste will be a factor as to whether significant cracking develops. It may be that rate of reaction in some aggregates choke off further destructive reaction by filling the cement paste with ASR gel. (i.e gel production :> gel diffusion = expansion). For each reactive aggregate type there is usually only a certain proportion of the rock that is considered reactive. For the Thames Valley gravel, it maybe that as nearly all the material is potentially reactive, this aggregate will react to such a degree that ASR gel is produced throughout the concrete, to such an extent that the localised development of strain and microcracking in particular reactive particles does not occur.

Petrographical examination of reactive concretes containing 100 % Thames Valley gravel, show evidence of ASR gel throughout the cement paste (i.e staining), but no evidence of specific aggregate particles showing expansive ASR-related microcracking. In appears therefore, that for ASR microcracking to develop in a concrete, the strain has to be confined to specific aggregate particles and not spread throughout. In a similar way, the occurrence ASR throughout a concrete as opposed to at specific reactive aggregate locations could also explain why the addition of a potentially reactive material like microsilica to a concrete actually stops

significant ASR microcracking developing.

Some aggregates such as silicified limestone or greywacke etc. only contain a small proportion (10 - 15 %) of material that would be considered reactive (Nixon et al. 1989) see 1.4.2.2. Therefore to obtain the greatest expansion the maximum amount of aggregate and thus reactive constituent must be added to the mix; hence a 100 % pessimum level is observed.

### 1.4.2.2 Reactive materials

Silica is found in many geological deposits in a wide range of crystal forms and sizes. Only disordered silica and / or fine particle size material react to any significant extent. As seen from the description of the reaction in section 1.2, silica is the only reactive constituent found in the aggregates that develop ASR. The many forms in which silica occurs are shown in Table 1.1 below, with a brief discussion of their source and ASR potential.

TABLE 1.1 - Forms of silica, ($Si O_4$) naturally found in aggregates.

| | |
|---|---|
| 1. Opal | - Very reactive, amorphous or disordered form of silica,very rare in UK rocks. |
| 2. Volcanic glass | - Very reactive non-crystalline silica rich material found in some volcanic rocks. |
| 3. Chalcedony | - Very fine grained silica with a distinctive fibrous microstructure found in some flints and cherts. Reactive. |
| 4. Cristobalite | - Very high temperature metastable form of silica found in acid volcanic rocks. Very reactive. |
| 5. Tridymite | - High temperature metastable form of quartz usually found in acidic volcanic rocks. Very reactive. |
| 6. Cryptocrystalline quartz | - Common crystalline quartz constituent of many UK rocks, (sub-microscopic size, < 0.5 $\mu$ms). Reactive. |
| 7. Microcrystalline quartz | - Common crystalline quartz constituent of many UK rocks, (visible microscopically, > 0.5 $\mu$ms). Reactive |
| 8. Vein quartz | - Coarse crystalline quartz, not known to suffer from ASR. |
| 9. Strained quartz | - Normal crystalline quartz which has experienced lattice deformation by metamorphism, (See section 1.4.2.3). |
| 10. Calcined Flint | - Man made aggregate used in ASR testing. Reactive. (consisting almost entirely of cristobalite). |
| 11. Fused silica | - Man made aggregate used in ASR testing. Reactive. |
| 12. Pyrex | - Glass, man made artificial aggregate. Reactive. |

Most of these various forms of silica can be identified petrographically (Mather, 1948 and Mielenz, 1954). Cryptocrystalline silica cannot be identified accurately using normal petrography as the grain size is too small, but bulk chemical, X-ray diffraction and SEM analysis can usually identify the material. Opal is the most reactive natural aggregate and can cause damage even in concentrations as low as 1 or 2 % of the mix. Opal is however, rare especially in the UK where only one example of ASR can be attributed to it (Cole ,1988). Hobbs (1986), feels that opaline material can be found in flint and chert aggregates of UK origin and it is this material that is considered to be reactive. This opinion is however, not widely held. In the UK at the present time cryptocrystalline and microcrystalline silica and chalcedony found in flint and cherts are considered the main reactive constituents.

Several workers (French, 1990, Blackwell, 1992, Zhang et al, 1990, Sibbick and Page, 1992) studying other UK aggregate types now consider the main reactive constituent in some reactive rocks to be a form of cryptocrystalline and microcrystalline silica found as either a cementing agent, as finely disseminated material in the matrix of the rock or as intercrystalline material found at coarser quartz crystal boundaries (See 1.4.2.3). The high temperature volcanic forms of silica can be found in UK aggregates, but they are a lot rarer than cherts and other rock types containing cryptocrystalline and microcrystalline quartz.

The reactivity of quartz is dependent on the increasing degree of crystal lattice disorder / breakage or reduced grain size. This relates to an increase in the amount of silica crystal surface area available to the ASR. The increasing amount of silica surface available to the reaction is therefore dependent on the number of crystal lattice deformations, the complexity of the crystal boundaries and the reduced size of the individual quartz crystals found.

Finally, French in his 1992 paper states:

> 'All rocks are considered to be possibly reactive. Those materials exhibiting significant levels of reaction at realistic alkali levels are characterised by the presence of a small percentage of silica minerals in particles of less than 5 micrometers in a structure which either porous or contains flaws such as fine cracking or microcracking developed by geological factors or in manufacture'.

### 1.4.2.3 Strained quartz as a reactive constituent

The present specifications and reports for the avoidance of ASR state an opinion along the lines presented below:

'That quartzes with large undulatory extinction angles are particularly prone to alkali-silica reaction when contained in rocks used as aggregate for concrete.'

(From The Concrete Society Report No. 30, 1987).

This was based on the views published by Mielenz (1954) and (1956), Brown (1955) and Dolar-Mantuani (1981). With this in mind a number of researchers have been trying to answer this still unconfirmed statement.

Strained quartz is known to occur in a number of different geological environments; granites and other quartz-bearing igneous rocks, sediments derived from such rocks and metaquartzites formed by metamorphism. Strained quartz is typified by undulatory extinction, which often appears as curtain-like shadows of non-uniform extinction, that pass over an individual grain as it is rotated under a polarising microscope with crossed nicols. The internal strain within the crystal lattice causes a displacement of the C-axes thus producing the undulatory extinction. This non-uniform extinction occurs as a result of line defects 'dislocations' in the crystal lattice. This structural mismatch within the grains mean that there is excess internal energy present and this means the quartz is more chemically reactive.

In Canada especially, a correlation between highly strained granitic rocks and alkali expansivity is well documented (Gratten-Bellew, 1987). Buck (1987) has tried to give some parameters for petrographic identification of strained quartz. Likewise, Andersen (1989) carried out a survey of 6 different concrete petrographers in Denmark to try and specify the measuring of undulatory extinction angles, (UEA) and thus relate that to the reactivity of aggregates. The methods of measuring this UEA angle are still debatable and subject to great variability. Andersen states that an aggregate containing 20 % of quartz grains with an UEA larger than 15$^{o}$ should be considered as potentially reactive. This belief that quartz exhibiting undulatory extinction is particularly susceptible to ASR, is based on a consideration that the internal strain energy arising from the presence of dislocations and sub grains increases the solubility and hence reactivity of quartz grains. There is little direct observational or experimental evidence that strained quartz gives rise to alkali-silica reaction in concrete. It is however considered that in some instances the occurrence of ASR in a concrete containing strained quartz is due to the increased occurrence of cryptocrystalline and micro-crystalline quartz grains at or on the sub grain boundaries and dislocation faces of the quartz crystals and it is these constituents that are in fact reactive (Andersen,1989). A detailed explanation of

strain in quartz and measuring the undulatory extinction angle of a crystal is given in West (1991).

Recently papers by Smith et al. (1992) and Grattan-Bellew (1992) both came to the conclusion that the relationship between a measured extinction angle of a quartz grain on a single plane microscope had very little bearing on the dislocation density that had developed in that crystal lattice and therefore would also have little bearing on relating the recorded undulatory extinction strain angle to the potential degree of reactivity. It was concluded that measuring of this extinction angle was of little direct relevance to ASR reactivity. Both papers made well founded recommendations for identifying the degree of strain a rock had undergone, by studying the quartz grains' metamorphic textures and grain sizes developed. They concluded that the potentially reactive constituent in these strained aggregates was probably micro and cryptocrystalline quartz found at the intergrain boundaries of the larger strained quartz crystals. The amount of this reactive silica material is dependent on the grain size, texture and therefore degree of strain that the rock has undergone.

The evidence in the U.K for a highly strained quartz bearing aggregate that is reactive due to the strained particles of quartz within it has up to now been inconclusive. For this reason the research described here includes testing of the most highly strained granitic aggregate in the country (see Table 2.2) (Source A.Smith, 1991, Leicester University, Pers Comm).

### 1.4.3 Cements

The second requirement to induce ASR is sufficient alkali. This is primarily derived from the cement, see section 1.3. Both sodium and potassium hydroxides are capable of attacking the silica to induce the reaction, so it is convenient to express the total alkali content present in cement and concrete as an equivalent sodium oxide content. This is calculated by the following equation:

$$(Na_2O)_e = Na_2O + 0.658 \times (K_2O)$$

$$\text{equivalent sodium oxide} = \text{sodium oxide content} + 0.658 \times \text{potassium oxide content}$$

(From BS4550: Part 3: Page 48, 1970)

The alkali contents of OPC cements generally range from 0.3 to 1.3 %, but higher levels have been recorded (Hobbs, 1988). Normal concretes made with a low alkali

cement (below 0.6 % $Na_2O_e$ ) and containing no other external alkali source have not to date been shown to have triggered ASR with normal UK aggregates (French, 1990a). The alkali content of a concrete is usually described in terms of kg/m$^3$ $Na_2O_e$. In the UK the alkali levels of concretes range from 1.5 to 7 kg/m$^3$ $Na_2O_e$. ASR has been seen to occur in concretes with alkali levels of less than 2.5 kg/m$^3$ $Na_2O_e$. However in these concretes the reaction was not considered significant (French,1990a). The most serious cases of ASR damage relate to mixes which had more than 4.5 kg/m$^3$ $Na_2O_e$ and are generally associated with mixes with very high cement contents (450 to 550 kg/m$^3$) (Inst. of Struct. Eng., 1988). The present recommended maximum total alkali content (derived from the cement paste, water, aggregates, additives and NaCl in the aggregate) at which it is felt significant ASR is unlikely to develop in UK concretes using UK aggregates is 3 Kg/m$^3$ $Na_2O_e$ (The Concrete Society, 1987). This limit is taken assuming the aggregates used do not include opal and to date no mainland UK aggregate has been discovered that contains significant amounts of opal. However, Hobbs (1986) does not take this view. A reduction of the total cement content of a mix, to bring down the alkali level below this figure can also be used for the avoidance of ASR provided, the strength required for the concrete is still within specification. Alkalis can also be slowly released from some types of aggregate containing feldspars, some micas, clays, glassy rocks and glass. In France this has led to serious AAR damage to a major dam (Greeman,1986) and in the UK it has also been felt that this feature may have contributed to the reaction in some cases.

Probably the simplest method of avoiding further cases of ASR would be to reduce the alkali content of the cements used. This is however, not as easy as it first appears as virtually all the raw materials used in the manufacture of cement from the clay, limestone, chalk and shale through to the coal used to heat traditional kilns contribute some alkali to the cement product. In the recent past a certain amount of alkali material was lost by volatilising it out of the raw materials and venting into the atmosphere with the exhaust gases and dust. This practice is no longer environmentally acceptable so currently all the particulate material, (alkali rich dust) is electrostatically removed from the waste gases and returned to the cement product increasing its alkali content (Warning and Johansen, 1983). One method used to reduce this problem is by the use of a high sulphur content fuel in the kiln, this leads to the formation of an increased amount of alkali sulphates in the clinker where the alkalis remain. This results in clinker leaving the kiln with higher alkali contents much of which is chemically bonded into these alkali sulphate phases and

therefore less accessible to the ASR, which usually obtains alkali directly from the pore solution. Another method of reducing the alkalinity of a mix is by the replacement of some of the high alkali cement by another material such as pfa or slag (see section 1.4.5).

### 1.4.4 Water and other environmental conditions

The third component required for the occurrence of ASR expansion is water. This is usually derived directly from environmental sources such as rain, river or sea water, ground water and heavy condensation or humidity. It has been reported that a reactive concrete left in a dry environment and condition will not suffer from ASR expansion (Vivian, 1951 and The Concrete Society, 1983). If this fact is applied to the design of new concrete structures, then the avoidance of moisture concentrating features, such as ponding on flat roofs, open joints and any other design flaws leaving free water next to any concrete surface should reduce the potential for the development of ASR in that structure. The up-keep of drainage channels, pipe work, weep holes and guttering etc. during the service life of the building or structure, should also alleviate, if not stop the occurrence of ASR in that concrete structure.

The total removal of free water from a potentially reactive concrete will alleviate, if not stop the reaction. To date there has been little success in this by coating concretes to stop further ingress of water into the concrete (Kojima et al. 1992). Water by its very nature will tend to get behind such coatings and once there, the coating may actually reduce loss of water from the surface layer of concrete by evaporation (Blight, 1991). It is unlikely that all the free water can be totally removed from a concrete structure in a field environment prior to the placing one of these coatings.

The temperature of the environment can also have a great influence on the rate and even maybe the extent of ASR developed. Gudmundsson (1975), determined that the reaction stopped at 10$^{o}$C and below and the maximum expansion developed at 38$^{o}$C. This fact has been used by many workers to produce rapid test methods for potentially ASR reactive concretes and mortars (British Standards Institution, 1990). Hobbs in recent work (1992) has tentatively suggested that a time relationship to complete expansion exists between tests carried out on identical reactive concretes at 38$^{o}$C, 20$^{o}$C and external exposure of 7 : 4 : 1. These observations are still, however, looked upon with some degree of suspicion as they are based on only

one lithological aggregate type and have been interpreted from expansion results still to be completed. This work has also been used as evidence of different alkali thresholds for significant reaction at different reaction temperatures. Hobbs states:



This point is however, not established and requires a lot of further study. There is also some evidence that cyclic heating and cooling can accelerate the reaction further and this is being looked at in this work.

Specific environmental circumstances can lead to alkali migration which in turn may induce or accentuate ASR on a localised basis (Nixon et al. 1979; Gutt and Nixon, 1979 and Page et al. 1992). For example evidence is coming to light of ASR induced by cathodic protection which locally can cause alkali migrations to the cathode region of the protected concrete so leaving that area more susceptible to ASR (Sergi and Page, 1991). The replacement of damaged concrete with high alkali non-reactive repair material has also been recently observed to induced localised ASR in the host concrete due to the migration of alkali from one material to the other. Research underway at Aston University has shown the possibility of inducing ASR by alkali migration using a number of different methods.

### 1.4.5 Additions of Pulverised fuel ash, (pfa)

As already briefly mentioned (see section 1.4.3), the addition of a cement replacement material to a concrete can help to reduce the total alkali content and therefore avoid significant ASR cracking in a concrete. This material can be any suitable hydraulic or pozzolanic * material. The mechanisms involved can be highly complex, though they are thought to involve the dilution of the alkalis in the cement paste and / or an increase the fineness of the cement paste microstructure so in the process maybe increasing the strength of the concrete. This may have the affect of reducing the ability of Na+, K+, Cl- and OH- ions to diffuse through the paste, therefore reducing the capacity to continue the ASR. Many different pozzolanic materials have been used with cements for blending. These include burnt rice husks, burnt clay, broken up tiles, microsilica, (silica fume), ground up blast furnace slags and the one used in this research pulverised fuel ash.

* - A pozzolan is a material of siliceous or siliceous / aluminate composition which possess little or no cementitious value but in a finely divided form and in the presents of moisture, chemically react with $Ca(OH)_2$ at ordinary temperatures to form compounds possessing cementitious properties.

Pulverised fuel ash is a high glass content waste product from the electrical industry and is produced in large quantities by thermal power stations which burn pulverised coal as a fuel. Pfa reacts pozzolanically at normal temperatures but at a slower rate than Portland cement. World production of fly ash (pfa) is huge around 400 million tonnes per year and so its beneficial use in the concrete industry is a sound environmental and economic prospect.

Pfa consists of glassy spherical particles of size 1 to 100 $\mu$m, with the majority being under 20 $\mu$m. An ash's physical and chemical properties are dependent on the type of coal burnt and the efficiency of the burning. Many workers have looked at various aspects of pfa's ASR suppressing abilities (Rogers, 1986, Duncan et al. 1973, Page and Vennesland, 1983, Nixon and Gaze, 1983, Thomas et al. 1992). A whole section of the recent 9th International conference on AAR was devoted to the study of pfa and other replacement materials with respect to AAR suppression.
However, there are at least two examples where concretes containing pfa have still been affected by ASR. In the McPherson test road project in Kansas, USA, the concrete pavement containing pfa was found to contain a greater number of ASR induced transverse cracks than the equivalent OPC concrete (Lerch,1959). In Japan, a number of supporting piers on the Hanshin Expressway that contain about 20 % pfa are cracked as a result of ASR. Therefore this method of ASR avoidance must be taken as potentially suspect (Imai et al.1987).

Partial replacement of a cement by pfa can affect the physical and chemical properties of the concrete, including the hydroxyl ion content and hence the ASR reactivity of the mix. Because of the varied chemistry of pfa's, some naturally contain a lot of internal alkalis. These alkalis are bound in the glassy phases and are released at a rate much slower than a Portland cement. British pfa's have been chemically analysed and found to have total alkali contents ranging from 0.75 to 4.6 % kg/m$^3$ $Na_2O_e$ by mass (Smith and Halliwell, 1979). This is significantly higher than for UK Portland cements, (0.3 to 1.1 %). If any of this alkali in the pfa can be released in the concrete mix then it could potentially accentuate the reaction. Many workers have however also shown the benefits of pfa replacements (Thomas et al. 1992; Blackwell et al. 1992; Page and Vennesland, 1983; Nixon and Gaze, 1983).

Nixon and Page (1987) have reviewed the results of studies of the hydroxyl and alkali ion determinations in expressed cement and concrete pore solutions from mixes containing pfa. They observed that three factors determined the hydroxyl ion concentration of the pore solution in pfa mixes. These were:

1. Alkali content of the pfa.
2. The fineness of the pfa.
3. Alkali content of the Portland cement.

It was found that in the case of high alkali cements the total hydroxyl ion content was reduced significantly compared to the equivalent OPC mix. However, with a low alkali cement the partial replacement of cement by pfa was ineffective in reducing the total hydroxyl ion concentration. As the ASR reactivity of a mix is related to the hydroxyl ion concentration of the pore solution (see section 1.2) it follows that the addition of pfa is only beneficial to the suppression of ASR in high alkali mixes.

The benefit of including pulverised fuel ash in low alkali systems is not so clear. From work carried out by Hobbs (1986) and Kolleck et al. (1986) it has been established that in the presence of pfa, deleterious expansion of mortars can occur at lower alkali contents than would be expected if only the OPC alkali contribution was important. All the testing above, was carried out using opaline or other highly reactive aggregates with low alkali thresholds for significant reaction. However, as most natural aggregates appear to only be reactive in high alkali mixes (>5.2 kg/m$^3$ $Na_2O_e$, Hobbs, 1992a) then the benefits of pfa replacements in UK concretes seem substantial.

Recent work still to be published has confirmed this previous evidence (Nixon et al. 1987) that in concretes containing replacement pfa there may be an alkali contribution from the pfa after 1 year. The new research has shown ASR can be induced in a calcined flint mix at low alkali levels (2.5 kg/m$^3$ $Na_2O_e$), which are just below the alkali threshold for that material, when a high alkali pfa is used as the replacement material. A further similar study was carried out at the same time using Thames Valley gravel aggregate as the reactive material. This aggregate is known to have an initial alkali threshold for significant reaction of around 5.2 kg/m$^3$ $Na_2O_e$ (Nixon et al. 1989) and at the time was considered the UK's most reactive aggregate when added at the correct pessimum level. The pfa additions were seen to at least initially increase the OH ion concentration of the concretes, but not sufficiently to induce reaction in mixes with initial alkali contents below the alkali

threshold of 5.2 kg/m$^3$ $Na_2O_e$ (Sadeghzadeh, 1993). The effects pfa's additions have on the $Ca(OH)_2$ concentration of pore solutions in a potentially reactive concretes are also still unclear.

### 1.4.6 Air entrainment of concretes

It has been observed by experimentation and observation of field concretes that air entrainment may suppress the alkali silica reaction as well as improve a concretes freeze / thaw resistance. Early work by Jensen et al. (1984) found that in tests on mortar bars immersed in salt solution at 50°C, the introduction of 4 % volume of air did not prevent ASR cracking, but reduced the expansion by about 40 %. Petrographic analysis indicated that many of the air voids were full of alkali-silica gel. If this does occur to a significant extent in practice the bubbles may no longer be effective in improving the resistance of the concrete to freeze-thaw action. To date however, there still appears to have been no published work carried out on the topic in the U.K and no work could be found that had been carried out on 'real' concretes (Hobbs, 1988 page 49-50).

## 1.5. Accentuating the Alkali-silica reaction, (ASR).

The main topic discussed here is the possible contribution made to the alkali-silica reaction by alkali derived from deicing salt. In the UK, North America and Europe deicing salts consisting mainly of sodium chloride are added to roads and bridges in winter. In the UK an average of 4.49 tonnes of salt per km per annum, have been added to road pavements (County Surveyors' Society, 1985). Over a period of time therefore a great concentration of deicing salt has developed in the concrete pavements and structures of Britain's roads. This is confirmed by the recent large number of cases of chloride attack reported on many of these structures. The possibility has also therefore been frequently suggested that deicing salt may enhance the alkalinity of the concrete and so exacerbate the ASR (Byrd, 1985). Aggregates especially those of sea-dredged origin can also contain a proportion of sodium chloride. If this salt is not washed out, which was the case up until fairly recently, then the aggregate can contain up to 0.105 % sodium chloride (Gutt and Collins, 1987). Any of the effects observed on the ASR for concretes in a deicing salt environment should also be considered for concretes containing unwashed sea dredged aggregates.

### 1.5.1 Effects of sodium chloride on the alkali silica reaction.

From the discussion in section 1.2. it is apparent that the alkali content of the pore solution is increased significantly by complex reactions between alkali sulphates and other phase minerals in the original cement. If sodium chloride is added to the mix water or enters from an external reservoir such as deicing salts, equivalent reactions can theoretically take place in which a calcium chloro-aluminate or chloro-sulpo-aluminate complex is precipitated and in the process the OH ion concentration of the pore solution is further increased. This reaction is shown in a simplified form below:

NaCl + $C_3A$ ---------- Cl bonds to $C_3A$ (To form Friedel's salts) , this releases OH ions
Salt + Tricalcium silicate

---------- Na from salt bonds to newly released OH ions

To form extra NaOH which is added to
pore solution increasing its alkalinity
until this is sufficiently raised to initiate ASR.

Mehta found when sodium chloride is present in the aggregate or mix water, the tricalcium aluminate ($C_3A$) in Portland cement may react with chlorides, taking some chlorides out of solution into the compound, $C_3A.CaCl_2.10H_2O$ (Mehta,1980). The compound taking some of this chloride out of solution was further analysed to produce a general composition of $C_3A.CaCl_2.H_{10}$ and is now frequently termed Friedel's salt (Page,1986). In this chemical process further sodium hydroxide is formed, which increases the hydroxyl ion concentration of the pore solution and therefore presumably increases the potential ASR reactivity of concretes containing this cement. Another simpler possible reaction between deicing salt and $Ca(OH)_2$ (Portlandite) is shown below:

$$Ca(OH)_2 + NaCl \longrightarrow Na+ + OH- + CaCl_2$$

PORTLANDITE + SALT ----------> SODIUM + HYDROXYL

It is felt by many observers and researchers that if salt, (NaCl) is added to concrete by such means as deicing salts in winter, then this will exacerbate any reaction in the concrete by adding its alkali load to that already present (Swamy, 1988).

Hobbs (1987) stated that if NaCl was added to a potentially reactive, but sound two year old concrete, the NaCl will not cause ASR. However, if NaCl is added to wet concrete at the time of mixing it will induce ASR. It is now reasonably well

documented that the addition of NaCl at the mixing stage can induce expansion due to ASR (Nixon et.al. 1988). Nixon (1987) also stated that increasing percentage Cl ion additions to a concrete increases the hydroxyl ion concentration of the pore solution and so increasing the alkalinity and the potential reactivity of the mix. Mehta (1978) carrying out work with mortar bars found that when sodium chloride was added to a mix such that the equivalent $Na_2O$ % was 0.92 % significant expansion due to ASR was found to develop, whereas no significant expansion occurred when the cement alone with an alkali level of 0.42 % $Na_2O_e$ was used.

Kawamura et al. (1990) carried out work on mortars to investigate the effects that sodium and calcium chlorides had on the alkali-silica reaction.He found that addition of NaCl and also $CaCl_2$ increased the amounts of expansion due to ASR by a factor of 3 and 1.5 to 2 times respectively. Therefore the addition of $CaCl_2$ a commercial accelerator (for increased early strength and shorter setting time) to the mortar is actually increasing the ASR developed despite a reduction in the OH ion concentration. Kawamura felt that the Cl ion is playing a significant role in the development of ASR, acting as a kind of catalyst.

As the $CaCl_2$ can also bond to the $C_3A$ in a similar manner to that previously described with deicing salt, it can also produce hydroxide. However, instead of producing a NaOH addition to the pore solution so enhancing potential reactivity, solid $Ca(OH)_2$ will be precipitated. As has been recorded previously (Chatterji et al. 1986) a limited addition of $Ca(OH)_2$ to a concrete is required to accentuate or initiate ASR and therefore this might explain why the addition of $CaCl_2$ to these mortars will accentuate the reaction.

Hobbs states in his 1988 book:



No mention has been made as to possible movements in the initial alkali threshold for significant reaction caused by placing potentially reactive concretes in a deicing salt rich environment. This is a major area looked at in the research described in this thesis.

It is worth pointing out here that in Denmark the addition of salt to many public

indoor swimming pools is believed to have been a major factor in the deterioration of a number of concrete swimming pools due to ASR (Petersen, 1983). Sibbick and West (1989) whilst carrying out a survey of concrete road pavements in the U.K for signs of ASR, identified the reaction in a number of road sites. They found it to be most prevalent in the areas next to the contraction joints of the pavement, these being the areas most affected by deicing salts and water penetration.They suggested that the deicing salts were accentuating the reaction in an otherwise probably non-reactive concrete (low initial alkali content mix and 100 % Thames Valley gravel aggregate). They were, however, unable to prove this categorically. A further more detailed study backed up this idea, with a detailed alkali and chloride analysis of another reactive concrete pavement which related the results to the locations of greatest microcracking and ASR (Sibbick and West,1992).

To date there is however, still little direct evidence on the effects of sodium chloride introduced from the outside after the concrete has already hardened (Kawamura et al. 1988 and Jensen et al. 1982). Chatterji (1978) exposed mortar cubes which had been cured for 28 days in water to a saturated sodium chloride solution at 50°C and showed that mortars containing reactive aggregate expanded whereas those made with a non-reactive material did not expand significantly. The cement used was low in alkali so that any observed reaction could only be attributed to alkali's from the sodium chloride. Nishibayashi and Yamura (1987) also found that potentially reactive mortars with added NaOH expanded greatly when exposed to seawater at 40°C.

In work published at the recent 1992 conference on AAR Kawamura et al. (1992) working with mortars containing opaline aggregates immersed in NaCl made a number of important conclusions from expansion and chemical tests. He found:

1. A small change in reactive component content, alkali concentration and local environments where concrete structures are located, brings about a drastic change in the degree of damage due to ASR.

2. In concretes with a greater alkali content than the threshold for significant reaction, the smaller the amount of alkali found above this figure the greater is the severity of the damage due to ASR caused by NaCl. *

3. The NaCl concentration affects the degree of deterioration due to ASR.

4. Even reactive aggregate-bearing concretes with low amounts of initial alkali may be damaged in a saline environment.

5. A chemical reaction, in which Cl ions are consumed and OH ions are released

seems to occur within some opal-bearing mortars during immersion in 1 molar NaCl solution. However, this phenomenon appears not to be related to the expansion of the mortars in the NaCl solution.

6. Considerable amounts of $Ca(OH)_2$ are dissipated during the immersion in 1 molar NaCl solution in all the mortars containing reactive aggregate, but not those with inert aggregate.

* -This conclusion has been reworded to make the point clearer, but is still of great importance to the later work discussed here as a similar feature has been detected. The points made above are referred to later as they are felt to have some bearing on the observations made in this work.

Finally, recent work carried at BCA using only chert-rich aggregates has found no evidence of the ASR being accentuated by deicing salts in outdoor exposure conditions (Hobbs, 1992b). Clearly there is much uncertainty over this issue and the present research will be aimed at elucidating the problem. In the UK at present it is suggested that an initial alkali level of less than 3 kg/m$^3$ $Na_2O_e$ in a concrete can be regarded as 'unreactive' (Concrete Society,1987). However, this only takes account of alkalis derived from the cement paste pore solution. If the above mentioned ideas for external sources of alkali accentuating ASR is found to be correct, then this relatively subjective figure of a 'safe' alkali level can be regarded as very suspect.

## 1.6 Purpose of Investigation

It is well established that some British aggregates exhibit alkali aggregate reaction but differences in the mechanism and effects of reaction involving lithologically varied aggregates are relatively unknown. Furthermore, it has been suspected that deicing salts have been accentuating and in some cases initiating ASR in otherwise non-reacting UK concretes, but there is a lack of clear evidence about this. In order to obtain improved understanding of these phenomena, the present research has been undertaken with the following main objectives:

1. To determine the initial alkali thresholds required by the various aggregates to induce significant ASR.

2. To identify the source materials in these aggregates causing the AAR reaction and thereby determine the type of reaction initiating the observed expansions.

3. To establish whether aggregates containing strained quartz are reactive and, if so, whether the reactive constituent is the strained quartz or some other element of the aggregate.

4. To determine the affects of immersion in salt solution on concretes of varying initial alkali content and containing different reactive aggregates. This may also establish if the initial alkali threshold for a concrete has any bearing on the affects the NaCl has on the ASR.

5. To establish by chemical analysis and petrography why ASR develops differently when the concretes are immersed in salt solution.

6. To determine whether alkalis' from high alkali pfa can contribute to and exacerbate any ASR in low alkali threshold aggregate mixes.

7. To establish if the ASR retardant qualities of air entrainment in a concrete are a life long or just a temporary feature of the material.

8. To determine if ASR in an air entrained concrete affects the freeze / thaw resistance of the material.

9. To identify the variations in ASR gel composition due to using either different reactive aggregates, alkali levels and salt environment.

10. To identify petrographically and by use of the EMP changes noted in some reactive cement pastes in saline environmental conditions and to explain the relevant observations.

## 1.7 Plan of presentation

Following the review presented in this chapter, the thesis contains the following parts:

Chapter two details the materials used and experimental methods employed in this work.

Chapter three describes the experimental work undertaken to establish the alkali threshold for significant expansion for each of the coarse aggregates. It also

describes the petrographical analysis used to establish cause of expansion and the source of reaction in the aggregate.

Chapter four explains the methods employed to establish the effects of salt solution in a number of experimental situations, on some of the reactive aggregates studied in chapter three. Compositional profiles through the concrete prisms are discussed and petrographical analysis is used to interpret the observed variations in expansion results.

Chapter five discusses the effects of cement replacement by high alkali pfa's on concretes containing reactive aggregates. Pore solution analysis of these concretes is employed to ascertain whether alkalis from the pfa are contributing to the total amounts available to any ASR.

Chapter six describes the affects of air entrainment on the degree of expansion occurring in concretes containing reactive aggregates. The results obtained at 38°C are compared to the behaviour of identical mixes placed in a field environment.

Chapter seven describes the results of electron microprobe analysis of ASR gels developed by different reactive aggregates at various alkali levels, immersed in distilled water and salt solution and also some analyses of the associated cement pastes and aggregates.

Chapter eight presents the general conclusions and recommendations for future work.

# CHAPTER 2

## Experimental Materials and techniques

### 2.1 Materials

### 2.1.1 Cement

A single Portland Cement (PC) was used throughout the experimental work to make the concretes. The cement was a white cement called 'Snowcrete' provided by Blue Circle Industries. Table 2.1 shows a detailed chemical analysis of the cement as a percentage by weight of the constituent oxides and the calculated constituent cement minerals.

TABLE 2.1 : Chemical Analysis of Portland Cement and constituent cement minerals present.

| $CaO$ | $SiO_2$ | $Al_2O_3$ | $Fe_2O_3$ | $SO_3$ | $MgO$ | $Na_2O$ | $K_2O$ | Ignition Loss |
|---|---|---|---|---|---|---|---|---|
| 66.02 | 22.55 | 4.87 | 0.31 | 3.16 | 0.27 | 0.14 | 0.28 | 1.55 |

$C_3S$ = 51.5 %  $C_2S$ = 25.8 %  $C_3A$ = 12.4 %  $C_4AF$ = 0.94 %

(Calculated by method described in Lea, 1970, page 116).

This cement was used because of its low total alkali content (0.324% $Na_2O_e$), which meant that a suitable range of alkali levels could be produced by the addition of NaOH to the mix water. It also has a higher than normal $C_3A$ content (12.4 %). This high $C_3A$ content means it maybe more susceptible to the creation of extra OH ions by the chemical reaction between the $C_3A$ and deicing salt discussed briefly in section 1.5.1.

### 2.1.2 Aggregates

Eight lithologically varied United Kingdom aggregates were used in this work, six of which have been shown to exhibit alkali aggregate reaction in field structures. The seventh aggregate, a strained granitic rock, from Anglesey, North Wales was included as it has been shown recently to be heavily strained, exhibiting an undulatory extinction angle (UEA) of 31.5$^o$ based on the Dolar-Mantuani method

(1983), (Source A. Smith, Leicester University). Including this rock in the testing may help answer the question of whether highly strained quartz is itself ASR reactive.

TABLE 2.2 : Aggregates used in work.

| NAME | LITHOLOGY & AGE | LOCATION | AFFECTED STRUCTURE. |
|---|---|---|---|
| Maentwrog greywacke | Greywacke, Lr. Cambrian. | Maentwrog, North Wales. | Maentwrog Dam. |
| Horrocksford limestone | Silicified limestone, Carboniferous. | Clitheroe, Lancashire. | Various bridge beams. |
| Dry Rigg siltstone | Chloritic siltstone, Silurian. | Horton in Ribblesdale, North Yorkshire. | Padiham Bypass. |
| Venn Quarry siltstone | Quartz rich iron stained siltstone, Carboniferous. | Venn Quarry, Nr Barnstable, Devon. | None reported. |
| Trent Valley gravel | Polymictic gravel contains chert, quartz and quartzites, Quaternary. | Repton gravel pit, Derbyshire. | Midlands Links. |
| Thames Valley gravel | Mainly flint with some vein quartz and quartzites, Quaternary. | Theale gravel pit, Berkshire. | Old section of M40, Oxon. |
| Anglesey granite | Heavily altered and metamorphosed granite, Pre-cambrian. | Gwyndy Quarry, Llandrygarn, Anglesey. | None known. |
| Cheddar limestone | Fossiliferous limestone, Carboniferous. | Cheddar, Somerset | None known. |

The Cheddar limestone was used as the inert fine (<5mm) aggregate as well as one of the coarse aggregates.

The last rock included in the series was Cheddar limestone, a non-reactive aggregate which was also used as the inert fine aggregate constituent of the concrete mixes used. This rock was included to dispel the possibility that the expansions observed could produced by other environmental causes or ASR in the fine aggregate. A brief summary of information on these rocks is shown in Table 2.2.

A more detailed petrographical description is given in Appendix 1.

Once the aggregates had been collected and all relevant geological data obtained they were stored in dry sealed bins in preparation for mixing. In all the aggregates studied with the exception of the Cheddar limestone, constituents were noted petrographically that could be potentially ASR reactive (Appendix 1).

### 2.1.3 Pulverised Fuel Ashes (Pfa's)

Two pulverised fuel ashes (Pfa's) were used as cement replacement materials for stage 3 of the research programme (see chapter 5). The chemical compositions of the two ashes are shown in Table 2.3. The Pfa's were provided by the Building Research Station and are thought to represent typical medium and high alkali content materials, the Fiddlers Ferry Pfa containing 3.08% $Na_2O_e$ and the West Burton Pfa containing 4.00% $Na_2O_e$.

TABLE 2.3 : Chemical Analysis of the two pulverised fuel ashes (%).

| | CaO | $SiO_2$ | $Al_2O_3$ | $Fe_2O_3$ | $SO_3$ | MgO | $Na_2O$ | $K_2O$ | LOI |
|---|---|---|---|---|---|---|---|---|---|
| Fiddler's Ferry (FF) No. 913. | 2.31 | 52.40 | 29.40 | 9.20 | 0.68 | 1.50 | 0.84 | 3.40 | 4.40 |
| West Burton (WB) No. 901. | 1.48 | 51.00 | 25.30 | 9.92 | 0.79 | 1.38 | 1.58 | 3.69 | 3.69 |

## 2.2 Experimental techniques

The initial stages of this research was carried out using expansion test prisms (as described in the draft BS 812 part 123 (1990) made up from the eight aggregates described above. To these concretes were added a quantity of NaOH in the mix water to produce concretes of specific alkali content (See Chapter 3).

### 2.2.1 Mix design

All stages of the work took place using mixes containing the reactive constituent in the coarse aggregate (20 to 5 mm) only. This was decided after discussion with Dr. W. French, Queen Mary's College, London. He felt that though results on the reactivity of aggregates were more rapidly obtainable for expansion testing carried

out on finer (<5mm ) aggregate, greater amounts of expansion could obtained using a coarse aggregate over longer periods of time. The petrographical identification of ASR sites, product and form would be easier using only a reactive coarse aggregate. A lot of research has been carried out using mortar and fine aggregate concretes, therefore it was also considered of benefit to study more 'realistic' reactive coarse aggregate concretes.

By using a non-reactive fine aggregate, it is clear that any ASR observed in a particular sample is derived from the coarse aggregate only, so the overall analysis is not confused by having secondary sources of reactivity present in the fine aggregate. The only disadvantage to using a non-reactive fine aggregate, is that the concrete will therefore contain less than 100 % reactive aggregate and this can often reduce the total expansion recorded, as many aggregates tend to have 100 % pessimum levels (see section 1.4.2.1). Consultation with Dr. P. Nixon of the Building Research Station helped set the maximum pessimum value for the Thames Valley Gravel at 50 % of the coarse aggregate. It was felt this figure was closest to a pessimum value using only a coarse reactive aggregate and was most comparable with the other aggregates which were all considered to have 100 % pessimum levels. The initial requirements of the mix design were to include a realistic volume of cement, coarse and fine aggregates similar to that found in field structures. After a series of trial mixes, the eventual design mixes used were as shown in Table 2.4.

In all cases only deionised water was used in the mixes. The proportions of these mixes were initially calculated using, 'Design of normal concrete mixes', BRE publication BR106 (1988). To these mixes were added specific amounts of NaOH to produce the required alkali levels as shown in chapters 3, 4, 5 and 6.

TABLE 2.4 : Mix design for aggregates with various specific gravity to produce two expansion prisms.

A. Specific gravity 2.7

1. Maentwrog greywacke.
2. Horrocksford limestone.
3. Dry Rigg siltstone.
4. Venn Quarry siltstone.
5. Anglesey granite.
6. Cheddar limestone (inert).

MIX PROPORTIONS:

| | | | |
|---|---|---|---|
| Cement | = | 1.238 kg | => 400 kg/$m^3$. |
| Water | = | 0.619 kg | => 200 kg/$m^3$. |
| Coarse Aggregate | = | 3.975 kg | =>1285 kg/$m^3$. |
| Fine Aggregate Inert | = | 1.701 kg | => 550 kg/$m^3$. |
| TOTAL MIX MASS | = | 7.533 kg. | |

Water / Cement ratio = 0.5 Aggregate / Cement = 5 to 1.

Pessimum : All 100 %.

B. Specific gravity 2.6

1. Trent Valley gravel.
2. Thames Valley gravel.

MIX PROPORTIONS:

| | | | |
|---|---|---|---|
| Cement | = | 1.238 kg | => 400 kg/$m^3$. |
| Water | = | 0.619 kg | => 200 kg/$m^3$. |
| Coarse Aggregate | = | 3.790 kg | =>1225 kg/$m^3$. |
| Fine Aggregate Inert | = | 1.624 kg | => 525 kg/$m^3$. |
| TOTAL MIX MASS | = | 7.271 kg. | |

Water / Cement ratio = 0.5 Aggregate / Cement = 5 to 1.

Pessimum : Trent Valley gravel 100 %, Thames Valley gravel 50 % of coarse aggregate which is equivalent to 30 % of the total aggregate content.

### 2.2.2 Mixing Procedure

The mix components were batched by weight in a dry state. For a number of the aggregates which were collected from closed or non producing quarries the 20 to 5 mm coarse aggregate had to be made up by the addition of the following sieved aggregate sizes.

TABLE 2.5 : Percentages of various aggregates sizes added to produce a 20 to 5mm graded concreting aggregate.

| | | |
|---|---|---|
| 20mm | - | 35 % |
| 14mm | - | 25 % |
| 10mm | - | 25 % |
| 6mm | - | 15 % |

The two prisms for each mix were made up in accordance with the British Standard BS1881: Part 5 (1970). The prisms were made up to the dimensions, 75 X 75 X 250 mm.

The dry constituents of the concrete mixes were first mixed by a mechanical mixer for 2 minutes to ensure an even distribution of the components. The mixing water, along with the dissolved NaOH additions was added to the concrete mix which was then mixed for a further 1.5 minutes. After this period the mix was agitated by hand mixing with a trowel before being mechanically mixed for a further 3.5 minutes. Once mixed, the concrete was added to the moulds in three even layers. After each layer was placed in the prism moulds, the moulds were placed on a vibrating table for 1 minute. No tamping was carried out on the prisms. The top surface of the prism was hand trowelled to a smooth finish. Once this was complete the prisms were cured under a plastic sheet to keep moisture loss to a minimum in a constant 20°C± 2 temperature room. After 24 hours the prisms were demoulded, cleaned and numbered. Demec points were then stuck to the upper (in most cases) surface of the prism at a distance of 200 mm. This completed, the prisms were left to cure for a further 6 days above water and under a plastic sheet at room temperature.

### 2.2.3 Expansion tests

After 7 days the prisms were measured accurately between their Demec points, using a dial gauge accurate to $9.9 \times 10^{-4}$ % strain. The dial gauge is a portable

extensometer measuring the distance between two metallic discs, (Demec points) glued to the surface of the concrete. Once measured the prisms were wrapped in an absorbent towelling material and wetted with approximately 200 ml of distilled water. This water was added to later as required. The prism, towelling and water were triple bagged in plastic bags and sealed.The prisms were placed in a temperature controlled room at 38°C ± 2. The prisms were taken out of this temperature controlled room 24 hours prior to being measured each month.This was done to allow thermal expansion effects to be removed. The prisms of all the different aggregate mixes were seen to expand rapidly during the first week as they took up some of the surrounding water. These first week expansion figures were taken as the zero point for further measurements. The prisms were usually measured once a month.

The second stage of the work involved exposure of identical prisms to various saline environments as summarised below:

1. Prisms were totally immersed in salt solution, (2 mol NaCl / litre).
2. Prisms were totally immersed in salt solution, (2 mol NaCl / litre) for 1 month then left dry for 1 month.
3. Prisms were half immersed in salt solution, (2 mol NaCl / litre) and half left dry, but still within the sealed plastic container.
4. Prisms were totally immersed in deionised water.
5. Prisms were left totally dry in air (25 % relative humidity).

None of these prisms were wrapped or treated in any way. In the case of the prisms half immersed in salt solution (environment 3) sets of Demec points were stuck to the top and bottom of the prisms. A pair of Demec points 50 mm apart were also added to the side of the prism covering the area in which the salt solution / air interface occurs. All the testing was carried at 38°C and all prisms were left for 24 hours at room temperature before being measured.

The third stage of work involved the replacement of some of the cement by Pfa. The alterations to the mix design and alkali addition are described in chapter 5. These prisms were wrapped and stored in the same manner as those described above for chapter 3.

During summer the high outside temperatures on occasions showed up in higher than expected expansion figures, these abnormalities were taken into account. It was found that the effect of temperature on expansion was in the order of 0.001 % strain per degree centigrade. This figure was based on the expansion results of

non-reacting prisms in July 1991 when the outside temperature was 28°C + (see Table 2.6).

TABLE 2.6: Expansion data, (%) strain for various non-reacting (DR) siltstone prisms, which show the effects of the high summer measuring temperatures (28°C+).

| Sample letter and alkali level. | 2.0 kg A | 2.0 kg B | 2.5 kg A | 2.5 kg B | Average % change |
|---|---|---|---|---|---|
| July 1991, (28°C+) | 0.01089 % | 0.00990 % | 0.01089 % | 0.01188 % | 0.01089 % |
| December 1991, (20°C±2) | 0.00495 % | 0.00099 % | 0.00396 % | 0.00198 % | 0.00297 % |

The average difference in percentage strain between July 1991 and normal room temperature was 0.00792 %. Therefore, the 8°C+ rise in measuring temperature for July 1991, means that for each degree rise the strain recorded was increased by 0.001 %+.

## 2.3. Chemical analysis of concretes

After some of the concrete prisms had been tested for 15 months in differing saline environments, it was necessary to carry out chemical analyses of the prisms from their outer surface into the centre and in one particular environment (see chapter 4) to have a complete traverse from top to bottom. To carry out the chemical analysis the prisms were firstly sawn into 5 or 8 slices approximately 7 or 9 mm thick of dimensions 30 x 35 mm that ran from the outer surface inwards avoiding the effects of the other prism faces (see Figure 2.1 page 196). These slices were numbered, bagged and dried at 80°C for 48 hours. The slices were individually crushed in a small ball crusher and passed through a 600 $\mu$m sieve. The powdered sample was then dried at 110°C for a further 24 hours.

The sample was now ready to be analysed for Cl -, Na+ and K+ ions. Once thoroughly mixed to produce a homogeneous material, approximately 5 grammes of the powder was weighed into a 200 ml glass beaker, the amount of powder being recorded to the nearest 0.01 grammes. The powdered concrete was dispersed in a small amount of deionised water after which 10 ml of concentrated nitric acid was added. To this solution was added warm deionised water to make up

a total volume of 100 ml. This solution was then heated just to boiling, after which it was taken off the heat and left to cool in a fume cabinet for 3 to 4 hours. Once cool the solution was filtered and diluted with deionised water to make up 500 ml of solution. At this point some solution samples were ready to be analysed. Other solutions, however, were diluted as required.

### 2.3.1 Chloride testing

The free chloride ion concentrations of the samples were determined by a colorimetric method using a Beckman Model 24 double beam spectrophotometer. 10 ml of the solution, diluted as required, was placed into a test tube to which the colorimetric reagents were added. These were in the form 2 ml of 0.25 Molar ferric ammonium sulphate, $[Fe(NH_4)\ (SO_4)_2.12H_2O]$ in 9 Molar nitric acid and 2 ml of saturated mercuric thiocynate in absolute ethanol. The solutions were allowed to stand for ten minutes while the colour developed. The colour intensity relates to the chloride ion concentration, due to the formation of a highly coloured complex involving the chloride ions (Vogel, 1961). The spectrophotometer measures the absorption of light at a specific wavelength, namely 460 nanometres. This coloured solution is then added to a small glass sample cell and a light beam is passed through it. The difference in the light absorbed between a blank (clear) and test solution was proportional to the concentration of chloride ions present.

Using a calibration curve produced using standard chloride solutions the molarities of the test solutions can be calculated. The chloride content figure for a particular test solution can alternatively be obtained by using the following equation mathematically obtained from the graph shown in Figure 2.2, page 197:

$$Y = \frac{54.78\ X - 2.73}{100}$$

Where X is the Light absorption (ABS) figure for that solution obtained from the spectrophotometer (i.e 0.123) and Y is the required unknown chloride concentration in mmol per litre.

From this figure of the chloride concentrations in mmol / litre, it was possible to calculate the same result as a percent chloride, ($Cl^-$ ion %) as shown below.

1. Cl concentration in mmol /litre is for example 0.06 mmol / litre. Take this concentration and multiple it by the amount of solution that has been made up, for example 500 ml.

$$0.06\ X\ 0.5 = 0.03\ mmol$$

2. Take this figure and divide it by the mass of the initial powdered concrete sample, (5.23 grams), to give your Cl concentration per gram of material.

$$\frac{0.03}{5.23} = 5.736 \text{ X } 10^{-3} \text{ mmol / g}$$

3. Multiply by molar weight equivalent for Cl (1 mmol Cl = 0.0355g Cl).

$$5.736\text{X}10^{-3} \text{ X } 0.0355 = 2.036 \text{ X } 10^{-4} \text{ g / g.}$$

4. Multiply by X100 to get a percentage %.

$$2.036 \text{ X}10^{-4} \text{ X } 100 = \underline{\textbf{0.02 \%}} \text{ Cl by weight of sample.}$$

A number of sample solutions were slightly milky due to fine suspended particulates; in these cases the solution was allowed to settle before any analysis took place.

### 2.3.2 Sodium and potassium testing

The sodium and potassium contents of the sample solutions were determined by flame photometry. Duplicate specimens of the solution were made up and diluted accurately as required, to allow the recorded sodium and potassium concentration to be located in the range of concentrations over which the flame photometry method of analysis were linear. To produce this, a series of standard calibration solutions was made up to 1, 2, 4, 6, 8, and 10 parts per million (ppm) of Na and K. These standard calibration solutions were made up from a master standard equivalent to 500 ppm, produced from an analytical grade sodium and potassium solution and diluted as required. Calibration from these standard solutions was carried out before and after each series of tests to ensure accuracy. A graph of the standard Na / K ppm solutions were plotted against the recorded flame intensity figures (Figure 2.3). The required Na and K concentration readings for the test solutions were taken directly from this graph, prior to correction for the dilution rate used with that solution. These Na and K results in parts per million, ppm were also calculated for ease of display as $Na_2O$ %and $K_2O$ %, by the following method.

1. Take the parts per million figure (5 ppm for example) for a litre of solution and divide by the mass of your initial sample, and multiply by X100 to give you a figure of percentage Na or K cations.

$$\frac{0.005}{5.23} \text{ X100} = 0.096 \text{ \% Na or K}$$

2. To make up Na or K to any oxide equivalent multiply by $\frac{Na_2O}{2Na} = \frac{23+23+16}{23+23} = \frac{62}{46}$

$$0.096 \times 1.348 = \underline{\mathbf{0.129\ \%}}\ Na_2O\ \%$$

OR $\frac{K_2O}{2K} = \frac{39+39+16}{39+39} = \frac{94}{78}$

$$0.096 \times 1.205 = \underline{\mathbf{0.116\ \%}}\ K_2O\ \%$$

This method of analysis is equivalent to that described in BS 1881: Part 124 (1988).

## 2.4 Pore solution expression and analysis

Part of the work required the addition of a number of pulverised fuel ashes (pfa's) to some potentially reactive concrete mixes. This has been observed to alter their potential ASR reactivity (See Chapter 5). As the alkalis in the pore solution are considered to be the primary source of alkalis for ASR, it was considered necessary that pore solutions be obtained from these concretes at a number of ages during the experimentation to establish the potential reactivity of those mixes at various times. This was carried by establishing the Na+, K+ and OH- ion concentration of the pore solution, which should relate directly to the potential reactivity of that concrete.

### 2.4.1 Pore solution expression

The pore water is the fluid within the pores of the hydrated cement structure that is able to be extracted from hardened pastes, mortars and concrete specimens by subjecting them to very high pressure. The specimens used for the extraction of pore solution were the same as those tested for expansion. Once the expansion testing time of the prism was complete, the prism was cut using a diamond saw to produce a piece of concrete of dimensions, 75 X 75 X 100 mm. This was then washed in deionised water, dried and wrapped in a plastic bag. The concrete sample was then crushed whilst still in the plastic bag by a hydraulic press. The crushed concrete was then passed through a 5 mm sieve which removed most of the aggregate particles. The finely crushed concrete was then loaded into the pore solution expression apparatus. The construction of the press is similar to that first described by Longuet, Burglen and Zelwer (1973) and is shown in Figure 2.4 in Appendix 2.

The crushed concrete sample was contained within a cylindrical vessel and subjected to pressure created by a free moving piston loaded by the hydraulic press used to crush the concrete sample. As some of the older samples, (1 year) contain little extractable pore solution the load was applied quickly increasing at a rate of up to 30 MPa per second to a maximum pressure of 600 MPa, this was done to avoid significant evaporation. This pressure was usually maintained for 30 minutes, but with the older samples up to two hours of pressure was sometimes required to produce a large enough volume of pore solution to carry out the full chemical analysis. Normally the pore solution ran straight into a sealed plastic vial avoiding excessive contact with the air and therefore possible carbonation. Occasionally, a slight vacuum produced using a plastic syringe was required to extract the pore fluid.

Although the pore solutions expressed represent only a small fraction the total evaporable water present in the specimens it is a reasonably accurate representation of the specimen. This observation was determined by experimental work carried out at Aston University (Hardon, 1983). It is appreciated that a small variation in the pore solution composition is possible as a result of the variations in the rate, magnitude and duration of the pressure applied to the sample. However, the effects are believed to be small (Silsbee et al. 1986).

### 2.4.2 Analysis of expressed pore solution

The expressed pore solutions were left for no longer than three hours before the analysis for the hydroxyl ion concentration was carried out. During this time the vials containing the pore solutions remained upright to allow any particles, if present to settle out. They also remained sealed to prevent carbonation. It was necessary that the solutions were tested for sodium, potassium and hydroxyl ion concentrations (See chapter 5). As for the analyses carried out on the powdered concrete samples the sodium and potassium ion concentrations were determined by flame photometry (See 2.3.2). The only significant difference was that the duplicate samples were made up by adding a 0.1 ml aliquot of pore solution to 100 ml of deionised water, which allowed the Na and K concentrations to be determined without further dilution. The hydroxyl ion concentration was measured by titration using phenolphthalein as an indicator. A 0.1 ml aliquot of pore solution was added to a small volume of deionised water and titrated against either 0.01 M or 0.005 M nitric acid to the end point of phenolphthalein. The quantity of acid required was measured using a 10 ml burette with 0.02 ml divisions which was found suitable for

use with all the pore solutions analysed in this work.

## 2.5 Petrographical analysis of test concrete

Once the concrete prisms had completed their expansion testing they were analysed for surface microcracking, gel exudations and the outer surfaces were photographed (see section 2.5.3). Two slices were then cut vertically through the centre of the prisms. One of these slices was 35 mm thick and this was used for bulk chemical analysis (See 2.3). The second slice was 15 mm thick and a petrographical thin section was produced from it.

### 2.5.1 Manufacture of a petrographical thin section

The slice of concrete was firstly dried out at 50°C for 48 hours. Once dry the concrete slice was placed in a vacuum impregnation unit and the whole chamber was evacuated for 3 to 4 hours or until a significant vacuum had developed. After this time a fluorescent araldite resin was added to the chamber and allowed to cover the concrete sample in vacua. A short time after this the vacuum pump was switched off and air allowed back into the chamber. The return of air pressure caused the fluorescent resin to be drawn into the concrete along any fissures, cracks or voids present. In the area of concrete immediately adjacent to the original surface, the vacuum was strong enough to actually draw the resin into the capillary porosity of the cement paste. After a few minutes the concrete slice was removed from the chamber and left for between 5 to 8 hours to allow the resin to harden. The resulting concrete sample was held together by the resin and all the voids and microcracks etc. would be shown up clearly by the fluorescence dye.

Once the resin was hard the cut surface of the concrete was ground to an almost mirror like finish on a lapping plate using a 15 and 9 $\mu$m aluminium oxide abrasive powders suspended in ethane diol lubricant. These materials were used to avoid the dangers of washing the water based ASR gel out of the thin section. This polished face was then cleaned and stuck down to a ground glass slide. Once the concrete was stuck the excess material was cut off back face leaving a slice of concrete approximately 250 $\mu$m thick stuck to the glass slide. This face was then ground down on the lapping plate to a final standard thickness of 30 $\mu$ms. Once a cover glass was stuck to this slide it is ready for petrographical examination.

### 2.5.2 Petrographical examination

The thin sections were examined using a normal transmitted light polarising microscope. Petrography allows for the identification and confirmation of a number of features of the alkali silica reaction which cannot usually be seen by other means. These include: (i) aggregate lithology and relationship to any ASR; (ii) cement type, condition, carbonation, water / cement ratio etc.; (iii) occurrence of other degenerative minerals or products such as ettringite from sulphate attack; (iv) microcracking, type, degree, form and location and (v) ASR gel, amount, location and form. From these and other macro-observations a good basis can be made for the interpretation of any ASR affected concrete. Full details of the petrographical examinations of the concretes in this study are given throughout this thesis.

### 2.5.3 Other visual techniques used with the alkali silica reaction

Two further techniques were employed to examine the reacted concretes on a larger scale. Firstly the off-cuts from the manufacture of the thin sections were polished to a fine face using 15 $\mu$m aluminium oxide powder. This face was then photographed in a dark room, using only an ultra-violet light source and a long exposure time (Marshall and Walker, 1978 and Hobbs, 1988, page 89). As most of the microcracks had been previously filed by an araldite resin containing a fluorescent dye, all the microcracks and voids were shown clearly (plates 3.12 to 3.15). These photos give a good impression of the the overall microcrack networks in relation to the different aggregates used and their location in the prism.

The final technique employed was the staining of ASR gel present in the test concretes with a UV light sensitive material (Natesaiyer and Hover, 1988). Once the expansion testing was complete a further slice was cut from the concrete prism. This was cleaned but left wet, as this technique produces better results in a wet condition. After putting on eye protection and rubber gloves, uranyl acetate solution was added to the surface using a sprayer. The protective clothing was especially important here as the uranyl acetate releases a low level of gamma radiation. Only a momentary application of a solution film was necessary to wet the surface with solution adequately. The uranyl acetate solution is comprised of dilute acetic acid which was 5 ml of glacial acetic acid to deionised water making up 200 ml. To this was added 5 g of uranyl acetate; this was warmed but not boiled until the powder had fully dissolved. The solution was then stored in a closed plastic bottle.

After 5 minutes the solution was rinsed off the concrete surface using deionised water as any ASR gel present would have reacted. The sample was then taken to a dark room and viewed using a UV light source. Photographs were also taken in this environment, but viewing is easier by eye. Any alkali silica gel present on the surface was shown up by a yellowish-green fluorescence along the microcracks and voids in which it maybe found. In this technique the uranyl ions in the acetate solution substitute for alkali in the gel thereby imparting its fluorescent colour when viewed in UV light. Some fluorescence is taken up by alkalis in the cement paste, but the much lower concentrations of these in the paste means that the gel is far more clearly seen under UV light conditions.

## 2.6 Electron microprobe analysis

An electron microprobe was used to analyse the composition of the alkali silica gels produced by the ASR in various mixes in this work. In electron microprobe analysis electron bombardment is used to generate X-rays in the sample area to be analysed. From the wavelength and intensity of the lines in the X-ray spectrum the elements present may be identified and their concentrations estimated. The use of a finely focused electron beam (5 $\mu$m diameter) gives the technique its particular advantage of enabling chemical analyses to be obtained on a very small scale such as the ASR gel material found in the microcracks of the concretes in this study. The electron beam when analysing only penetrates to a depth of about 1 $\mu$m into the sample material. In the process it leaves a small mark which can be seen after the analysis is complete. For accurate quantitative analysis the intensities of the X-ray lines from the sample are compared with those from standard samples of known composition (Reed, 1975). Once set up the microprobe is able to analyse a great number of points on a sample automatically. For this reason a relatively large number of analysed points has been used on each sample and this makes the results obtained statistically reliable. The concrete to be analysed is made into a polished thin section of normal 30 $\mu$m thickness, but the polishing is obtained using a 1 $\mu$m diameter diamond powder.

The electron microprobe used for the work was a Jeol JXA-8600 Superprobe located in the Geology Department of Leicester University who have kindly allowed this work to be undertaken there.

A number of other experimental techniques were used during specific parts of this work, and these are described in detail where required.

# CHAPTER 3

## Calculation of alkali thresholds for selected UK aggregates

### 3.1 Introduction

In recent years a number of lithologically varied UK aggregates have been shown to be susceptible to the alkali silica reaction. These have a greater geographical range than previously studied aggregates and therefore may be of concern to future construction work.

In the UK research work has been carried out on the Thames and Trent Valley river gravels which have been considered potentially the most reactive land-based UK aggregates presently produced. However, in the case of the Thames Valley gravel the occurrence of reactive concretes with near-pessimum proportions will be very rare in field structures. To date only one case has been reported in which Thames Valley gravel has been responsible for ASR induced cracking and in this structure the ASR was considered to be a secondary feature (Sibbick and West, 1989).

In view of the continuing use of other lithologically varied aggregate types in concrete, it should be of benefit to identify the initial levels of alkali required in the original concrete mixes to initiate a significant ASR. From this information it should be possible to compare the amounts and rates of expansion developed by each aggregate type in rapid test conditions and these results should help in the avoidance of further cases of ASR.

Using petrographical examination it is possible to identify the causes of the expansion seen in these concretes and to explain why certain aggregates should be more reactive than others. In a few cases the cause of the expansions observed is still debated (Hobbs,1990). With this in mind extra chemical and petrographical tests have been carried out on particular concretes to confirm the cause of the observed expansions (see section 3.7).

### 3.2 Experimental method

Expansion testing of concrete prisms has been a common method for assessing ASR in the UK. The rates of expansion in a concrete prism considered to represent significant ASR are some what poorly defined. The method of expansion testing used in this work was in accordance with British Standards Institution specification

(1983, 1987 and 1990) which has also been successfully used by researchers at the Building Research Station for some years. They consider that if the amount of expansion recorded exceeds 0.05 % strain after 6 months then, 'some degree of ASR has occurred'. If the amount of expansion recorded exceeds 0.1 % strain after 12 months, then the aggregate mix should be regarded as 'reactive'. In Canada, however, the AAR reactivity of a concrete mix is considered significant if a strain of 0.04 % is achieved at any age in 38°C and 100 % RH, for concretes subjected to severe exposure conditions (CAN /CSA-A23.1-M90, CAN /CSA-A23.2-M90, 1990). On the other hand Hobbs (1992a) suggests that only concretes exhibiting greater than 0.25 % strain after 12 months at 38°C and 100 % RH will show significant ASR in field exposure. From this information it is apparent that even an expansion figure considered to be representative of significant AAR reaction is still unresolved. However, as visible surface microcracking usually appears at >0.05 % strain, the figure of 0.05 % strain after 12 months at 38°C and 100 % RH will be taken, at least in the first stage of this research, to indicate that substantial expansion of the concrete has taken place.

Concrete prisms for this work were made following the mix design described in section 2.2.1. The various total alkali contents for the mixes were produced by adding NaOH to the alkalis already present in the cement.

TABLE 3.1: Chemical analysis of the OPC 'Snowcrete' from Blue Circle cement for sodium and potassium

| | | |
|---|---|---|
| $Na_2O$ | = | 0.14 % |
| $K_2O$ | = | 0.28 % |

$Na_2O$ equivalent $= Na_2O\ \% + (0.658 \times K_2O\ \%)$.

$Na_2O$ equivalent $= 0.14\ \% + (0.658 \times 0.28\ \%)$.

% $Na_2O$ equivalent = **0.32 %**

(Calculated from BS4550: Part 2: 1970, clause 16.2).

Based on previous knowledge of the alkali levels that were required to initiate the ASR the mixes were made up with alkali levels ranging from 2 kg/m$^3$ to 7 kg/m$^3$ $Na_2O$ equivalent. For the Thames Valley gravel aggregate it is well documented

that significant expansion does not occur below 5.2 kg/m$^3$ $Na_2O_e$ (Nixon et al. 1986) and therefore in these cases some low alkali level mixes could be omitted.

However, with reference to some of the other aggregate types, French (1990) has previously stated :

> 'Significant amounts of reaction involving cracking and gel production have been encountered with alkali concentrations between 2.5 and 3.5 kg/m$^3$.'

After consultation with Dr. French and Dr. Nixon the ranges of the alkali level for each aggregate type to be studied were decided upon as shown in Table 3.2.

TABLE 3.2: Alkali levels of mixes made up for each of the aggregates (expressed in $Na_2O_e$).

| | |
|---|---|
| 1. Dry Rigg siltstone, | 2.0 to 7.0 kg/m$^3$ |
| 2. Horrocksford limestone, | 2.0 to 7.0 kg/m$^3$ |
| 3. Maentwrog greywacke, | 2.0 to 7.0 kg/m$^3$ |
| 4. Trent Valley gravel, | 2.0 to 7.0 kg/m$^3$ |
| 5. Venn Quarry siltstone, | 4.5 to 7.0 kg/m$^3$ |
| 6. Thames Valley gravel, | 4.5 to 7.0 kg/m$^3$ |
| 7. Anglesey granite, | 4.5 to 7.0 kg/m$^3$ |
| 8. Cheddar limestone, | 4.5 to 7.0 kg/m$^3$ |

## 3.3 Alkali addition calculations

The amounts of NaOH which had to be added to a mix to obtain the correct alkali levels were calculated as shown in the example below:

1. Cement content of the concrete = 400 kg/m$^3$

Alkali content of cement = 0.32 % $Na_2O_e$.

Alkali derived from cement in a mix = 400 x 0.32 = 1.29 kg/m$^3$ $Na_2O_e$

2. If the required alkali content for a particular concrete is 4.0 kg/m$^3$

Alkali addition required = 4.0 - 1.29 = 2.71 kg/m$^3$ $Na_2O_e$

3. As this alkali is added to the mix water (200 kg/m$^3$) the required concentration is,

$\frac{2.71}{200} \times 1000 = \underline{13.55}$ g $Na_2O_e$ / litre.

4. This is equivalent in to,

$\frac{80}{62} \times 13.55g = \underline{17.48}$ g NaOH / litre.

5. The required water for 2 prisms mix = 0.62 litres

The required NaOH addition for this mix is :

$$17.439 \times 0.62 = \underline{\mathbf{10.80}}\ g$$

Similar calculations yielded the following table of NaOH additions:

TABLE3.3: NaOH additions for concretes of varied alkali content.

| Required alkali level, kg/m$^3$ | Required $Na_2O_e$ / litre. (grammes) | Required NaOH /litre. (grammes) | Required NaOH in water for 2 prisms. (grammes) |
|---|---|---|---|
| 2.0 | 3.52 | 4.54 | 2.81 |
| 2.5 | 6.02 | 7.76 | 4.80 |
| 3.0 | 8.52 | 10.99 | 6.80 |
| 3.5 | 11.02 | 14.21 | 8.80 |
| 4.0 | 13.52 | 17.44 | 10.80 |
| 4.5 | 16.02 | 20.67 | 12.79 |
| 5.0 | 18.52 | 23.89 | 14.79 |
| 5.5 | 21.02 | 27.12 | 16.79 |
| 6.0 | 23.52 | 30.34 | 18.78 |
| 7.0 | 28.52 | 36.79 | 22.78 |

The relevant amounts of NaOH were added to the mix water and allowed to dissolve fully. The various concrete prisms were then made up in accordance with the relevant British Standards (British Standards Institute, 1970 and 1990) as described in section 2.2.2.

## 3.4 Expansion testing of concrete prisms

The concrete prisms were then tested as described in section 2.2.3. At monthly intervals they were removed from the 38°C ± 2°C environment and allowed to cool to normal laboratory temperature (20°C ± 2°C) for 24 hours prior to being measured. The strains recorded over a period of up to 12 months are shown in Figures 3.1 to 3.9. The times when surface microcracking was first observed was also recorded and these are summarised in Table 3.5.

### 3.4.1 Result of expansion tests using variable alkali contents

In Figure 3.1, the behaviour of some of the aggregates in mixes of constant high alkali level (7 kg/m$^3$ $Na_2O_e$) are compared. It is apparent that the Thames and Trent Valley gravels, which have often been considered amongst the more reactive land-based UK aggregates (French, 1990a) suffer relatively modest expansions in comparison with those recorded for some of the other less well-documented aggregates studied here. These lithologically varied aggregates are therefore more susceptible to ASR than the chert-rich gravels. It is apparent from all the figures shown that all of the coarse aggregates studied with the exception of the control material, inert limestone, gave rise to substantial expansions of the concrete prisms directly related to the initial alkali contents of the mixes. Amongst the more interesting expansion results are those obtained for the strained granite (Figure 3.5). This rock has never previously been examined for its AAR potential. Clearly it is affected quite severely by an expansive alkali dependent reaction, the cause of which is discussed later in the petrographical analysis (Section 3.5).

Figures 3.10 to 3.16, shows the expansion results after 12 months for all the different prisms at the various initial alkali levels of the various aggregate mixes. These graphs can on occasions be of greater use in identification of a minimum level of alkali inducing significant reaction. The lowest alkali levels, (expressed in terms of $Na_2O_e$) at which appreciable expansion and visible surface microcracking were detected for each aggregate were as follows, with the corresponding minimum alkali levels required to produce expansions in excess of 0.05 % within six months shown in brackets :

| | | |
|---|---|---|
| Siltstone | - 3.5 kg/m$^3$ | (4.5 kg/m$^3$ ) |
| Silicified Limestone | - 3.5 kg/m$^3$ | (4.0 kg/m$^3$ ) |
| Greywacke | - 4.5 kg/m$^3$ | (6.0 kg/m$^3$ ) |
| Strained Granite | - 4.5 kg/m$^3$ | (6.0 kg/m$^3$ ) |
| Venn Quarry Siltstone | - 7.0 kg/m$^3$ | (Not detected) |
| Thames Valley Gravel | - 6.0 kg/m$^3$ | (Not detected) |
| Trent Valley Gravel | - 7.0 kg/m$^3$ | (Not detected) |
| Cheddar Limestone | - None | (INERT) |

Note: An expansion greater than 0.05 % within six months storage at 38°C has previously been proposed as a criterion signifying ASR in concrete prisms (Concrete Society, 1987).

A conclusion that can be made from these various test results is that ASR may be induced in concretes made from certain British aggregates at alkali contents as low as 3.5 - 4 kg/m$^3$, expressed in terms of $Na_2O_e$ (Sibbick and Page, 1992b). In view of this, the present recommendations for minimising the risk of AAR in the UK (Concrete Society, 1987) which call for a limit of 3 kg/m$^3$ $Na_2O_e$ on alkali derived from concrete mix materials, do not seem unduly conservative.

## 3.5 Petrographical analysis

Mixes containing the aggregate types shown above were examined petrographically to ascertain the source and cause of the AAR identified from the expansion test data.

### 3.5.1 Dry Rigg Siltstone

Petrographical analysis of specimens containing siltstone coarse aggregate, which had suffered expansion, exhibited microcracking to an extent that increased with the increasing alkali content of the concrete.The microcrack networks were expansive in form, but also showed a preference to follow the inherent cleavage of the rock in a stepped form and to run along the long axis of the aggregate particles, a feature common amongst many reactive greywackes. By tracing the networks back to their origin, the centres of expansion were located within the siltstone (Plate 3.1). Alkali-silica gel was found extensively throughout the concrete, as plug like deposits at the aggregate/cement paste interface, within voids, and as side deposits on many of the microcracks in the cement paste. Alkali-silica gel was also found within the siltstone aggregate but was quite rare in this location. The source of

reactivity appeared to be microcrystalline quartz spread throughout the rock matrix and as bands running sub-parallel to the rock's inherent cleavage (Plate 3.2). The concrete satisfies all the petrographical criteria to confirm that the major cause of expansion was ASR. No ettringite was detected in any of the sections examined.

### 3.5.2 Horrocksford Limestone

Specimens containing silicified limestone aggregate tended to contain more large microcracks (>100 $\mu$ms wide) than the siltstone concrete and a lot more of the overall microcrack network involved peripheral cracks running on the edges of the coarse limestone particles, 'pseudo-adhesion cracks' (Plate 3.3). The microcracking network, though unusual, was still of an expansive form and tended to run along the long axis of the aggregate particles.The centres of this expansion were traced back to the coarse silicified limestone aggregate. Where areas of the limestone were richer in chert, the microcracking appeared more severe (Plate 3.4). The darker bituminous-rich particles were seen to be more heavily cracked and to be associated with greater amounts of alkali-silica gel than lighter material. The gel was either light brown to orange in colour or colourless and contained clearly visible banding. Voids and microcracks in the cement matrix were localities where deposits of alkali-silica gel tended to accumulate, but gel was also found in large amounts in specific coarse aggregate particles. The most likely source of the ASR in this concrete would be the chert found widely throughout the rock as infills and inclusions. This chert was often so finely disseminated in the matrix calcite that observation microscopically was very difficult. No ettringite was identified in these concretes.

### 3.5.3 Maentwrog Greywacke

The greywacke aggregate concretes expanded less severely than those already discussed (Figure 3.5) and petrographical analysis confirmed that the amount of visible microcracking was noticeably reduced. Tracing the microcracks back to their source revealed the overall network to be expansive in nature with the centres of expansion within the coarse greywacke aggregate. Close examination showed that the microcracks progressively reduced in size and split up as they entered the greywacke particles. This type of ASR induced microcracking has been observed elsewhere in mylonitic rocks (Lagerblad and Tragardh, 1992).The microcracks eventually became indistinct from the linear features of the fine matrix minerals. These microcracks did not generally split the larger clastic materials in the

greywacke but passed around them. Though ASR gel was observed, it was relatively rare in comparison to that seen in the previous concretes examined. The most common location for the gel was in voids. Here it took a number of unusual layered and spherical forms. It was also found as plug-like deposits at the aggregate / cement paste interface. These petrographical observations are consistent with the view that ASR contributes to the expansion caused by greywacke aggregates, but further work is needed to assess the possible role of an alkali-silicate reaction mechanism (Gillot et al.1973) for the particular aggregate studied in the present work. Recent studies conducted elsewhere (Blackwell, 1992 and Zhang et al. 1990) have suggested that ASR, rather than alkali-silicate reaction, is likely to be the predominant cause of expansion.

### 3.5.4 Anglesey Granite

The strained granite (Figure 3.6) showed a form of microcracking similar to that seen in the greywacke mixes. The rock has been so heavily metamorphosed that it should really be classified as a schist or in parts even a mylonite. The concrete contained networks of expansive microcracks centred on the strained granite coarse aggregate particles and originating from microcrystalline areas of quartz in the rock matrix. This material is all that now remains of heavily shattered larger quartz crystals that had undergone extreme strain and therefore contained a high density of dislocations and undulatory extinction. The microcracking was also frequently seen associated with secondary recrystallised quartz in some fractures in the rock. Cracks did not usually run through the larger quartz crystals even when they were clearly very heavily strained. It was also apparent that the microcracks had a preference to run along bands of chlorite and muscovite found in veins or fractures in the rock, parallel to these minerals' cleavage direction. This type of ASR induced microcracking has been observed elsewhere in similar rocks (Lagerblad and Tragardh, 1992). Alkali silica gel was clearly identified in all the samples examined. Gel was most commonly found in voids in the cement paste, but was also seen in microcracks in both aggregate and cement paste. The gel was colourless or brown and on occasions, appeared to have occurred in two separate pulse 'generations'. Clearly all petrographical criteria have been met to indicate that the strained granite had undergone a form of ASR and the most likely source for this reaction was the microcrystalline quartz found throughout the rock. No evidence was found of the larger strained quartz crystals being reactive.

### 3.5.5 Venn Quarry Siltstone

The petrographical analysis of specimens containing Venn Quarry siltstone coarse aggregate, only showed noticeable microcracking caused by ASR in the 7 Kg/m$^3$ $Na_2O_e$ specimens. In all the concrete samples examined, extensive microcrack networks were observed running throughout the cement paste. These were associated with large open adhesion cracks surrounding most of the coarse aggregate particles. These paste and adhesion cracks were found associated with areas of higher water / cement ratio paste and it is felt that the cause of cracking in these concretes was dry shrinkage due to the use of an over-dry aggregate at the mixing stage.

The microcrack networks caused by ASR were dominated by microcracks running subparallel to the inherent cleavage in the siltstone as seen in the Dry Rigg samples. Though quite limited in these slides the reaction centres were all seen in the siltstone. Alkali-silica gel was rarely found in these concretes, usually being located in voids in the paste and occasionally as side deposits on adhesion microcracks running around the coarse aggregate particles. Alkali-silica gel was found within the siltstone aggregate but was very rare. The source of reactivity is probably the microcrystalline and cryptocrystalline quartz spread throughout the rock matrix (See Appendix 1) though direct proof of this is difficult due to the low level of reactivity encountered. A small amount of ettringite was detected in all of the sections examined and this was generally located in voids though occasionally it was found in cement paste microcracks or adhesion cracks. It is not felt the ettringite contributed to the damage observed for this concrete because, firstly there was insufficient ettringite to create the amounts of expansion detected and secondly it was not found associated with any of the expansive microcracking. In general this was a sound concrete and even in the high alkali mixes the microcracking was clearly not significant enough to cause excessive expansion though ASR is at least a contributory cause of distress.

### 3.5.6 Trent Valley Gravel

Evidence of limited alkali silica reaction was observed in the 6 and 7 Kg/m$^3$ $Na_2O_e$ mixes. The 4.5 Kg/m$^3$ $Na_2O_e$ mix contained non-reacted chert particles, which appear 'unstable', these aggregate particles contained many small discontinuous microcracks, which may have developed due to a small amount of early age ASR. Generally only the chert exhibited the effects of ASR displaying typical divergent

microcrack systems centred on the coarse chert aggregate particles seen in the concrete. A few of the metaquartzites and quartzites particles contained single microcracks that continued out into the cement paste and contained small amounts of gel at the aggregate / paste interface. These microcracks were not divergent or bifurcating, but showed evidence of some expansion related to them. A number of adhesion cracks were noted surrounding the quartzites and these were often filled by ASR gel. Overall the microcracking was limited, but still typical of ASR in a chert-bearing aggregate. Most expansion centres were located in the chert particles and a few quartzites also show some evidence of being reactive. These reactive quartzites were usually connected to the overall ASR network by straight open microcracks as shown in Plate 3.7. Some shrinkage cracks were also observed. The cherts also appeared to occasionally contain some chalcedonic silica as well as the normal reactive cryptocrystalline quartz. A few voids in the cement paste contained ASR gel. The ASR gel in this concrete was often dirty containing fine aggregate and cement paste debris. It was also often dark in colour, occasionally even appearing a reddish / brown presumably as a result of taking up taking some of the red / brown iron staining seen in many of the quartzites and chert.

### 3.5.7 Thames Valley Gravel

In view of the known pessimum associated with this aggregate type, only 50% of the coarse aggregate was actually composed of the Thames Valley gravel. Most of this aggregate was made up of flint (Cretaceous age chert). Evidence of limited alkali silica reaction was only observed in the 7 Kg/m$^3$ $Na_2O_e$ mix. The microcrack network displayed the typical divergent bifurcating structure typical of ASR in chert-rich aggregates. Some of the more reactive chert particles were porous and iron stained. As has been observed previously there was little evidence of gel in the aggregate particles, but some porous areas of the chert contained a milky pseudocrystalline silica-rich substance that has previously been attributed to a pseudo-gel like material (Pettifer, 1990). Some typical ASR gel was identified in fine edge deposits on some adhesion microcracks and in cement paste voids. This gel material was of variable colour and highly desiccated. In general this did not appear to be a particularly reactive concrete.

### 3.5.8 Cheddar Limestone

Petrographical analysis of the Cheddar limestone was carried out only on the 7 kg/m$^3$ $Na_2O_e$ sample. No evidence was observed of any deleterious activity in this

concrete. All the aggregate appeared sound and contained only a few microcracks. A few adhesion cracks were observed running around the coarse aggregate particles. The cement paste was in a sound condition with a low capillary porosity. The only significant feature observed in this concrete was a number of shrinkage cracks. There was no evidence of alkali-silica reaction.

## 3.6 Chemical analysis for sulphate attack

Due to the unusual form that the ASR took in the Dry Rigg siltstone and especially the Horrocksford limestone as described above section 3.5 and the due to the large amount of elemental sulphur recorded in the bulk chemical analysis of the aggregates (Appendix 4) sulphate attack has been proposed as the major cause of the expansion and microcracking in these concretes, with ASR only a contributory factor in the damage (Hobbs, 1990). To assess this suggestion, sulphate content tests were carried out on powdered samples from the test prisms. The results of this work are summarised in Table 3.4.

### 3.6.1 Chemical determination of sulphate content

Calculation of the sulphate content of the test concrete was carried as described in BS1881: Part 124 (1988). Once the concretes had completed their expansion tests a piece of concrete of approximately 250 grams mass was cut from the prism and dried for 24 hours at 110°C. The concrete sample was then crushed and passed through a 600 $\mu$m sieve. This powdered sample was then dried for a further 24 hours at 110°C. Following this two $5 \pm 0.005$ g samples were accurately weighed into a 400 ml beaker. The powdered concrete was then dispersed with 50 ml of deionised water to which 10 ml of concentrated hydrochloric acid was added. This was immediately covered as some samples, especially those containing limestone aggregate, effervesced vigorously. To this solution was added 50 ml of deionised water, which was then covered and boiled gently for 10 minutes. The solution was left too cool and then filtered through a fine filter paper (No.1), the residue being washed through thoroughly with hot dilute HCl. Three drops of methyl red indicator were then added and the filtrate was heated again until it was boiling. Dilute ammonium hydroxide was then added to this solution to neutralise the acidity, this changed its colour to yellow. When this colour change had occurred 1 ml of concentrated HCl ml was immediately added. To this boiling solution 10 ml of barium chloride solution was then added dropwise. This caused the precipitation of any sulphates in the solution as barium sulphate. The solution was then

continuously boiled for a further 5 minutes and then kept just below its boiling point for a further 30 minutes after which it was allowed to cool to room temperature. The solution was then filtered through a sintered glass crucible filter, grade 4, which had been previously weighed accurately to the nearest 0.001 g. The precipitate remains on the filter which is then oven dried and reweighed, the difference in mass being the amount of barium sulphate now present.

The sulphate content of the concrete (G) expressed as a percentage $SO_3$ is calculated from the equation shown below, which was derived from the relevant British Standard:

$$G = \frac{L}{M_d} \times 34.3$$

Where, L is the mass of barium sulphate remaining in the filter in grammes.

$M_d$ is the mass of the concrete sample used in grammes.

and 34.3 represents the multiplication figure required to express the $BaSO_4$ content as a percentage $SO_3$.

$$\frac{SO_3}{BaSO_4} = \frac{32+3(16)}{137+32+4(16)} = \frac{80}{233} \times 100 = \mathbf{34.3}$$

### 3.6.2 Results of the chemical analysis

The results show no indication of an increase in sulphate content proportional to the increasing alkali content and therefore the strain / expansion as shown in Figures 3.2 and 3.3. The relatively low figures for $SO_3$ content suggest sulphate attack is unlikely to have caused a large amounts of the expansion seen in the prisms.

TABLE 3.4: Sulphate contents of ASR reacted concrete prisms.

| Sample Name. | Sulphate content (Expressed as $SO_3$) Average of 2 analyses samples. |
|---|---|
| Siltstone 3.5 kg/m$^3$ | 0.62 % |
| Siltstone 5.0 kg/m$^3$ | 0.61 % |
| Siltstone 7.0 kg/m$^3$ | 0.64 % |
| Silicified limestone 3.5 kg/m$^3$ | 0.71 % |
| Silicified limestone 5.0 kg/m$^3$ | 0.60 % |
| Silicified limestone 7.0 kg/m$^3$ | 0.55 % |
| Siltstone Aggregate | 0.047 % |
| Silicified Limestone Aggregate | 0.039 % |
| OPC White cement | 3.592 % |

(Test carried in accordance with BS1881 pt 124 page 17: 1988).

## 3.7 Petrographical analysis for sulphate attack

Normal petrographical analysis showed that whilst large amounts of ASR gel and associated expansive microcracking were clearly seen, there was little or no evidence for the occurrence of ettringite in any of the concretes examined. The possibility however, still existed of microcrystalline ettringite being present in the cement paste. The occurrence of numerous peripheral microcracks surrounding the Horrocksford limestone, which was thought to be indicative of sulphate attack is not sufficient evidence by itself (Pettifer, 1986). With this in mind a second technique was used to determine the occurrence of sulphate minerals in the cement paste.

### 3.7.1 Staining of sulphate minerals in petrographical thin section

The second technique involved staining an otherwise normal petrographical thin section (Poole and Thomas, 1975). In this process once the thin section has been ground down to the required thickness of 30 $\mu$m, the sample is immersed for two minutes in a mixed solution of barium chloride and potassium permanganate in water. The best results are obtained with a 2 : 1 ratio barium chloride to potassium

permanganate in a 6 % mixed solution. The colouration due to excess permanganate is then removed by washing the sample in a saturated solution of oxalic acid. The procedure described above is satisfactory for the identification of sulphates gypsum, anhydrite and ettringite but does not differentiate between them. Examination of the thin section revealed no evidence for the staining of any ettringite or other needle like crystals in the paste. The cement paste did take on the stain to a limited degree throughout, however, this was considered to represent the sulphate minerals such as finer calcium sulphoferrites / aluminates and dihydrate $CaSO_4.2H_20$ normally found in cement paste. Other stain methods can differentiate these minerals, but it was felt that this was not necessary in this case.

It should also be pointed out here that the pyrites, ( $4[FeS_2]$, $4[CuFeS_2]$ ) commonly observed in the siltstone and silicified limestone and considered to be the only inherent minerals in the aggregates capable of producing the high sulphur contents recorded in bulk chemical analysis, showed no evidence of chemical or physical breakup in the concretes or in fresh condition. In conclusion it was felt there was no evidence to substantiate the claim that the recorded expansions were due to sulphate attack.

## 3.8 Inspection of concrete prisms

Visual inspection was carried during each measuring session to identify the time when the prisms first showed surface microcracks. The results of this work are summarised in table 3.5. Occasionally an unusual feature such as a 'pop out' occurred on the surface of the prism and this was also recorded. The occurrence of ASR gel exuded on to the prism surface was a common feature and helped confirm ASR as the cause of the recorded expansion.

From this information, it is interesting to note the long times to commencement of microcracking in the Trent Valley gravel (RP) and low alkali Maentwrog greywacke mixes. When this is examined along with the corresponding expansion time graphs, (Figures 3.4 and 3.5) it becomes apparent that ASR in these aggregates which is just starting may be just as destructive in the long term as that developed by the other aggregates over a shorter period. It was interesting to note the early age (4 months) at which all the Thames Valley gravel (TV) prisms that were going to expand actually started. This aggregate had a known approximate alkali threshold of >5.2 kg/m$^3$ $Na_2O_e$. Based on these two facts it seems that the Thames Valley gravel concretes that were potentially able to react had so within a short period of

time. The longer testing period had no affect on the degree of this concretes reactivity or alkali threshold for significant reaction. This relatively quick time for the reaction to develop maybe true for many of the other aggregate types. Due to the leaching of alkalis from concretes over time, it seems that most of the potential reactivity (expansion) in these prisms occurred within the first 3 to 4 months, after which time the leaching had lowered the alkali content of the concretes to a level below the alkali thresholds. Therefore after a short period of rapid ASR reactivity, further reaction would be unlikely to develop, unless a secondary source of alkali is brought into contact with the concrete.

TABLE 3.5: Number of months to appearance of first visible microcracks. (For aggregate type see abbreviations at front.)

| Alkali level of mix. (In kg/m$^3$ $Na_2O_e$) | AGGREGATE TYPE | | | | | | |
|---|---|---|---|---|---|---|---|
| | DR | HL | MD | RP | AG | TV | VQ |
| 2.0 | 0 | 0 | 0 | 0 | 0 | 0 | 0 |
| 2.5 | 0 | 0 | 0 | 0 | 0 | 0 | 0 |
| 3.0 | 0 | 0 | 12 | 0 | 0 | 0 | 0 |
| 3.5 | 4 | 5 | 11 | 0 | 0 | 0 | 0 |
| 4.0 | 3 | 4 | 11 | 0 | 0 | 0 | 0 |
| 4.5 | 2 | 4 | 7 | 0 | 8 | 0 | 0 |
| 5.0 | 2 | 3 | 6 | 0 | 5 | 0 | 0 |
| 5.5 | 2 | 4 | 6 | 0 | 5 | 0 | 0 |
| 6.0 | 2 | 3 | 4 | 12 | 5 | 4 | 0 |
| 7.0 | 2 | 3 | 7 | 6 | 4 | 4 | 7 |

### 3.8.1 Forms of microcracking at completion of expansion testing

Once the expansion testing was complete and the prisms had been allowed to dry, they were photographed before being cut up or crushed for other testing. The first feature observed on the prism surfaces, was that the form of microcracking changed with the alkali level of the concrete. Plates 3.8 and 3.11 show the concrete prisms after 1 year made from the siltstone (DR) and silicified limestone (HL) at the various alkali levels shown. The degree and form of the microcracking becomes more severe the higher the alkali level. The 3.5 kg/m$^3$ $Na_2O$ e mixes with Dry Rigg and Horrocksford aggregate are characterised by a single large crack running the length of the prism whilst the higher alkali mixes develop more and more complex forms of the 'map cracking' considered typical of ASR. The single long crack observed on these 3.5 kg/m$^3$ $Na_2O_e$ mixes is also found for all the other aggregate

types in the concrete mixes just above their alkali thresholds for significant reaction. Based on this observation it may be possible to decide how close an ASR affected prism is to its alkali threshold and therefore the degree of further deterioration of the concrete that could occur.

### 3.8.2 Internal microcracking studied on a macroscale

The microcracking in the various concrete mixes was also studied with a macroscale viewer using a fluorescent resin impregnated into the microcracks and observed under a UV light by the method described in section 2.5.3. The resulting photographs are shown in Plates 3.12 to 3.15. Clearly, as with the photographs taken of the prisms outer surface (see section 3.8.1) there is a progressive increase in the amount of microcracking / expansion with an increase in initial alkali level of the mix.

Different deleterious activities in a concrete produce different forms of microcracking (Pettifer, 1986). With experience these different forms can be identified. For example, expanding aggregate or paste shrinkage produce numerous adhesion cracks surrounding the aggregate particles (on specific edges in some circumstances). The Venn quarry siltstone mix (Plate 3.12) which it is now felt was too dry when made, shows an extensive network of adhesion cracks with associated porous paste areas and a few limited expansive type ASR cracks associated with the siltstone cleavage. Inspection of the photographs show fairly extensive microcrack networks especially in the higher alkali mixes. There are specific features of the ASR microcracking in each particular aggregate type and these can be identified by this method as well as the usual petrographical method. The association of the microcracking in the siltstone (metamorphosed) to the aggregate's inherent cleavage is clear (Plate 3.13). The preference of the microcracks to run on the edge of the coarse aggregate particles, 'pseudo-adhesion cracks' are also noted (Plate 3.14), though petrography is still required to confirm that these were associated with the ASR.

The limited amounts of ASR that occurred in the Thames and Trent Valley gravel mixes is confirmed by the general lack of microcracks in these concretes. However, the reaction had occurred to a limited degree in some of the flint aggregate particles where the microcracking exhibits the divergent bifurcating form so typical of ASR in chert aggregates. The quartzites in the mix are seen to contain single straight microcracks running out into the paste as were also observed in the thin section

(Plate 3.15).

The main contribution this method of inspection makes is in the identification of ASR when it is observed in an unusual form. In the silicified limestone mixes the observed microcracking appears to be composed mainly of interconnected adhesion cracks, as has been observed by other workers (Pettifer, 1986 and Hobbs, 1990). This type of cracking has been found associated with sulphate attack derived from sulphate-rich aggregates (see 3.6). Closer inspection however, reveals numerous finer microcracks in the silicified limestone coarse aggregate itself, which then connect to the surrounding adhesion cracks. This helps confirm ASR as the primary cause of expansion in this concrete.

It should be pointed out that deleterious features such as frost attack often exhibit identical microcrack systems to ASR and so petrographical examination is still required to confirm a primary case of ASR.

#### 3.8.2.1 Possible use for this method of examination in field structures affected by ASR.

For some time it has been considered feasible to use image analysis to pick out the recorded area of microcracking and the total microcrack length in the image by placing a fluorescent dye in the resin used to make up the thin sections (West, 1988). Once a satisfactory value for the degree of microcracking (in that image) is obtained, it may be possible to correlate this with the degree of strain recorded for that prism.

It is hoped that this method of identification of the internal microcracking may help in the rapid inspection of field structures potentially suffering from ASR. The microcracking observed in a core taken from a structure, should give an approximate indication of the degree of expansion / deterioration that has been experienced by that concrete. It can also be used to indicate whether ASR should be considered as a possible cause of the damage observed. If ASR is suspected a petrographical analysis will still be required to confirm it as the primary cause of microcracking.

### 3.8.3 Testing of prisms for the presence of alkali silica gel

By the method described in section 2.5.3, it was possible to stain any alkali silica gel present on a concrete specimen with an ultra-violet light sensitive material

(uranyl acetate). When these concrete samples are examined in a dark room under a UV light source the gel gives off a fluorescence which can be seen or photographed relatively easily.

The first obvious conclusion that can drawn from observing such gel sites is that ASR has occurred to some extent in that particular concrete. The second feature that can be of use, is that the sites of large areas of ASR gel can be observed without the need for a petrographical thin section. Therefore in a concrete structure which may be suffering from ASR, a quick test of the concrete can be carried out, without the need for a core to be taken. If the aggregate types in the concrete can be distinguished easily by eye; by finding the location of the fluorescent ASR gel and its relation to the aggregates suffering expansive cracking, then it should be possible to make a reasonably good initial interpretation of which aggregate type is causing the ASR. This method of inspection of possible ASR affected structures can be relatively quick and cheap at least for initial inspections. However, for a full examination and interpretation of an ASR reacted concrete a petrographical analysis would still be required (Stark, 1991).

## 3.9 Discussion

The expansion test results show considerable variations in the degree of recorded expansion / reaction and the initial alkali thresholds to cause significant reaction with the various aggregates used. These results are very much in line with remarks made by French (1990b) that are not actually found in published sources. The variations observed can be attributed to a number of factors; variations in the rocks' physical and chemical properties, type of reactive constituent and the different amounts of reactive constituents in each aggregate. In these particular concrete mixes all other factors affecting the concrete except the coarse aggregate source should be constant. These initial expansion tests were carried out over 12 months after which time most of the mixes appear to have completed their expansion. The completion of the ASR in some of the concretes has to be as a result of the depletion of one or more of the reactants (alkali, water, reactive silica) to such a level that further gel formation ceases. Clearly, as the prisms were still wet at the end of the testing the free water supply was still present. Petrographical observation of the reactive aggregates and further tests carried in stage 2 (Chapter 4) with an extra alkali source over a longer period of time, showed greater expansions with identical initial alkali levels meaning there was still significant quantities of reactive silica available in the aggregates. These facts imply that ASR ceased in these stage

1 prisms as a result of insufficient alkalis. The ASR itself depletes the pore solution of OH ions. Leaching of alkalis into the distilled water surrounding the prisms was also considered significant in reducing the amount of alkalis available for the ASR. The surrounding water had pH levels of 13 to 14 when the expansion testing was completed. If extra alkalis are available to the reaction, gel formation and expansion will continue.

A single sample of concrete from a 7 kg/m$^3$ $Na_2O_e$ siltstone (DR) mix was sliced in the same manner as described in 2.3, to determine a chemical compositional profile. The results of this are shown in figure 3.17. This clearly shows the depletion that has occurred in alkali metals content, especially near the outer edge (and therefore presumably hydroxyl concentration) since the concrete was first mixed. The initial alkali content of this 7 kg/m$^3$ $Na_2O_e$ concrete was 0.29 %$Na_2O_e$ therefore, only the central part of the prism contains anything like the original alkali metals content. From the expansion data for that prism (Figure 3.2) it appears that most of the reaction available in that concrete was complete and this would therefore presumably be due to loss of alkalis to the ASR due to leaching.

The fact that all this expansion testing was carried out at 38°C may give cause for concern, as it has been suggested the results may not be reliable as indicators of equivalent ASR reactivity in field structures. Examination of identical ASR reactive concretes tested at 38°C and 20°C, show a difference in the form the expansion takes with time. Recently Hobbs (1992) has suggested that:

> 'Storage at 38°C leads to deleterious expansion at lower original alkali contents than for similar concretes stored at 20°C or exposed externally'.

Whilst this work does not attempt to suggest there is a direct relationship between testing at 38°C, 20°C and external exposure, there is no evidence to support the hypothesis that the initial alkali thresholds required to induce significant reaction are altered by testing at these different temperatures. Direct estimates for field structures affected by ASR, containing some of the aggregates included in this study have indicated that the original alkali contents of these concretes at the time of construction were 3.3 to 2.7 kg/m$^3$ $Na_2O_e$, (Sibbick and West, 1992). Though in this structure additional alkalis have since been derived from deicing salts, these concretes still initially had alkali contents well below the presently accepted alkali level required to induce ASR with UK aggregates namely >5.0 kg/m$^3$ $Na_2O_e$

In all the concretes examined ASR was identified as the primary cause of the recorded expansions. For each aggregate type the probable reactive constituents were identified and these are summarised in Table 3.6.

TABLE 3.6 : Reactive constituent of each aggregate.

| | |
|---|---|
| 1. Siltstone (DR) | - Microcrystalline quartz found throughout the aggregate matrix and as bands running through the rock. |
| 2. Silicified limestone (HL) | - Chert inclusions and cryptocrystalline quartz throughout the matrix. |
| 3. Greywacke (MD) | - Crypto / Microcrystalline quartz in matrix and and larger quartz crystal boundaries. |
| 4. Trent Valley gravel (RP) | - Porous chert and some microcrystalline quartz found in the quartzites. |
| 5. Strained granite (AG) | - Microcrystalline quartz located at the edge of highly strained large quartz crystals and as part of highly textured areas. |
| 6. Thames Valley gravel (TV) | - Highly porous white 'patina' chert / Flint. |
| 7. Siltstone (VQ) | - Microcrystalline quartz found throughout the aggregate matrix. |

In the concretes containing the highly strained granite rock, (AG) once evidence had been found of significant ASR, the question that immediately came to mind was:

> 'Does the highly strained quartz show any evidence of being the source of ASR reactivity ?'

The petrographical analysis indicated that the large strained quartz crystals, showed no evidence of involvement in the ASR. As with the greywacke aggregate, the expansion centres were traced back to the microcrystalline matrix material of the rock. In these areas significant quantities of microcrystalline quartz could be identified, some being highly sutured, having a very high surface area to volume ratios, making its potential for reactivity significant. The development of the microcrack networks from these microcrystalline matrix regions suggests this microcrystalline quartz is the source of reactivity, not the larger highly strained quartz crystals.

The various aggregates displayed different forms of microcracking due to the ASR. A diagrammatic summary of these various forms is shown in Figure 3.18. As has already been discussed briefly, each aggregate exhibits a different form of cracking dependent on its lithological features. The microcracking in the siltstone aggregates is affected by their internal cleavages and fine bedding planes along which many microcracks are seen to run. These aggregates still display a typical expansive network, but it is altered by the rock's individual lithology. The silicified limestone contains numerous bifurcating adhesion cracks running around the edge of individual particles just within the aggregate, 'Pseudo-adhesion cracks'. Apart from these adhesion cracks surrounding each particle there were also divergent microcrack networks leaving the body of the aggregate heading away from areas particularly rich in chert and cryptocrystalline silica. The evidence for the existence of this cryptocrystalline quartz is based on a comparison of the bulk chemical analysis silica content, compared with the amount of microcrystalline quartz observed petrographically. Apart from the specific source aggregate for these microcracks, the network took on a form typical of most ASR. The greywacke tends to contain ASR microcracks that disappear into the fine matrix of the aggregate once they are deeply within the rock material. Some particles do also exhibit divergent networks and some microcracks typically run the length of the long axis of flaky aggregate particles. A similar form of microcracking was also demonstrated by the strained granite aggregate with the microcrack network centred on areas of fine crystalline quartz and other minerals in the matrix material. This fine matrix material was formed by the same high grade metamorphism that gave rise to the large highly strained quartz crystals, the complexed textures, and the distinctive undulatory extinction seen in some of the quartz. The Trent Valley gravel exhibited two types of microcracking. First, divergent bifurcating networks filled with gel centred on cherty particles were seen. This is the most typical form of microcracking observed in most reactive concretes in the UK. Secondly, a number of the various types of quartzite contained single microcracks often containing a little gel, which just continued straight out into the cement paste. The final reactive aggregate was the Thames Valley gravel that exhibited the typical divergent bifurcating networks filled with gel centred on cherty particles which were usually the only reactive constituents of this aggregate.

## 3.10 Conclusions

1. Alkali silica reaction is the cause of all the significant expansion observed in the concretes in this study. No evidence was found of any other contributory deleterious process affecting the concrete prisms.

2. The reactive constituents for all the aggregates were identified from petrographical analysis. In all cases the reactive constituent was either crypto- or microcrystalline quartz or chert.

3. The highly strained quartz-rich granitic aggregate (AG) shows significant expansion due to ASR. The highly strained quartz was not itself reactive, but the physical geological processes that form strained quartz, also result in the formation of microcrystalline quartz at the edge of larger quartz crystals and highly foliated textures in this fine quartz which results in increased potential reactivity. The reactive constituent was the microcrystalline quartz

4. The completion of the reaction / expansion was due to the depletion of alkalis in the concrete in all cases studied.

5. Significant alkali-silica reaction has occurred in UK aggregate concrete mixes at 38°C with initial alkali contents of between 3.5 and 4.5 kg/m$^3$ $Na_2O_e$. A relationship of these results to testing at 20°C and in external exposure conditions is not proposed, but the initial alkali threshold figures for these concretes are in line with alkali content estimates carried out on ASR affected structures containing these aggregates in the real environment.

6. The alkali threshold for significant reaction varies from one aggregate source to another. This work confirms that chert-rich aggregates do not exhibit significant expansion at less than 5 kg/m$^3$ $Na_2O_e$ in a 38°C environment.

7. Unless or until it becomes practicable to introduce different permissible alkali limits for concretes made from specific groups of UK aggregates, the present recommendations for minimising the risk of ASR in the UK which call for a limit of 3 kg/m$^3$ $Na_2O_e$ of alkalis derived from concrete mix materials do not seem unduly conservative.

# CHAPTER 4

## Effects of de-icing salt on the alkali-silica reaction in hardened concretes.

### 4.1 Introduction

The effects of de-icing salt on ASR are still not fully understood. Laboratory testing has shown that when NaCl is added to the mix water of a potentially reactive concrete, it can cause ASR expansion to develop, whereas in the same concrete without the salt none occurs (Nixon et al. 1988). Previous work on field concretes has indicated that de-icing salts appear to accentuate or even initiate ASR in otherwise marginally reactive or non reactive mixes (Sibbick and West,1992). However, the rate, form and strain associated with ASR developed in these saline environments, compared directly with identical concretes placed in a distilled water environment, has still to be studied. It was proposed that this work should establish the extent to which de-icing salt contributes to the development of ASR expansion. The initial work involved making up concrete prisms with alkali levels well above, on and just below each aggregate's initial alkali threshold for significant reaction. Once the testing in the saline environments had been completed, chemical profile analysis and petrography was carried out in an attempt to clarify the causes of any variations observed in the ASR developed.

### 4.2 Experimental method

The expansion testing method was similar to that used in chapter 3, the main difference being the environments in which the prisms were stored during testing.

#### 4.2.1 Mix initial alkali thresholds

This work initially involved the production of concrete prisms of just below, just above and well above the initial alkali threshold for significant ASR with each aggregate in the study. From the results obtained in the earlier work described in chapter 3, it is possible to establish the approximate initial alkali thresholds for the four reactive aggregates used in this part of the study and these are shown in Table 4.1. The concrete expansion prisms were made up and cured in the same manner as described in 2.2.1 and 2.2.2. The initial alkali contents of the concretes were produced by the addition of NaOH pellets to the mix water as described in 3.3. Ten concrete prisms were made up at one time from a single batch mix for each

aggregate type and at all of the required alkali levels, so reducing the possibility of error in the mixing stage.

TABLE 4.1: Approximate initial alkali thresholds to produce significant reaction with each aggregate and the alkali levels of the concrete mixes used in this stage of the work.

| Aggregate name. | Alkali threshold for significant ASR to occur. | Total alkali levels of concrete mixes. |
|---|---|---|
| 1. Dry Rigg siltstone | 3.5 Kg/$m^3$ | 3.0, 3.5 and 7.0 Kg/$m^3$ |
| 2. Horrocksford limestone | 3.5 Kg/$m^3$ | 3.0, 3.5 and 7.0 Kg/$m^3$ |
| 3. Maentwrog greywacke | 4.5 Kg/$m^3$ | 4.0, 4.5 and 7.0 Kg/$m^3$ |
| 4. Trent Valley gravel | 6.0 Kg/$m^3$ | 5.5, 6.0 and 7.0 Kg/$m^3$ |

(All figures are expressed in $Na_2O_e$)

### 4.2.2 Saline environments

Once fully cured, numbered pairs of these prisms were placed in the following environmental situations within sealed plastic containers.

1. Prisms were totally immersed in salt solution, (2 mol NaCl /litre).

2. Prisms were totally immersed in salt solution, (2 mol NaCl / litre) for 1 month then left to dry in air for 1 month.

3. Prisms were half immersed in salt solution, (2 mol NaCl / litre) and half left exposed to air within a sealed plastic container.

4. Prisms were totally immersed in deionised water.

5. Prisms were left totally dry in air at 25 % relative humidity.

(All the testing was carried out at 38°C).

These various saline environments and situations were intended to simulate the field conditions experienced by typical concrete structures. The first environment (total immersion of already hardened concrete in salt solution) was used to establish the extent if any, of ASR development in comparison to that observed previously in chapter 3. The second environmental situation was used to see if wet / dry cycling in a saline environment could be a contributory factor to the accentuation of the reaction beyond what may be encountered in a saline

environment. This environment was considered to mimic the intertidal conditions that may be experienced by some concrete structures. The third situation with half the prism in and half out of salt solution in moist air was included to see if the effects of the de-icing salt on ASR could be passed on by alkali or salt migration into an area of the concrete prism, which would otherwise be non-reactive due to its low initial alkali content. It was also intended to identify where the reaction develops to its greatest extent since it has been felt that extensive ASR may occur at the interface between a liquid and air environment, where salt will be concentrated by localised drying out (Nixon and Gillson, 1986). The distilled water test environment was also included in this stage of the work for direct comparison with the standard expansion prism test method used for calculation of the initial alkali thresholds in chapter 3. The final two prisms were placed in the 38°C room and left dry. These prisms could later be used as reference non-reacted concretes and as such could be used for direct comparison of microcracking, chemical profiling and the cement paste condition if required.

2 molar NaCl was used as it was considered a reasonably strong solution but not unrepresentative of concentrations experienced under certain condition of field exposure. This figure is still considerably less than that found in ponding points and joints etc. in real structures. In these circumstances a concentration of up to 7 molar NaCl / litre has been recorded (Wood 1992b).

None of the prisms were wrapped or treated in any way prior to testing. In the case of the prisms half immersed in salt solution, demec points were stuck to the top and bottom of the prisms. A pair of demec points 50 mm apart was also attached to the side of the prism covering the area in which the salt solution / air interface occurs as shown in Figure 4.1. Measurements were taken on each of the three sets of demec points monthly and the results are discussed in section 4.3.3. Unlike the expansion testing carried out in chapter 3 to establish the initial alkali thresholds for significant reaction which continued for 12 months, the prisms in this work were all tested for at least 15 months and some considerably longer. This was done to see more fully the effects of ASR in the slower, (even at 38°C) reacting aggregates, to gauge what might be the maximum possible expansion / strain developed and to discover what causes the ASR expansion to cease.

## 4.3 Results of expansion testing.

All the prisms were measured for expansion for up to 15 months after which most

were cut up for chemical profiling and for petrographical analyses. For each aggregate type the medium alkali level concrete samples were left to continue testing until it was felt they had completed their expansion.

### 4.3.1 Expansion results for the prisms immersed in salt solution and distilled water.

A summary of the expansion tests for the prisms totally immersed in salt solution compared with the equivalent prisms immersed in distilled water for 15 months are shown in Figures 4.2 to 4.5. From these graphs it is possible to see that when the various concretes were immersed in the distilled water the three different initial alkali level mixes expanded more or less directly in proportion to their initial alkali content. This would be expected, based on the results obtained previously in chapter 3. These expansion results confirm that the initial alkali thresholds for significant reaction (taken as >0.05% strain) obtained for each aggregate in chapter 3 were more or less correct. The 'revised' thresholds for the aggregate mixes tested by total immersion in distilled water are; Dry Rigg siltstone, slightly greater than 3.5 kg/m$^3$ $Na_2O_e$, Horrocksford limestone, slightly greater than 3.5 kg/m$^3$ $Na_2O_e$, Maentwrog greywacke, less than 4 kg/m$^3$ $Na_2O_e$ and finally the Trent Valley gravel, just below 7 kg/m$^3$ $Na_2O_e$.

When the expansion results for the same concretes immersed in salt solution are compared, it is apparent that they have not behaved in the same way with regard to their initial alkali levels and the degree of expansion recorded. The results for the Dry Rigg siltstone mixes (Figure 4.2) show that at 7 kg/m$^3$ $Na_2O_e$ there is a slight increase in the recorded expansion of the prisms in the salt solution compared with those immersed in distilled water. The extra expansion recorded for the salt solution prisms is 0.104 %. This result taken by itself, is in line with what it might be expected to happen if the external source of salt is contributing alkalis by the method described in section 1.5.1. However, the amounts of extra expansion recorded for the lower initial alkali mixes in the salt solution is far greater than that recorded for the 7 kg/m$^3$ $Na_2O_e$ mix. The greatest expansion is recorded for the 3.5 $Na_2O_e$ mix when placed in salt solution. The total expansion at 15 months was 0.424 %. A similar effect is also observed in the Horrocksford limestone mixes (Figure 4.3) though with lower expansion recorded for each mix. The greatest expansion recorded for the Horrocksford limestone was also with the 3.5 kg/m$^3$ $Na_2O_e$ mix immersed salt solution and this was 0.240 % after 15 months. There is clearly an

anomaly here which needs to be understood.

The Maentwrog greywacke concretes (Figure 4.4) show different behaviour in the salt solution. As each individual prism in the pairs had approximately the same total expansions these results would appear to be reliable and unaffected by a single rogue result. At 7 kg/m$^3$ $Na_2O_e$ the amount of expansion is less for the prisms in the salt solution compared to those in the distilled water. However, the amount of expansion recorded for the lower initial alkali mixes (4 and 4.5 kg/m$^3$ $Na_2O_e$ ) in the salt solution was still greater than that recorded for the 7 kg/m$^3$ $Na_2O_e$ mix and far greater than the expansions recorded for equivalent alkali concretes immersed in distilled water. The greatest expansion recorded for the Maentwrog greywacke was for the 4 kg/m$^3$ $Na_2O_e$ mix and that was 0.149 % after 15 months. Unfortunately this was the lowest alkali level included in the work. It is also worth pointing out the slow, but apparently continuing expansions observed for all the Maentwrog prisms beyond the 15 months shown in Figure 4.4. This aggregate seems to be especially slow to react even at 38°C and in salt solution or distilled water.

The results in chapter 3 also indicated a slower reaction rate and a higher initial alkali threshold for the Trent Valley gravel compared to the other aggregates included in the work. In this stage of the work, the 7 kg/m$^3$ $Na_2O_e$ mixes show the same increase in recorded expansion in the salt solution compared to immersion in distilled water, exhibited by the other aggregates (Figure 4.5). However, the greatest recorded expansion after 15 months (0.09 %) was found for the 6 kg/m$^3$ $Na_2O_e$ mix in salt solution. The 5.5 kg/m$^3$ $Na_2O_e$ mix did not react even in the salt solution and may therefore represent a concrete of too low initial alkali level to initiate ASR even in salt solution. It seems even a slowly reacting aggregate like this can develop accentuated ASR in salt solution at lower initial alkali levels than in distilled water. In distilled water the leaching of alkalis can be a great suppressor of the ASR problem, especially over the long periods of time which will be required by these slowly reacting aggregates (Structural Engineer, 1988).

In Figure 4.6 the expansion results at 15 months are plotted against the three initial alkali levels of the Dry Rigg and Trent Valley gravel concretes. The graph appears to suggest that a specific 'pessimum' initial alkali level may exist for these aggregates when placed in a salt solution. This pessimum point is not by any means related to the results of ASR expansion in distilled water or any aggregate content pessimum that may exist. In distilled water the greatest recorded expansion

occurs at the highest initial alkali level as might be expected. There appears to be no similar relation of the initial alkali content of these concretes to the recorded expansion in salt solution. In the Dry Rigg concrete mixes this point of maximum expansion (pessimum) when placed in salt solution appears to be around 3.5 kg/m$^3$ $Na_2O_e$ (equivalent to the alkali threshold in distilled water) based on the limited number of alkali levels studied.

Figure 4.7 shows the equivalent graph for the Horrocksford limestone aggregate at 15 months. With the Horrocksford aggregate there is also evidence of a pessimum initial alkali level at around 3.5 kg/m$^3$ $Na_2O_e$, though again this is based only on a limited number of points.

Figure 4.8 shows the equivalent graph for the Maentwrog greywacke with the greatest expansion recorded for the 4 kg/m$^3$ $Na_2O_e$ mix. The fact that the 7 kg/m$^3$ $Na_2O_e$ mix when placed in salt solution expanded less than in the distilled water is as yet unexplained. Based on the limited number of points available it is possible to suggest the 'initial alkali threshold pessimum' for the greywacke in salt solution is probably less than 4 kg/m$^3$ $Na_2O_e$, though this is still somewhat speculative. Finally, the results for the Trent Valley gravel, which are included on Figures 4.6 to 4.8 for comparison suggest an 'initial alkali threshold pessimum' of 6 kg/m$^3$ $Na_2O_e$ when the concretes are immersed in salt solution.

#### 4.3.1.1 Conclusions on comparison of expansion results for immersion in salt solution and distilled water.

The results obtained in Figures 4.6 to 4.8 indicate that an initial alkali level 'pessimum' exists for each aggregate when it is placed in salt solution. This pessimum point is apparently related to the initial alkali threshold required to initiate significant (>0.05 % strain after 12 months) reaction in distilled water. Furthermore these pessimum points appear for some aggregates to be located (close to or even below) the present 3 kg/m$^3$ $Na_2O_e$ UK initial alkali content limit recommended for the avoidance of ASR in new concrete structures (Concrete Society, 1987). This work does not provide any judgment as to what might occur in the future to concretes containing similar aggregates with initial alkali contents in the range 2 to 3 kg/m$^3$ $Na_2O_e$ and this represents an interesting area for further research.

One of the clearer results is that all the potentially reactive aggregates appear to have excess quantities of silica available to react within them, assuming there is a sufficient supply of alkali and water to continue the ASR.

### 4.3.2 Comparison of expansion test results for prisms subjected to wet / dry cycling and permanently immersed in a saline environment.

Figures 4.9 to 4.12, give a summary of the expansion results obtained for prisms immersed permanently in salt solution compared to those for specimens exposed to cycling (one month immersed in salt solution, one month left dry in air). These figures show, characteristically stepped increases in percentage strain for the prisms cycled between immersion in salt solution and air contrasted with the continuous curves obtained by those permanently immersed in salt solution. From these graphs it appears the overall strains in the two environments can often be somewhat different. By plotting the percentage strain at 15 months against initial alkali levels of the concretes (Figure 4.13 and 4.14) it is possible to see a number of features related to the specific aggregate mixes used more easily.

Figure 4.13, shows the expansions plotted for the Dry Rigg siltstone and Trent Valley gravel. The recorded expansions for the siltstone mixes in the wet / dry cycling environment are more or less the same as those for prisms totally immersed in salt solution. It is interesting however, that these two sets of results appear to be mirror images of each other. With the wet / dry cycled prisms the greatest percentage strain was found with the 7 Kg/m$^3$ $Na_2O_e$ mix and this expansion decreases with a reduction in the initial alkali content of the mix. As with the samples immersed permanently in salt solution the amounts of expansion are still very high, all being greater than 0.32 % strain. The alkali level at which the greatest expansion occurs is different from that for the samples permanently immersed in salt solution.

The Trent Valley gravel mixes placed in the wet / dry cycling environment all show significantly enhanced expansion in comparison to those prisms totally immersed in salt solution. Extrapolation from these result to lower alkali levels suggest that the wet / dry cycling in salt solution may lower the initial alkali threshold for significant ASR in the Trent Valley gravel concrete mixes to approximately 4.5 Kg/m$^3$ $Na_2O_e$, compared to 7 Kg/m$^3$ $Na_2O_e$ in distilled water and 5.75 Kg/m$^3$ $Na_2O_e$ when totally immersed in salt solution. This lowering of the initial alkali level for significant reaction in wet / dry cycled prisms is only observed in this graph with the Trent

Valley gravel. With the (DR) aggregate the expansions appear to remain constant or even too slightly increase with a lower alkali levels. The reason for this reduced figure with Trent Valley gravel aggregate, may be due to paste drying shrinkage cracks and the greater reduction in paste to aggregate bond developed when using a rounded river gravel aggregate. This might mean a greater number of adhesion cracks formed around the coarse aggregate particles, which could result in increased alkali / chloride ion diffusion (see section 4.4.5) through the concrete, so increasing the potential for ASR reactivity.

Figure 4.14, shows the equivalent data for the Horrocksford limestone and Maentwrog greywacke. The effect of the wet / dry cycling in salt solution on the Horrocksford limestone is negligible, though interestingly the data is again a mirror image of the results for the totally immersed specimens. As for the samples immersed permanently in salt solution the amounts of expansion are still very high, all being greater than 0.22 %. As with the Dry Rigg concretes, the effects of the salt solution either by total immersion or wet / dry cycling, on the low initial alkali mixes (3 Kg/m$^3$ $Na_2O_e$) are still not understood. The Maentwrog greywacke mixes also exhibit a mirror image of the data for the prisms totally immersed in salt solution. Extrapolation of the expansion results to lower initial alkali levels suggest that the wet / dry cycling in salt solution may lower the initial alkali threshold for significant ASR in Maentwrog greywacke mixes to approximately 2.5 Kg/m$^3$ $Na_2O_e$ (compared to 3.5 Kg/m$^3$ $Na_2O_e$ in distilled water). This possible lowering of the initial alkali level for significant reaction in wet /dry cycled prisms is not fully understood for this aggregate, but may be related to the slower rate of reaction exhibited by this material and increased diffusion of chlorides through the greater number of drying shrinkage paste cracks.

In conclusion it seems that the wet / dry cycling in salt solution has little effect compared to total immersion in salt solution for the extremely reactive Dry Rigg and Horrocksford aggregates. However, the effect on the less reactive Trent Valley gravel and the slowly reactive Maentwrog greywacke is quite different. For both materials it appears they have reduced initial alkali thresholds for significant reaction when they are placed in the wet / dry cycling environment. In all the wet / dry cycled prisms, significant ASR expansion was encountered, even in prisms that did not expand when totally immersed in salt solution (i.e RP25.5A/B). The degree of ASR expansion could also be increased locally by the concentration of alkali / salt in the pore solution ahead of the dried-out surface zone, which it is felt could be a contributory effect of the wetting and drying. The evidence from the expansion

data, chemical analysis (section 4.4.5) and petrography (section 4.5.3) was all negative. It is considered that such a concentration of salt / alkali with an associated increase in ASR probably occurs, however, the examination techniques used here are carried out on too large a scale to identify such a narrow band of increased reaction. The observed mirror images for the expansion data developed by the Dry Rigg, Horrocksford and Maentwrog aggregates, in the salt solution and the wet /dry cycled prisms are still unexplained.

### 4.3.3 Expansion analysis of prisms half immersed in salt solution and half in humid air.

Expansion measurements were taken from pairs of demec points placed on the upper, lower and side faces of the prisms included in this part of the research Figure 4.1. The pair of demec points placed on the side of the prism were only 50 mm apart and therefore a separate dial gauge was required to measure the expansion in this area (see section 2.2.3). A summary of the expansion results is given in Figures 4.15 to 4.18. A summary of the data taken at 15 months is also shown in Figures 4.19 and 4.20.

Figure 4.15, shows the effects of half immersing a 7 and 3 Kg/m$^3$ $Na_2O_e$ mix containing Dry Rigg siltstone in salt solution. First, as expected the dry surfaces show the lowest recorded expansions. The 7 Kg/m$^3$ $Na_2O_e$ mix dry face has expanded by 0.183 % and this is significantly less than the results for the equivalent prism totally immersed in distilled water (0.222 %, Figure 4.2). This has probably occurred because the only moisture available to the reaction was obtained from the surrounding humid air, capillary migration upwards from the submerged part of concrete and some limited splashing from the salt solution. The 3 Kg/m$^3$ $Na_2O_e$ mix dry face has expanded to almost the same extent as the 7 Kg/m$^3$ $Na_2O_e$ mix dry face. Extra alkali would be required, however, to initiate the ASR in this 3 Kg/m$^3$ $Na_2O_e$ sample and this has presumably to be derived either from splashes of the salt solution, in which case any ASR will be a very localised surface effect or by the migration of NaCl upwards through and around the concrete prism. Evidence for these different methods may be obtained from later petrographical and chemical analysis. The expansions recorded on the wetted surfaces are roughly equivalent to those obtained for the equivalent prisms permanently immersed in salt solution (see section 4.3.1). The most surprising feature was the very high expansions recorded on the side faces of the prisms. This is the area where the moist air to salt solution interface was located. In this area the recorded expansions of the various

mixes were more or less equal, regardless of their initial alkali content.

It has been observed previously that the greatest ASR develops in real structures just on or above areas of wet ground or moisture etc. (Nixon and Gillson, 1986). This is an area in which any NaCl present is also likely to concentrate due to evaporation and therefore it may be richer in alkalis, if the reaction between the $C_3A$ and NaCl previously discussed is actually occurring. This is one possible reason for the occurrence of a high expansion in this area. A second explanation is that the Dry Rigg siltstone, has a tendency to produce elongated 'flaky' aggregate particles which form parallel to the rock's inherent cleavage. These elongated particles tend to aline themselves up with the horizontal, when placed in moulds. As a lot of the ASR expansion developed in this siltstone is derived from cleavage orientated microcracks and microquartz bands that run subparallel to this cleavage (section 3.5.1), it follows that a greatest amount of expansion will occur perpendicular to the cleavage and therefore towards the top of the expansion prism and across the side face demec points.

Figure 4.16, shows the effects of half-immersing 7 and 3 $Kg/m^3$ $Na_2O_e$ specimens containing Horrocksford limestone in salt solution. As with the Dry Rigg siltstone the dry faces show the least expansion and these are virtually identical even though the two mixes contain different initial alkali contents. The wetted faces and side faces all show similar expansions. As for the Dry Rigg siltstone, the 3 $Kg/m^3$ $Na_2O_e$ mix shows significant expansions on the dry, wet and side faces even though the initial mix was below the initial alkali threshold for significant ASR for this aggregate. This would suggest not only that the NaCl has developed ASR in an otherwise non-reactive mix, but also the NaCl has diffused through the concrete to develop ASR in material well away (30 to 40 mm) from the salt-immersed concrete. Petrographical and chemical analysis will confirm or dispel this idea later.

Figure 4.17, shows the effects of half-immersing 7 and 4 $Kg/m^3$ $Na_2O_e$ specimens containing Maentwrog greywacke in salt solution. The two equivalent sets of demec points on these prisms show remarkably similar expansions considering the different initial alkali levels of the two mixes. The two dry faces have expanded equally as might be expected, but interestingly the 4 $Kg/m^3$ $Na_2O_e$ mix should be virtually non-reactive assuming no alkali contribution from the salt solution. This is clearly not the case and so it would appear that as for the other low alkali mixes there is a contribution of alkali by the mechanisms already described. The wetted faces also have virtually identical expansions recorded. The side faces

interestingly, have the same high expansion levels observed for the Dry Rigg siltstone. However, unlike the siltstone this aggregate does not contain a significant cleavage or elongation tendency, so the cause of the increased localised expansion is either due to the localised concentrations of salt due to evaporation etc. or some other undiscovered mechanism.

Finally, Figure 4.18, shows the effects of half-immersing 7 and 6 Kg/m$^3$ $Na_2O_e$ specimens containing Trent Valley gravel in salt solution. The behaviour of these prisms is more in line with their initial alkali levels and appears to have less to do with the effects of salt solution as observed in sections 4.3.1 and 4.3.2. The low reactivity of this aggregate and the overall shortage of moisture on the dry faces mean these areas have the lowest recorded expansions, but they do occur in the correct order with respect to their initial alkali levels. The other faces also expanded in relation to their initial alkali levels. The side faces both show significant expansion but this is not greater than is recorded for the wetted surfaces and is probably related to the initial alkali content of the mix. Most of these observations can be seen clearly in Figures 4.19 and 4.20.

### 4.3.4 Expansion results of selected concrete samples over longer periods of time.

It was noted that all the concretes continued to expand for up to 15 months and this was most apparent for the Maentwrog greywacke mixes. The observation of continued expansion was also made with the bagged prisms used in chapter 3. With these facts in mind, expansion testing was continued for as long as was felt necessary using the middle initial alkali level samples for each aggregate type. Figures 4.21 to 4.24, show the continued expansion results for one alkali level with each of the reactive aggregates for a period as long as was considered necessary. The salt solutions were not replaced and all testing continued at 38°C in sealed plastic containers.

Figure 4.21, shows the long term expansion results for the 3.5 kg/m$^3$ $Na_2O_e$ Dry Rigg siltstone concretes. It is apparent from this graph that most of the expansion potential is now complete in the samples immersed in salt solution (SS) with little significant increase occurring from 20 months onwards. The extent of the expansion trend in the wet / dry cycled prisms also began to reduce markedly in the last few months. The cycled prisms containing Dry Rigg siltstone never show anything like the expansion totals developed by the prism totally immersed in salt solution. The

concrete prisms immersed in distilled water (DW) still have not obtained a level of expansion considered to represent significant ASR.

Figure 4.22, shows the long term expansion results for the 3.5 kg/m$^3$ $Na_2O_e$ Horrocksford limestone concretes. It is apparent that the expansion potential of this aggregate when placed in salt solution was virtually complete after 17 months. The cycled prisms are also showing reduced expansion rates, which give a total expansion almost equivalent to the samples totally immersed in salt solution. Though the expansion developed in distilled water (DW) was very slow, by 18 months the expansion total would be considered to represent a significant case of ASR.

Figure 4.23, shows the long term expansion results for the 4.5 kg/m$^3$ $Na_2O_e$ Maentwrog greywacke concretes. Expansion in all the samples was continuing at a slow but constant rate up to 18 months. In the samples immersed in salt solution 36 % of the total expansion measured has developed since the concrete was 12 months old, whereas in the distilled water immersed samples 26 % of extra expansion has occurred. At the completion of expansion testing some expansion was still continuing with this aggregate type.

Finally Figure 4.24, shows the long term expansion results for the 6 kg/m$^3$ $Na_2O_e$ Trent Valley gravel concretes. No significant expansion is seen to develop in the distilled water immersed samples (DW) even over the longer periods of time used here. Both sets of concrete prisms immersed totally in salt solution and wet / dry cycled in salt solution show slow but continued expansion with time. At the completion of expansion testing some expansion was still continuing with this aggregate type.

These results show that expansion testing at 38°C should be continued for at least 24 months if a reliable figure for maximum potential expansion in saline and distilled water environments is to be obtained using the various reactive aggregates. If so any comparison of these results with field concretes as proposed by Hobbs (1992b) could not be made for up to 14 years (24 months to completion of most of the expansion multiplied by 7) as the development of the expansion potential in these slower reacting concrete mixes, could not have developed until that time. Hobb's proposed time relationship between expansion testing carried out at 38°C and external exposure conditions gives a ratio of 1:7. However, this was developed only using data from a series of chert-based rapid reactivity mixes and

therefore will have little bearing on any relationship between the times to completion of expansions with the slower reacting aggregates such as the Maentwrog greywacke (MD) in the various test environments.

### 4.3.5 Expansion test results for the prisms immersed in distilled water compared to equivalent prisms, wrapped in damp cloth and triple bagged

Figures 4.25 and 4.26, show the differences in expansion recorded for identical prisms immersed in distilled water compared with those wrapped in moist cloth and triple bagged as described in chapter 3. All these expansion tests were carried out at 38°C. The results show a significant degree of variation between the test methods.

The Dry Rigg siltstone specimens of high alkali content show greater expansion when tested by the triple bagged method than when simply immersed in distilled water. The 3 kg/m$^3$ $Na_2O_e$ siltstone specimens show virtually no expansion and the results for the two test regimes are almost equivalent. The Horrocksford limestone mixes on the other hand are remarkably consistent in both test regimes. The Maentwrog greywacke mixes exhibit surprisingly varied expansion results, when comparing the two test regimes. Finally the Trent Valley gravel mixes show slightly greater expansions with the lower alkali levels for the bagged prisms compared to those immersed in distilled water.

In general it appears that the bagging technique produced raised expansion results and lower initial alkali thresholds for significant reaction. The most likely reason for the difference encountered is the greater leaching of alkalis from the prisms when they are placed in the large volume of distilled water. The leaching of alkalis over longer periods of time in field structures should be even more substantial and therefore the bagging technique and to a lesser degree the immersion in distilled water may produce significant ASR expansion at initial alkali levels below those encountered in field structures. Further work would be required to establish whether this is so.

Clearly testing of concrete prisms under controlled conditions at 38°C may be somewhat unrealistic as a basis for a method of recommending the initial alkali contents of new structural concrete. However, the requirement for a relatively rapid test and the need for a margin of safety with regard to the initial alkali contents of a

mix, means these accelerated methods still have a useful role in deciding the present limits.

### 4.3.6 Discussion

Figures 4.27 to 4.29, show hypothetical expansions in distilled water, salt solution, and wet / dry cycling in salt solution for various aggregates in relation to their initial alkali contents with tests carried out at 38°C.

Figure 4.27, shows the predicted effects of increasing initial alkali contents of concrete mixes on the expansions recorded for various aggregates placed in distilled water. The higher the initial alkali content of a mix the higher the total expansion developed. This is pretty much in line with the present ideas regarding ASR, disregarding the effects of aggregate pessimum. The parallel near linear nature of the various guidelines is of course highly speculative as the expansion to time trends of many mixes will be curved dependent on other variables such as temperature and humidity, as shown by the real curves plotted.

Figure 4.28, shows the predicted effects of increasing initial alkali contents of concrete mixes on the expansions recorded for various aggregates when placed in salt solution. According to this figure each aggregate will be represented by a line on which a pessimum or point of greatest expansion can be observed. The few real data points available from this work suggest that with more reactive aggregates, the point of greatest expansion appears to migrate towards lower initial alkali content concrete mixes. These 'pessimum points' appear to be located near the alkali threshold for significant reaction when the same mix is immersed in distilled water. This indicates that reactive aggregates such as the Dry Rigg siltstone will expand more severely in the salt solution with concretes containing lower initial alkali contents may be at levels even below the present 3 kg UK limit.

Finally, Figure 4.29, shows the predicted effects of increasing initial alkali contents of concrete mixes on the expansions recorded for various aggregates when the prisms are placed in a wet / dry cycled environment using salt solution. In this case each aggregate is represented by a line on which its potential expansion for different initial alkali levels is recorded. This does not produce a migrating pessimum point as seen in figure 4.28. However, it does show a migration to lower levels of the initial alkali content required for significant reaction with these lower reactivity aggregates. Variations in the rate of reactivity of an aggregate appear to

have a great effect on the potential expansion of a mix in this wet / dry cycled environment. It seems that this test regime, though carried out in laboratory conditions at 38°C is reasonably in line with a real life situation and therefore may have a relevance for the future avoidance of ASR in saline environments.

For example it may help explain why some low reactivity UK aggregates such as the Trent Valley gravel (RP) are found in many ASR affected structures with calculated initial alkali levels well below the apparent alkali threshold for significant reaction with that aggregate (Based on 38°C testing in distilled water). It is appreciated that all these suggestions are very speculative, but they may be a good starting point for further study into the phenomena established by this work.

### 4.3.7 Conclusions on expansion testing.

The main conclusions that can be drawn from this work with regard to the expansion tests described above are:

1. The immersion of already potentially reactive concretes in salt solution accentuates the ASR-induced expansion, whilst for concretes with initial alkali contents below that required to initiate expansion when immersed in distilled water, immersion in salt solution promotes significant ASR. In saline environments the greatest expansions were developed by concretes of relatively low initial alkali content, at or near the initial alkali thresholds for significant ASR in distilled water. The expansions developed suggested that each aggregate may have an "initial alkali content pessimum" for its greatest reaction / expansion when placed in salt solution.

2. The wet / dry cycling of the prisms in salt solution has little effect on the highly reactive aggregates, (DR and HL) in comparison to total immersion in salt solution. The expansion recorded was very high for all the initial alkali levels studied. However, with the less reactive / slower reacting aggregates, (MD and RP) the effect of this environment was to lower the initial alkali threshold for significant reaction even further than by just immersing the prisms in salt solution.

3. Significant expansion, presumably due to ASR, was found in all the prisms half immersed in salt solution. The greatest expansion was found in the lower concrete, totally immersed in salt solution. However, significant expansions were also recorded for the upper dry faces, even in potentially non-reactive low initial alkali

prisms. The source of alkalis causing this expansion is presumably either salt solution splashed on to the top surface from the main reservoir or alkalis that have diffused through and / or around the prism. The expansion recorded at the salt solution to air interface areas were large for all the prisms. However, the expansion observed here on the Dry Rigg siltstone and Maentwrog greywacke prisms were the greatest expansions recorded for those prisms. Possible reasons for this are discussed and confirmed in section 4.4.3.

4. The tests carried out on concrete samples containing the MD greywacke and RP river gravel aggregate immersed in distilled water and salt solution showed that slow expansion continues in these concretes over a long period of time. The rapid testing of these or similar materials for alkali-silica reactivity may prove to be difficult.

5. The long term expansion test results show that all the mixes have potentially more expansion remaining in them than is recorded after 15 months. If sufficient alkalis remain or are added, it appears that expansion will continue in the 38°C and 100% RH environment for at least 24 months. With a resupply of alkalis from a source such as de-icing salts, many ASR affected structures could continue to react for a lot longer than has previously been considered. Expansion developed in all the prisms tested except the Trent Valley gravel mix containing 5.5 kg/$m^3$ alkali when it was placed in distilled water.

6. The degree of expansion and the initial alkali contents required for significant reaction, is not only dependent on the occurrence of salt solution in the environment, but also the environmental circumstances in which the concrete is placed. The wet / dry cycling environment was included to give these laboratory based experiments a closer relationship to the environment encountered by many real structures. It appears to lower the initial alkali content for significant reaction still further than by just immersing the samples in salt solution. This observation is true most especially for aggregates of relatively low reactivity many of which are still used in the UK.

## 4.4 Chemical analysis of concrete prisms.

Chemical analysis was carried out on each of the prisms, for $Cl^-$, $Na^+$, and $K^+$. A series of slices of the concrete were taken from the outer surfaces to the centres of the specimens by the method described in section 2.3. For clarity and to aid

comparison with other chemical analysis data the results for the alkali metals are shown as oxides. These chemical analyses were carried to help to explain why the unusual expansion results recorded in section 4.3 occurred. It was hoped this work might show differences in chemical compositions developed in the prisms using the different reactive aggregates and indicate whether the different initial alkali levels of the concretes and the various environments in which they are placed have any significant effects. In section 4.3, it was apparent that by placing the concrete prisms in salt solution the ASR was either accentuated in an expansive concrete or initiated in an otherwise non-expansive concrete.

### 4.4.1 Chloride profiles

Figure 4.30, shows the chloride contents of all the various mixes which were permanently immersed in salt solution. This graph shows that chloride diffusion towards the centre of the prisms was greatest in the low alkali mixes regardless of the aggregate type. The diffusion of the chlorides from the surrounding 2 molar NaCl solution into the central area of the prism would have been virtually complete after approximately 3.5 years, based on work by Sergi et al. 1991 using similar materials. This work by Sergi produced a 'typical' chloride concentration profile of similar appearance to those established by the 7 Kg/m$^3$ $Na_2O_e$ mixes in this work. All the 7 Kg/m$^3$ $Na_2O_e$ mixes have remarkably consistent Cl ion profile. The reasons for these higher concentrations of chloride penetrated into the centre of the lower alkali mixes is however, still unknown. It was suggested by Page (1993) that the ASR gel that would develop rapidly in the 7 Kg/m$^3$ $Na_2O_e$ mixes may be blocking up the cement paste capillary porosity so reducing its permeability.

The lower alkali mixes are initially unable to react significantly before obtaining extra alkalis from the NaCl diffusing inwards. Therefore in the central area of the low alkali prisms little ASR gel will develop until NaCl has diffused into the area. The Cl ion concentration in these central areas is surprisingly constant around 0.3 Cl %. This is itself equivalent to an alkali addition of 6.4 Kg/m$^3$ $Na_2O_e$. Following a recent article in New Civil Engineer the following points were raised:

Could highly ASR reactive concrete be of benefit to a structure by first, suppressing the Cl ion diffusion into the body of the concrete and second by having extremely high alkali contents, both reducing the potential for corrosion of the reinforcement. After all the structural and strength reducing effects of ASR are now considered by some workers to be minimal (New Civil Engineer, 26 November 1992).

In conclusion it seems that the diffusion of NaCl into the concretes is affected either by the alkali level of an initial concrete mix or more likely by the ASR occurring in that mix.

### 4.4.2 Chemical analysis of prisms immersed in salt solution

Figures 4.31 to 4.33, show the chemical profiles for all the various mixes when totally immersed in salt solution. A feature that remains constant throughout all the mixes is the relatively consistent figure for $Na_2O$ content in the central zones of the prisms regardless of their initial alkali content. The $Na_2O$ contents all range from 0.3 to 0.4 %, with some slight increases in the surface regions, presumably due to increased local NaCl contents (see equivalent Cl % profiles). As the 3 and 4 $Kg/m^3$ $Na_2O_e$ mixes are equivalent to 0.12 % and 0.16 % $Na_2O_e$ respectively when calculated as a percentages, from the plotted data it appears that the main source of the high internal $Na_2O$ contents measured in these low initial alkali content mixes were derived from the NaCl that has diffused into the central zone (see Figure 4.31 to 4.33).

The addition of the initial alkali level of a 3 $Kg/m^3$ $Na_2O_e$ mix (0.12 % $Na_2O_e$) to that derived from the salt (average Cl content for central region of 3 $kg/m^3$ Dry Rigg prism is 0.341 %, which is equivalent if derived from NaCl to 0.298 % $Na_2O$) gives a total $Na_2O$ figure of 0.418 %. This figure is not greatly different from that recorded on the profile and assuming slight leaching of original $Na^+$ cations into the surrounding salt solution, the figures would appear to be roughly equivalent.

The other interesting feature noted is the raised $K_2O$ contents observed in the Dry Rigg siltstone mixes (Figures 4.31). These $K_2O$ figures show evidence of slight leaching towards the outer surface, but they are still much higher figures than would be expected, based on the equivalent results for the Horrocksford limestone (Figure 4.32) and to a lesser extent the Maentwrog greywacke (Figure 4.33). The large initial addition of NaOH pellets at the mixing stage, means that variable but large amounts of $Na_2O$ would be expected in all the concretes analysed. However, no additions of $K_2O$ were used, so any increase has to be as a result of release from the various coarse aggregates when placed in the concrete. With this in mind, chemical analyses equivalent to those described in section 2.3, were carried out on powdered fresh aggregate samples, see section 4.4.3.

Figures 4.32 and 4.33, show remarkably similar results for their Cl and $Na_2O$ percentage profiles. Their $K_2O$ contents are well below those recorded for the Dry Rigg mixes and represent a figure not greatly different from a calculated $K_2O$ content, based purely on the initial $K_2O$ content of cement used to made up the concrete prisms which was 0.046 % $K_2O$ (see Table 2.1). In all the prisms immersed in salt solution the $Na_2O$ % is enhanced in the surface regions, as expected.

### 4.4.3 Chemical analysis of reactive aggregates

As a result of the findings shown above with regard to the potassium contents of the concrete mixes, a number of chemical analyses were carried out on freshly crushed rock aggregate samples. Only the reactive aggregates used in stage 2 of the work were analysed and the results of those chemical analyses are shown below in Table 4.2:

TABLE 4.2 : Chemical analysis of coarse aggregates leached with nitric acid or water.

| | Chemical analysis by removal in nitric acid. | | | Chemical analysis by release in water over 48 hours. | |
|---|---|---|---|---|---|
| | $Cl^-$% | $Na_2O$% | $K_2O$% | $Na_2O$% | $K_2O$% |
| Dry Rigg siltstone | 0.027 | 0.032 | 0.176 | 0.00074 | 0.00132 |
| Horrocksford limestone | 0.027 | 0.047 | 0.071 | 0.00036 | 0.00027 |
| Maentwrog greywacke | 0.015 | 0.120 | 0.208 | 0.00035 | 0.00026 |
| Trent Valley gravel | 0.015 | 0.040 | 0.144 | 0.00020 | 0.00012 |

The results obtained for the release of constituents in the water were obtained in the same manner as described in section 2.3 except that the samples were left for 48 hours immersed in water in a manner similar to that described in BS1881: part 124, (1988). Nitric acid extraction was carried for between 3 to 4 hours, until the solution was cool.

It is apparent from these results, that some potassium is being released from the aggregates when extracted in nitric acid or distilled water. If even a small amount of potassium can be released in distilled water over the period of 48 hours, it seems likely that significant quantities could be released when the aggregate is placed in concrete and it is therefore quite possible that this source of additional alkali will

become available for the ASR. If this is case, then the potential reactivity of the Dry Rigg siltstone will be significantly enhanced and the initial alkali threshold required for significant reaction will be reduced. Discussion of these results with other researchers (Blackwell, 1993) confirmed that that they appeared to be surprisingly high and therefore similar tests on the alkali contents were carried at the Building Research Station using the same powdered samples of aggregate. The results of these tests are shown in Table 4.3 in appendix 4. These alkali test results also showed similar surprisingly high alkali levels, and therefore confirmed the initial observation of a high release of alkalis from some of these aggregates.

The detected $K_2O$ % contents released from the powdered concretes (Figures 4.31 to 4.39) were well below the levels expected based purely on the releases of alkalis by the equivalent powdered aggregates. The potassium contents of the concrete mixes obtained by extraction in nitric acid, were lower than would be expected, if all the potassium potentially able to be released from the aggregates (Table 4.2) actually occurred when the aggregates were placed in the concrete mixes. This suggested that either the method of releasing potassium by leaching in nitric acid was releasing potassium which would otherwise remain bonded in the silicate minerals and therefore be unavailable to the reaction or that the potassium is not being released in the highly alkali environment of a concrete.

Consideration as to source of this potassium released from the coarse aggregates, strongly suggests that the layered minerals, muscovite and sericite, ($4[KAl_2.\{AlSi_3O_{10}\}.\{OH\}_2]$ ) found abundantly in the Dry Rigg rock's matrix are the most likely cause. In these minerals the potassium is located between the various strongly bonded layers of the silicate and would therefore presumably be more easily removed from the mineral especially in highly aggressive environments such as nitric acid (Battey, 1981, page 273). Petrographical inspection of the Maentwrog greywacke also reveals a high percentage of muscovite / sericite in that rock's matrix. Interestingly, the result of the chemical analysis for this aggregate (Table 4.2) also shows a high potassium content released for the greywacke in acid. However, in general the potassium content figures for the Maentwrog greywacke concretes are generally not significantly higher than would be expected with any other aggregate using this cement. Therefore, it seems that only in the Dry Rigg siltstone mixes can significant quantities of potassium be released into the concrete. This may be due to the heavily cleaved and fine platey nature of the Dry Rigg siltstone in comparison to the other aggregates. Interestingly it is also only the Dry Rigg siltstone that releases 'significant' potassium into the distilled water over 48 hours

(Table 4.2).

In concretes, the pore solution always contains a small amount of free $Ca(OH)_2$ as well as NaOH and KOH. The replacement of these $Ca^{2+}$ cations with the now free $K^+$ derived from the aggregate could be a possible method by which this $K^+$ could enter the pore solution, so increasing the alkalinity and so accentuating the ASR developed in concretes containing these aggregates. Work by Sergi (1986) has shown that $K^+$ can only enter the pore solution if a source of $OH^-$ (or other soluble anions) is available. Solid portlandite ($Ca(OH)_2$) precipitated in the cement paste is such a source. This process was seen to continue until the large amounts of portlandite naturally found in the cement paste were used up. In this way large amounts of extra KOH could become available to the ASR using aggregates with a potential to release potassium.

When considering the importance of these high $K_2O$ percentage results on the potential reactivity of these Dry Rigg siltstone mixes, it is worth noting the analysis of pore solutions from equivalent normal OPC concretes containing DR aggregate, described in chapter 5 (see Table 4.3 ).

TABLE 4.3 : Chemical analysis of pore solution in millimoles per litre from normal OPC mix containing Dry Rigg siltstone over time.

| | $Na_2O$ mmol / litre | $K_2O$ mmol / litre | $OH^-$ mmol / litre |
|---|---|---|---|
| 1 day | 713.40 | 94.72 | 752.00 |
| 7 days | 717.75 | 92.80 | 700.17 |
| 28 days | 543.75 | 67.84 | 484.30 |
| 183 days | 247.95 | 29.44 | 218.00 |

Pore solution from OPC concrete with Dry Rigg siltstone aggregate and the highest alkali content.

In these concretes the $K^+$ concentration of the pore solution was observed to be relatively low and reduced over time presumably due to normal leaching. Therefore although the chemical analysis of the powdered concretes show a high potassium % figure, the lack of significant potassium detected in the pore solution suggests it may have been used up by the ASR and is therefore likely to have been a major cause of the high expansions and low initial alkali thresholds detected with the Dry

Rigg siltstone concrete samples. If $K^+$ is being consumed by ASR, it will not be detected in the pore solution of a reacted concrete, but will be detected in a bulk chemical analysis of the concrete which would include the desiccated ASR gel containing the potassium.

### 4.4.4 Chemical analysis of prisms immersed in distilled water.

Figures 4.34 to 4.36, show the chemical profiles of all the prisms immersed in distilled water. Unlike the prisms immersed in salt solution, where contributions of alkalis from the salt appears to be a major element affecting the overall profiles, in these prisms significant leaching of the alkalis into the surrounding water appears to be the major factor. Later analysis of the distilled water confirmed that large amounts of alkalis were leached during the expansion testing. For example the small amount of distilled water placed in the plastic bags for the work described in chapter 3, usually had pH's in the range 12.8 to 13.1 after the testing.

Figure 4.34, shows the chemical profiles for the Dry Rigg siltstone prisms. As with all the other samples immersed in distilled water there were virtually no Cl ions detected and this is in line with what might be expected using a 'normal' UK land-based crushed rock aggregate. The $Na_2O$ percentage is seen to reduce towards the outer edge of the prisms for both mixes. Leaching of the alkalis into the water has almost certainly caused this effect. In the 3 $Kg/m^3$ $Na_2O_e$ mix the central region contains almost the initial alkali content of the mix (i.e 0.12 % $Na_2O_e$ ) suggesting little leaching from that zone. Whereas, the 7 $Kg/m^3$ $Na_2O_e$ mix, is seen to be significantly depleted in sodium throughout its profile. As with the prism immersed in salt solution (Fig 4.31) the recorded potassium contents for the DR prisms are well above those observed for the other aggregate types and the possible causes of this have been discussed already in section 4.4.3.

Figure 4.35, which refers to the Horrocksford limestone mix shows significant leaching of the sodium from the outer surfaces of the prism only in the 7 $Kg/m^3$ $Na_2O_e$ mix. The 3 $Kg/m^3$ $Na_2O_e$ mix appears to have a slightly reduced, but constant figure of $Na_2O$ % throughout its profile compared to the initial mix levels. The potassium contents are small and almost constant (approximately equivalent to the potassium content derived directly from the cement at mixing).

Figure 4.36, which shows mixes containing the Maentwrog greywacke also shows significant leaching of the sodium from the outer surfaces of the prism in both the 4

and 7 Kg/m$^3$ $Na_2O_e$ mixes. The 7 Kg/m$^3$ $Na_2O_e$ mix is significantly depleted in sodium throughout its profile compared to its initial mix level. The 4 Kg/m$^3$ $Na_2O_e$ mix appears to have retained all its initial sodium content in its central zone. The potassium contents of both mixes appear slightly raised, above what might be expected if the only potassium source available were that derived directly from the cement and this is again most probably a result of some release of alkalis from the coarse aggregate.

### 4.4.5 Chemical analysis of prisms cyclically immersed in salt solution for 1 month and then left dry in air for 1 month.

Figures 4.37 to 4.39, show the chemical profiles of the various concrete prisms when exposed to cycles of salt solution for 1 month and dry air for 1 month. The initial observation that applies to all the different aggregate types, is that the penetration of the 7 Kg/m$^3$ $Na_2O_e$ prism mixes by Cl ions is far greater in depth and concentration than observed for the prisms permanently immersed in salt solution, (see 4.4.1). The equivalent 3 and 4 Kg/m$^3$ $Na_2O_e$ mixes also appear generally to have higher Cl ion contents than those of the equivalent prisms immersed in salt solution. The most likely reason for these observations is simply the effect of capillary suction caused by surface drying.

Figure 4.37, shows the chemical profiles for the Dry Rigg siltstone prisms. As with all the other Dry Rigg prisms an enriched figure for the $K_2O$ content is observed in both mixes and this does not appear to be significantly affected by leaching. The chloride contents were both high especially in the outer region though as might be expected they do decline slightly towards the centres. The central zone of the 3 Kg/m$^3$ $Na_2O_e$ mix has a relatively constant Cl ion content of around 0.52 %, whilst in the 7 Kg/m$^3$ $Na_2O_e$ mix, the Cl ion content remains above 0.5 % throughout the profile. The $Na_2O$ % profiles both run parallel to their equivalent Cl % profiles. From the position of these two profiles, it appears that the majority of the $Na_2O$ content in the 3 Kg/m$^3$ $Na_2O_e$ mix is derived directly from the salt with exception of a small zone in the very centre. The $Na_2O$ content of the 7 Kg/m$^3$ $Na_2O_e$ mix, however, is derived from both the salt solution and the initial alkali content of the mix.

Figures 4.38 and 4.39, show the chemical profiles for the Horrocksford limestone and Maentwrog greywacke mixes respectively. The results confirm the observations made above for the Dry Rigg mixes. The compositional profiles analysis described

here showed no evidence of any localised alkali / salt concentrations ahead of the dried-out surface zone. It is however, considered quite probable that such a feature exists, although it would be too narrow to be detected using this method of analysis.

### 4.4.6 Chemical analysis of prisms half immersed in salt solution and half in moist air.

Figures 4.40 to 4.42, show the chemical profiles of the concrete prisms containing the various aggregate types, half immersed in salt solution. The depths shown are taken from the top dry surface and run right through the prism to the bottom surface, which was fully immersed in salt solution. All three graphs show a consistency throughout for their results. The Cl % profiles always show high concentrations in the wetted area of the 7 Kg/m$^3$ $Na_2O_e$ mix which decline to virtually nothing in the central part of the dry upper area of the prisms. The top surface figures for Cl % are always slightly raised and this probably represents the migration of NaCl in from the outer face where splashing with salt solution or migration of salt solution around the prism edges, could have caused a local increase in chloride concentration. The 3 Kg/m$^3$ $Na_2O_e$ mixes show similar Cl % concentrations at the outer faces, but also have much higher chloride concentrations internally in both the wetted and dry central areas. The $Na_2O$ % profiles indicate that the $Na_2O$ content in the 3 and 4 Kg/m$^3$ $Na_2O_e$ mixes is largely derived largely from the salt solution (see Table 4.3), whereas that in the 7 Kg/m$^3$ $Na_2O_e$ mix it is derived largely from the original initial alkali content of the mix. From these results, it is possible to infer that any ASR found in the internal areas of the low alkali prisms was caused directly by alkalis derived from the NaCl that has migrated into the prism centre under the influence of the well developed hydraulic gradients present in all the prisms in this section of the work. This can also be confirmed because these concretes would be non-expansive without this extra external source of alkali. Clearly, as the dry area of the prism was not intentionally soaked with salt solution a lot of the NaCl must therefore have migrated through the concrete from the salt solution immersed region of the prism.

In conclusion, it appears ASR can develop in concrete some distance from a source of de-icing salts or equivalent due to migration and diffusion of NaCl solution through the material. The petrographical analysis described in section 4.5.4 can be used to confirm whether or not ASR has fully developed in these areas of the prisms or whether they are just showing ASR as a secondary cause of microcracking.

TABLE 4.4: The internal, (8 to 36 mm depth) $Na_2O$ %contents of the upper regions the prisms half immersed in salt solution.

| Mix name. | $Cl^-$ % | $Na_2O$ % derived from NaCl | $Na_2O$ % | % Difference |
|---|---|---|---|---|
| DR 3 kg mix | 0.212 | 0.186 | 0.255 | +0.069 |
| DR 7 kg mix | 0.020 | 0.018 | 0.219 | +0.201 |
| HL 3 kg mix | 0.176 | 0.154 | 0.221 | +0.067 |
| HL 7 kg mix | 0.025 | 0.022 | 0.263 | +0.241 |
| MD 4 kg mix | 0.100 | 0.088 | 0.178 | +0.090 |
| MD 7 kg mix | 0.028 | 0.025 | 0.310 | +0.285 |
| RP 7 kg mix | 0.068 | 0.060 | 0.267 | +0.207 |

### 4.4.7 Discussion

The evidence from the work in this chapter strongly suggests that ASR can be accentuated or even initiated in a hardened potentially reactive concrete exposed to external sources of NaCl. Table 4.4 in appendix 4, shows the extent to which the total internal alkali content of the various mixes studied is accentuated by immersion in salt solution.

From this data it is clear that concretes with lower initial alkali contents are more susceptible to the diffusion of NaCl into the central regions of the material. Therefore the diffusion of NaCl into a potentially reactive low initial alkali mix is of greater concern with respect to ASR initiation than into an already expansive high alkali concrete. The high alkali reactive concrete will react / expand slightly more when placed in a saline solution. However, the low alkali concrete will not only react, but will expand to an even greater degree than the high alkali mix. It is also apparent that the different reactive aggregates are affected to differing degrees with respect to ASR by immersion in salt solution.

It may be that the avoidance of certain mixes containing aggregates particularly prone to the effects of de-icing salts should be recommended in particular circumstances in which the heavy usage of de-icing salts is required, i.e concrete

road pavements. The addition of such a clause to those already present in specifications for the avoidance of ASR, may help especially where the availability of aggregate types for construction is reduced.

## 4.5 Petrographical analysis

Petrographical analysis was carried out on a selected number of the concrete prisms to ascertain the following: the causes of the observed differences in the expansion results; the degree of ASR; the form, volume and location of ASR gel; other changes to the cement paste or unusual features specific to particular test environments. The full details of the petrographical analysis are shown in Appendix 6. The various aggregates included in this stage of the work all exhibited varying degrees of the ASR in most environments. However, a number of observations that were made apply to all the concretes studied in each specific environment and these are described below.

### 4.5.1 Concretes immersed in distilled water

The petrography of all the concrete mixes immersed in distilled water showed that ASR occurred to the same extent as observed by the petrography carried out on the prisms examined for stage 1 of this work (Chapter 3).

The high alkali 7 kg/m$^3$ $Na_2O_e$ mixes all showed a degree of ASR in line with the equivalent mixes studied in chapter 3. The Dry Rigg siltstone / 3 kg/m$^3$ $Na_2O_e$ mix showed no evidence of ASR confirming that the initial alkali threshold for significant reaction with this aggregate is between 3 and 3.5 kg/m $Na_2O_e$. The Horrocksford limestone / 3 kg/m $Na_2O_e$ and Maentwrog / 4 kg/m $Na_2O_e$ mixes immersed in distilled water both showed evidence of very limited ASR, but in neither case could it be classified as significant reaction. The Trent Valley gravel / 5.5 kg/m $Na_2O_e$ mix was not thin sectioned as the expansion results clearly showed no evidence of ASR expansion (Figure 4.5). In all the concrete prisms immersed in distilled water, the cement paste was slightly stained around the paste microcracks by the injection of ASR gel into the capillary porosity of the paste. However, the majority of the paste appeared as typical hydrated OPC with a high alite to belite ratio and the staining would be regarded as limited (Plate 4.1). The degree of surface carbonation was also generally low.

### 4.5.2 Concretes immersed in salt solution

The petrographical inspection of the prisms immersed in salt solution revealed in general far more extensive microcracking and evidence of the ASR than observed in the equivalent prisms immersed in distilled water. The volume of ASR gel was noticeably increased compared to the other prisms. This increase in the degree of reaction for each mix confirmed the surprisingly high increases in expansion seen in section 4.3.1 and in the process also confirmed ASR to be the primary cause of the expansion in each case. The most extensive ASR was actually found in the 3 kg/m $Na_2O_e$ concrete mix containing Dry Rigg siltstone (Plates 4.2 and 4.3). The main difference seen between these concretes and the prisms immersed in distilled water was the massive increase in the degree of cement paste staining or darkening observed (Plate 4.4). This darkening of the cement paste is almost total in most of the samples with only small core areas of unaffected paste observed deep within the central parts of some concretes (Trent Valley gravel 7 kg/m $Na_2O_e$ prism).

#### 4.5.2.1 Effects on the cement pastes of immersion in salt solution when studying an ASR reactive concrete

Petrographical examination of cement paste cannot usually determine the $C_3A$ phase crystals individually as they are found as a constituent of the very fine dark matrix material of the paste (Lea, 1970, page 101). Close examination of the cement paste in this work shows a high alite ($C_3S$) to belite ($C_2S$) ratio, the size of these unhydrated crystals often being quite large (40 to 70 $\mu$m). Because this concrete was made up with a 'white cement' (see section 2.1.1) it was expected to contain a large proportion of the $C_3A$ phase. $C_3A$ is, however, best observed in polished sections of the unhydrated clinker grains where it can be etched by KOH (Lea, 1970).

The immersion of these concretes in salt solution has no discernible effect on the large alite and belite phase minerals. However, in the area of cement paste directly adjacent to the paste microcracks a localised area of high capillary porosity is seen to develop (Plate 4.5). This area is usually filled by the fluorescent araldite resin used to impregnate the concrete samples prior to thin sectioning. This area was also seen to contain fine granular calcite crystals in the more highly porous areas of the paste.

Two possible explanations are proposed to explain the occurrence of this high capillary porosity. First, it is suggested that this localised high capillary porosity could be due to the partial replacement of the $C_3A$ phase, when it comes into contact with the salt solution. This forms Friedel's salt (Calcium chloro-aluminate) which in the process releases further NaOH into the cement paste pore solution. Friedel's salt is also considered to be unidentifiable in thin sections as it will presumably become just another constituent of the fine cement paste matrix. This process, however, may result in some reduction of the volume of material present due to the loss of NaOH to the pore solution, hence the increased porosity.
This hypothesis may presumably be tested by either producing a polished section of the relevant area of the paste surrounding a microcrack in which the identification of the $C_3A$ will be easier or by X-ray diffraction analysis of suitable powdered samples of the affected concrete.

Alternatively, the localised high porosity may be due to portlandite depletion as discussed by Kawamura (1992). He has shown by chemical analysis that large amounts of $Ca(OH)_2$ were dissipated by an ASR reactive mortar when immersed in salt solution, whereas this did not happen when an inert aggregate was used. Portlandite can be easily identified in hardened concretes as large prismatic crystals exhibiting high polarisation colour under crossed nicols. These crystals are often observed in voids and microcracks in the paste. However, identification of small scale $Ca(OH)_2$ crystals in the finer matrix material is difficult as petrographically the fine calcite added as part of the limestone fine aggregate has a dispersive affect on the optical properties of other minerals in the paste and as such we cannot confirm the cause of the observed increase in capillary porosity.

One possible method of identifying $Ca(OH)_2$ in a specific area is by a combination of differential thermal analysis (DTA) and thermogravimetric analysis (TG). This should produce evidence of differences in $Ca(OH)_2$ content between cement paste samples taken from adjacent to the microcracks in a salt solution immersed sample and an identical sample immersed in distilled water. A problem will, however, remain as to a reliable method of collecting suitable paste samples presumably from a polished thin section of the concrete.

### 4.5.3 Concretes cyclically immersed in salt solution for one month then left dry in air for one month.

The alkali-silica reaction was found extensively in all the prisms placed in this

environment. The degree of microcracking was usually more substantial than that seen in the concretes permanently immersed in salt solution. However, much of the microcracking seen in the cement paste was due primarily to drying shrinkage (Plate 4.6) and is therefore unrelated to the ASR. This high degree of paste microcracking has caused greater diffusion of Cl ions and presumably Na (section 4.4.5) cations into the prisms than was seen in the other concrete samples studied. The darkening of the cement paste due to the injection of ASR gel is also more severe in these samples and this is a result of the increased diffusion in these pastes for ASR gel as well as Cl ions and alkali cations. In general, though more heavily microcracked, these concrete samples have experienced slightly less ASR than those samples immersed permanently in salt solution. Though ASR gel is found widely in these samples the microcracking directly related to ASR appears to be reduced.

It might be that some of the strain induced in these concretes by the ASR gel is actually dissipated by the drying shrinkage paste microcracking. The localised increase in capillary porosity of the paste adjacent to the paste microcracks is again apparent and widespread. There was no noticeable increase in the extent of ASR microcracking in the area ahead of any dried-out surface zone in which salt / alkali may have been concentrated. However, that does not mean this localised concentration does not exist.

### 4.5.4 Concretes half immersed in salt solution and half left in moist air.

These samples behaved more or less as might be expected. The ASR was extensive in all the specimens examined. The degree of reaction was seen to be reduced locally in the central regions of the upper part of the prisms, of the low initial alkali level mixes. The lower wetted areas were seen to have extensive ASR microcracking and staining of the cement paste by the injection of ASR gel. This staining was vastly reduced, compared to the samples discussed in sections 4.5.2 and 4.5.3, but was still clearly present even in the central and upper regions of the prisms.

A number of the of low initial alkali content samples developed extensive ASR related microcrack networks in the lower area immersed in salt solution and these networks could be traced into the upper areas, which were generally less reactive in their central regions. One of the more interesting aspects of these slides was

seen in the Dry Rigg siltstone 3 Kg/m$^3$ $Na_2O_e$ mix where cubic sub-isotropic salt crystals were observed in a microcrack in a coarse aggregate particle near the original edge of the prism (Plate 4.7 and section 4.6). This is a confirmation that the salt is penetrating the concrete / aggregate.

### 4.5.5 Conclusions from the petrographical analysis.

From the petrographical observations recorded above a number of conclusions can be drawn.

1. If there was no salt solution available there would have been no ASR developed in the Dry Rigg siltstone 3 Kg/m$^3$ $Na_2O_e$ mix. The ASR developed in the Horrocksford limestone 3 Kg/m$^3$ $Na_2O_e$ mix and the Maentwrog greywacke 4 Kg mix could not be classified as significant reaction in the absence of salt solution.

2. Extensive ASR was observed in all the concrete prisms immersed in salt solution. The immersion of the various prisms produced a staining of the cement paste due to the injection of large volumes of ASR gel into the capillary porosity surrounding the paste microcracks. An increase in the capillary porosity of the cement paste was seen adjacent to the paste microcracks.

3. The wet / dry cycling of the concrete prisms in salt solution gave the impression of greater reaction due to the increased number of drying shrinkage cracks. These cracks may allow dissipation of strain induced in the ASR-affected concretes by releasing a proportion of gel into the paste, where it is injected under pressure into the capillary porosity giving overall a greater staining than was observed for the prisms totally immersed in salt solution.

4. In the prisms half immersed in salt solution, there was evidence of microcrack networks initiating in the wetted salt solution region and continuing up into the dry half of the prism. These microcracks would be a good path for the migration of alkalis to the upper parts of the prism in the same manner as discussed above with respect to drying shrinkage cracks. Chemical analysis appears to confirm that alkalis were reaching the upper central regions of the prisms.

5. Under conditions of saline exposure the most extensive ASR appeared petrographically to be developed by mixes with an initial alkali content near the aggregate's threshold for significant reaction.

TABLE 4.5: Extent of ASR observed by petrographical analysis. Number represents the visual extent of ASR in the range 1 to 10.

| Mix initial alkali level | 3 / 4 Kg/m$^3$ $Na_2O_e$ mix | 7 Kg/m$^3$ $Na_2O_e$ mix |
|---|---|---|
| **Dry Rigg siltstone** | | |
| Distilled water immersion | 0 | 7 |
| Salt solution immersion | 10 | 8-9 |
| Salt solution / dry cycling | 8-9 | 7-8 |
| Half in salt solution and half dry | 6 in dry<br>7-8 in wet | 7-8 in dry<br>8-9 in wet |
| **Horrocksford limestone** | | |
| Distilled water immersion | 1 | 6 |
| Salt solution immersion | 7-8 | 8 |
| Salt solution /dry cycling | 8-9 | 8 |
| Half in salt solution half dry | 4 in dry<br>6-7 in wet | 6 in dry<br>7 in wet |
| **Maentwrog greywacke** | | |
| Distilled water immersion | 5 | 6 |
| Salt solution immersion | 7 | 7 |
| Salt solution /dry cycling | 6-7 | 8 |
| Half in salt solution half dry | 4 in dry<br>7 in wet | 5 in dry<br>6 in wet |
| **Trent Valley gravel** | 7 Kg/m$^3$ $Na_2O_e$ mix only | |
| Distilled water immersion | 4 | |
| Salt solution immersion | 4 | |
| Salt solution /dry cycling | 5 | |
| Half in salt solution half dry | 2 in dry<br>3 in wet | |

## 4.6 Discussion.

Combining the observations made by chemical, petrographical and expansion analysis, the following suggestions can be made.

In all the 7 kg mixes immersed in salt solution the alkali-silica reaction would occur regardless of any ingress of NaCl solution as there were sufficient alkalis present from the initial mix. This ASR will form large amounts of ASR gel which will be

injected into the cement paste filling the capillary porosity. This reduces the ability of the paste to diffuse Cl and $Na^+$ ions into the central area of the prisms .

However, in the identical 7 kg prisms placed in the cycled environment, the diffusion of Cl ions into the central area of the prism was increased significantly due to the large numbers of drying shrinkage microcracks. These paste cracks allowed the salt solution easy access to the central areas of the concrete. This observation was further proof that the saturation of the cement paste with ASR gel, was the main cause of the reduce diffusion of ions into the other ASR reactive concretes totally immersed salt solution.

In the 3 and 4 kg mixes no significant ASR was able to develop initially and therefore the diffusion of NaCl continued at the rate seen in any 'normal' concrete. The diffusion of $Na^+$ and Cl mainly occurs in this initial stage of the testing. As the NaCl was now entering the concrete, it was able to initiate bonding of the Cl ions with the $C_3A$ (section 2.1.1), this formed the mineral calcium chloro-aluminate. In the process of forming this mineral, hydroxyl ions were released and these were bonded to the associated $Na^+$ also diffusing into the paste. This forms NaOH which raises the pore solution alkalinity, until it is sufficiently high to initiate the ASR for that particular aggregate. Once ASR had started the paste will become filled with ASR gel and the diffusion of NaCl should be reduced though the ASR microcracks will allow some limited diffusion. The ASR can only develop in these mixes after the bonding of the Cl ions with the $C_3A$. The process which appears to be occurring is shown below:

NaCl —— enters non reacting

concrete cement paste by diffusion —Cl - bonds to — ($C_3A$) to form $C_3A.Cl$ complexes

I

I_____ Na+ Diffuses slightly slower _____

I

OH - released

I

NaOH forms and enhances pore solution alkalinity.

(The rate and extent of this reaction maybe temperature dependent)

It is considered that the use of a sulphate resistant cement (SRPC) with its associated lower $C_3A$ content, may have a limiting effect on the degree of ASR expansion developed due to the reaction discussed above being more limited. The darkening / staining of the cement paste can only really be attributed to the injection

of ASR gel into the paste capillary porosity. However, it should be pointed out a similar feature has frequently been observed in concretes associated with sulphate attack derived from ground water percolation (Pettifer, 1993). It is very unlikely that this is the case here.

In this work NaOH enrichment of the pore solution by the reaction between NaCl and the $C_3A$ phase forming calcium chloro-aluminate etc. occurs as described above has caused the accentuations and initiations of the ASR observed.
The paste microcracks formed by ASR and drying shrinkage will continue to allow salt solution containing dissolved carbon dioxide to enter the cement paste. This $CO_2$ entering the system will in effect locally neutralise the alkalis (NaOH and KOH) in the paste pore solution surrounding the microcrack, therefore stop further ASR locally. In the process, the lowering of the alkali level may also allow the carbonation of the portlandite in cement paste matrix on a localised basis. In this process a precipitation of $CaCO_3$ should be observed in the cement paste, which is coming into direct contact with the NaCl solution diffusing inwards, the most likely site of this occurrence would be adjacent to paste microcracks.

Petrographical analysis shows clearly the increase in the capillary porosity of the cement paste in the area directly adjacent to the paste microcracks suggesting the removal of some initial constituent of the cement paste and secondly it is seen that this area contains fine granular calcite crystals now impregnated in the araldite resin (Plate 4.9). This fine calcite could of course be due to an overall carbonation of the concrete and not just this localised affect. These observations may be the physical evidence required for the depletion of $Ca(OH)_2$ from the cement paste matrix.

Unfortunately, in all the concrete prisms made up for this work, the observation of primary hydrated portlandite in the cement paste was not possible. This is because an inert limestone fine aggregate (5 mm to dust) was used to make up the concretes, this places very calcite dust particles into the cement paste matrix and this has the effect of masking (syntaxial overgrowths) or removing any primary portlandite present by the process termed epitaxy. This feature has been observed before in similar mixes and means the detection of fine portlandite in cement paste is impossible (Pettifer, 1993). Epitaxy is a process by which one mineral (namely calcite in this case) is able to grow in lattice continuously with another (in this case portlandite) thus totally masking the interface from optical detection (Plate 4.1). This process has been observed previously by Farran (1956).

Primary portlandite can usually be observed in a hydrated cement paste as small poorly formed, (anhedral) prisms / rhombi of first order yellow to orange polarisation colour, often located in small adhesion cracks and surrounding aggregate particles, though they can be found throughout some paste. However, because of the process described above no primary portlandite is observed in these cement pastes; the only portlandite detected was of secondary crystallisation found in some air voids along with ettringite and thaumasite.

The testing of a broken surface of this concrete with phenolphthalein solution showed a local depletion in hydroxyl ion concentration in the area surrounding the fine paste cracks. This confirms that calcite crystallisation should be feasible in the area adjacent to the paste cracks. Carbonation of the original surface of the prisms was relatively minor, whereas the calcite deposits described above though on a very fine crystal scale (20 to 60 $\mu$m) are found deep within the concrete well away from surface influences, next to drying shrinkage and ASR related paste microcracks.

Therefore in summary, it is possible that the observation of $Ca(OH)_2$ depletion in an ASR reactive mortar made previously by Kawamura, may occur as a result of a secondary reaction between $Ca(OH)_2$ in the cement paste and $CO_2$ and $H_2O$ in the salt solution, which may form late stage calcite crystallisation and an associated increased capillary porosity. ASR may continue unaffected in the vicinity of the reactive aggregate particles, until sufficient microcracking has developed to allow large volumes of dissolved $CO_2$ in the salt solution to enter, so ending further ASR by lowering the alkalinity and also in the process starting up carbonation of the $Ca(OH)_2$. This theory can be questioned, however, by work carried out by Buck and Mather (1978) which reported a tendency of calcium to move initially into the high alkaline ASR gels of a reactive concrete, leaving an area of cement paste depleted in calcium hydroxide surrounding the microcracks, regardless of the involvement of salt solution in the reaction.

The creation of large volumes of ASR gel in the initial stage of the reaction as is seen in some of these concretes, will result in a reduced diffusion of chlorides and alkali ions through the paste and therefore except in areas adjacent to the paste cracks the process described above should not occur and a small amount of further ASR will develop, until a balance of sorts is obtained between the reactive concrete and the 'carbonated' $Ca(OH)_2$ depleted material is accomplished. The

petrographical evidence for the depletion of something in the cement paste is clearly present, what this might be is still unknown. However, none of the petrographical evidence really disproves any of this ideas postulated.

The discovery by petrography of residual salt in the thin sections was an unexpected, but useful method of confirming the presents of that material at some depth into the concrete prism (Plate 4.7). In the same voids as the salt crystals, fine colourless needle-like crystals were also seen. These crystals were of an unknown mineral, not unlike ettringite. It was considered possible that they may be a form of the calcium chloro aluminates (Friedel's salts). The petrographical identification of these minerals has never apparently been reported and as such no real knowledge exists on the subject. Pettifer (1993) felt after observing the crystals in question, that these could well be calcium chloro-aluminate or chloro-sulpo-aluminate complexes as discussed, as though they were clearly not ettringite (calcium sulpo aluminate) they exhibit similar low birefringence and this would presumably be what might be derived from a Tricalcium aluminate ($C_3A$) and chloride ($Cl^-$) based mineral. French (1991) has shown very similar crystals developed in a chloride ingressed concrete under a scanning electron microscope (SEM) and he has infers these crystals were Friedel's salt.

Finally, in all the thin sections analysed a general lack of ASR gel in the reactive aggregate particles was observed. Some ASR gel was seen in these particles, but these were generally in small residual microcrack edge deposits. As the microcracks in this location all exhibit expansive divergent patterns the gel forming these must have been present once. This observation has been made previously on real structural concretes.

Many EMP analysis (Chapter 7 and Laing et al. 1992) have shown that gels located in the reactive aggregate were usually $Na^+$ or $K^+$ rich, whereas cement paste, aggregate to paste interface areas and void gels were $Ca^{2+}$ rich. Calcium rich gels appear to be more viscous and therefore should also be harder. This means they should also be more retainable in the thin sectioning process. The sodium and potassium rich gels are however, of lower viscosity and are therefore lost far more easily by the thin sectioning process. As this work progressed the quality of the thin sectioning process improved and therefore the amounts of residual ASR gel located in the reactive aggregate increased. In the Maentwrog greywacke for example, very little ASR gel was detected in the stage 1 / chapter 3 work, however, by the end of the stage 2 work described here a reduced but significant quantity of

ASR gel was usually found within the coarse aggregate particles.

## 4.7 Ideas for further work

Further work could help to establish if any of the suggestions made above with regard to the localised paste porosity surrounding the microcracks in the cement paste are correct. This work includes:

1. The uranyl acetate staining method (see section 2.6) could be used to detect ASR gel in the highly stained cement paste of petrographical thin sections. To accomplish this a high grade UV microscope will be required, as the fluorescence developed by any ASR gel in the paste would be very low.

2. The production of polished sections of the concrete prisms, which are then etched with KOH can be used to identify the location of any $C_3A$ phase crystals present in the cement paste. Close examination of the areas of high capillary porosity paste surrounding the paste microcracks may reveal the $C_3A$ depletion already discussed.

3. Electron microprobe analysis of the same areas of paste will also show any significant depletions in either $Ca(OH)_2$ or $C_3A$.

## 4.8 Conclusions.

1. The immersion of an already ASR expansive concrete in salt solution accentuates the ASR. In concretes with initial alkali contents below that normally required to initiate expansion, immersion in salt solution may induce even greater ASR expansion than that referred to in the previous case.

2. The greatest expansions in salt solution were developed in concretes with moderate initial alkali contents (at or near the initial alkali thresholds for the particular aggregate when placed in distilled water). From the expansions developed it appears each aggregate has an "initial alkali content pessimum" for its greatest expansion when placed in salt solution.

3. The wet / dry cycling of the prisms in salt solution had little effect on the highly reactive aggregates (DR and HL) in comparison to permanent immersion in salt

solution. However, with the less reactive / slower reacting aggregates (MD and RP) the effect was to lower the initial alkali threshold for significant reaction even further than that associated with simple immersion in salt solution. This wet / dry cycling of the prisms produced an increased number of drying shrinkage paste cracks. The formation of these allowed the dissipation of some of the strain induced in the concretes by releasing more of the expansive ASR gel into these finer paste microcracks so reducing the total expansion potential in comparison to the equivalent samples permanently immersed in salt solution. In the process, this also allowed increased NaCl diffusion into the concretes so the expansions were still raised in comparison to those immersed in distilled water.

4. Significant ASR expansion was found in all the prisms half immersed in salt solution. The greatest expansion was found in the lower region of the concrete immersed in the salt solution. However, ASR expansion was also recorded for the upper face, even for the low initial alkali prisms. In these prisms there was evidence of microcrack networks initiating in the lower immersed areas and extending into the upper halves. These microcracks may have promoted the transport of NaCl and alkalis into the upper parts of the prisms.

5. The expansion test performed with concrete samples containing the MD and RP aggregates, showed that in certain circumstances there was a slow release of ASR that may continue over a long period of time. The rapid testing of these or similar materials for alkali-silica reactivity may therefore prove inadequate.

6. If sufficient alkalis remain or are added to the concrete ASR expansion may continue in a 38°C / 100 % RH environment for up to 24 months with all the aggregates included in this study. It therefore seems likely that in the presence of a supply of alkalis from de-icing salts, many ASR affected structures could continue to exhibit expansion over many years.

7. In the high alkali mixes the diffusion of Cl ions into the concrete is apparently impeded due to the early age injection of ASR gel into the capillary porosity of the cement paste. In the low alkali mixes the diffusion of Cl ions continues as in a 'normal' non-reacting concrete. This allows the Cl ions to bond with the $C_3A$ phase releasing extra hydroxyl ions which participate in the later age ASR. The high capillary porosity observed in the cement paste, surrounding paste microcracks when the concretes are placed in salt solution could be due to the depletion of either $C_3A$ or $Ca(OH)_2$ from the paste.

8. The high water soluble and acid soluble potassium contents released by the Dry Rigg siltstone and Maentwrog greywacke aggregates could be due to a release of weakly bonded potassium cations from the layered silicates muscovite, sericite etc. found in the aggregate. However, the lack of a significant quantity of K+ in equivalent pore solution analyses suggest that, either the potassium is not being released when the aggregate is in a concrete or that it has been lost or used up by the ASR. Whatever the explanation is for these high potassium contents, they may be a subsidiary reason for the high reactivity of these two aggregates.

# CHAPTER 5

## Additions of pulverised fuel ash to ASR susceptible concretes

### 5.1 Introduction

It has been observed in previous work by Nixon et al. (1984) that the addition of pulverised fuel ash (pfa) to ASR reactive concrete mixes made from high alkali cement reduces the hydroxyl ion concentration of the pore solution substantially and so reduces the potential reactivity of the mix, (section 1.4.5). However, with concrete made from low alkali cements there was a net contribution of hydroxyl ions to the pore solution at all ages up to one year when high alkali pfa was included, presumably by the addition of alkalis derived from the pfa itself.

With these results in mind, ASR expansion testing was carried out with low alkali concretes containing pfa as a partial cement replacement and calcined flint aggregate, which has a low initial alkali threshold for ASR (Hobbs, 1991 unpublished results). The results showed that some extra alkalis were being released from the pfa and causing increased ASR compared to an equivalent OPC mix. Similar testing with the reactive Thames Valley gravel aggregate however, showed no significant difference in the reactivity of the concrete (No significant ASR developed in either the pfa or OPC mixes). It was felt this was most probably because Thames Valley gravel and other similar chert-rich aggregates develop significant ASR only at high initial alkali levels, i.e >5.0 kg/m$^3$ $Na_2O_e$ which is well above the lower alkali levels at which some contribution of alkalis from the pfa has been established. Therefore, if a natural UK aggregate was identified that exhibited ASR at lower alkali levels than with the Thames Valley gravel, then additional alkali derived from the pfa may be expected to accentuate the reaction in a concrete with an initial alkali threshold just below that required for ASR with a normal OPC mix.

As a result of the work described in chapter 3, it was established that a number of UK aggregates develop significant ASR at alkali levels of between 3.5 and 4.5 kg/m$^3$ $Na_2O_e$. These aggregates were used to establish, whether alkali contribution from medium or high alkali pfa's could cause the development of ASR in an otherwise stable concrete. The main objective of this work was to see what effect partial replacement of the cement with pfa had on the pore solution alkali concentrations.

## 5.2 Experimental method

### 5.2.1 Mix design

Concrete mixes containing a 25 % replacement of the cement by pulverised fuel ash (pfa) were made up using the two most reactive aggregates included in this study (see section 3.4 ). The two aggregates used were the Dry Rigg siltstone (DR) and the Horrocksford silicified limestone (HL). Pfa replacement mixes were made up at initial alkali levels of 3, 4, 5 and 6 kg/m$^3$ $Na_2O_e$. A 25 % replacement of pfa was applied as it was hoped this work could be used in collaboration with results obtained by the Building Research Station, using the same pfa materials. Two British pfa's were used with alkali contents of 3.08 % and 4.00 % $Na_2O_e$, as these were thought to represent a typical medium and high alkali pfa (see section 2.1.3).

---

TABLE 5.1 : Calculation of the NaOH addition required to produce the various alkali content mixes, assuming no contribution of alkali from the pfa's.

---

To calculate the quantity of NaOH to be added to the mix, the following procedure was used.

1. Cement content =300 kg/m$^3$, and the alkali content of cement = 0.324 % $Na_2O_e$. Therefore, the amount of alkali derived from the cement in the mix is:

$$300 \times 0.324\ \% = \underline{\mathbf{0.973}}\ \text{kg/m}^3\ Na_2O_e$$

2. Required alkali for a mix is = 3 kg/m$^3$ $Na_2O_e$. Therefore, the alkali addition still required is:

$$3 - 0.973 = \underline{\mathbf{2.027}}\ \text{kg/m}^3\ Na_2O_e$$

3. This alkali was placed in 184 kg/m$^3$ of water in the mix to give a concentration of:

$$\frac{2.027}{184} \times 1000 = \underline{\mathbf{11.016}}\ \text{g } Na_2O_e \text{ / litre.}$$

4. This is equivalent to:

$$\frac{80}{62} \times 11.016\ \text{g} = \underline{\mathbf{14.214}}\ \text{g NaOH / litre.}$$

5. Water required for 2 prisms mix is 0.568 litres. Therefore, the required addition of NaOH for 2 prism mix is:

$$14.214\ \text{g} \times 0.568 = \underline{\mathbf{8.07}}\ \text{g of NaOH.}$$

Results of similar calculations for the various concrete mixes are as shown below :

| Required alkali level in $Na_2O_e$. | Required addition of NaOH. in water for 2 prisms. |
|---|---|
| 3 kg/m$^3$ | 8.07 g |
| 4 kg/m$^3$ | 12.06 g |
| 5 kg/m$^3$ | 16.04 g |
| 6 kg/m$^3$ | 20.02 g |

No alkali contributions from the pfa or aggregate were included in the initial alkali audits for this work. However, because of the inclusion of a 25 % replacement of the cement by pfa a recalculation of required additions of NaOH and mix designs had to be made (See Table 5.1). These changes in mix design also cause minor alterations to the water / cement and aggregate / cement ratios as shown in table 5.2.

TABLE 5.2 : Mix design for aggregates with specific gravity of approximately 2.7, to produce 2 prisms.

| MIX PROPORTIONS: | For 1m$^3$ of concrete | For 2 prisms |
|---|---|---|
| 20-5 mm coarse aggregate | =1296 kg/m$^3$ | = 4.01 kg |
| Inert <5mm fine aggregate | =555 kg/m$^3$ | = 1.717 kg |
| Free water content | =184 kg/m$^3$ | = 0.568 kg |
| Cement content | =300 kg/m$^3$ | = 0.928 kg |
| Fly ash (pfa) | =100 kg/m$^3$ | = 0.309 kg |
| TOTAL MIX MASS | | = 7.533 kg |

Calculated from original mix with replacement of 25% of cement by pfa.

| | |
|---|---|
| Water / cement + pfa ratio | = 0.46 |
| aggregate / cement + pfa ratio | = 6 to 1. |

Two different pfa's were used to study the effects of compositional variations between them.The two pfa's were from the Fiddlers Ferry and West Burton power stations. If the alkalis in these two pfa's are all included in the total alkali content of the concretes the results would be as shown in Table 5.3.

TABLE 5.3: Total alkali contents in $Na_2O_e$ for the various mixes assuming all the alkalis in the pfa to be available to the reaction.

| Alkali level assuming no contribution from the pfa. | Alkali level with West Burton pfa | Alkali level with Fiddler's Ferry pfa |
|---|---|---|
| 3.0 kg/m$^3$ | 7.0 kg/m$^3$ | 6.08 kg/m$^3$ |
| 4.0 kg/m$^3$ | 8.0 kg/m$^3$ | 7.08 kg/m$^3$ |
| 5.0 kg/m$^3$ | 9.0 kg/m$^3$ | 8.08 kg/m$^3$ |
| 6.0 kg/m$^3$ | 10.0 kg/m$^3$ | 9.08 kg/m$^3$ |

### 5.2.2 Expansion testing

The concrete mixes were made up and stored in the same manner as described in sections 2.2.2 and 2.2.3, part 1. The prisms were measured for 1 year, after which they were analysed for pore solution composition and by petrographic microscopy. The majority of the pore solution analyses were carried out on identical prisms that were made up and tested later, but were not included in the expansion measurements.

## 5.3 Expansion test results

The expansion test results are shown in Figures 5.1 to 5.8.

### 5.3.1 Dry Rigg siltstone concretes

Figures 5.1 and 5.2, show that the addition of the two pfa's to the high alkali, 5 and 6 kg/m$^3$ $Na_2O_e$ mixes containing the (DR) siltstone aggregate, significantly reduced the amount of expansion recorded. In all these mixes the expansions were still large enough to be considered significant (>0.05 % after 1 year).

Figure 5.3, shows the expansion results for the low alkali mixes with the (DR) siltstone aggregate and a 25 % cement replacement with high alkali pfa (West Burton). The 4 kg/m$^3$ $Na_2O_e$ mixes with and without the pfa replacement show virtually identical expansions after 1 year. Both mixes would be classified as of borderline reactivity showing strains of around 0.05 %. The expansion results for the 3 kg/m$^3$ $Na_2O_e$ mixes show a slightly larger expansion in the pfa replacement

mix compared with the normal OPC mix. The percentage strain difference between the two mixes is 0.014 %. Neither mix is however, considered to show enough strain to be classified as suffering significant ASR. The expansion data for both concrete prisms made for each mix was similar, so it seems unlikely that the data is flawed by a rogue result.

Figure 5.4, shows the expansion results for the low alkali mixes with a 25 % cement replacement with medium alkali content pfa (Fiddler's Ferry). The results show a negligible difference in the expansion of the 4 kg/m$^3$ $Na_2O_e$ mixes, with and without the pfa replacement. Both mixes would be classified as of borderline expansiveness concretes showing approximately 0.05 % strain after 1 year. The 3 kg/m$^3$ $Na_2O_e$ mix with pfa however, shows virtually no expansion and is also slightly less expansive than the normal OPC 3 kg/m$^3$ $Na_2O_e$ mix.

### 5.3.2 Horrocksford limestone concretes

The equivalent mixes using the (HL) silicified limestone as the reactive aggregate are shown in Figures 5.5 to 5.8. Again, there is a noticeable increase in the recorded expansion of the high alkali (WB) pfa mix at 3 kg/m$^3$ $Na_2O_e$ compared to the normal OPC mix (Figure 5.5). The difference in percentage strain between these two mixes is 0.017 %. The expansion is however, still not enough to be considered a significant case of ASR. The difference in the recorded percentage strain, between the 3 kg/m$^3$ $Na_2O_e$ Fiddlers Ferry pfa and normal OPC mix is negligible (Figure 5.7). For the rest of the mixes containing the silicified limestone, the 25 % replacement of the cement by pfa retarded all the expansions recorded, as compared with the equivalent OPC concretes. This occurs to such a degree that only one of the other pfa mixes expands enough to be considered to have suffered significant ASR, that being the 6 kg/m$^3$ $Na_2O_e$ mix containing the West Burton pfa (Figure 5.6).

### 5.3.3 Summary

A summary of the results discussed above is given in table 5.4. and also displayed in Figure 5.9. Taking an overview of these results, it is apparent that the pfa's (of both medium and high alkali content) have a reducing effect on the expansions of the high alkali concretes (5 kg or 6 kg/m$^3$ $Na_2O_e$). Though the pfa additions reduced the expansion there was still a significant level recorded in all the (DR)

siltstone aggregate high alkali mixes. At 4 kg/m$^3$ $Na_2O_e$ pfa produced no detectable suppression of the expansion in the siltstone mixes. In both the 3 kg/m$^3$ $Na_2O_e$ siltstone and silicified limestone mixes there was a net increase of expansion in the high alkali pfa (WB) mix as compared to the equivalent normal OPC mixes and virtually no difference in the expansions for the medium alkali content pfa (FF) mixes. It is therefore probable that the release of alkalis from the pfa's maybe the cause of the observed increases in expansion.

TABLE 5.4 : Comparison of expansion data for the OPC and pfa mixes, shown as % strain average of two prisms after 12 months.

| Dry Rigg siltstone | OPC mix | West Burton, | DIFF | Fiddler's Ferry, | DIFF |
|---|---|---|---|---|---|
| 3.0 kg/m$^3$ | 0.011 | 0.025 | (+0.014) | 0.002 | (-0.009) |
| 4.0 kg/m$^3$ | 0.053 | 0.048 | (-0.005) | 0.045 | (-0.008) |
| 5.0 kg/m$^3$ | 0.131 | 0.075 | (-0.056) | 0.065 | (-0.066) |
| 6.0 kg/m$^3$ | 0.232 | 0.109 | (-0.123) | 0.111 | (-0.121) |
| Horrocksford limestone | | | | | |
| 3.0 kg/m$^3$ | 0.003 | 0.020 | (+0.017) | -0.001 | (-0.004) |
| 4.0 kg/m$^3$ | 0.099 | 0.040 | (-0.059) | 0.003 | (-0.096) |
| 5.0 kg/m$^3$ | 0.149 | 0.045 | (-0.104) | 0.023 | (-0.126) |
| 6.0 kg/m$^3$ | 0.121 | 0.057 | (-0.064) | 0.044 | (-0.077) |

Finally there is some evidence from the work described in section 4.4.3, to suggest that some alkali may be released from aggregates, especially the (DR) siltstone and Maentwrog greywacke (MD) and this may result in another alkali contribution to the total alkali content of those mixes. Similar effects on recorded expansions have been found by Blackwell (1993) using the same pfa's and Maentwrog greywacke as the reactive aggregate.

## 5.4 Pore solution analysis results

The reactivity of concrete mixes with sufficient water and reactive silica, is dependent on the amount of alkali present and its availability for the reaction. Unless an external source of alkali is present (see chapter 4 ) the alkali used up by the ASR is derived directly from the pore solution of the concrete. Measurements of the pore solution composition should indicate therefore whether the various alkali

level pfa mixes analysed in this study, were a more or less potentially reactive than the equivalent OPC mixes.

The composition of the pore solution in a concrete will alter with time and so some impression may be obtained as to the levels of sodium, potassium and hydroxyl concentration at which the reaction stops in the various mixes. In this study the pore solutions were expressed from the hardened concrete by the method described in section 2.4.1 and the chemical analyses for $Na^+$, $K^+$ and $OH^-$ were carried out as described in section 2.4.2. The pore solution was expressed from the concrete mixes at 1,7, 28, 183 and 365 days. The results are presented in millimoles per litre (mmol / litre) (see Appendix 5).

As ASR is a chemical reaction involving consumption of hydroxyl ions, the measurement of the hydroxyl concentration of the pore solution should be a good indicator of the amount of alkali available to the reaction from the pore solution and therefore the potential reactivity remaining in that concrete. Calculation of the sodium and potassium content is a second method of identifying the amount of alkali available in the pore solution for reaction. As virtually all the alkali metals in the pore solution will be associated with hydroxyl ions to produce an electrical balance a calculation of the total alkali metal content should be more or less equivalent to the hydroxyl ion concentration (Nixon et al. 1986). The pore solution data obtained is recorded in detail in appendix 5 and Figures 5.10 to 5.17.

### 5.4.1 Evolution of pore solution composition with time

Figures 5.10 to 5.13, show the changes that occurred in the pore solution composition with time. The sodium cation concentrations (Figure 5.10) shows an initial (1 to 7 days) enrichment in the pfa samples compared with the OPC mixes, though this appears to be lost by 28 days, with little difference between the two mix types. Extrapolation of the OPC mix data to 365 days suggests the pfa mixes will again be significantly in surplus over the OPC mixes. The equivalent graph for the hydroxyl ion concentrations (Figure 5.11) show a net enrichment for all the pfa mixes, at all ages in comparison to the OPC mixes. Though this data again appears to show the greatest hydroxyl enrichment at the very early and late ages.

Finally, in some ways the most significant of these graphs (Figure 5.12) shows the equivalent data for the potassium cation concentrations. This shows a gradual increase in the $K^+$ cation concentration for the first 28 days after which there is a

slight gradual decline. When it is considered that the pfa's alkali contents are made up mainly of potassium (FF pfa alkali content = 80 % $K_2O$, and WB pfa alkali content = 70 % $K_2O$, see section 2.1.3) it seems quite reasonable that the majority of alkalis released into the pore solution from these pfa's should be potassium as this would reflect the high K / Na ratio of the pfa. It been previously shown that potassium is more easily stripped from aggregates and minerals than sodium and is then detected in raised potassium levels of the relevant concrete pore solution (Greeman, 1986). The results for potassium concentration in the pore solution over time also confirm this observation. Assuming a loss of some potassium hydroxide to the ASR and leaching to a similar extent as seen with the sodium concentration, it appears that the release of potassium from the pfa continued constantly throughout the expansion test. Its contribution to the total alkali content however, will only be noticeably positive during the first 28 days, the period often considered most crucial to the ASR reactivity of a mix. Interestingly, the greatest differences in potassium concentrations were found in the low alkali content pfa mixes. The release of more alkali from the pfa in the lower alkali mixes is what was anticipated would be shown from this work, if the pore solution alkali concentration relates directly to the degree of ASR expansion developed. This is clearly the case when considering potassium only. Some researchers working in this field have speculated that potassium hydroxide is potentially more 'reactive' than sodium hydroxide (Blackwell, 1993). The higher level of potassium seen in the lower alkali mixes can only really result in raised reactivity. In Figure 5.13 the late age 3 kg mix combined alkali concentration (Na+K) is virtually identical to the 6 kg mix due largely to this extra potassium derived from the pfa and therefore by this late age the two mixes will have almost equal low potential reactivity. The main period of expansion developed by the 6 kg mix occurs relatively early, between 2 to 6 months, whilst in the 3 kg mix the little expansion that does develop occurs later, mainly between 8 and 10 months. The loss of alkali material both sodium and potassium by leaching, ASR etc. will occur in both mixes, but will be most significant in the 6 kg mix with the higher initial alkali content and therefore further significant expansion ceases quite early (8 months). In the 3 kg mix, however, the slow release of the potassium with time allows this loss of alkali due to leaching (and slight ASR) to be reduced and therefore the limited expansion that develops is at later ages (Figure 5.3). Overall as the amount of potassium in the pore solution is relatively small in comparison to sodium the only significant contribution it makes is to slightly increase the long term pore solution total alkali concentration (Figure 5.13). This will probably result in continued slightly increased late age ASR expansion, so its contribution will still be significant.

### 5.4.2 Variations in the pore solution composition at specific dates with different initial alkali levels

Figures 5.14 to 5.17, show the difference in pore solution compositional data for each initial alkali level at each of the measuring ages. Figure 5.14, shows the results of the pore solution analyses carried out on the 1 day old concretes. This graph shows a net contribution of hydroxyl ion and alkali metal cations to all the pfa mixes, most especially those containing the high alkali (WB) pfa. No trends are apparent with regard to the initial alkali levels of the concrete. A good correlation can be seen between the total alkali metal cation content and the equivalent hydroxyl ion concentration, which suggests most of these constituents are found in the pore solution as sodium or potassium hydroxides.

Figure 5.15, shows the results of the pore solution analyses carried out on the 7 day old concretes. With the exception of the hydroxyl ion concentrations in the medium alkali pfa (FF) mixes all the results all show a net increase in the contribution of alkali metals and hydroxyl ion molarity compared to equivalent OPC mixes. The low alkali pfa, (FF) mixes total alkali metal cation concentrations are seen to behave almost as has been postulated, with enrichment in the low initial alkali mix compared to the higher levels. However, even these low alkali mixes are still reduced in alkali metal cation concentrations compared to the equivalent OPC mixes.

Figure 5.16, shows the results of the pore solution analyses carried out on the 28 day old concretes. This graph exhibits the trends that were expected to develop if the theories suggested previously were going too be proved valid. The hydroxyl and alkali metal concentrations of the low alkali pfa (FF) mixes show a net decline at higher initial alkali levels compared to the equivalent OPC mixes. However, the high alkali pfa (WB) mixes exhibit a fairly static positive differences at the various initial alkali levels. The 28 day results show a general coming together of the various pfa and OPC equivalent mix results (see also Figures 5.10 to 5.13).

Finally, Figure 5.17, shows the results of the pore solution analyses carried out on the 183 day old concretes. By now the total concentrations of hydroxyl and alkali metals are much reduced (Appendix 5, Figures 5.10 to 5.13). All the pfa mix results show a net contribution of hydroxyl ions and alkali metal cations compared to the equivalent OPC mixes. Though importantly there is also a noticeable drop off in the

differences recorded at the higher initial alkali levels with the high alkali pfa mixes, (WB).

A direct relationship between the pore solution concentrations and the rates of expansion / reaction in the various was not seen. Therefore, it seems unlikely that it exists, especially as other factors related to the reactivity pfa mixes are also involved. It should be pointed out the the compositional differences shown in Figure 5.17 were calculated using OPC 183 day results and 365 day pfa mix results. Based on extrapolation of the results in Figures 5.10 to 5.13, this should result in a slight lowering of the differences recorded between the two mixes, as the OPC mixes seem to be losing their $OH^-$ and Na+K concentrations more rapidly.

### 5.4.3 Differences between the two reactive aggregates.

Table 5.5, shows the effects on the pore solution concentrations of using different reactive aggregates. Comparison of the two aggregate mixes at 1 year shows that the (HL) limestone mixes have consistently higher hydroxyl and sodium plus potassium concentrations in their pore solutions than the equivalent (DR) siltstone mixes. As the (DR) siltstone is more reactive than the (HL) limestone, those concretes have used up larger amounts of hydroxyl, sodium and potassium available from their pore solution than the other equivalent mixes (Figures 5.1 and 5.8).

TABLE 5.5 : Difference between pore solution results for Dry Rigg siltstone and Horrocksford limestone mixes after one year (HL-DR).

| | Na+ | K+ | OH - | (Na+K) |
|---|---|---|---|---|
| **West Burton pfa mixes** | | | | |
| 3.0 kg/m$^3$ $Na_2O_e$. | +34.8 | +15.4 | +35.5 | +50.2 |
| 4.0 kg/m$^3$ $Na_2O_e$. | +50.0 | +42.9 | +60.0 | +55.8 |
| 5.0 kg/m$^3$ $Na_2O_e$. | +50.0 | +5.8 | +26.5 | +55.8 |
| 6.0 kg/m$^3$ $Na_2O_e$. | +128.3 | +23.7 | +91.0 | +152.0 |
| **Fiddler's Ferry pfa mixes** | | | | |
| 3.0 kg/m$^3$ $Na_2O_e$. | +21.8 | +18.6 | +8.0 | +40.3 |
| 4.0 kg/m$^3$ $Na_2O_e$. | +75.0 | +27.5 | +68.0 | +102.6 |
| 5.0 kg/m$^3$ $Na_2O_e$. | +88.1 | +25.0 | +73.0 | +113.0 |
| 6.0 kg/m$^3$ $Na_2O_e$. | +47.9 | +7.0 | +43.0 | +54.9 |

### 5.4.4 Summary of results of pore solution analysis

The pore solution chemical analysis carried out as part of this work showed a number of specific features:

1. In the 1 day old concretes, there was a net contribution of hydroxyl ions and alkali metal cations to the pore solutions of all the pfa mixes compared to the equivalent OPC mixes, regardless of initial alkali content of the mix, which was surprising when considering the slow pozzolanic reaction of pfa at the room temperature in which the concrete was cured. No relationship could be identified between the initial alkali content of the mixes and their pore solution concentrations. The hydroxyl and alkali metal concentrations for each mix were similar, suggesting most of these constituents were found in the forms NaOH and KOH. The medium and high alkali pfa mixes were always seen as the lower and higher pore solution concentrations respectively.

2. In the 7 day old concretes, there was a little contributory effect by the additions of pfa to the concrete mixes and no apparent relationship to the initial alkali content of the concrete. The medium alkali pfa (FF) mixes almost exhibit the suspected

enrichment of hydroxyl ions at lower initial alkali contents. However, in general the hydroxyl ion concentrations are virtually equivalent to or even reduced in comparison to the equivalent OPC mixes. The alkali metal cation concentrations all show enrichment in both the pfa mixes, unrelated to initial alkali content. This may imply the alkali metals have been released from the pfa, but are not at present found as hydroxides.

3. In the 28 day old concretes, the addition of the medium alkali pfa (FF) showed a slight retarding affect on the hydroxyl ion and alkali metal cation concentrations for the high initial alkali mixes (5 and 6 kg/m$^3$ $Na_2O_e$) in comparison to the equivalent OPC mixes. However, this observation was not made for the high alkali pfa (WB) mixes which broadly, show a slight increase in hydroxyl ion and the alkali metal cation concentration towards the lower initial alkali levels (3 and 4 kg/m$^3$ $Na_2O_e$ mixes) during this first month of the pore solution testing.

4. The 183 day results show enrichment of hydroxyl and alkali metals in all the pfa mixes regardless of the initial alkali levels and type of pfa used. There is a marked reduction in the differences of both constituents observed for the high initial alkali mixes containing high alkali pfa (WB) compared to the equivalent OPC mixes.

5. The alkali metals and hydroxyl concentrations of the pore solutions for the medium (FF) and high (WB) alkali pfa's mixes were always related to each other with regard to the various concentrations (i.e one pfa mix was above or below the other pfa mix in relation to their total alkali contents).This suggests the chemical analyses of the pore solution was accurate and reliable. The differences observed between the pore solutions of the OPC and pfa mixes were similar to those observed in equivalent work using Thames Valley gravel (see section 5.4.5).

6. The majority of the alkali released from the pfa's was potassium. Therefore there is a net contribution of potassium to the pore solution at virtually all ages, except 1 day. This contribution appears to be most significant in the older age concretes, when the total alkali concentration is much lower. The release of potassium was greatest in the lower alkali mixes, but the reasons for this are still unknown.

7. In summary these pore solution results are inconclusive and this suggests the problem being studied is more complex than initially thought or due to factors other than pore solution alkalinity, see section 5.5. The fact that the siltstone mixes did not show similar pore solution concentration behaviour to that seen using Thames

Valley gravel (see section 5.4.5) could be a result of the significant ASR occurring in the Dry Rigg siltstone concretes (see 5.5). In the complex chemical reactions now envisaged for these reactive pfa concretes, the movements, releases and removal of hydroxyl ions and alkali metals cations from the pore solution, pfa and even aggregates is still to be fully understood.

### 5.4.5 Comparison to similar results using a Thames Valley gravel aggregate

Similar work only using the Thames Valley gravel has also been carried out at Aston University for the Department of the Environment (DOE) (Sadeghzadeh, 1993). Thames Valley gravel was used as at the time it was considered, by some researchers to be the most reactive UK aggregate, when used in a suitable pessimum proportion. The results of the pore solution analyses carried out in this DOE work, for concretes containing identical types and amounts of pfa as used in this research are summarised in Figures 5.18 to 5.22. The initial alkali contents for the concretes in the DOE work was established by using of cements of differing alkali content rather than by the addition of NaOH to the mix water. From this additional data using Thames Valley gravel, it is possible to make the following comments.

1. In the high initial alkali mixes the addition of pfa to a concrete in general reduced the hydroxyl ion and alkali metal cation concentrations in the pore solution, so reducing that concretes potential for reactivity at the later stages. The reason for this this remain unresolved, but it has been suggested that either the pfa results in a greater percentage of CSH gel which takes up more alkalis, or that it modifies the ASR gel composition to allow a greater take up of alkali ions (Nixon et al. 1984).

2. In low alkali mixes the addition of pfa to the concrete enhanced the hydroxyl ion and alkali metal cation concentrations in the pore solution, so increasing the potential reactivity of that concrete depending on the occurrence of an aggregate with an alkali threshold as low as 2.2 kg/m$^3$ $Na_2O_e$. Materials which are reactive at these low alkali levels are relatively rare but do exist. Such materials include natural opal and calcined flint, which is a man made aggregate previously used in similar experiments to evaluate the effect of pfa on ASR.

3. ASR in Thames Valley gravel concretes has been observed to be most rapid during the first few days after which it slows. Therefore as there appears to be a net contribution of alkalis to low alkali concretes during this period enhanced ASR could develop in the pfa mixes. However, the reasons for no observed ASR in the concretes made up for this work would be the fact that Thames Valley gravel requires an initial alkali threshold of at least 5 kg/m$^3$ $Na_2O_e$ to initiate significant reaction, well above anything developed here.

4. The different pfa's produced different pore solution characteristics the causes of which are still not fully understood.

If the effects observed on the pore solution concentrations in these concrete samples are correct, then the addition of pfa to concretes containing similar high initial alkali threshold reactive aggregates, such as Thames and Trent Valley gravels will be of benefit as a further method of suppressing ASR. However, the effects on other potentially reactive aggregates with low to medium alkali thresholds for significant reaction (3 to 4.5 kg/m$^3$ $Na_2O_e$) are still unclear.

## 5.5 Petrographical analysis

Petrographical thin sections were made up of the 4 and 6 kg/m$^3$ $Na_2O_e$ mixes containing both West Burton and Fiddler's Ferry pfa's after 12 months. The alkali silica reaction was observed to have occurred in all the thin sections examined. The reactive material was the DR siltstone coarse aggregate and the ASR took the usual forms of divergent, expansive microcracking seen with this aggregate as described previously in section 3.5.1. Apart from the usual form the ASR took within the reactive aggregate particles the slides were observed to be quite different. A summary of these findings is shown below.

### 5.5.1 Sample No. DRWB16.0A

1. Dry Rigg aggregate, 6.0 kg/m$^3$ $Na_2O_e$ mix, with West Burton pfa replacement. SCALE OF REACTION = 4.

This slide contained a dark grey / black cement paste unlike those observed previously in chapter 3. Some pfa particles were clearly visible as dark spheroids clusters and blobs of size range 100 to less than 5 $\mu$m diameter (Plate 5.1). A number of orange / brown glassy spheres were observed in this and all the other concretes containing pfa and it was felt this material was also a form of the pfa. Some 'smudging' of the darker pfa spheroids edges was observed, (as in all the other slides examined) and it was thought this might represent a limited localised pozzolanic reaction with the cement paste or that the particular pfa particle was only partially included in the thin section. There was overall a surprising lack of paste cracks due to plastic shrinkage compared to the other pfa slides examined. Carbonation was confined to a thin original edge region (50 to 100 $\mu$ms wide) which penetrated in a little deeper down the short surface microcracks. The paste was on the whole a dark, low porosity, low air void content and sound material.

There were a number of adhesion cracks on the coarse aggregate and these were generally finer than seen in other non-pfa concretes. These adhesion cracks were thought to represent localised aggregate / paste debonding, maybe due to a drier initial paste mix. The adhesion cracks were a typical location for the occurrence of ASR gel. The evidence of ASR was found extensively in the coarse aggregate particles throughout this slide. However, little of this ASR-related microcracking continued into the cement paste for any great distance. The pseudo-adhesion cracks running around the periphery of the coarse aggregate, as described previously in section 3.5.1, were the main type of ASR cracking observed and these were usually devoid of ASR gel. The majority of gel was found in paste voids and adhesion cracks. The finer size of the observed adhesion cracks may be further evidence for the differences in the cement paste microstructure caused by the addition of pfa. In summary this was a sound dense (low porosity) concrete with ASR developed in the coarse aggregate. Little of the microcracking present occurred in the cement paste which was in general uncracked and uncarbonated. The amount of expansion recorded for this prism (0.109 % strain after 12 months) seems high in comparison to the amount of microcracking and ASR gel detected. Therefore the majority of the expansion could be due to finer undetected microcracks and expansion solely within the cement paste.

### 5.5.2 Sample No. DRWB14.0A

Dry Rigg aggregate, 4.0 kg/m$^3$ $Na_2O_e$ mix, with West Burton pfa replacement. SCALE OF REACTION = 3.

The most substantial difference compared to the 6 kg/m$^3$ $Na_2O_e$ mix is the increase in paste cracks and associated carbonation. The area of the cement paste surrounding the paste microcracks has a higher capillary porosity. Though there are areas of the cement paste that are still as dark as the 6 kg/m$^3$ $Na_2O_e$ mix, a great deal is now highly carbonated and microcracked (Plate 5.2). This fine paste microcracking does not appear to be particularly damaging to the concrete, but is fairly continuous and is most probably the result of small scale cement paste shrinkage. This localised microcracking and associated carbonation gives this paste a patchy appearance.

The amount of ASR-induced microcracking observed in the coarse aggregate specifically is actually greater than that seen in the 6 kg/m$^3$ $Na_2O_e$ mix. However,

even less of this microcracking continues into the cement paste or to the outer surfaces of the prism. One major crack system caused by ASR is observed to run sub-parallel to one of the original outer surfaces of the prism for about 25 mm this was however, unique in the slide. Though the effects of ASR can be easily identified in this slide, the damage it causes to the concrete as a whole was negligible and this was unusual when compared with the relatively high expansion figure (0.046 % strain after 12 months) for this prism.

### 5.5.3 Sample No. DRFF16.0A

Dry Rigg aggregate, 6.0 kg/m$^3$ $Na_2O_e$ mix, with Fiddler's Ferry pfa replacement. SCALE OF REACTION = 2.

Unlike the West Burton pfa 6 kg mix this concrete shows evidence of heavy carbonation of the cement paste. This carbonation was patchy in appearance and was usually associated with the paste and adhesion cracks but was also observed surrounding some coarse and fine aggregate particles. The fine paste microcracking was very extensive and was frequently connected to adhesion cracks. The carbonation was associated with areas of high capillary porosity cement paste. The highly carbonated / depleted nature of this concrete gives the thin section a creamy brown overall colour (Plate 5.3). No ettringite was observed in this concrete. ASR microcracking was well developed in the siltstone coarse aggregate. The most common forms of microcracking were pseudo-adhesion cracks, followed by microcracks running along the long axis of the aggregate particles, running with the cleavage of the rock and finally the typical divergent expansive type microcrack systems. ASR gel was rare in this slide, but was observed in some paste voids, adhesion cracks and as 'plug-like deposits' in microcracks at the aggregate to cement paste boundary. Much of the ASR induced microcracking in the coarse aggregate did not continue into the cement paste.

### 5.5.4 Sample No. DRFF14.0A

Dry Rigg aggregate, 4.0 kg/m$^3$ $Na_2O_e$ mix, with Fiddler's Ferry pfa replacement. SCALE OF REACTION = 1 or less.

Only a few coarse aggregate particles show evidence of ASR . The main feature exhibited by this slide was an extensive number of adhesion cracks connected to dry shrinkage paste cracks. These paste cracks were associated with heavy

carbonation / depletion and localised high capillary porosity of the cement paste (Plate 5.4). There were still however, areas of darker unaffected cement paste. There was no evidence of large expansive ASR cracks developed in this concrete. The few ASR related microcracks seen were small and not particularly extensive, few even leave the reacted aggregate particles. ASR gel was observed in a few paste voids, some appears to have been recrystallised to an alkali silicate rich mineral or had been carbonated.

### 5.5.5 Conclusions on petrography of pfa mixes.

ASR has occurred in all the slides examined and the development of microcracking in the coarse aggregate particles seems extensive and related directly to the initial alkali content of the mix. It is however, clear that these microcrack systems do not extend over the concrete as a whole, many appear to just stop at or near the boundary of the aggregate particle with the cement paste. Therefore, though ASR has occurred in these concretes changes in the cement paste microstructure presumably caused by the addition of pfa seems to stop microcrack networks developing beyond the reactive aggregate particles.

The amount of ASR gel observed is noticeably reduced, especially gel injected into the capillary porosity of the cement paste (see section 4.5.2). This may well be due to the reduced average particle size of the cement paste with a pfa replacement, which will result in a more subdivided network of capillary pores and therefore less ease of access for the gel to enter the cement paste microstructure. The number of reacted aggregate particles is clearly still related to the initial alkali content of the mix. However, the number of microcracks reaching the surface of the concrete is vastly reduced. Because of the addition of the pfa these cement pastes have a finer microstructure and this may reduce the large scale 'fracturing' of it, in some as yet unknown manner. The recorded expansion must therefore be a result of ASR expansion from the coarse aggregate particles released via the fine paste microcracks. Maybe the less viscous alkali-rich expansive ASR gels could be drawn into this finer paste microstructure so dissipating its volume rapidly, therefore lowering the strain it places on the surrounding concrete and in the process stopping any microcracking of the paste. However, no cement paste staining due to injection with ASR gel could be identified. This does not however, mean the process above is not occurring, as the increase in the colour / darkness and other changes in the paste form could mask any injected gel.

## 5.6 Discussion

The expansion test results show an increased expansion for the low initial alkali concretes containing high alkali pfa compared with the equivalent OPC mix, though this increased expansion is still not enough to be considered significant. The expansion-reducing effects of the pfa's additions on the 4 kg mixes is negligible when compared to the equivalent OPC mix, whilst the high initial alkali mixes show reduced expansion with the pfa mixes.

In general the high alkali pfa, enriched the pore solution hydroxyl and alkali metal concentrations of all the mixes, regardless of the initial alkali content. Whereas, the medium alkali pfa mixes showed unaltered or even slightly reduced concentrations of hydroxyl and alkali metals, especially at higher initial alkali levels. When these results are compared with the expansion data, it is apparent that something else, other than the pore solution alkalinity is affecting the reactivity of the pfa mixes.

The addition of pfa to a concrete appears to 'dry out' the early mixes causing a slight initial shrinkage to all the prisms (see Figure 5.1 to 5.8) and later drying shrinkage paste cracks. It also may reduce the diffusion rates of ions in the paste and alter its mechanical properties. It may be that these features are significant in reducing the effects of ASR reactivity in mixes containing a partial replacement of cement with pfa.

The petrography showed that some degree of ASR had occurred in all the concretes examined. However, though a lot of the potentially reactive particles showed evidence for the reaction, only a little cracking due to ASR developed externally in the cement paste. Though the addition of pfa clearly affects the pore solution compositions, it appears that the ASR develops internally within the coarse aggregate particles regardless. Therefore, it may be the effects of the pfa replacement on the cement paste microstructure, that are the main reasons for the reduced expansions observed in high alkali mixes. The diffusion / migration of the alkali laden pore solution in the cement paste towards the reactive aggregate particles, maybe affected by the addition of the pfa to the concretes. The addition of the pfa should reduce the capillary porosity total volume in the cement paste. Therefore the overall ability of the pore solution to reach the reactive aggregate particles should be reduced.

Importantly, these comments do not alter the fact that increases were observed in

the expansions measured for the 3 kg mixes containing the high alkali pfa (WB). The pore solution data showed a net contribution of hydroxyl ion and alkali metal cations especially in the lower initial alkali mixes, so presumably there was still a greater potential for increased ASR reactivity in this mix. Throughout the testing there was a constant small release of potassium from the pfa's and this was most pronounced in the low alkali (WB) pfa mixes. It might be that this extra potassium rather than the sodium caused the slight increase observed in expansion results seen in the later stages of the testing. However, an explanation of why the lower alkali (WB) pfa mix should consistently release more potassium is unknown.

In the high alkali mixes (5 and 6 kg) some ASR will occur regardless of any alkali addition from the pfa. Therefore, ASR occurs in these concretes though at a reduced level compared to the equivalent OPC mixes, perhaps because of the reduced diffusion of the pore solution through the cement paste towards the aggregate particles. In the 3 kg mix the concrete will not develop significant reaction at this initial alkali level in a normal OPC mix. However, in releasing potassium into the pore solution, the pfa leaves this concrete mix potentially ASR reactive. Therefore, limited ASR due to the alkalis derived from the pfa occurs in the reactive aggregate particles. However, due to the alterations to the capillary pores of the cement paste discussed above, the ASR was largely confined to the aggregate particles which locally expand and form a few minor associated paste cracks. The lack of significant quantities of high alkali pore solution reaching the reactive aggregate particles due to the reduced diffusion of the cement paste, means the expansion was very limited and localised.

If this theory is valid, the measured increase in expansion developed by the 3 kg pfa mix (or other equivalent borderline alkali threshold mixes) will always remain limited, as the reduced diffusion of pore solution in this cement paste should stop significant ASR, until such a time as the leaching of alkalis from the concrete will retard any further ASR. If this is the case then the partial replacement of cement by a pfa, (even a high alkali one) will be of benefit to the suppression of ASR with real reactive aggregates, such as DR siltstone.

The pozzolanic reaction between pfa and $Ca(OH)_2$ may also have a bearing on reducing the ASR developed in a mix by removing a requirement for the occurrence of significant ASR namely portlandite, (Diamond, 1989, Duchesne and Berube, 1992). However, this aspect of pfa / ASR research has not been studied here.

It has been frequently shown that a limited amount of calcium [source $Ca(OH)_2$] is required by ASR gel in order to initiate deleterious expansion, see section 7.5.1, page 175. The full understanding of these results is still not fully accomplished. The effects of pfa on ASR are clearly not as simple as initial considered.

## 5.7 Conclusions

1. The concrete prism expansion test results showed that the replacement of 25 % of the cement with pfa's reduces the amount of recorded expansion in high initial alkali concretes significantly. Many of these prisms would however, still be considered to be suffering from a significant case of ASR.

2. The expansion test results for low alkali concretes containing both pfa's showed no discernible increase or decrease in expansion recorded for the 4 kg mixes compared to the equivalent OPC mix. Both these mixes would be regarded as borderline reactive concretes.

3. With the 3 kg mixes the expansion recorded was greater for the high alkali pfa (WB) mix compared with the normal OPC mix, which showed no expansion. However, the amount of expansion recorded was still significantly below that considered to represent significant ASR (>0.05 % strain after 12 months). The equivalent medium alkali pfa (FF) mixes showed no expansion.

4. The pore solution analysis data, showed that in general the high alkali pfa enriched the pore solution hydroxyl and alkali metal concentrations of all the mixes, in comparison to the equivalent OPC mixes, regardless of the initial alkali content. The medium alkali pfa mixes showed unaltered or even slightly reduced concentrations of hydroxyl and alkali metals, especially for the higher initial alkali mixes.

5. Study of the pore solution data at the different ages, showed some evidence of trends developing in relation to the initial alkali contents of the concretes. However, these compositional trends did not remain valid for more than one or two analyses.

6. The majority of the alkali released from the pfa's was potassium. Therefore there is a net contribution of potassium to the pore solution at virtually all ages, except 1 day. This contribution appears to be more significant in the older age concretes when the total alkali concentration is much lower due to leaching, but this is also a

time when most ASR would have been complete. The greatest release of potassium was found in the lower alkali (WB) pfa mix and this was the probable explanation for the slight increase shown in the expansion developed at late ages in the 3 kg mix containing (WB) pfa. An explanation of why this has occurred is still unclear.

7. In general the pore solution results are inconclusive and this suggests the problem being studied is more complex than initially thought. The fact that the various aggregates mixes did not show similar pore solution concentration behaviour could be as a result of the variable amounts of ASR occurring or alkalis released from the coarse aggregate (section 4.4.3). In the complex chemical reactions now envisaged for these reactive pfa concretes, the movements, releases and removal of hydroxyl ions and alkali metals cations from the pore solution, pfa and even aggregates are not understood.

8. The petrographical analysis showed that ASR located specifically in the reactive aggregate particles was observed in all the thin sections examined. It may be that the lack of evidence for ASR microcracking in the cement paste is due largely to the effect pfa has on the physical and chemical properties of the cement paste and also that the pfa-containing paste is altered so the observation of ASR gel staining etc. is no longer possible.

9. The hydroxyl concentration of the pore solution was enhanced with all the low alkali mixes containing the high alkali pfa (WB), for all the analyses carried out. This was however, not the case for the higher initial alkali mixes. The medium and high alkali pfa's gave pore solution results that indicate a release of alkali from the pfa's proportional to their initial alkali content.

# CHAPTER 6

## Effects of air entrainment on the alkali-silica reaction

### 6.1 Introduction

Air entrainment (AE) which is the addition of a small percentage of air bubbles to a concrete's cement paste is primarily used to improve a concretes freeze / thaw resistance. It has been observed in experimental mixes using ASR reactive mortars that the addition of air entrainment to a mix has a reducing effect on the development of ASR expansion (Jensen et al. 1984). It is now also fairly widely assumed that this air entrainment will reduce the longer term effects of ASR. Discussion of these observations with Dr T. Miyagawa (1991) of Kyoto University, however, revealed that unpublished Japanese work on reactive aggregate concretes has shown that, though in the short term ASR was significantly suppressed in concretes with high air entrainment, over a longer period of time the effects were lost and the concretes continued to expand. This later initiation of ASR presumably occurs in the concrete once all the air voids have been filled with ASR gel. It is the aim of this work to establish which of these observations on the effects of air entrainment on the degree of ASR is correct. Petrographical analysis of the reactive concretes will be used to establish by what method the air entrainment actually reduces the expansion developed by the reaction.

### 6.2 Experimental method

With these considerations regarding the effects of air entrainment on ASR in mind, concrete prisms were made up at two initial alkali levels, well above and just above the thresholds for significant reaction with the most reactive aggregate used. These prisms were made up with various levels of air entrainment and the same mix design was used as described in section 2.2.1. As a proportion of each mix had to be tested for its air content prior to making up the prisms a concrete batch equivalent to six prisms was made for each mix design. This was carried out so that the concrete tested for its air content was not actually used to make the expansion prisms. The air entrainment agent (AEA) used was SIKA-AER and this was added to the mix water to make up a total water volume equivalent to the original design mix as described in 2.2.1. The suggested initial trial dosage of AEA for typical levels of AE was 25 ml per 50 kg of cement. Using a diluted form of this AEA as a starting point the actual levels of AE in the concrete mixes were made up as shown in Table

Missing page(s) from the bound copy

expansion results were taken monthly for 15 months in the same manner as described in section 2.2.3, the results shown being the average for two prisms.

The effect that the ASR occurring in air entrained concrete has on its freeze / thaw resistance remains unknown. The reliability of expansion testing carried out at 38°C for direct comparison with the reactivity of real concrete structures is still unresolved. With these problems in mind therefore, a series of air entrained concrete prisms equivalent to those described for the 38°C testing were placed in external exposure conditions to see if any ASR or freeze / thaw damage developed during the period of research.

## 6.3 Expansion test results

The expansion results for the prisms tested at 38°C are shown in Figures 6.2 and 6.3. The expansion data at 15 months plotted against the levels of air entrainment levels are shown in Figures 6.4 and 6.5

Figure 6.2, shows the expansion data for all the 7 kg/m$^3$ $Na_2O_e$ mixes with different degrees of air entrainment. All the prisms have expanded vigorously due to the ASR. The total range of expansions recorded were from 0.206 % to 0.275 %. The sequence in which the various air entrainment level mixes occur with respect to the total expansion are more or less as might be expected with the maximum expansion developed in the lower air entrained concrete and the minimum expansion in the highest. All the expansion curves have a similar trend and appear to be levelling out towards the end of the testing period, suggesting little further expansion is likely to occur. The amount of ASR gel that could potentially be taken up by the air voids in a concrete mix is relatively small. Therefore, if a large amount of ASR occurs, these air voids will be quickly swamped with gel and 'normal' ASR expansion may commence. The amount of eventual expansion developed in the prisms should be roughly proportional to the volume of ASR gel available to induce the strain. Therefore, as the higher air entrainment mixes have taken up greater proportions of the ASR gel in the air voids, then these mixes should have generally lower levels of strain than seen in the lower air entrainment mixes. Examination of these expansion results show this idea to be correct.

Figure 6.3, shows the expansion data for all the 3.5 kg/m$^3$ $Na_2O_e$ mixes with different degrees of air entrainment. In this graph only the 1.7 % air entrainment

prisms would be considered to have experienced significant ASR (i.e 0.068 % and >0.05 % strain after 12 months). All the other prisms show expansion rates in the range 0.020 to 0.024 % and are ordered regardless of their air entrainment levels. Importantly, though the expansion results do not show significant ASR related expansion in the mixes of greater than 1.7 % AE, close inspection of the prisms revealed a few surface microcracks similar to those in borderline reactive mixes (section 3.8.1) on the 3.7 % and 6.6 % air entrainment prisms on surfaces other than those with demec measuring points.

Probably the most significant feature noted is seen on the expansion curve for the mix containing 1.7 % air entrainment. The expansion recorded with time continues in a similar manner / trend to that seen in the other mixes until month four. Here a change in the rate and amount of ASR expansion is observed, which does not occur in the other mixes. As this concrete contains the lowest level of air entrainment produced (1.7%) it would presumably be the concrete in which the voids would be most likely to totally fill with gel, in which case this would be the first and possibly the only 3.5 kg/m$^3$ $Na_2O_e$ mix in which significant ASR could occur. This change in the rate of expansion increase, may either represent the time at which all the voids were filled by ASR gel and therefore strain had to occur; or the time at which the take up of ASR gel / strain by the voidage is not sufficient to stop the development of ASR expansion throughout the concrete prism.

Figure 6.4 and 6.5, show the expansion data at 15 months for all the 3.5 and 7 kg/m$^3$ $Na_2O_e$ mixes respectively with the different degrees of air entrainment. The 3.5 kg/m$^3$ $Na_2O_e$ mixes (Figure 6.4) exhibit a distinct change in the trend of the plots in between the results of the 1.7 % and 3.7 % mixes. This observation is probably due to one of the factors discussed previously. The 7 kg/m$^3$ $Na_2O_e$ mixes (Figure 6.5) show no distinct trend alteration throughout the graph. The trend of the results show a gradual decrease in the recorded expansions with higher levels of air entrainment. The line trend may represent an increasing volume of the expansive gel being taken up by the progressively larger percentages of air voids in the cement paste. Clearly, the extreme ASR developed in these concrete mixes produce large volumes of gel. By extrapolation of the trend shown in the graph, it can be considered that an air entrainment level of between 30 and 35 % will be required to stop significant reaction (< 0.05 % strain) in 7 kg/m$^3$ $Na_2O_e$ mixes containing the Dry Rigg siltstone. This figure of air entrainment is unfeasible in a real concrete mix and also the likelihood of a real concrete containing an initial alkali level of 7

kg/m$^3$ $Na_2O_e$ very small. This observation is therefore, only used as a broad indicator of what maybe going on within these concretes with respect to the take up of ASR gel by the air voids.

Therefore, in summary the addition of the air entrainment agent (AEA) to the ASR reactive concretes reduced the degree of ASR expansion recorded. For the 3.5 kg/m$^3$ $Na_2O_e$ mix (borderline alkali threshold) an air entrainment level of 3.7 % caused a 72 % reduction in the recorded expansion compared with the 1.7 % mix. This reduction in the expansion of the 3.7 % and higher air entrainment mixes, means these mixes would no longer be classified as suffering from significant ASR. For the 7 kg/m$^3$ $Na_2O_e$ mix (high alkali) an air entrainment level of 8.0 % reduced the recorded expansion by 25 % compared to the 1.7 % AE mix. All the 7 kg/m$^3$ $Na_2O_e$ prisms regardless of AEL would however, still be classified as suffering from significant ASR.

## 6.4 Petrographical analysis

Petrographical analyses were carried out on two of the air entrained concretes to establish what affect the air entrainment was having on the ASR expansion developed. The first thin section was taken from a concrete containing 7 kg/m$^3$ $Na_2O_e$ which is well above this aggregates alkali threshold for significant ASR. This mix also had an air entrainment level of 2.3 %. The amount of expansion developed by this particular concrete prism after 15 months was 0.217 % (Sample No. DR37.06DA). The other thin section was taken from a concrete containing 3.5 kg/m$^3$ $Na_2O_e$ which is on the alkali threshold for significant expansion with this aggregate. This mix had an air entrainment level of 6.6 %. The amount of expansion developed by this particular concrete prism after 15 months was 0.024 % (Sample No. DR33.56DA).

### 6.4.1 7 kg/m$^3$ $Na_2O_e$ mix containing 2.3 % air entrainment

This concrete showed strong evidence of ASR developing throughout the slide originating in the DR siltstone coarse aggregate. The amount of microcracking and associated ASR gel was similar to that observed previously in the equivalent non air-entrained 7 kg mix examined in chapter 3. The ASR took the usual forms observed when studying this particular aggregate (i.e mainly pseudo-adhesion microcracks running with the cleavage and divergent microcrack systems, see

Figure 3.17). A lot of the paste microcracks were surrounded by a region of cement paste injected with ASR gel.

The cement paste was typical of most OPC and looked like all the non-saline immersed concrete samples previously studied in this research (Plate 6.1). The degree of carbonation associated with the original surface and paste microcracks was low. Though slightly higher than in a normal OPC mix, the number and volume of air voids seemed low. The majority of the 2.3 % total void volume appeared to be made up from a small number of larger (>1mm diameter) voids semi-spherical. The air voids were often, but not always totally filled with ASR gel (Plate 6.2). These gel filled voids were connected to cement paste microcracks from which gel could occasionally be seen to exude into the void space. A number of other voids showed a partial filling with ASR gel and these exhibit the now well documented gravity flow feature. These partially gel filled voids were usually connected to the cement paste microcrack network. Finally, there were a few voids empty of ASR gel, which contained small deposits of secondary portlandite and ettringite crystallisation (see section 6.4.2). In this concrete any ASR related paste microcracking that did not meet one of the limited number of air voids continued through the concrete, causing ASR expansion until it reached an outer prism surface.

It appears that the cement paste in the area immediately adjacent (< 20 $\mu$m) to the air voids has a raised capillary porosity and this area is often filled with ASR gel (i.e shows gel stained cement paste). The lack of a significant number of air voids however, means this increased capillary porosity of the cement paste surrounding the air voids is a localised effect and therefore, the take up of ASR gel by this increased porosity will not be particularly great. Though many of the air voids are totally filled with gel many are only partially filled or even empty. This is what might be expected as only voids actually intercepted by a ASR related microcrack would fill with gel if it migrates along microcracks rather than exudes through cement paste. The general lack of air voids means the associated surrounding higher capillary porosity paste was also limited and therefore, little gel could be taken up in this area by exudation of the gel through the cement paste. Therefore, in this concrete the strain and microcracking developed by the ASR gel will continue to occur. The air voids will reduce the ASR expansion developed but will not stop it.

In summary, though the air voids and surrounding high capillary porosity cement paste took up some of the ASR gel entering the cement paste via the microcracks, there was such a large volume of gel being produced in this concrete that the ASR

expansion developed could only be reduced slightly, not stopped.

### 6.4.2 3.5 kg/m$^3$ $Na_2O_e$ mix containing 6.6 % air entrainment

The amount of ASR microcracking and volume of associated gel developed by this concrete was vastly reduced in comparison to the 7 kg mix. However, the limited ASR that has developed was typical of that seen in other DR siltstone concretes. The cement paste was lighter in colour and this may indicate an overall higher capillary porosity, especially around the voids and microcracks. This increased capillary porosity was however, not considered to be significant to the suppression of ASR expansion in this concrete.

The most noticeably new feature displayed by this concrete was the large increase in the number of finer (<1mm diameter) air voids (Plate 6.3). The larger voids seen previously in the 7 kg mix were also still present in this concrete. Very few of the air voids of either size contained ASR gel, however, many contained a partial infill of secondary portlandite and ettringite, which suggests a moisture flowed through this concrete. Tracing the few ASR related microcracks across the concrete, it was apparent that many were lost or stop on entering groups or individual air voids (Plate 6.4). It was in these locations that limited amounts of ASR gel were observed within the voids. Much of the ASR gel found in these voids appeared to have been recrystallised to form an alkali-silica crystallised mineral. The loss of these few ASR-related microcracks into air void groups means little significant expansion due to ASR could develop. Therefore in concrete with a high air void content, any ASR related microcracks will usually meet air voids, where it will release its expansive gel so dissipating its strain and stopping the further development of the microcrack. In this manner the ASR gel is lost into the air void and the surrounding area of high capillary porosity paste. The petrographical examination of this concrete showed that most of the gel filled air voids also had a surrounding area of gel filled higher capillary porosity paste. In this manner the expansive gel will be further removed from the microcracks and in the process stop further expansion.

The secondary minerals portlandite and ettringite seen in many of the air voids have presumably been deposited during the percolation of water through the concrete (Plate 6.5). This assumption is confirmed as air voids with these mineral growths are found in areas / zones of the cement paste associated with the microcracks and higher capillary porosity cement paste, evidence for which is given by the pastes deeper impregnation with the fluorescent resin in those particular

areas (Plate 6.3). In the other areas of cement paste not containing microcracks or fluorescent resin, the air voids are totally empty (see parts of Plate 6.4). In the whole slide only a single ASR related microcrack actually reaches the original surface of the prism. In this crack the ASR gel and the surrounding cement paste are heavily carbonated, indicating heavy penetration by air / water down the crack. Finally, a couple of problems that may develop with the infilling of the voids with secondary mineralisation as observed above, are that first the beneficial affects of air entrainment in freeze / thaw resistance could be lost and secondly a later age ASR induced by external alkalis such as de-icing salts (Chapter 4) could cause significant long term expansion.

In summary, the limited ASR microcracking developed by this concrete was arrested when the individual microcracks entered the numerous air voids, so dissipating gel and strain. The low potential reactivity of this mix and high air void content suggest little chance of significant ASR expansion developing. The proposed take up of some extra ASR gel by the raised capillary porosity area surrounding the air voids still appears to be a likely occurrence; however, the main factor in reducing the ASR in this concrete and any other AE concrete appears to be the interception of the ASR related microcracks with air voids and therefore the dissipation of the gel / strain into them.

### 6.4.3 Petrography conclusions

From the petrographical examinations, it appears:

1. Air entrainment will stop or reduce ASR, not by completely filling all the voids with the expansive gel, but by dissipating the strain into specific voids.

2. Once there, the gel then losses its potential to create further ASR microcracking by taking up $Ca(OH)_2$ from the cement paste (see chapters 4 and 7).

3. Only air voids actually encountered by the ASR related microcracking contain any ASR gel.

4. In the highly reactive 7 kg mix the volume of ASR gel was too great and the number of air voids too small to have a significant effect on the expansion developed. In the borderline reactive 3.5 kg mix the volume of gel was so low and the number of voids so high that significant ASR microcracks could not develop

except at a few locations.

5. In the same manner as air entrainment suppresses the effects of frost by allowing the growth / strain induced by ice crystals to dissipate into the spheres, so the migration of the gel into these spheres dissipates a large amount of the gel strain.

Factors affecting the ASR expansion in an air-entrained concrete:

| | |
|---|---|
| 1. Volume of ASR gel | ] Due to ASR |
| 2. Rate of gel formation / microcrack development | ] |
| 3. Air void content | } |
| 4. Size of air voids | } |
| 5. Capillary porosity of cement paste | }Due to mix design |
| 6. Spacing factor | } |

## 6.5 Expansion result for prisms left in external exposure conditions

Figures 6.6 and 6.7, show the results at the completion time for this research of equivalent air entrained concrete prisms left in external exposure conditions. During this period the prisms have experienced only one moderately severe winter (see months 10 to 14) and therefore the air entrainment is still considered to be fully functional as to date no significant ASR has been detected in these prisms. The occurrence of significant ASR in the higher alkali prisms should have started after around 14 to 18 months if the 1: 7 time ratio of 38°C testing to external exposure testing proposed by Hobbs (1992b) is to be regarded as accurate. With this in mind the expansion testing of these prisms will be continued and be reported on at a later date. As of July 1993, 17 months after the beginning of testing all the concrete prisms appeared to be sound uncracked and unaffected by ASR and unaffected by the previous winter frosts.

## 6.6 Discussion

The test results of work carried out at the British Cement Association show that in a series of concretes containing opaline silica as the reactive aggregate at various levels of air entrainment, the air entrainment reduces the expansion developed but did not prevent deleterious expansion from occurring. In this work Hobbs (1988) has suggested that the changes seen in the form of the expansion curves at a

specific age could represent a point when the air voids in these concretes become filled by ASR gel. A similar feature is observed for the 3.5 kg mixes expansion-versus time trends in this work. Hobbs felt that if this is occurring then the freeze / thaw resistance of the concretes will be also reduced as stated by Jensen et al. (1984).

In the 7 kg/m$^3$ $Na_2O_e$ mixes the amount of ASR gel developed was, as expected, far larger than that seen for the equivalent 3.5 kg/m$^3$ $Na_2O_e$ mixes. With the 7 kg/m$^3$ $Na_2O_e$ mixes in this work the amount of ASR gel / expansion available is probably far too high for significant absorption of ASR gel into the cement paste air voids to have any great effect on the recorded expansion. However, there were differences recorded and these may represent the filling up of the differing degrees of air entrainment with ASR gel. In the highly reactive 7 kg/m$^3$ $Na_2O_e$ prisms most of the ASR gel should be found in the air voids and the amount of recorded expansion in each mix should therefore be roughly inversely proportional to the total volume of air voids. However, in general the 7 kg/m$^3$ $Na_2O_e$ mixes were far too reactive to be significantly affected by the air entrainment. The degree of strain developed by the 3.5 kg/m$^3$ $Na_2O_e$ mixes was affected by air entrainment levels of greater than 1.7 %. The close proximity of this mix's initial alkali content to that aggregates initial alkali threshold for significant expansion, means that an increased volume of ASR gel would be required to cause significant ASR expansion.

Unfortunately, this might easily be accomplished in a field structure by the addition of alkalis from an external source such as deicing salt. This would raise the reactivity level of that mix (section 4.3.1), thus the gel would fill more of the air voids and ASR would commence at a higher level of air entrainment. Therefore if ASR is to be avoided with this concrete in a saline environment the air entrainment levels should be raised. The air entrainment may lower the recorded expansion in rough proportion to the air void content of a particular mix.

The air entrainment of a reactive concrete mix will suppress some of the ASR expansion in most cases dependent on the level of air entrainment and the degree of reactivity, however, the reason for this are still questionable. The results in this research show that increased air entrainment reduces the expansive affects of ASR. This appears to be caused by the partial filling up of some of the air voids in the various concrete mixes with the ASR gel. To fill the air voids the ASR gel has to get in there in the first place and this is accomplished by either migration of the gel through microcracks, themselves caused by ASR or exudation of the gel through

the cement paste. Clearly, based on the petrographical examination, the fact that all air voids filled with gel are connected to a paste microcrack and that little of the paste shows evidence of gel exudation, it seems probable that the method of filling the voids with gel is by migration through the paste microcracks. Therefore the ASR is dissipated by a loss of gel / strain into specific voids rather than a complete filling of the whole concrete voidage with ASR gel. It is the formation of the fine cracks by ASR that is recorded as the limited strain, approximately 0.02 % after 15 months seen in the expansion results of all the 'non-reacted' concretes.

The occurrence of a high air void content in a concrete will result in the localised dissipation of gel induced strain into the specific voids. This will lower the recorded expansions in proportion to the number of localised releases of ASR gel, (air voids) from microcracks developing at specific reactive particles and migrating out into the cement paste. Therefore the resultant concrete should contain evidence of reacting particles with microcracks stopping / dissipating at the first void or voids they encounter, in which a deposit of gel should also be seen. Many of the air voids will however, be empty and have no significant effect on reducing the reactivity / expansion of a specific mix. The higher the air entrainment of a mix the greater the number of ASR related microcrack encounters with air voids and therefore the greater the reduction measured in the recorded strain. This indicates that the critical factor is the 'spacing factor' or size distribution of the air voids, which incidentally was also what determines the freeze / thaw resistance.

It was observed in the petrographical examination that the cement paste in the area surrounding each air voids had a higher water / cement ratio than the rest of the paste and therefore had a locally raised capillary porosity. Therefore, if the mix has a high air entrainment level, there is an increased air void content and associated increase in the porosity of the cement paste. A rise in the porosity of a cement paste improves the rate of ASR gel exudation into the paste surrounding the air voids and therefore indirectly also reduces the amount of strain induced by the reaction. If this theory is correct it would result in an increase in cement paste staining with the ASR gel and localised injections of the ASR gel into the air voids. The petrographical examination, however, only showed a localised impregnation of the cement paste surrounding the air voids and therefore it is unlike that the take up of expansive ASR gel by the cement paste is the major reason for the depleted strain induced in these air-entrained reactive concretes.

Most present day UK concrete pavements are air entrained. As the vast majority of

ASR reactive aggregates used in the UK do not react at particularly low initial alkali levels (usually >5.0 kg/m$^3$ $Na_2O_e$) and generally concrete pavements contain moderate cement contents, the initiation of ASR is relatively unlikely. If a limited case of ASR was to develop in a concrete pavement, then the 4 % to 5 % air entrainment presently placed in most UK pavements should absorb this ASR gel without any obvious deleterious effects to the concrete. However, the use of some of the more reactive aggregates discussed in chapter 3 and heavy winter salting of air entrained concrete pavements containing these materials may initiate a reduced, but still significant deleterious level of ASR.

The effect that the partial filling the air voids with ASR gel seen in this work has on the freeze / thaw resistance of the concrete, has not been studied in this work. However, it seems highly probable that the removal of the voids, by filling them with ASR gel or even secondary portlandite and ettringite as seen petrographically will reduce the voidage of the upper concrete area into which the ice crystals formed during cold weather can grow. This will clearly therefore remove some of the benefit of the air entrainment to the concrete with regard to its freeze / thaw resistance. In all the concretes studied here the ASR was felt to have stopped as a result of leaching of the alkalis into the surrounding distilled water.

Further work with air entrained mixes containing the higher reactivity aggregates , when placed in a saline environment should be of interest in covering an area of potential problem with respect to the continuing avoidance of ASR in concrete pavements exposed to winter deicing salts.

## 6.7 Conclusions

1. The addition of air entrainment reduced the expansion developed due to ASR. The closer the mix was to the alkali threshold for significant reaction the greater was reducing effect of air entrainment.

2. In the highly reactive 7 kg mixes the amount of ASR gel totally swamped the relatively low level of air entrainment and therefore the expansion induced was only slightly reduced by an amount proportional to the total air entrainment level of the concrete. An air entrainment level of 8.0 % reduced the recorded expansion by 25 % compared to the 1.7 % AE mix. To remove the effects of significant ASR expansion from this 7 kg mix an unrealistically high air-entrainment level of between 30 to 35 % would be required.

3. In the borderline reactive 3.5 kg concrete all levels of air entrainment above 1.7 % effectively prevented significant expansion due to ASR. With the 1.7 % AE concrete the trend of the expansion verses time graph showed a distinct positive change from the other mixes after four months and it is considered this may represent the time at which the production of gel / strain became too great to be all taken up by the air voids with the result that an increased rate of expansion developed. The air entrainment level of 3.7 % caused a 72 % reduction in the recorded expansion compared with the 1.7 % mix.

4. The petrographical examination showed the 7 kg mix to contain relatively few voids; however, many of these were full or partially filled with ASR gel. All the gel-filled voids were connected to ASR related microcracks and there was little evidence for the exudation of significant quantities of ASR gel into the voids via the cement paste. The ASR in this concrete was considerable.

5. The petrographical examination showed the 3.5 kg mix contained numerous voids few of which contained ASR gel. Those that did contain gel were connected to the ASR related microcracks present and the gel was usually recrystallised. The other voids were frequently totally empty or contained secondary portlandite and ettringite mineralisation, due to water percolation. The ASR in this concrete was very limited and would not be considered significant.

# CHAPTER 7

## Analysis by electron microprobe (EMP) of the alkali-silica gels formed by various aggregates and environmental conditions

### 7.1 Introduction

Since the alkali-silica reaction was first established as a problem in the early 1940's, numerous chemical analyses have been carried out on the expansive gel product. An interaction between the alkalis in a concrete's pore solution and reactive silica in some aggregates produces a hygroscopic alkali-silica gel which swells on the absorption of water from the environment causing expansion in the concrete. These gels vary considerably in composition, depending on the composition of the initial alkali pore fluids, themselves usually solely dependent on the cement alkali content and probably on the nature of the particular form of reactive silica, temperature and concentration of reactants (Poole, 1992b).

The work described was initially carried out on four different reactive aggregate concretes, in which all the other variables are constant. In these circumstances it was therefore felt, it may be possible to establish whether any compositional differences occur in the ASR gel formed by using different reactive aggregates. The main objective of this work, however, was to establish whether the immersion of concretes containing reactive aggregates in salt solution affects the composition of the ASR gels developed. Some explanation of the occurrence of the 'initial alkali pessimum' developed by these concretes was also required. The EMP analysis of these ASR-affected concretes was intended to establish whether the composition of the cement pastes in the various test environments was altered.

Previous study of ASR gel compositions has shown that when they were first exposed to air by breaking open a concrete the gels were transparent and resinous in appearance with viscosity between that of motor oil and resin. This type of gel would be able to flow along microcracks and enter cement paste air voids as is frequently seen. However, when left open to the air these gels rapidly carbonate and harden to a white desiccated powdery material often exhibiting shrinkage cracking. Therefore in any detailed compositional analyses of the ASR gels, care must always be taken to avoid the excessive carbonation. Earlier analyses of ASR gel has shown a wide range of potential compositions (Poole, 1992a) though basically they are made up of varying proportions of Na, K, Si, Ca, Mg and $H_2O$,

though of course the latter can not be detected in EMP analysis. It has become fairly well established that the chemical variations developed by ASR gels and the effect that these have on the expansions developed are more complex than initially thought. A compositional variation between high alkali gels located in the reactive aggregate and 'harder' more calcic material found in the cement paste has been frequently observed (Verbeck and Gramlich, 1955). However, the effect this and other compositional variations in the gel have on the degree of reactivity has still to be established.

## 7.2 Experimental method

The ASR gel analyses discussed here were carried out using a Jeol JXA-8600 Superprobe (Electron microprobe). The use of this electron microprobe allows for the accurate analysis of an area of down 5 $\mu$m diameter. This allows the fine edge deposits and thin crack gels found within aggregate particles to be analysed accurately. For the EMP analysis to be carried out the first requirement is a normal petrographical thin section of about 35$\mu$m, which at this stage is slightly thicker than those used in petrography. This thin section is then polished using diamond powders of progressively decreasing size, down to a final fine polish with 0.25 $\mu$m powder to a completed slide thickness of 30 $\mu$m. The completed polished sections were left in a desiccator when not being analysed to keep paste and ASR gel carbonation to a minimum.

The polished section was analysed initially by manual controls at which point some analyses were carried to confirm that the materials being analysed were real ASR gels. Each suspected ASR gel site was initially examined with a polarising microscope built into the EMP device to confirm that it was a gel site and not some other constituent being analysed. A quick check was also made to confirm the point at which the analysing electron beam was actually hitting the sample. These simple checks were useful for confirming the accuracy of the gel analyses produced (Appendix 7). Once each site had been established petrographically as ASR gel, a large number were programmed into a computer together which ran the EMP analyses automatically.

Care was needed in making a correct interpretation of the results obtained. The EMP requires the samples to be fully desiccated. Also many ASR gel specimens are partially carbonated by exposure to air before analysis. Finally, with modern computer-corrected microanalyses, as used here, the results obtained are also

normalised to 100 % for the elements determined with those elements below atomic number 11 such as carbon and lithium not being detected.

## 7.3 Results of electron microprobe analyses of concretes containing different reactive aggregates

The complete list of the EMP analyses used in this work is shown in appendix 7. The compositional analyses shown in the figures are triangular plots of three constituent elements ratioed against each other (ternary phase diagrams) these were used as they were felt to be a good method of observing distinct changes in the composition of the ASR gels derived from microcracks / voids in the cement paste and also ASR gels derived from within the reactive and non-reactive aggregate particles. The dominant constituents of the ASR gels were usually $SiO_2$, CaO, $Na_2O$ and $K_2O$ and therefore suitable plots including these are shown in most diagrams concerning the distilled water immersed environmental mixes described in this section.

### 7.3.1 Dry Rigg siltstone concrete immersed in distilled water

The concrete analysed here, contained the Dry Rigg siltstone coarse aggregate, had an initial alkali content of 7 kg/m$^3$ $Na_2O_e$ and was wrapped in damp cloth and triple bagged for the duration of its expansion testing (see chapter 3). The expansion recorded at 12 months was 0.304 % (Sample No. DR17.0B).

Figure 7.1, shows the analyses of ASR gels that are located in the reactive siltstone coarse aggregate (CA). The combined sodium and potassium contents have been enhanced ten times in all the graphs studied. This is done to visually pull the plotted gel compositions away from one edge of the ternary diagrams. Even the gels from specific locations clearly have a fairly diverse range of compositions. Removing the few spurious points as possible errors in the interpretation of the source gel area, there remains a major grouping of gel compositions. The majority of plotted points lie close on the $SiO_2$ to $(Na_2O+ K_2O)*10$ line suggesting the gels found in the coarse aggregate are dominantly silica and alkali rich with a little calcium also present. The majority of gels fall in the range; $SiO_2$ = 25 - 90 %, $(Na_2O+ K_2O)$ = 4 - 6 % and CaO = < 35 %. The observed medium to high CaO concentration seen in some analyses may represent carbonated paste or gels in the vicinity of the aggregate to cement paste interface. In conclusion the coarse aggregate gels are dominantly silica rich, alkali rich, calcium poor materials. As with all the following

chemical analyses no interpretation can be made on the amounts of water in each gel and therefore the expansivity potential of the product.

Figure 7.2, shows the equivalent plot for the ASR gels found in the cement paste microcracks (CP). Clearly, there are again a few spurious results, but the majority show an increased CaO content to the detriment of mainly silica, but also the alkali content. These gels are therefore, dominantly calcium rich and alkali poor. This increased CaO content of cement paste ASR gels (CP) has been noted previously (Chatterji et al. 1986, Diamond et al. 1981, Laing et al. 1992 etc.) and been attributed to the uptake of $Ca(OH)_2$ from the paste by the gel so reducing its fluidity (Verbeck and Gramlich,1955). However, a correlation between this reduced fluidity as demonstrated synthetically by Diamond et al. (1981) and any internal swelling developed was never found. Buck and Mather (1978) have shown that $Ca(OH)_2$ was depleted from the areas of cement paste surrounding the microcracks containing the CaO enriched ASR gel. These findings all indicate that CaO enrichment of the gels was not the only factor affecting their swelling behaviour. Interestingly, there is a fairly distinct overlap observed between the two different gel suites, (CA and CP) which suggests a complete transgression of compositions, unlike the phase separation postulated by Laing et al. (1992). Laing states that once a critical level of calcium is exceeded a phase change appears to occur. The existence of a phase boundary in CP gels unlike those plotted above has been supported by Macphee et al. (1989). Macphee suggests an incomplete range of solid solubilities between (CA) gels and (CP) gels exists. Examination of some of the other gel analyses graphs shown in this work however, does indicate the occurrence of a phase boundary as postulated (Laing et al. 1992).

Figure 7.3, shows the ternary diagram plots for the same ASR gels with the compositional end members being $SiO_2$, $Al_2O_3$*10 and Cl*100. The lack of any detected chloride in many of the gels means the total number of point plotted is significantly reduced. The main reason for the inclusion of this data is for comparison with the salt solution immersed concretes discussed later. The graph does show a slight take up $Al_2O_3$ in the gels recorded particularly in those derived from the cement paste. The high $C_3A$ content in this cement paste and the apparent slight take up of such materials by the gels appears to give some broad indication of the cement paste composition through which the gels have passed. This will be of greatest benefit in the direct comparison of the two concretes immersed in salt solution (see section 7.4). No significant chloride was detected in the gels and this is in line with what would be expected of a concrete placed in distilled water.

As a confirmation of previous petrography, analyses of cement pastes from adjacent to the ASR gel filled paste microcracks compared with pastes well away from the microcracks (see appendix 7) showed a depletion in CaO associated with portlandite loss and a slight alkali increase caused by the take up of some ASR gel into the area of cement paste next to the microcracks which appears to have increased capillary porosity based on petrographic evidence, see section 4.5.2 (plots of these cement pastes are not shown).

### 7.3.2 Analyses of other ASR reactive aggregate concretes immersed in distilled water

The two concretes analyses described here contained the Horrocksford limestone and Anglesey granite coarse aggregate and both had initial alkali contents of 7 kg/m$^3$ $Na_2O_e$. Both expansion test prisms were wrapped in damp cloth and triple bagged for the duration of expansion testing (see chapter 3). The expansions recorded at 12 months were 0.189 % and 0.179 % for the Horrocksford and Anglesey aggregates respectively (Sample No. HL17.0A and AG17.0A). The equivalent concrete containing the Maentwrog greywacke was also initially included in this study. However, as has been observed previously in chapter 3, not a great deal of ASR gel was detected using this aggregate and therefore the few results obtained are not included here.

### 7.3.3 Horrocksford limestone concrete immersed in distilled water

Figure 7.4, shows the chemical composition of gels from the within the coarse aggregate (CA) and the cement paste (CP) and a number of aggregate analyses (A). Taken together the gel points show a trend from a high silica / alkali gel to virtually pure CaO. The majority of coarse aggregate gels (CA) are high silica / alkali compositions, even in this silicified limestone. Whereas the paste gels (CP) are dominantly CaO and $SiO_2$ with a little alkali also present. The aggregate analyses are dominated by CaO as might be expected, but the chert material ($SiO_2$) present in the rock is also clearly detected in the overall results. The overall gel compositions from the various locations (CA and CP) are very similar to those seen with the Dry Rigg siltstone (Figure 7.1 and 7.2).

Figure 7.5, shows the equivalent graph with $SiO_2$, $Al_2O_3$*10 and Cl*100 as end members. Analyses of typical cement paste (PU) are also shown on the plot. The

cement paste analyses are typified by a low Cl content, and medium $Al_2O_3$ content and a high $SiO_2$ content. This is as might be expected from from the high $C_3A$ content white cement used in all these concretes (see Table 2.1). It is worth noting the compositional position of these cement pastes compared to those studied later. The ASR gels all appear to take up some $Al_2O_3$ especially the CA gels which is rather surprising, but it may represent a constituent element in the limestone i.e clay minerals rather than material taken from the cement paste. The CP gels contain Cl and $Al_2O_3$ contents more or less equivalent to the cement paste itself.

### 7.3.4 Anglesey granite concretes immersed in distilled water

Figure 7.6, shows the chemical composition of ASR gels from within the coarse aggregate particles (CA) and the cement paste (CP) of concrete containing Anglesey granite. Points representing the coarse aggregate (A) and cement paste (PU) analyses are also recorded. The plotted points show that the CA gels have a composition not greatly different from many of the coarse aggregate analyses (A), these being high in $SiO_2$, medium alkali and generally low in CaO content. The paste gels (CP) however, again show an enrichment in CaO, associated mainly with a loss in alkali. The cement paste analyses show a composition not greatly different from the cement paste gels (CP). The aggregate analyses are quite widely spread and represent analyses points on the different minerals that made up the granite,i.e (quartz = silica, feldspars = (calcium / potassium / sodium) alumino-silicates, micas = layered alkali alumino-silicates and calcite veining = calcium)

Figure 7.7, shows the equivalent ASR gels, aggregate and cement paste, plotted against different compositional end members. These components were $SiO_2$, $Al_2O_3$*10, Cl*100. The results are rather inconclusive and are specifically for comparison with the samples immersed in salt solution. However, a consistent but low level of enrichment of the cement paste and the cement paste gels with Cl at the expense of $SiO_2$ and $Al_2O_3$ is noted. The CA gels and aggregate analysis remain just off the $Al_2O_3$ to $SiO_2$ line and therefore do contain a little Cl. The source of this chloride is unknown.

### 7.3.5 Summary

When comparing the gel compositions obtained for the various aggregate mixes, it is apparent that the location of the gel in the concrete is of far greater importance to the overall composition trend than the original reactive aggregate type. In each

concrete the gel located in the coarse aggregate (CA) was dominantly high silica, medium alkali and medium / low calcium content. Whereas the gels found in the cement paste (CP) were dominantly high calcium, medium silica and low alkali content.

On the $SiO_2$: $Al_2O_3$: Cl ternary diagrams the cement pastes and (CP) gels of all these concretes immersed in distilled water, showed little enrichment in chloride and were mainly found in compositional range, $Al_2O_3$ = 1 to 6 % and $SiO_2$ = 10 to 32 % and this is where they should be expected to plot, based on their initial bulk chemistry (see section 2.1.1). A specific EMP analysis may land on particular cement paste phase mineral ($C_3S$, $C_2S$, $C_3A$) and this will determine the absolute extremes that may expected in these point analyses. More detailed analyses ( not shown) of the cement pastes in this work confirmed these observations.

## 7.4 Electron microprobe (EMP) analysis of concretes immersed in salt solution

The work described in chapter 4, established that ASR could be accentuated in 7 kg initial alkali mixes by immersion in salt solution. It also showed that when a potentially non-reactive 3 kg alkali mix containing the Dry Rigg siltstone was immersed in salt solution, significant ASR developed. Somewhat surprisingly however, the expansion and reaction developed in the 3 kg mix was significantly greater than that developed in the 7 kg mix. The earlier chemical and petrographical analysis of the two concretes has established possible reasons for the extent of ASR developed (see chapter 4). With these results in mind and the observation made earlier in section 7.3 with regard to the composition of the various ASR gels developed, it was considered of interest to establish compositionally, what types of gel were causing the different degrees of reaction / expansion recorded and also to establish whether the alterations to the cement paste discussed in section 4.5.2.1, were actually occurring. Was the composition of the gels developed important in establishing why the extra ASR induced expansion occurred in the 3 kg mix ?

Therefore with these questions in mind, once the expansion testing, chemical and petrographical analysis of the concretes in question were complete, a full EMP analysis of the ASR gels developed was carried out, the results of which are discussed below.

### 7.4.1 Dry Rigg siltstone concrete with 7 kg of alkali

The concrete prism used in this analysis was immersed for 15 months in salt solution (2 mol NaCl / litre). The total expansion developed was 0.366 % (Sample No. DR27.0B).

#### 7.4.1.1 $SiO_2$ : ($Na_2O+K_2O$) : CaO ternary diagram

Figures 7.8 and 7.9, show ternary diagrams of the gel compositions with $SiO_2$, ($Na_2O+K_2O$)*10, CaO as the end members. These graphs show the development of two distinct groups of gel compositions. The first graph (figure 7.8) is composed entirely of coarse aggregate located gels (CA) and these were all lower calcium (<17 %) materials with high silica (30-75 %) and alkali (<10 %) contents. The silica to alkali ratio is also seen to be quite variable. It seemed that the majority of these gels contain only a small, but significant amount of calcium, leaving the area of typical gel compositions just off the $SiO_2$ to ($Na_2O+K_2O$)*10 line.

In the second graph (Figure 7.9) all the CP gel compositions are plotted, these show a general migration of the gel compositions. Beginning with high alkali / silica and low calcium gels, located in the approximate area where most of the CA gels from the concretes immersed in distilled water (Figure 7.1 to 7.7) were found. The gel compositional trend is initially seen to migrate towards the silica end member, indicating initial silica enrichment and alkali depletion. At a point approximately half along the alkali to silica axis (which does not represent a 50: 50 compositional ratio) the trend changes and the compositions head towards the CaO end member away from the alkali to silica axis, indicating a depletion in silica and alkali, with enrichment in calcium. The end gel composition of this migration has a very low alkali, medium silica and medium calcium content, i.e compositionally very like cement paste, CSH gel. There is a suggestion of a compositional gap / phase boundary in the gels between the CaO rich end and the rest. Overall, though the two gel suites (CA and CP) overlap to some degree they are quite distinct in compositional range.

In general the forms that the gel composition ternary diagrams displayed here, are broadly equivalent to those observed in the equivalent concrete mix immersed in distilled water (see section 7.3.1). The CA gels are all of low calcium and high silica / alkali composition, whilst, the CP gels are usually of high calcium, medium silica and low alkali content, though a significant group of gels of low calcium and high

silica / alkali composition were also detected; the significance of these is discussed later.

#### 7.4.1.2 $SiO_2$ : $Al_2O_3$ : Cl ternary diagram

Figure 7.10, shows a ternary diagram of the same ASR gels along with a number of cement paste (PU) and aggregate (A) analyses with different compositional end members. In this diagram three distinct regions of compositional plots can be observed. First, in the area adjacent to the $SiO_2$ end member a region of analyses dominantly made up of CA gel compositional plots can be seen. A few CA plots can also be observed running along the $SiO_2$ : $Al_2O_3$ line indicating that little or no chloride is present in those gels. Therefore in general the CA gels are $SiO_2$ rich, with no significant Cl and occasionally some $Al_2O_3$ detected.

The second area representing the CP gels covers a large part of the diagram and represents $Al_2O_3$ enriched gels, with lower amounts of $SiO_2$ and some variable but, significant take up of chloride. Finally a few points representing typical cement paste analyses (PU), show a high chloride take up, a lower $Al_2O_3$ content than the ASR gels and a reduced silica content, all of which appears to be typical of the high $C_3A$ cement used in this concrete, see section 7.3. A linear traverse of compositional points can be made from the CA (silica rich) gels to the CP (alumina and chloride enriched) gels to the final cement paste analyses (lower alumina, further enrichment in chloride). In the reaction occurring in this concrete, ASR gels which begin (CA) as silica-rich materials, on entering the cement paste they take up alumina and chlorides (CP), so compositionally they are heading towards the cement pastes (PU) which are even more chloride and alumina rich.

#### 7.4.1.3 $SO_3$ : $Al_2O_3$ : Cl ternary diagram

Finally Figure 7.11, shows a ternary diagram for the cement paste ASR gels (CP) along with a number of cement paste (PU) and ettringite (ETT) analyses with different compositional end members. The removal of silica from the compositional ternary diagram allows variations detected in the other lower percentage constituents to be more clearly emphasised. In this graph there is a strong bias of the cement paste analyses and CP gels towards the alumina end member. A few CP gels are also observed that show a strong chloride content and though these are not very numerous they should still be considered significant. Though not plotted here the equivalent CA gels were also clearly alumina rich, chloride poor,

see Figure 7.10.

A relationship has often been observed between the ASR and ettringite formation at higher temperatures / late stage and this may suggest a connection exists between $SO_3$ content and the ASR reactivity of a concrete (Herr, 1992). Unfortunately none of the areas in this slide analysed as possible sulphate minerals turned out to be real ettringite as appears on the equivalent graph for the 3 kg mix (Figure 7.16). Therefore in general, the cement paste (PU) and ASR gel located within microcracks in the cement paste (CP) are mainly high alumina and low chloride content materials, though a few high chloride content ASR gels were also recorded.

### 7.4.2 Dry Rigg siltstone concrete with 3 kg of alkali

The concrete prism used in this analysis was immersed for 15 months in salt solution (2 mol NaCl / litre). The total expansion developed was 0.394 % (Sample No. DR23.0A).

#### 7.4.2.1 $SiO_2$ : ($Na_2O$+$K_2O$) : CaO ternary diagram

Figures 7.12 and 7.13, show ternary diagrams of the gel compositions with $SiO_2$, ($Na_2O$+$K_2O$)*10 and CaO as the end members. The trends of compositional plots for gels in this concrete are distinctly different from any observed previously. Two regions of gel compositions are clearly present; however, the plots of CA gel suite (Figure 7.12) and CP gel suite (Figure 7.13) occur in both compositional areas.

More specifically the area of CA gels plot in regions of slightly lower alkali content than the CP gels, which in general are more alkali enriched than observed in any of the CP gels studied previously. The two areas of ASR gel compositional plots are distinctly separate and presumably therefore have a phase separation present between them dependent on the calcium content (Laing et al. 1992). In general therefore, the CA gels are compositionally more inclined towards the $SiO_2$ end member, whereas the CP gels are more inclined towards the alkali end member. The compositional areas show medium and low calcium contents and do not compositionally behave like the gels analysed previously. There is overall a lack of calcium enriched gels in the 3 kg concrete.

### 7.4.2.2 $SiO_2$ : $Al_2O_3$ : Cl ternary diagram

Figure 7.14, shows a ternary diagram plot of the same ASR gels along with a number of cement paste (PU) and aggregate (A) analyses with different compositional end members. As this figure is comparable with that described in section 7.4.1.2 (Figure 7.10) clearly significant differences have occurred. The first most noticeable observation is the large depletion of alumina in all the samples in comparison with the 7 kg mix discussed previously. The CA gels have a reduced silica content, a more or less equivalent or slightly reduced alumina content and a large increase in chloride uptake. The CP gels are all largely confined to an area near the silica : chloride line indicating a massive loss of alumina compared with the 7 kg mix. The plots for the cement paste (PU) are more or less equivalent to those developed in the 7 kg mix with a high uptake of chlorides, low silica and medium low alumina contents. Figure 7.15, demonstrates the same graph with the alumina contents enhanced by fifty times and shows more clearly a traverse from CA gels, (low alumina, medium chloride, and medium silica) to CP gels (very low alumina, high chloride and high to low silica). The main observation in the 3 kg mix therefore is the large depletion in alumina content, most especially in the CP gels.

In these concretes the ASR gels therefore begin (CA) as medium silica and chloride, alumina poor materials, on entering the cement paste they become more depleted in alumina and slightly more enriched in chlorides and silica (CP), so compositionally they are heading away from the cement paste (PU) and alumina end member towards the silica : chloride line indicating chloride and silica enrichment.

### 7.4.2.3 $SO_3$ : $Al_2O_3$ : Cl ternary diagram

Figure 7.16, shows a ternary diagram for the cement paste gels (CP) along with a number of cement pastes (PU) and ettringite (ETT) analyses with different compositional end members. The main observation made here is the migration of the CP gel plots away from the alumina end member, as also seen in Figure 7.14 towards chloride enrichment (i.e the opposite of the 7 kg mix). The chloride content has increased at the expense of alumina. The cement paste (PU) analyses plot further away from the chloride end member and therefore are compositionally not greatly different from the cement pastes examined in the equivalent 7 kg mix immersed in salt solution. In general therefore the CP gels here are enriched in

chloride and depleted in alumina. Two analyses of ettringite are also shown, with a preponderance of $SO_3$ and alumina with only a little chloride detected; however, no relationship with the ASR gel or cement paste analyses could be detected.

### 7.4.3 Comparison of the two concretes immersed in salt solution

Figure 7.17, gives a summary of the compositional differences between the two siltstone concretes when immersed in salt solution. In the $SiO_2$ : $(Na_2O+K_2O)$ : CaO ternary diagrams, the 7 kg mix behaves in a similar manner to that observed for the equivalent mix immersed in distilled water. The CA gels are generally silica and alkali rich, calcium poor, whilst the CP gels have a more varied range of compositions, initially being a typical CA gel composition (when immersed in distilled water), then migrating towards more silica rich gels and eventually developing calcium rich gels with an associated depletion in alkali. This observation of calcium enrichment in the CP gels has been made previously and is thought to represent $Ca(OH)_2$ take up by the gels once in the cement paste. This causes an increased viscosity and presumably therefore the end of further expansion within that gel. It is considered that the rapid production of the CA alkali rich calcium poor gels is a major factor causing the development of ASR expansion and concrete microcracking originating in the coarse aggregate particles.

The 3 kg mix shows the development of two distinct gel compositional areas. These two areas do not relate to the CA and CP gels specifically, but are made up of both gel suites. No distinct calcium enrichment of the CP gels is observed. The main feature noted is a slight compositional shift of the CP gels towards the alkali end member in comparison to the CA gels, (i.e on average the CP gels contain more alkali). An examination of the two $SiO_2$ : $Al_2O_3$ : Cl ternary diagrams, shows distinct differences between the two concretes. These are summarised in Table 7.1.

In the 7 kg mix, the CA gels are dominantly silica rich, with a few containing some alumina and no chloride. The CP gels are enriched in alumina and slightly with chloride at the expense of silica, whilst the cement paste itself is further depleted in silica. The ASR gel compositions migrate away from silica towards alumina and chloride (i.e towards the cement paste composition). In the 3 kg mix there is an overall chloride take up by the gels and a very large depletion in alumina in comparison to the 7 kg mix. The cement paste analyses are similar to that observed for the 7 kg mix. The CP gels are slightly more depleted in alumina and more enriched in chloride than the CA gels. The ASR gel compositions migrate away

from alumina composition towards silica and chloride enrichment (i.e away from cement paste composition).

TABLE 7.1: ASR Gel compositional variation between the two DR siltstone mixes immersed in salt solution.

7 kg mix

| CA gel | -------- | CP gel | ------ | Cement paste (PU) |
|---|---|---|---|---|
| Silica rich, Cl poor | | Silica depletion, Al enriched | | Chloride enrichment |
| (Si - H, Al - L+M, Cl - L) | | (Si - M, Al - M, Cl - M) | | (Si - L, Al - L, Cl - H) |

3 kg mix

| CA gel | -------- | CP gel | -------- | Cement paste (PU) |
|---|---|---|---|---|
| Silica, chloride rich | | Alumina depleted | | Chloride enrichment |
| (Si - M, Al - L, Cl - M) | | (Si - M+H, Al - VL, Cl - M+H) | | (Si - L, Al - L, Cl - H) |

N.B Scaling of very low, (VL) low, (L) medium, (M) and high (H) are based purely on what is shown on these graphs, actual percentage values are not discussed here.

Finally, with the $SO_3$ : $Al_2O_3$ : Cl ternary diagrams the CP gels in the two mixes were shown to be compositionally distinct. The CP gel in the 7 kg mix was rich in alumina, whereas the 3 kg mix CP gel was rich in chloride. The CA gels in each mix show similar features to the equivalent CP gels. No significant trend towards $SO_3$ was detected and therefore any relationship discussed elsewhere with regard to sulphate attack and ASR is not occurring in these mixes.

## 7.5 Discussion

The composition of the ASR gels examined from the two concrete mixes immersed in salt solution were observed to vary greatly. The 7 kg mix gels often exhibit compositional features similar to those observed by the equivalent mixes immersed in distilled water (see section 7.3.1). This 7 kg mix would have developed significant ASR at 38°C regardless of whether it was immersed in salt solution, whereas the 3 kg mix would not have reacted at all (section 4.6).

### 7.5.1 The role of $Ca(OH)_2$ in ASR

It has been suspected that the take up of $Ca(OH)_2$ by an ASR gel on entering the cement paste is the reason for the frequently observed raised levels of CaO

detected in the cement paste (CP) gel's (Verbeck and Gramlich, 1955). This raised CaO content increases the gels viscosity (Diamond et al. 1981), therefore reducing its flowability and the expansion associated with it. This idea has, however, to date not been fully proven.

The CP gels in the 7 kg mix show CaO enrichment and so taking the opinion stated above, that calcium reduces the expansion and increases the viscosity of a gel, it follows that some of the 7 kg CP gels are no longer expansive and therefore will not flow, migrate or cause further expansion.If the more alkali-rich CA gels flow into the paste they will with time take up $Ca(OH)_2$ and become more calcic, therefore stopping further flow and the associated expansion. The $SiO_2$ : ($Na_2O$+$K_20$) : CaO ternary diagram also shows a number of CP gels of typical CA gel composition and these may represent 'newly' injected gel material. However, they are more likely to represent the few CP gels of higher alkali and chloride content seen in Figure 7.11. In the equivalent concrete mix immersed in distilled water, the uptake of $Ca(OH)_2$ from the cement paste into the ASR gels may slow and eventually stop further ASR expansion, if the production of 'fresh' high alkali expansive gel in the coarse aggregate reduces below the amount / rate of CaO up take by other cement paste located ASR gels. The take up of the $Ca(OH)_2$ from the paste into gel will in effect, make the ASR gel more like a cement paste (Power and Steinour, 1955) and therefore it maybe the limiting factor on the degree of ASR expansion developed in a particular mix.

It has however, been postulated that $Ca(OH)_2$ is a requirement of ASR (Chatterji et al. 1986b)a view now endorsed by results from Diamond (1989) and Davis and Oberholster (1988). Thaulow et al. (1989) however, state that:

> 'It appears that a low amount of calcium causes gel to be very fluid which causes it to be exuded, (causing expansive reaction). On the other hand, a high content of calcium gives the gel binding properties similar to that of hydrated cement paste. These observations suggest that there is only a narrow range of calcium content in a gel that give it the right viscosity to be expansive and deleterious in a concrete.'

With this comment in mind, similar expansion tests to those carried out for this work using the same Dry Rigg siltstone reactive coarse aggregate with an initial alkali content of 4 kg/m$^3$ $Na_2O_e$ and the addition of set amounts of $Ca(OH)_2$ were also carried out at Aston University and these gave rather conflicting results (Table 7.2). These expansion results show that the addition of 5 % $Ca(OH)_2$ actually accentuates the reaction, whereas, the addition of 10 % $Ca(OH)_2$ reduces it to a

level below that seen with the normal OPC mix.

TABLE 7.2: Concrete prism expansion test results, Dry Rigg siltstone coarse aggregate and 4 kg/m$^3$ $Na_2O_e$. Tests carried out at 38°C and 50°C triple bagged in 100 % RH.

| Mix design | Percentage (%) strain after 12 months | |
|---|---|---|
| | 38°C | 50°C |
| 0 % $Ca(OH)_2$ addition | 0.067 % | 0.103 % |
| 5 % $Ca(OH)_2$ addition | 0.132 % | 0.107 % |
| 10 % $Ca(OH)_2$ addition | 0.040 % | 0.064 % |

(Data taken from unpublished work at Aston University, Dept. of Civil Eng.)

This seems to confirm Thaulow's observations that only a small amount of $Ca(OH)_2$ is required to initiate / accentuate the ASR in a reactive concrete. The 0 % $Ca(OH)_2$ mix, will of course have some $Ca(OH)_2$ already present in its cement paste / pore solution and this causes some ASR to develop regardless of additions. The 10 % $Ca(OH)_2$ addition mix appears to be above the narrow band of calcium addition required for ASR accentuation and therefore the effect of the extra $Ca(OH)_2$ is to reduce the ASR expansion by causing some the ASR gel formed to act as a binding / cementing agent once in the cement paste rather than an expansive gel. These results however, are not fully understood and therefore further work is still required to establish why these unusual affects occur with $Ca(OH)_2$ additions on the extent of ASR expansion developed by a particular mix.

Kawamura (1992) has previously shown the cement pastes of ASR reactive mortars are depleted in $Ca(OH)_2$ when immersed in salt solution and it may be that this $Ca(OH)_2$ is the source of the small amount of $Ca(OH)_2$ that appears to be required to initiate expansive ASR. However, the equivalent alkali metal contents may well have been raised when the concrete is immersed in salt solution and this has caused the increased ASR. The lack of calcium rich gels in this 3 kg mix implies that there should be a greater potential for expansion in this concrete if the assumption that only a small amount of $Ca(OH)_2$ uptake by the gels is required for them to develop significant ASR expansion. The expansion results obtained (see 4.3.1) seem to confirm this observation. Thaulow et al. (1989) have also shown by the petrography of concretes immersed in saline environments that such $Ca(OH)_2$

depletions in the cement paste can be seen. An explanation of why larger amounts of the $Ca(OH)_2$ are not taken up by the gels so stopping expansive reaction is unknown. However, it may relate to the particulars of this mix, namely the large amounts of extra NaOH available to the gels in the pore solution derived directly from the $C_3A$ to chloride reaction already discussed.

The work discussed earlier carried out by Thaulow et al. (1989) and the unpublished work carried out at Aston University, imply that though some $Ca(OH)_2$ is required for expansive ASR a large amount will cause the gels to become calcic and take on bonding / cementing properties rather than expansion. Therefore, the low calcium levels detected in most of the CA and CP gels in the 3 kg mix should represent the equivalent of a low $Ca(OH)_2$ addition to the gels that will cause the most expansive ASR. A large $Ca(OH)_2$ addition to a potentially reactive mix along with a partial replacement of Pfa for example, should alleviate any ASR.

Finally on the topic of calcium up take by ASR gels Poole (1992b) has stated:

> 'In a real concrete, pore fluids are principally composed of strong sodium or potassium hydroxide solutions but calcium ions are also freely available. Thus as the gel swells on absorption of water the network opens sufficiently to allow calcium ions to penetrate into the gel where they can replace the alkali ions thus regenerating the alkali pore fluids which allow the reaction to continue while the gel gradually becomes increasingly calcium rich and loses its capacity to produce swelling pressures.'

### 7.5.2 Occurrence of alumina and chloride in the ASR gel

The $SiO_2 : Al_2O_3 : Cl$ ternary diagram shows an increase in the alumina uptake by gels in the cement paste of the 7 kg mix. This might be as expected of a reactive concrete containing a large amount of the cement phase mineral, tricalcium aluminate ($C_3A$). Some of this $C_3A$ will react with chloride ions entering the concrete as part of the salt solution to create more NaOH for the pore solution (see section 4.6). However, as shown from the chemical profile analyses in section 4.4, only a few Cl ions are actually entering the centre of the 7 kg concrete mix. This is now considered to be due to reduced Cl diffusion through the cement paste, this itself being a result of the cement paste being filled up with the calcium-rich viscous ASR gel (see section 7.4.1.1).

It follows therefore, that both gel suites and the cement paste in this concrete should have a relatively low chloride content and the cement paste should not have lost a

great deal of the alumina present in the original mix. Any alumina released by the reaction between $C_3A$ and chloride will be bonded chemically into Friedel's salt which remains in the cement paste. However, in this particular case, little of this reaction has taken place and therefore the majority of the alumina has remained in the paste as $C_3A$ hydrates. Finally it has been shown that alumina is more soluble in higher alkali solutions and this may be a simpler explanation of the higher alumina content observed in the 7 kg mix in comparison to the 3 kg mix. The $SO_3$ : $Al_2O_3$ : Cl, ternary diagram also confirms the high alumina content in both the CP gel and the cement paste of this mix.

The gel compositional results described for the 7 kg mix clearly do not apply to the 3 kg mix. In the 3 kg mix, the gels do not show the enrichment in calcium seen in all the 7 kg mix CP gels. All the gels analysed in general, show a high alkali, high silica and medium to low calcium content. The only difference detected between the two gel suites (CP and CA) in the $SiO_2$ : ($Na_2O$+$K_2O$) : CaO ternary diagram was a slight alkali enrichment in the CP gels (Figure 7.12 and 7.13). As the gels in this concrete are not particularly enriched in calcium, it follows that the increased viscosity and associated slowing of expansion / reaction etc. normally found with a high calcium content does not develop significantly in this concrete. As both the CA and CP gels are alkali / silica rich (but do also contain the required small amount of calcium) they are more fluid, therefore flow 'rapidly' reaching more of the concretes volume and the induce the larger overall expansions recorded. The slight alkali enrichment of the CP gels in comparison to the CA gels could be attributed to a net gain of alkalis from the now NaOH enriched cement paste pore solution or from the NaCl in salt solution which was the fluid constituent of these gels (see 4.4).

The $SiO_2$ : $Al_2O_3$ : Cl ternary diagram shows that both gel suites in the 3 kg mix are heavily depleted in alumina in comparison to the 7 kg mix. This feature may relate to the requirement for the initiation of ASR in the 3 kg concrete of an initial reaction between $C_3A$ (alumina source) and chloride derived directly from the salt solution now well diffused into the concrete, which forms the extra NaOH required (see section 4.6) to initiate the reaction. Therefore the lack of a significant quantity of free alumina in the paste due to $C_3A$ depletion will result in little alumina being taken up by the ASR gel injected into it (a lot of the alumina in the paste will be bonded into Friedel's salt). Obviously, as the $C_3A$ was originally in the cement paste, the greatest depletion of $C_3A$ should be from there and therefore any ASR gels in the paste (CP) will be particularly depleted in alumina. Of course the cement paste should show some limited alumina depletion and this is also observed (Figure 7.11

and 7.14). This does not really explain why the $C_3A$ content should be affected by the initial alkali content of the concretes, but clearly it is and shall need to be explained by further study.

The 7 kg mix gels show little evidence for the involvement of chlorides in their composition. This is due first to the lack of chloride entering the concrete (reduced diffusion of Cl ions due to ASR gel injected into the capillary porosity of the cement paste) and secondly because the ASR developed in this concrete regardless of the $C_3A$ to NaCl reaction, therefore only a little of this supplementary reaction occurred; hence only the slight increase in ASR expansion developed and the lack of significant alumina depletion and chloride enrichment was observed.

In the 3 kg mix however, large amounts of chloride are detected in the gels most especially the CP gels now also heavily depleted in alumina. So the ASR developed in this concrete is due primarily to the extra NaOH developed by the reaction between the $C_3A$ (hence depletion in alumina in gels) and the NaCl. The $SO_3$ : $Al_2O_3$ : Cl ternary diagram confirms the high chloride uptake by the 3 kg CP gels. This high chloride concentration found in the ASR gels, most especially the CP gel occurs because the pore solution and salt solution entering this concrete are heavily laden with salt, therefore any ASR gel formed using this water will have a high chloride content. Further evidence for the lack of salt solution entering the 7 kg mix can be taken from the low chloride content of the gels formed. Interestingly, both cement pastes, (3 or 7 kg mixes) appear to have taken up some residual Cl ions, which are now presumably now part of Friedel's salt derived from the reaction between NaCl and the $C_3A$ cement paste phase. The alumina and chloride content that remains may confirm that the Friedel's salt remains in the cement paste.

### 7.5.3 Theory on types ASR gel and expansion caused in saline conditions

From these results showing two compositionally distinct ASR gel suites it is possible to establish a theory on the unusual ASR that develops (Chapter 4) in saline environments.

In a concrete of higher initial alkali content (7 kg mix), ASR due to that alkali occurs rapidly, in the process filling the cement paste with ASR gel and therefore stopping the significant diffusion of sodium chlorides into the concrete. This reduced diffusion means that the ASR caused by the alkalis derived directly from the salt ($C_3A$+ NaCl

reaction) is negligible, whilst the ASR due to the initial alkali in the mix is significant.

The process for the development of ASR in a lower (borderline threshold) alkali concrete mixes in salt solution is, however, different and can be taken as a combination of the two parts. First the ASR due to alkalis derived from the salt solution as is described above with the resulting high expansions and secondly by taking the limited ASR due to the internal initial alkali content of the concrete occurring in higher initial alkali mixes. This limited internal alkali derived ASR (small amount of ASR gel) only causes a slightly reduced diffusion of the NaCl into the concrete. Therefore, with concretes of intermediate to borderline threshold initial alkali level immersed in salt solution, some ASR expansion should develop due to its internal initial alkalis (as seen in the distilled water immersed and 7 kg mix) and some ASR expansion should develop due to the reaction between $C_3A$ and NaCl as discussed frequently above. This combination of ASR from the two sources may result in the greatest development of ASR expansions, in concretes of borderline reactivity initial alkali threshold contents, being immersed in salt solution.

In a concrete of lower initial alkali content (below that concrete's initial alkali threshold), ASR due to that internal alkali does not occur at all. However, because of the improved diffusion of NaCl through this cement paste, due to a lack of ASR gel in it, then the ASR caused by the alkalis derived directly from the salt ($C_3A$+ NaCl reaction) is greatly enhanced.

This conclusion is remarkably close to the concluding observations made for the concretes tested in chapter 4. Those results indicated that an initial alkali content pessimum appears to develop for each reactive aggregate type when it is immersed in salt solution. Hence if this theory is correct, the ASR developed in such concretes would be a combination of ASR due to the initial alkali in a concrete mix and ASR due to a reaction between the NaCl in solution and $C_3A$ in the cement paste producing extra NaOH. In the process the total expansion developed would be greater than that developed by either type of ASR (see Table 7.3) in higher or lower alkali mixes.

The idea of compositionally distinct gel suites being developed by the two types of ASR is interesting in the fact, that if further research was carried out in this field it may lead to a method of establishing the cause of ASR in field structures. For example in a disputed case of compensation for ASR occurring in a structure, the confirmation that the ASR is due primarily to de-icing salts or the internal alkali

content of mix will be useful in establishing blame.
It may also be useful in explaining the number of field structures with low initial alkali contents that still show the effects of ASR, due to the fact that the ASR is primarily due to deicing salts developed in an otherwise non-reactive concretes.

---

TABLE 7.3: Dry Rigg siltstone expansion results, (Figures are an average of two prisms).

---

1. 3.0 kg mix = ASR due to salt solution primarily,
Expansion at 15 months = 0.384 %

(Initial alkali level below that aggregate's threshold. Expansive ASR gel mainly alumina poor, chloride rich)

2. 3.5 kg mix = ASR due to salt solution and initial alkali content,
Expansion at 15 months = 0.424 %

(Borderline initial alkali level for that aggregate, Expansive ASR a combination of both gel types)

3. 7.0 kg mix = ASR mainly due to initial alkali content + a little salt solution,
Expansion at 15 month = 0.326 %

(Well above initial alkali threshold, but ASR gel in paste reduces NaCl diffusion hence reduced level of ASR due to the salt solution. Expansive ASR gel mainly alumina rich chloride poor)

Expansion (%) developed.

| Mix alkali | ASR (SS) | ASR (IA) | TOTAL EXPANSION |
|---|---|---|---|
| 3.0 kg | 0.384 % | 0.000 % | 0.384 % |
| 3.5 kg | (0.384 %) | 0.021 % | 0.424 % (0.384 + 0.021 = 0.405 %) * |
| 7.0 kg | (0.104 %) | 0.222 % | 0.326 % (0.326 - 0.222 = 0.104 %) * |
| | | | or (0.104 + 0.222 = 0.326 %)* |

ASR (SS) - ASR due to salt solution
ASR (IA) - ASR due to internal alkalis. (as in distilled water)

* - Surprisingly close. Expansion figures seem to confirm results

---

## 7.6 Conclusions

1. The composition of the ASR gel varies dependent on location in the concrete. Gels from within aggregate particles (CA) appear to generally be alkali and silica rich, calcium poor, whilst the gels from within the cement paste (CP) are calcium rich, medium silica and alkali poor. This increasing calcium content in the cement paste gels may result in increased viscosity and reduced gel migration / flow and therefore less expansion.

2. The use of different reactive coarse aggregates produced remarkably similar CA and CP gel compositions. All the various concretes regardless of aggregate type showed the well documented calcium enrichment in the cement paste gels.

3. The Dry Rigg siltstone 7 kg mix when immersed in salt solution, shows similar CA and CP gel compositions to the equivalent mixes immersed in distilled water. Therefore, it follows that the ASR developed here is due primarily to the internal initial alkalis in the concrete mix and not the alkali derived from the salt solution.

4. Evidence for this is based on the low chloride content of the CP gels. However, a few of these CP gels also show compositional similarities to the 3 kg mix CP gels (i.e high Cl content) and these have been caused by alkalis derived from the salt solution. The high alumina content of the 7 kg mix CP gels is probably due to the greater solubility of alumina in higher alkali mixes or a lack of reaction between $C_3A$ and $Cl^-$ taking place in this mix.

5. The Dry Rigg siltstone 3 kg mix when immersed in salt solution, shows very different results. The CP and CA gels do not show strong calcium enrichment; all the gels were of high silica, high alkali content, which suggests they would all remain fluid and continue to be expansive. All the gels, especially CP gels are depleted in alumina and enriched in chloride. This suggests the reaction between $C_3A$ and chloride which results in an increased NaOH concentration in the pore solution is required to initiate the ASR in this concrete.

6. The chloride enrichment of the 3 kg gel occurs as a result of using salt solution as the hydrous element of the gel formation. The associated depletion in alumina may occur as a result of using up $C_3A$ in the cement paste by the reaction with NaCl already described. The analysis of the cement paste seems to confirm this opinion.

7. The gel compositional results suggest that ASR could continue to occur in the 3 kg mix concretes until the take up of large amounts of $Ca(OH)_2$ by the CP gels stops further expansion. If the expansion and associated CA gel production developed in the aggregate particles, is greater than the solidification of CP gels due to the take up of extra $Ca(OH)_2$, then expansion will continue letting more alkali rich (CA) gel out into the cement paste, thus causing further expansion. On the basis of this suggestion an increased initial large addition of $Ca(OH)_2$ might lower the effects of the alkali-silica reaction.

8. The compositional behaviour of the lower alkali mixes (below the aggregate's initial alkali threshold), when immersed in salt solution is remarkably different from that seen with the other concretes with or without the salt solution. This might help to suggest why some real structural concretes with low initial alkali contents have suffered significant ASR in saline conditions.

9. Two compositionally distinct suites of ASR gels can be identified in reactive concretes immersed in salt solution. One originating from ASR derived from the internal alkalis in the concrete is alumina rich, chloride poor. The second due to ASR caused by NaCl entering the concrete is alumina poor, chloride rich.

10. On the silica, alumina, chloride ternary diagrams for the concretes immersed in salt solution, the 7 kg mix composition of gels tend (CA to CP) away from silica, towards the cement paste composition. However, the 3 kg mix composition of gels tend (CA to CP) away from alumina and away from the cement paste composition

# CHAPTER 8

## General conclusions and recommendations for further work

### 8.1 Conclusions

1. The reactive constituents for all the reactive aggregates were identified or at least inferred to be either crypto / microcrystalline quartz or chert. The highly strained quartz-rich granitic aggregate (AG) shows significant expansion due to ASR. However, the highly strained quartz was not itself seen to be reactive, but the physical geological processes that form the strained quartz, also result in the formation of microcrystalline quartz at the edge of larger quartz crystals and highly foliated textures in this fine quartz which results in increased potential reactivity. The reactive constituent was again microcrystalline quartz.

2. Whether the reactive concretes were immersed in distilled water or wrapped in damp cloth and triple bagged the cause of the cessation of the ASR expansion was the depletion of alkalis in the concrete and not the shortage of reactive silica or moisture.

3. Significant alkali-silica reaction has occurred in UK aggregate concrete mixes at 38°C 100 % RH with initial alkali contents of between 3.5 and 7.0 kg/m$^3$ $Na_2O_e$. This lower figure is well below any alkali level previously published for specific UK aggregates. A relationship of these results to those that may be obtained by testing at 20°C and in external exposure conditions is not proposed but these initial alkali figures are in line with many alkali content measurements carried out on ASR affected structures in the real environment. The alkali threshold for significant ASR varies from one aggregate source to another. This work also confirms that chert-rich aggregates do not exhibit significant expansion at less than 5 kg/m$^3$ $Na_2O_e$ in a 38°C environment.

4. Unless or until it becomes practicable to introduce different permissible alkali limits for concretes made from specific groups of UK aggregates, the present recommendations for minimising the risk of ASR in the UK which call for a limit of 3 kg/m$^3$ $Na_2O_e$ of alkalis derived from concrete mix materials do not seem unduly conservative.

5. The immersion of already potentially reactive concretes in salt solution

accentuates the ASR. In concretes not expanding significantly, due to their initial alkali contents being below that required to sustain reaction, immersion in salt solution initiates even greater ASR expansion than for concretes of higher initial alkali level. The greatest expansions were developed in concretes with initial alkali contents at or near the initial alkali threshold for significant ASR with that aggregate mix when placed in distilled water. From the expansion results it appears each aggregate has an "initial alkali content pessimum" for its greatest expansion when placed in salt solution. For the DR and HL aggregates this pessimum is on or just above the present UK initial alkali content limit. The wet /dry cycling of the prisms in salt solution was shown to have little effect on the highly reactive aggregates, (DR and HL) in comparison to total immersion in salt solution. However, with the less reactive / slower reacting aggregates, (MD and RP) the effect was to lower the initial alkali threshold for significant reaction even further than by just immersion in salt solution.

6. The expansion test carried out on concrete samples containing the MD and RP aggregates, showed that when they were immersed in distilled water or salt solution there is a slow development of ASR that continued over a long period of time. The rapid testing of these or similar materials for alkali-silica reactivity may thus prove doubtful. If sufficient alkalis remain or are added, it appears ASR expansion will continue in the 38°C, 100% RH environment for up to 24 months with all the aggregates used in this study. Therefore with a resupply of alkalis from deicing salts many ASR affected structures could continue to react for longer than has previously been considered.

7. Concretes containing lower initial alkali contents suffer less ASR induced by the initial alkali content of a mix, but are more susceptible to diffusion of NaCl into the central areas of concrete specimens. The addition of NaCl to a potentially reactive low initial alkali mix is of greater concern with respect to ASR initiation than the same addition to an already reacting high alkali concrete. In the high alkali mixes the diffusion of Cl ions into the concrete is significantly impeded due to the injection of ASR gel into the capillary porosity of the cement paste. In the low alkali mixes the diffusion of Cl ions continues as in any normal concrete. This allows the Cl ions to bond with the $C_3A$ phase which then releases extra hydroxyl ions which initiates the ASR.

8. The high $K_2O$ contents recorded for the Dry Rigg siltstone and Maentwrog greywacke aggregates could be due to a release of potassium cations from the

muscovite, sericite etc. in the aggregate particles when they were placed in acid or water. However, the lack of a significant quantity of K cations in the pore solution analyses suggest either the potassium is not released when the aggregate is in a concrete (highly alkali environment) or that it has been used by the ASR in preference to the sodium. The apparent release of this potassium from some of the reactive aggregates may be an extra reason for the high reactivity and low alkali thresholds of those aggregates.

9. The concrete prism expansion tests carried out with a replacement of 25 % of the cement with pfa's, show a reduced amount of recorded expansion in high initial alkali concretes. Most of these prisms would still be considered to be suffering from significant ASR. The expansion test results for the 4 kg/m$^3$ $Na_2O_e$ mixes containing both medium and high alkali pfa's showed no discernible change in expansion compared to the equivalent OPC mix. Both mixes would still be regarded as borderline reactive concretes. However, with the 3 kg/m$^3$ $Na_2O_e$ mixes the expansion recorded was greater for the high alkali pfa mix compared with the normal OPC mix. The amount of expansion was still significantly below that considered to represent significant ASR. The equivalent medium alkali pfa mixes showed no expansion.

10. The pore solution analysis data, showed that in general the high alkali pfa enriched the pore solution hydroxyl and alkali metal concentrations of all the mixes, in comparison to the equivalent OPC mixes, regardless of the initial alkali content. By contrast, the medium alkali pfa mixes showed negligible or even slightly reduced concentrations of hydroxyl and alkali metal ions, especially in the higher initial alkali mixes.

11. The majority of the alkali released from the pfa's was potassium. Therefore, there was a net contribution of potassium to the pore solution at all ages, except 1 day. This contribution appears to be most significant in the older age concretes when the total alkali concentration is significantly reduced due to leaching. The greatest release of potassium was found in the lower alkali mixes containing high alkali pfa and this was the probable explanation for the late age increase in the expansion developed in the 3 kg/m$^3$ $Na_2O_e$ mix containing high alkali pfa. In general the pore solution results are inconclusive and this suggests the problem being studied is more complex than initially thought.

12. The petrographical analysis of all the pfa concrete mixes, showed that ASR

microcracking was located mainly in the reactive aggregate particles. It may be that the lack of evidence for ASR microcracking in the cement paste is due largely to the effects the pfa has on the physical and chemical properties of the cement paste.

13. The addition of air entrainment reduced the expansion developed due to ASR. The closer the mix was to the alkali threshold for significant reaction the greater was reducing effect of the air entrainment. In the highly reactive 7 kg/m$^3$ $Na_2O_e$ mix the amount of ASR gel totally swamped the relatively low level of air entrainment and therefore the expansion induced was only slightly reduced in proportion to the total air entrainment level of the concrete. In the borderline reactive 3.5 kg/m$^3$ $Na_2O_e$ concrete all levels of air entrainment above 1.7 % prevented significant expansion due to ASR. With the 1.7 % AE concrete the trend of the expansion verses time graph shows a distinct change from the other mixes after four months.

14. For the 3.5 kg/m$^3$ $Na_2O_e$ mix an air entrainment level of 3.7 % caused a 72 % reduction in the recorded expansion compared with the 1.7 % mix and that means the mix would no longer be classified as suffering significant ASR expansion. For the 7 kg/m$^3$ $Na_2O_e$ mix an air entrainment level of 8.0 % reduced the recorded expansion by 25 % compared to the 1.7 % AE mix. All the 7 kg/m$^3$ $Na_2O_e$ prisms regardless of the level of air entrainment would still be classified as suffering significant ASR. To remove the effects of significant ASR expansion from the 7 kg/m$^3$ $Na_2O_e$ mix an unrealistically high air entrainment level of between 30 to 35 % would be required.

15. The petrographical examinations showed the 7 kg/m$^3$ $Na_2O_e$ mix to contain only a few large voids; however, most of these were full or partially filled with ASR gel. All the gel filled voids were connected to ASR related microcracks, there was little evidence for the exudation of significant quantities of ASR gel into the voids via the cement paste. The ASR occurring in this concrete was considerable. The 3.5 kg/m$^3$ $Na_2O_e$ mix contained numerous small voids, few of which contained ASR gel. Those that did contain gel were connected to the ASR related microcracks present and the gel was usually recrystallised. The other voids were frequently totally empty or contained secondary portlandite and ettringite mineralisation. The ASR in this concrete was very limited and would not be considered significant.

16. The reduction in the strain induced by ASR in the air entrained concretes was due primarily to the dissipation of gel / strain into air voids intercepted by expansive

ASR related microcracks. As not all the voids were filled with gel, exudation of the gel through the cement paste did not seem a likely method of explaining the reduced expansions. The petrographical evidence also confirmed this by only revealing significant localised exudation of gel into the higher capillary porosity cement paste surrounding the air voids.

17. The composition of the ASR gels varies dependent on their location in the concrete. Gels located in the reactive coarse aggregate appear generally to be alkali and silica rich, calcium poor, whilst the gels found in the cement paste are calcium rich, medium silica and alkali poor. This increasing calcium content in the cement paste gels results in increased viscosity and reduced gel migration / flow and therefore maybe less expansion. The use of lithologically different reactive coarse aggregates produced remarkably similar gel compositions.

18. The Dry Rigg siltstone 7 kg/m$^3$ $Na_2O_e$ mix when immersed in salt solution, shows similar, coarse aggregate and cement paste gel compositions to the mix immersed in distilled water. Therefore, it follows that the ASR developed is due primarily to internal initial alkalis in the concrete mix and not the alkali derived from the salt solution. Evidence for this is based on the low chloride content of the gels. The high alumina content of the 7 kg/m$^3$ $Na_2O_e$ mix gels is most probably due to the greater solubility of alumina in higher alkali mixes.

19. The Dry Rigg siltstone 3 kg/m$^3$ $Na_2O_e$ mix when immersed in salt solution, shows very different results. None of the ASR gels show strong calcium enrichment; all the gels were high silica, high alkali gels, which suggests they would remain fluid and continue to be expansive. All the gels, especially cement paste gels are depleted in alumina and enriched in chloride. The chloride enrichment of the 3 kg/m$^3$ $Na_2O_e$ gel occurs as a result of using salt solution as the hydrous element of the gel formation.

20. The behaviour of the low alkali (3 kg/m$^3$ $Na_2O_e$) Dry Rigg siltstone immersed in salt solution is remarkably different from that seen with the all other concretes with and without the salt solution. This might help to explain why some real structural concretes with low alkali content have been shown to suffer significant ASR in saline conditions.

21. Two compositionally distinct suites of ASR gels can be identified in reactive concretes immersed in salt solution. The first suite originates from ASR derived

directly from the internal alkalis in the concrete (alumina rich, chloride poor), whilst the second suite is due to ASR caused by the NaCl entering the concrete prisms (alumina poor, chloride rich).

22. These two compositionally different ASR gel suites may explain why the initial alkali level pessimum postulated in chapter 4, actually occurs in salt solutions. In high alkali mixes ASR due to the initial internal alkali occurs, filling the concrete with gel, so reducing diffusion of NaCl and in the process, slowing or stopping the ASR due to salt solution. In a low alkali mix little ASR occurs due to the internal alkali content; therefore NaCl diffusion proceeds at a 'normal' rate and ASR due to the salt solution develops fully. In an intermediate borderline alkali threshold mix, some ASR will develop due to the internal alkalis of the mix. However, the little gel formed will only slow the diffusion of NaCl slightly and therefore ASR due to the salt solution will also occur. In this manner the greatest expansions / ASR developed by the concretes in the salt solution will occur with the intermediate alkali mixes, hence accounting for the position of the initial alkali content pessimum.

## 8.2 Recommendations for further work

Research in the field of alkali-silica reaction (ASR) has been underway for many years. Over this period the number of specific areas of study have become progressively greater and therefore many ASR related topics have not even been mentioned in this research. Some aspects of ASR research have, however, now been fully covered and a general understanding is complete. Research into a subject to answer specific questions often gives the required answers, but in the process also creates a series of new unresolved observations or questions, which themselves need to be answered (eg. the effects of salt on the alkali silica reaction). The work described in this thesis set out to clarify a series of unresolved areas of ASR research (see section 1.6). In the process, a number of interesting phenomena were observed the results which, though unusual, should be explainable by further research.

With regard to ASR developed specifically with UK aggregates up until recently flint and chert-bearing materials were considered to be the most reactive mainland UK aggregates, developing significant ASR at initial alkali levels of greater than 5.0 kg/m$^3$ $Na_2O_e$. The work described in chapter 3 showed that significant ASR can develop with lithologically varied aggregates at initial alkali levels down to between 3.5 and 4.5 kg/m$^3$ $Na_2O_e$ at 38°C and 100 % relative humidity. Further work

establishing the initial alkali threshold for significant ASR with either specific aggregate sources or reactive lithologies would be of great use in establishing the sort of alkali levels that could be considered 'safe' when using specific aggregates mixes.

Along these lines, Livesey (1992) has proposed raising the initial alkali level to 4 kg/m$^3$ $Na_2O_e$ for concrete mixes containing chert-based aggregates. The work described in chapter 3 suggests that this would probably be a safe option; however, it also confirms that for some aggregate types the present 3 kg/m$^3$ $Na_2O_e$ limit is not unduly conservative and therefore remains of benefit in the avoidance of new cases of ASR. It also remains unknown whether this proposed 4 kg/m$^3$ $Na_2O_e$ limit for chert aggregates would be 'safe' in the presence of deicing salts. Further expansion testing of chert-based aggregates immersed in salt solution and tested at 38°C, 20°C and in external exposure conditions will help answer this dilemma.

Wood (1992a) when commenting on the results described here states:

> "The implication of studies of the variation of the alkali level on expansion, like that of this work, is that we need to grade aggregates by test expansion threshold alkali level. We must abandon trying to discriminate in the vast grey area between 'reactive' and 'non-reactive' aggregates."

He then uses the alkali thresholds of the various aggregates to propose a direct statistical relationship of the 38°C test results to the occurrence of significant ASR in field structures leaving a large margin of error. He concludes:

> "Should alkali thresholds change with aggregate? Further field and laboratory tests are needed to develop this and to relate it to the more promising of the proliferating range of rapid chemical and hot mortar bar tests which are appropriate for monitoring production week by week."

Wood also presents the question as to the reliability of the present 3 Kg/m$^3$ $Na_2O_e$ limit when using these aggregates especially as some ASR affected structures containing them have been shown to have initial alkali levels of around 3 Kg/m$^3$ $Na_2O_e$. This suggests that we should be more cautious with some non-chert aggregate types, particularly in vulnerable structures like dams, tunnels and foundations.

Concrete prism expansion results obtained at 38°C and 100 % RH showing

significant ASR with various aggregate mixes, are of interest in establishing a range of alkali levels over which ASR may develop with specific aggregate types and this may therefore remain a reliable and relatively rapid ASR test method. However, some researchers continue to feel that testing at these raised temperatures have little direct bearing on the ASR developed in field structures and that ASR may even develop at lower initial alkali levels at 38°C than at normal ambient temperatures.

Therefore, to establish the reliability of 38°C prism tests, it is proposed that further work be carried out with a series of different lithology reactive aggregates (not just chert-based materials as has been already started) in identical prisms placed in 20°C and external exposure conditions, to settle these continuing questions on the reliability 38°C expansion tests.

A problematic area that will continue in this field of research concerns the slower reactive aggregates such as the Maentwrog greywacke and Trent valley gravel. Even in the 38°C test environment these aggregates did not develop significant expansion (>0.05 % strain) due to ASR, until well into their second year (see chapter 4). Therefore the testing of such materials for ASR reactivity continues to be a problem. Establishment of a test method for these slower reacting aggregates will still be required in the future; after all, the Maentwrog dam in North Wales which contains one such aggregate remains one of the worst cases of ASR presently found in the UK.

Most researchers agree that the usual source of alkalis used by ASR to cause the expansion is NaOH and KOH found in the cement paste pore solution. Therefore altering the initial alkali content of a mix by the addition of these hydroxides to the initial mix water appears to be a valid method of creating different mix alkali levels. However, some researchers contend this and therefore only carry out ASR expansion testing using concretes made up using cements of different initial alkali content; this of course creates other variables to be considered. Therefore further work should be carried out to compare the expansion prism results for a series of known reactive aggregate mixes. The first set having variable alkali contents created by the addition of alkalis (NaOH and KOH) to the mix water, and the second set having variable alkali contents using cements of different alkali content, all the other mix variables will remain constant. This work would establish if these methods of alkali content variation to a concrete mix are comparable, with respect to the degree of expansion, alkalis available to the reaction in the pore solution and the form that the ASR takes. This information will be obtained by the use of pore

solution analysis and petrography.

The main objective of the research in this thesis was to establish accurately the effects of NaCl solution on the alkali silica reaction developed by the various reactive aggregates in different initial alkali level mixes. The work has revealed the existence of an 'initial alkali content pessimum' for the various aggregate types, when they were immersed in salt solution. This pessimum appears to be usually found near the initial alkali threshold for significant reaction, for the equivalent mix when it is immersed in distilled water. It is hoped that further work will elucidate the phenomenon and test the hypothesis proposed in chapter 7.

This work will involve the testing of a series of concrete prisms, containing the same aggregates (as described in chapter 3) at medium to low alkali levels. Cements containing different quantities of $C_3A$ shall be used to establish the extent to which the $C_3A$, NaCl reaction discussed previously is actually causing the ASR expansion. It is also hoped to establish the lower limits of alkali content at which significant ASR is able to develop in various salt solutions. Once the expansion testing is complete, petrographic and chemical analysis will be used to establish if the observations made in chapter 4 remain valid at lower alkali levels.

The chemical profile analysis in chapter 4 revealed an interesting reduction in the diffusion of chlorides into the prisms with increased ASR. Further work on similar concretes could be carried out to estimate the diffusion coefficient for the chloride ions migrating into these reactive prisms. Further analysis of the pore solution composition and electron microprobe study of the ASR gel compositions shall be used to help establish; the remaining reactivity of the various mixes with time and to also confirm the hypothesis proposed in chapter 7.

At 38°C the accentuation and initiation of ASR by immersion in salt solution has been proven. However, the development of a similar feature at 20°C and in external exposure conditions has still to be shown. Therefore the proposed expansion testing described above, will also be carried out at 20°C to confirm any observations made at 38°C. Once this is established a further piece of research is proposed in which concrete cores taken from ASR reactive structures containing similar aggregates to those in the prisms are placed in various salt solutions and tested for expansion. A possible correlation of all the expansion results and other analysis carried out on these cores with the concrete prisms is intended.

[This particular proposal for further work has been submitted to SERC and confirmation has now been received for the commencement of the project in October 1993].

The experimental work in chapter 4 established potassium was being released from some of the reactive aggregates. Further work should be undertaken to establish whether this potassium released by immersion of the aggregates / concretes in acids and water are actually also released from the aggregates, whilst they are in the highly alkaline environment of concrete. If this is found to be the case, then the form in which this potassium is found and its potential availability for the alkali-silica reaction needs to be assessed.

The work in chapter 7 using EMP analysis of the various ASR gels, established that two compositionally different ASR gel suites exist in concretes immersed in salt solution. Further EMP analysis of borderline alkali threshold reactive concretes could be used to confirm the existence of an 'initial alkali pessimum' as postulated previously. If the two compositional gel suites are found to make up more equal percentages of the total number of gels analysed (i.e the larger total expansion is due to a combination of both gel suites together rather than just one) then this will confirm the proposed reason for the observed pessimum. Further detailed EMP analyses of the various cement pastes could also be used to establish if $Ca(OH)_2$ and $C_3A$ are being depleted and the fate of the alumina in the lower alkali mixes.

**Figure 1.1 Locations of a number of well documented structures affected by ASR and some of the ASR reactive aggregate deposits. (Information has been obtained from a number of sources).**

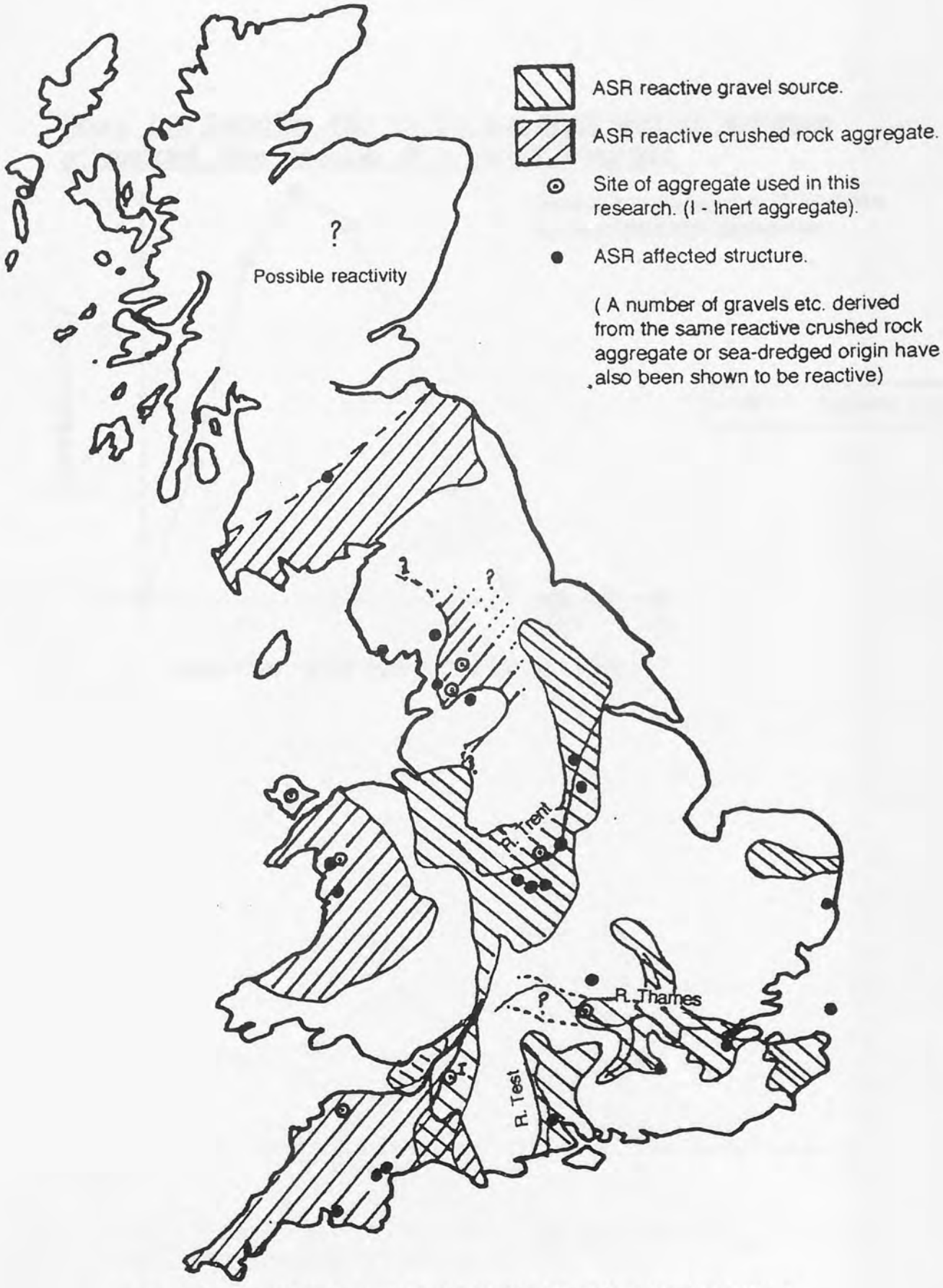


N.B Cases of ASR have also been found in Northern Ireland and Jersey.

**Figure 1.2: Expansion (%) Vs Percentage of reactive aggregate at constant time. Example of a typical 'pessimum'.**

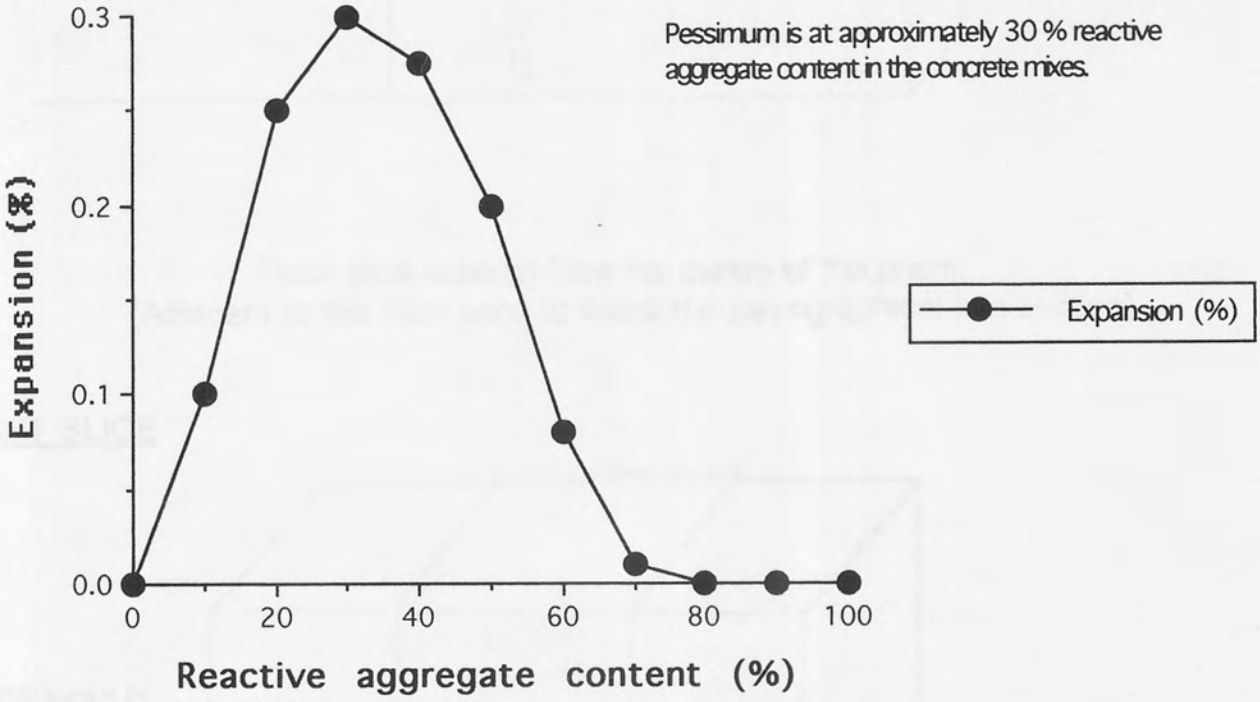

**Figure 2.1 Diagram shows the position from which the slices of concrete prism for profile chemical analysis were taken.**

Original prism

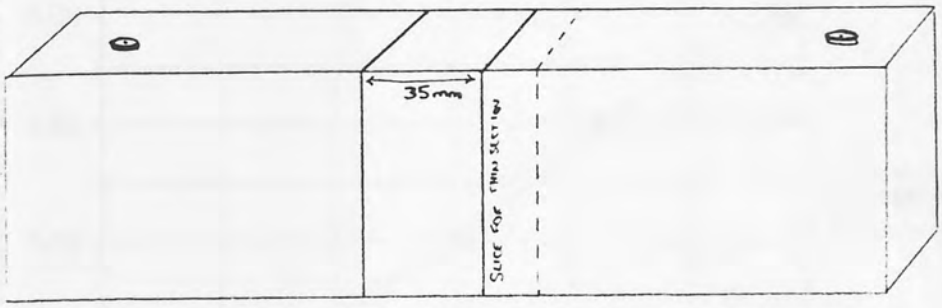


Thick slice is taken from the centre of the prism.
(Adjacent to the slice used to make the petrographical thin section).

CUT SLICE

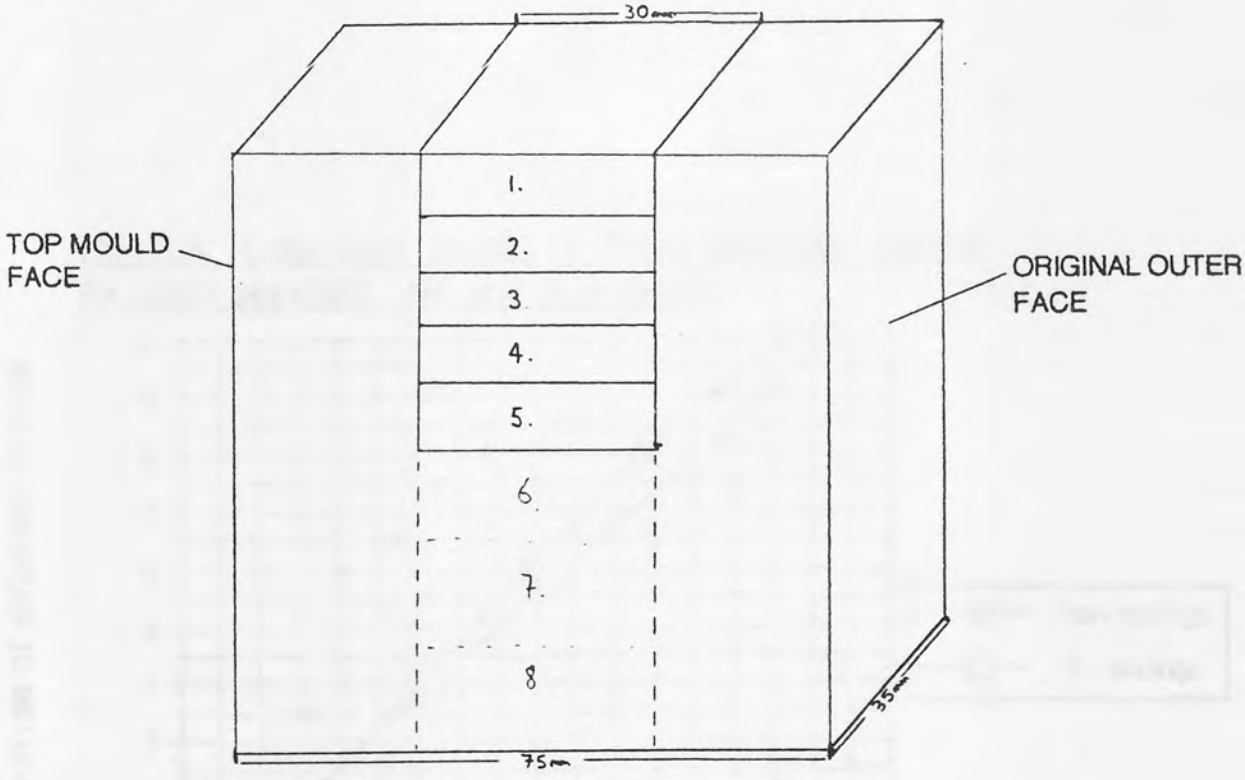


Slices 1 to 5 are for the typical analysis, whilst 1 to 8 are for samples analysed in section 4.4.6.

Taking into account the loss of some material to the saw cut, each slice for analysis measured approximately, 30 X 35 X 7 mm.

FIG 2.2: Calibration curve to produce chloride contents of solution as (mmol/litre).

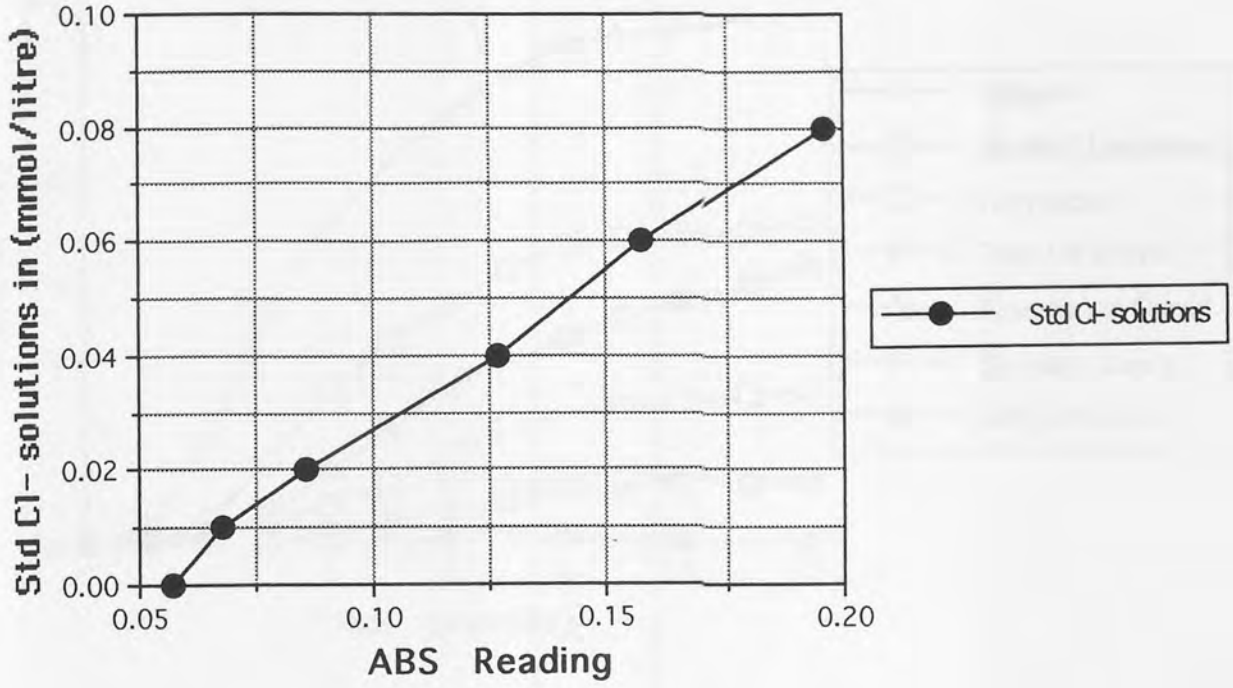


FIG 2.3: Calibration graph of flame intensity figures for each standard Na and K solution.

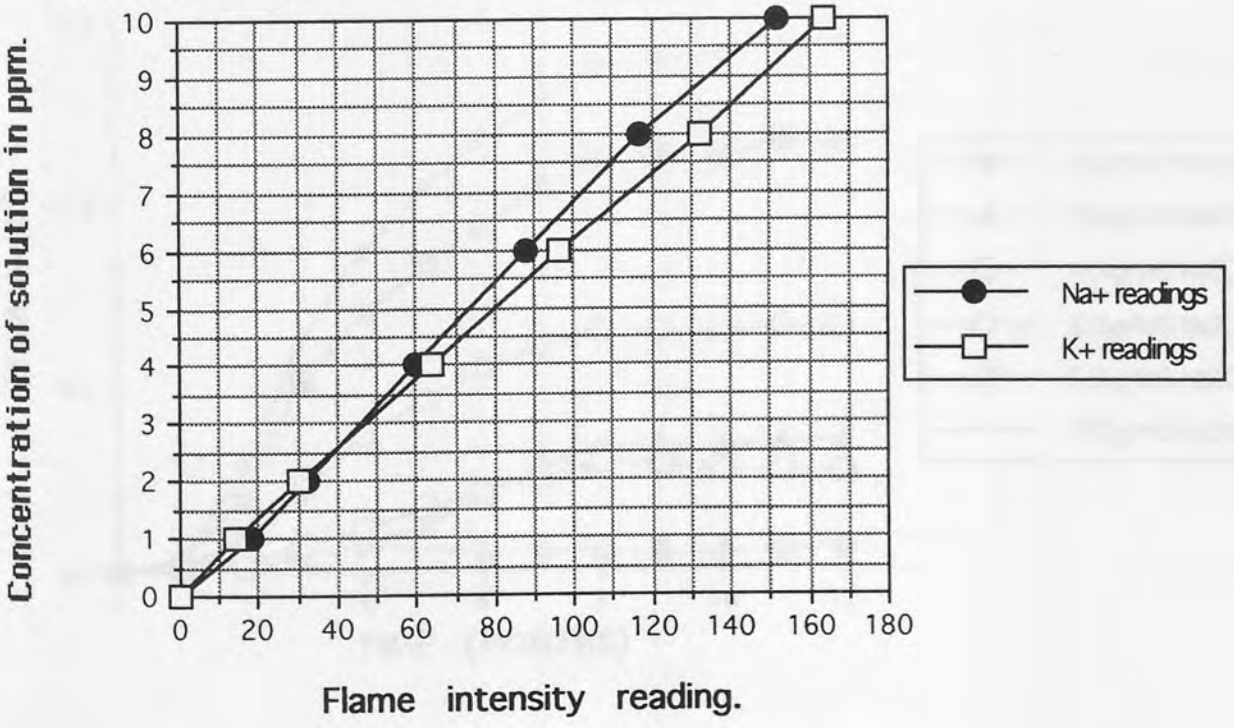

FIG 3.1: Expansion (%) Vs time. For all the aggregate mixes at an initial alkali level 7 kg/m3 Na2O equivalent. Tested at 38oC and 100% RH.

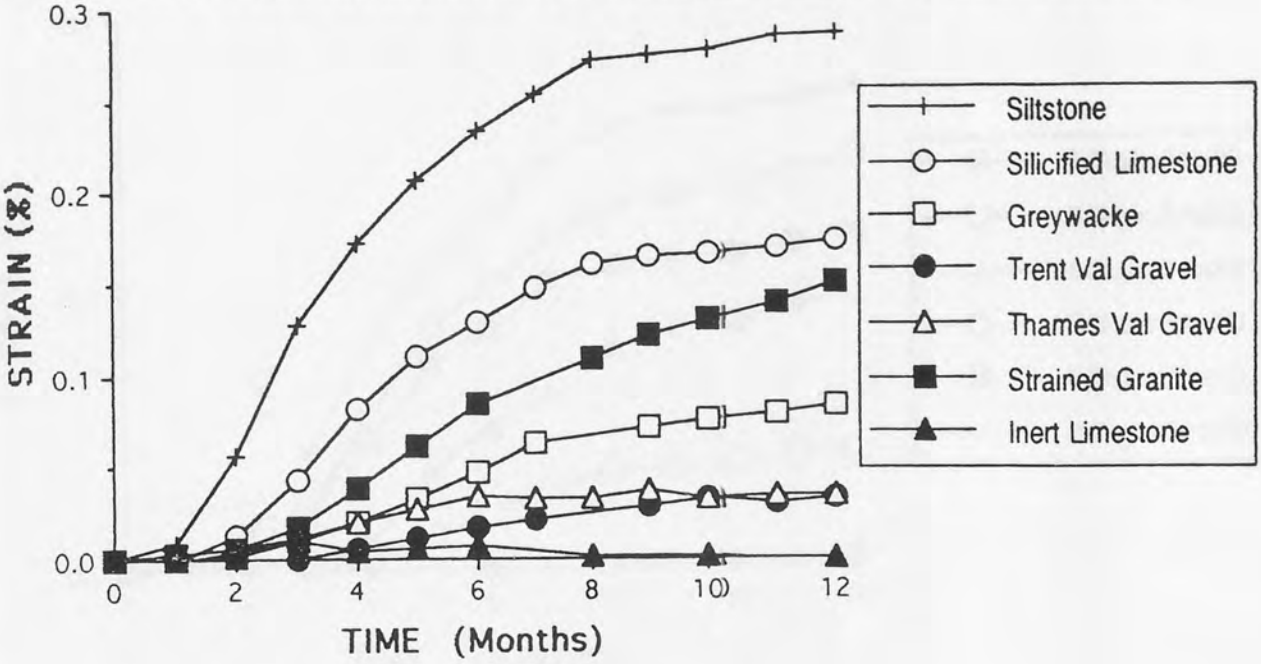


FIG 3.2: Expansion (%) Vs time. For (DR) siltstone mixes at various initial alkali levels. Tested at 38oC and 100% RH.

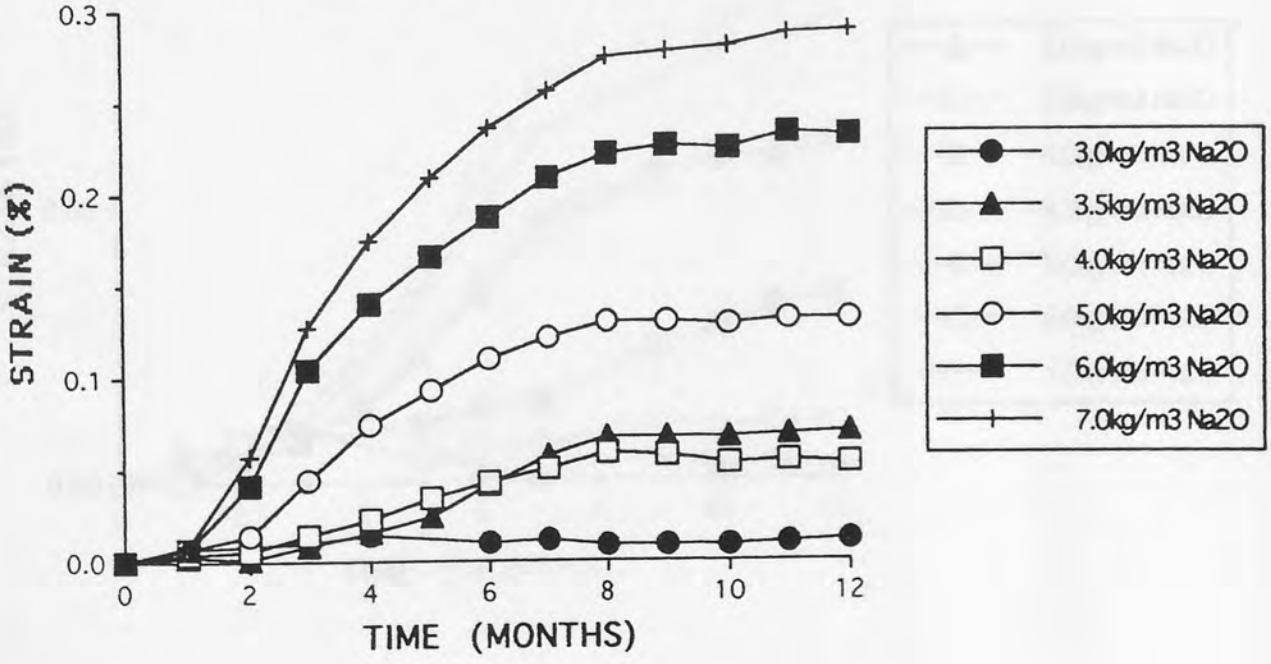

FIG 3.3: Expansion (%) Vs time. For (HL) limestone mixes at various initial alkali levels. Tested at 38oC and 100% RH.

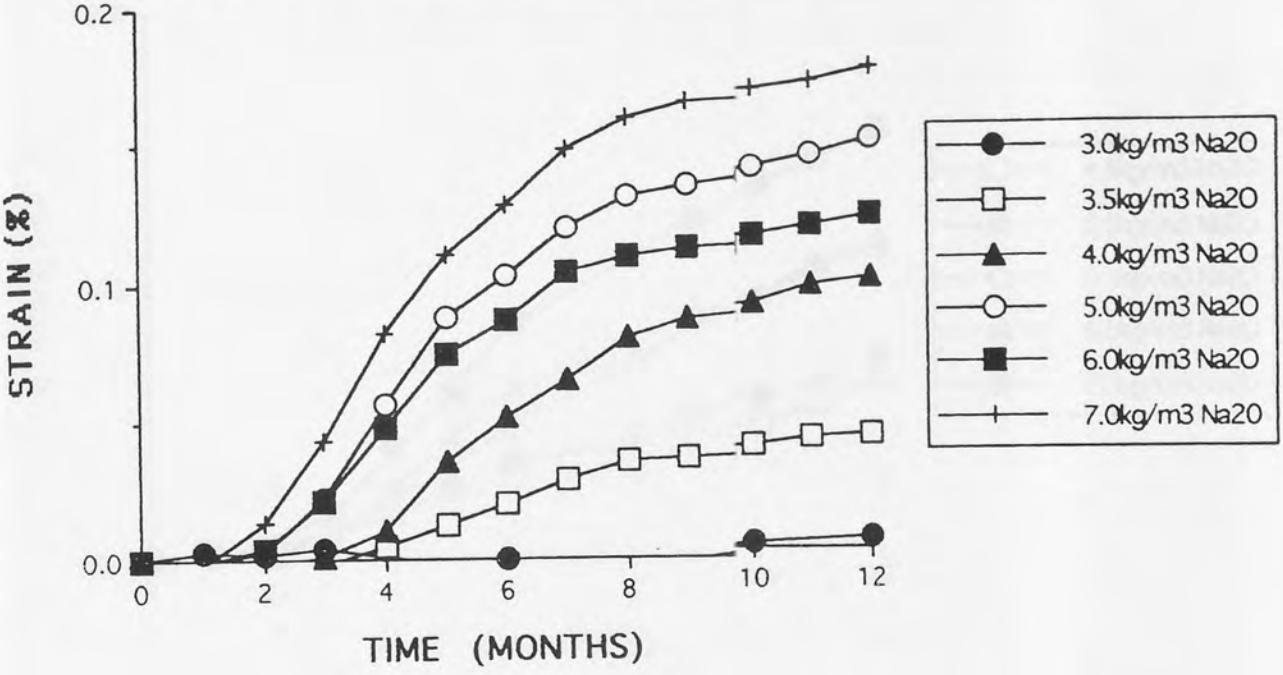


FIG 3.4: Expansion (%) Vs time. For (MD) greywacke mixes at various initial alkali levels. Tested at 38oC and 100% RH.

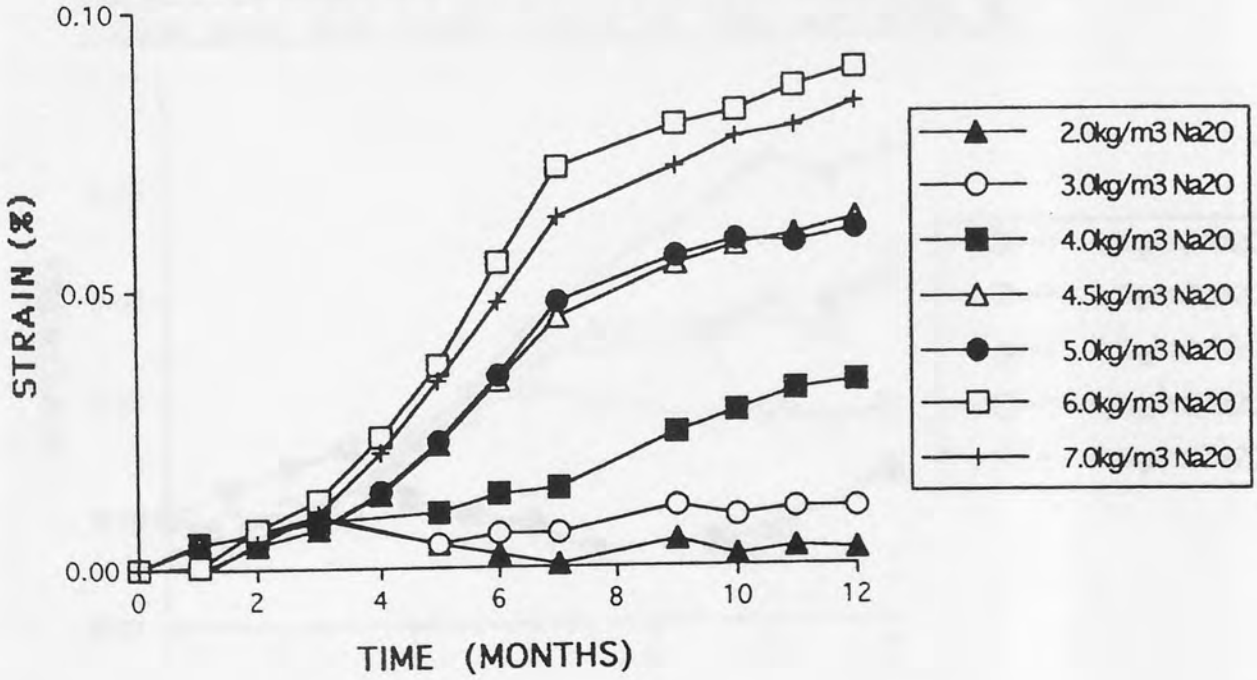

FIG 3.5: Expansion (%) Vs time. For (AG) strained granite mixes at various initial alkali levels. Tested at 38oC and 100% RH.

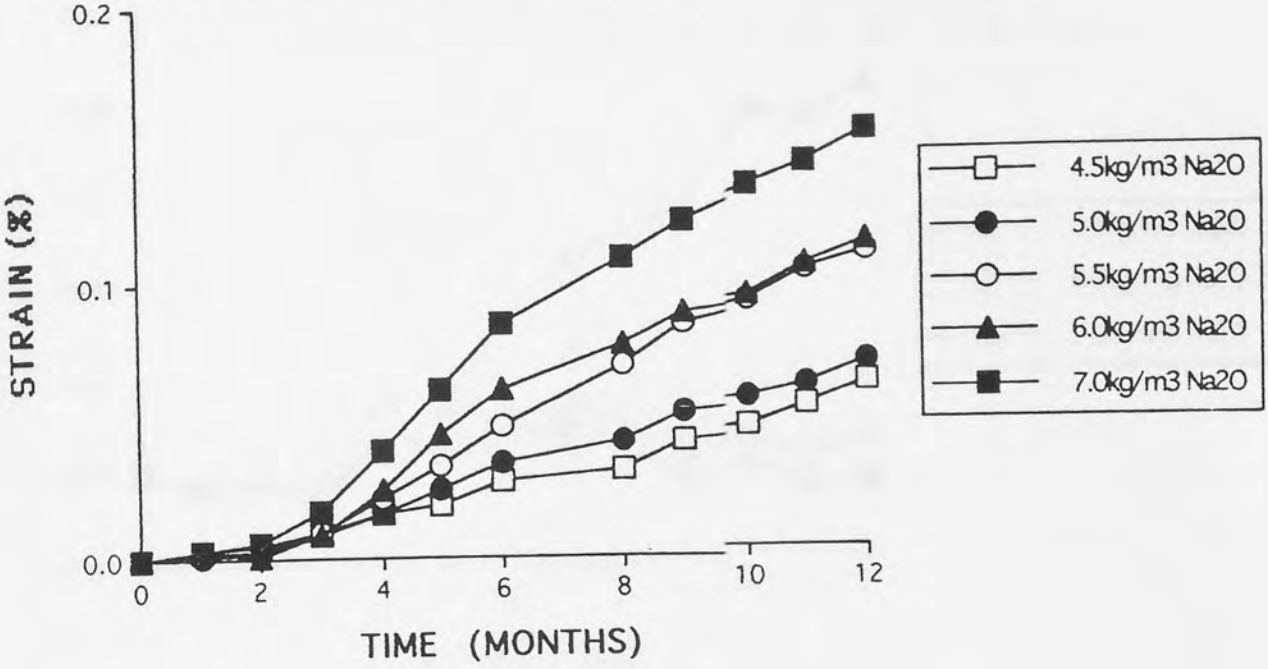


FIG 3.6: Expansion (%) Vs time. For (RP) river gravel mixes at various initial alkali levels. Tested at 38oC and 100% RH.

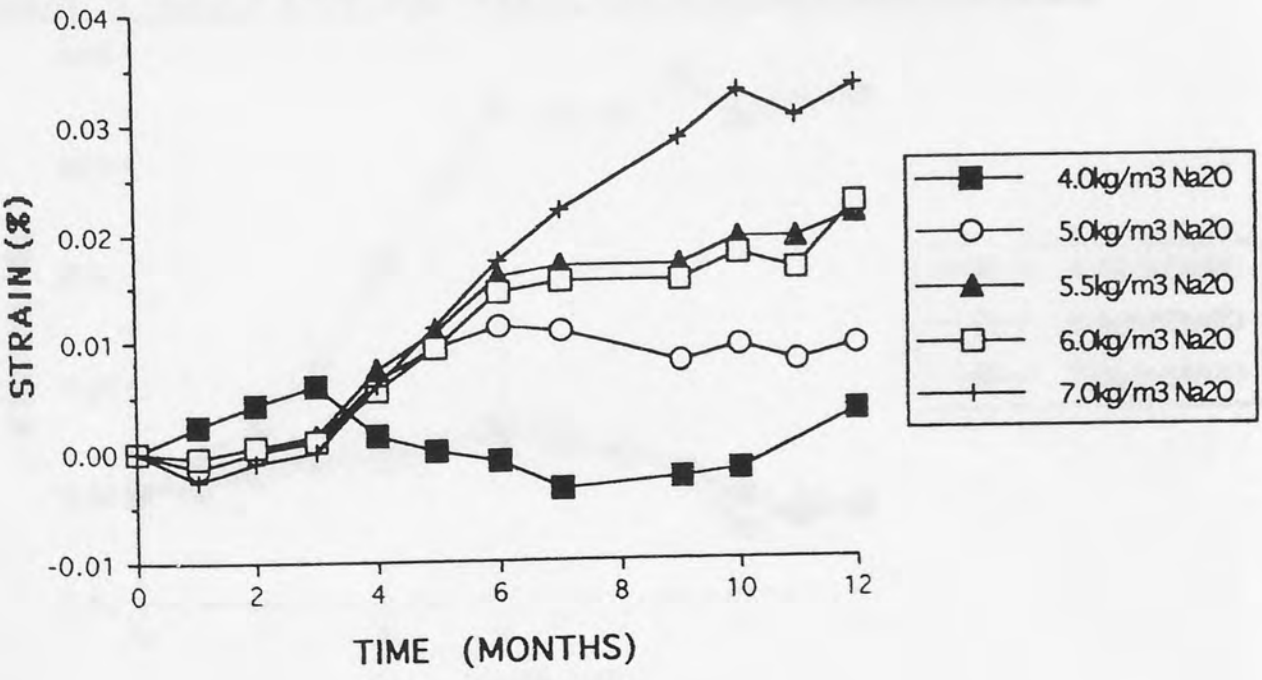

FIG 3.7: Expansion (%) Vs time. For (VQ) siltstone mixes at various initial alkali levels. Tested at 38oC and 100% RH.

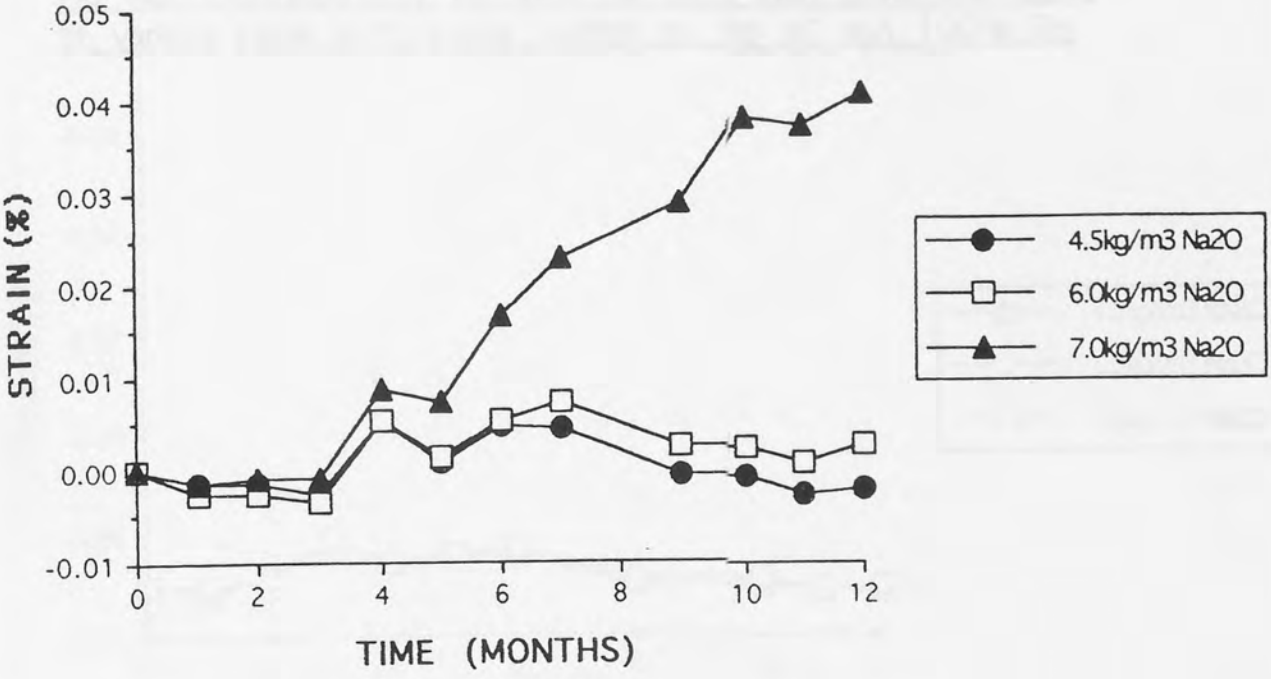


FIG 3.8: Expansion (%) Vs time. For 50% coarse aggregate (TV) gravel mixes at various initial alkali levels. Tested at 38oC and 100% RH.

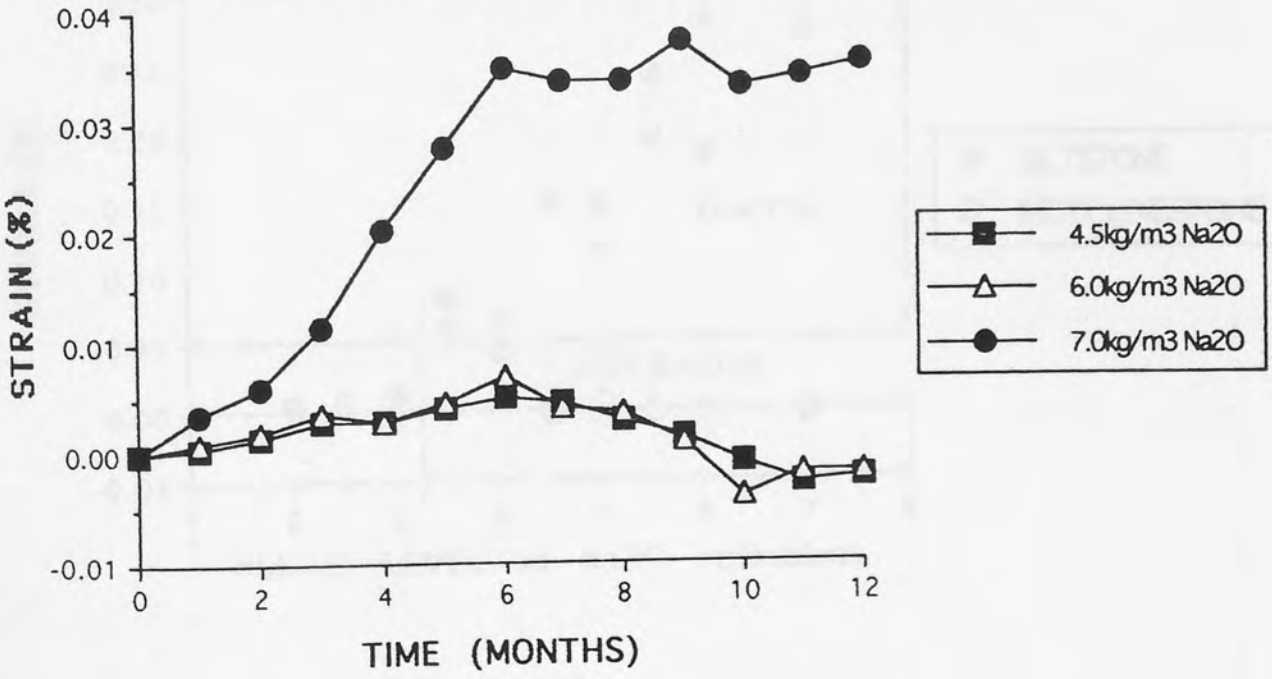

FIG 3.9: Expansion (%) Vs time. For (CL)) inert limestone mixes at various initial alkali levels. Tested at 38 oC and 100% RH.

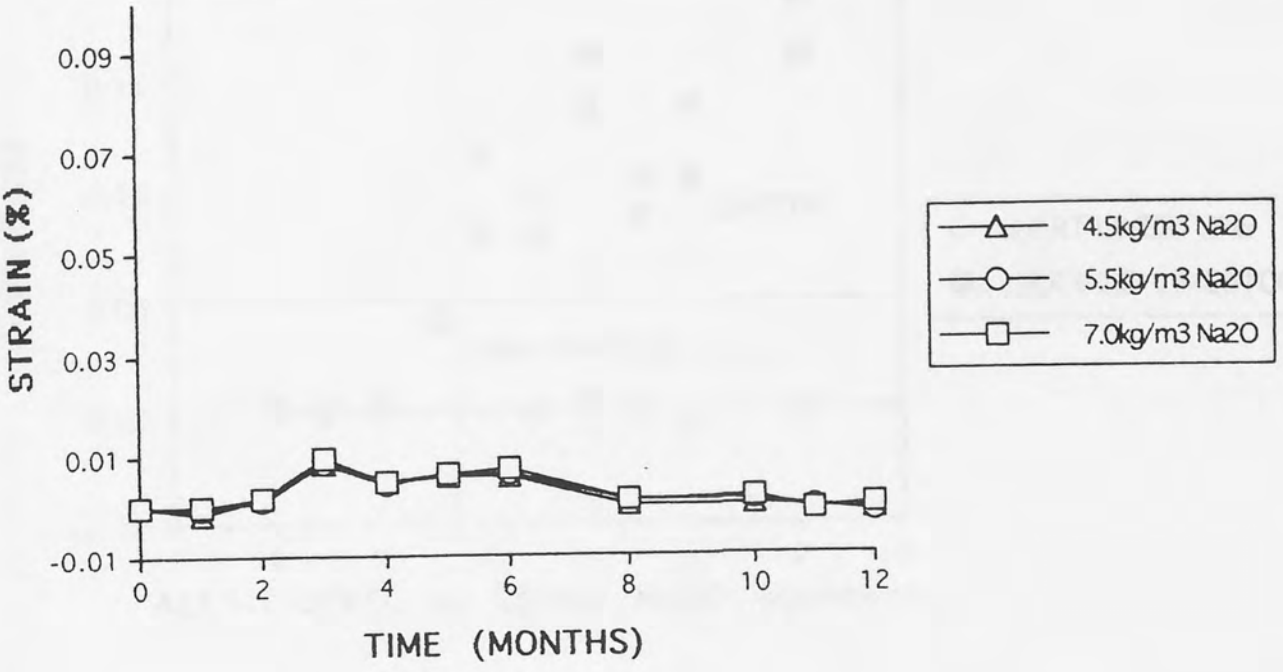


FIG 3.10: Expansion of siltstone and inert aggregate concrete prisms at various alkali levels after 12 months.

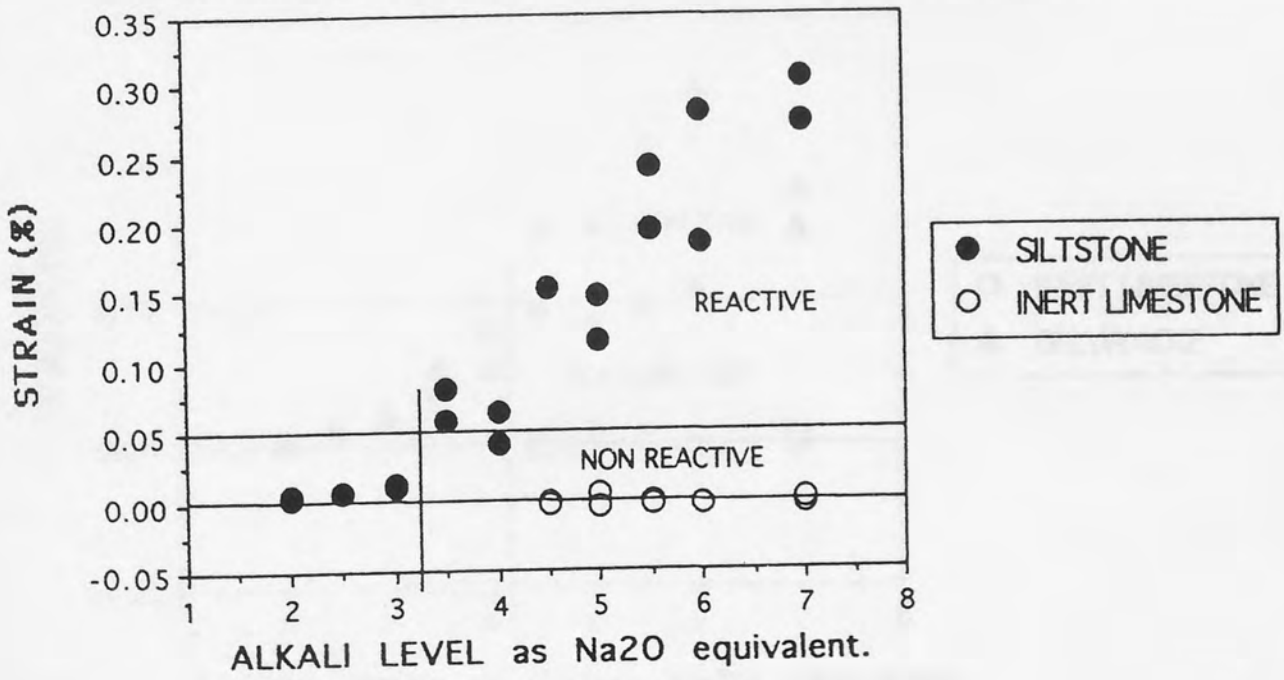

FIG 3.11: Expansion of silicified limestone and inert aggregate concrete prisms at different alkali levels after 12 months.

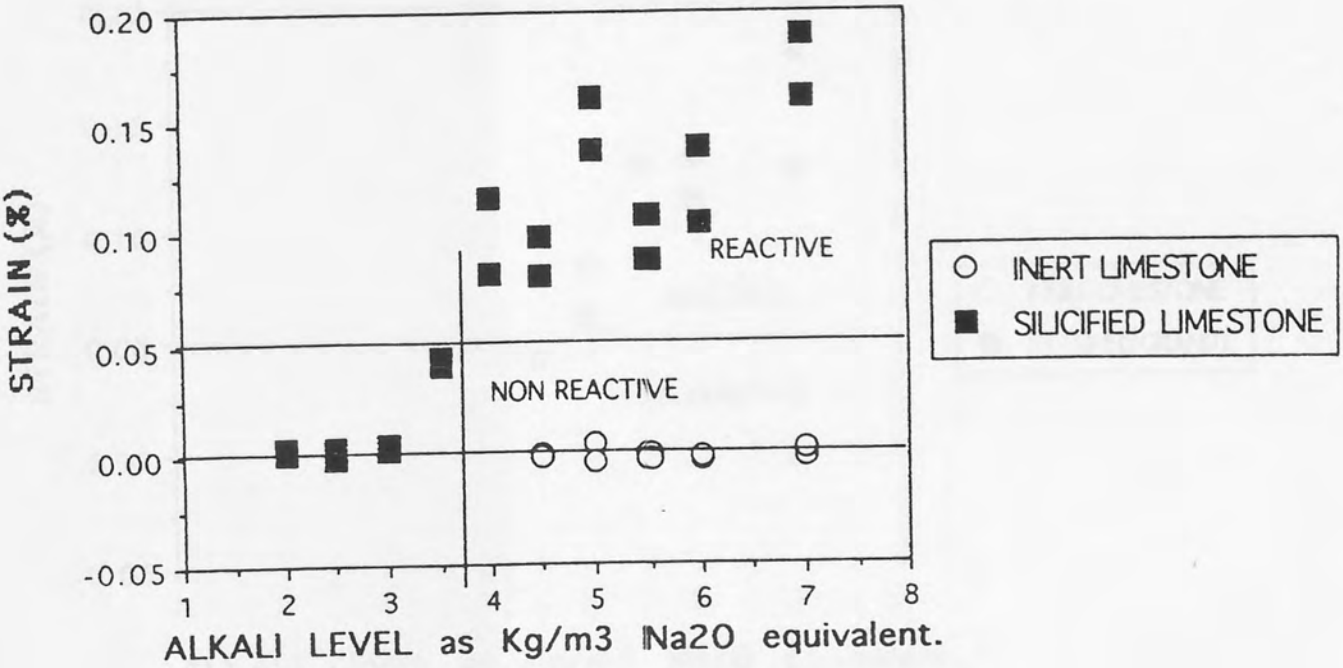


FIG 3.12: Expansion of greywacke and inert aggregate concrete prisms at different alkali levels after 12 months.

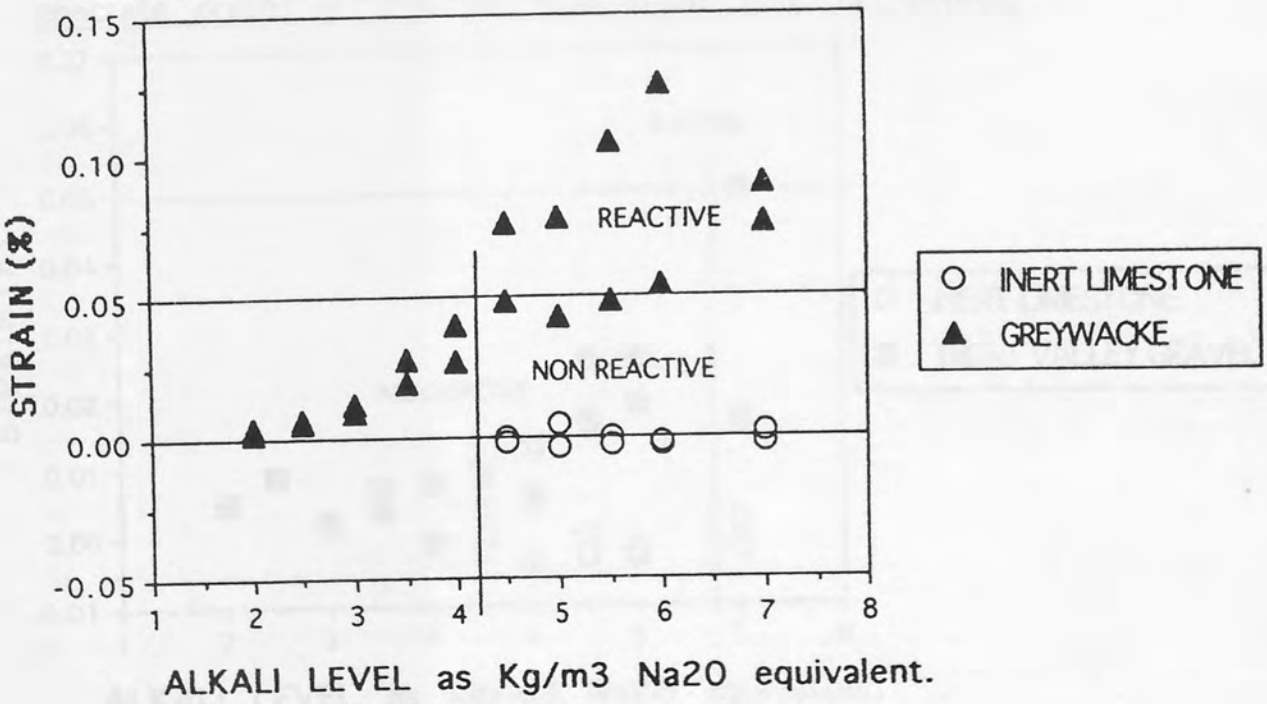

FIG 3.13: Expansion of strained granite and inert aggregate concrete prisms at different alkali levels after 12 months.

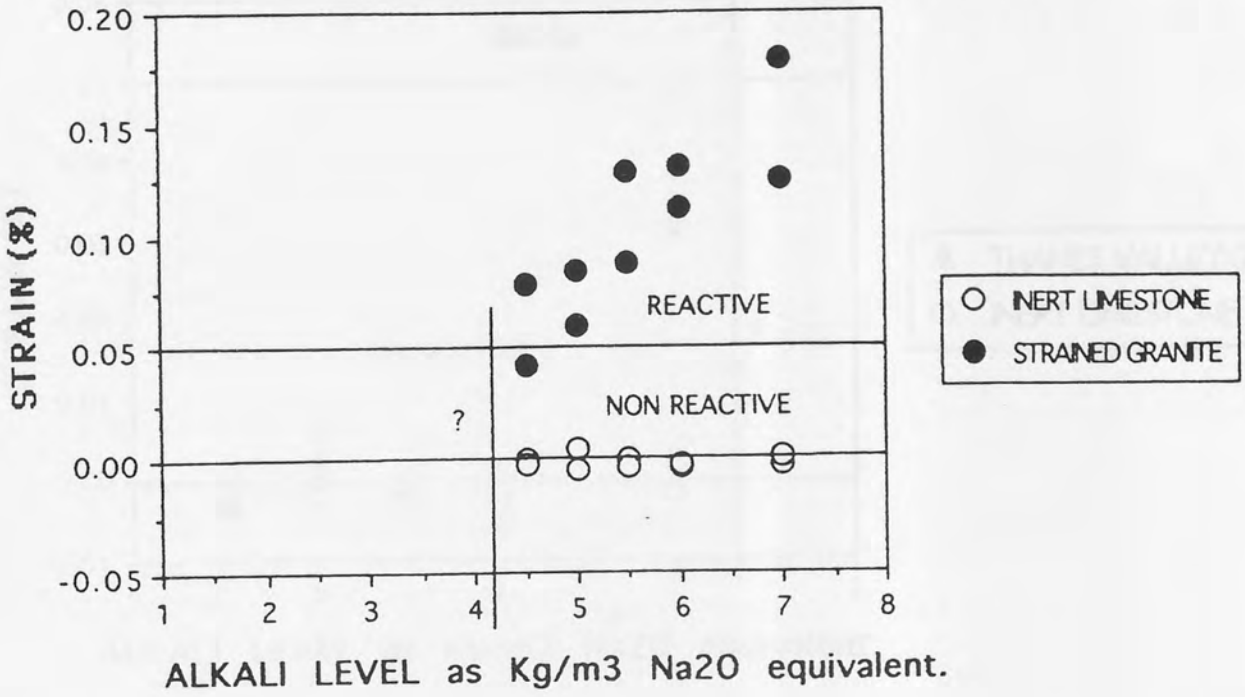


FIG 3.14: Expansion of Trent Valley gravel and inert aggregate concrete prisms at different alkali levels after 12 months.

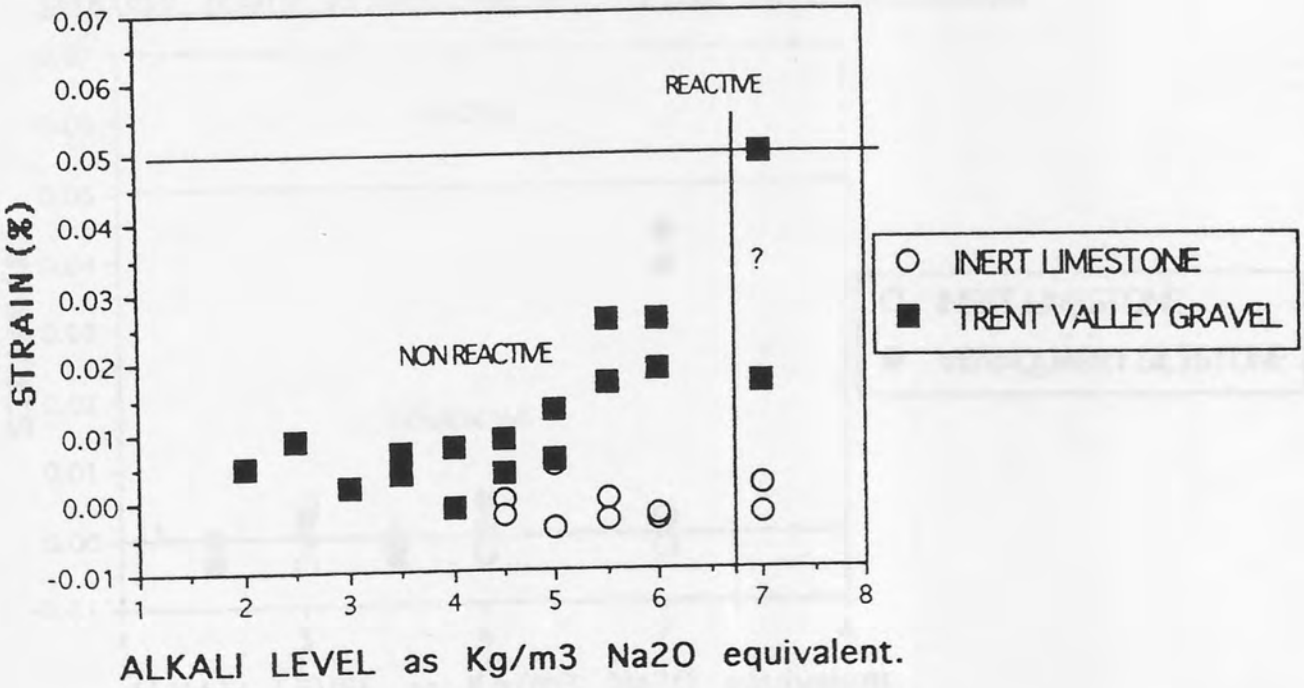

FIG 3.15: Expansion of Thames Valley gravel and inert aggregate concrete prisms at different alkali levels after 12 months.

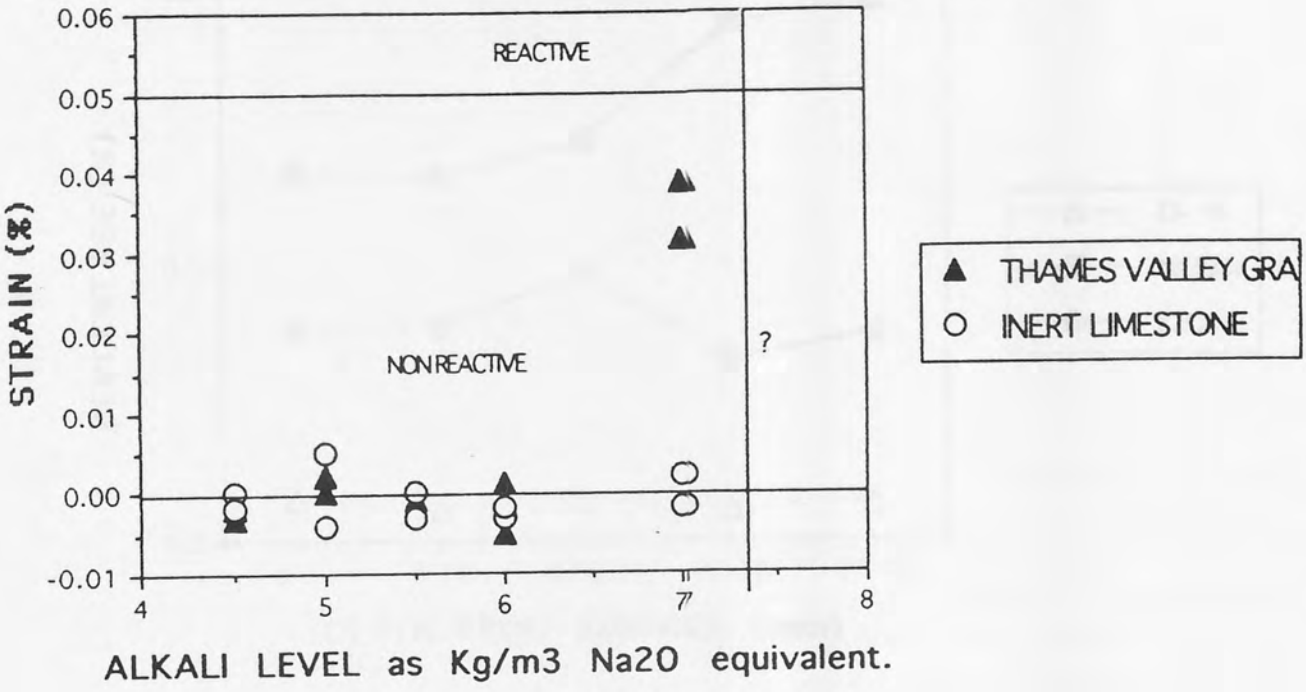


FIG 3.16: Expansion of Venn Quarry siltstone and inert aggregate concrete prisms at different alkali levels after 12 months.

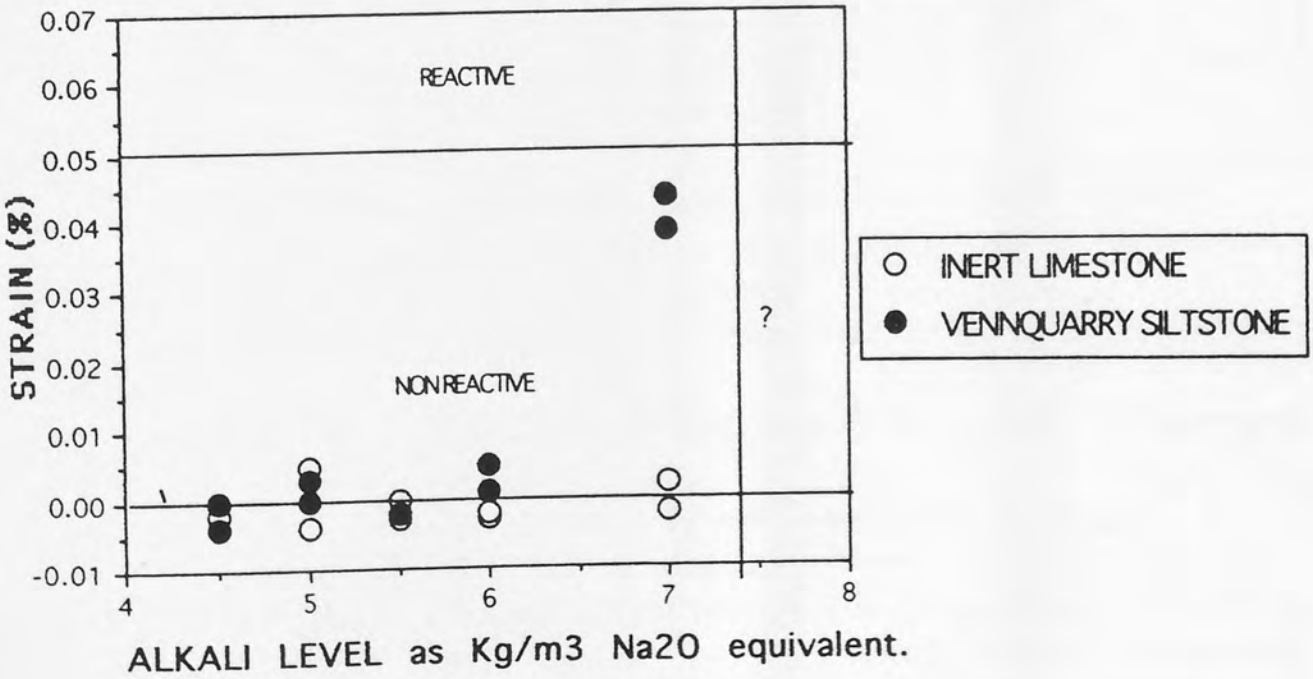

FIG 3.17: Chemical profile through a (DR) siltstone concrete prism with initial alkali content of 7 kg/m3 Na2Oe. Taken after 12 months of testing.

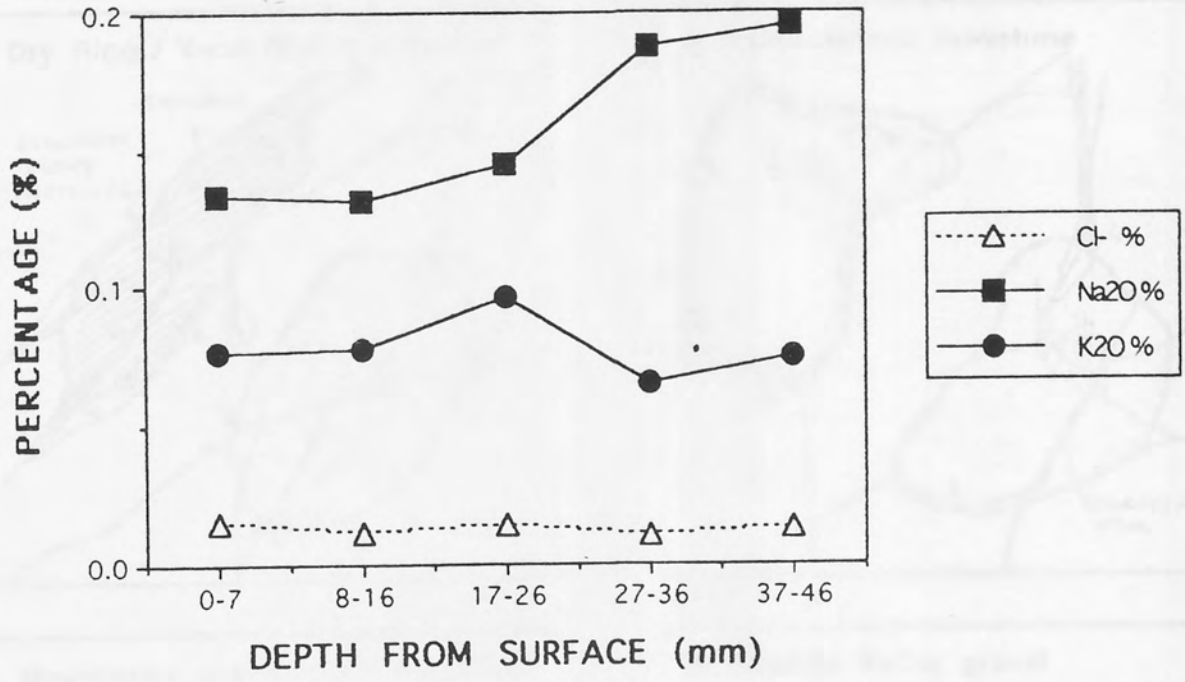

**FIGURE 3.18: Diagrammatic sketch of the various forms of ASR microcracking taken by the reactive aggregates.**

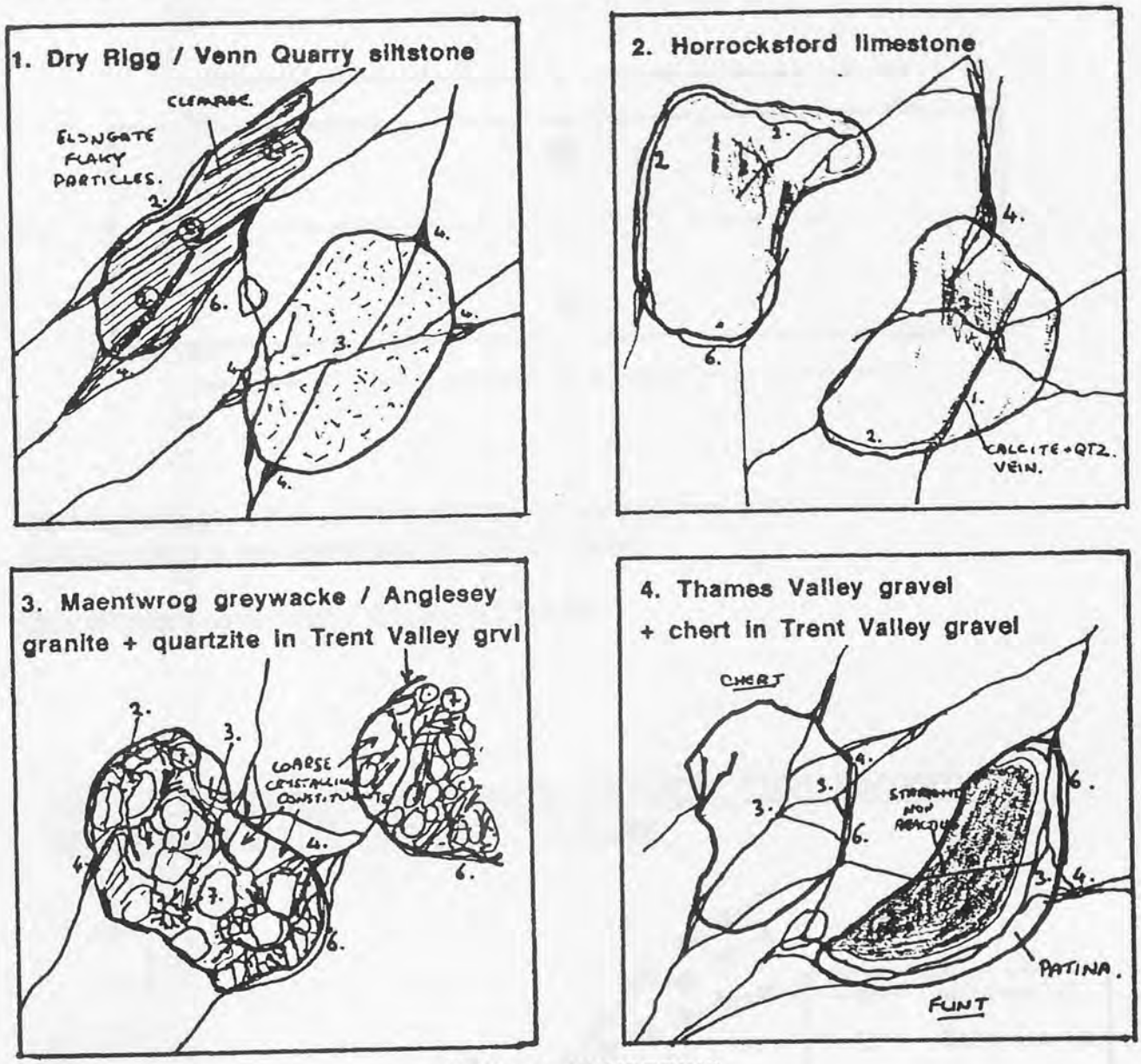


**KEY TO NUMBERING**

1. Microcracks developing from area or band rich in microcrystalline quartz.
2. Pseudoadhesion cracks, (Microcracks located in the vicinity of the aggregate particle edge but, still with the aggregate material).
3. Divergent microcrack system centred on areas rich in chert or micro crystalline quartz.
4. Dendritic patterns of microcracks and 'plug deposit' of gel found as microcrack leaves aggregate particle for cement paste.
5. Microcracking running with the rocks inherent cleavage or lineations.
6. Involvement of adhesion cracks in overall ASR network.
7. Loss of progressively finer microcracks into the finer clastic material in the rocks matrix, (Minerals here usually include; quartz, muscovite, sericite and chlorite). Microcracking still divergent and does not affect the coarse clastic material that may include strained quartz.

(ALL SHOW A TENDANCY TO HAVE MICROCRACKS RUNNING WITH THE LONG AXIS OF THE AGGREGATE PARTICLE).

**Figure 4.1 Diagram showing the positions of the various sets of demec points on the concrete prisms, half immersed in salt solution and half left dry.**

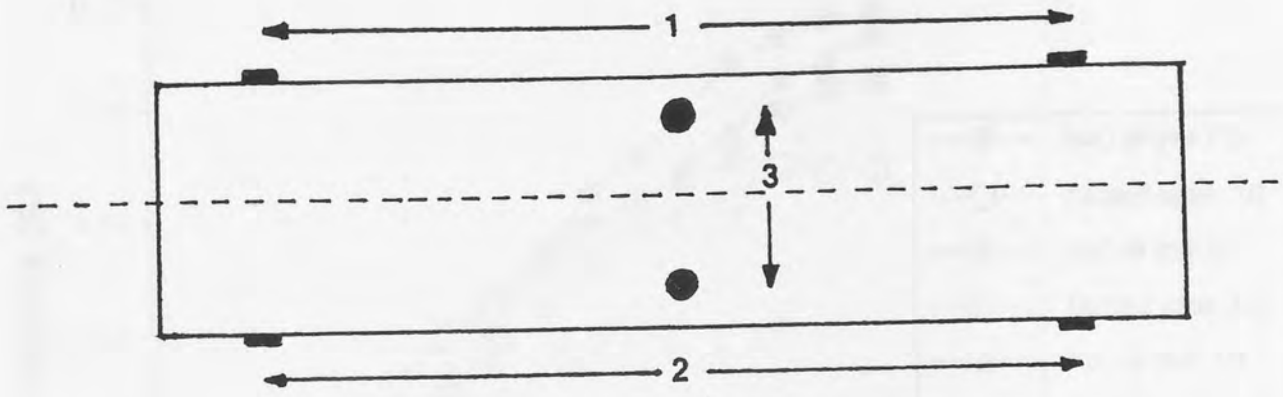


Demec point pairs 1 and 2 are approximately 200 mm apart.
Demec points 3 are approximately 50 mm apart.

Overall prism dimensions 250 X 75 X 75mm.

FIG 4.2: Expansion (%) Vs time (DR) SILTSTONE MIXES IMMERSED IN DISTILLED WATER AND SALT SOLUTION.

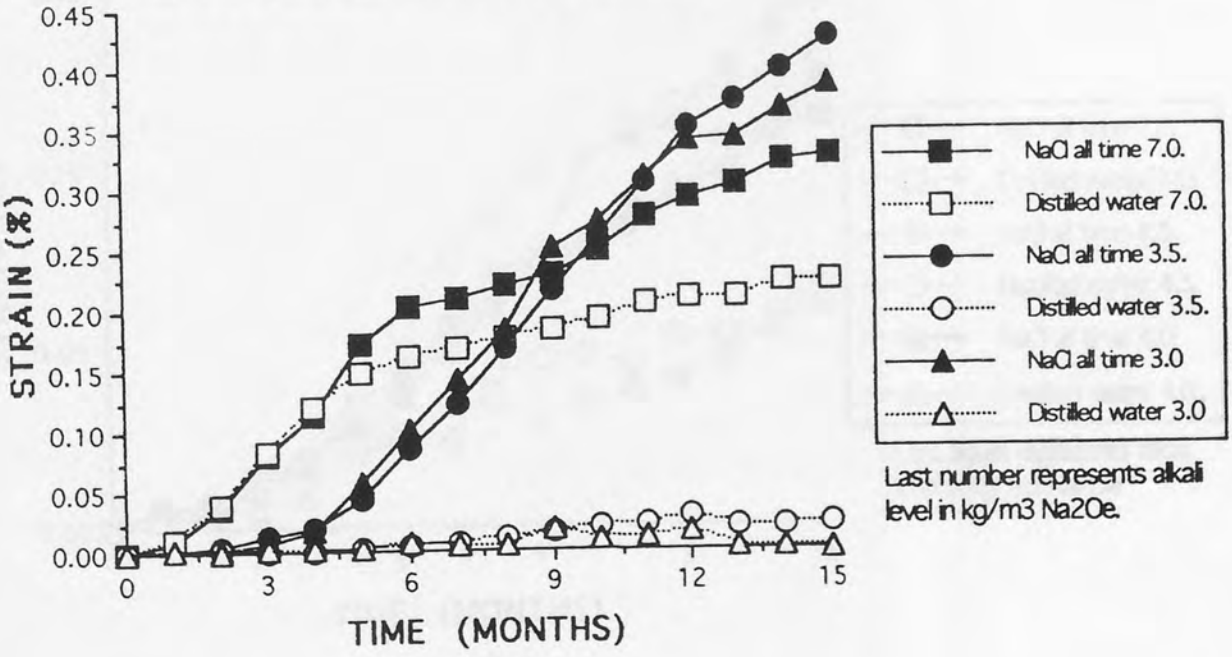

FIG 4.3: Expansion (%) Vs time (HL) LIMESTONE MIXES IMMERSED IN DISTILLED WATER AND SALT SOLUTION.

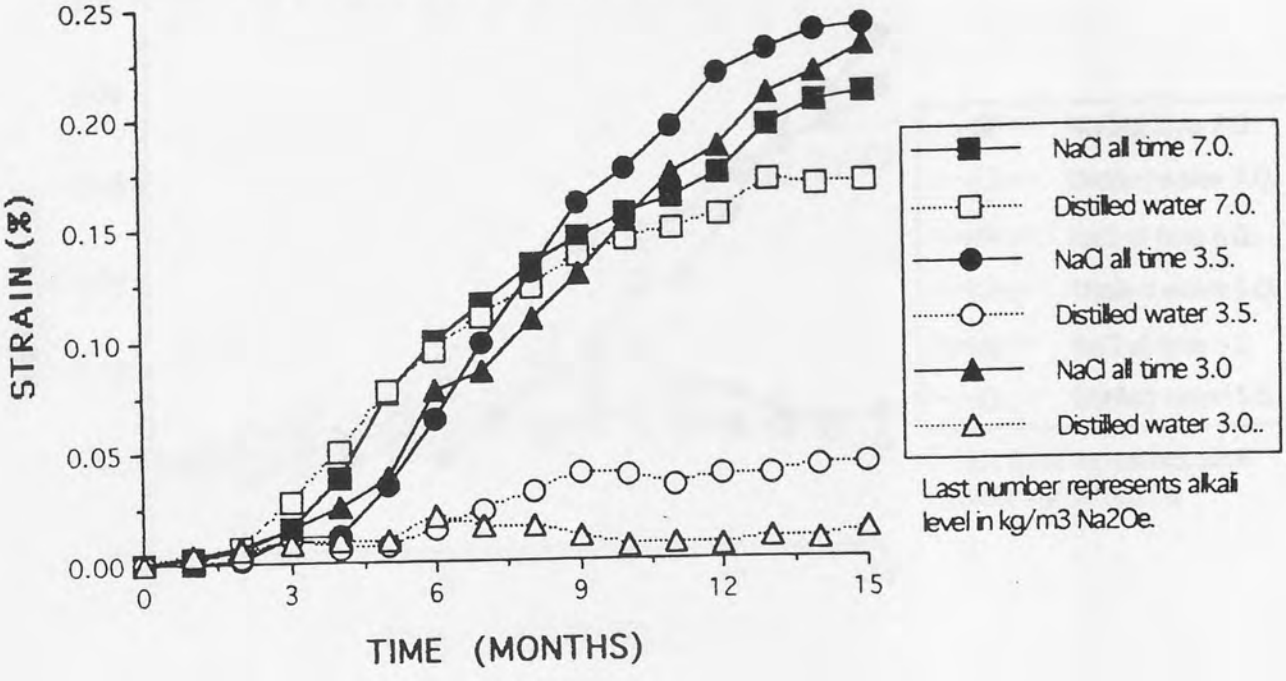


FIG 4.4: Expansion (%) Vs time (MD) GREYWACKE MIXES IMMERSED IN DISTILLED WATER AND SALT SOLUTION.

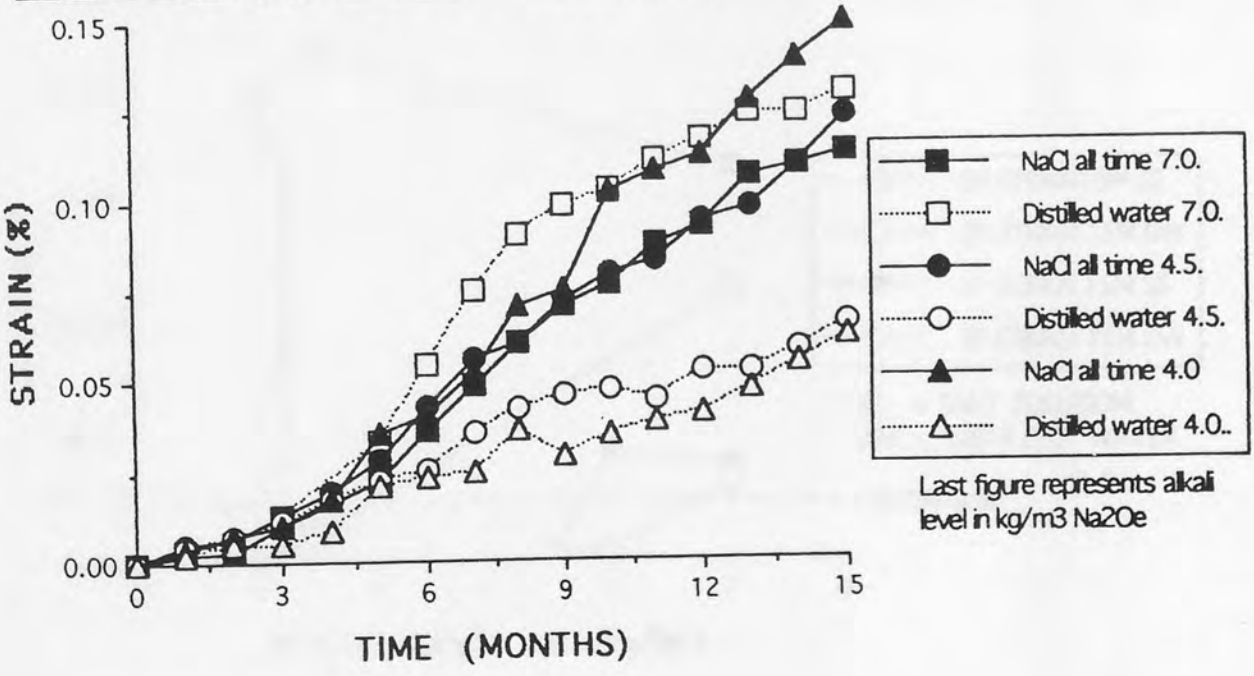

FIG 4.5: Expansion Vs time (RP) GRAVEL MIXES IMMERSED IN DISTILLED WATER AND SALT SOLUTION.

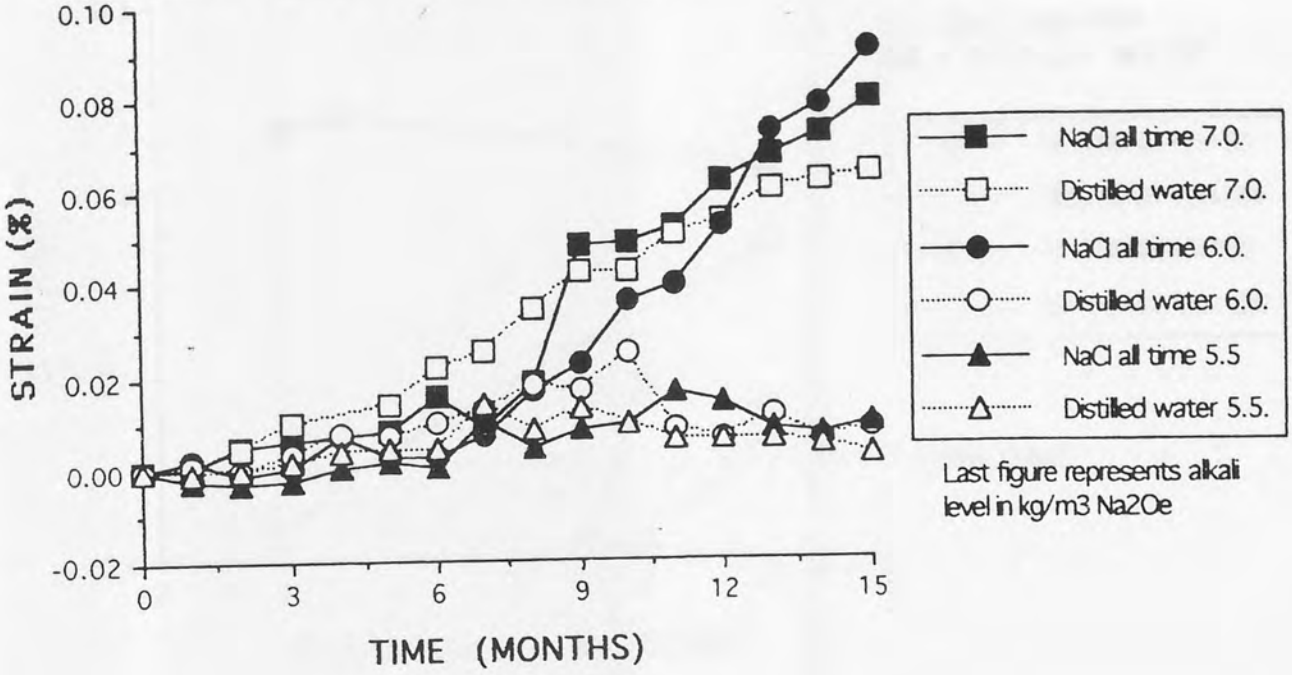


FIG 4.6: Effects of external salt solution on an ASR reactive siltstone (DR) and chert rich gravel (RP) after 15 months.

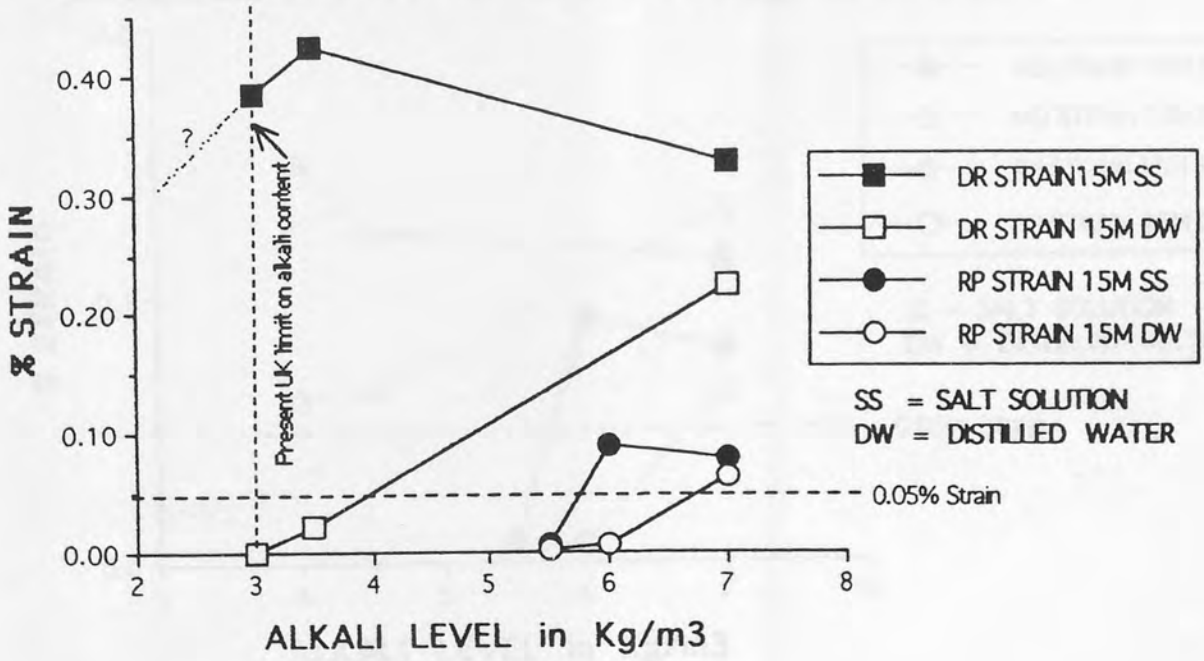

FIG 4.7: Effects of external salt solution on ASR reactive silicified limestone (HL) and a chert rich gravel (RP) after 15 months.

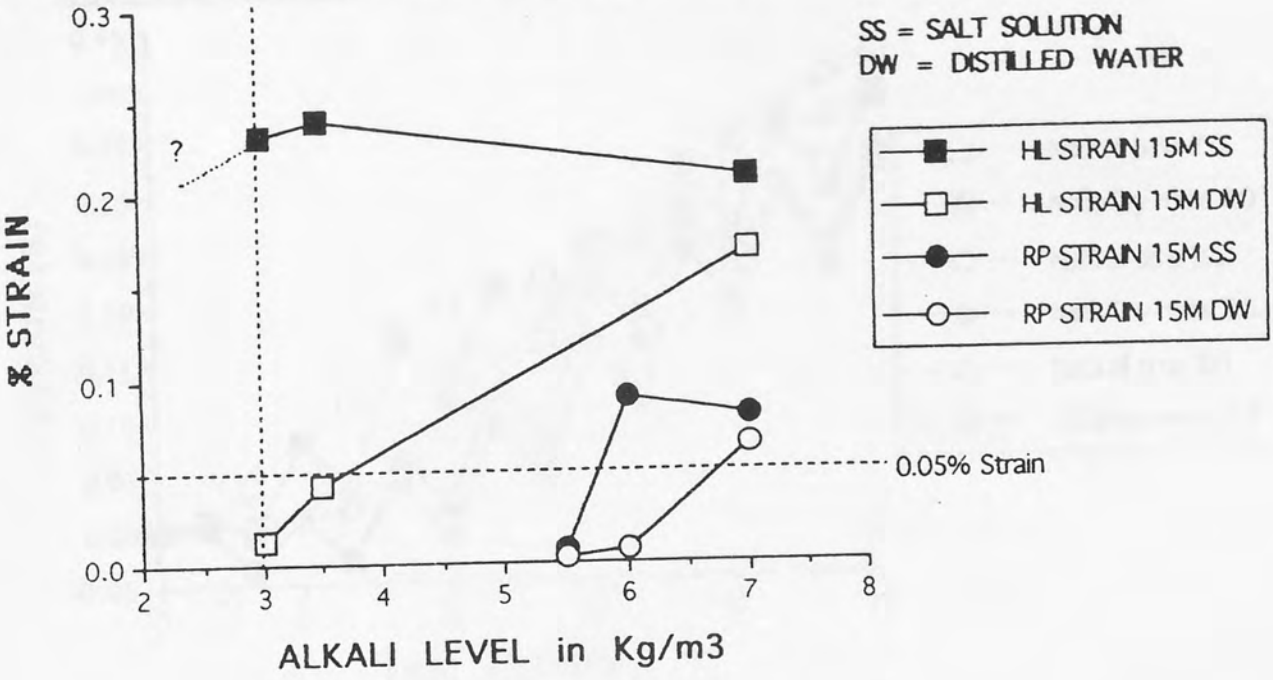


FIG 4.8: Effects of external salt solution on an ASR reactive greywacke (MD) and a chert rich gravel (RP) after 15 months.

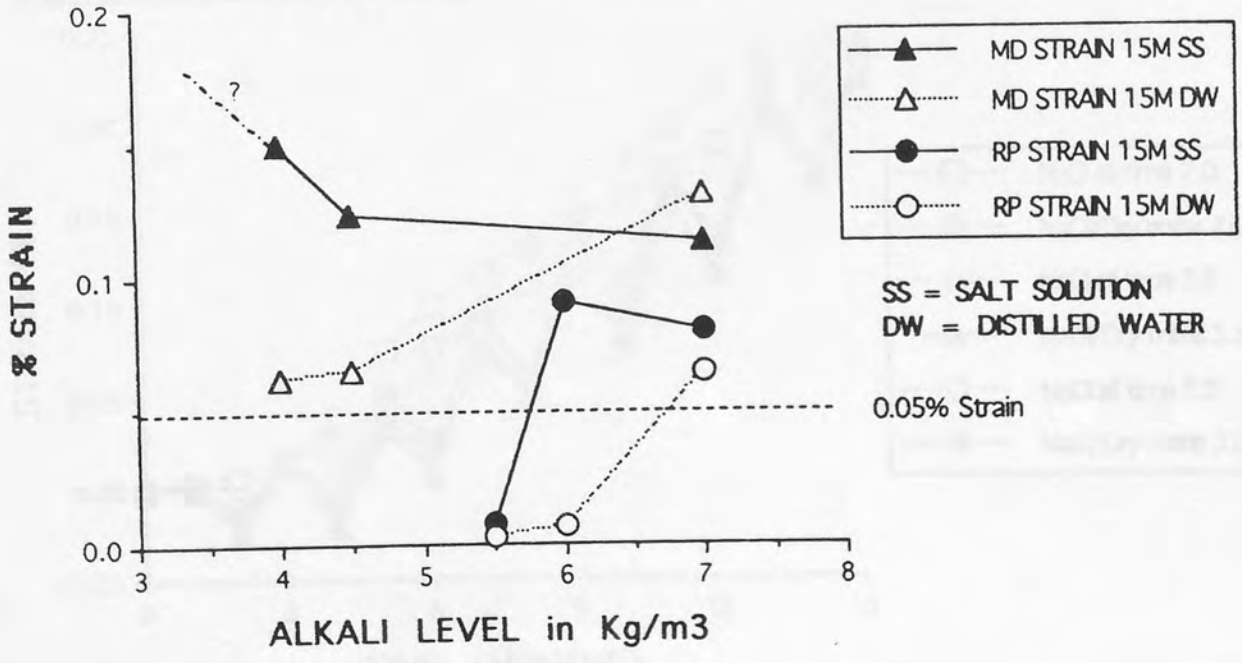

FIG 4.9: Expansion Vs time (DR) SILTSTONE MIXES IMMERSED IN SALT SOLUTION AND WET / DRY CYCLED IN SALT SOLUTION.

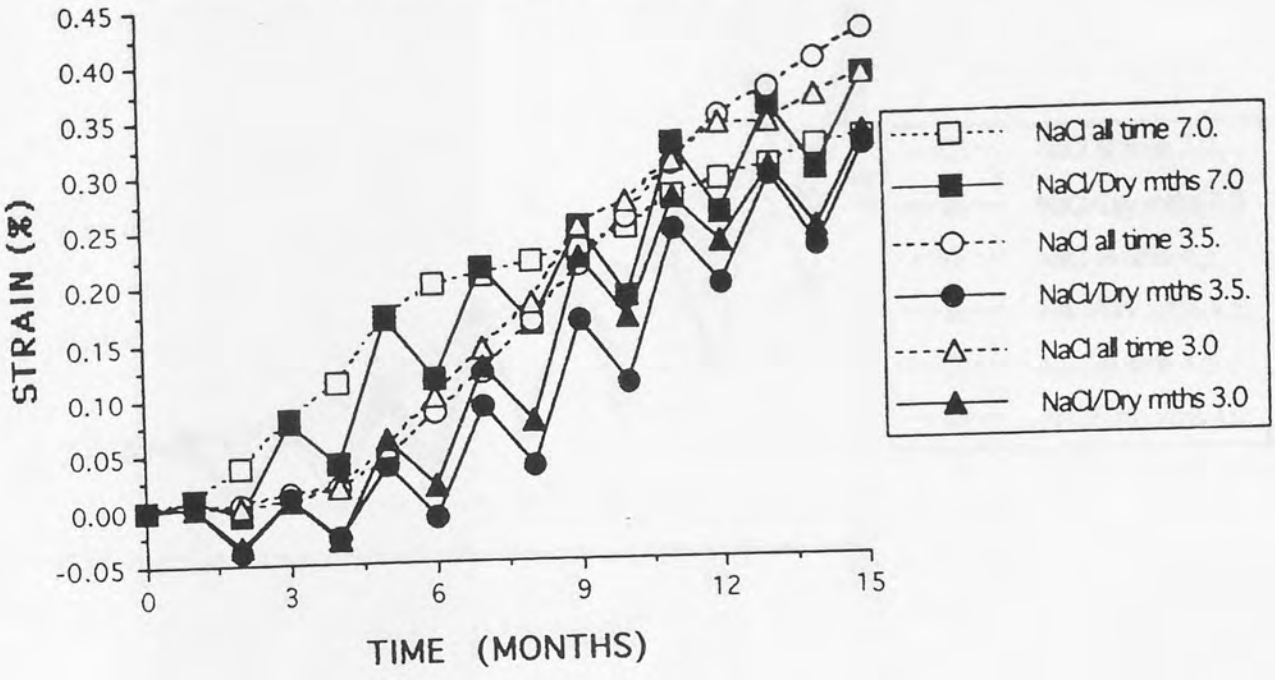


FIG 4.10: Expansion (%) Vs time (HL) LIMESTONE MIXES IMMERSED IN SALT SOLUTION AND WET / DRY CYCLED IN SALT SOLUTION.

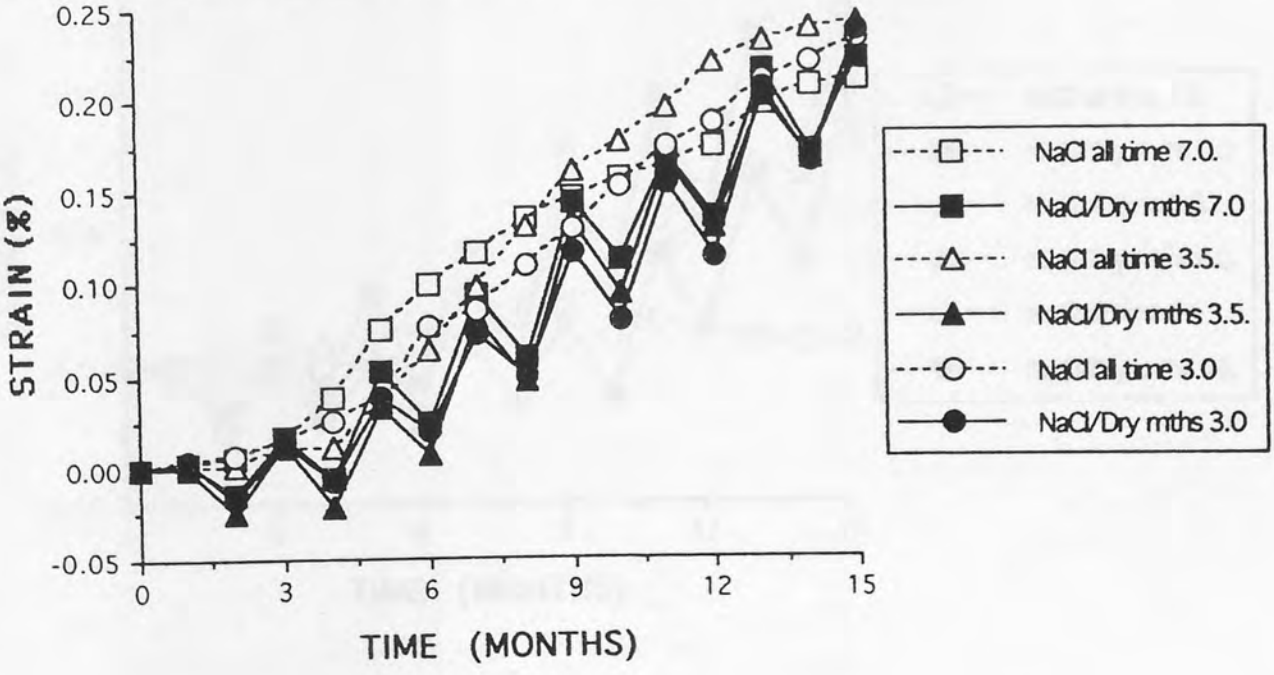

FIG 4.11: Expansion (%) Vs time (MD) GREYWACKE MIXES IMMERSED IN SALT SOLUTION AND WET / DRY CYCLED IN SALT SOLUTION.

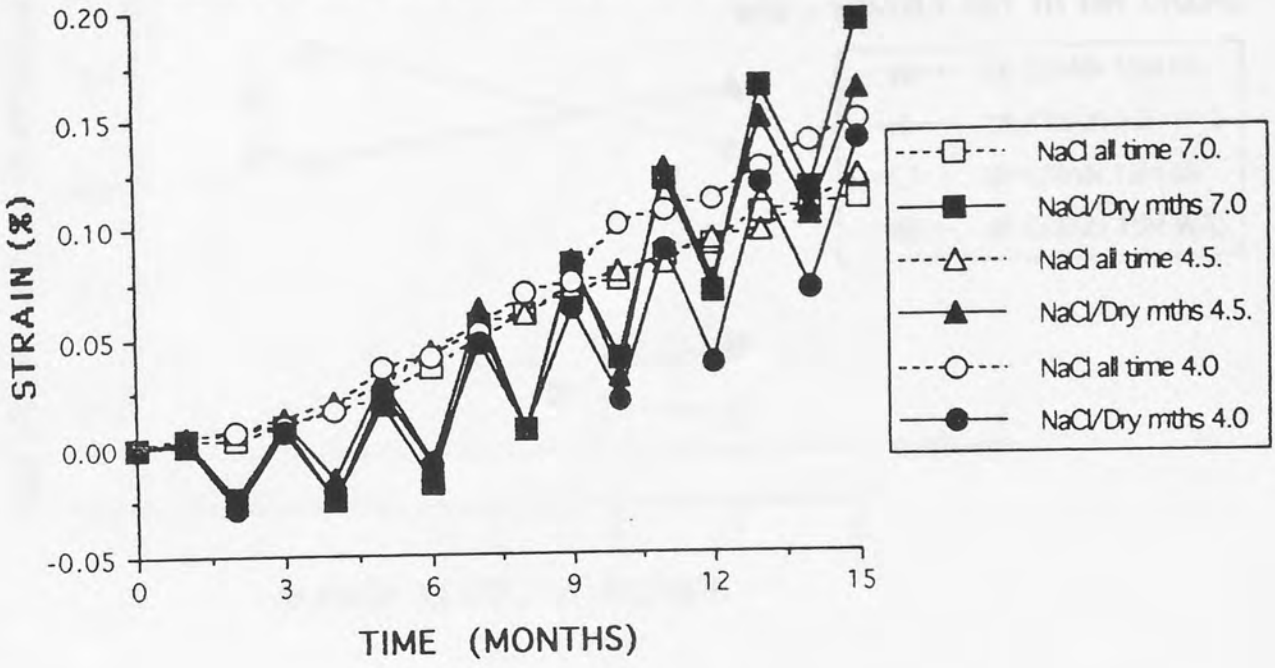


FIG 4.12: Expansion (%) Vs time (RP) GRAVEL MIXES IMMERSED IN SALT SOLUTION AND WET / DRY CYCLED IN SALT SOLUTION.

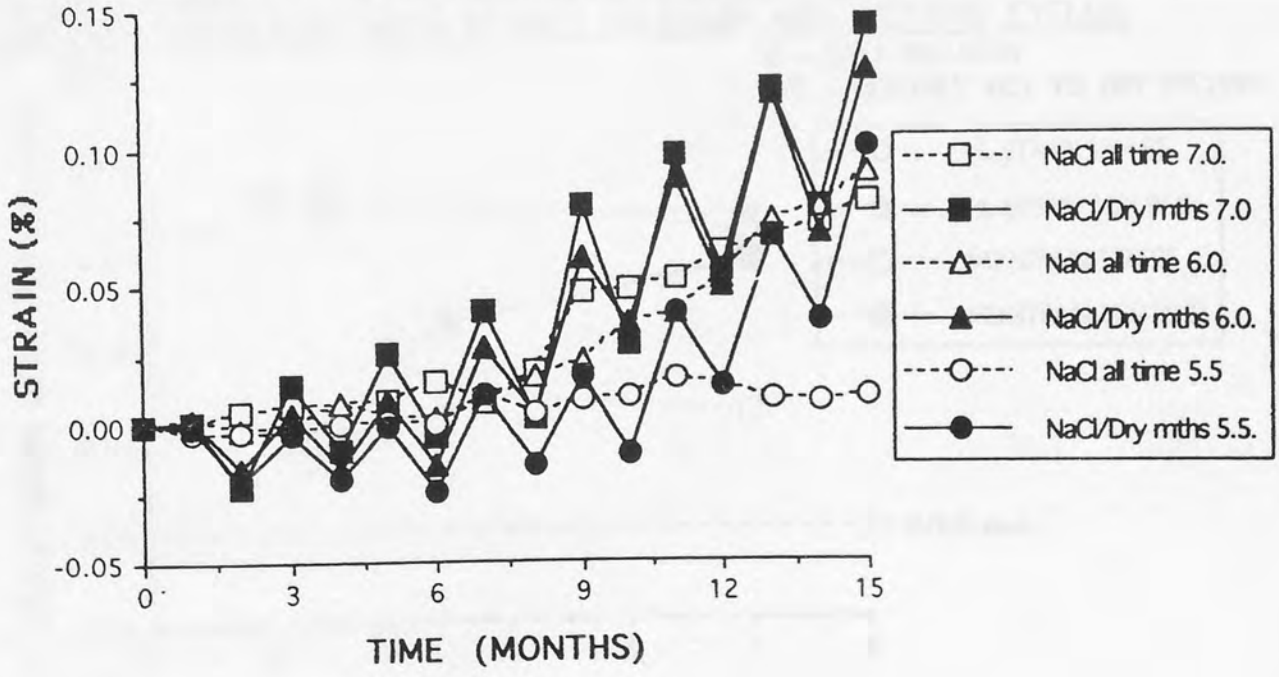

FIG 4.13: Expansion (%) at 15 months Vs initial alkali content FOR (DR) SILTSTONE AND (RP) GRAVEL MIXES IN SALT SOLUTION AND WET/DRY CYCLED.

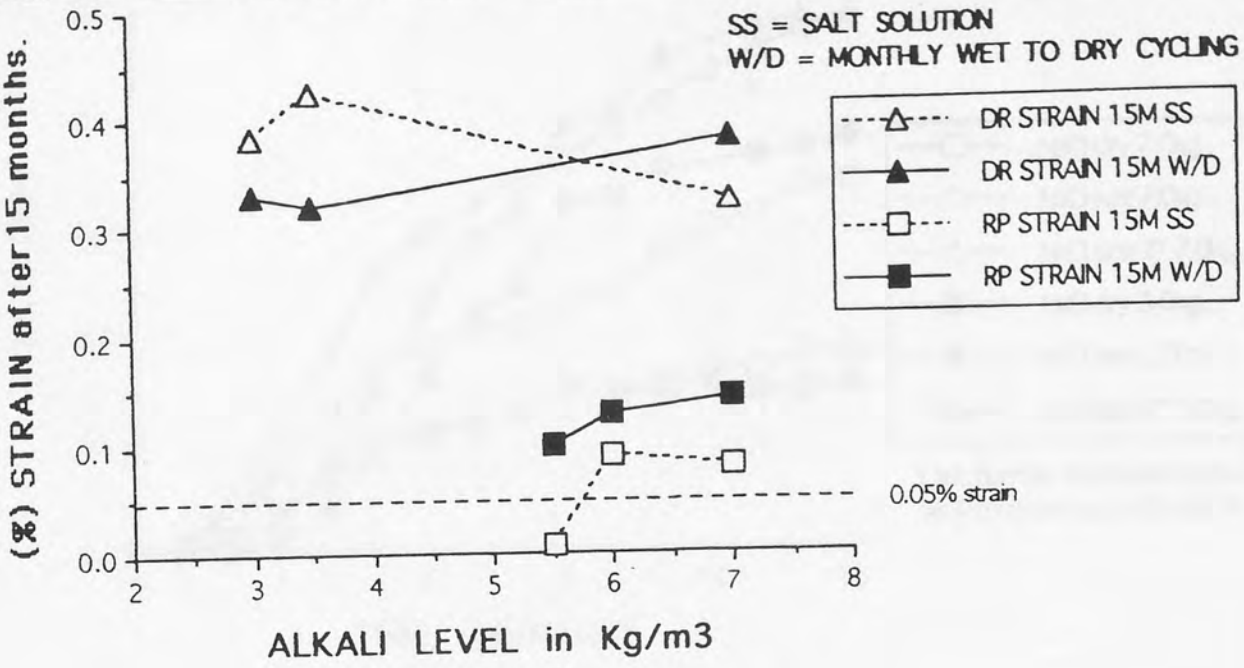


FIG 4.14: Expansion (%) at 15 months Vs initial alkali content (HL) LIMESTONE AND (MD) GREYWACKE MIXES IN SALT SOLUTION AND WET/DRY CYCLED.

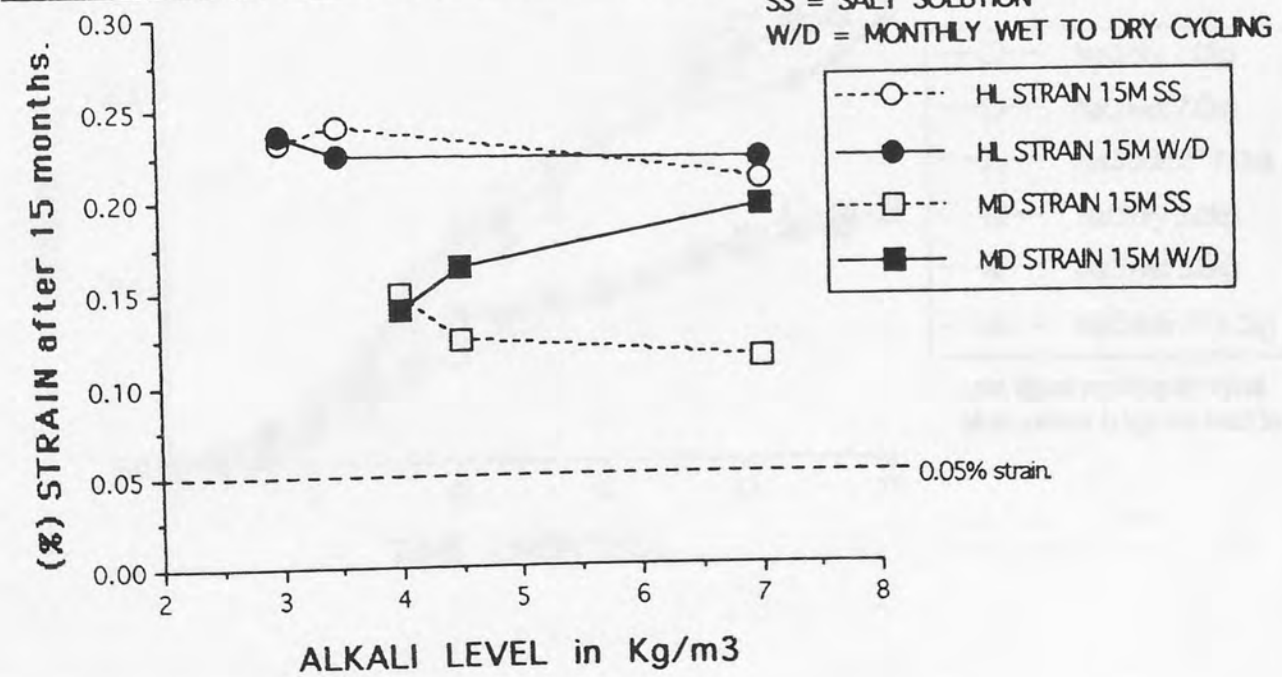

FIG 4.15: Expansion (%) Vs time TWO (DR) SILTSTONE MIXES HALF IMMERSED IN SALT SOLUTION.

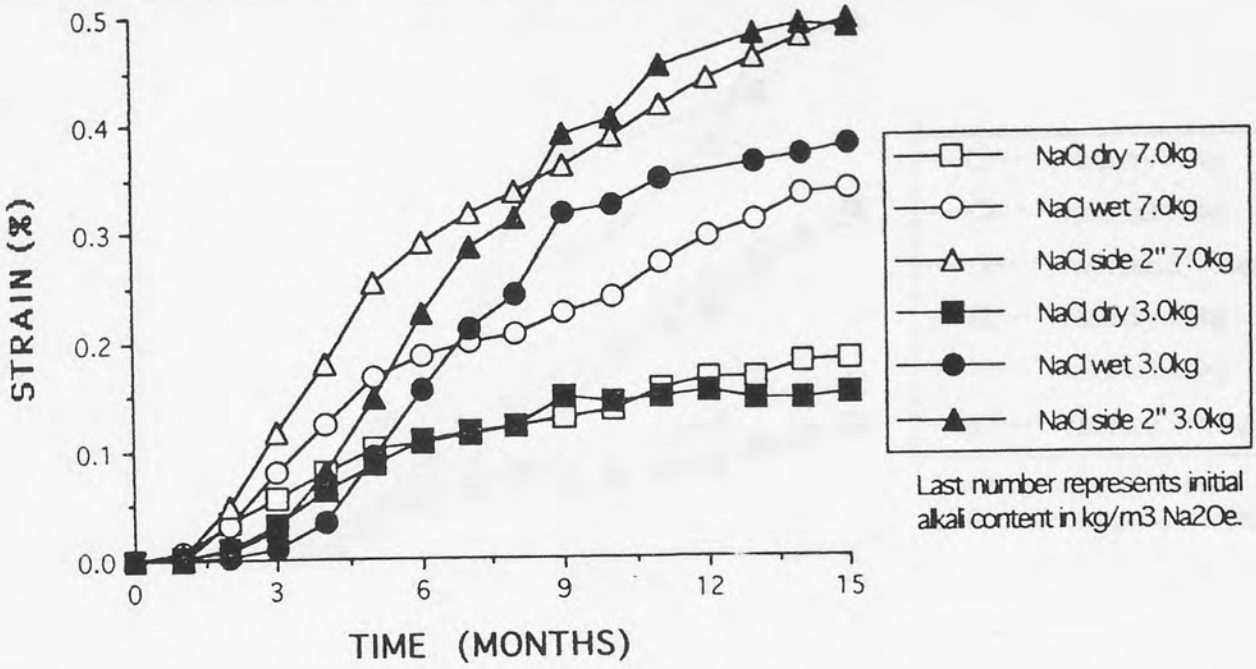


FIG 4.16: Expansion (%) Vs time TWO (HL) LIMESTONE MIXES HALF IMMERSED IN SALT SOLUTION.

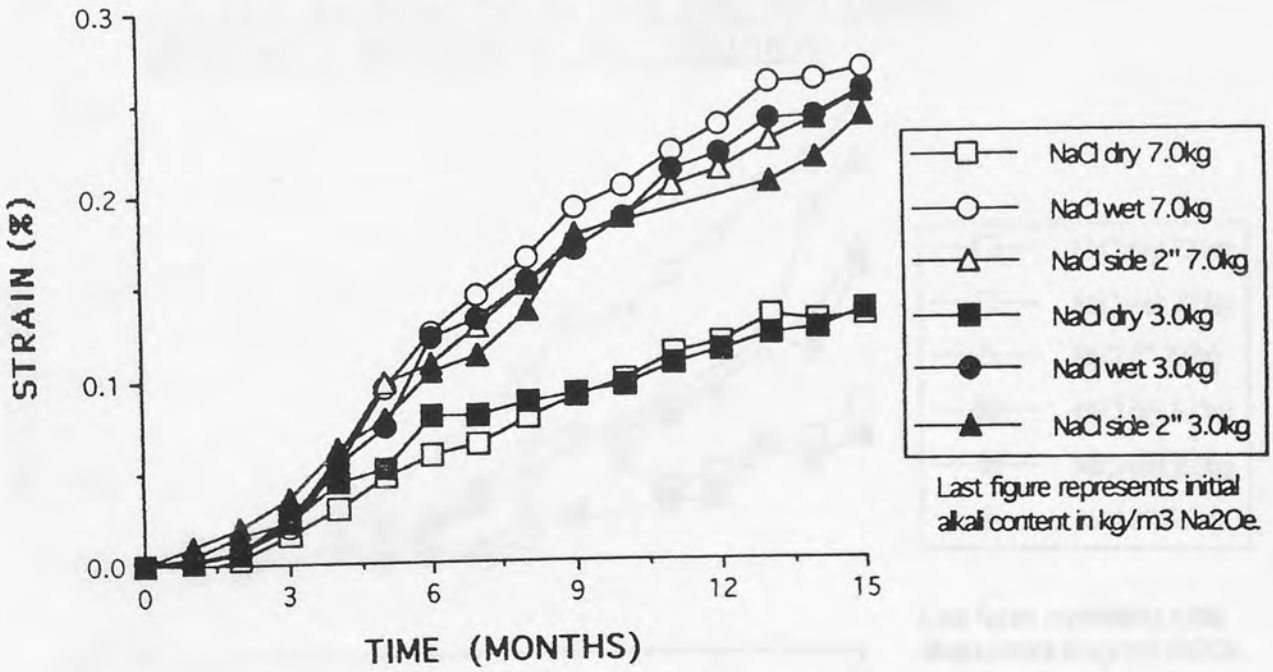

FIG 4.17: Expansion (%) Vs time TWO (MD) GREYWACKE MIXES HALF IMMERSED IN SALT SOLUTION.

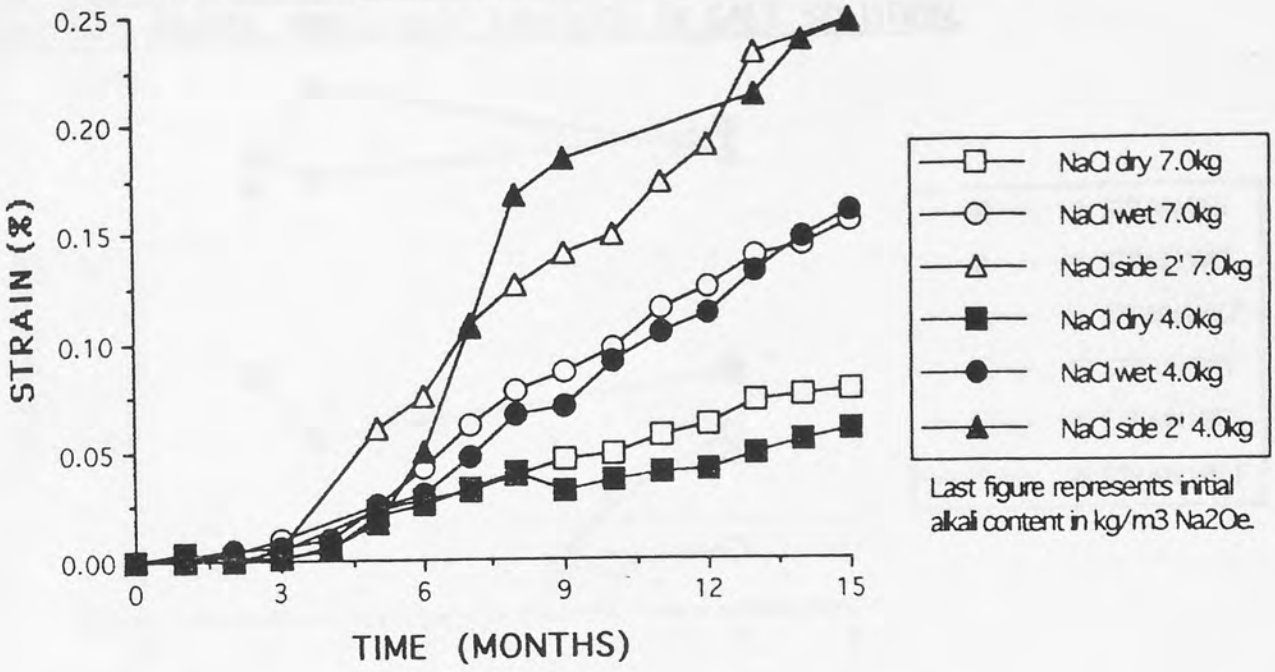


FIG 4.18: Expansion (%) Vs time TWO (RP) GRAVEL MIXES HALF IMMERSED IN SALT SOLUTION.

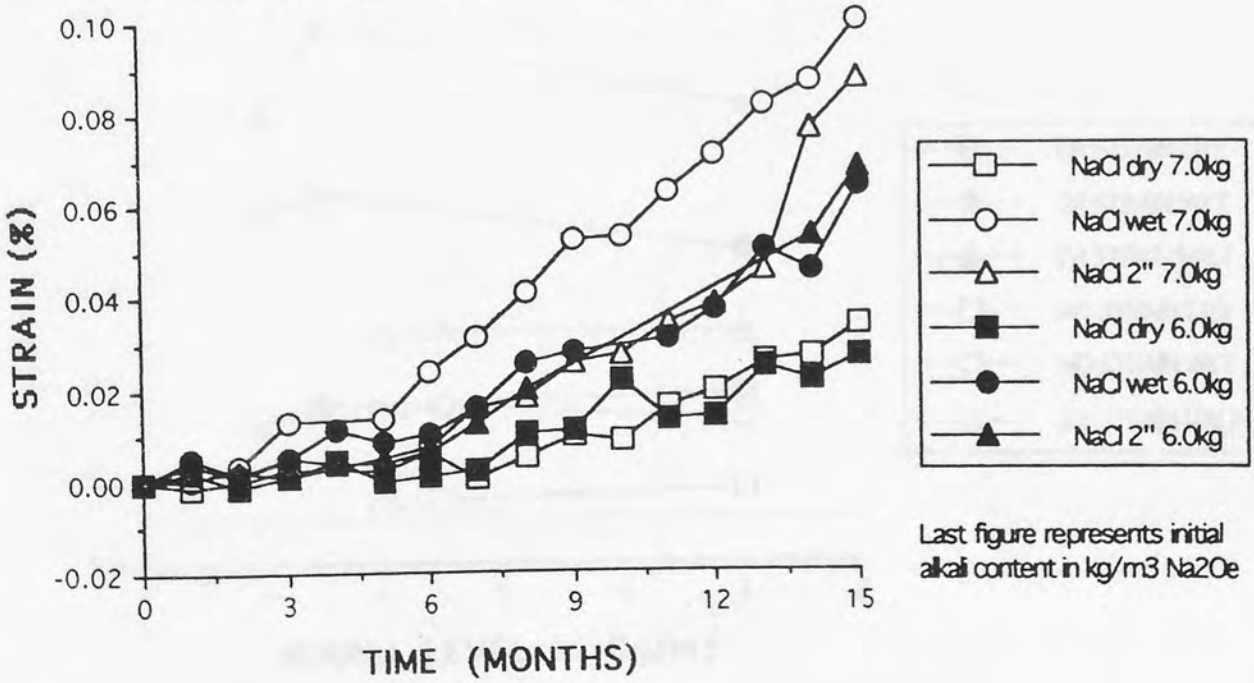

FIG 4.19: Expansion (%) Vs Alkali level at 15 months. (HL) LIMESTONE AND (RP) GRAVEL MIXES HALF IMMERSED IN SALT SOLUTION.

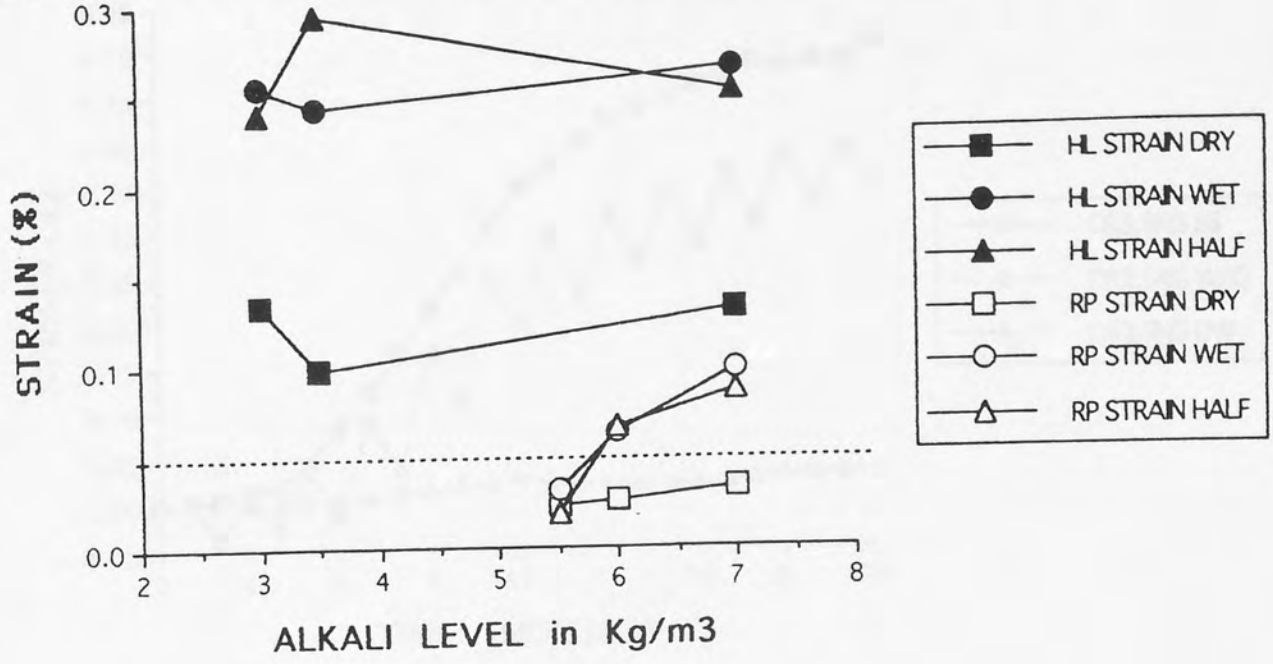


FIG 4.20: Expansion (%) Vs Alkali level at 15 months. (DR) SILTSTONE AND (MD) GREYWACKE MIXES HALF IMMERSED IN SALT SOLUTION.

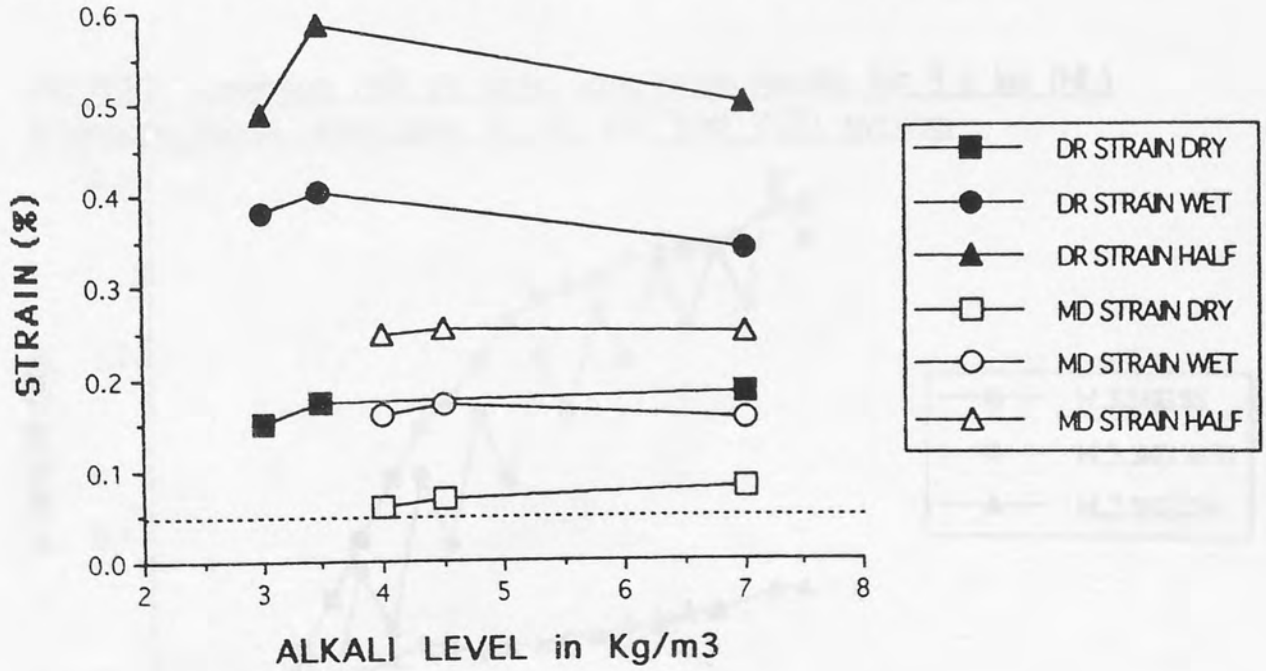

FIG 4.21: Expansion (%) Vs time. Long term results for 3.5 kg (DR) siltstone mixes. Immersion in SS DW and W/D cycling.

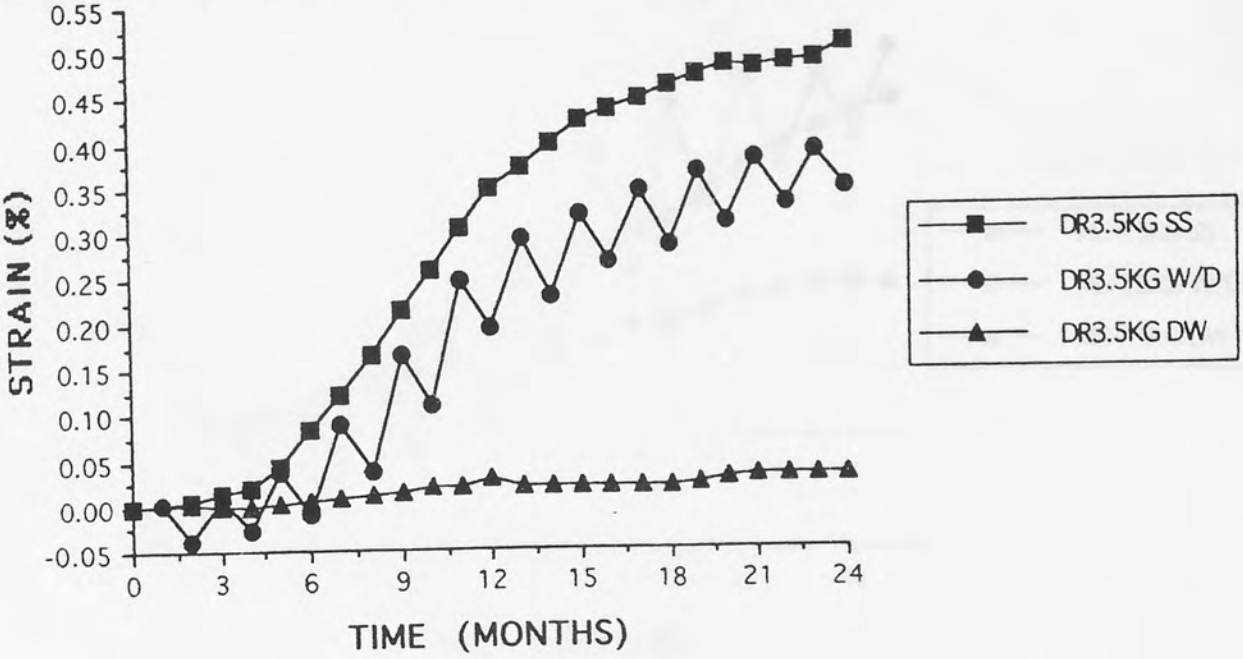


FIG 4.22: Expansion (%) Vs time. Long term results for 3.5 kg (HL) limestone mixes. Immersion in SS, DW and W/D cycling.

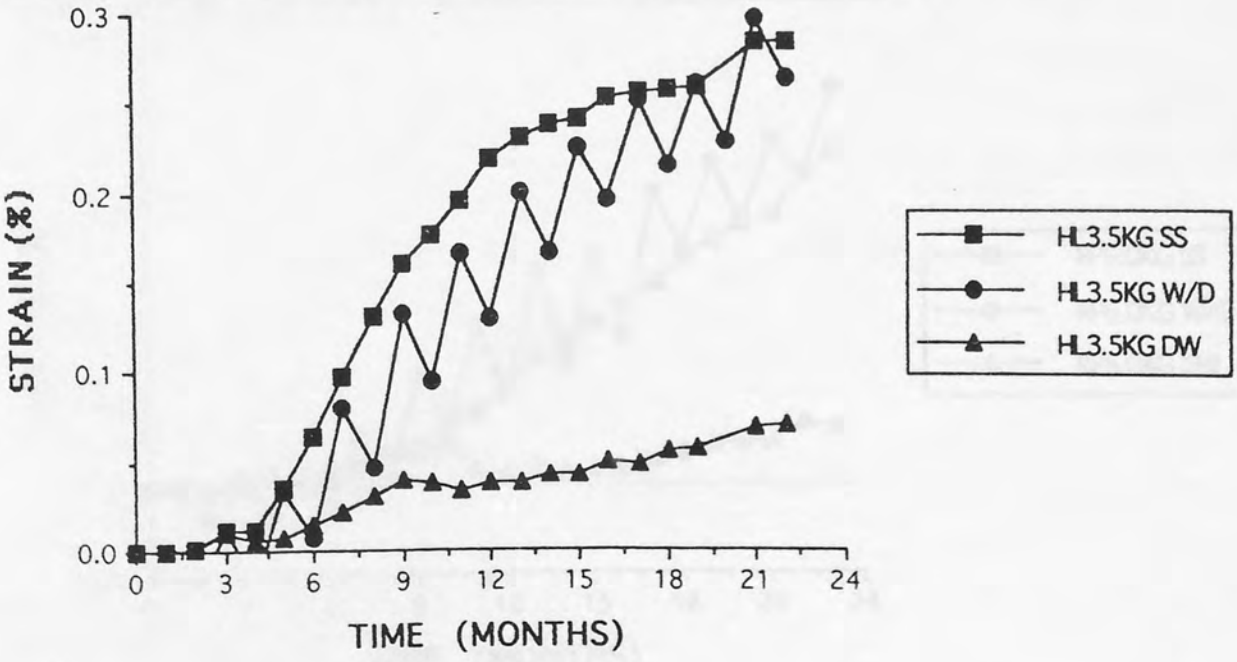

FIG 4.23: Expansion Vs time. Long term results for 4.5 kg (MD) greywacke mixes. Immersion in SS, DW and W/D cycling.

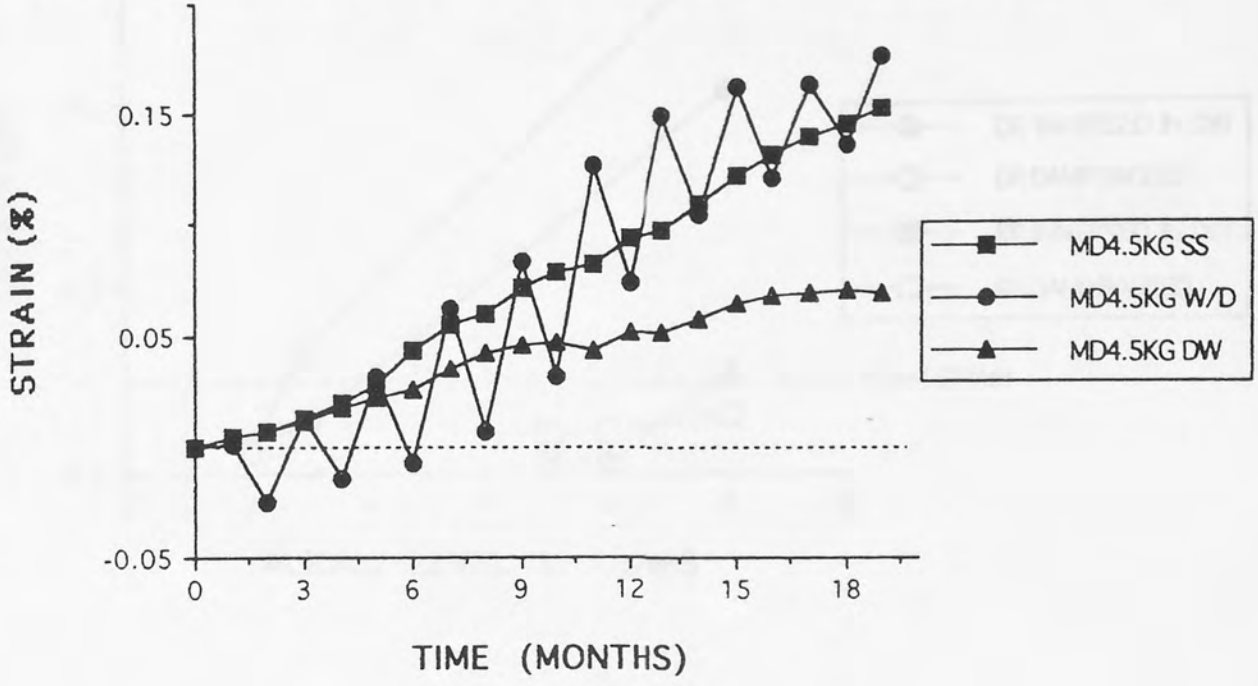


FIG 4.24: Expansion (%) Vs time. Long term 6.0 kg results for (RP) gravel mixes. Immersion in SS, DW and W/D cycling.

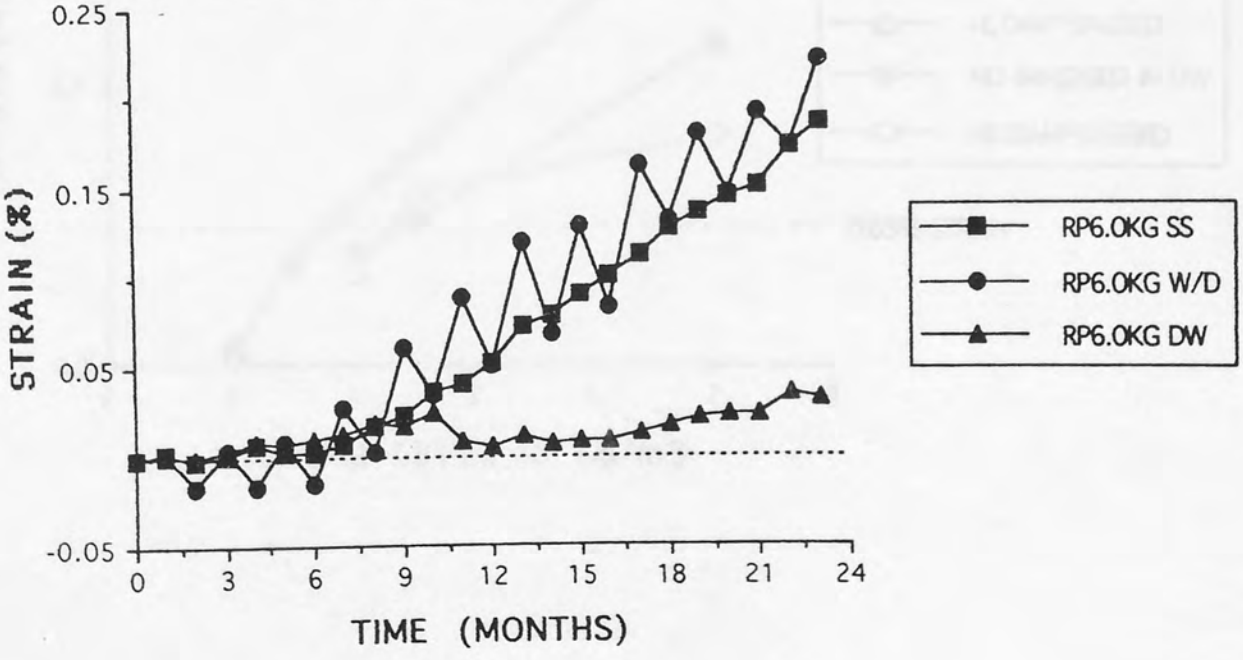

FIG 4.25: Expansion (%) Vs Alkali level, (15 MTHS). COMPARISON OF (DR) AND (RP) MIXES IMMERSED IN DISTILLED WATER OR TRIPLE BAGGED IN MOIST CLOTH.

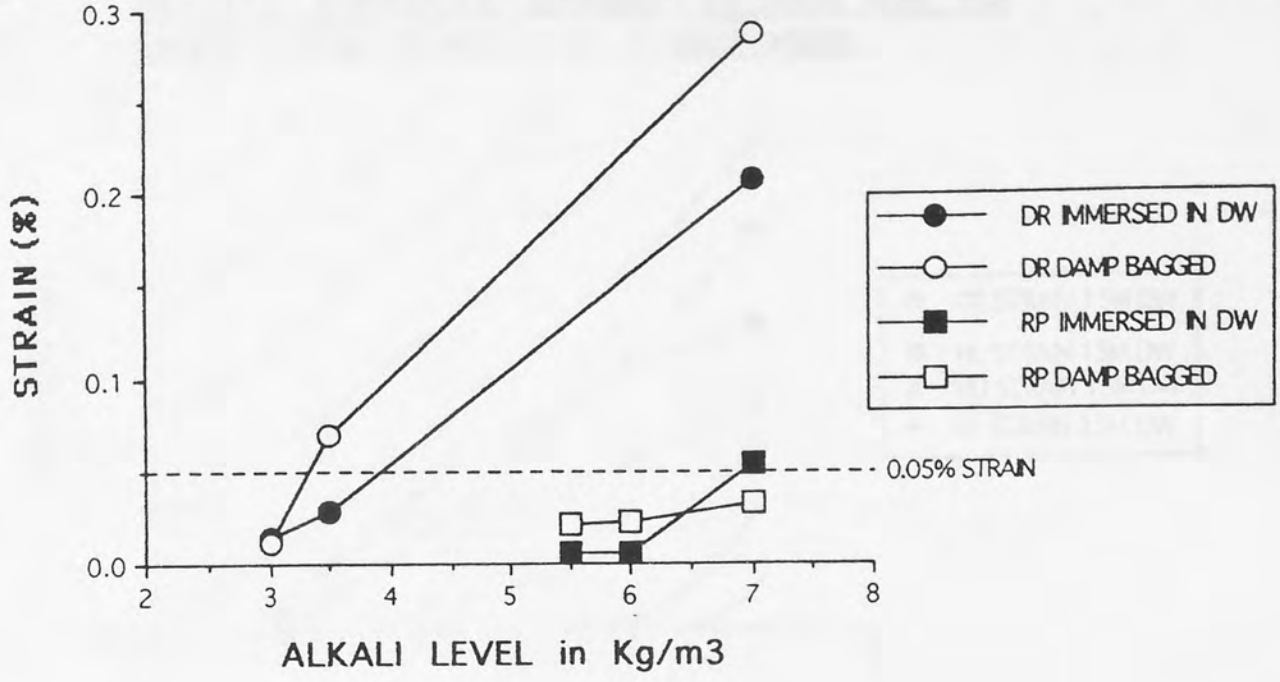


FIG 4.26: Expansion (%) Vs Alkali level, (15 MTHS). COMPARISON OF (HL) AND (MD) MIXES IMMERSED IN DISTILLED WATER OR TRIPLE BAGGED IN MOIST CLOTH.

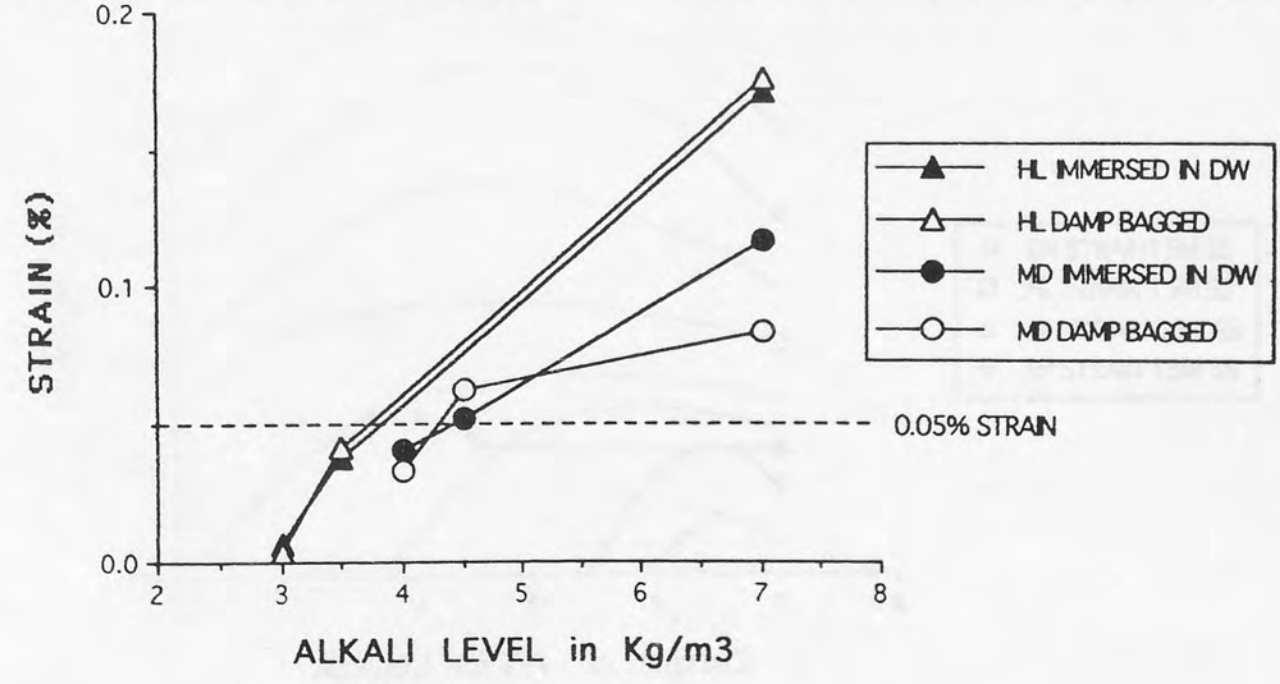

FIG 4.27: Hypothetical Expansion Vs Alkali level. For various mixes immersed in distilled water.

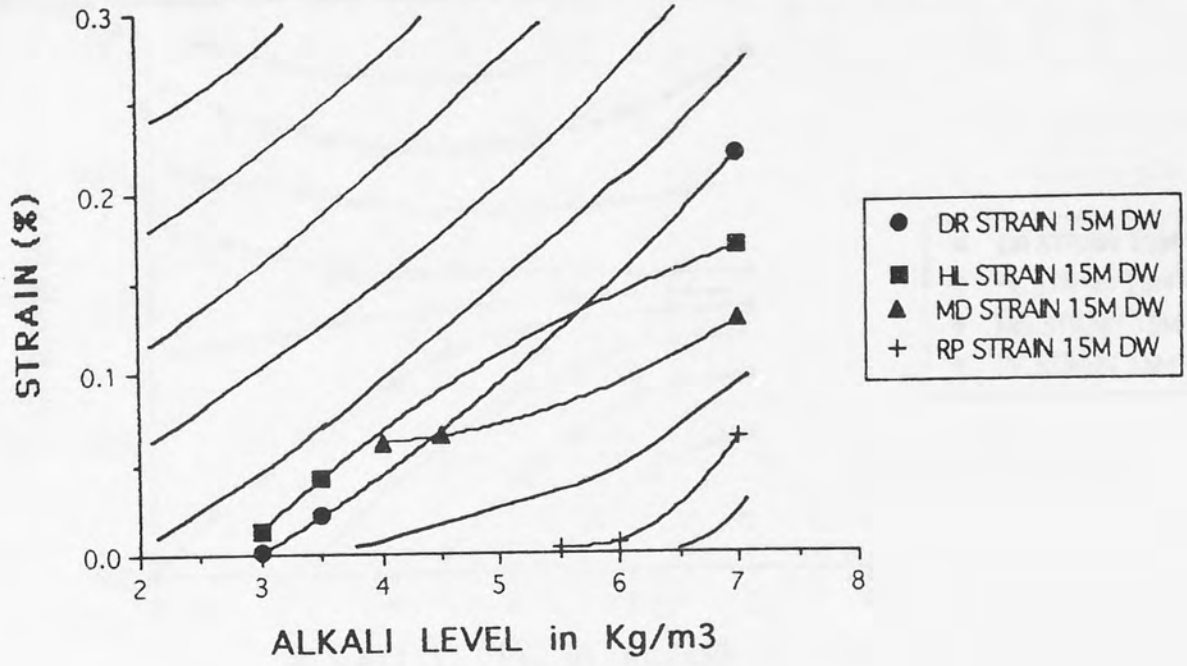


FIG 4.28: Hypothetical Expansion (%) Vs Alkali level data for various mixes immersed in salt solution.

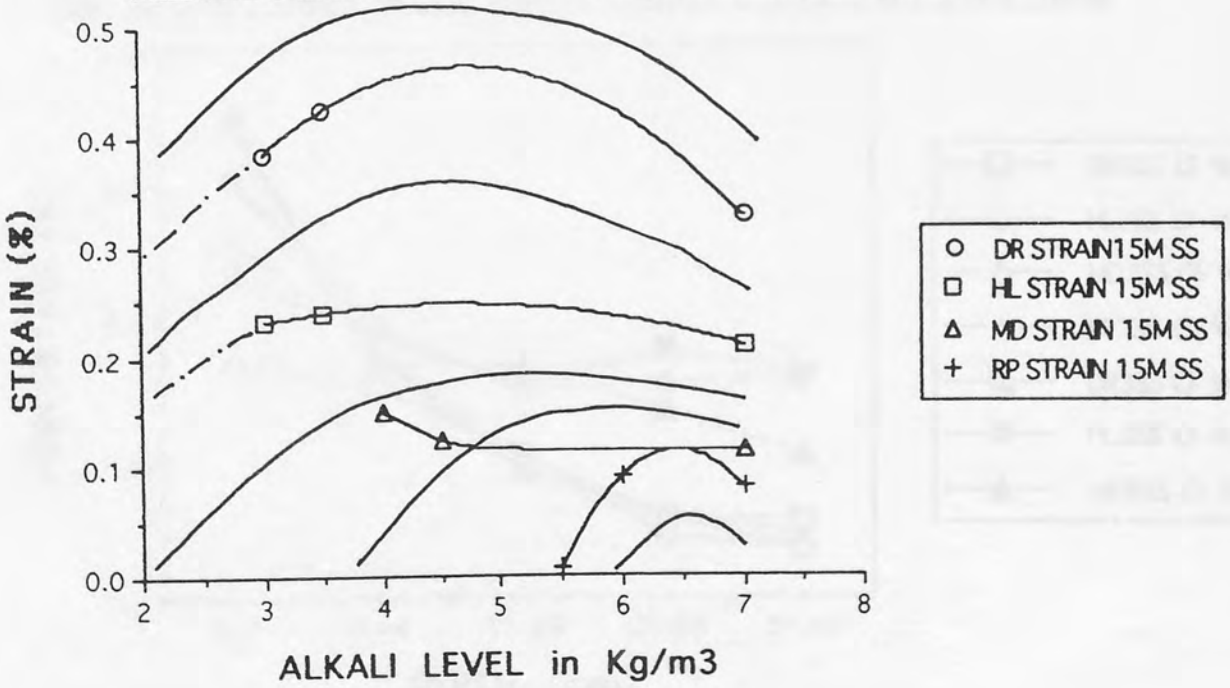

FIG 4.29: Hypothetical Expansion (%) Vs Alkali level data for various mixes immersed in salt solution for 1 month then left dry for 1 month.

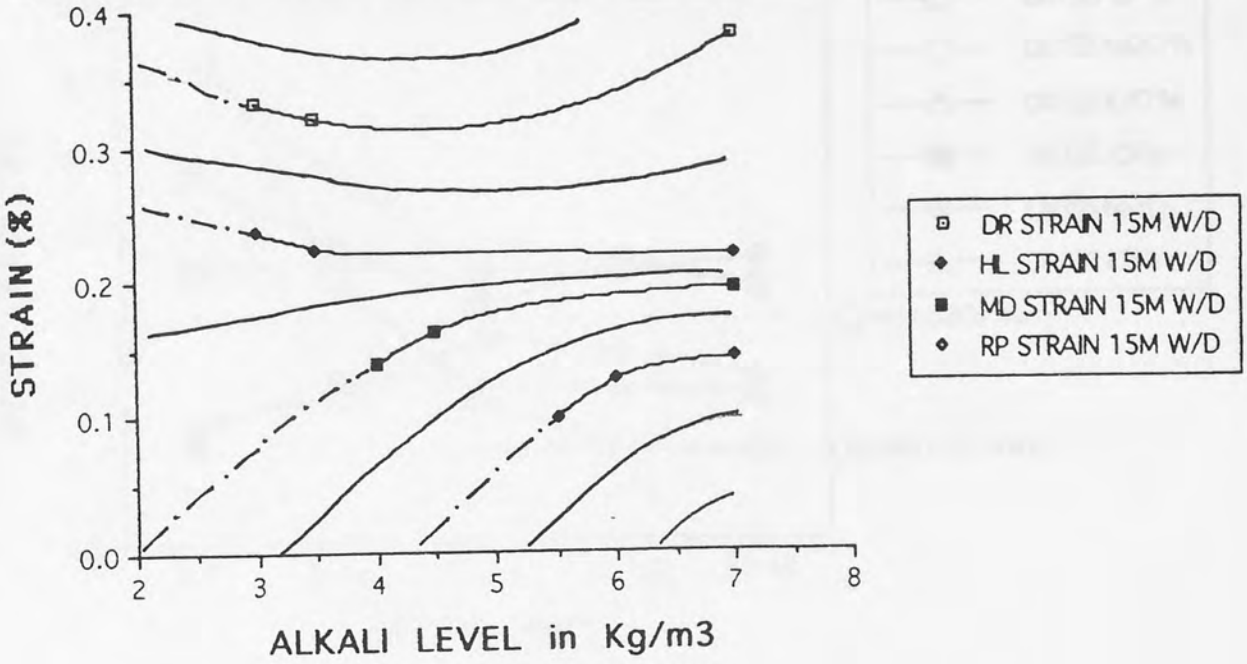


FIG 4.30: Chloride profiles through all prisms immersed in salt solution. Taken at 15 months, depth in mm from outer face.

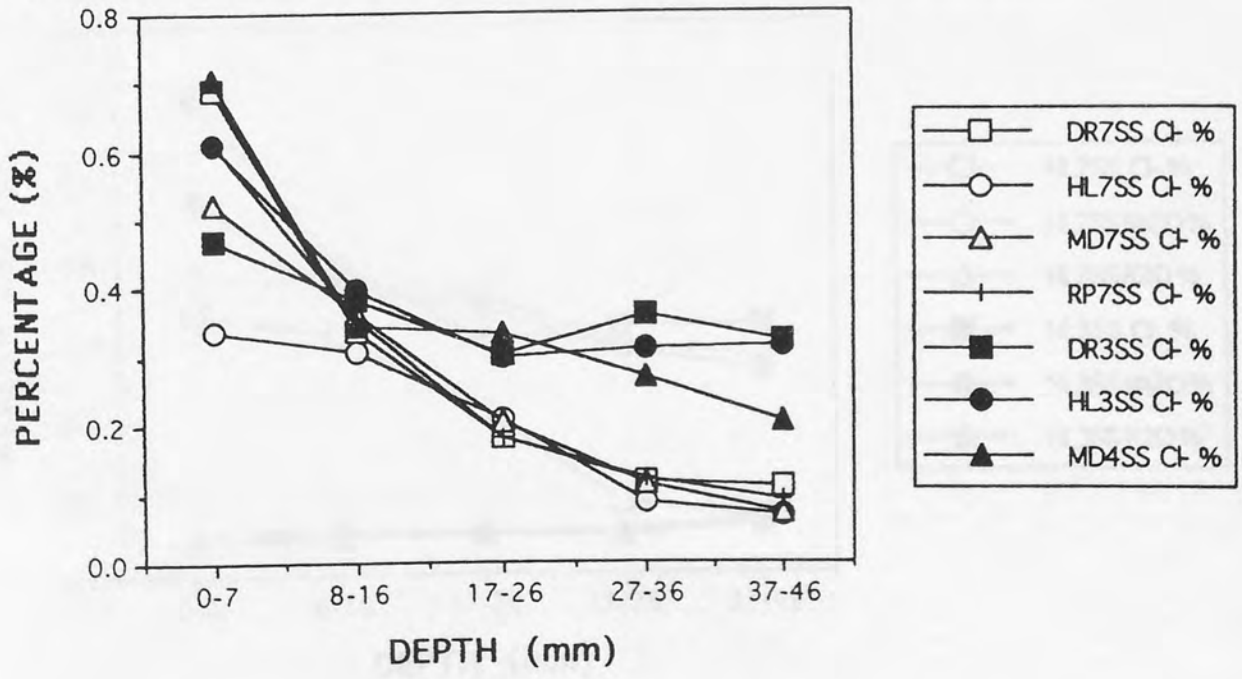

FIG 4.31: Chemical profiles for two (DR) siltstone mixes immersed in salt solution. Depth from outer face to centre.

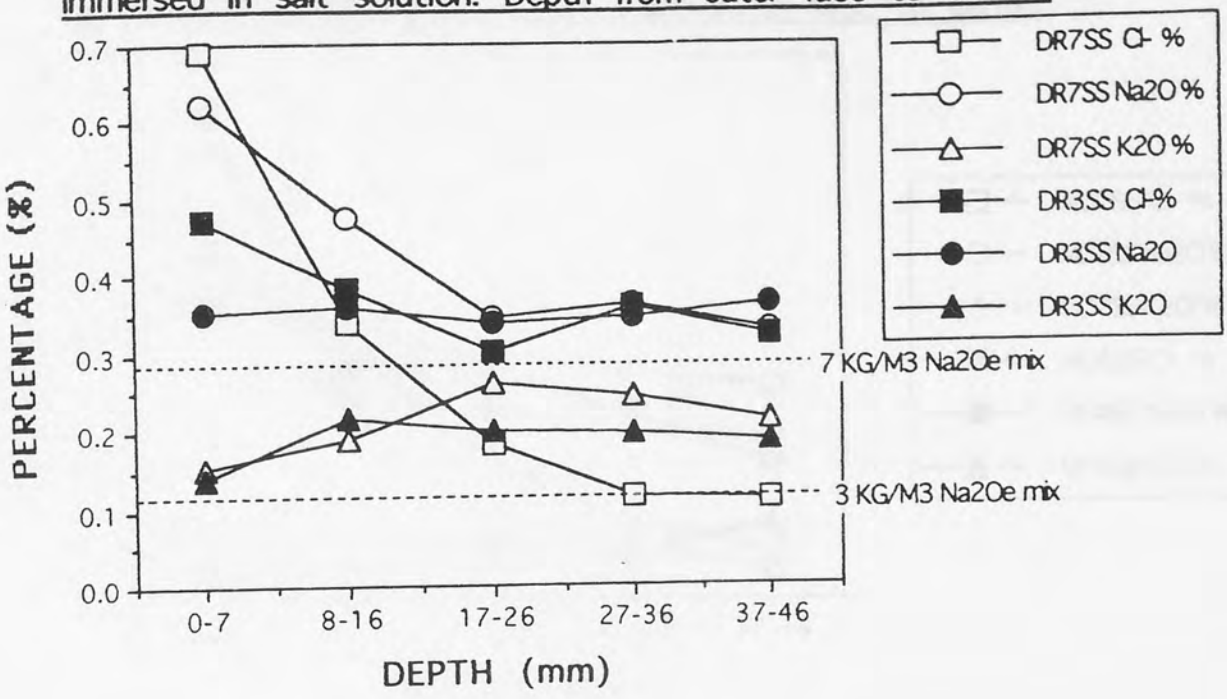


FIG 4.32: Chemical profiles for two (HL) limestone mixes immersed in salt solution. Depth from outer face to centre.

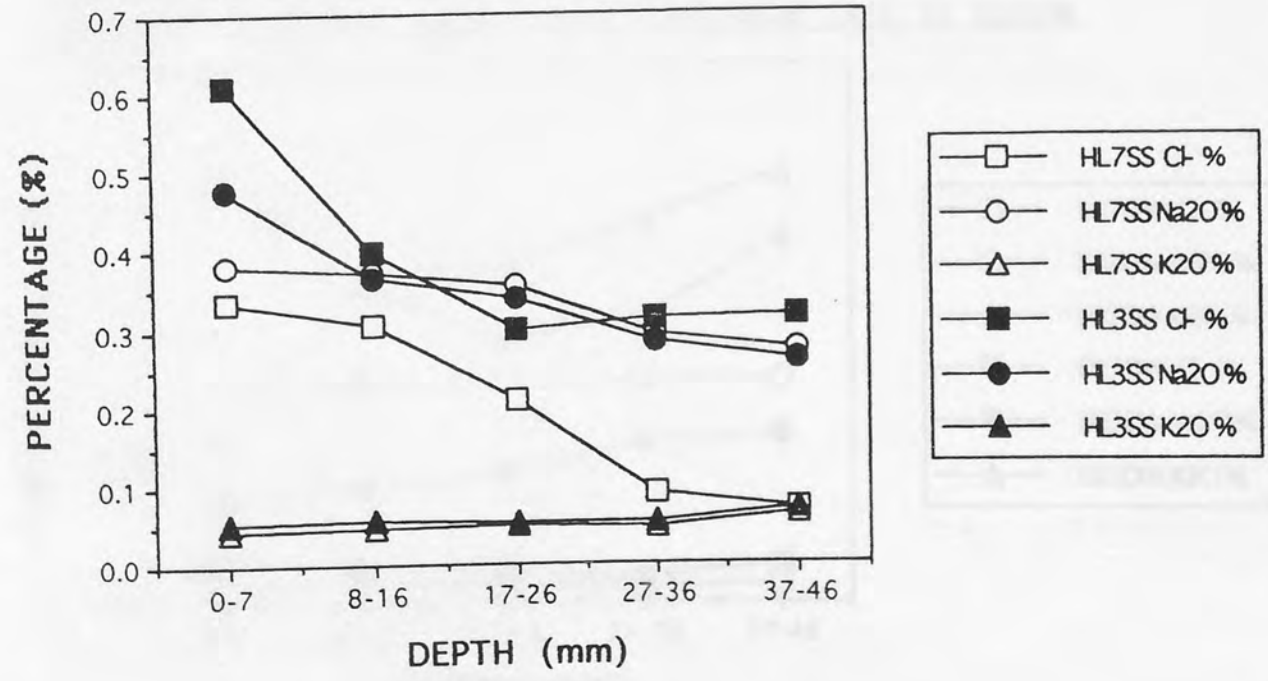

FIG 4.33: Chemical profiles of two (MD) greywacke mixes immersed in salt solution. Depth from outer face to centre.

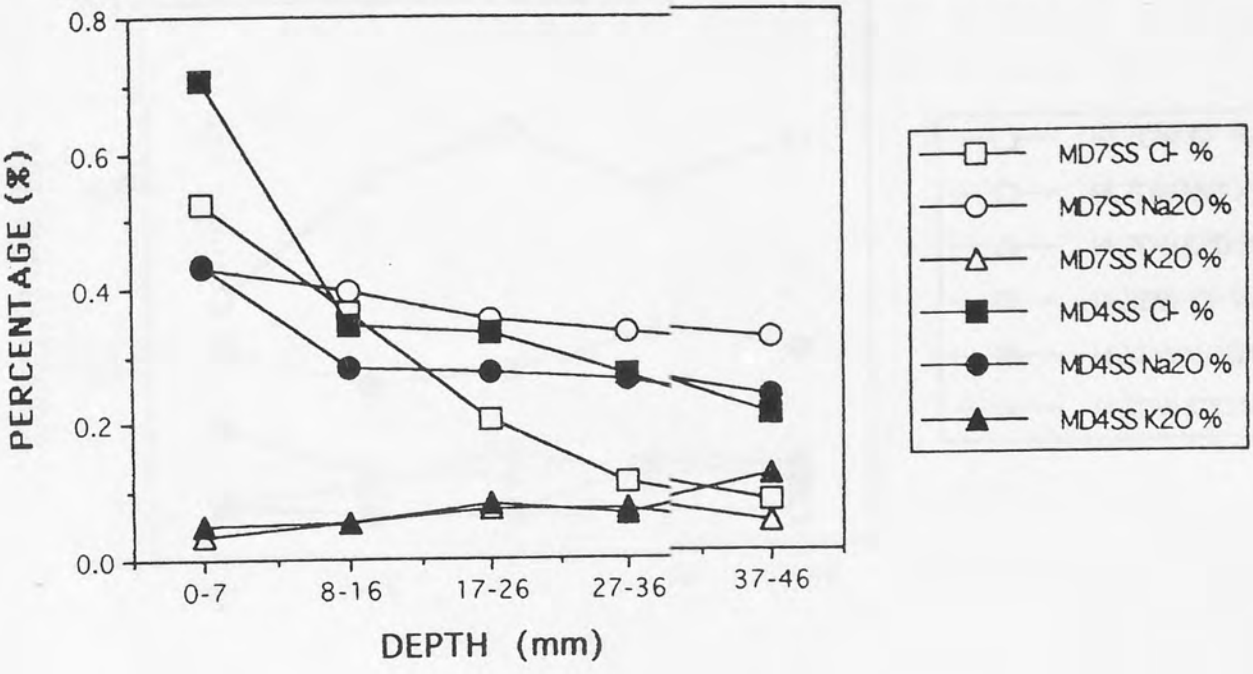


FIG 4.34: Chemical profiles of two (DR) siltstone mixes immersed in distilled water. Depth from outer face to centre.

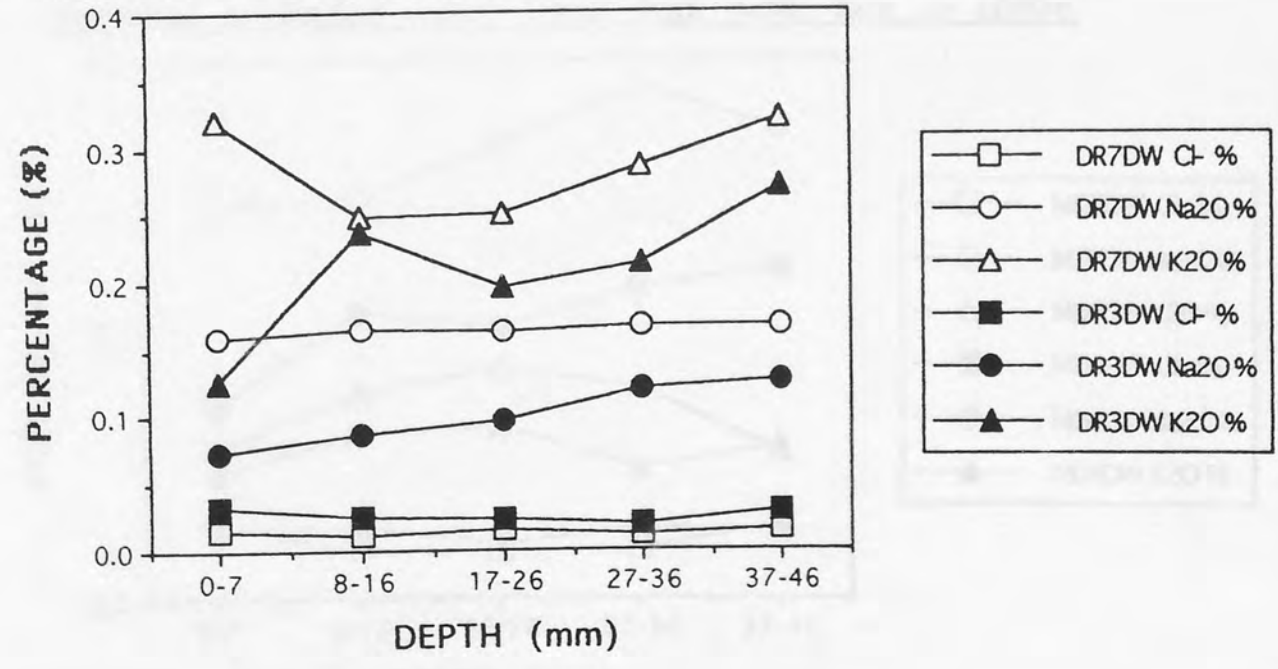

FIG 4.35: Chemical profiles of two (HL) limestone mixes immersed in distilled water. Depth from outer face to centre.

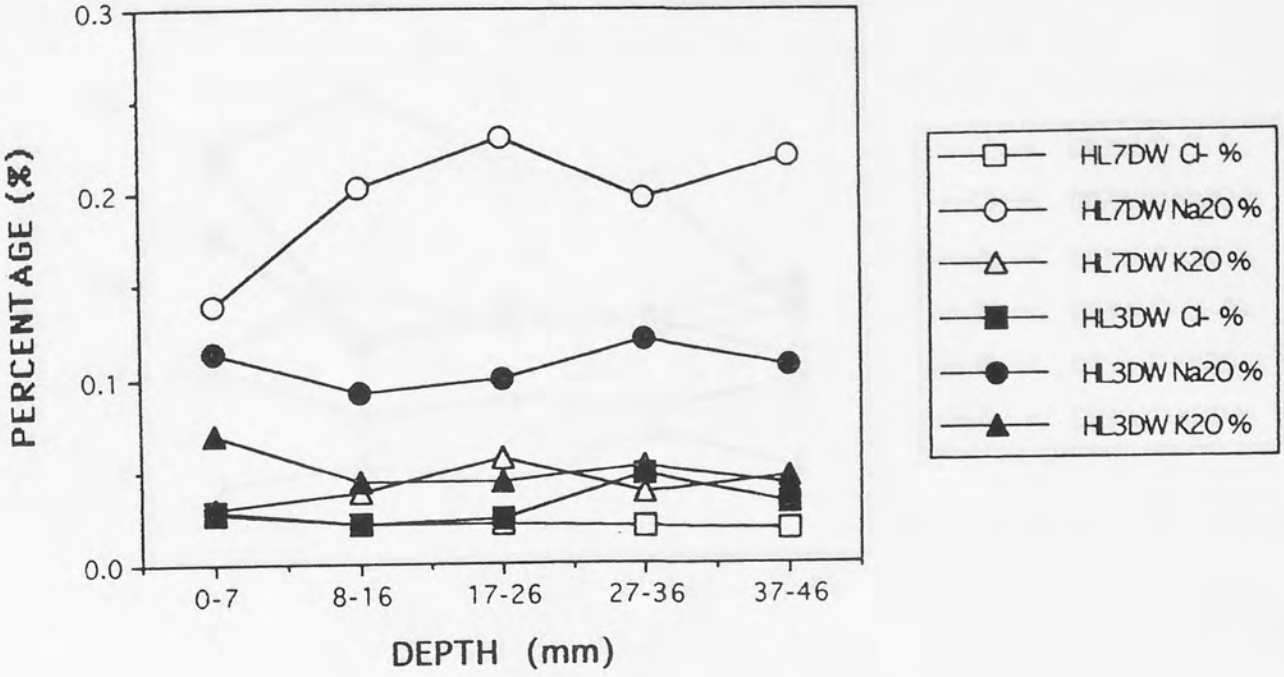


FIG 4.36: Chemical profiles from two (MD) greywacke mixes immersed in distilled water. Depth from outer face to centre.

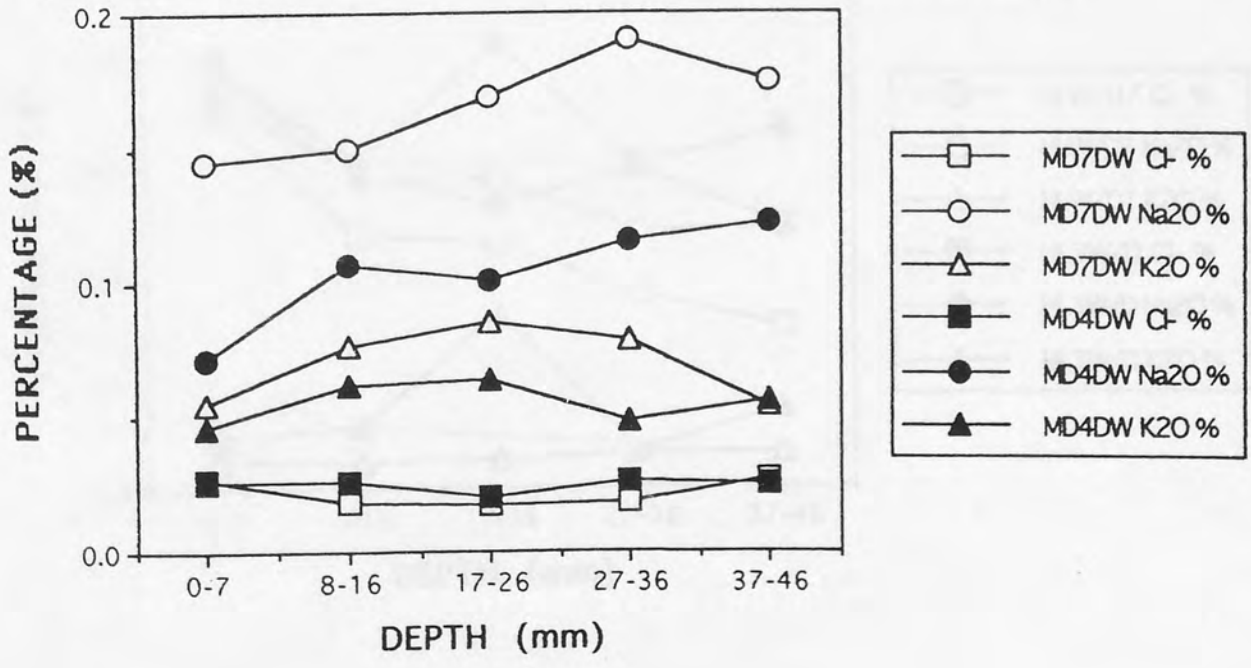

FIG 4.37: Chemical profiles from two (DR) siltstone mixes. Immersed in salt solution for 1 month then 1 month dry.

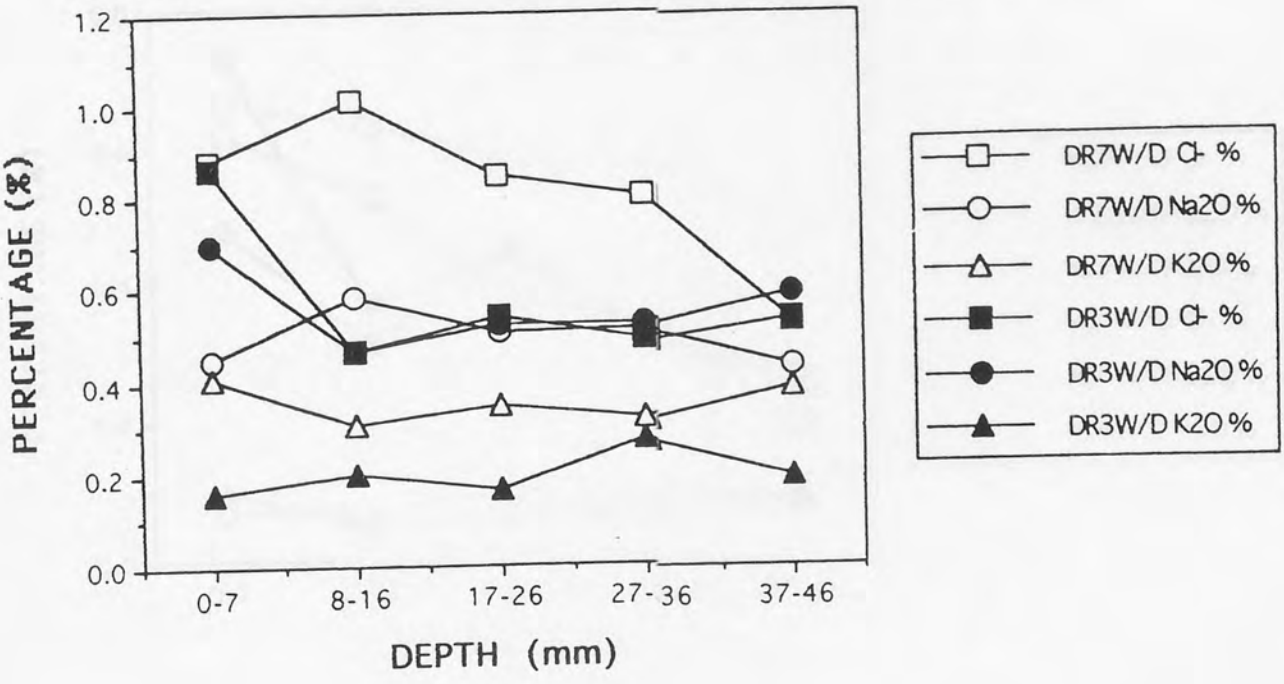


FIG 4.38: Chemical profiles from two (HL) limestone mixes. Immersed in salt solution for 1 month then 1 month dry.

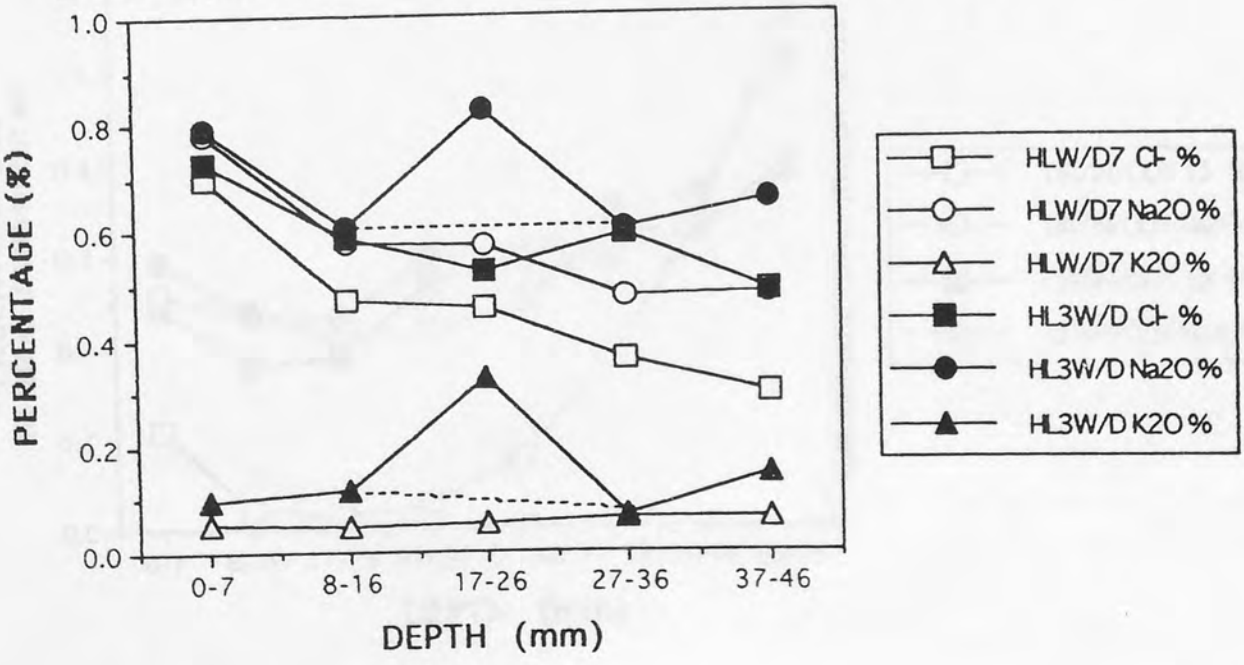

FIG 4.39: Chemical profiles of two (MD) greywacke mixes. Immersed in salt solution for 1 month and dry for 1 month.

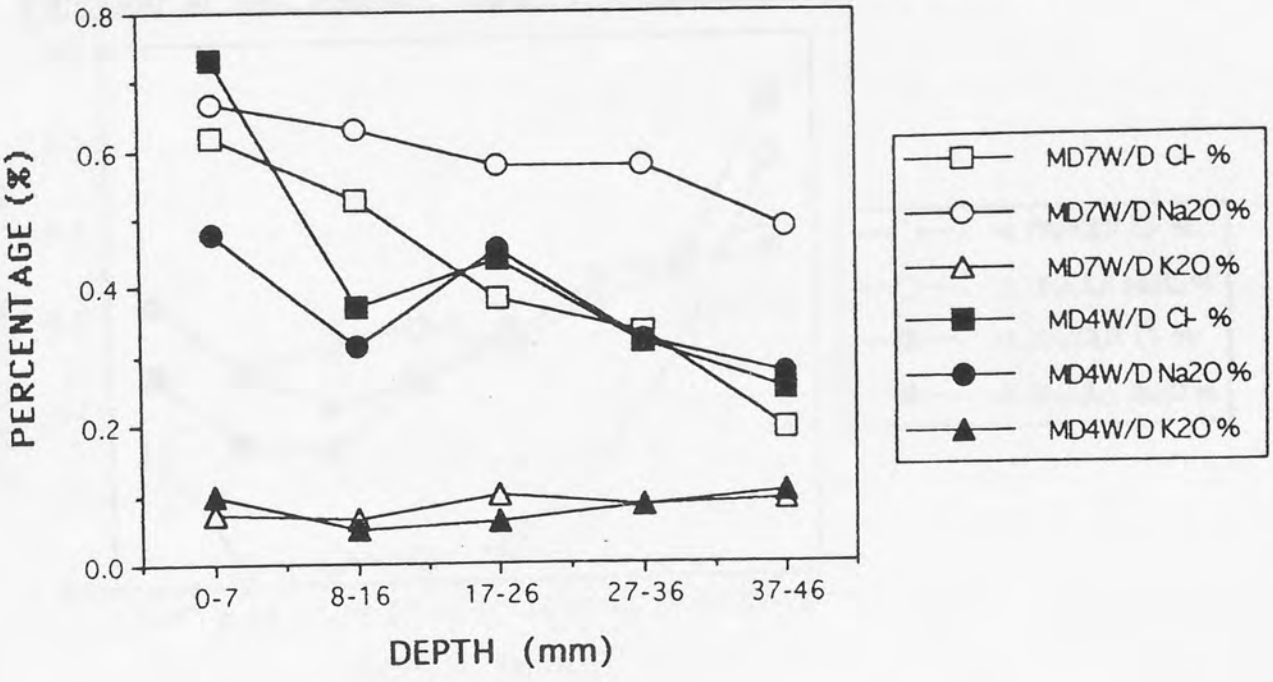


FIG 4.40: Chemical profiles through two (DR) siltstone mixes half immersed in salt solution. Depth taken from top to bottom.

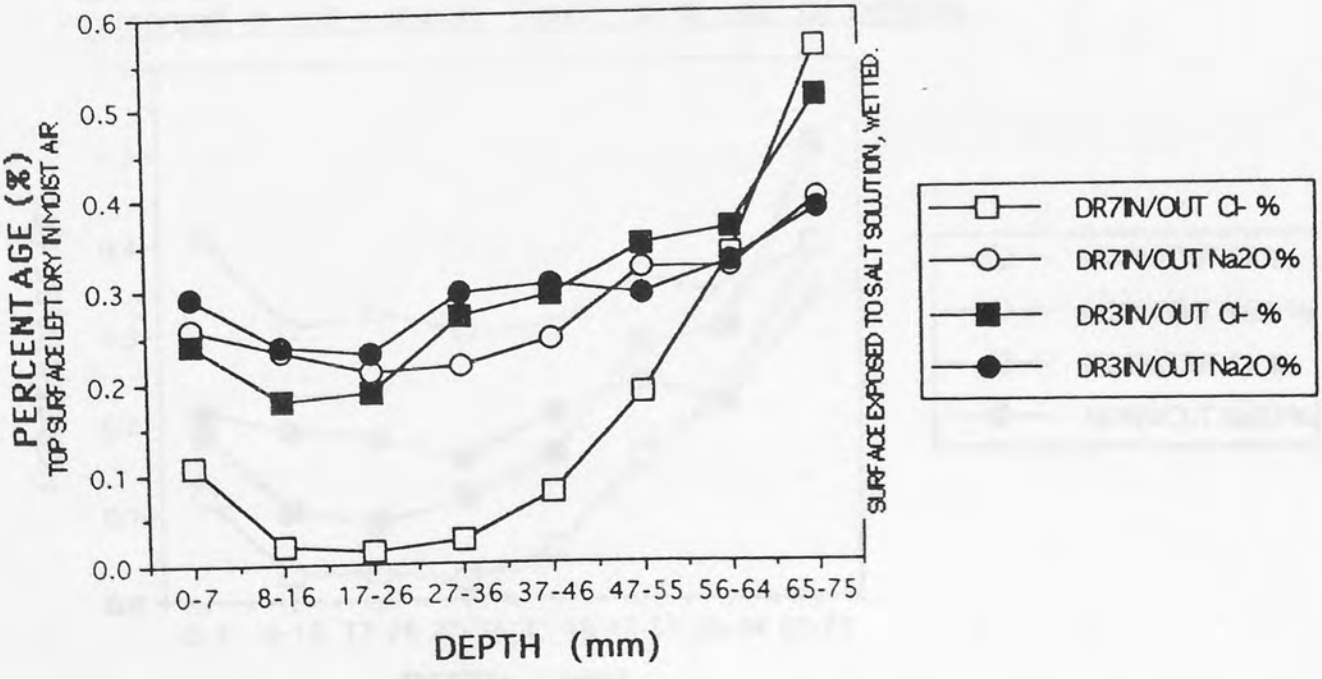

FIG 4.41: Chemical profiles of two (HL) limestone mixes half immersed in salt solution. Depth from top to bottom.

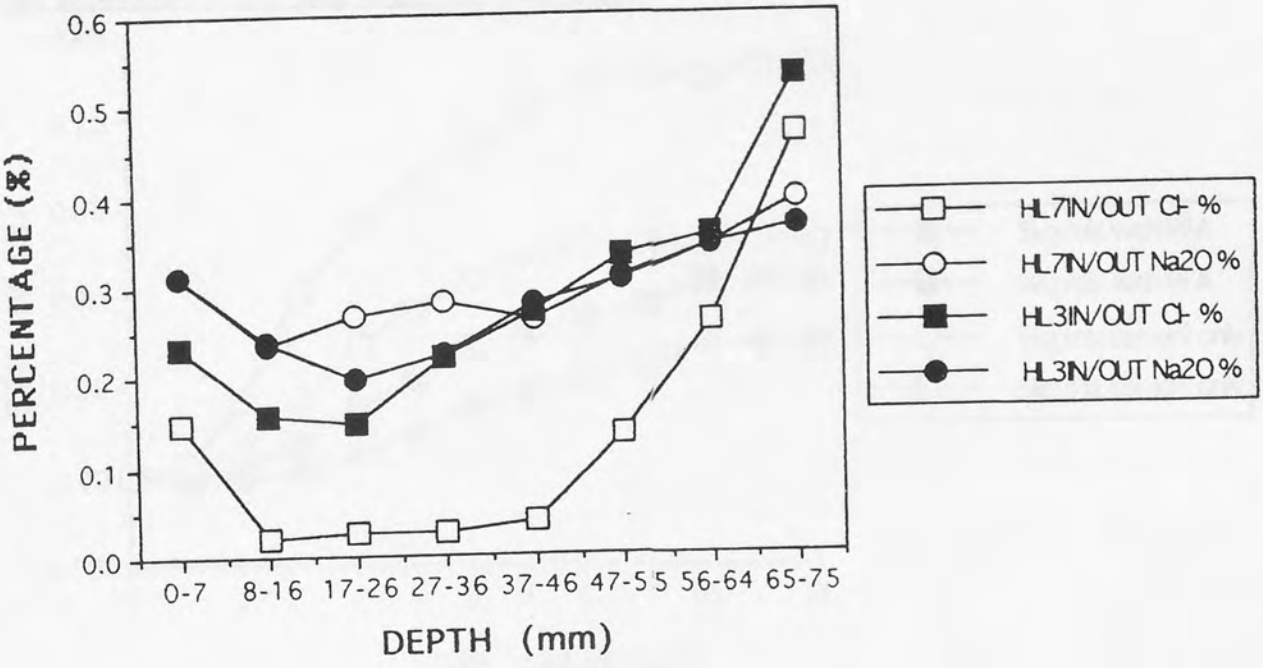


FIG 4.42: Chemical profiles from two (MD) greywacke mixes immersed in salt solution. Depth taken top to bottom.

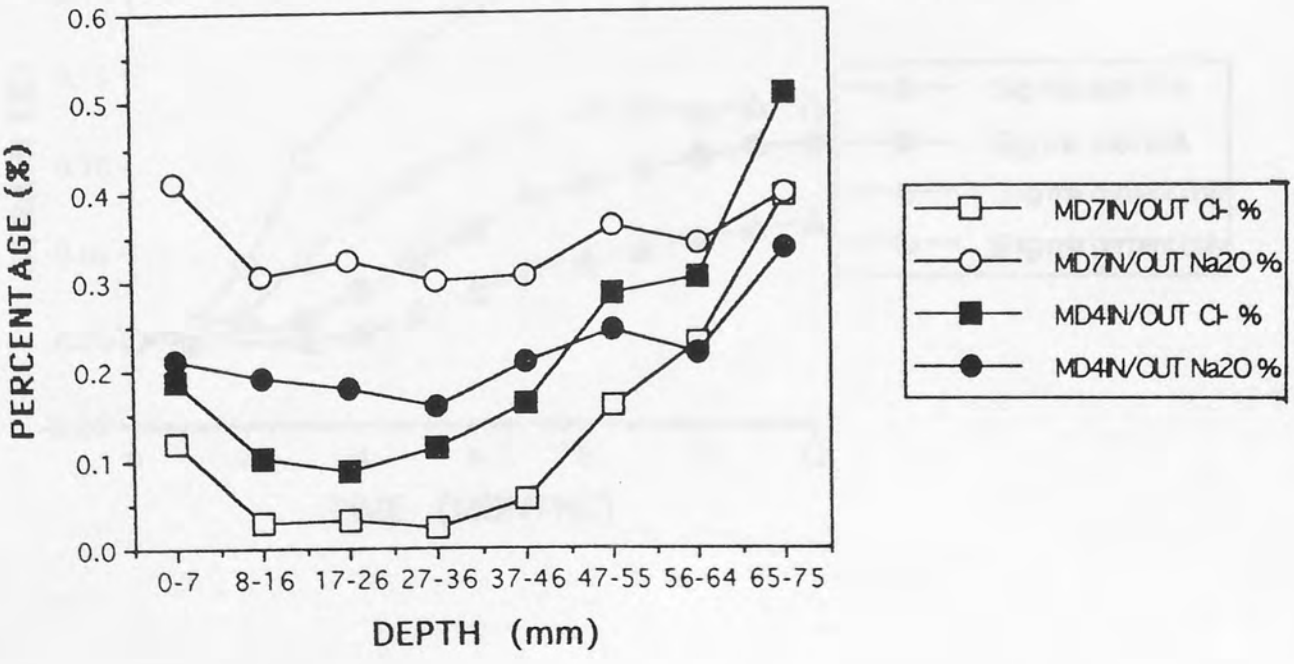

FIG 5.1: Expansion (%) Vs time. (DR) SILTSTONE MIXES WITH 25% REPLACEMENT OF CEMENT BY WB PFA.

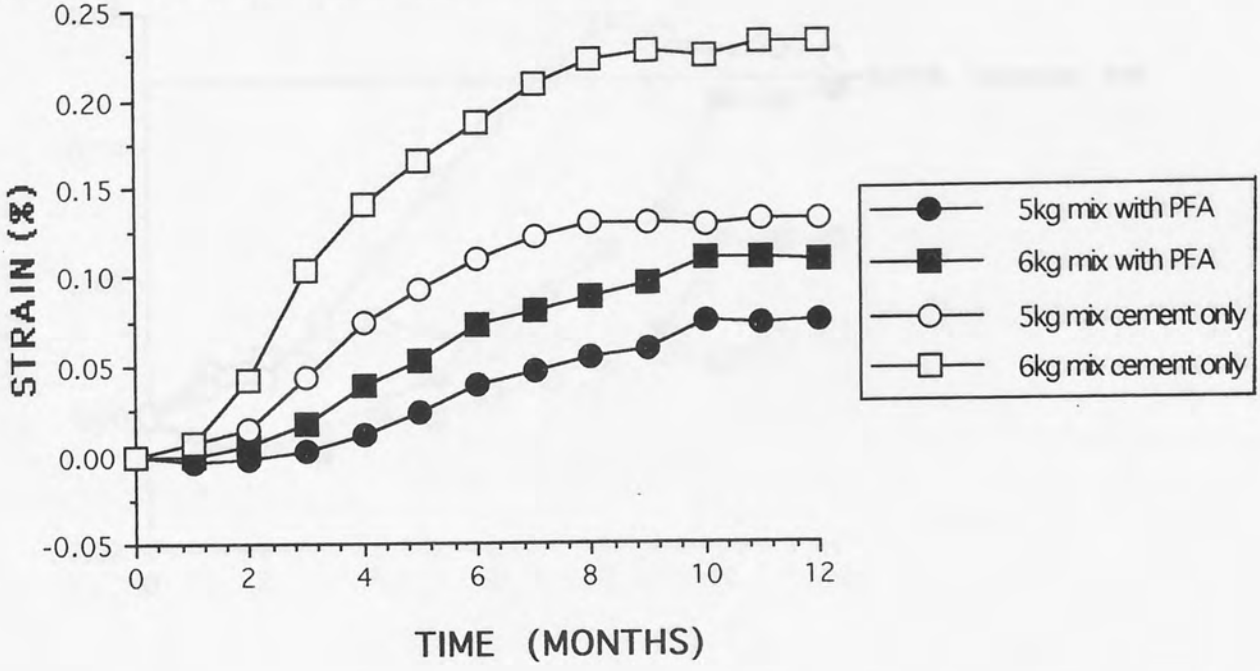


FIG 5.2: Expansion (%) Vs time. (DR) SILTSTONE MIXES WITH 25% REPLACEMENT OF CEMENT BY FF PFA.

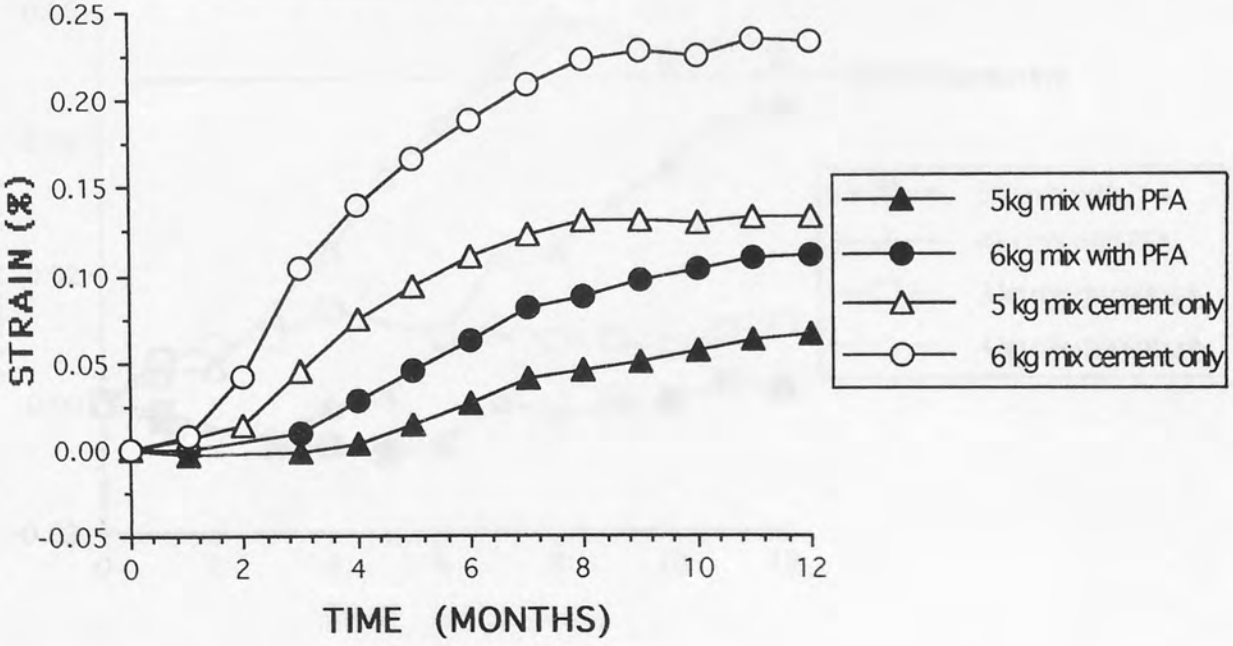

FIG 5.3: Expansion (%) Vs time. (DR) SILTSTONE MIXES WITH 25% REPLACEMENT OF CEMENT BY WB PFA.

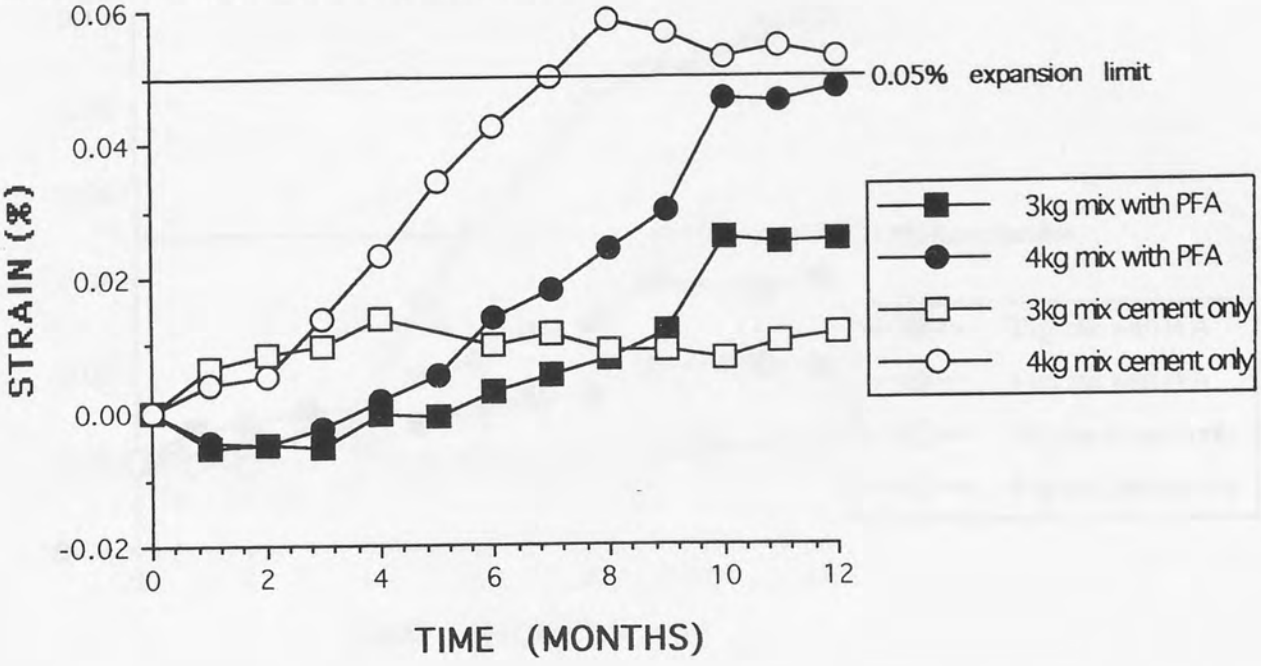


FIG 5.4: Expansion (%) Vs time. (DR) SILTSTONE MIXES WITH 25% REPLACEMENT OF CEMENT BY FF PFA.

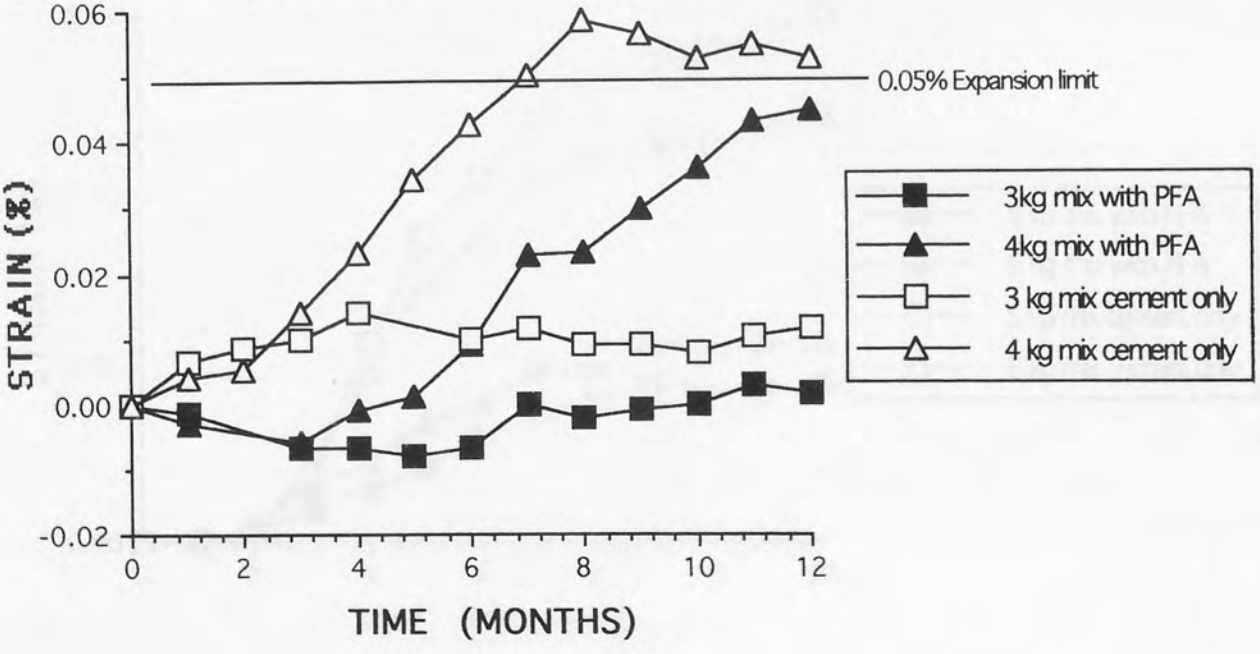

FIG 5.5: Expansion (%) Vs time. (HL) LIMESTONE MIXES WITH 25% REPLACEMENT OF CEMENT BY WB PFA.

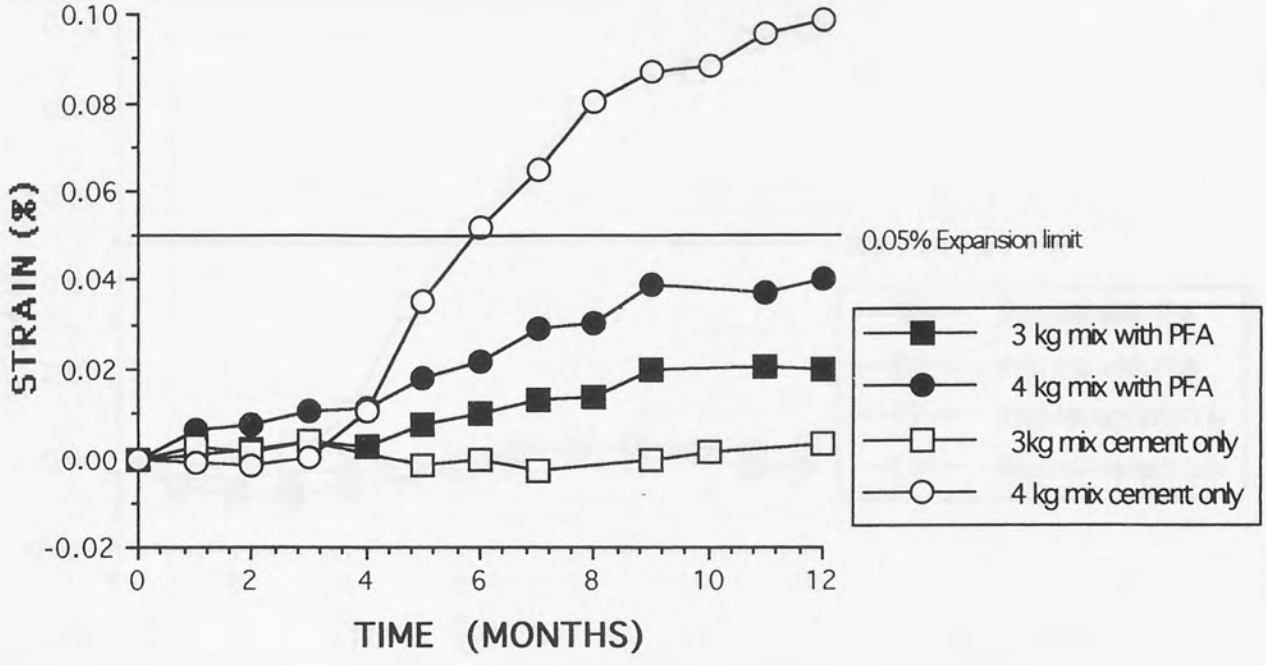


FIG 5.6: Expansion (%) Vs time. (HL) LIMESTONE MIXES WITH 25% REPLACEMENT OF CEMENT BY WB PFA.

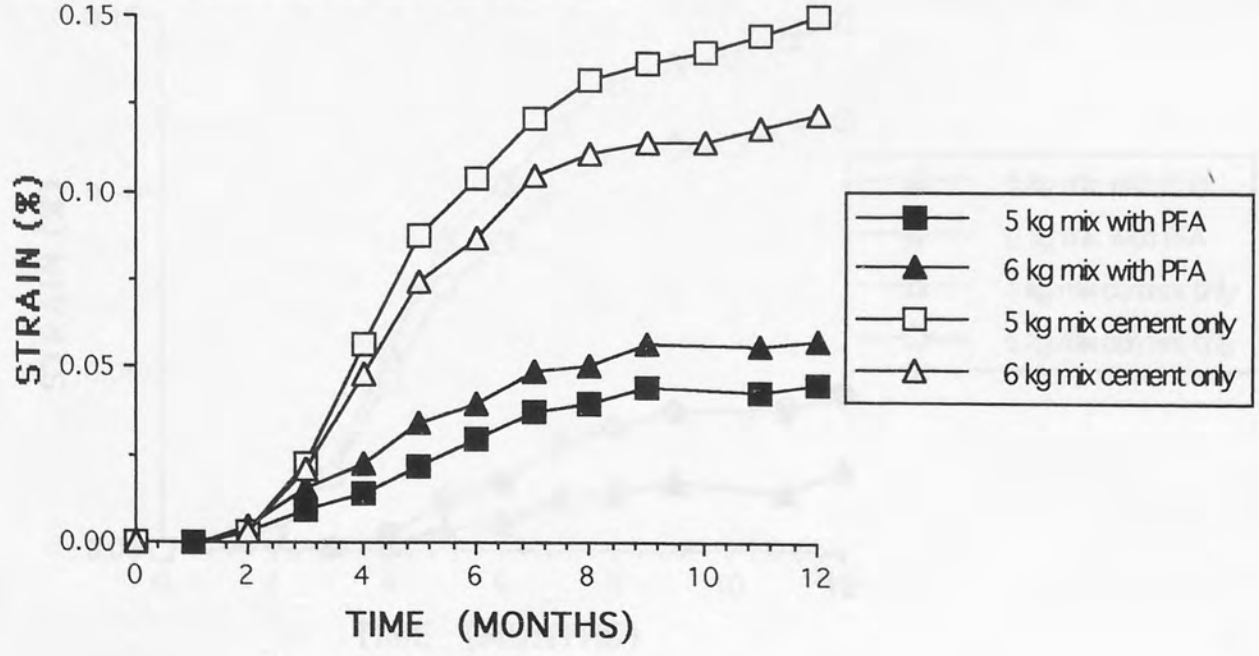

FIG 5.7: Expansion (%) Vs time. (HL) LIMESTONE MIXES WITH 25% REPLACEMENT OF CEMENT BY FF PFA.

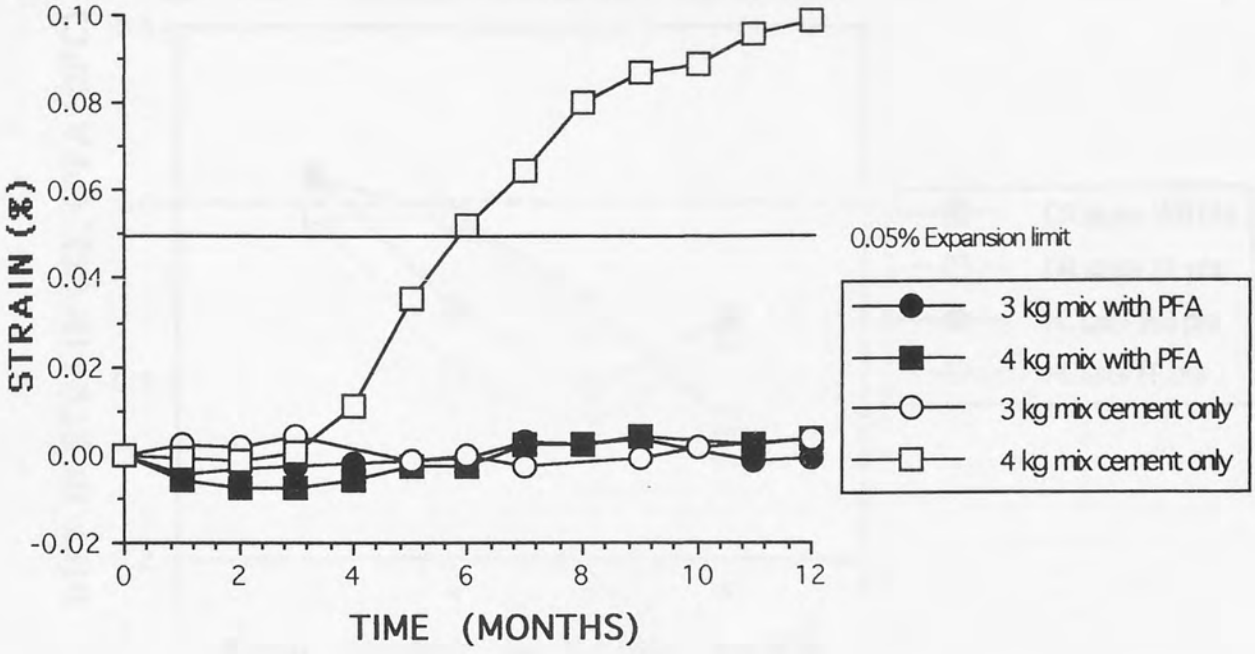


FIG 5.8: Expansion (%) Vs time. (HL) LIMESTONE MIXES WITH 25% REPLACEMENT OF CEMENT BY FF PFA.

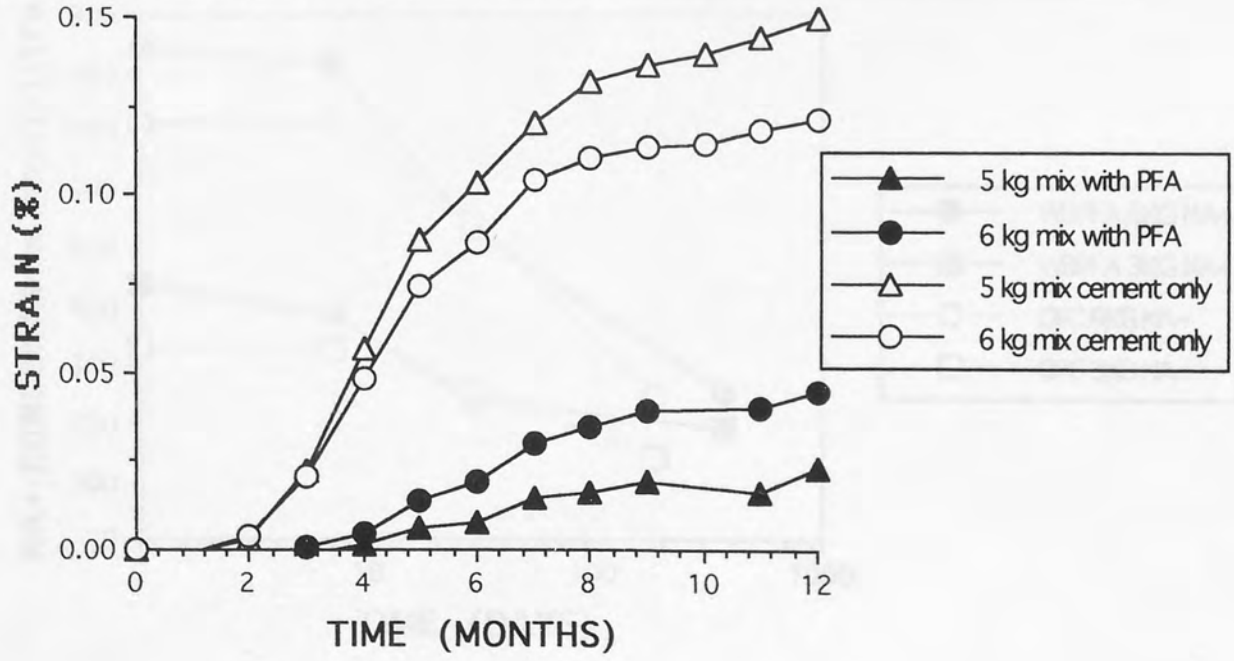

FIG 5.9: DIFFERENCE IN STRAIN (%) BETWEEN OPC AND VARIOUS PFA REPLACEMENT MIXES.

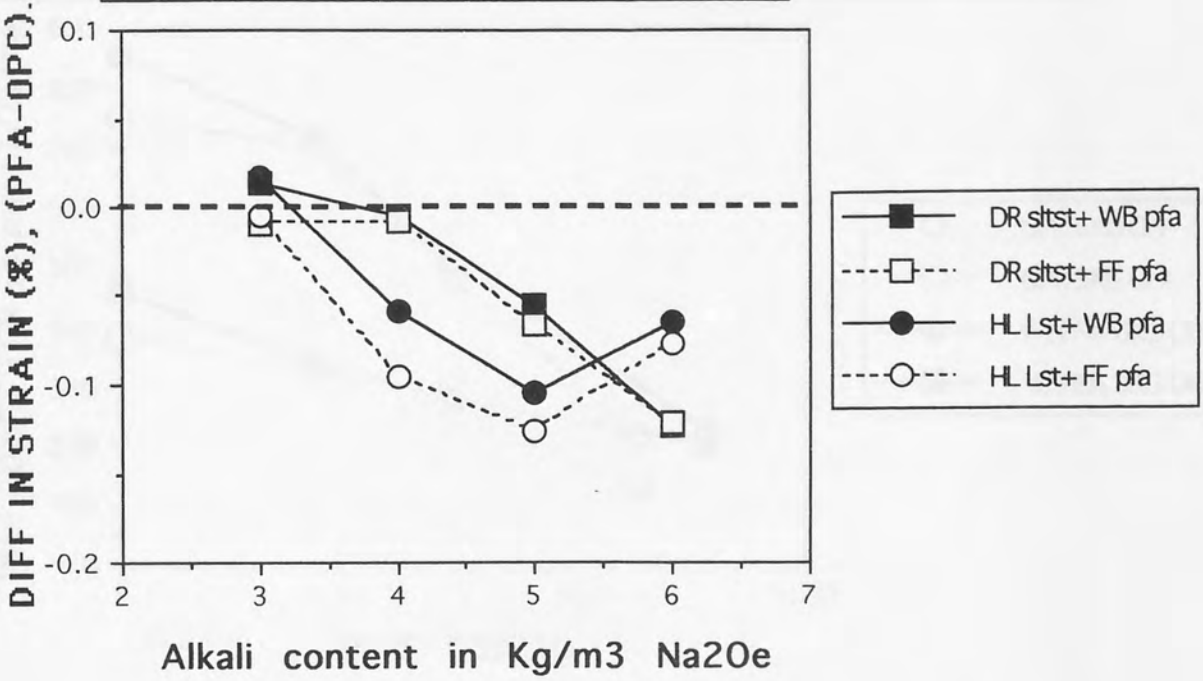


FIG 5.10: Change in NA data with time for pore solutions in the 3 and 6 kg mixes containing high alkali (WB) pfa and a normal OPC.

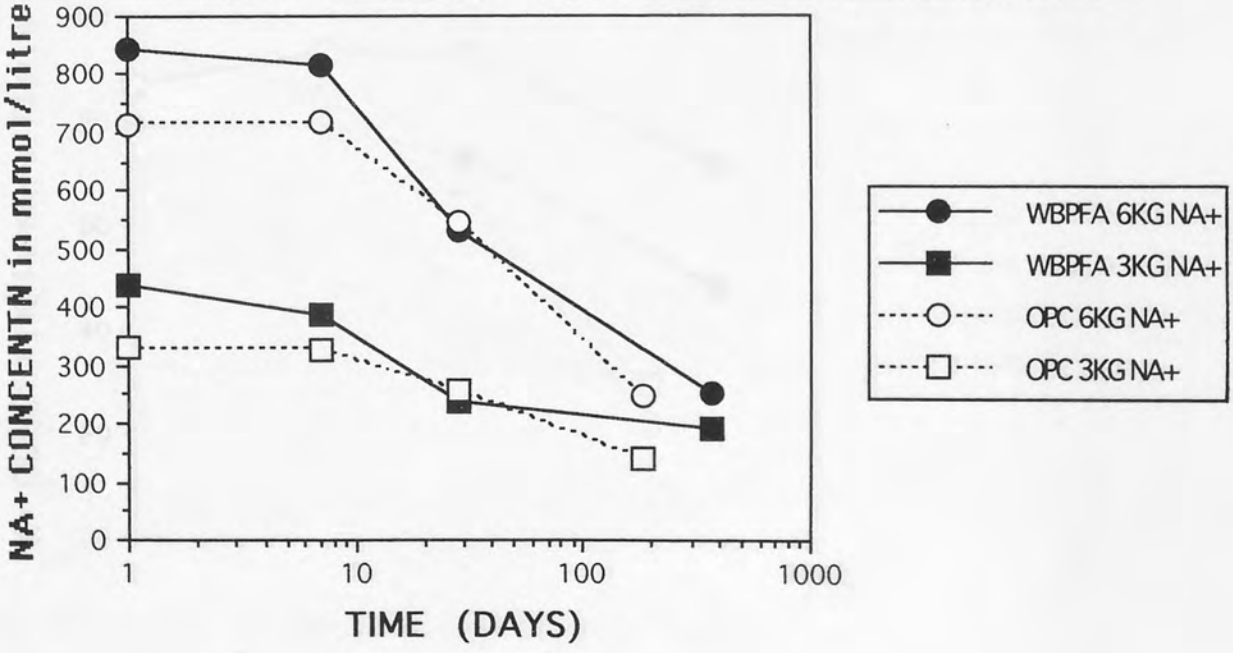

FIG 5.11: Changes in OH data with time for pore solutions in 3 and 6 kg mixes containing high alkali (WB) pfa and a normal OPC.

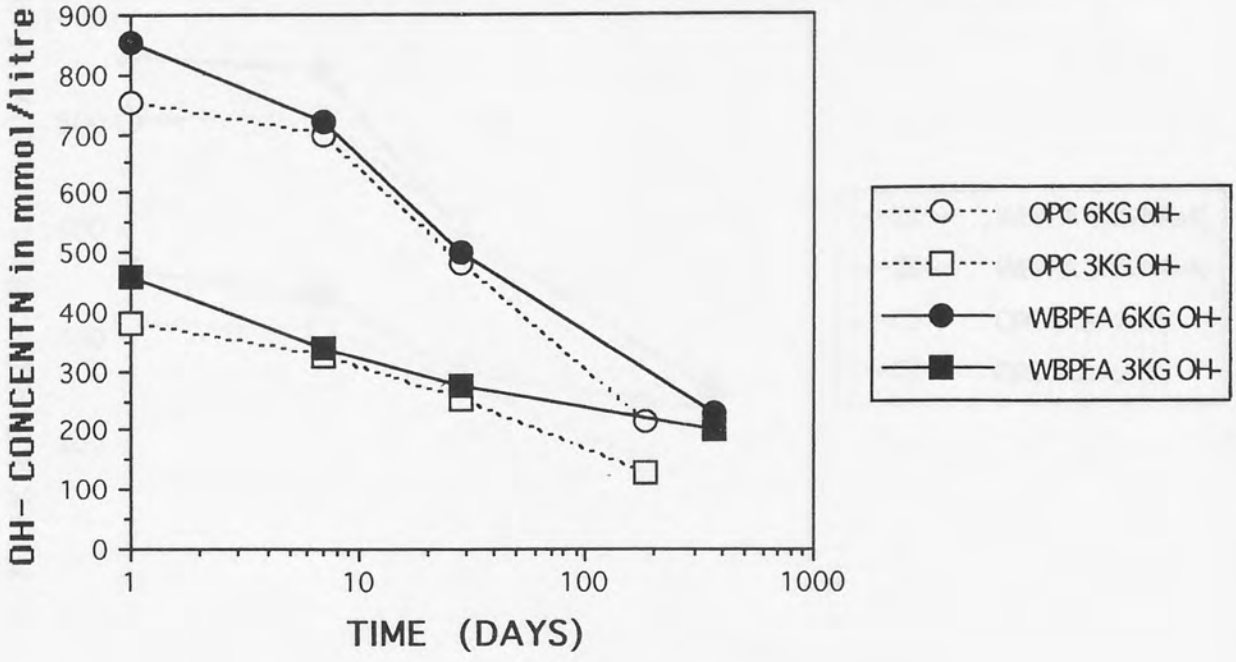


FIG 5.12: Changes in K data with time for pore solutions in 3 and 6 kg mixes containing high alkali (WB) pfa and a normal OPC.

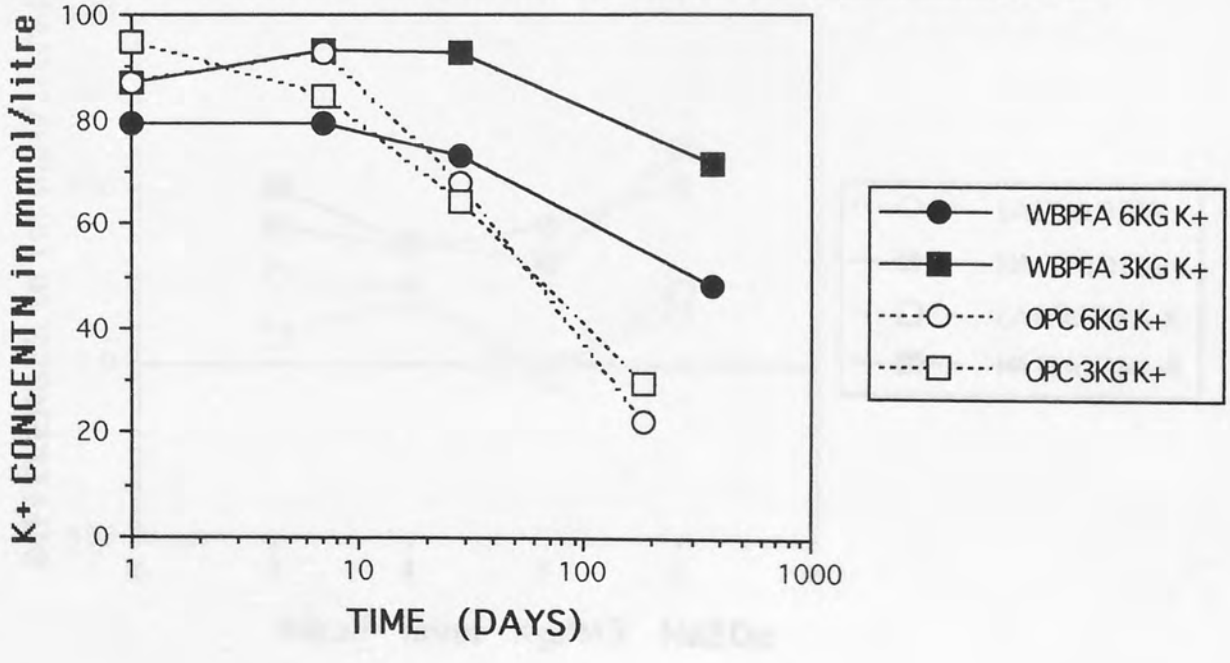

FIG 5.13: Changes in Na+K data with time for pore solutions in 3 and 6 kg mixes containing high alkali (WB) pfa and a normal OPC.

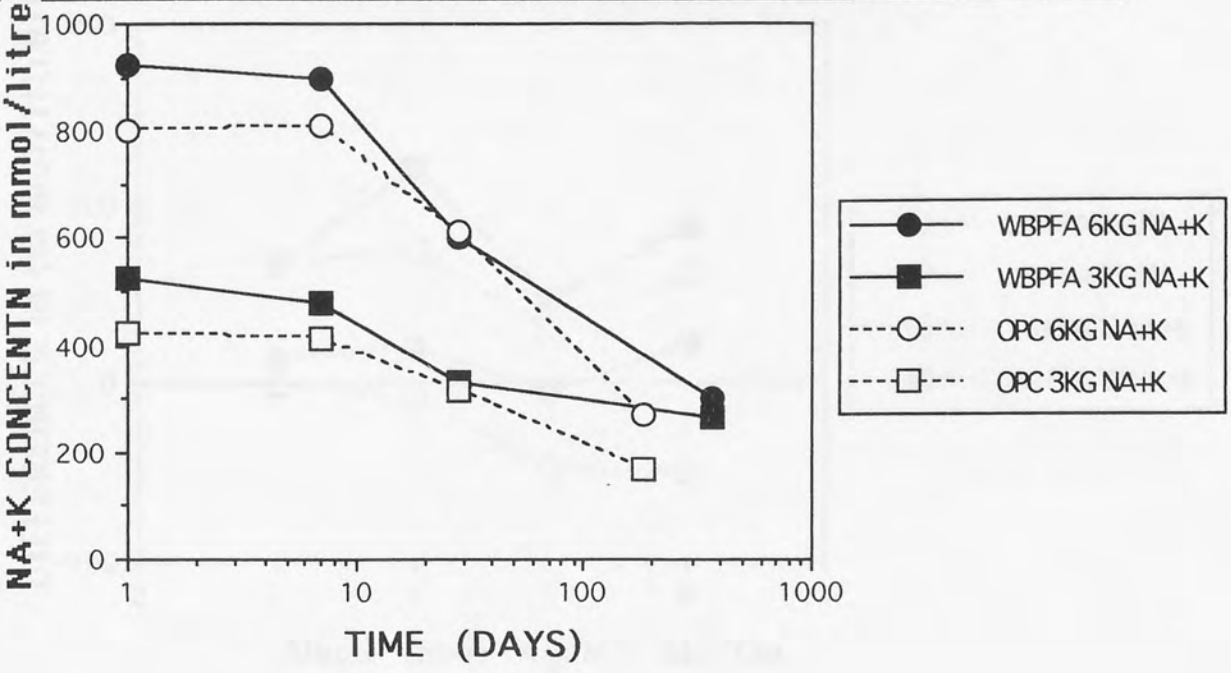


FIG 5.14: Differences between Pfa and OPC mixes pore solution concentrations with siltstone reactive aggregate at 1 day.

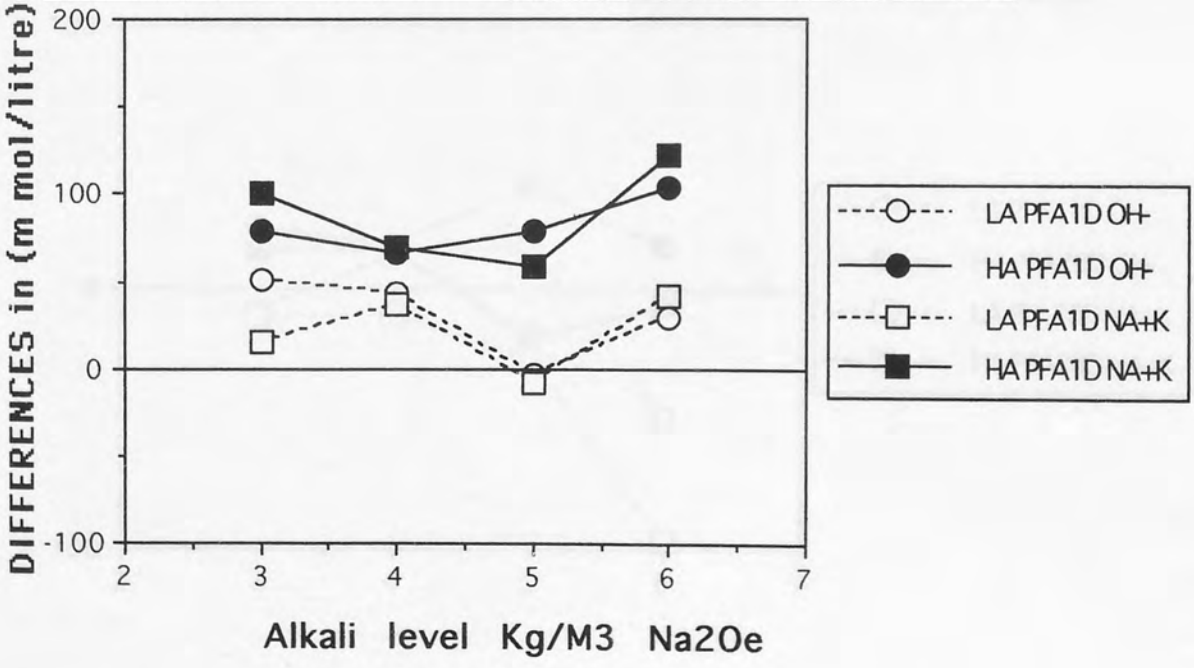

FIG 5.15: Differences between Pfa and OPC mixes pore solution concentration with siltstone reactive aggregate at 7 days.

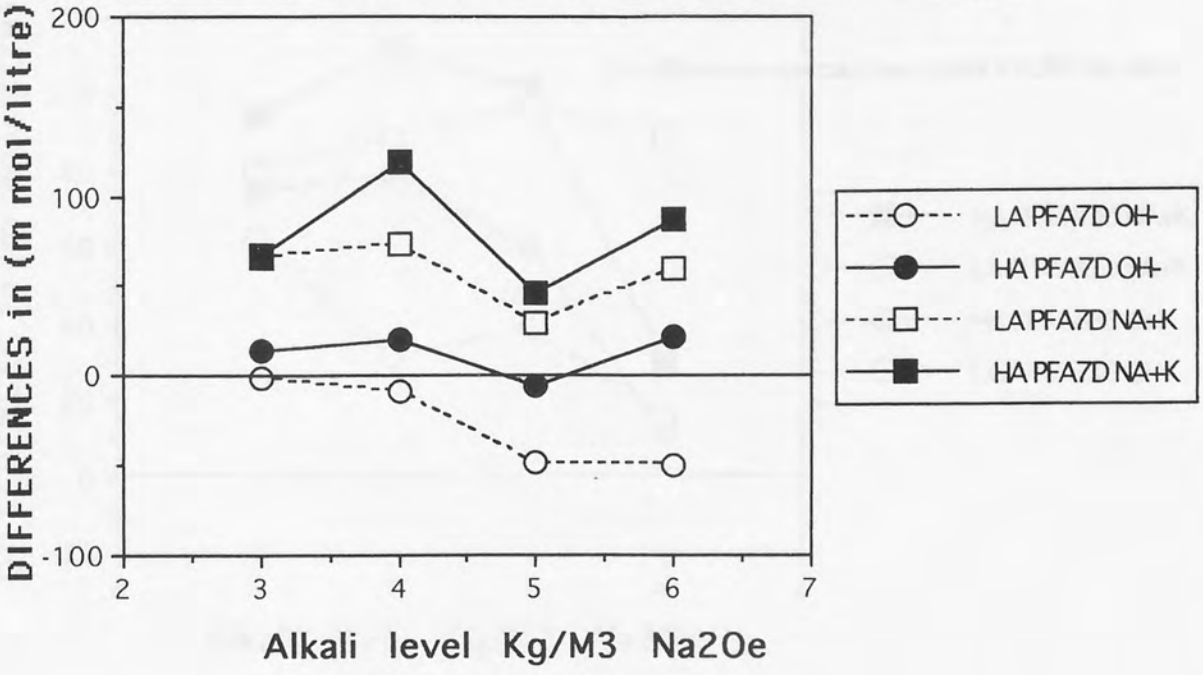


FIG 5.16: Differences between Pfa and OPC mixes pore solution concentrations with a siltstone reactive aggreagte at 28 days.

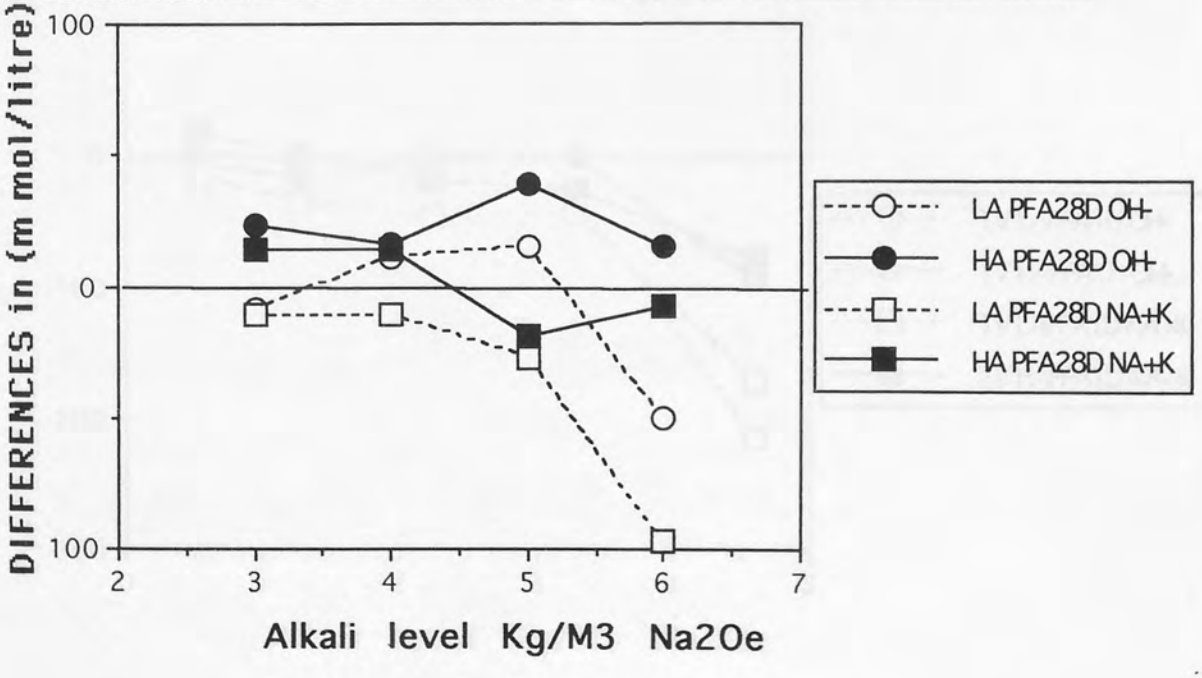

FIG 5.17: Differences between Pfa and OPC mixes pore solution concentrations with a siltstone aggregate at 183 days.

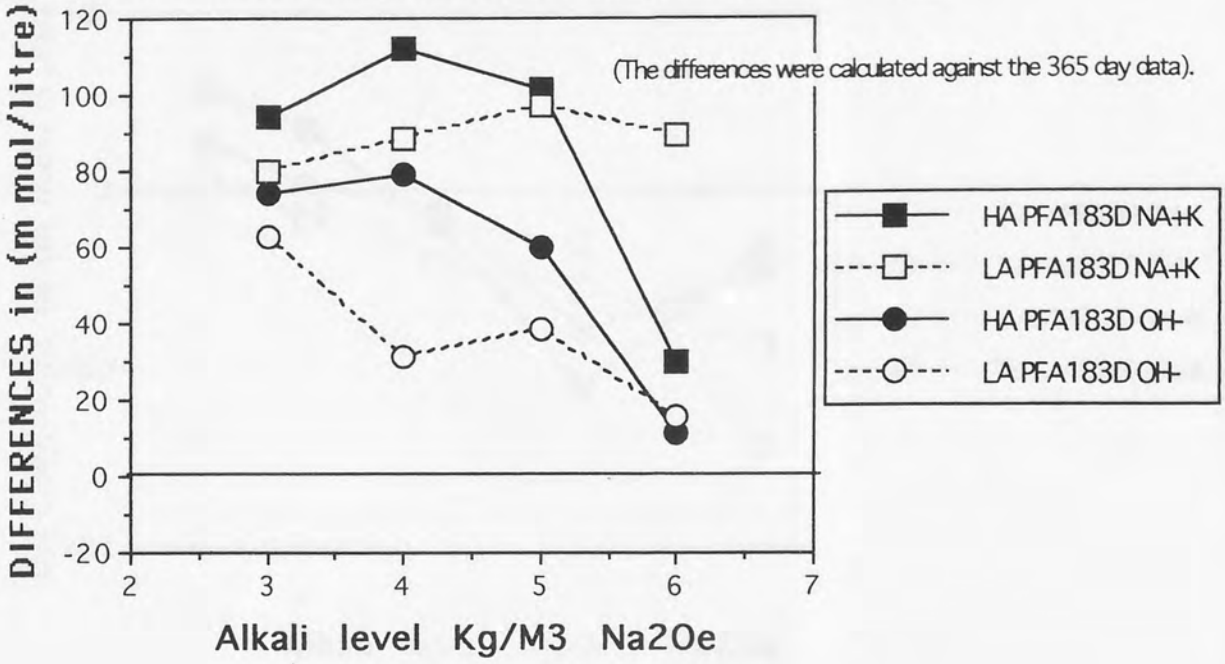


FIG 5.18: Differences between Pfa and OPC mixes pore solution concentrations with chert reactive aggregate at 1 day.

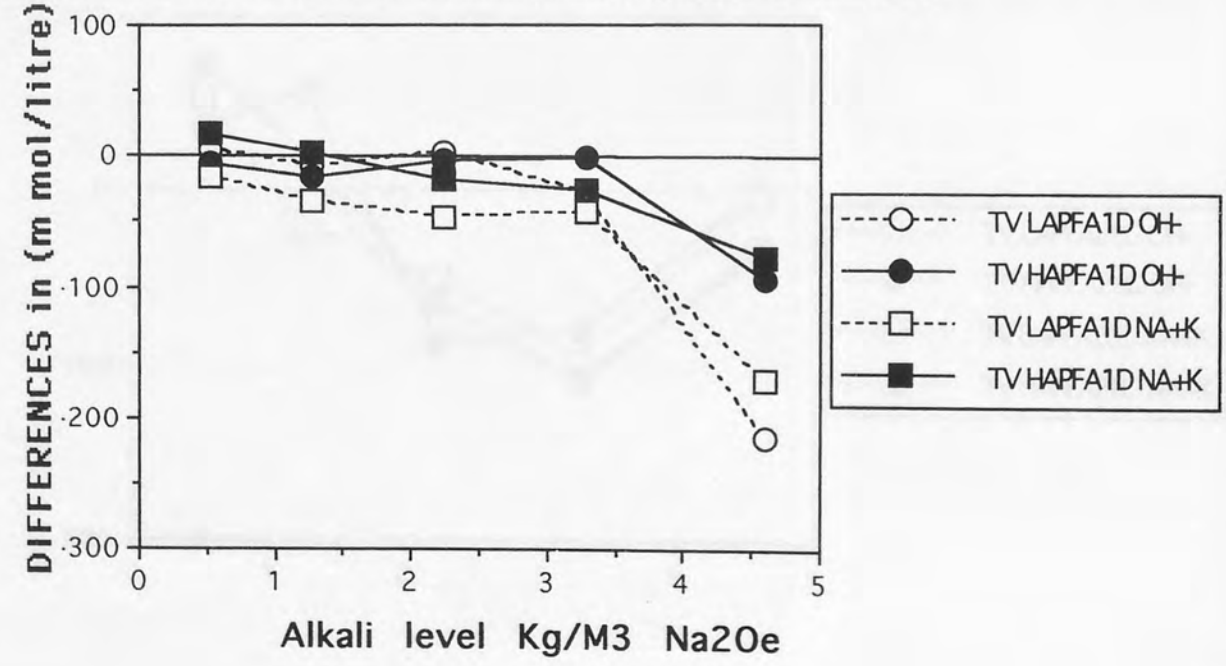

FIG 5.19: Differences between Pfa and OPC mixes pore solution concentration with chert reactive aggregate at 7 days.

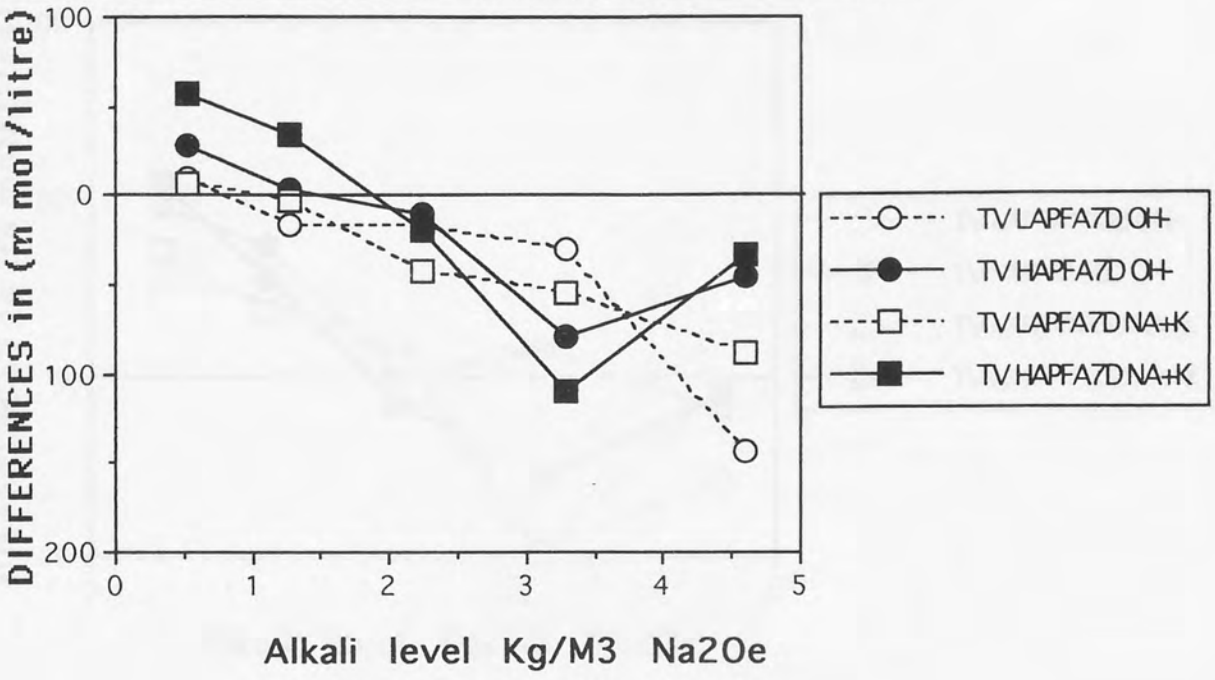


FIG 5.20: Differences between Pfa and OPC mixes pore solution concentration with chert reactive aggregate at 28 days.

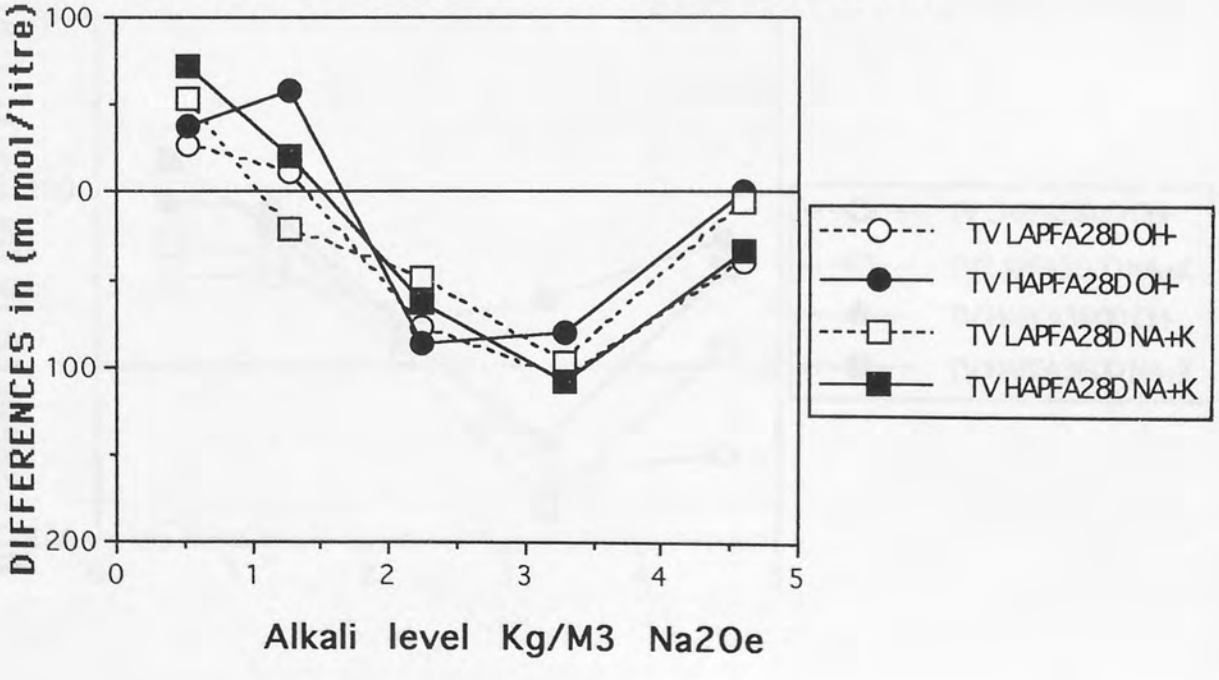

FIG 5.21: Differences between Pfa and OPC mixes pore solution concentration with chert aggregate at 180 days

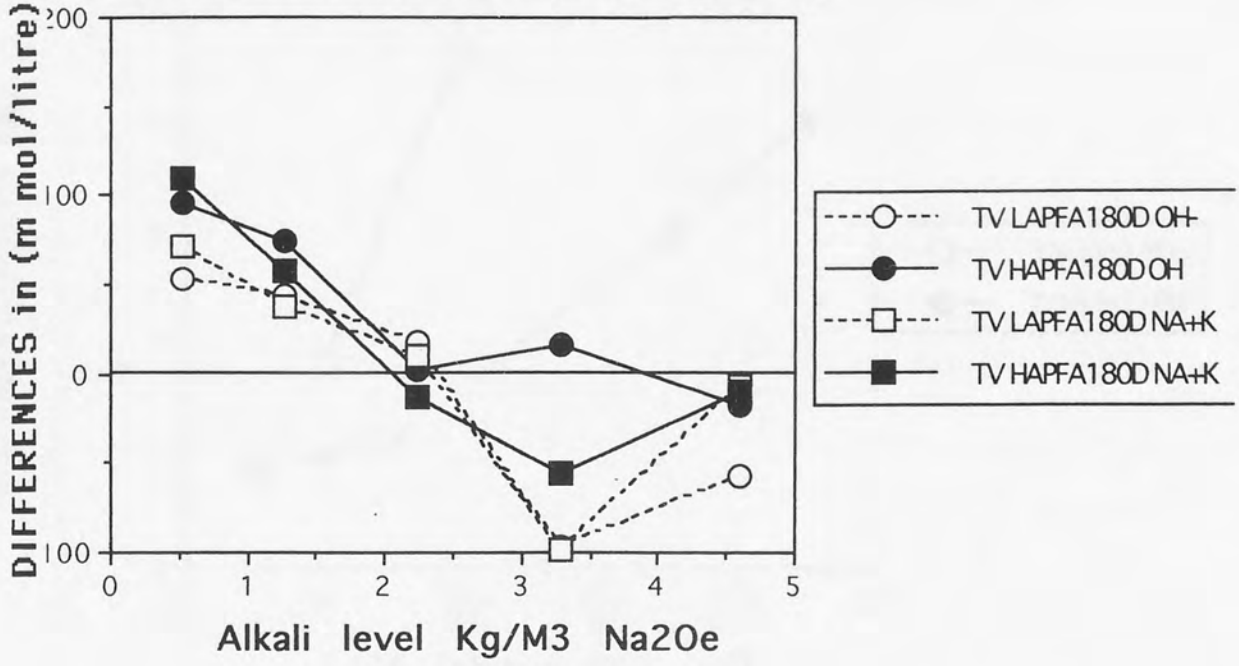


FIG 5.22: Differences between Pfa and OPC mixes pore solution concentration with chert aggregate at 360 days.

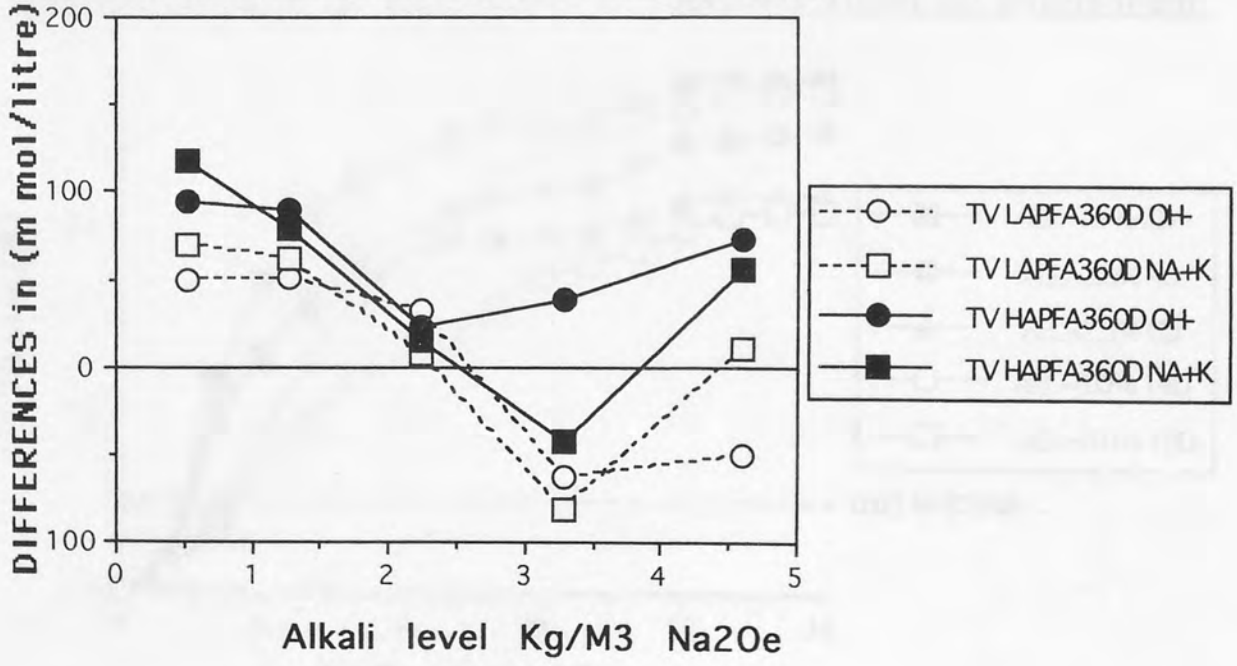

FIG 6.1: CALCULATED AIR ENTRAINMENT OF VARIOUS MIXES USED. (AEA addition are for 4 prisms)

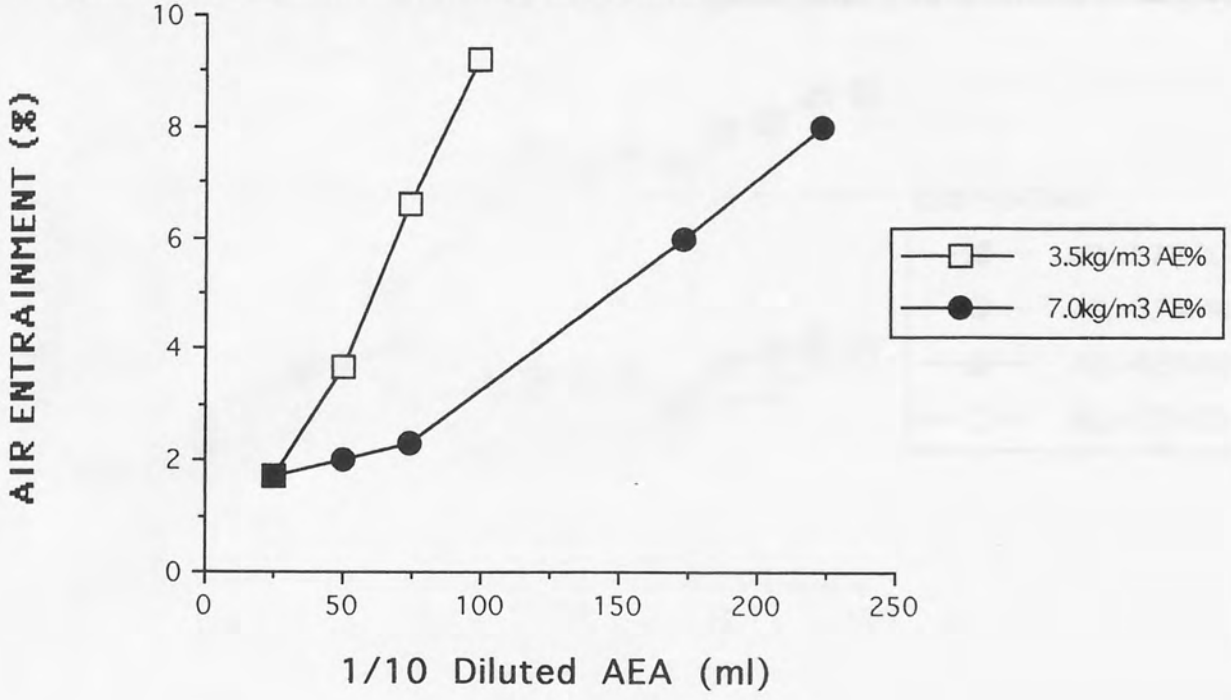


FIG 6.2: Expansion (%) Vs time for 7kg alkali (DR) siltstone mixes at different levels of air entrainment in 38oC and 100% RH environment.

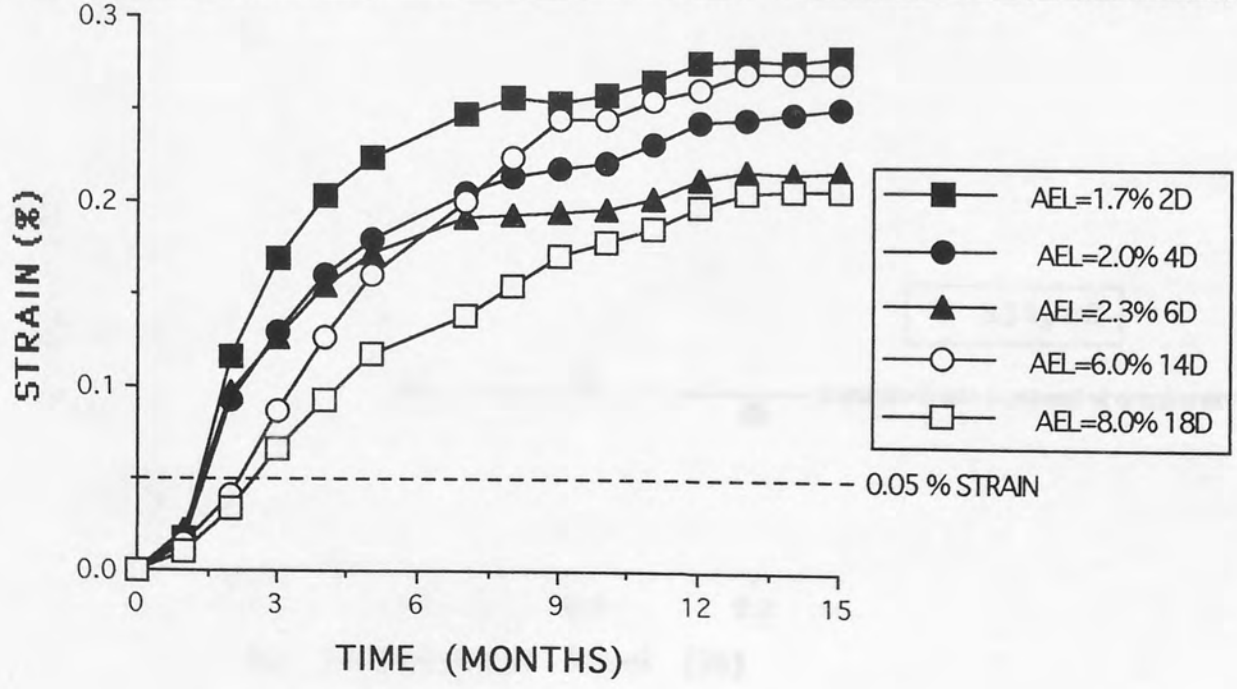

FIGURE 6.3: Expansion (%) Vs time for 3.5 kg alkali (DR) siltstone mixes at different levels of air entrainment in 38oC and 100% RH environment.

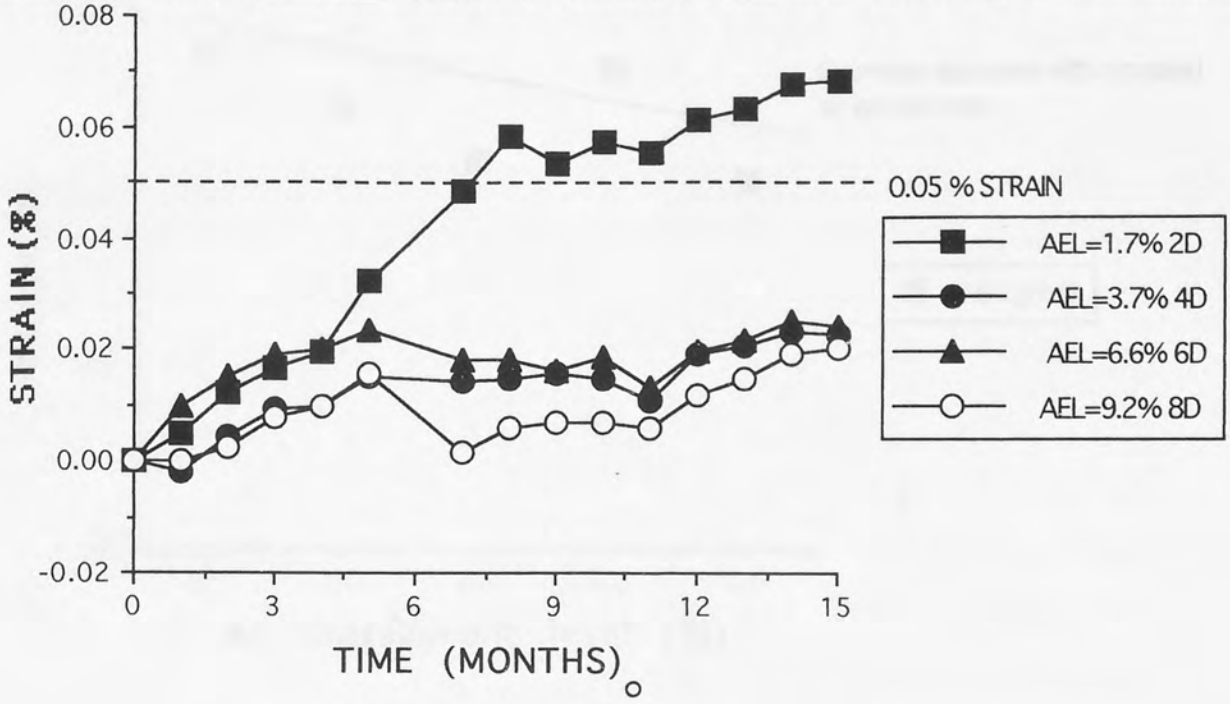


FIG 6.4 : Expansion (%) at 15 months Vs level of air entrainment. For 3.5 kg alkali (DR) siltstone mixes in 38oC and 100% RH.

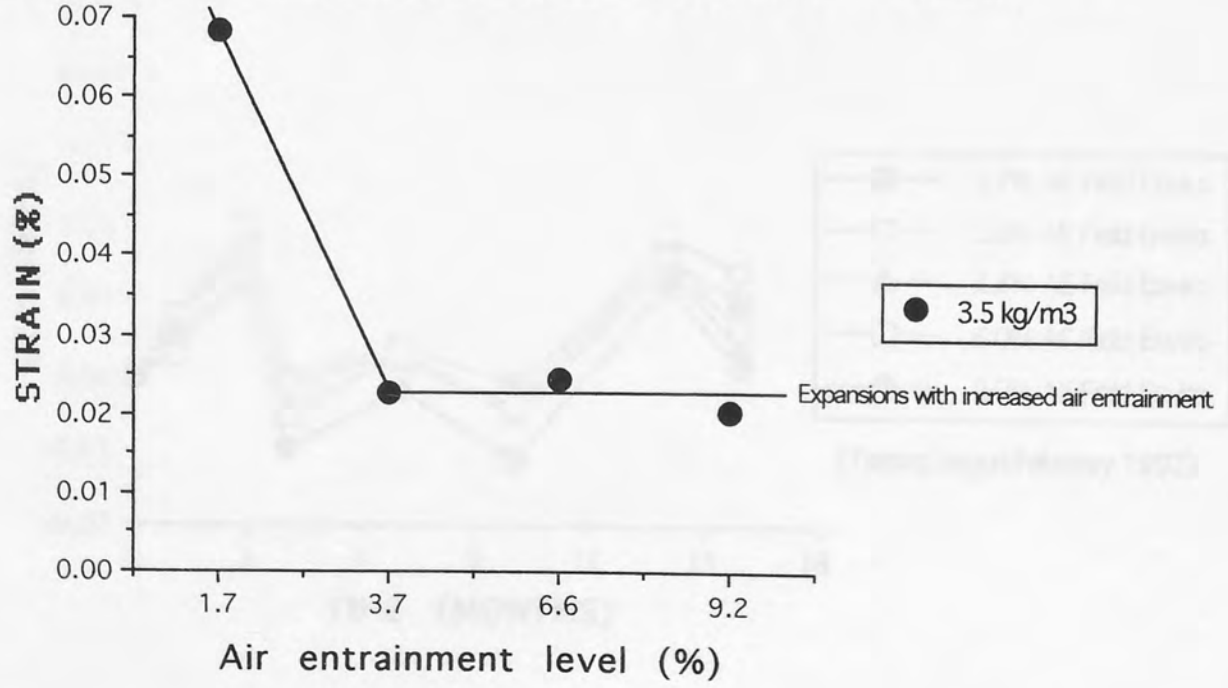

FIG 6.5: Exapansion (%) at 15 months Vs level of air entrainment. For 7 kg alkali (DR) siltstone mixes in 38oC and 100% RH.

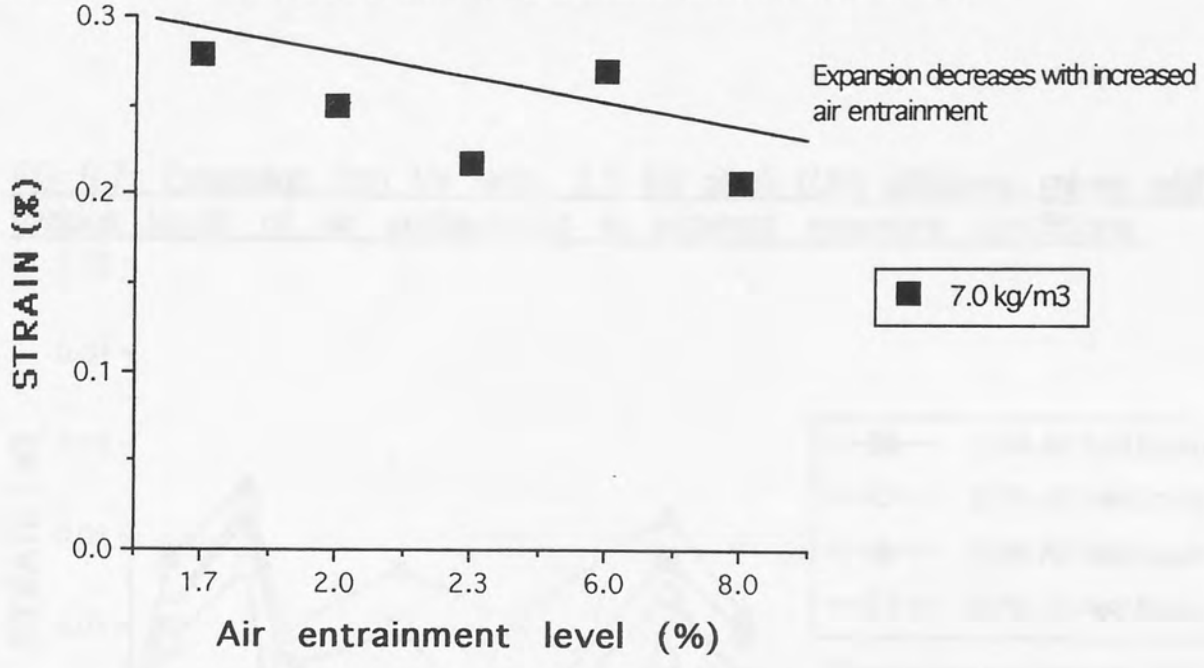


FIG 6.6: Expansion Vs time. 7 kg alkali (DR) siltstone mixes with various levels of air entrainment in external exposure conditions.

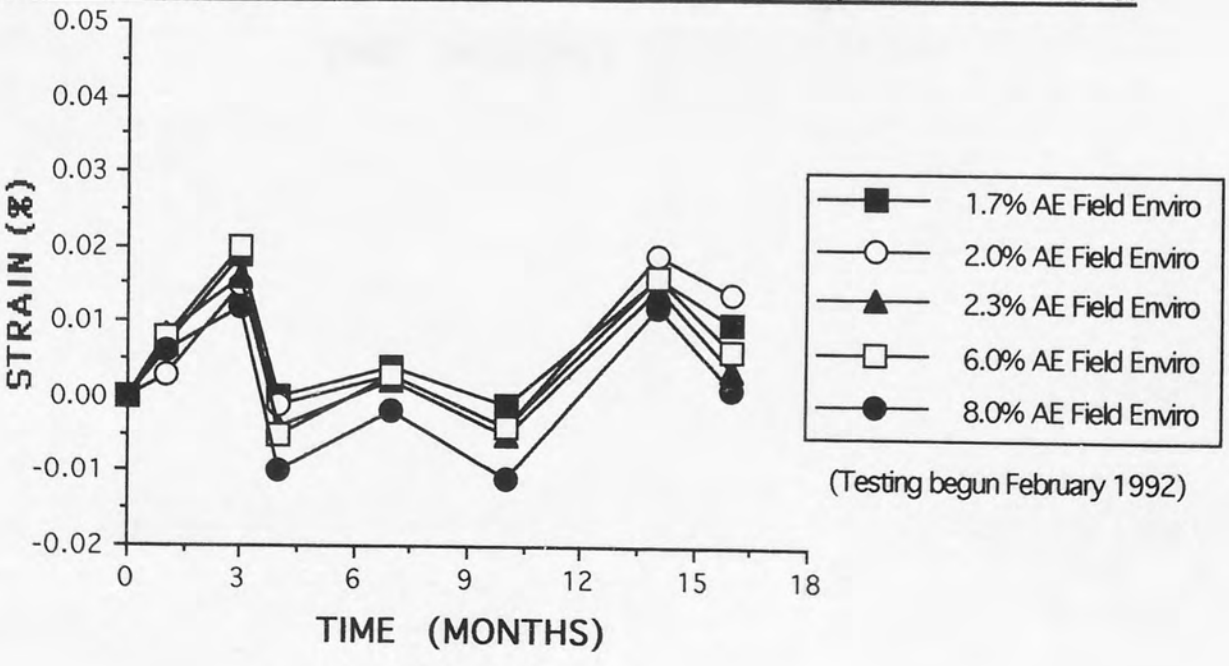

FIG 6.7: Expansion (%) Vs time. 3.5 kg alkali (DR) siltstone mixes with various levels of air entrainment in external exposure conditions.

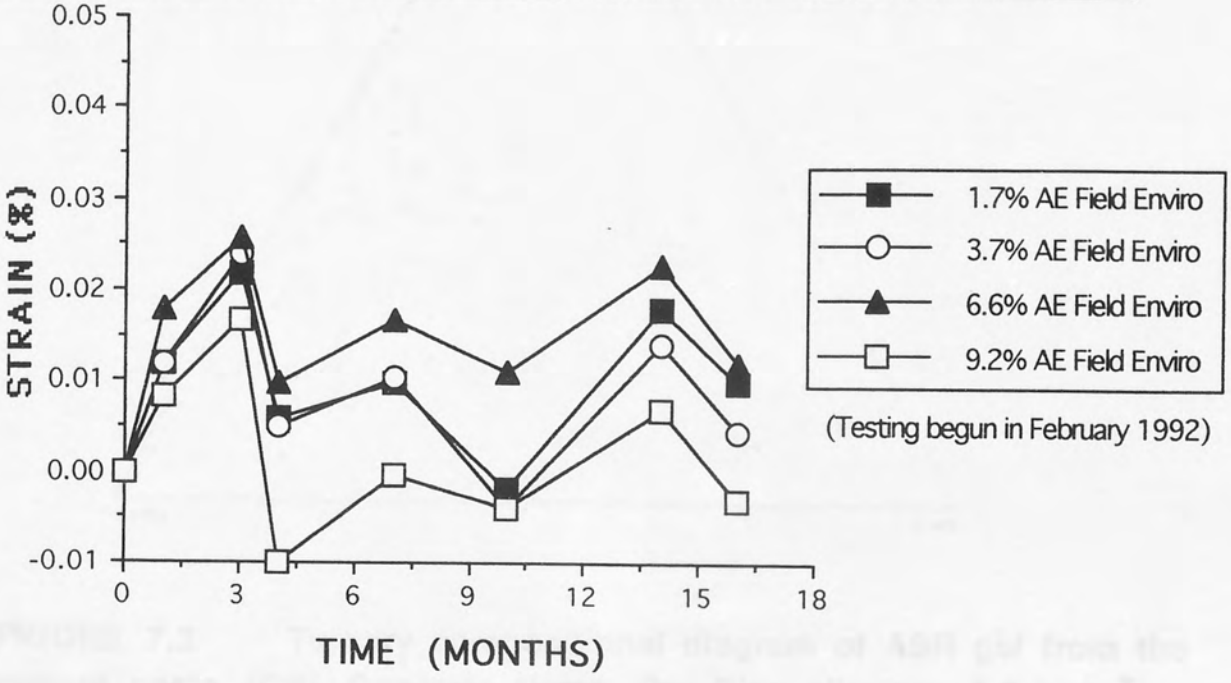

**FIGURE 7.1** Ternary compositional diagram of ASR gel from within coarse aggregate particles, (CA). Concrete Name: Dry Rigg siltstone 7.0 kg/m$^3$ $Na_2O_e$ immersed in distilled water for 12 months.

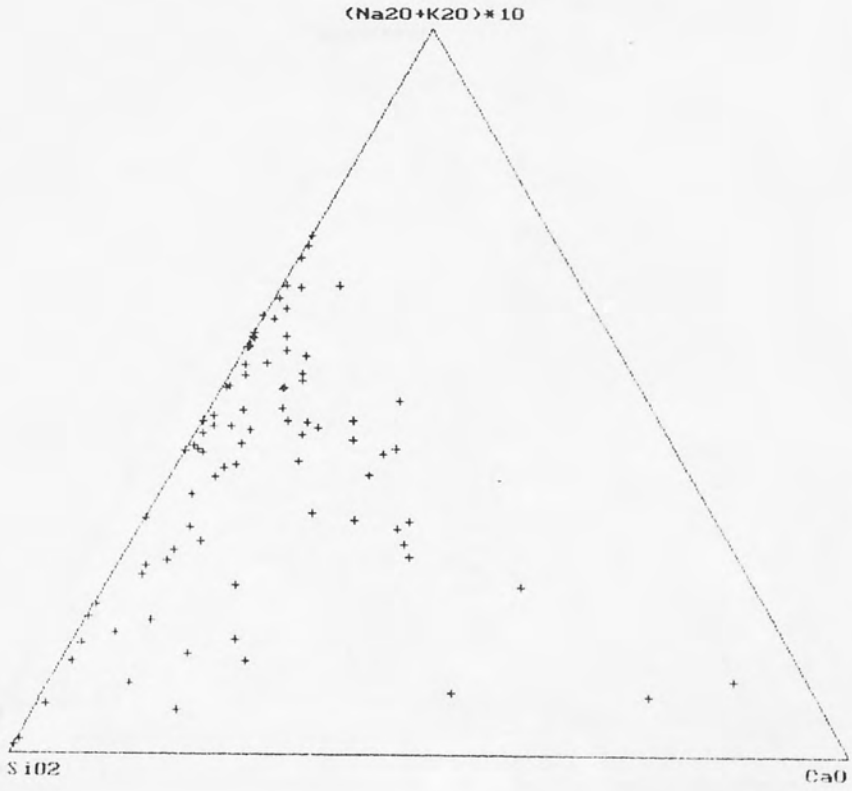


**FIGURE 7.2** Ternary compositional diagram of ASR gel from the cement paste, (CP). Concrete Name: Dry Rigg siltstone 7.0 kg/m$^3$ $Na_2O_e$ immersed in distilled water for 12 months.

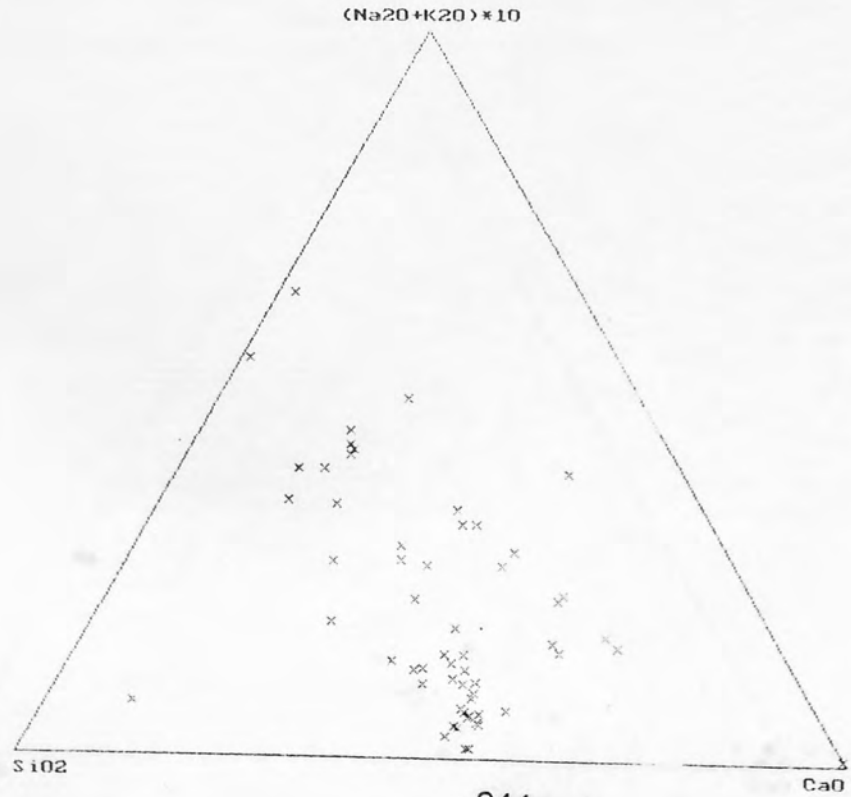

**FIGURE 7.3: Ternary compositional diagram, $SiO_2$: $Al_2O_3$: Cl of ASR gel from within coarse aggregate particles, (CA) cement paste, (CP). Concrete Name: Dry Rigg siltstone 7 kg/m$^3$ $Na_2O_e$ immersed in distilled water for 12 months.**

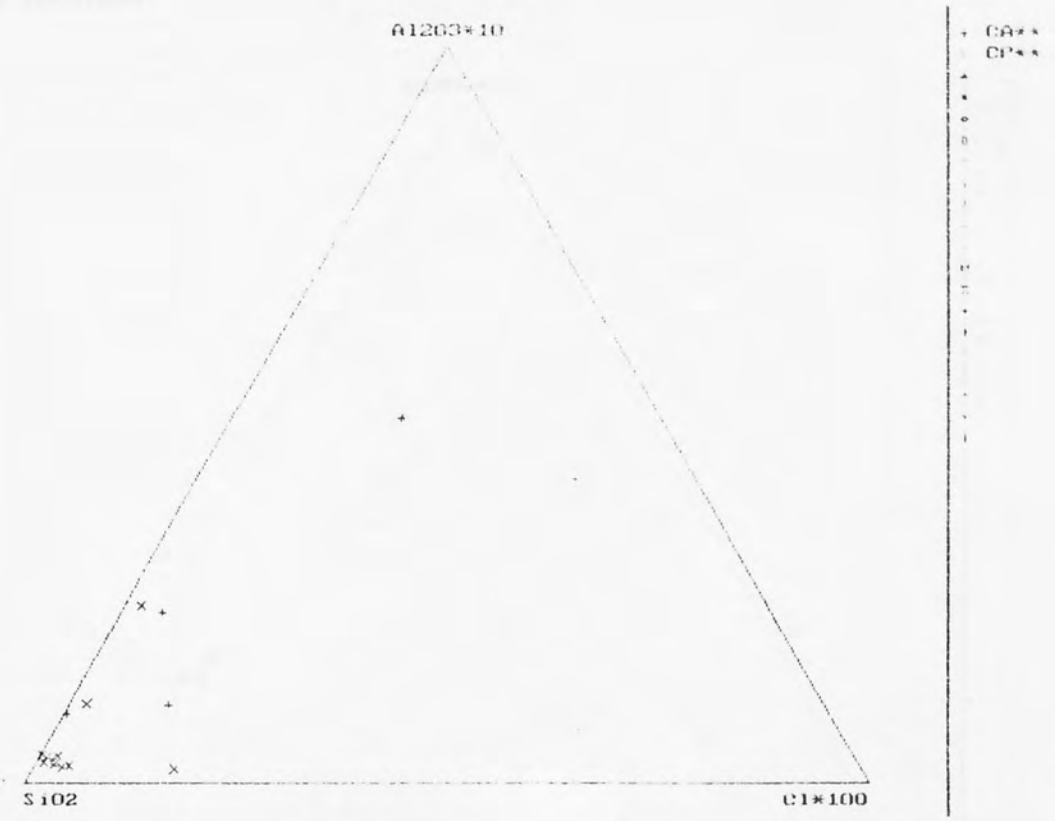


**FIGURE 7.4: Ternary compositional diagram, $SiO_2$: $Na_2O+K_2O$: CaO of ASR gel from within coarse aggregate particles, (CA) cement paste, (CP) and aggregate analyses. Concrete Name: Horrocksford limestone 7 kg/m$^3$ $Na_2O_e$ immersed in distilled water for 12 months.**

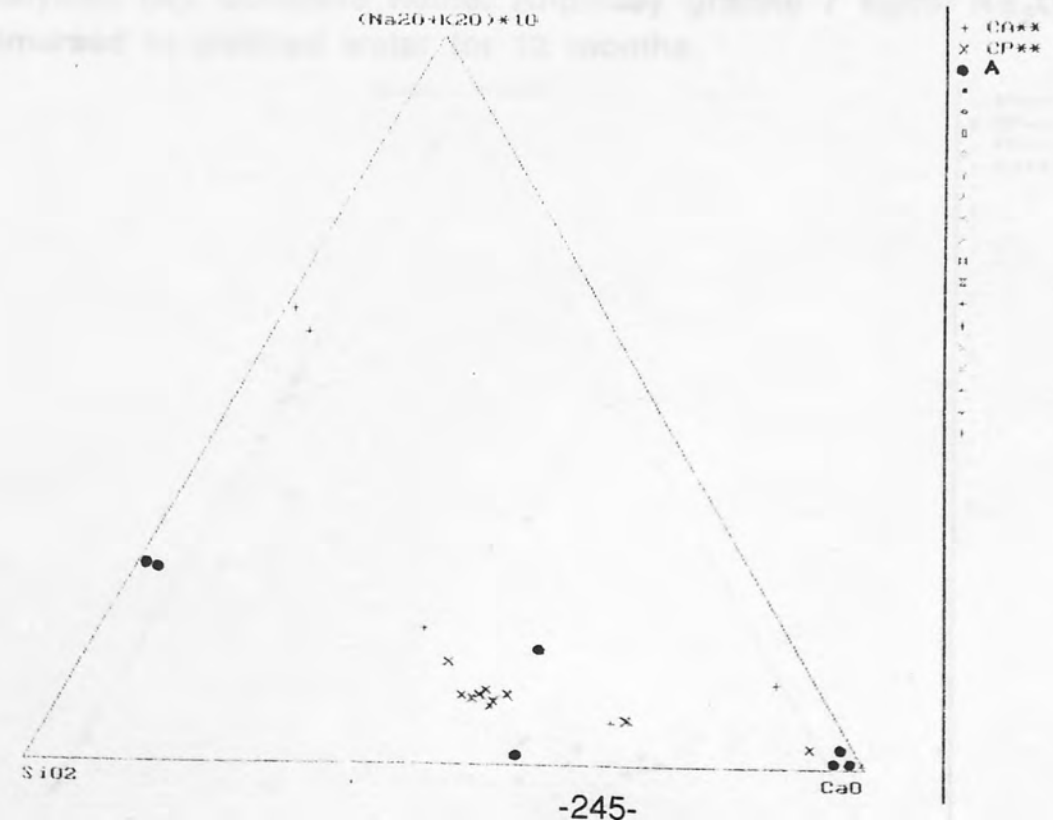

**FIGURE 7.5: Ternary compositional diagram, $SiO_2$: $Al_2O_3$: Cl of ASR gel from within coarse aggregate particles, (CA) cement paste, (CP) and normal cement paste, (PU) analyses. Concrete Name: Horrocksford limestone 7 kg/m$^3$ $Na_2O_e$ immersed in distilled water for 12 months.**

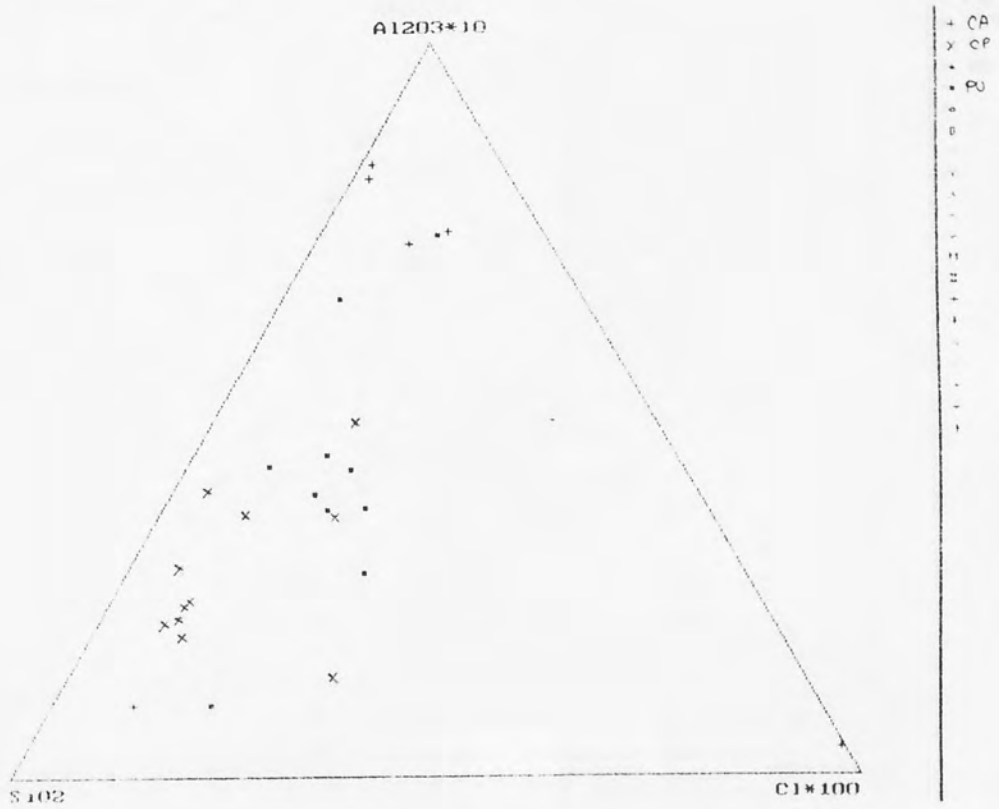


**FIGURE 7.6: Ternary compositional diagram, $SiO_2$: $Na_2O+K_2O$: CaO of ASR gel from within the cement paste, (CP) within coarse aggregate particles, (CA) normal cement paste, (PU) and bulk aggregate analyses, (A). Concrete Name: Anglesey granite 7 kg/m$^3$ $Na_2O_e$ immersed in distilled water for 12 months.**

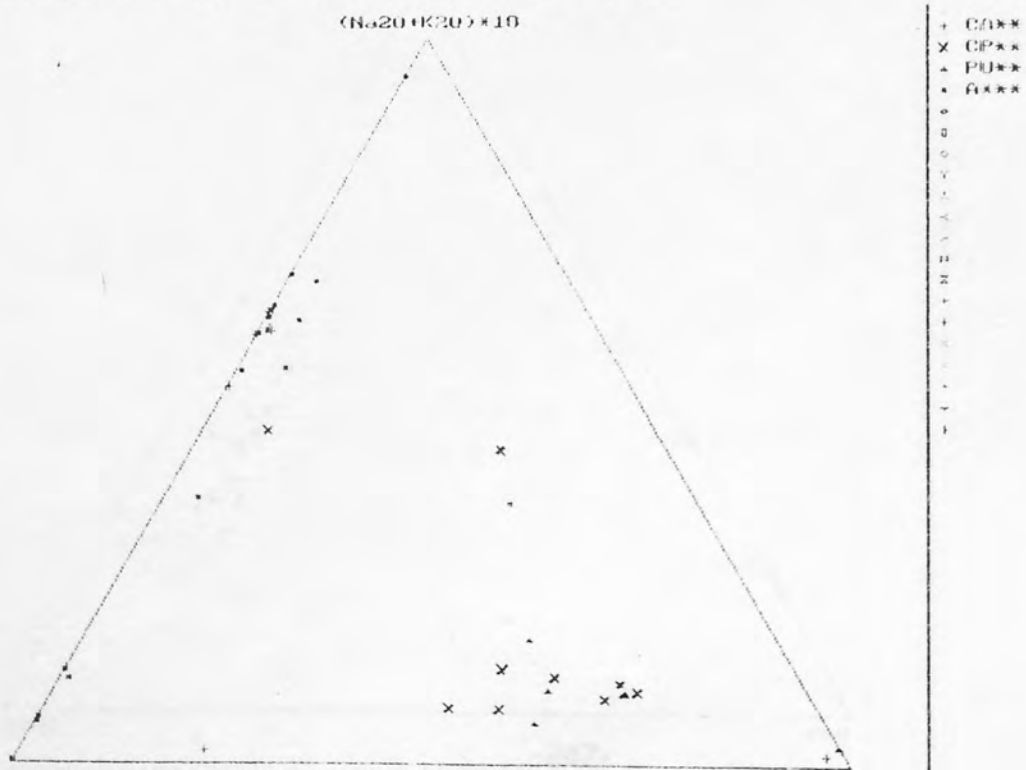

**FIGURE 7.7: Ternary compositional diagram, $SiO_2$: $Al_3O_2$: Cl of ASR gel from within cement paste, (CP) within coarse aggregate particles, (CA) normal cement paste, (PU) and bulk aggregate analyses, (A). Concrete Name: Anglesey granite 7 kg/m$^3$ $Na_2O_e$ immersed in distilled water for 12 months.**

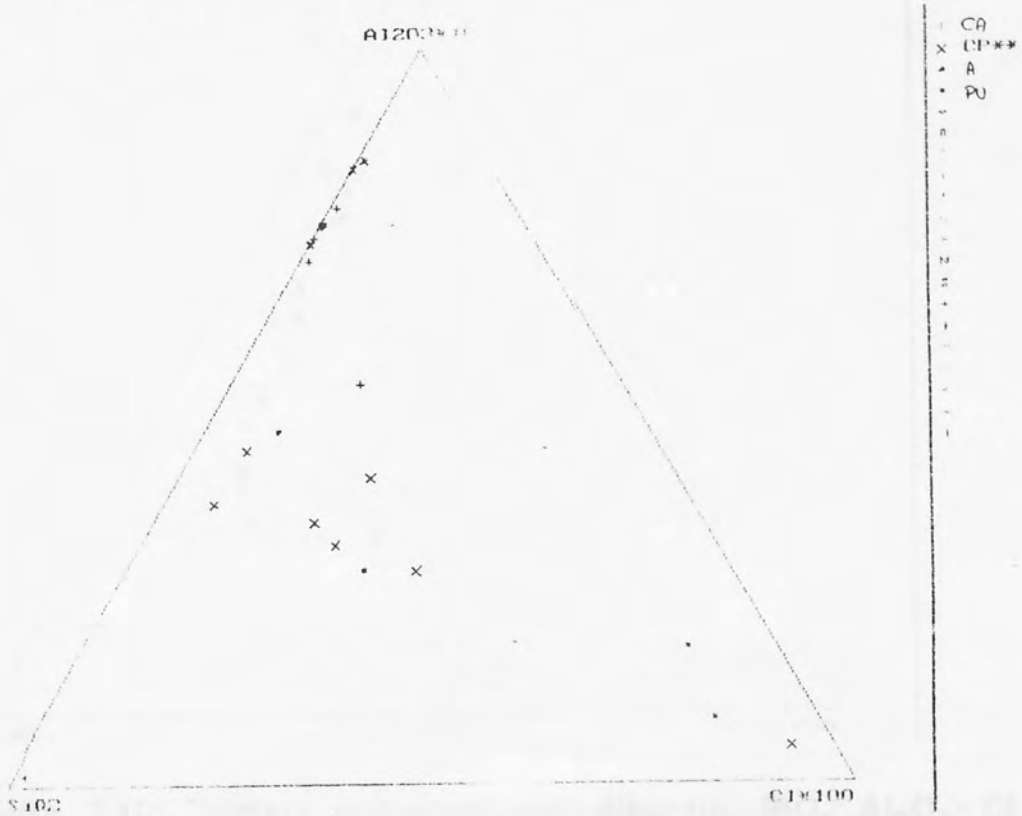


**FIGURE 7.8: Ternary compositional diagram, $SiO_2$: $Na_2O+K_2O$: CaO of ASR gel from within coarse aggregate particles, (CA). Concrete Name: Dry Rigg siltstone 7 kg/m$^3$ $Na_2O_e$ immersed in salt solution for 15 months.**

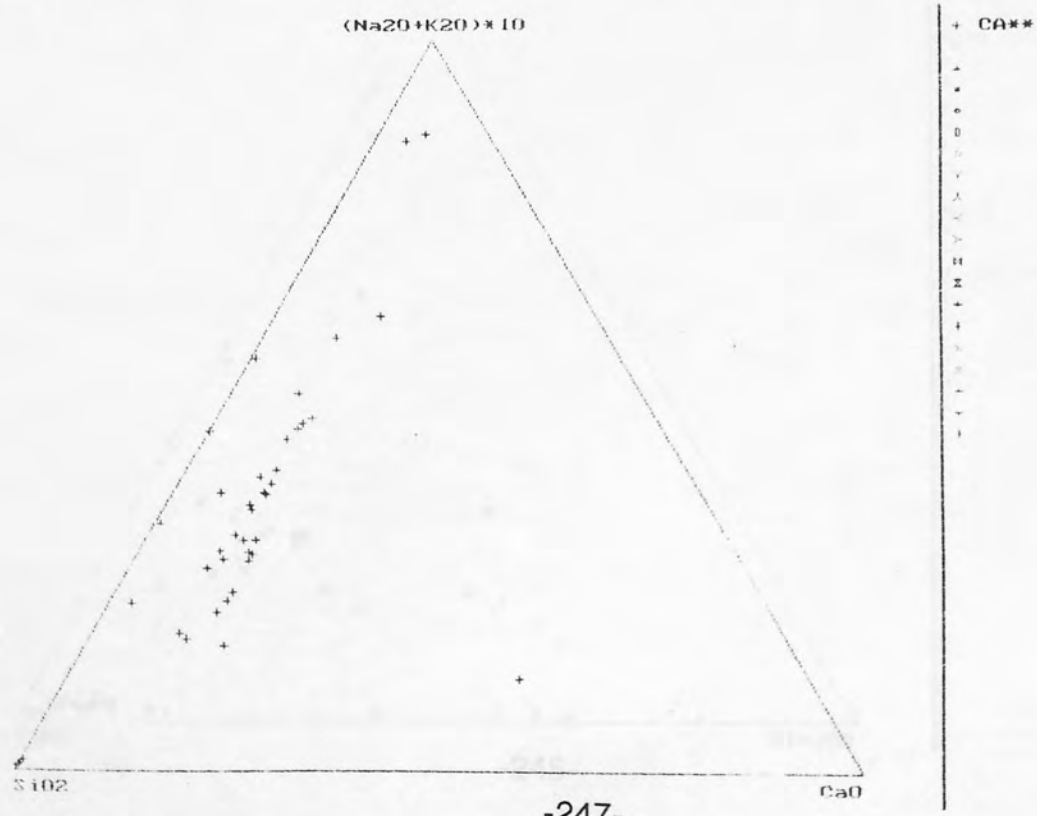

**FIGURE 7.9: Ternary compositional diagram, $SiO_2$: $Na_2O+K_2O$: CaO of ASR gel from within cement paste, (CP). Concrete Name: Dry Rigg siltstone 7 kg/m$^3$ $Na_2O_e$ immersed in salt solution for 15 months.**

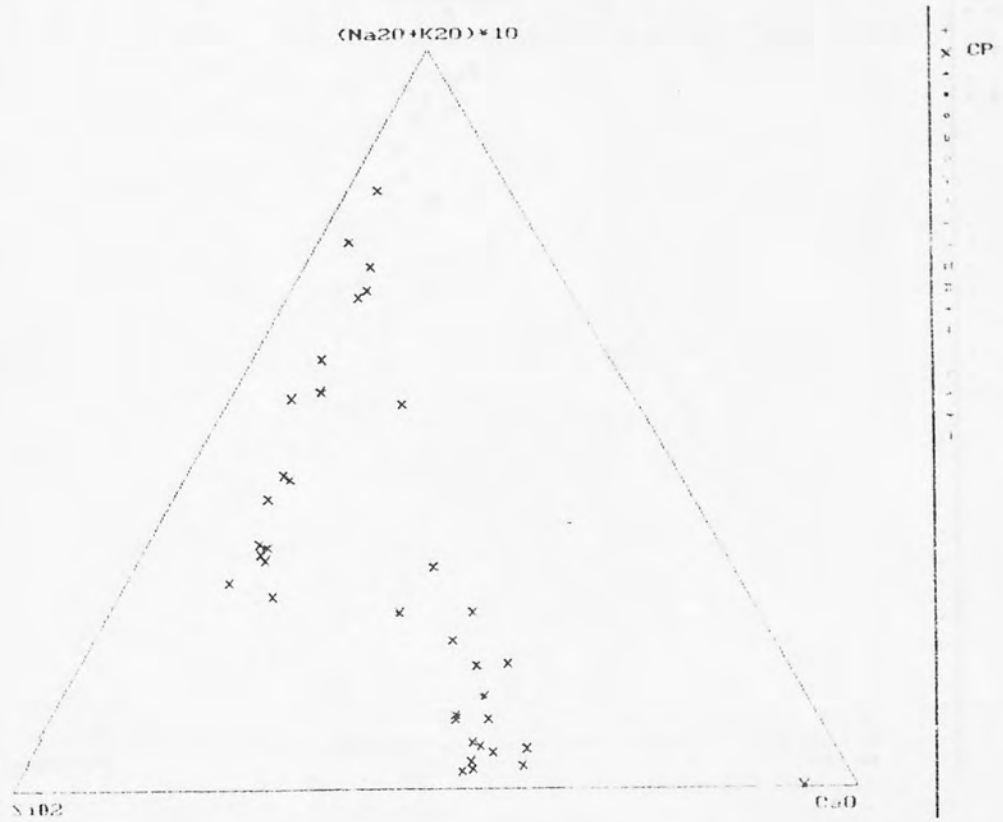


**FIGURE 7.10: Ternary compositional diagram, $SiO_2$: $Al_2O_3$: Cl of ASR gel from within cement paste, (CP) within coarse aggregate particles, (CA) and normal cement paste, (PU) analyses. Concrete Name: Dry Rigg siltstone 7 kg/m$^3$ $Na_2O_e$ immersed in salt solution for 15 months.**

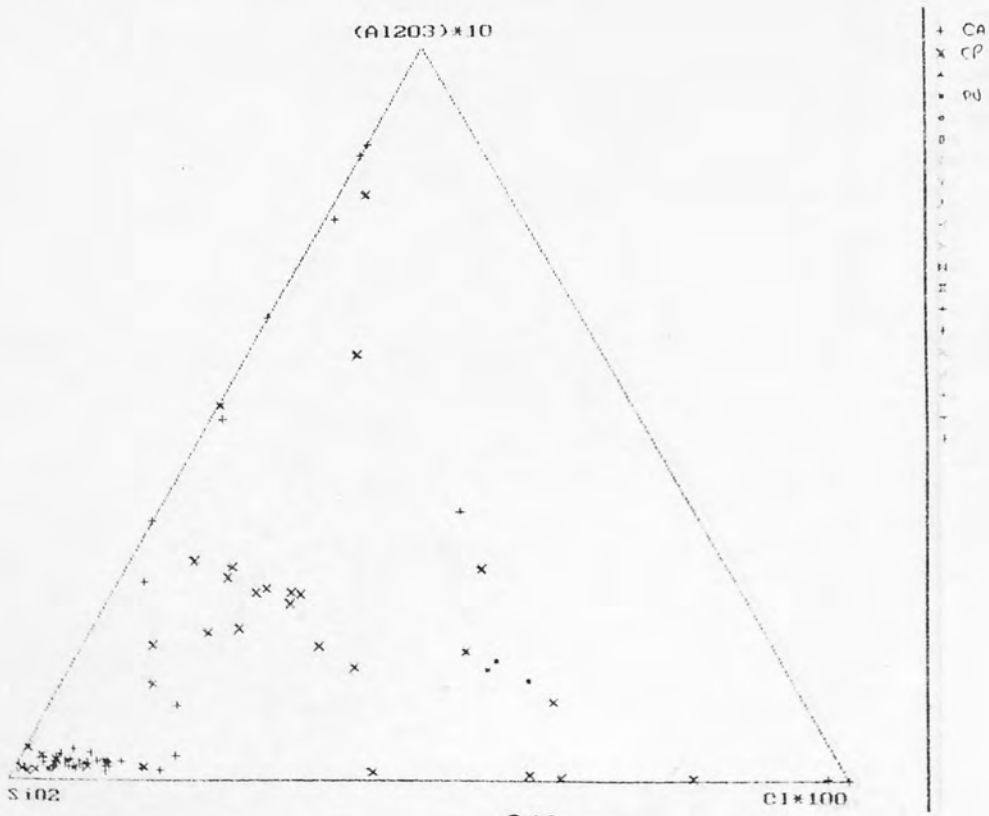

**FIGURE 7.11: Ternary compositional diagram, $SO_3$: $Al_2O_3$: Cl of ASR gel from within cement paste, (CP) ettringite, (ETT) and normal cement paste, (PU) analyses. Concrete Name: Dry Rigg siltstone 7 kg/m$^3$ $Na_2O_e$ immersed in salt solution for 15 months.**

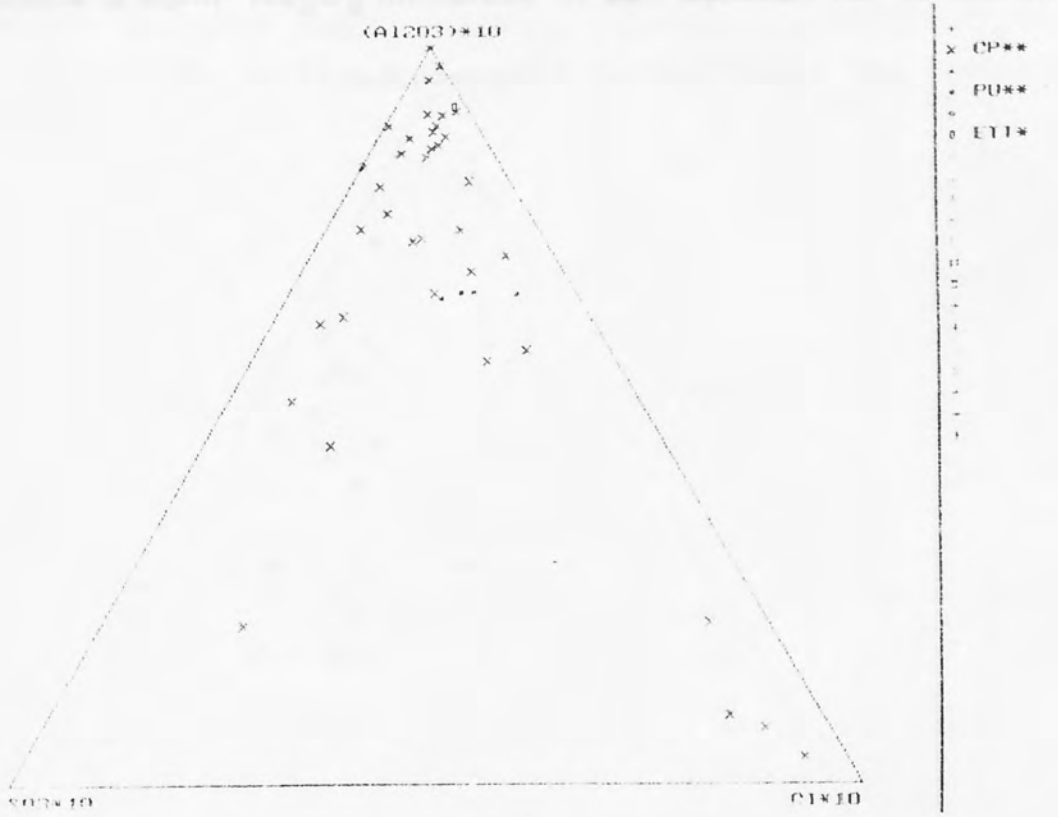


**FIGURE 7.12: Ternary compositional diagram, $SiO_2$: $Na_2O+K_2O$: CaO of ASR gel from within coarse aggregate particles, (CA). Concrete Name: Dry Rigg siltstone 3 kg/m$^3$ $Na_2O_e$ immersed in salt solution for 15 months.**

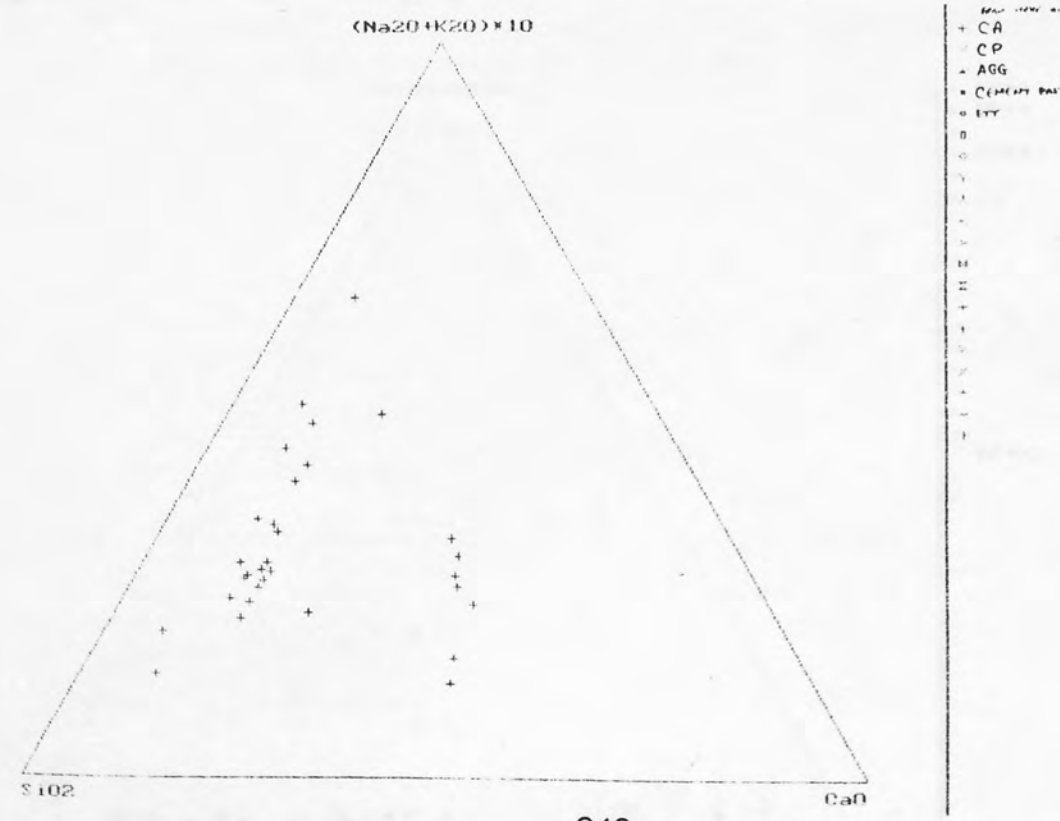

**FIGURE 7.13: Ternary compositional diagram, $SiO_2$: $Na_2O+K_2O$: CaO of ASR gel from within cement paste, (CP). Concrete Name: Dry Rigg siltstone 3 kg/m$^3$ $Na_2O_e$ immersed in salt solution for 15 months.**

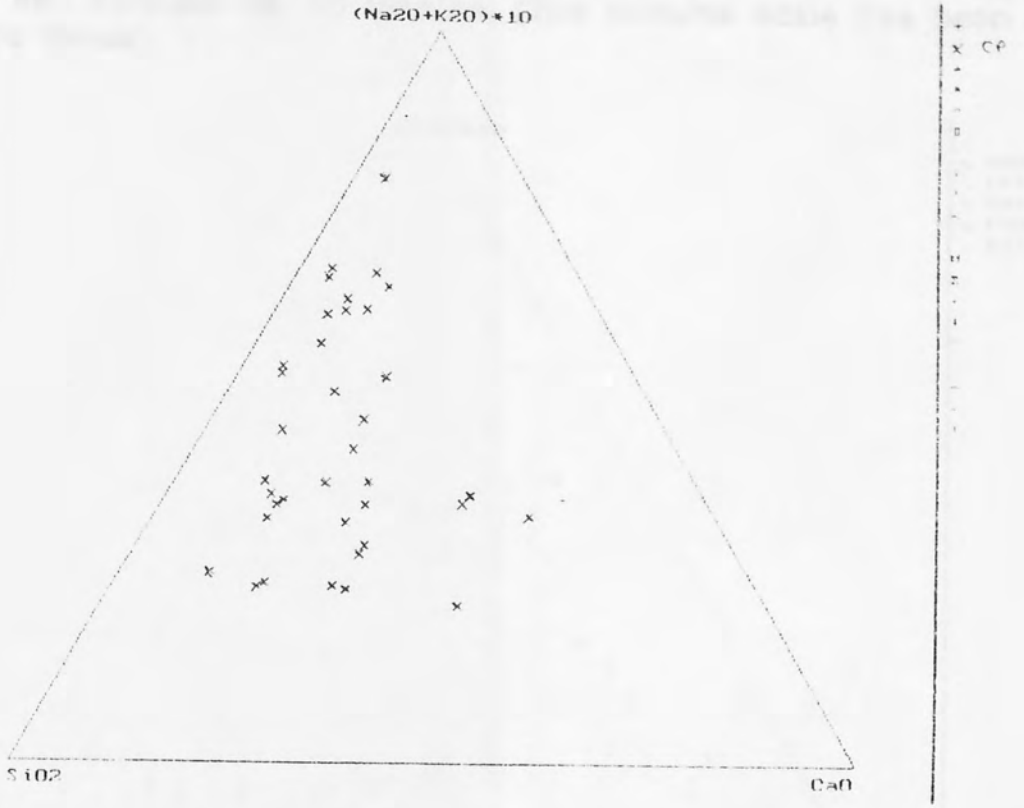


**FIGURE 7.14: Ternary compositional diagram, $SiO_2$: $Al_2O_3$: Cl of ASR gel from within cement paste, (CP) within coarse aggregate particles, (CA) and normal cement paste, (PU) analyses. Concrete Name: Dry Rigg siltstone 3 kg/m$^3$ $Na_2O_e$ immersed in salt solution for 15 months.**

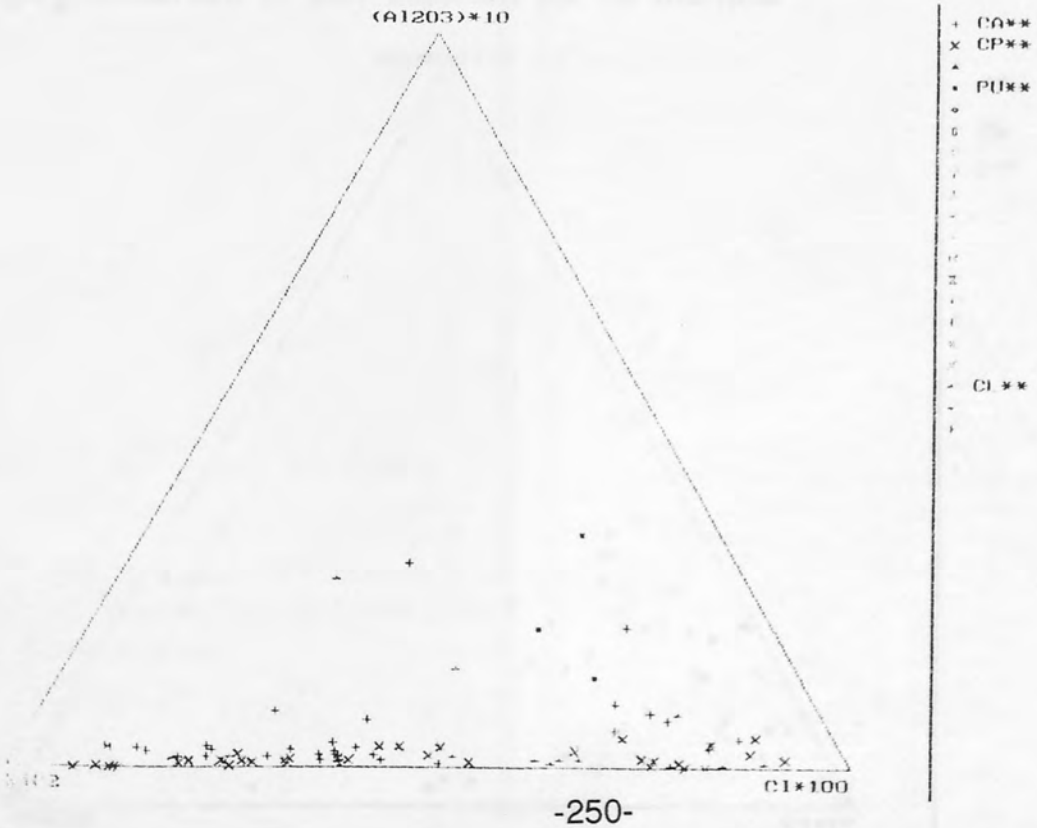

**FIGURE 7.15: Ternary compositional diagram, $SiO_2$: $Al_2O_3$: Cl of ASR gel from within cement paste, (CP) within coarse aggregate particles, (CA) ettringite, (ETT) aggregate (A) and normal cement paste, (PU) analyses. Concrete Name: Dry Rigg siltstone 3 kg/m$^3$ $Na_2O_e$ immersed in salt solution for 15 months. (The alumina scale has been expanded five times).**

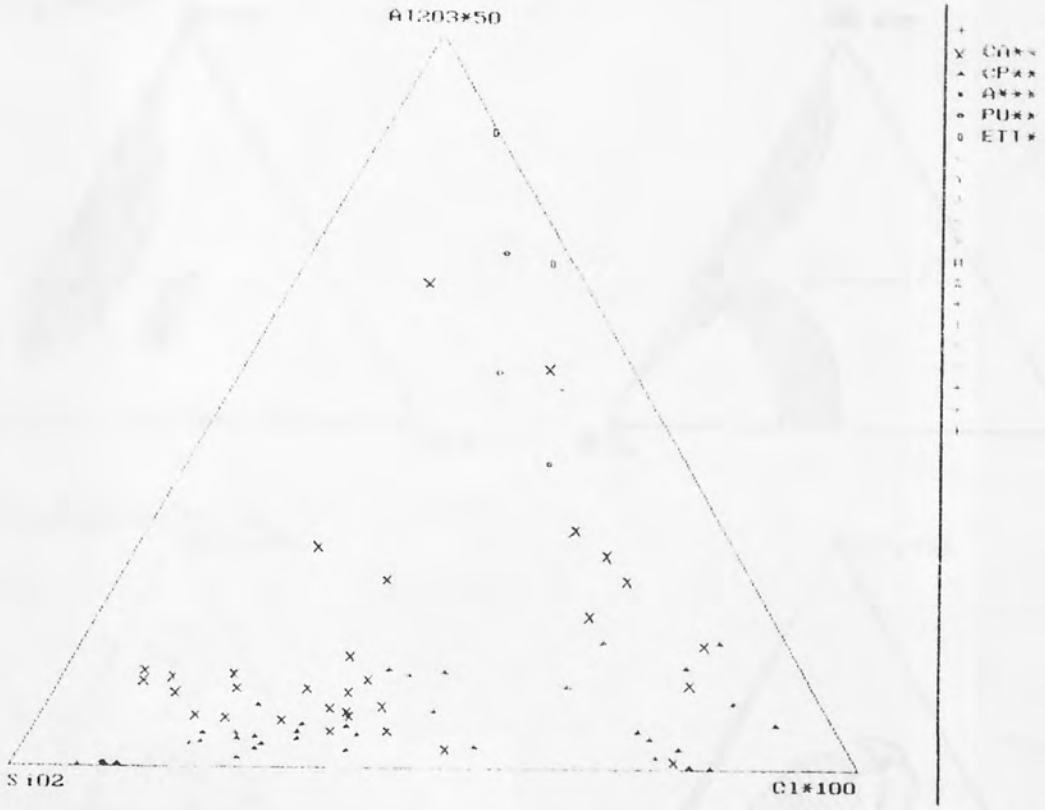


**FIGURE 7.16: Ternary compositional diagram, $SO_3$: $Al_2O_3$: Cl of ASR gel from within cement paste, (CP) ettringite, (ETT) and normal cement paste, (PU) analyses. Concrete Name: Dry Rigg siltstone 3 kg/m$^3$ $Na_2O_e$ immersed in salt solution for 15 months.**

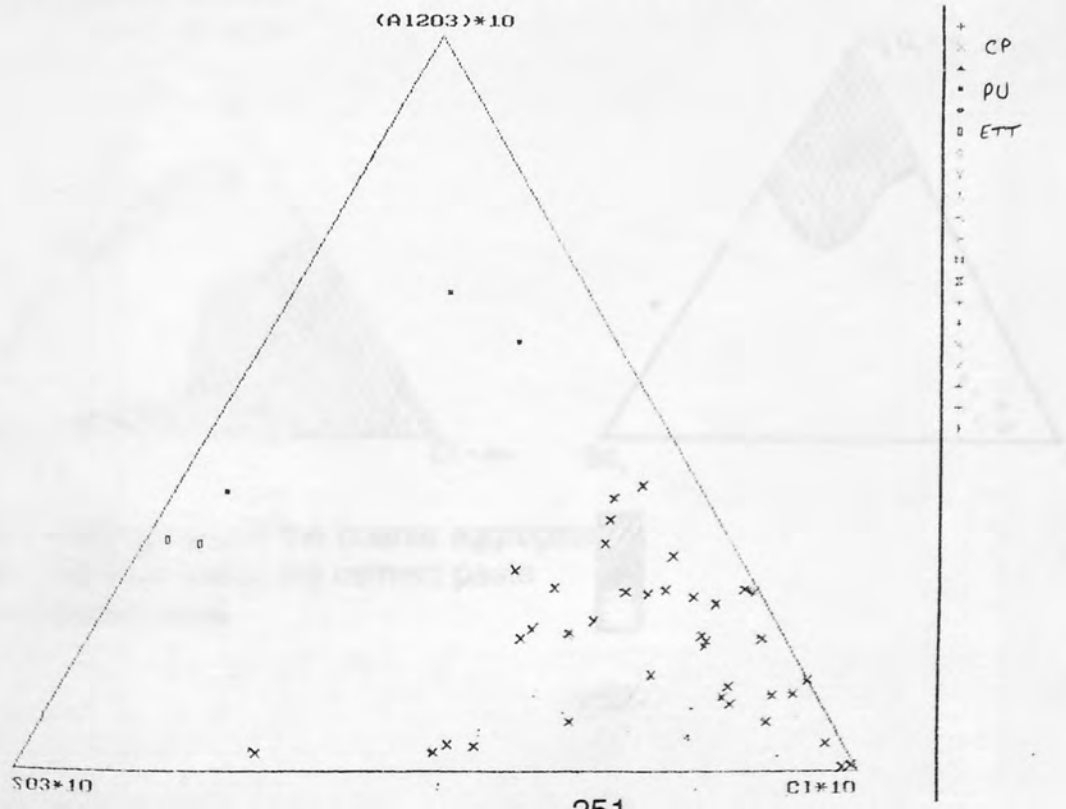

**FIGURE 7.17: Summary of electron microprobe (EMP) analyses of ASR gels and cement pastes from the two Dry Rigg siltstone concretes immersed in salt solution.**

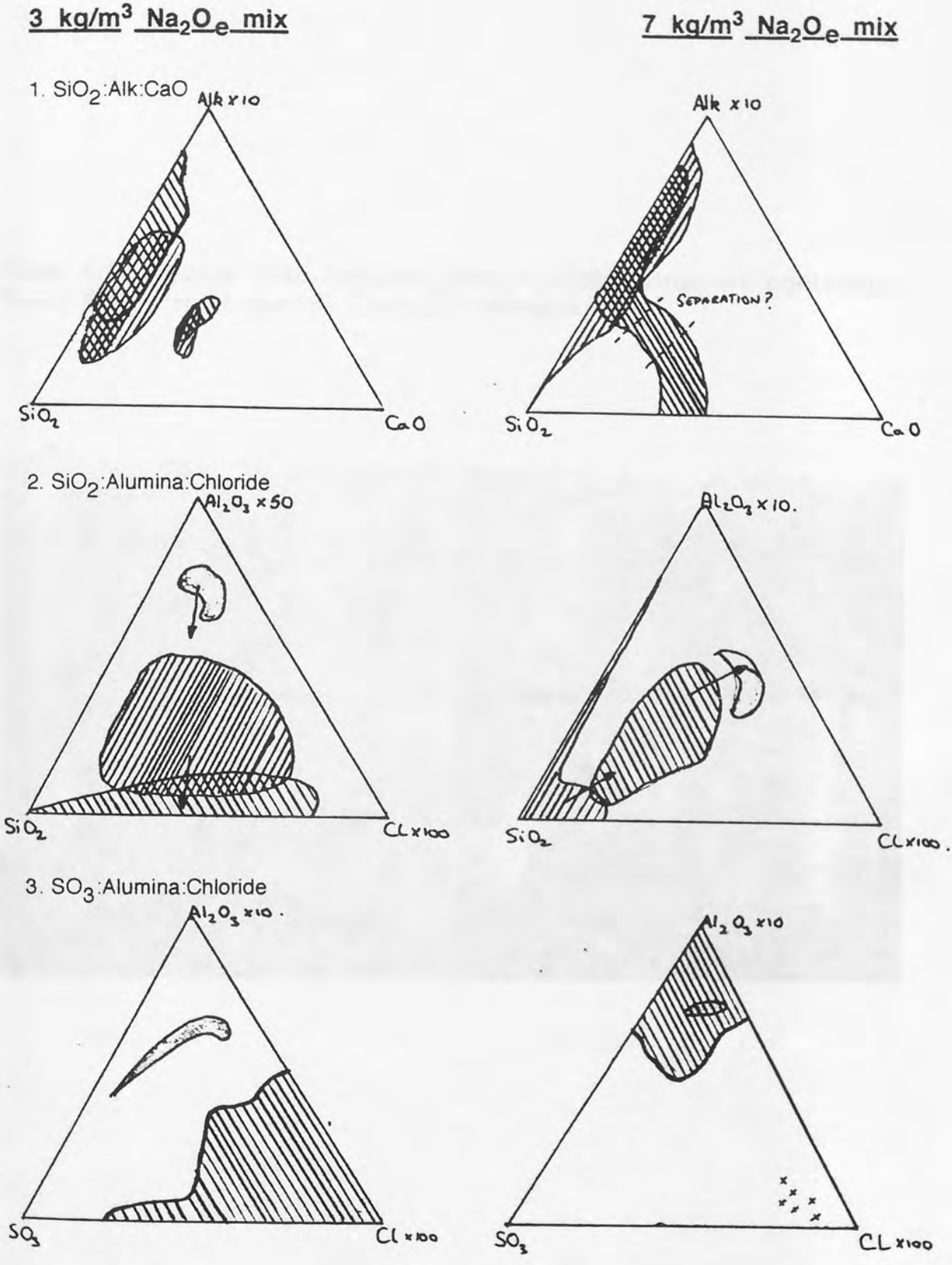


CA - Gel from within the coarse aggregate
CP - Gel from within the cement paste
P - Cement paste

**Plate 1.1 Typical map cracking from a bridge structure containing Trent Valley river gravel. Location Warwickshire.**

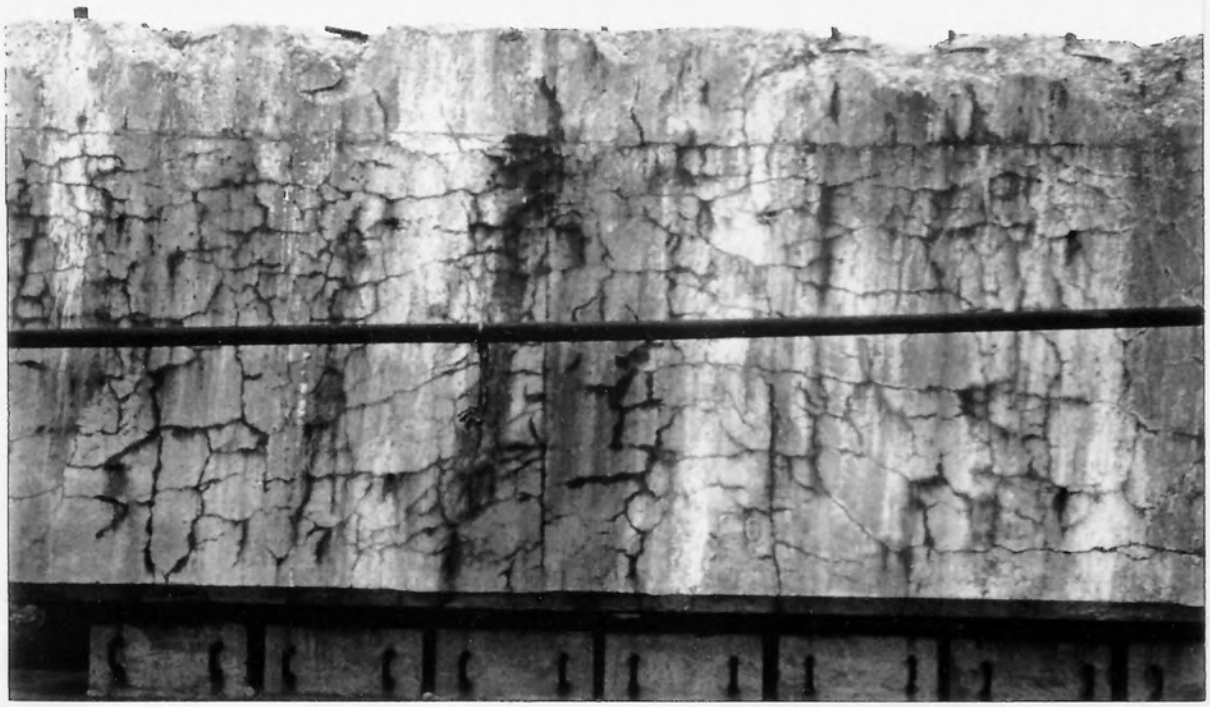

Plate 1.2 Typical map cracking from the surface of a concrete road pavement containing Dry Rigg siltstone. Location Lancashire.

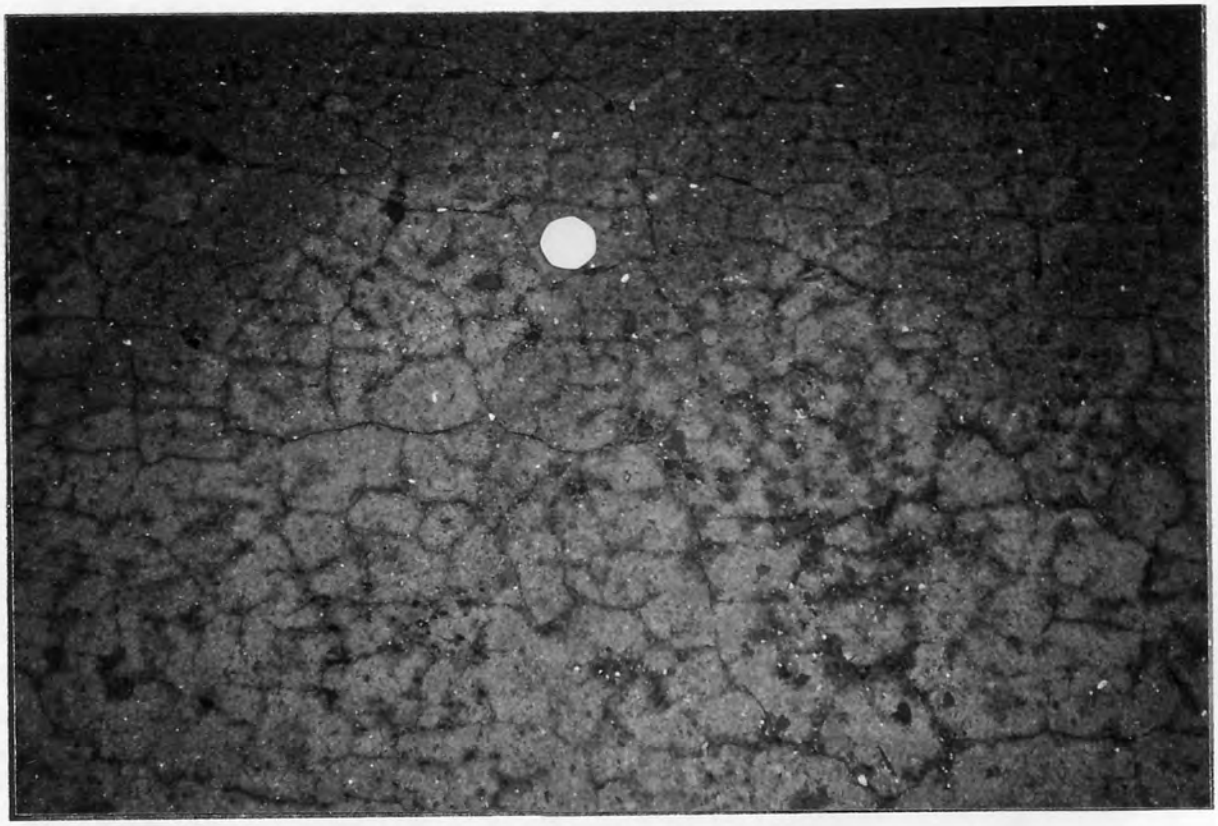

Plate 1.3 Sweaty moist area of concrete surface, feature often associated with ASR reactive aggregate. This core was taken from a road pavement in Lancashire and contains Horrocksford limestone.

Plate 3.1 Divergent expansive microcracking originating in the siltstone coarse aggregate. Dry Rigg siltstone mix,7 kg/m$^3$ $Na_2O_e$ (plane polarised light, X40 Mag).

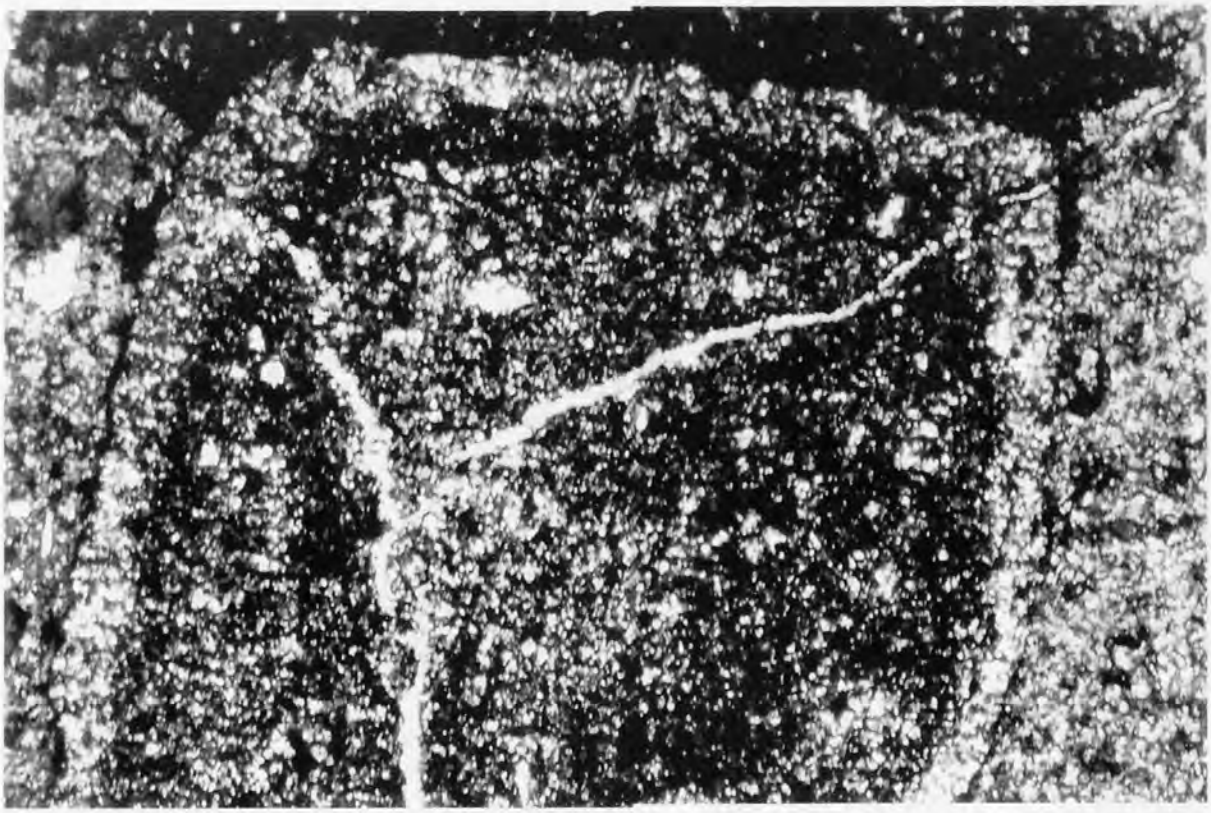

Plate 3.2 ASR microcracking in the siltstone coarse aggregate, some is observed to run preferentially with the cleavage and bedding of the rock. Dry Rigg siltstone mix,7 kg/m$^3$ $Na_2O_e$ (plane polarised light, X40 Mag).

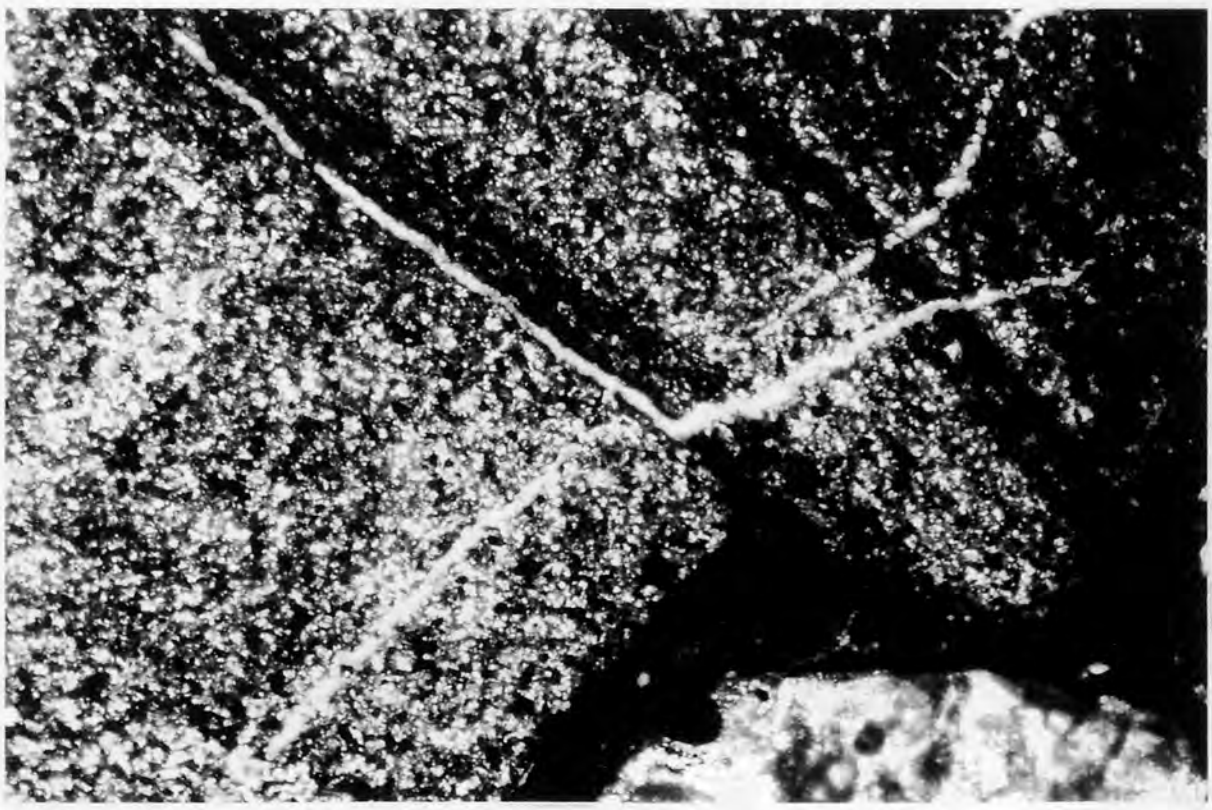

Plate 3.3 Pseudo-adhesion cracks running around the periphery of a reactive aggregate particle, but still within the aggregate material as opposed to the cement paste. Horrocksford limestone mix,7 kg/m$^3$ $Na_2O_e$ (plane polarised light, X40 Mag).

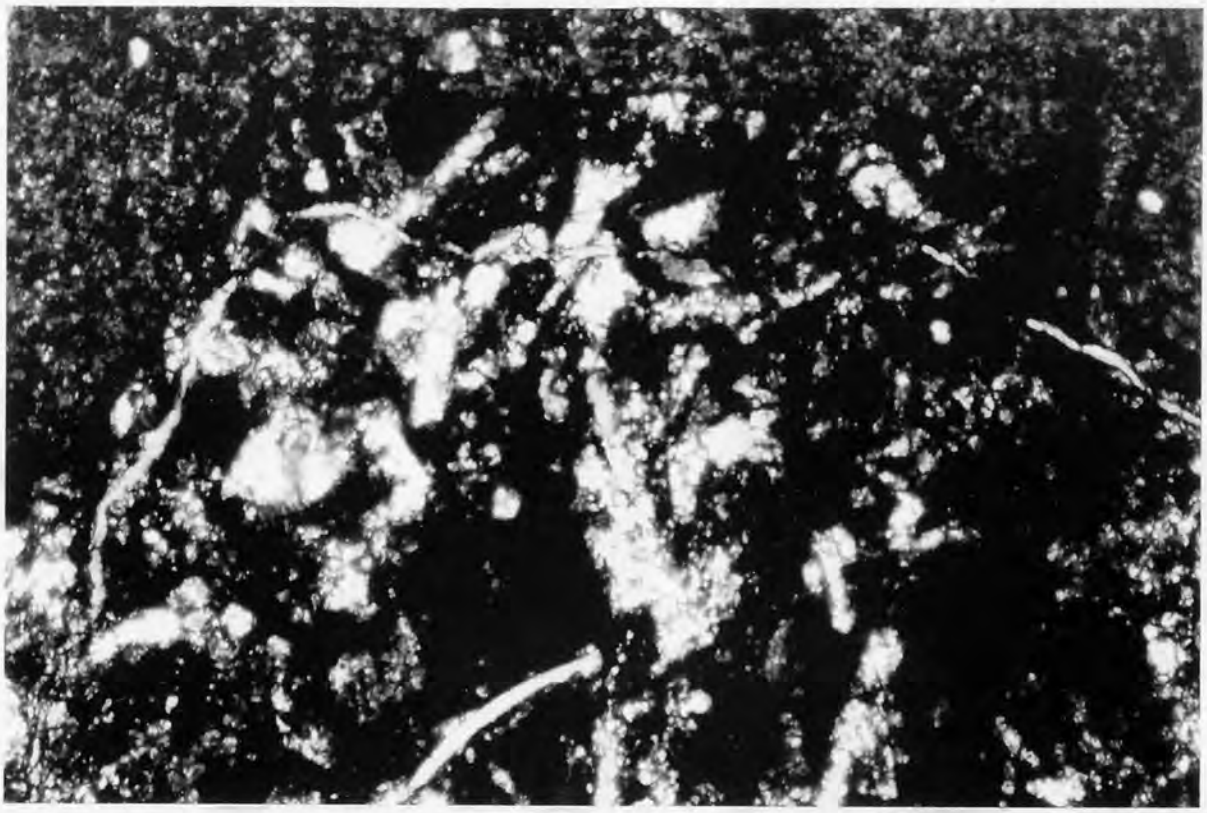

Plate 3.4 Expansive ASR microcracking centred on the silicified limestone coarse aggregate. Horrocksford limestone mix,7 kg/m$^3$ $Na_2O_e$ (plane polarised light, X40 Mag).

Plate 3.5 Expansion centre within the greywacke coarse aggregate running around larger clastic material. Finer microcracks from which the expansive ASR develops are found to dissipate into the microcrystalline quartz and sericite matrix material. Greywacke mix,7 kg/m$^3$ $Na_2O_e$ (plane polarised light, X40 Mag).

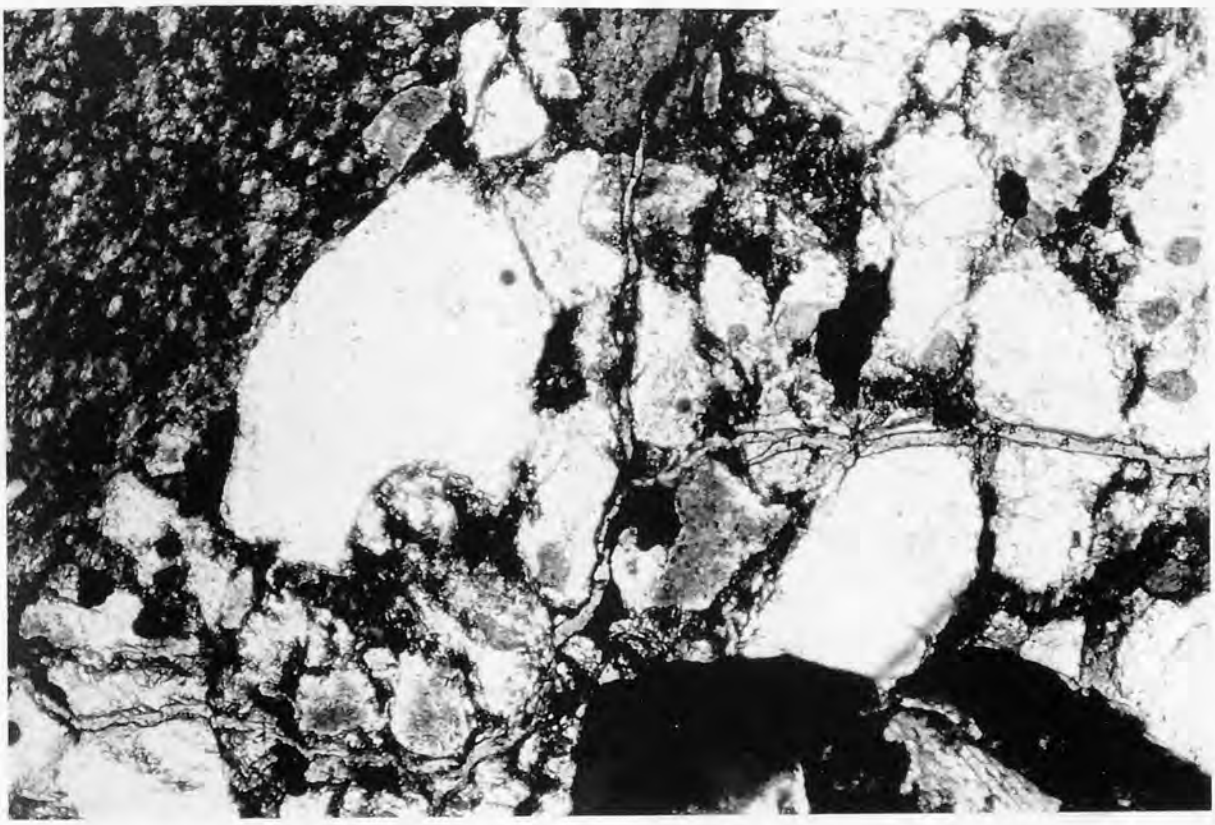

Plate 3.6 ASR microcracking similar to that observed in the greywacke aggregate. Source of reaction appears to be the fine siliceous matrix material. Strained granite mix,7 kg/m$^3$ $Na_2O_e$ (plane polarised light, X100 Mag).

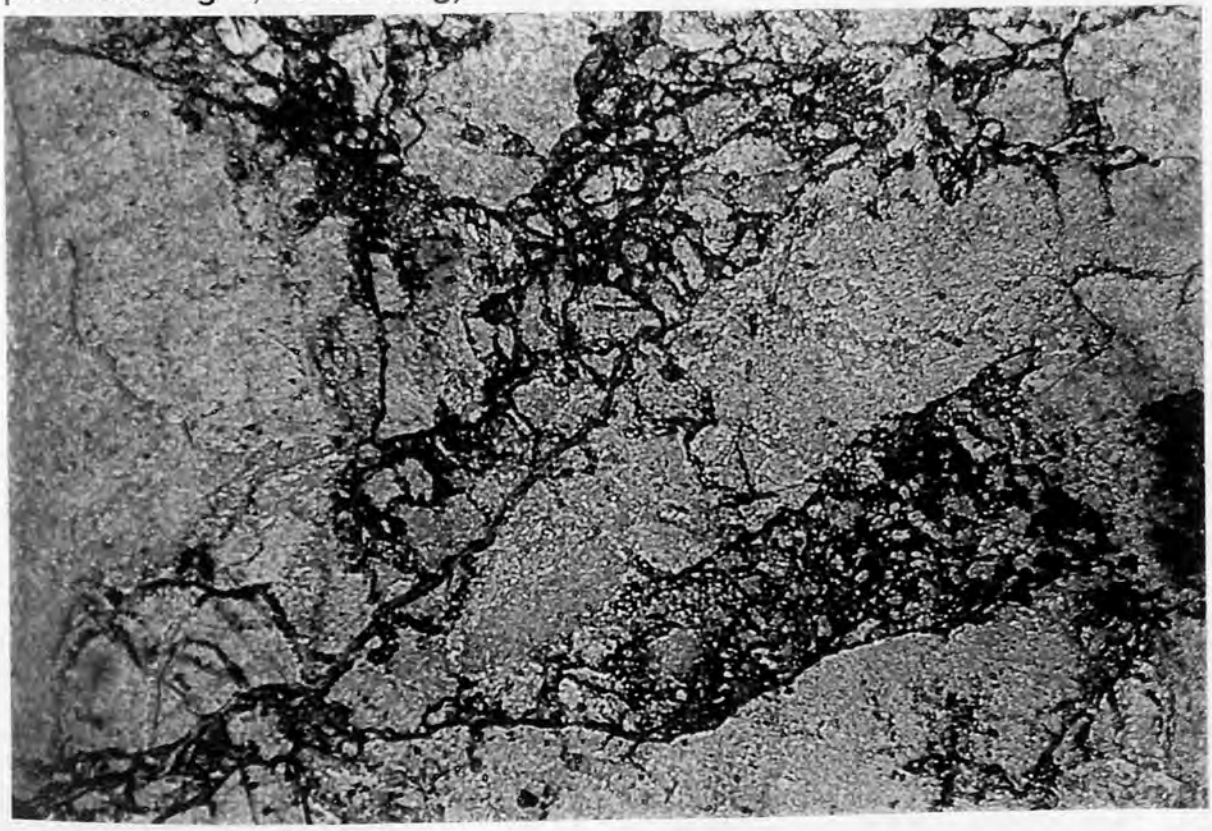

Plate 3.7 ASR microcracking passing from a chert to a metaquartzite particle. Both rock types show some evidence of reactivity. Note also the slight staining to the cement paste surrounding the microcrack. Trent Valley gravel mix,7 kg/m$^3$ $Na_2O_e$ (plane polarised light, X40 Mag).

Plate 3.12 Photograph taken in ultra-violet light of cut surface of concrete prism impregnated with fluorescent resin to show the microcracks and voids. Sample: Venn Quarry siltstone 7 kg/m$^3$ $Na_2O_e$ mix. Prism width 75 mm.

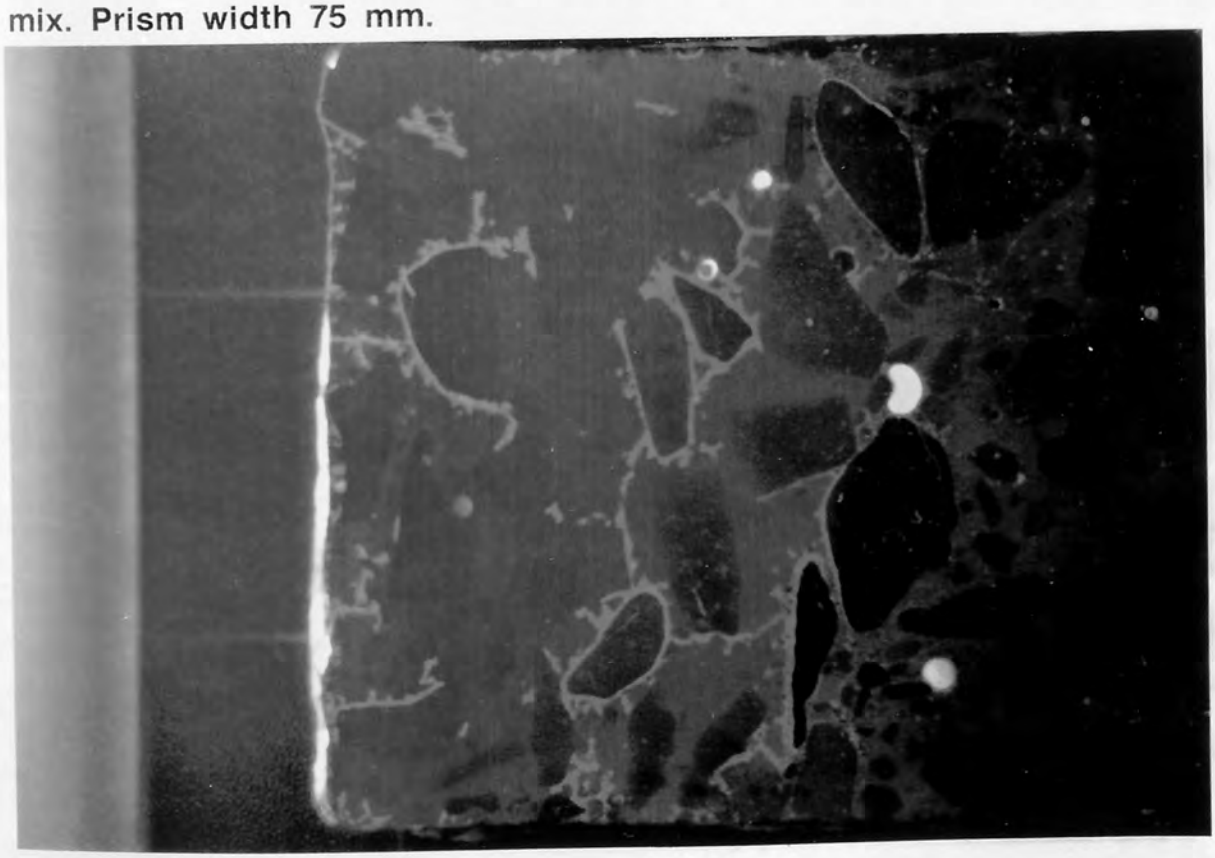

Plate 3.8 Shows the 3.5 kg/m$^3$ $Na_2O_e$ Horrocksford limestone concrete expansion prisms after 12 months triple bagged and wrapped in a moist towelling.

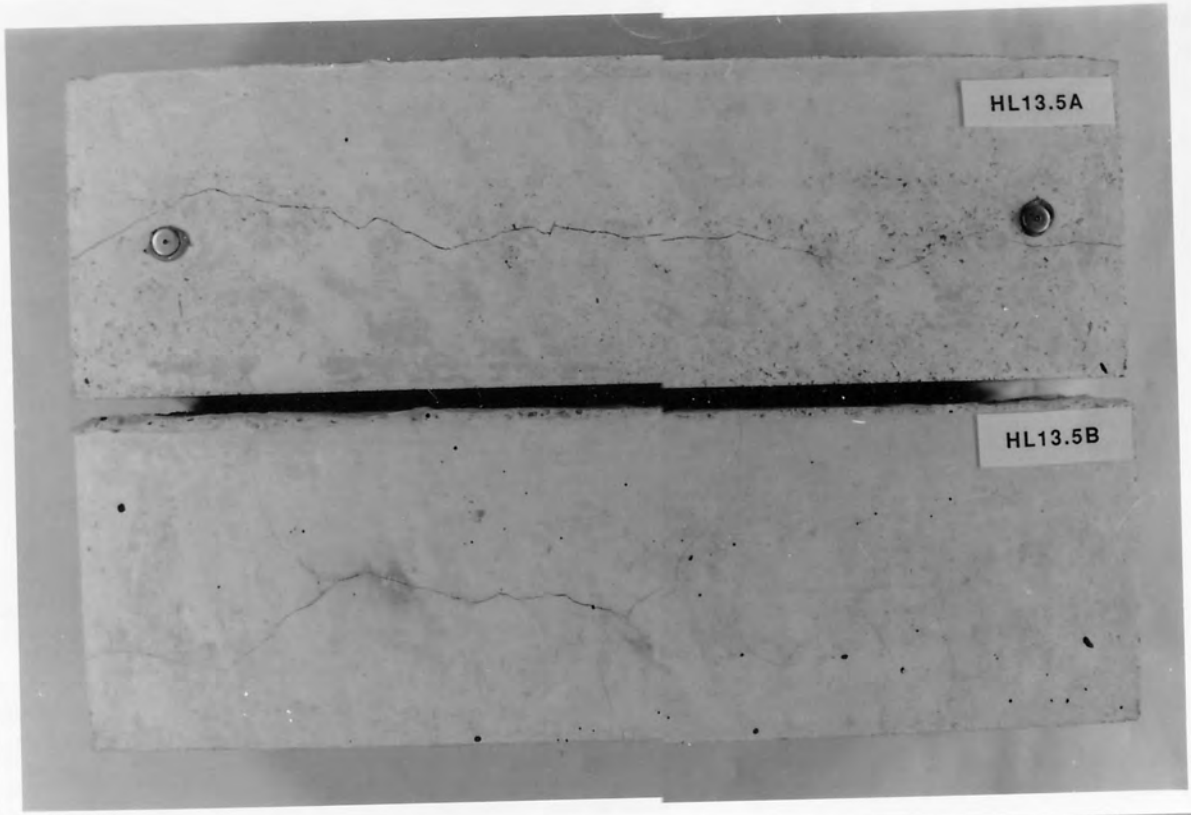


Plate 3.9 Shows the 4.5 kg/m$^3$ $Na_2O_e$ Horrocksford limestone concrete expansion prisms after 12 months triple bagged and wrapped in a moist towelling.

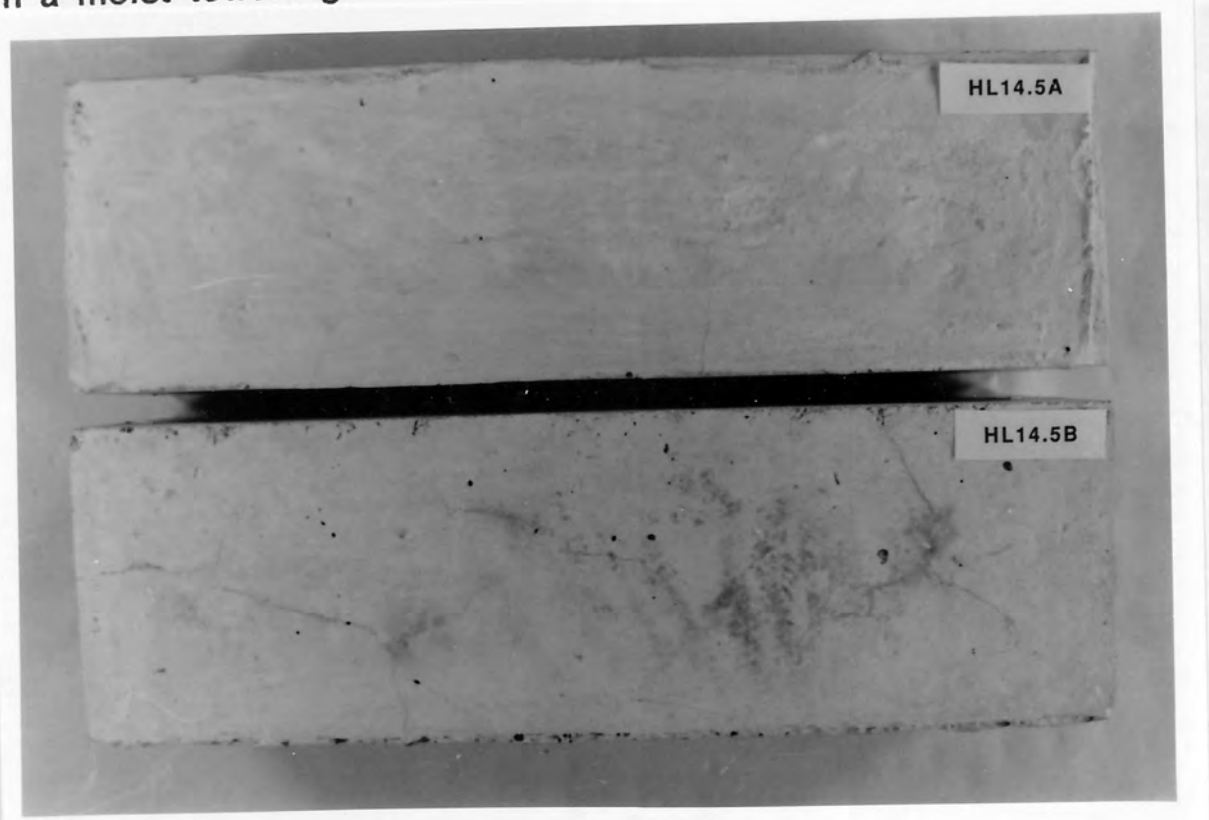

Plate 3.10 Shows the 3.5 kg/m$^3$ $Na_2O_e$ Dry Rigg siltstone concrete expansion prisms after 12 months triple bagged and wrapped in a moist towelling.

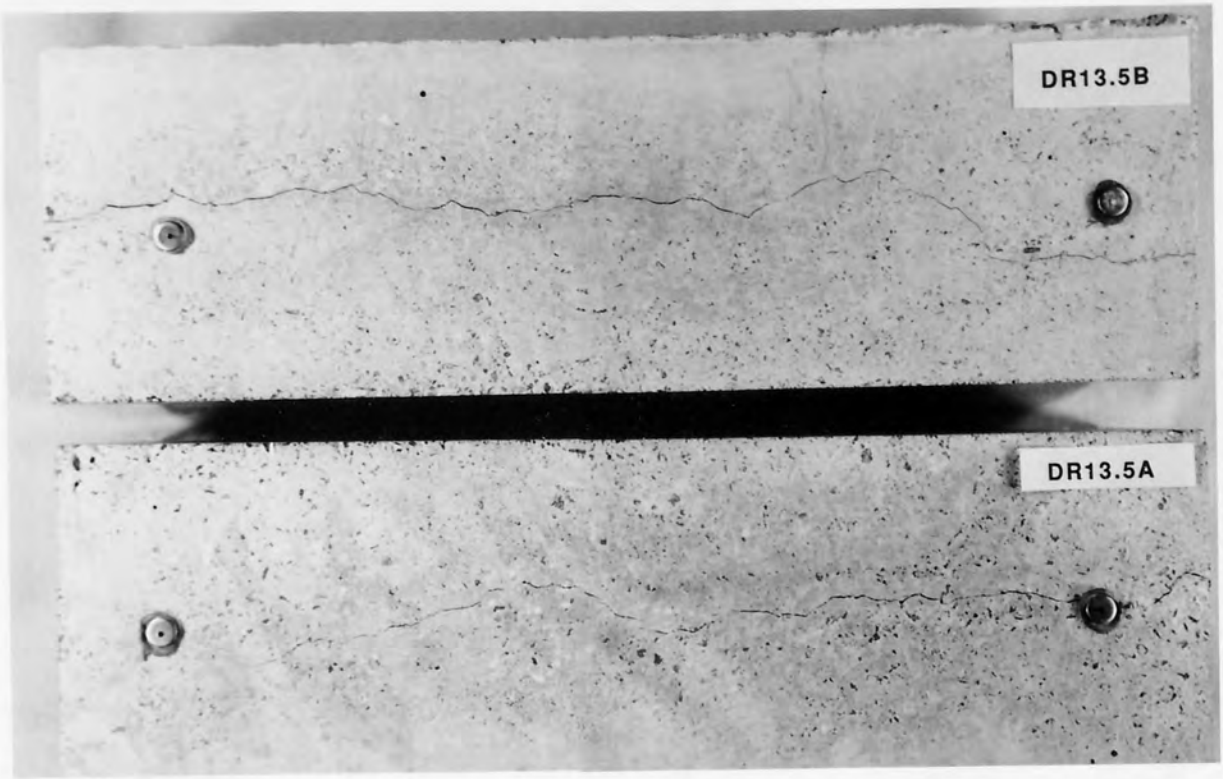


Plate 3.11 Shows the 5.0 kg/m$^3$ $Na_2O_e$ Dry Rigg siltstone concrete expansion prisms after 12 months triple bagged and wrapped in a moist towelling.

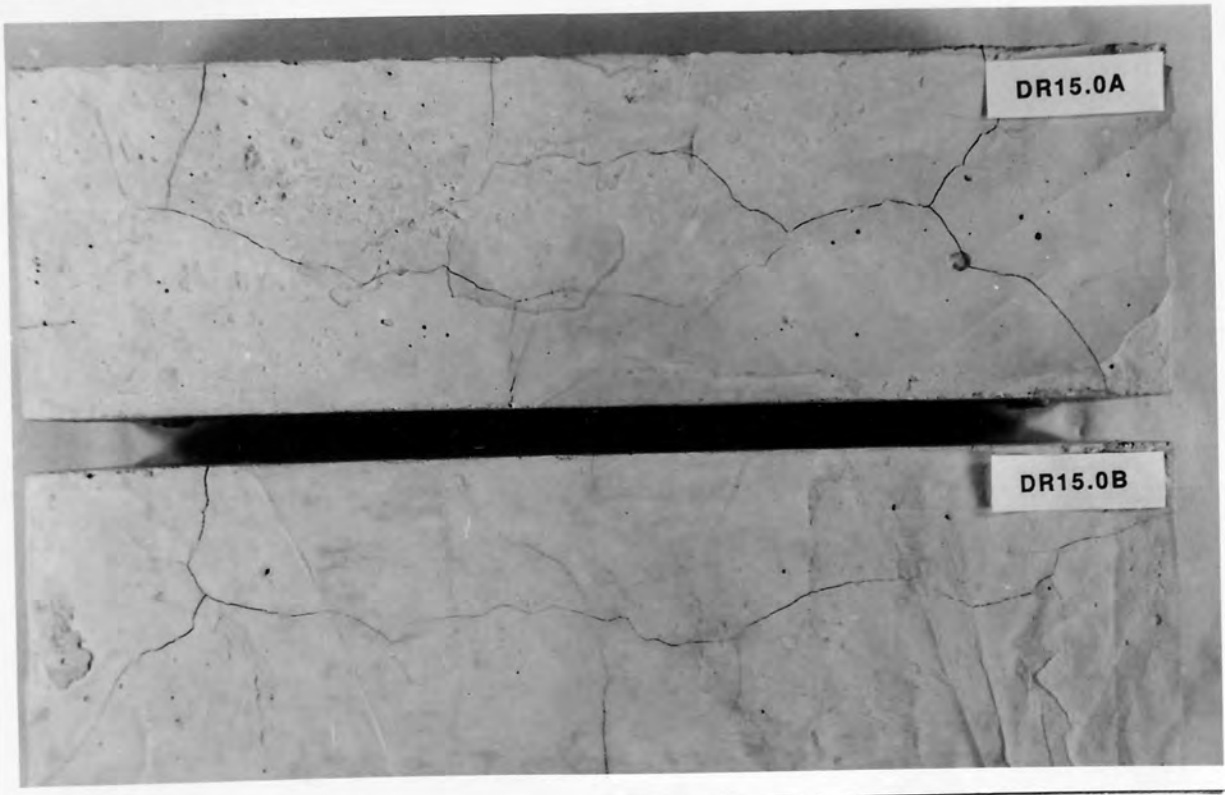

Plate 3.13 Photograph taken in ultra-violet light of cut surface of concrete prism impregnated with fluorescent resin to show the microcracks and voids. Sample: Dry Rigg siltstone 7 kg/m$^3$ $Na_2O_e$ mix. Prism width 75 mm.

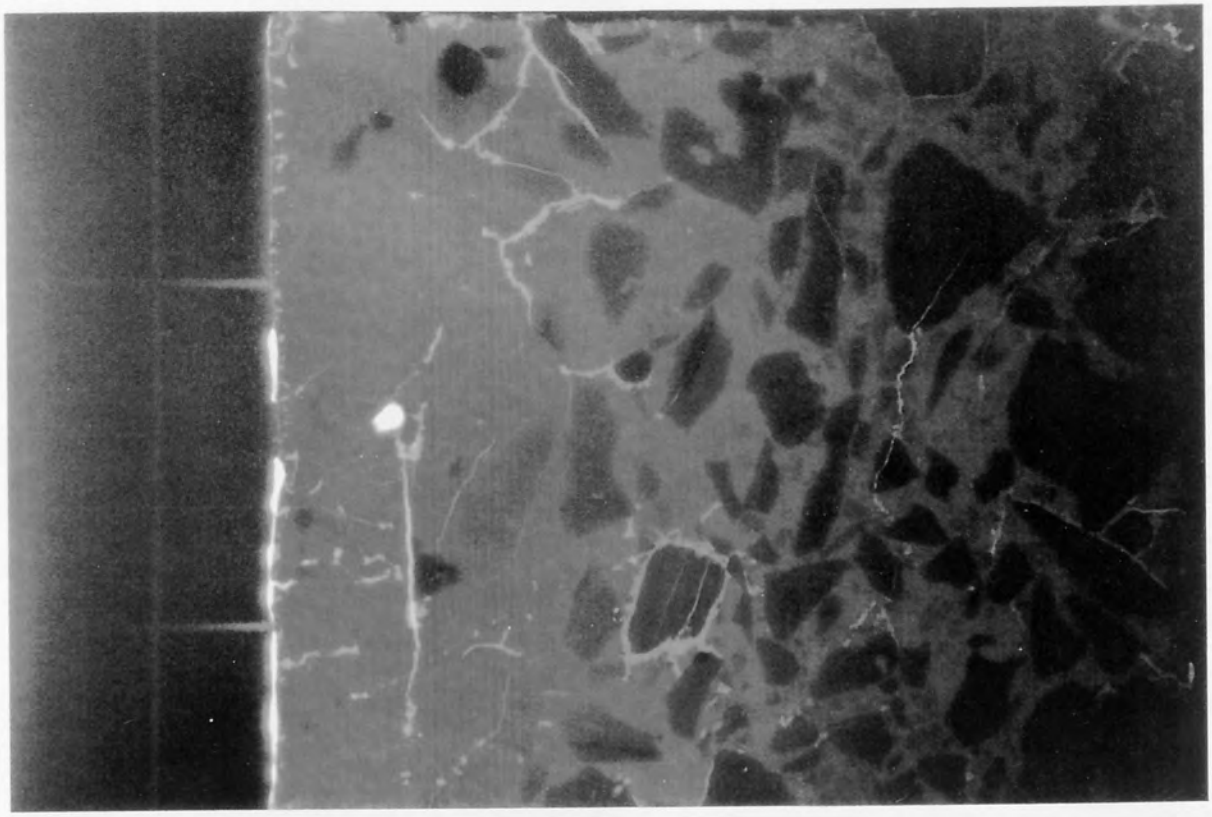

Plate 3.14 Photograph taken in ultra-violet light of cut surface of concrete prism impregnated with fluorescent resin to show the microcracks and voids. Sample: Horrocksford limestone 5 kg/m$^3$ $Na_2O_e$ mix. Prism width 75 mm.

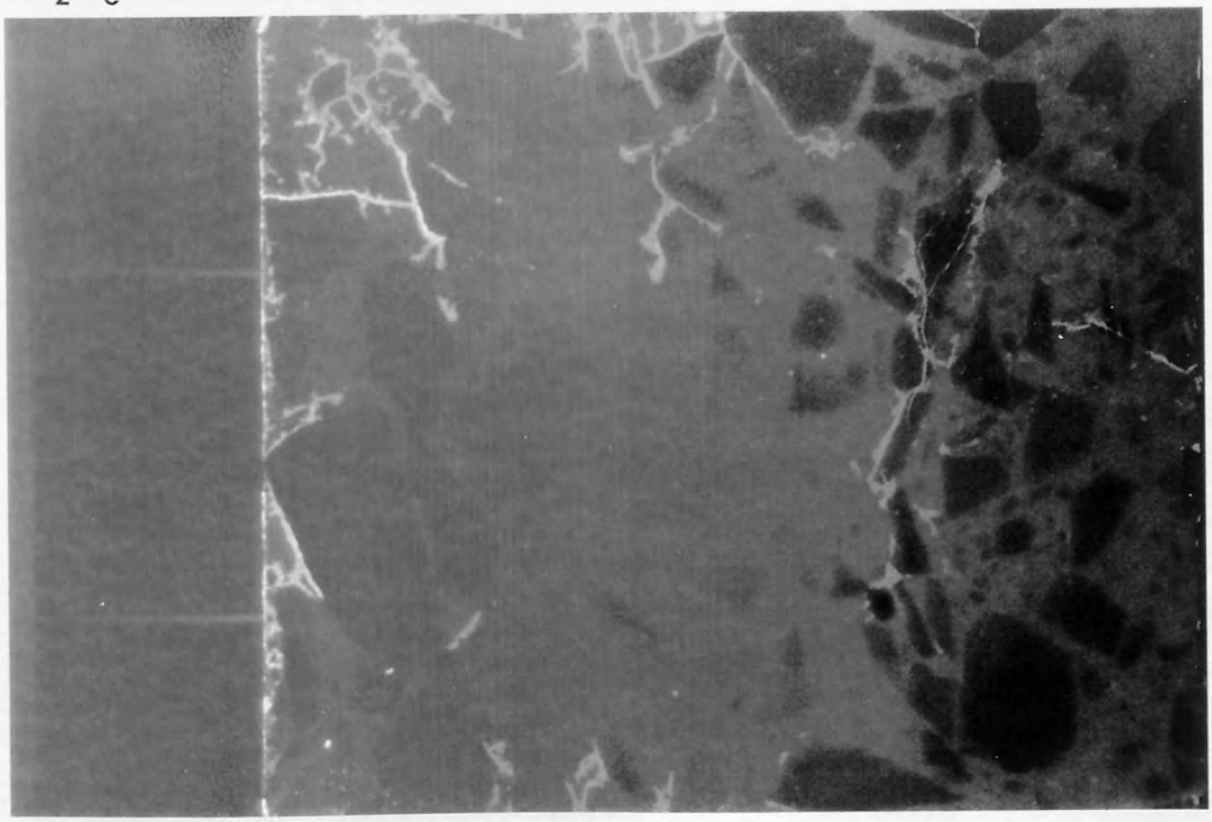

Plate 3.15 Photograph taken in ultra-violet light of cut surface of concrete prism impregnated with fluorescent resin to show the microcracks and voids. Sample: Trent Valley gravel 6 kg/m$^3$ $Na_2O_e$ mix. Prism width 75 mm.

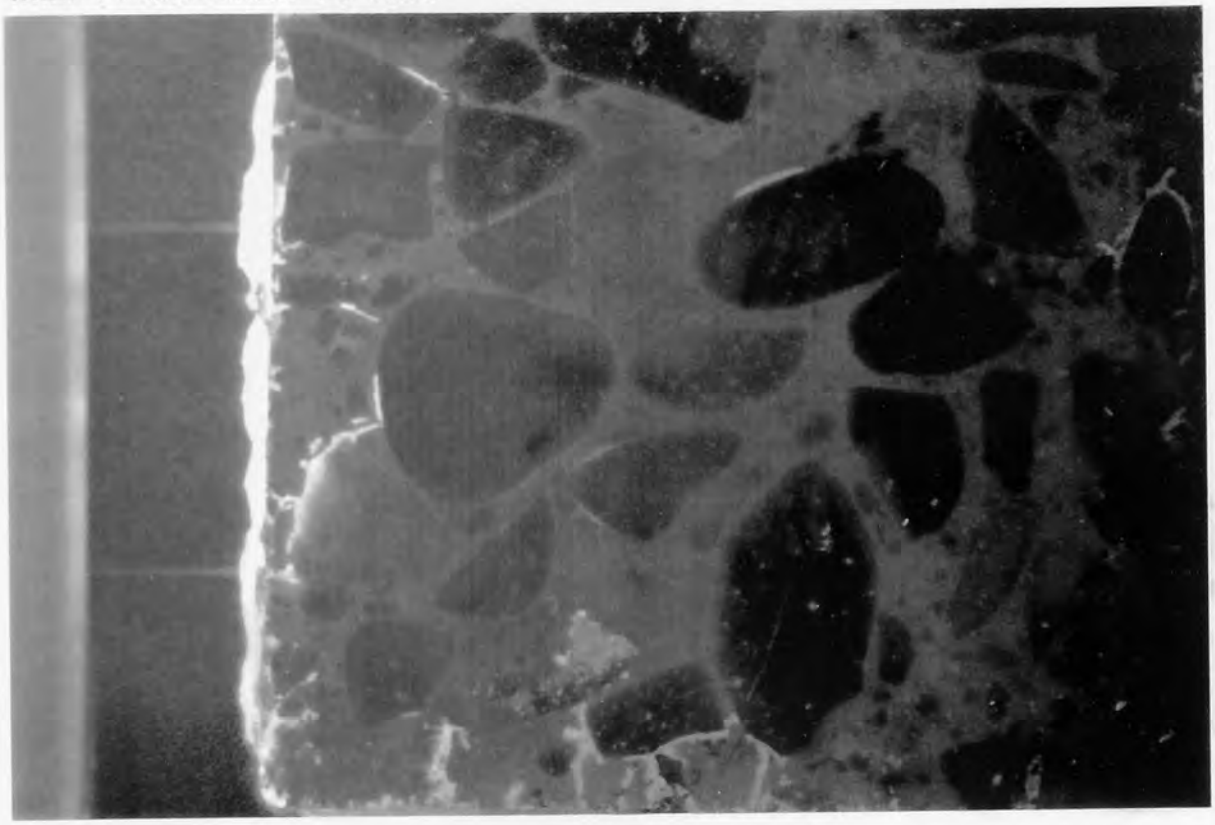

Plate 4.1 Close up of cement paste from concrete immersed in distilled water. No evidence of paste staining by ASR gel. Dry Rigg siltstone mix,3 kg/m$^3$ $Na_2O_e$ (Sample No. DR23.0H, plane polarised light, X200 Mag).

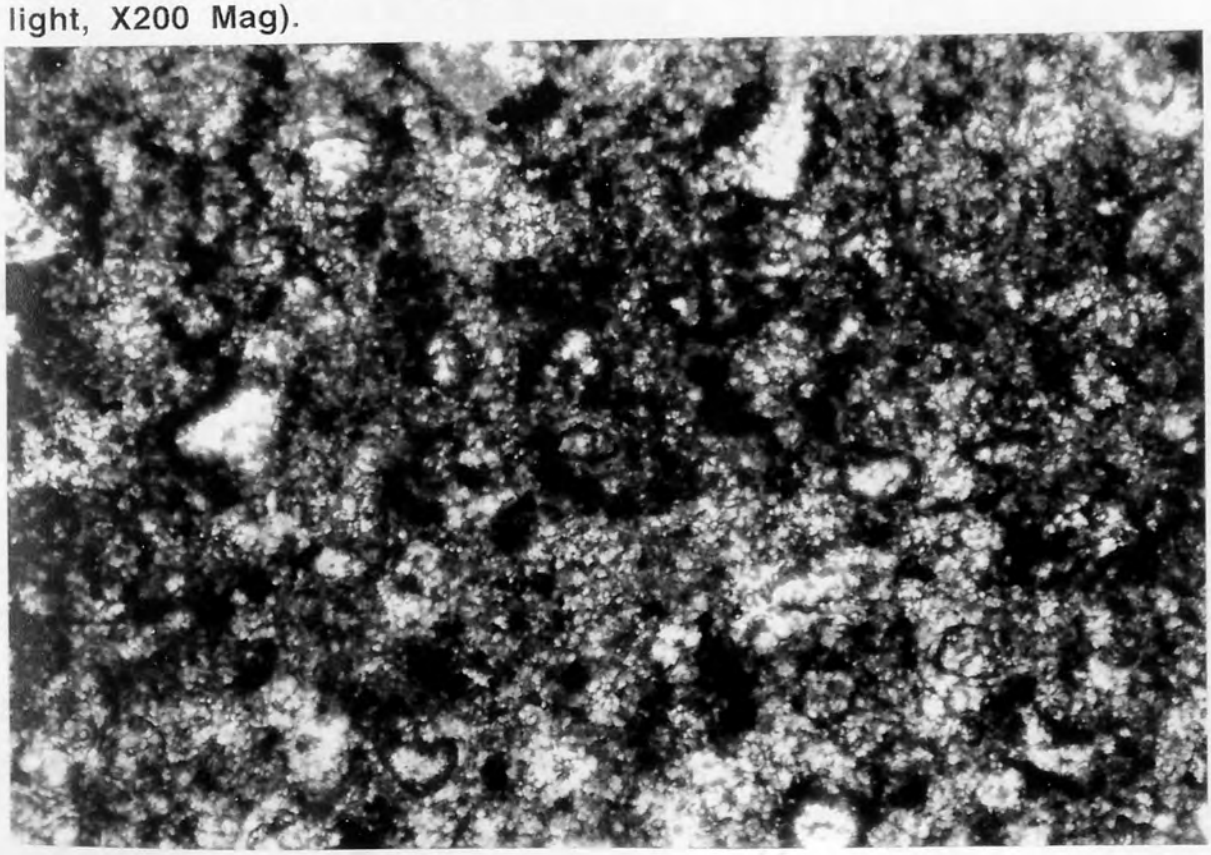

Plate 4.2 Extensive ASR microcracking containing some ASR gel, developed within the siltstone aggregate and continuing out into the surrounding cement paste. Dry Rigg siltstone mix,3 kg/m$^3$ $Na_2O_e$ (Sample No. DR23.0A, immersed in salt solution plane polarised light, X40 Mag).

Plate 4.3 ASR related microcracking running with the inherent cleavage and bedding of the siltstone aggregate. Dry Rigg siltstone mix,3 kg/m$^3$ $Na_2O_e$ (Sample No. DR23.0A, immersed in salt solution plane polarised light, X40 Mag).

Plate 4.4 Close up of cement paste from concrete immersed in salt solution. Milky blurred appearance to all dark interstitial material. Dry Rigg siltstone mix,3 kg/m$^3$ $Na_2O_e$ (Sample No. DR23.0A, plane polarised light, X200 Mag).

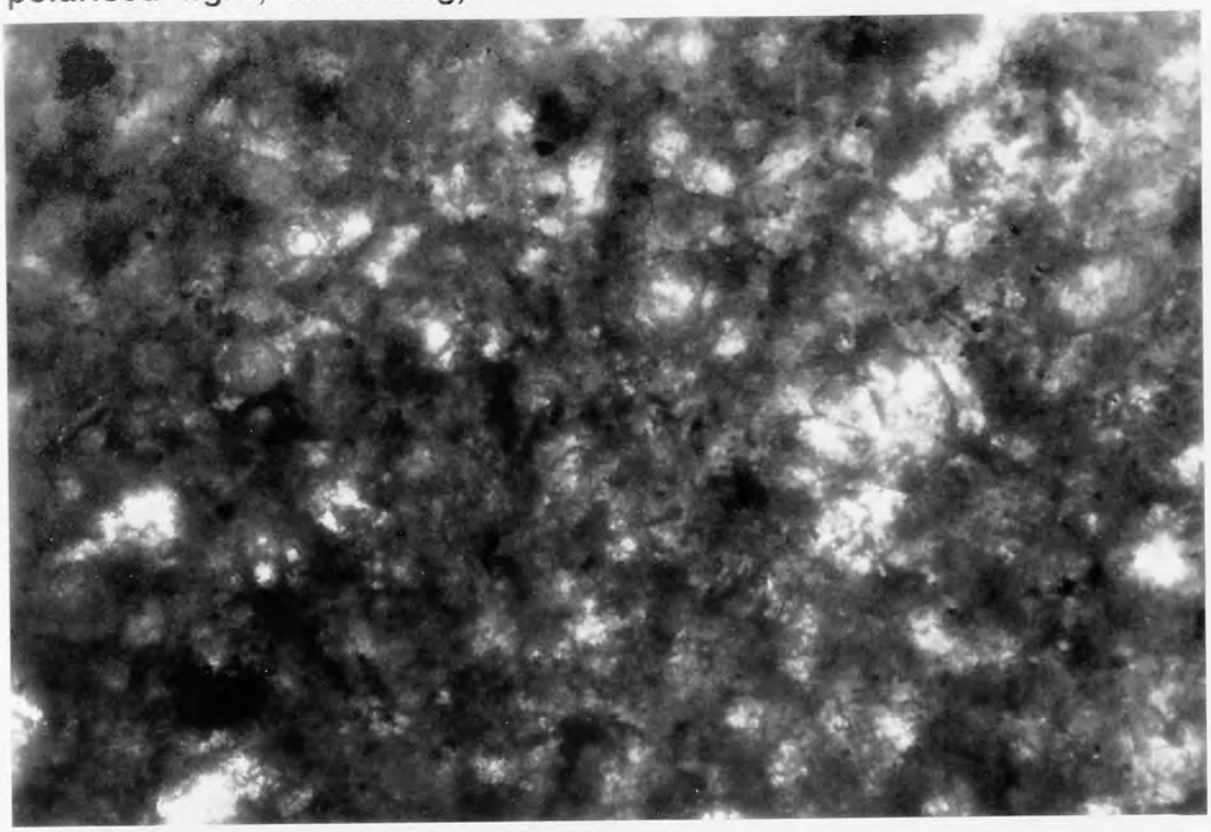

Plate 4.5 Area of apparently higher capillary porosity adjacent to the paste microcracks formed by the ASR. Area is often resin filled and contains what appears to be fine granular calcite. Dry Rigg siltstone mix,7 kg/m$^3$ $Na_2O_e$ (Sample No. DR27.0B, plane polarised light, X100 Mag).

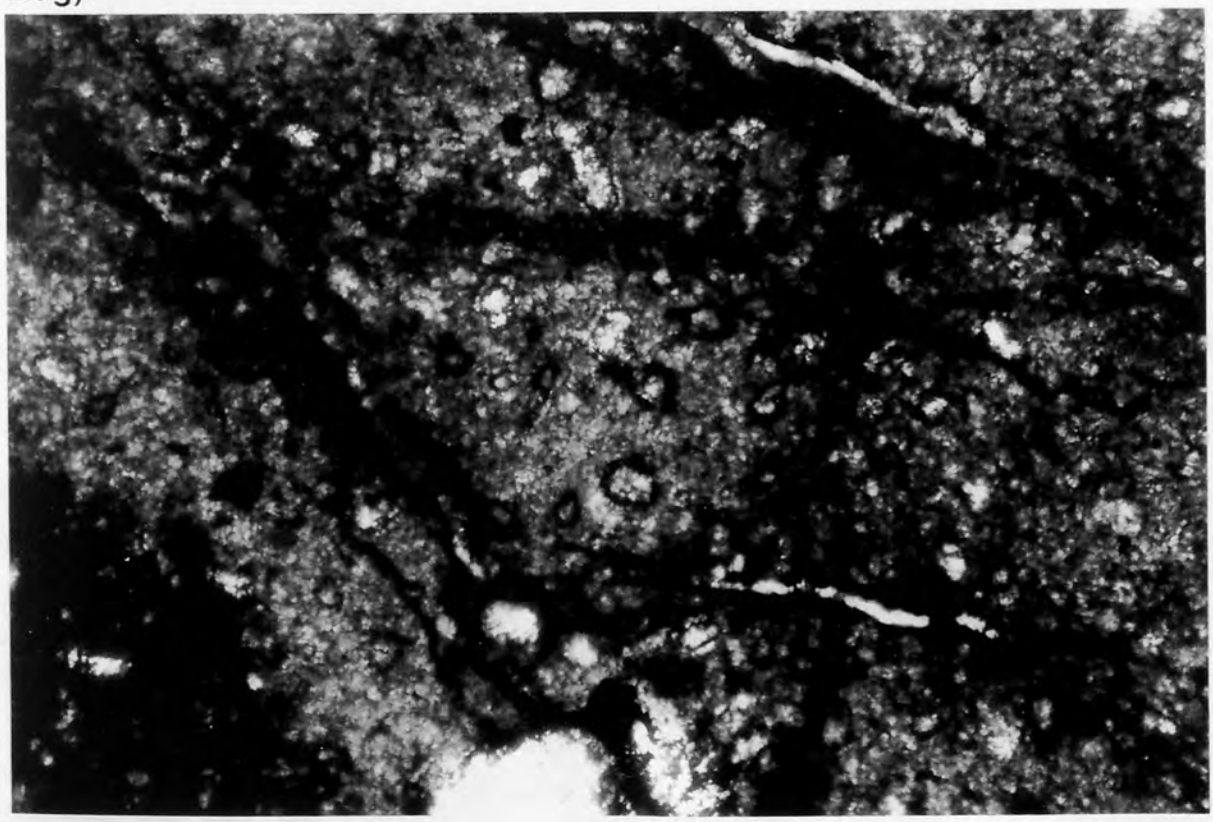

Plate 4.6 Dry shrinkage cement paste microcracking with associated stained, resin impregnated and normal PC paste. Horrocksford limestone mix,7 kg/m$^3$ $Na_2O_e$, immersed in salt solution for 1 month then 1 month dry. (Sample No. DR27.0C, plane polarised light, X40 Mag).

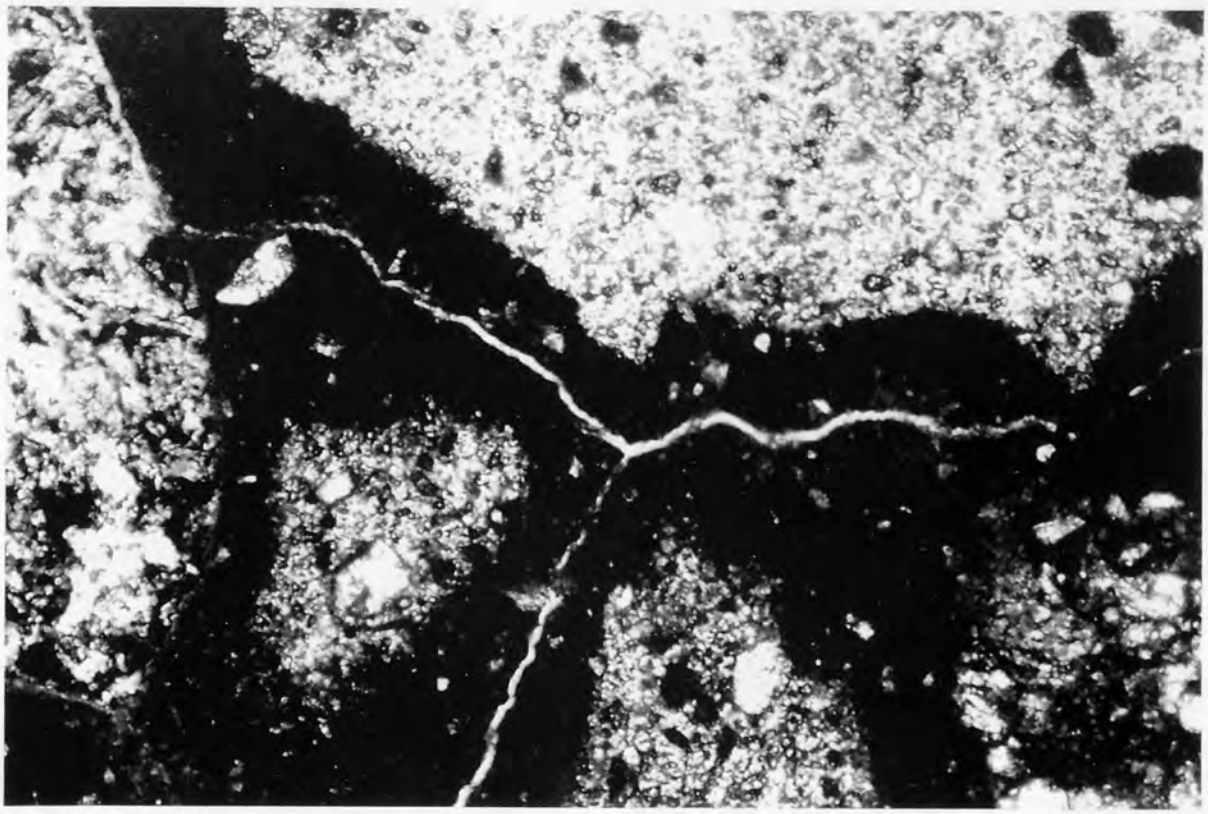

Plate 4.7 Small void and microcrack in the siltstone coarse aggregate containing sub-isotropic cubic NaCl and needle-like crystals of Friedel's salt (Calcium chloro-aluminate). Dry Rigg siltstone mix, 3 kg/m$^3$ $Na_2O_e$, half immersed in salt solution. (Sample No. DR23.0F. Taken in crossed polarised light with added sensitive tint plate [STP] X200 Mag).

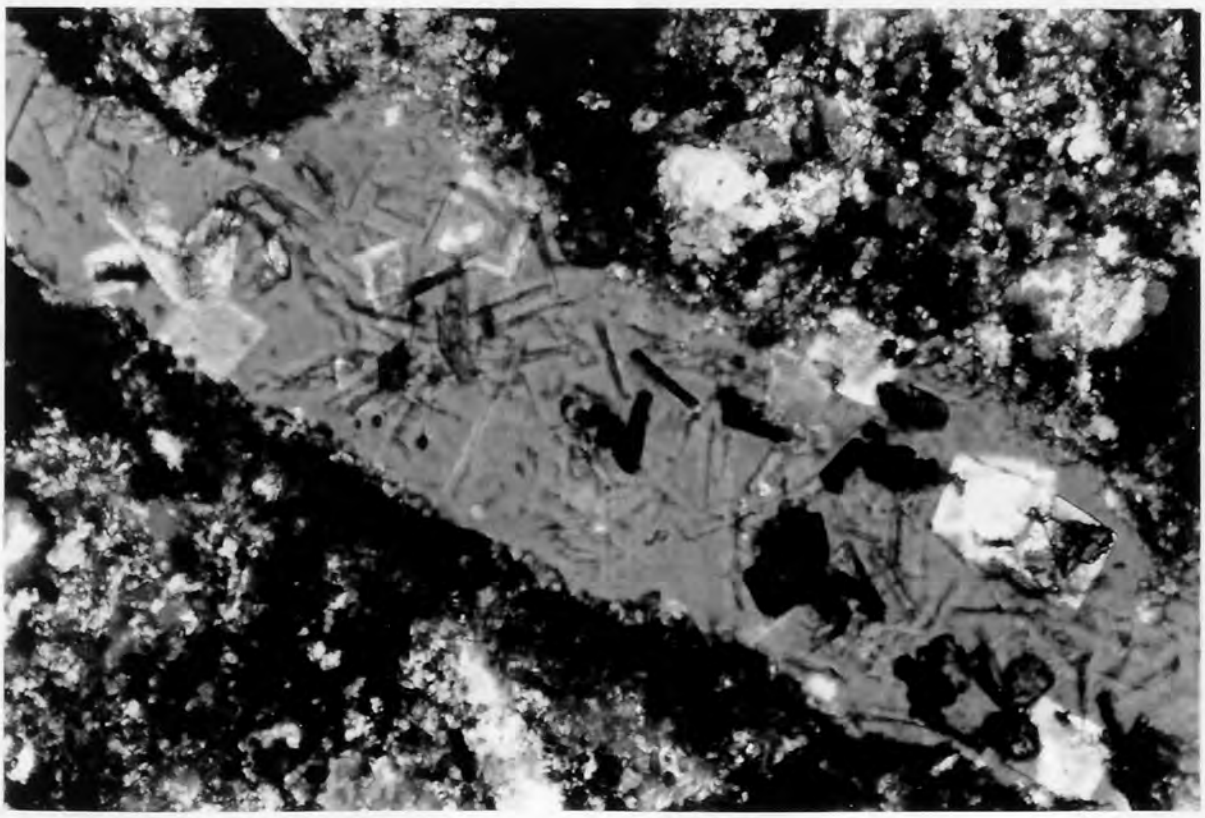

Plate 5.1 Close up of cement paste. Dry Rigg siltstone mix,6 kg/m$^3$ $Na_2O_e$, containing 25 % replacement of cement with high alkali WB pfa. (plane polarised light, X100 Mag).

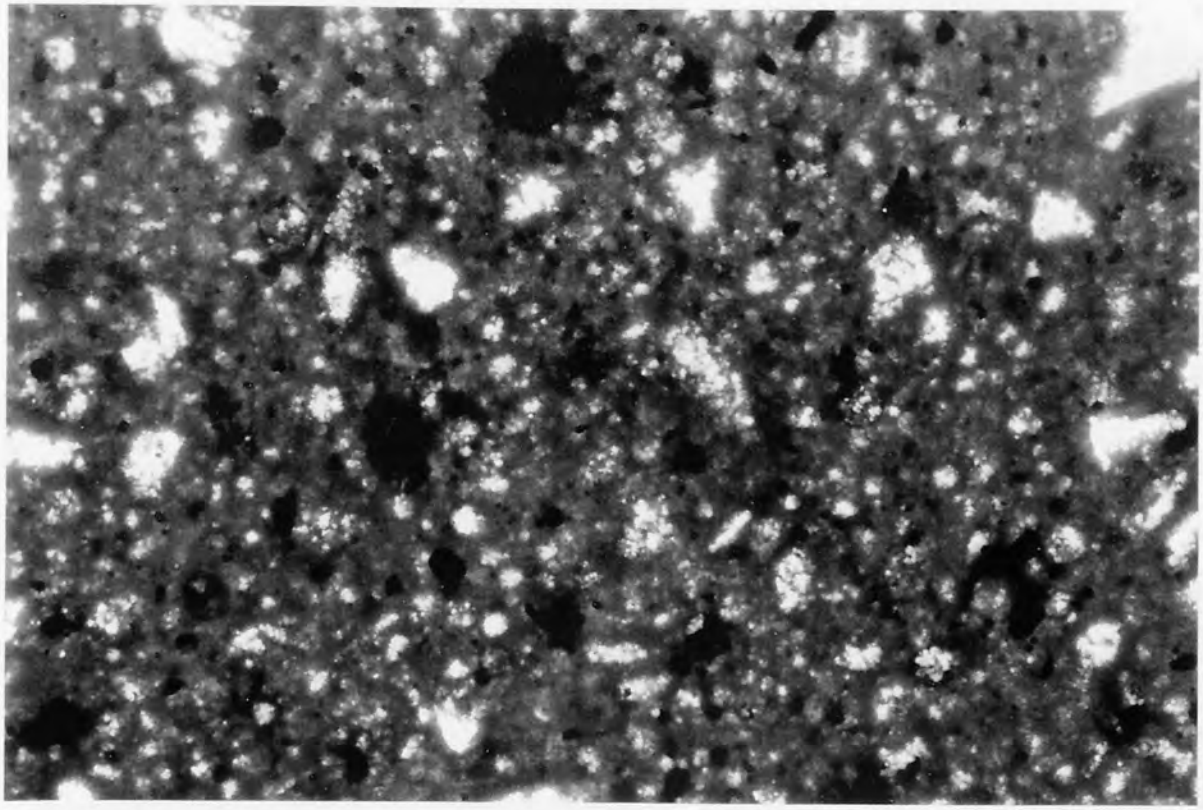

Plate 5.2 Close up of cement paste. Dry Rigg siltstone mix,4 kg/m$^3$ $Na_2O_e$, containing 25 % replacement of cement with high alkali WB pfa. (plane polarised light, X100 Mag).

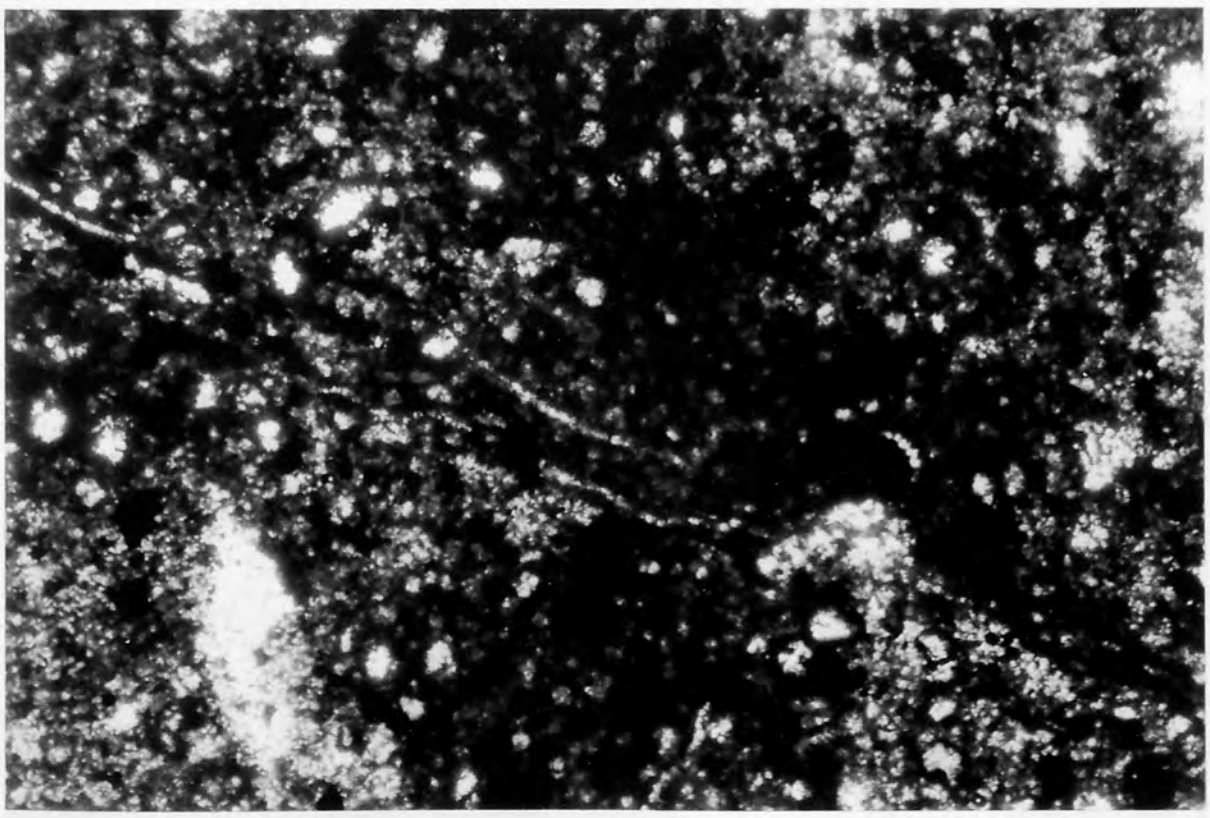

Plate 5.3 Close up of cement paste. Dry Rigg siltstone mix,4 kg/m$^3$ $Na_2O_e$, containing 25 % replacement of cement with medium alkali FF pfa. (plane polarised light, X100 Mag).

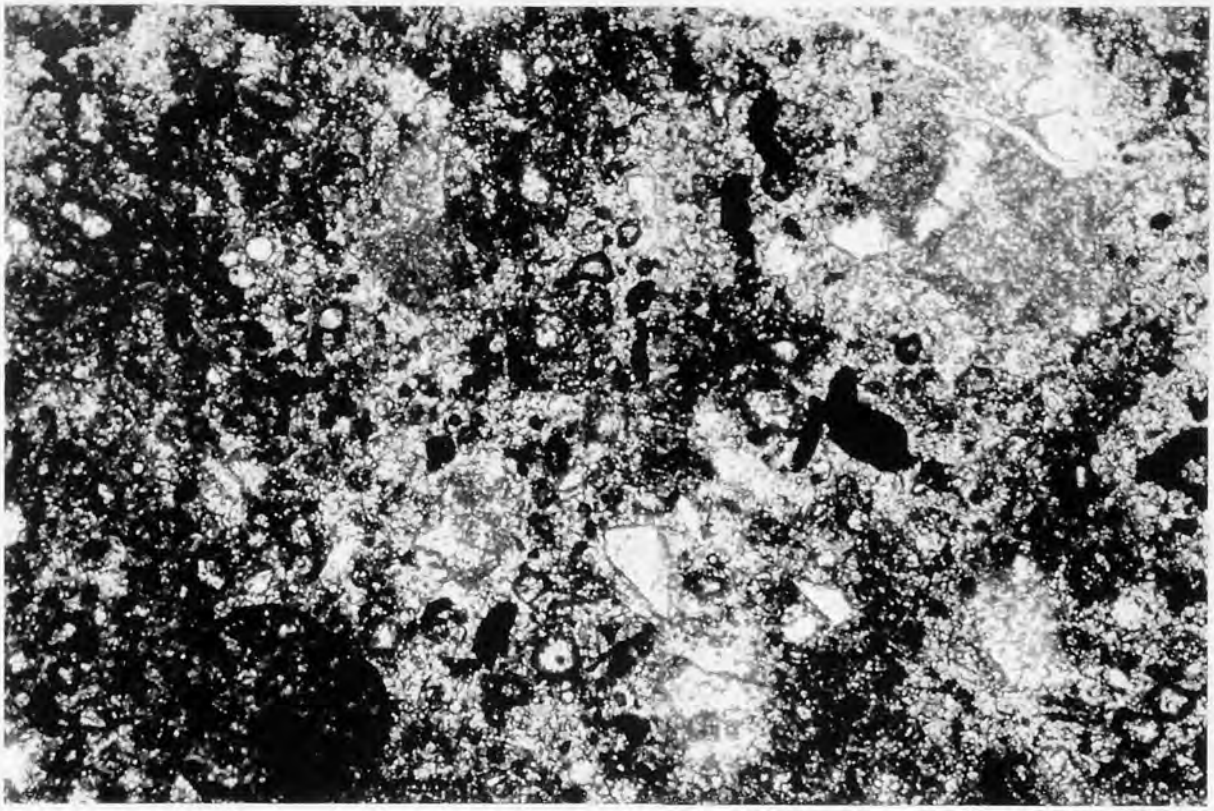

Plate 5.4 Close up of cement paste. Dry Rigg siltstone mix,6 kg/m$^3$ $Na_2O_e$, containing 25 % replacement of cement with medium alkali FF pfa. (plane polarised light, X100 Mag).

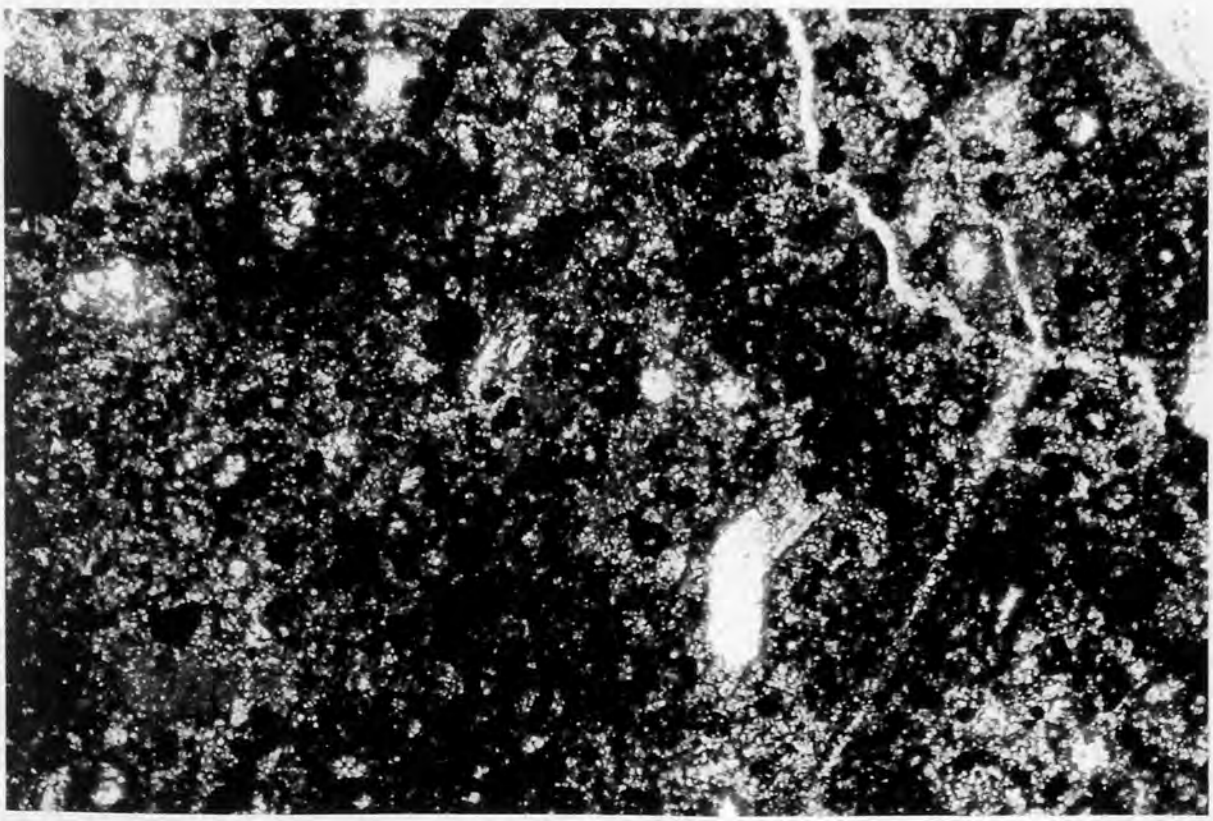

Plate 6.1 Close up of cement paste showing no ASR gel staining. High $C_3S$ content. Dry Rigg siltstone mix,7 kg/m$^3$ $Na_2O_e$, containing 2.3 % air entrainment. (plane polarised light, X100 Mag).

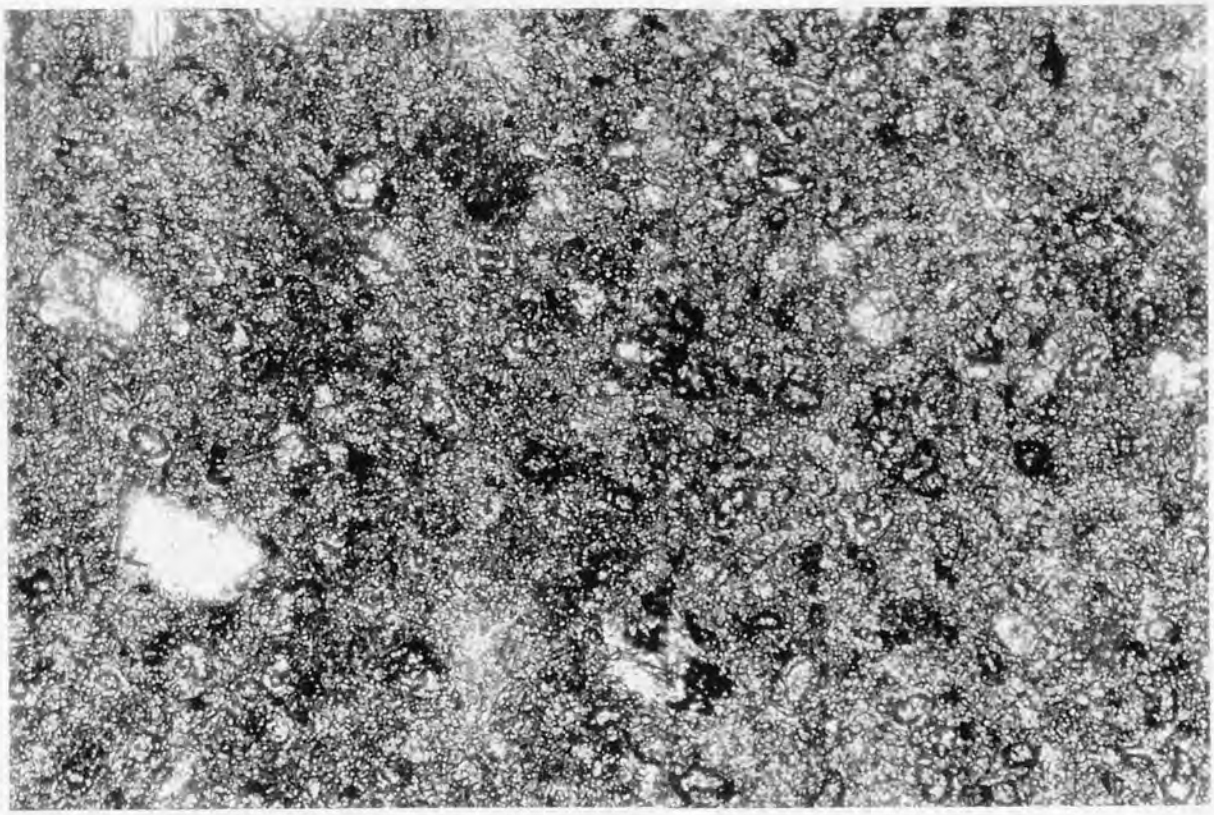

Plate 6.2 Partially ASR gel filled air voids near the original surface of the concrete prism. Note interception of void with microcrack of ASR origin leaving aggregate particle bottom right. Dry Rigg siltstone mix,7 kg/m$^3$ $Na_2O_e$, containing 2.3 % air entrainment. (plane polarised light, X40 Mag).

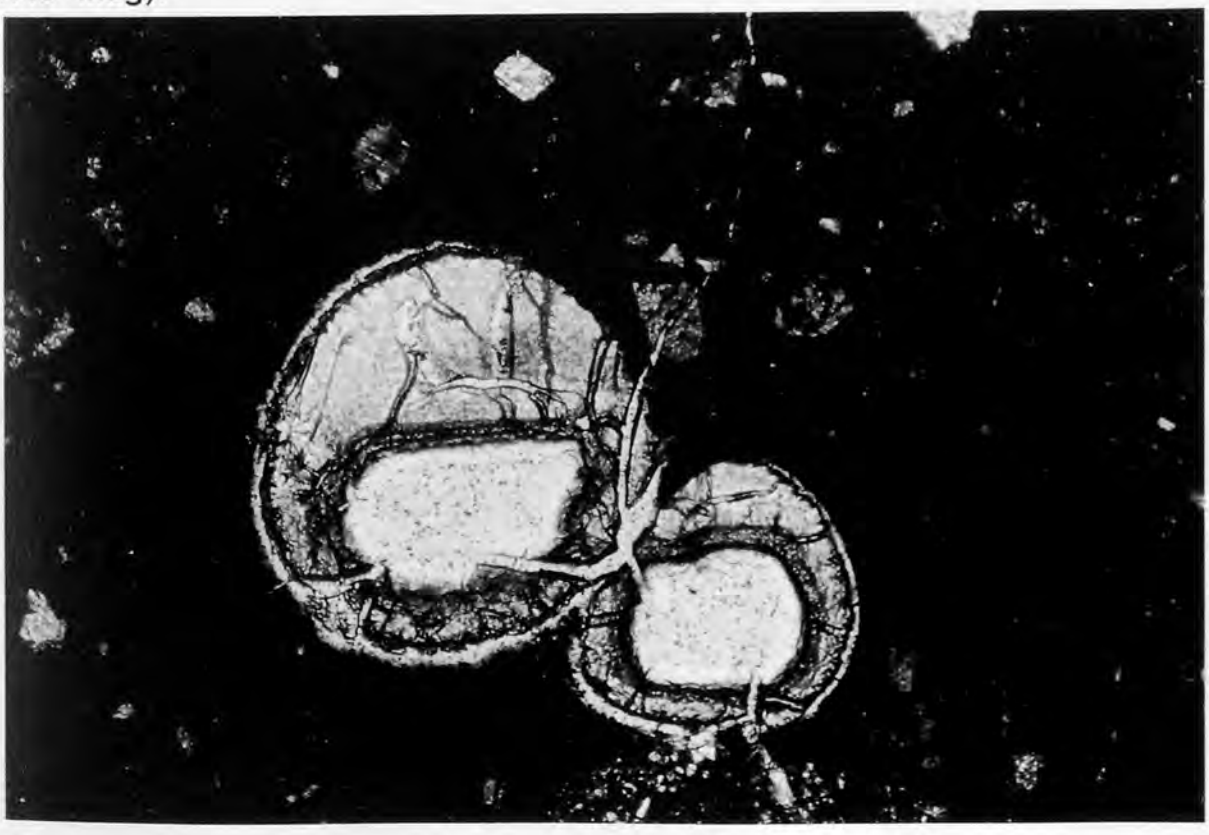

Plate 6.3 Numerous cement paste air voids associated with high capillary porosity paste. Voids in the vicinity of microcracks partly filled by portlandite and ettringite, indicating a flow of moisture. Dry Rigg siltstone mix,3.5 kg/m$^3$ $Na_2O_e$, containing 6.6 % air entrainment. (plane polarised light, X40 Mag).

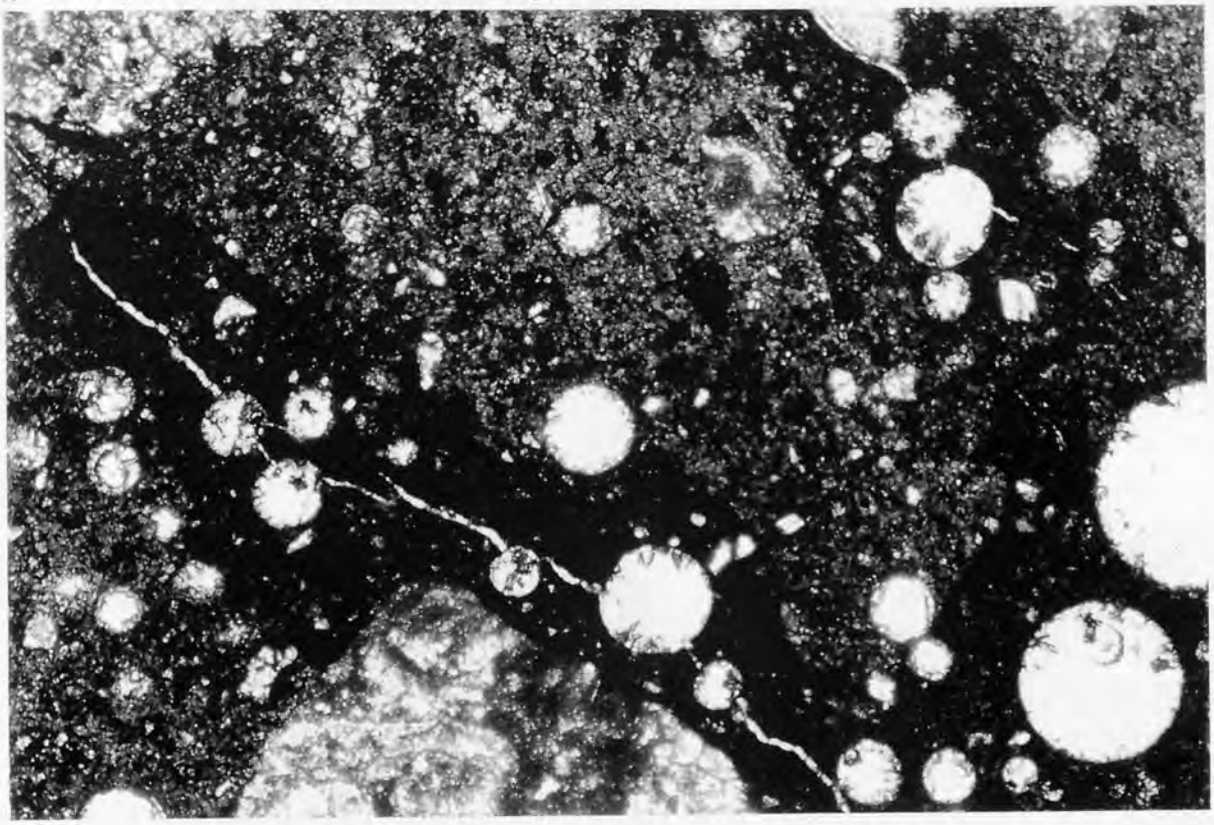

Plate 6.4 Dissipation of ASR microcrack on entering air voids. Also note the associated staining of the cement paste surrounding the microcrack. Dry Rigg siltstone mix,3.5 kg/m$^3$ $Na_2O_e$, containing 6.6 % air entrainment. (plane polarised light, X40 Mag).

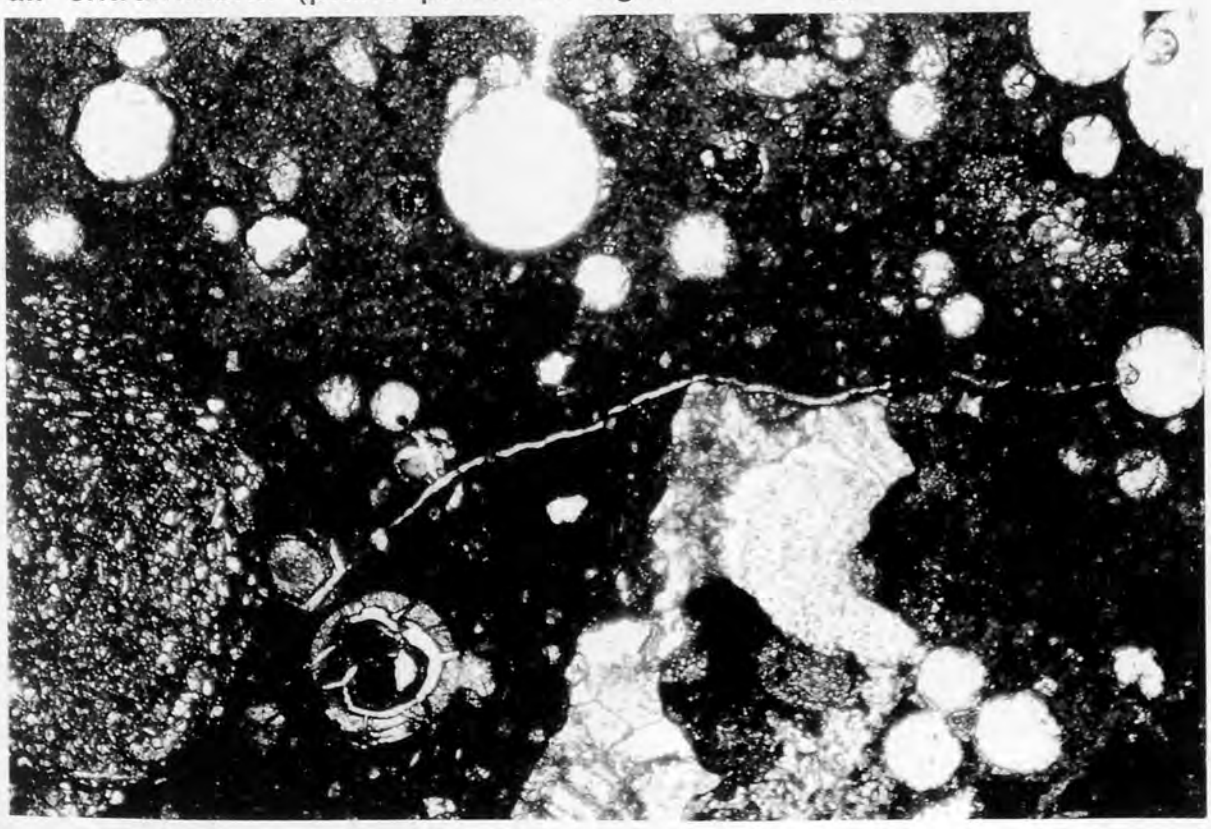

Plate 6.5 Secondary portlandite and ettringite infill to air voids. Presumably due to the percolation of moisture through the cement paste. Dry Rigg siltstone mix,3.5 kg/m$^3$ $Na_2O_e$, containing 6.6 % air entrainment. (crossed polarised light, X200 Mag).

## REFERENCES


ANDERSEN, K.T and Thaulow, N., (1989)
Proc. 8th Int. Conf. on alkali aggregate reaction, Kyoto, Japan. (Ed. K.Okada). The Society of Materials Science, Japan. pp 489-494.

ANON, (1980)
Concrete problems burst forth. New civil engineer, London, 24th April 1980, p 4.

ANON, (1984)
AAR problem now feared widespread. New civil engineer, London, 2nd August 1984, p 9.

BATTEY, M.H, (1981)
Mineralogy for students, Second edition. Longman Group Limited, Harlow, Essex.

BLACKWELL, B.Q., Thomas, M.D.A., Nixon, P.J., and Pettifer, K., (1992)
Proc. 9th. Int. Conf. on 'Alkali Aggregate Reaction in concrete', London. The Concrete Society, Slough, pp 102-109.

BLIGHT, G.E., (1991)
The moisture condition in an exposed structure damaged by alkali-silica reaction. Mag of Conc. Res.,43 , (157), pp 249-255.

BRITISH STANDARDS INSTITUTION. (1970)
Methods of testing hardened concrete for other than strength. The British Standard BS1881: Part 5: 1970. Determination of changes in length on drying and wetting. British Standards Institution, London, pp 17-27.

BRITISH STANDARDS INSTITUTION. (1970)
Methods of testing cements and aggregates. British Standards Institute, BS4550: Part 3. London.

BRITISH STANDARDS INSTITUTION. (1983)
Methods of determining the air content of a concrete. British Standards Institute, BS1881: Part 106. London.

BRITISH STANDARDS INSTITUTION. (1988)
Methods of testing hardened concrete for other than strength. Determination of chlorides, sodium and potassium oxide contents. British Standards Institute, London. BS1881: Part 124, 10.2 and 10.4, pp 17 - 18.

BRITISH STANDARDS INSTITUTION. (1990)
Testing aggregates. Alkali-silica reactivity. Concrete prism method. British Standards Institute, BS812: Part 123. London.

BROWN, L.S., (1955)
Some observations on the mechanics of alkali-aggregate reactions. ASTM Bulletin 205, NJ, USA, pp 40-56.

BUCK, A.D. and Mather, K., (1978)
Proc. 4th Int. Conf. on the effects of alkalis on concrete, Purdue University, West Lafayette, USA. Purdue University CE-MT-1-78. pp 73-77.

BUCK, A.D., (1987)
Proc. 7th Int. Conf. on Alkali-aggregate reaction, Ottawa, Canada. (Ed. P. Grattan-Bellew). Noyes Publications, NJ, USA. pp 419-423.

BUILDING RESEARCH ESTABLISHMENT, (1971)
Changes in the appearance of concrete on exposure. BRE, Digest 126. Building Research Station, Garston, Watford.

BUILDING RESEARCH STATION. (1988)
Design of normal concrete mixes. BRE Report BR106, Building Research Station, Garston ,Watford.

BUILDING RESEARCH STATION. (1988)
Alkali-aggregate reactions in concrete. Digest 330, Building Research Station, Garston, Watford.

BYRD,T., (1985)
Road salts new suspect in AAR epidemic. New civil engineer, 15th August 1985, pp 4-5.

BYRD, T., (1987)
'Concrete cancer' risk seriously understated. New civil engineer, 9th July 1987, pp 6-7.

BYRD, T., (1993)
Radiation fears grow over Maentwrog mud. New civil engineer, London, 29th July 1993, p 3.

CAN / CSA-A23.1-M90, CAN / CSA-A23.2-M90. (1990)
Concrete materials and methods of concrete construction. Methods of test for concrete. Canadian Standards Association, 178 Rexdale Boulevard, Rexdale, Ontario, Canada, M9W 1R3.

CHATTERJI, S., (1978)
An accelerated method for the detection of Alkali-Aggregate reactivity of aggregates. Cem. and Conc. Res., 8, pp 647-650.

CHATTERJI, S., Jensen, A.D., Thaulow, N., and Christiansen, P., (1986a)
Studies of alkali-silica reaction, Part 3. Cem. and Conc. Res., 16, pp 246-254.

CHATTERJI, S., Thaulow, N., Jensen, A.D., and Christiansen, P., (1986b)
Proc. 7th Int. Conf. on Alkali-aggregate reaction, Ottawa, Canada. (Ed. P. Grattan-Bellew). Noyes Publications, NJ, USA, pp 115-124.

COOMBES, H.L., (1976)
Proc. Symp. Effect of alkalis on properties of concrete, London. Cement and Concrete Association, Wexham Springs, Slough, pp 357-370.

COLE, R.G. and Horswill, P., (1988)
Alkali-silica reaction: Val de la Mare Dam, Jersey, case history. Proc. Inst. Civil Engineers, London, Part 1, 84, pp 1237-1259.

CONCRETE SOCIETY, (1985)
Alkali-silica reaction, new structures - specifying the answers, existing structures - diagnosis and assessment. One day conference, London. Concrete Society, Slough.

CONCRETE SOCIETY, (1987)
Alkali-silica reaction:minimising the risk of damage to concrete. Technical Report No.30. Concrete Society, Slough.

CORNELIUS, D.F., (1970)
Air-entrained concretes: a survey of factors affecting air content and a study of workability. Road research report LR363. Road research laboratory, Crowthorne.

COUNTY SURVEYORS' SOCIETY. (1985)
Report on ice warning systems. Report No 5/2. County Surveyor's Society.

DAVIS, G. and Oberholster, R.E., (1988)
Alkali-silica reaction products and their development. Cem. Conc. Res., 18, p 621.

DEPARTMENT OF TRANSPORT. (1988)
Draft addition of notes for guidance to the specification for highway works. Part 3, NG1001, HMSO, London, pp 19-20.

DENT GLASSER, L.S., (1979)
Osmotic pressure and swelling of gels. Cem. and Conc. Res., 9, (4), pp 515-517.

DIAMOND, S., (1975)
A review of alkali-silica reaction and expansion mechanisms 1: Alkalis in cement and in concrete pore solutions. Cem. and Conc. Res. 5, 4, pp 329-346.

DIAMOND, S., Barneyback, R.S. and Struble, L.J., (1981)
Proc. Conf. on Alkali Aggregate Reaction in concrete, Cape Town. National Building Research Institute, CSIR, Pretoria, South Africa. S252/22, p 1.

DIAMOND, S., (1989)
Proc. 8th Int. Conf. on Alkali Aggregate Reaction, Kyoto, Japan. (Ed. K. Okada). The Society of Materials Science, Japan, pp 83-94.

DIAMOND, S., (1992)
Proc. 9th. Int. Conf. on 'Alkali Aggregate Reaction in concrete', London. The Concrete Society, Slough, pp 269-278.

DOLAR-MANTUANI, L., (1983)
Handbook of concrete aggregates, Noyes Publications, New Jersey, USA.

DUCHESNE, J., and Berube, M.-A., (1992)
Proc. 9th. Int. Conf. on 'Alkali Aggregate Reaction in concrete', London. The Concrete Society, Slough. pp 287-297.

DUMBLETON, B., (1986)
Report pin points crack attack. New civil engineer, 12th June 1986, pp 24-25.

DUNCAN, M.A.G., Swenson, E.G., Gillot, J.E. and Foran, M.R., (1973)
Alkali aggregate reaction in Nova Scotia, Parts I, II, III and IV. Cem. and Conc. Res., 3, (1), pp 119-128.

FERRAN, J., (1956)
Contribution mineralogique a l' etude de l' adherrence entre les constituants hydrates des ciments et les materiaux enrobes: Second part. Revue des materiaux de construction, (492), pp 191-193.

FOOKES, P.G., Comerbach, C.D. and Cann, J., (1983)
Field investigations of concrete structures in South West England. Concrete, 17 (3), 54-58; 17 (4), 60-67; 18 (11), 12-18.

FRENCH, W.J., (1990a)
Observations on the alkali-aggregate reactions occurring in concrete structures in the United Kingdom. Paper given at the seminar on alkali-aggregate reaction - the European dimension, September 1990. Queen Mary and Westfield College, University of London. pp 57-67.

FRENCH, W.J., (1990b)
Queen Mary and Westfield College, University of London. Personnel communication.

FRENCH,W.J.(1991)
Concrete petrography: a review. The quarterly journal of engineering geology, London. 24, (1), pp 17-48

FRENCH, W.J., (1992)
Proc. 9th. Int. Conf. on 'Alkali Aggregate Reaction in concrete', London. The Concrete Society, Slough. pp 338-346.

GILLOT, J.E., (1975)
Alkali aggregate reactions in concrete. Engineering Geology. 9, (4), London. pp 303-326.

GRATTAN-BELLEW, P.E., (1987)
Proc. 7th Int. Conf. on Alkali-aggregate reaction, Ottawa, Canada. (Ed. P. Grattan-Bellew). Noyes Publications, NJ, USA. pp 434-439.

GRATTEN BELLEW, P.E., (1992)
Proc. 9th. Int. Conf. on 'Alkali Aggregate Reaction in concrete', London. The Concrete Society, Slough., pp 383-394.

GREEMAN, A., (1986)
French to abandon crumbling chambon. New Civil Engineer, 14th August 1986, pp 18-21.

GUDMUNDSSON, G., (1975)
Some investigations into alkali aggregate reaction: Cem. and Conc. Res. 5, (3), pp 211-219.

GUTT, W. and NIXON, P.J., (1979)
Alkali aggregate reactions in concrete in the UK. Conc. Mag. May 1979, pp 19-21.

GUTT, W. and Collins, R.J., (1987)
Sea-dredged aggregates in concrete. BRE Information Paper IP 7/87. Building Research Station, Garston, Watford.

HANSEN, W.C., (1944)
Studies relating to the mechanism by which alkali-aggregate reaction produces expansion in concrete. J. Am. Conc. Inst. Proc. 40, (3), pp 213-227.

HARDON, R.G., (1983)
Unpublished, Dept of Civil Engineering, Aston University, Birmingham, UK.

HERR, R. and Wiekler, W., (1992)
Proc. 9th. Int. Conf. on 'Alkali Aggregate Reaction in concrete', London. The Concrete Society, Slough. pp 440-450.

HOBBS, D.W. and Gutteridge,W.A., (1979)
Particle size of aggregate and its influence upon the expansion caused by the alkali-silica reaction. Mag. Conc. Res., 31, pp 235-242.

HOBBS,D.W., (1984)
Expansion of concrete due to the alkali-silica reaction. Struct. Eng. 62A, pp 26-34.

HOBBS, D.W., (1987)
Comment given at the meeting ' Alkali-silica reaction - The current scientific understanding. Society of Chemical industry, London. 19th Feb. 1987.

HOBBS, D.W., (1988)
Alkali-silica reaction in concrete, Thomas Telford Ltd. London.

HOBBS, D.W., (1990)
British Cement Association, Personnel communication.

HOBBS, D.W., (1991)
British Cement Association, Personal communication.

HOBBS, D.W., (1992a)
Proc. 9th. Int. Conf. on 'Alkali Aggregate Reaction in concrete', London. The Concrete Society, Slough. pp 451-460.

HOBBS, D.W., (1992b)
Deleterious alkali-silica reactivity of a number of UK aggregates and an examination of the draft BS concrete prism test. Report published by BCA on behalf of the Mineral Industry Research Organisation. British Cement Association, Wexham Springs, Slough, p 88.

IMAI, H., Yamasaki, T., Maehara, H. and Miyagawa, T., (1987)
Proc. 7th Int. Conf. on Alkali-aggregate reaction, Ottawa, Canada. (Ed. P. Grattan-Bellew). Noyes Publications, NJ, USA. pp 131-135.

INSTITUTION OF STRUCTURAL ENGINEERS. (1988)
Structural effects of alkali-silica reaction: Interim technical guidance on appraisal of existing structures. The Institution of structural engineers, Belgrave Street, London.

JENSEN, A.D., Chatterji, S., Christensen, N. and Thaulow, N., (1982)
Cem. and Conc. Res., 12, p 641.

JENSEN, A.D., Chatterji, S., Christensen, N. and Thaulow, N., (1984)
Studies of alkali-silica reaction-part II ,Effects of air entrainment on expansion.Cem. and Conc. Res., 14, pp 311-314.

JONES, F.E. and Tarleton, R.D., (1952 / 8)
Reactions between aggregates and cements, parts I - VI. National Building Studies Research Papers, Her Majesty's Stationary Office, London. No.14, 15, 17, 20 and 25.

KAWAMURA, M., Takemoto, K. and Teneshima, N., (1988)
Effects of Sodium chloride and sodium hydroxide from the surrounding solution on alkali-silica reaction in mortars containing fly ash. Mag of Conc. Res. 40, 144, pp 143-151.

KAWAMURA, M. and Makoto, I., (1990)
Characteristics of alkali-silica reaction in the presence of sodium and calcium chloride. Cem. and Conc. Res., 20, pp 757-766.

KAWAMURA, M., Igarashi, M., and Takeuchi, K., (1992)
Proc. 9th. Int. Conf. on 'Alkali Aggregate Reaction in concrete', London. The Concrete Society, Slough. pp 527-534.

KNUDESEN, T. and Thaulow, N., (1975)
Quantitative micro-analysis of alkali silica gel in concrete. Cem. and Conc. Res. 5, p 443.

KOJIMA, T., Miyagawa, T., Nakano, K., Yamaguchi, Y. and Kobayashi, S. (1992)
Proc. 9th. Int. Conf. on 'Alkali Aggregate Reaction in concrete', London. The Concrete Society, Slough. pp 550-555.

KOLLECK, J.J., Varna, S.P. and Zaris, C., (1986)
Proc. 8th Int. Congress Chemistry of cement, Rio de Janeiro, FINEP, Theme 3, IV, pp 183-189.

LAING, S.V., Scrivener, K.L. and Pratt, P.L., (1992)
Proc. 9th. Int. Conf. on 'Alkali Aggregate Reaction in concrete', London. The Concrete Society, Slough. pp 579-586.

LAGERBLAD, B. and Tragardh,J., (1992)
Proc. 9th. Int. Conf. on 'Alkali Aggregate Reaction in concrete', London. The Concrete Society, Slough. pp 570-578.

LAWRENCE, C.D., (1966)
Changes in composition of aqueous phase during hydration of cement pastes and suspensions, in special report 90. Highway Research Board, Washington D.C. Symposium on structure of Portland cement paste and concrete. p 492.

LEA, F.M., (1970)
The chemistry of cement and concrete, Third Edition. Edward Arnold (Publishers) Ltd., London.

LERCH, W., (1959)
A cement-aggregate reaction that occurs with certain sand-gravel aggregates. J. PCA Res and Dev. Lab., 1, (3), 42-50.

LIVESEY, P., (1992)
Alkalis in concrete. Paper presented at BCA informative seminar in Huddersfield, entitled, 'New developments in alkali-silica reaction in UK concretes'. 24th June.

LONGUET, P., Burglen, L. and Zelwer, A., (1973)
La phase liquide du ciment hydrate, Rev des materiaux de constructions et des travaux publics. Ciments et Betons 676, pp 35-41.

MACPHEE, D.E., Luke, K., Glasser, F.P., and Lachowski, E.E., (1989)
J. Am. Ceram. Soc. 72, p 646.

MARSHALL, B.F. and Walker, H.N., (1978)
Evaluation and adaptation of the Dobrolubov and Romer method of microscopic examination of hardened concrete. Virginia Highway and Transportation Council, VHTRC 78-R54.

MATHER, B., (1948)
Petrographic identification of reactive constituents in concrete aggregate. Proc. Am. Soc. Test and Mat., 48, pp 1120-1125.

MEHTA, P.K., (1978)
Proc. 4th Int. Conf. on the effects of alkalis in cement and concrete. Purdue University, West Lafayette, USA. Purdue University CE-MT-1-78. pp 229-234.

MEHTA, P.K., (1980)
Effects of cement composition on corrosion of reinforcing steel in concrete. American society for testing and materials, Special Technical publication 629, pp 12-19.

MIELENZ, R.C., (1954)
Petrographic examination of concrete aggregates. Proc. Am. Soc. Test and Mat., 54, pp 1188-1218.

MIYAGAWA, T., (1992)
Kyoto University, Japan,Personnel Communication.

MOORE, A.E., (1978)
Proc. 4th Int. Conf. on the effects of Alkalis in Cement and Concrete, Purdue University, West Lafayette, USA. Purdue University CE-MT-1-78. pp 363-365.

NATESSAIYER, K and Hover, K.C., (1988)
Insitu identification of ASR products in concrete. Cem. and Conc. Res. 18, pp 455-463

NIXON, P.J., Collins, R.J. and Rayment, P.L., (1979)
The concentration of alkalis by moisture migration in concrete - a factor influencing alkali aggregate reaction. Cem. and Conc. Res., 9, pp 417-423.

NIXON, P.J and Bollinghaus, R., (1983)
Proc. 6th Int. Conf. Alkalis in concrete, Copenhagen. edited by G.M. Idorn and S. Rostam. Danish Concrete Association, pp 329-336.

NIXON, P.J and Gaze, M.E., (1983)
Proc. 6th Int. Conf. Alkalis in concrete, Copenhagen. edited by G.M. Idorn and S. Rostam. Danish Concrete Association. pp 61- 68.

NIXON, P.J., Page, C.L., Bollinghaus, R. and Canham, I., (1984)
The effect of a pfa with a high alkali content on pore solution composition and alkali silica reaction. Mag of Conc. Res. 38, (134), pp 30-35.

NIXON, P.J. and Gillson, I.P., (1986)
Proc. 7th Int. Conf. on Alkali-aggregate reaction, Ottawa, Canada. (Ed. P. Grattan-Bellew). Noyes Publications, NJ, USA. pp 173-177.

NIXON, P.J., Page, C.L., Bollinghaus,R. and Canham, I., (1986)
The effect of PFA with a high total alkali content on pore solution composition and alkali-silica reaction. Mag. Conc. Res., 38, (134), pp 30-35.

NIXON, P.J., (1987)
Paper titled 'Pore solution Chemistry and alkali-silica reaction. at meeting entitled Alkali-silica reaction - The current scientific understanding. Society of Chemical industry, London. 19th Feb. 1987.

NIXON, P.J., Page, C.L., Canham, I. and Bollinghaus, R., (1988)
Influence of sodium chloride on the alkali-silica reaction. Advances in cement research, 1, (2), pp 99-106.

NIXON, P.J., Page, C.L., Hardcastle, J., Canham, I. and Pettifer, K., (1989)
Proc. 8th Int. Conf. on alkali aggregate reaction, Kyoto, Japan. (Ed. K.Okada). The Society of Materials Science, Japan. pp 129-134.

NIXON, P.J., (1990)
Building Research Station, Garston, Watford, Personnel communication.

PAGE, C.L and Vennesland,O., (1983)
Pore solution composition and chloride binding capacity of silica fume cement pastes. Materials and structures.16, pp 19-25.

PAGE, C.L., Sergi, G. and Thompson, D.M., (1992)
Proc. 9th. Int. Conf. on 'Alkali Aggregate Reaction in concrete', London. The Concrete Society, Slough. pp 774-781.

PAGE, C.L., (1993)
Dept of Civil Engineering, Aston University, Personnel communication.

PALMER, D., (1978)
Proc. 4th Int. Conf. Effect of alkalis in cement and concrete, Purdue University, West Lafayette, USA. Purdue University CE-MT-1-78. pp 285-298.

PARKINSON, J., (1981)
Cement changes blamed on concrete decay. New civil engineer, January 1981, p.21.

PATERSON, A.C., (1984)
The structural engineer in context. Struct. Eng. 62A, pp 335-342.

PETERSEN, S.E., (1983)
Proc. 6th. Int. Conf. Alkalis in concrete, Copenhagen. edited by G.M. Idorn and S. Rostam. Danish Concrete Association. pp 441-447.

PETTIFER, K., (1986)
Building Research Station, Watford, Personnel communication.

PETTIFER, K., (1990)
Building Research Station, Watford, Personal communication.

PETTIFER, K., (1993)
Building Research Station, Watford, Personnel Communication.

PIKE, R.G., Hubbard, D. and Insley,H., (1955)
Mechanisms of alkali aggregate reaction. Journal American Concrete Institute. Proceedings 52, (1), pp 13-34.

POOLE, A.B. and Thomas, A., (1975)
A staining technique for the identification of sulphates in aggregates and concretes. Mineralogical Magazine, 40, pp 315-316.

POOLE, A.B., (1992a)
Alkali-Aggregate reaction in concrete. Edited by R.N.Swamy, Publisher Blackie Ltd, Glasgow, pp 17 -19.

POOLE, A.B., (1992b)
Proc. 9th. Int. Conf. on 'Alkali Aggregate Reaction in concrete', London. The Concrete Society, Slough. pp 782-789.

POWER, T.C. and Steinour, H.H., (1955)
An interpretation of published researches on Alkali-aggregate reactivity. Parts I and II. J. Am. Conc. Inst. (Proc.), 51, 497, p 785.

RAYMENT, P.L., (1992)
Proc. 9th. Int. Conf. on 'Alkali Aggregate Reaction in concrete', London. The Concrete Society, Slough, pp 843-850.

REED, S.J.B., (1975)
Cambridge monographs on physics. Electron microprobe analysis. Cambridge University Press, Cambridge.

ROBBINS, J., (1992)
'Misleading' ASR claims slammed. New Civil Engineer, 26th November 1992, p 3.

ROGERS, C.A., (1986)
Proc. 7th Int. Conf. on Alkali-aggregate reaction, Ottawa, Canada. (Ed. P. Grattan-Bellew). Noyes Publications, NJ, USA. pp 259-263.

SADEGHZADEH, M., (1993)
The effect of pulverised fuel ash on the pore solution chemistry of concretes with reactive aggregate: Paper to be published.

SERGI, G., (1986)
Ph.D. thesis. Dept of Civil Engineering, Aston University, Birmingham, UK.

SERGI, G., Page, C.L. and Thompson, D.M., (1991)
Electrochemical induction of alkali-silica reaction in concrete. Materials and Structures, 24, pp 359-361.

SILSBEE, M. Malek, R.I.A. and Roy, D., (1986)
Composition of pore fluids extruded from slag cement pastes. Proc. 8th Int. Congress on the chemistry of cement, Rio De Janiero. pp 263-269.

SIBBICK, R.G., (1988)
Water absorption tests on flint gravels in concrete roads. Materials memorandum 186, Transport and road research laboratory, Crowthorne, (unpublished available on request).

SIBBICK, R.G. and West, G., (1989)
Examination of concrete from the M40 Motorway. Research report 197, Transport and road research laboratory, Crowthorne.

SIBBICK, R.G. and West, G., (1992).
Examination of concrete from the A6068, Padiham Bypass, Lancashire. Research report 304, Transport research laboratory, Crowthorne.

SIBBICK, R.G. and Page, C.L., (1992a)
Proc. 9th. Int. Conf. on 'Alkali Aggregate Reaction in concrete', London. The Concrete Society, Slough. pp 980-987.

SIBBICK, R.G. and Page, C.L., (1992b)
Threshold alkali contents for expansion of concretes containing British aggregates. Cem. and Conc. Res. 22, pp 990-994.

SMITH, A.C., (1991)
Leicester University, Personal communication.

SMITH, A.S.,Dunham, A.C and West, G., (1992)
Proc. 9th. Int. Conf. on 'Alkali Aggregate Reaction in concrete', London. The Concrete Society, Slough., pp 1001-1008.

SMITH, M.A. and Halliwell, F., (1979)
The application of the BS4550 test for pozzolanic cements containing pulverised fuel ashes. Mag. Conc. Res., 32, (108), pp 159-170.

STANTON, T.E., (1940)
Expansion of concrete through reaction with cement and aggregate. American Society of Civil Engineers: Proceedings 66, pp 1781-1811.

STANTON, T.E., (1942)
Expansion of concrete through reaction between cement and aggregate. American Society of Civil Engineers: Paper 2129, (107).

STARK, D., (1991)
Handbook for the identification of alkali-silica reactivity in highway structures. SHRP, National Research Council, Washington, D.C.

SWAMY, R.N. and Al-asali, M.M., (1988)
Alkali silica reaction-Sources of damage. Highways and Transportation, pp 24-29.

THAULOW, N., Holm, J. and Andersen, K.T., (1989)
Proc. 8th Int. Conf. on alkali aggregate reaction, Kyoto, Japan, (Ed. K.Okada). The Society of Materials Science, Japan. pp 573-581.

THOMAS, M.D.A., Blackwell,B.Q. and Pettifer, K., (1992)
Proc. 9th. Int. Conf. on 'Alkali Aggregate Reaction in concrete', London. The Concrete Society, Slough. pp 1059-1066.

VERBECK, G. and Gramlich, C., (1955)
Osmotic studies and hypothesis concerning alkali-aggregate reaction. ASTM: Proceedings 55, pp 1110-1120.

VIVIAN, H.E., (1950)
Studies in cement-aggregate reaction. XV: The reaction product of alkalis and opal. CSIRO, Melbourne, Australia. Bulletin 256, pp 60-82.

VIVIAN, H.E., (1951)
The effect on mortar expansion of particle size of the reactive component in the aggregate. Australian Journal Appl. Sci.: 2, (4), pp 488-494.

VOGEL, A.I., (1961)
Textbook of quantitative inorganic analysis. Longman, London.

WARNING, I. and Johansen, V., (1983)
Proc. 6th Int. Conf. on alkalis in concrete, Copenhagen. edited by G.M. Idorn and S. Rostam. Danish Concrete Association., pp 41-53.

WEBB, C., (1988)
Engineers take new measures to slow alkali aggregate reaction on afflicted Marsh Mills Viaducts. Highways, pp 27-33.

WEST, G., (1988)
Transport and Road Research Laboratory, Personnel communication.

WEST, G., (1991)
A note on undulatory extinction of quartz in granite. Quarterly journal of engineering geology, London. 24, pp 159-165.

WINNEY, M., (1980)
Alkali aggregate cracks up Plymouth car park. New civil engineer, 24th April 1980, pp 22-23.

WOOD, J.G.M., (1992a)
Some overseas experience of Alkali aggregate reaction and its prevention:- Specification for major projects: Bridges, Tunnels, and dams. Presentation to the ITBTP meeting, Paris, France.

WOOD, J.G.M., (1992b)
Structural studies and design Ltd., Personnel communication.

WORKING PARTY REPORT, (1983)
Minimising the risk of alkali-silica reaction: guidance notes. C and CA, Wexham Springs, Slough.

ZHANG, X., Blackwell, B.Q. and Groves, G.W., (1990)
The microstructure of reactive aggregates. Br.Ceramics.Trans.Journal. 89, pp 89-92.

# APPENDIX 1

## PETROGRAPHICAL EXAMINATION OF FRESH AGGREGATE SAMPLES

### CHEDDAR LIMESTONE

Light grey to cream limestone rock. Mainly fossiliferous, constituent fauna includes; Brachiopoda valves, Bryozoa stems, Corals, Gastropoda valves and small Ammonites. Some pelloidal and oolitic micrites often recrystallised. Some coarse calcite veining running through other limestone types. A redeposited form of limestone in a fine $CaCO_3$ cement also present. This rock was massively bedded and showed no evidence of having undergone significant deformation. Aggregate particles were generally uncracked internally. Some stylolites developed in the finer rock matrix which were shown up well by iron staining along the stylolite dissolution front. Rocks appeared dense with little porosity. Silica / chert / microcrystalline quartz were observed however this was relatively rare making up less than 1 % of the total rocks volume. This microquartz was generally found as an intergrowth with the calcium carbonate cement. Very fine quartz sand grains (50-100 $\mu$m) were seen occasionally, these were generally unstrained. In general the chert was found in the lighter coloured limestones, whilst the quartz sand grains were found more often in the darker more bituminous and muddy limestones. The amounts of silica were considered far to small to cause significant reaction in this aggregate.

The rock was of Lower Carboniferous age (360-320 million years).

### ANGLESEY GRANITE

Though called a granite in reality this aggregate was so heavily altered that its true classification was difficult. The rock was composed mainly of quartz, plagioclase, orthoclase, muscovite and some opaque particles. There was also some calcite in the form of veining and / or microcrack infills. Though in some areas the rock shows inherent igneous rock features other particles show well developed schistose and gneissous texture due to the very high degree of metamorphism they have undergone (Eclogite facies). These gniess' and schists have however, clearly been derived from a granitic rock prior to metamorphism. The feldspars showed a lot of alteration clay minerals and muscovite within them. The muscovite found in the veins and cracks of the rock may be an alteration product itself. The occurrence of microcline in the aggregate was further evidence for the recrystallisation in this rock. from a granitic material. The rock was highly fractured and these cracks and fracture zones have been filled by various minerals including calcite, Fe rich chlorite and muscovite. There was some recrystallised quartz found in centre of these cracks. Due to the alteration this rock exhibits larger crystals of quartz and feldspar surrounded by a mass of microquartz with veins / lineations of muscovite and chlorite with more microquartz running through them. There were also, some calcite veins present. This aggregate basically contained two different rock types; firstly a highly cleaved schistose rock made up of calcite, muscovite, quartz and chlorite with the quartz running in bands of rounded to sub rounded crystals unrelated to the cleavage. Second was a rock type of a more gniess appearance with remnant areas of feldspar and quartz from the previous rock now surrounded by veining and

microquartz.

The rock was of Pre Cambrian age (800-590 million years).

## DRY RIGG SILTSTONE

Generally a homogeneous dark grey chloritic siltstone containing quartz, chlorite, pyrite, muscovite, calcite and clay minerals, (sericite) all cemented together by fine silica and a little calcite. However, a few rather conglomeritic horizons could also be found in the quarry. There was a fair degree of variation in the grain size of the particles, which was typical of most greywackes / turbidites. This rock showed a well developed parallel cleavage. Microquartz veins and darker material bands probably made up of fine pyrite crystals were found running parallel /sub-parallel to this cleavage. There was also a smaller amount of calcite veining. Some coarse calcite was found as a secondary regrowth in some of the voids in the aggregate. Generally this aggregate was dense and had few significant voids. Larger pyrite cubes, (500-1000 $\mu$m) were seen frequently, though these appear sound and unaltered. The rock had undergone low 'chlorite' grade metamorphism and there was evidence that some of the quartz present had undergone limited strain. A few particles of a coarser calcareous gritstone / sandstone with a slight development of cleavage were also present.

The rock was of Lower Silurian age (438-421 million years).

## MAENTWROG GREYWACKE

Light grey green quartzo-feldspathic greywacke mainly composed of rounded quartz, feldspars and pyroxene particles; along with clasts of volcanic rock (acidic composition), microcline, hornblende, various quartzites and opaque minerals. There were also large areas of well crystallised chlorite, and muscovite / sericite spicules in the matrix. This phylosilicate matrix makes up the cementing agent for the particles described above. Some of the quartz was clearly strained. The rock was a complete jumble of particle types, sizes and shapes, this was all indicative of a typical greywacke. The recrystallisation and lineation of some areas of the muscovite / sericite matrix suggests some degree of metamorphism. A number of the constituent minerals have undergone a degree of alteration in part at least due to metamorphism. The rock had undergone lower 'greenschist facies' grade metamorphism. There were areas of the rock that appear to have a calcite and / or a clay cementing agent rather than those described above, however, the fine nature of this matrix makes true identification difficult. Though the majority of this aggregate was made up of the rock described, there was also a small percentage of a finer more silty rock exhibiting layering. This rock was composed of the same constituents as the coarser rock, but with a noticeably higher proportion of pyroxene and hornblende particles.

The rock was of Lower Cambrian age (590-540 million years).

## VENN QUARRY SILTSTONE

Made up of a number rock types which could all be classified as siltstones. All the particles were seen to have a thick layer (1mm) of dust on there surfaces. The first rock type identified was a quartz rich siltstone. This rock was of angular shape and

contained varying proportions of quartz (dominant), chert, feldspar and elongate muscovite flakes that developed a lineation within the rock. These various constituents were unsorted with regard to size and shape. Some of the quartz exhibited high undulatory extinction (UEA) but this was relatively rare. The degree of iron staining was the only variable factor in an otherwise uniform rock. The second rock identified was a finer more lineated siltstone. The constituent particles were more uniform in size and the rock more closely resembled the Dry Rigg siltstone described above, though there were however, less dark bands / lineation in this rock. This material was thought to probably be organic in origin. The major constituent was quartz which was often seen to be lineated this most probably representing the rocks bedding. Some aggregate particles were cracked, this was probably caused by water percolation and weathering at the quarry.

The rock was of Middle Carboniferous age (340-300 million years).

## HORROCKSFORD LIMESTONE

Light grey to dark brown highly silicified limestone composed mainly of calcite often as fossiliferous material. The fossiliferous material contains constituent faunas including; Brachiopoda valves, Bryozoa stems, Corals, Gastropoda valves and small Ammonites. There were also some pelloidal and oolitic micrites often recrystallised. Some coarse sparite calcite veining was observed running through other limestone types. There was also a high proportion of bituminous matter and quartz in this rock. Within the matrix were seen a few sand sized grains of vein quartz. The majority of the quartz was however, found as discrete cryptocrystalline masses of silica / chert within the matrix or as an infilling to some voids. The darker more bituminous limestone appeared to contain a higher percentage of chert than the lighter limestones. The chert comprised of up to 25 % of the total rock, though there may have been even more silica of extremely fine size in the matrix at present indistinct under a normal polarising microscope. Locally the chert content could be as high as 60 % in an individual grain. The rock was cemented by a calcite cement of micrite (fine) grain size.

The rock was of Lower Carboniferous age (360 -320 million years).

## THAMES VALLEY GRAVEL

Composed almost entirely of flint / chert (which is crypto to microcrystalline quartz / silica) with a small proportion of vein quartz and metaquartzites also present. These lesser constituents made no more than 5 % of the total aggregate. The flint had variable amounts of iron staining and porosity throughout. The white flints have very high coarser porosity whilst the brown and black flints have less porosity and this was of a finer average void size. A small amount of chalcedony was encountered in the flints as also were a few now silicified microfossils. Areas of slightly coarser crystallinity were also found in the flint though this would still be regarded as very fine (crypto to microcrystalline). Some calcite infills could be seen in voids in the flint particles. A few cracks can be identified running from the particle surfaces that were now filled by an iron mineral (Ilmenite). There were a few remnant areas of highly porous white / creamy material next to the 'pattina' on some flints. This was petrographically a different rock type from the flint and is usually found surrounding flint nodules when they were still in the chalk. The vein

quartz and metaquartzites tend to contain a high percentage of highly strained quartz crystals and also appear to be fresh and have no impurities.

The rock deposit was of Quaternary age (2 million years to present day).

## TRENT VALLEY GRAVEL

This was a typical river gravel from the Trent Valley area. The constituent rock particles were well rounded as would be expected from a fluvially derived gravel. The constituent rock types include; chert, metaquartzite, orthoquartzite, vein quartz, iron stained sandstone and a quartzose gneiss. There were a smaller number of metamorphosed greywackes and tuffs, (pyroclastic rock) now heavily quartz veined and altered. The dominant rock types were the various quartzites, though there was a significant amount of chert in this aggregate as well. Some of the quartzites contain secondary growths of micro-quartz between the pre-existing quartz particles. These rocks tend to be severely fractured and therefore contained many microcracks which are now heavily iron stained. Quartz sand grains within these rocks types, exhibiting at least a degree of strain were common. The vein quartz was composed of strained interlocking crystals with some microcrystalline quartz grains at the intergrain boundaries. The rock was generally pure, with only limited iron staining on the lattice dislocation boundaries. The cherts which were the most likely reactive rock type in the gravel were fine grained siliceous rocks of low porosity and were generally darker and more iron stained than Cretaceous flint.

The rock was of Quaternary age (2 million years to present day).

# APPENDIX 2

The construction of the pore press used for the expression of pore solution from the concretes.

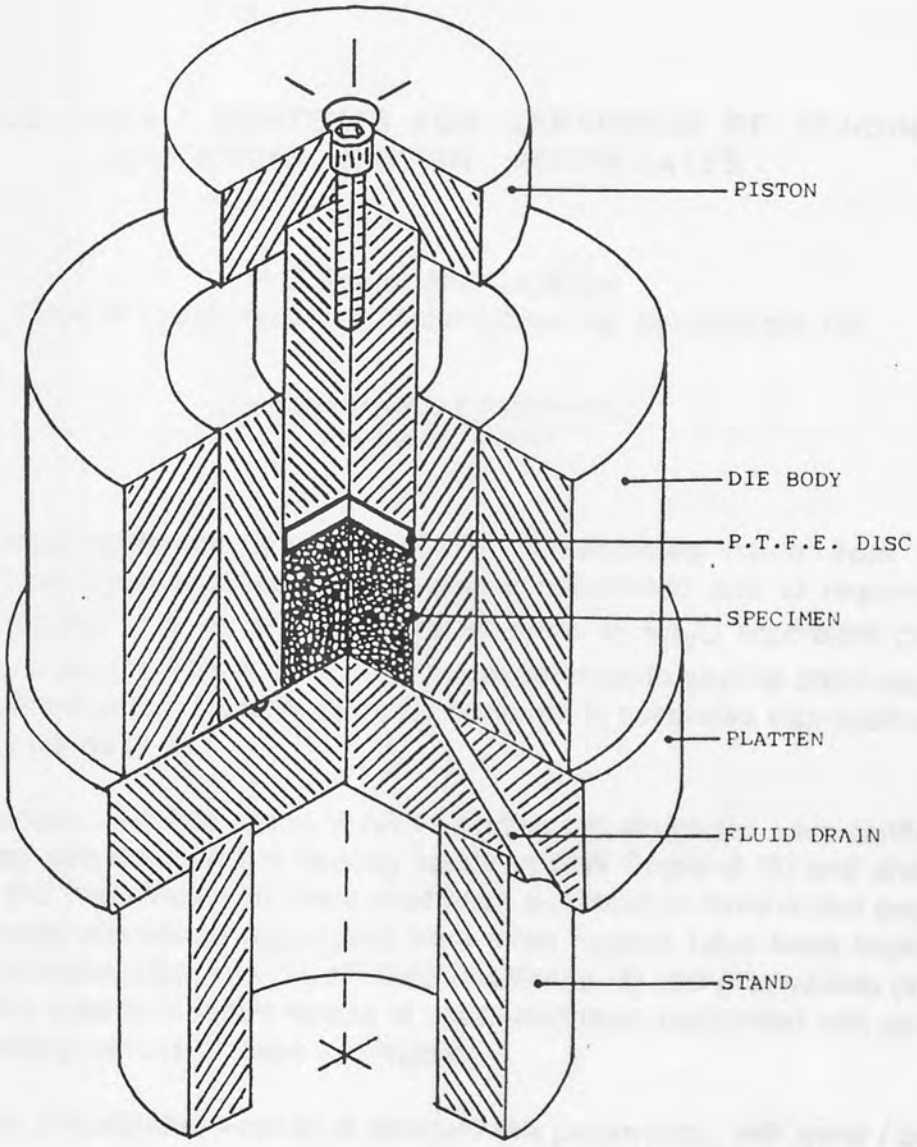

# APPENDIX 3

## Published work from study

CEMENT and CONCRETE RESEARCH. Vol. 22, pp. 990-994, 1992. Printed in the USA.
0008-8846/92. $5.00+00. 



Aston University

**Content has been removed for copyright reasons**

Aston University

**Content has been removed for copyright reasons**

Aston University

**Content has been removed for copyright reasons**

Aston University

**Content has been removed for copyright reasons**

Aston University

**Content has been removed for copyright reasons**

Aston University

**Content has been removed for copyright reasons**

CEMENT and CONCRETE RESEARCH. Vol. 23, pp. 495-499, 1993. Printed in the USA.
0008-8846/93. $6.00+00. 



Aston University

**Content has been removed for copyright reasons**

Aston University

**Content has been removed for copyright reasons**

Aston University

**Content has been removed for copyright reasons**

Aston University

**Content has been removed for copyright reasons**

# APPENDIX 4

Chemical analysis of the Dry Rigg siltstone and Horrocksford limestone aggregates.

| | Dry Rigg siltstone (%) | Horrocksford limestone (%) |
|---|---|---|
| $SiO_2$ | 56.65 | 14.19 * |
| $Al_2O_3$ | 22.29 | 3.52 |
| $Fe_2O_3$ | 3.23 | 1.65 |
| CaO | 5.03 | 41.77 |
| MgO | 3.18 | 1.64 |
| $SO_3$ | - | 1.23 @ |
| $K_2O$ | 0.17 | 0.56 |
| $Na_2O$ | 0.24 | 0.30 |
| Loss on ignition at 1000°C | 7.08 | |
| $Na_2O$ equivalent | 0.35 | 0.67 |

* - The this is an average representing a typical sample of Horrocksford limestone.

The chemical analysis of the sample collected and used for this work is shown below:

@ - This figure was different to that calculated in section 3.6.2

Chemical analysis of Horrocksford limestone used in this work. This aggregate was deliberately picked from an area of the quarry of higher than normal silica content.

| | |
|---|---|
| $SiO_2$ | - > 25.52 % |
| $Al_2O_3$ | - 1.63 % |
| $Fe_2O_3$ | - 1.52 % |
| CaO | - < 40.80 % |
| MgO | - 0.92 % |
| $SO_3$ | - 0.31 % |
| $K_2O$ | - 0.10 % |
| $Na_2O$ | - 0.08 % |
| Cl - | - 0.013 % |

$Na_2O$ equivalent - 0.146 %

This chemical analysis was kindly carried by Castle Cement (Ribblesdale) Ltd. on the 30 th October 1990.

TABLE 4.6: Comparison of the chemical analysis of the central areas, (37-46 mm) of the various prisms, before and after immersion in salt solution.

| Mix Name. | $Cl^-$ | $Na_2O$ | $K_2O$ | $Na_2O_e$ |
|---|---|---|---|---|
| 1. After immersion in salt solution | | | | |
| DR 3 kg mix | 0.322% | 0.364% | 0.187% | 0.487% |
| DR 7 kg mix | 0.111% | 0.330% | 0.213% | 0.470% |
| HL 3 kg mix | 0.314% | 0.258% | 0.070% | 0.304% |
| HL 7 kg mix | 0.070% | 0.272% | 0.062% | 0.313% |
| MD 4 kg mix | 0.203% | 0.229% | 0.114% | 0.304% |
| MD 7 kg mix | 0.073% | 0.313% | 0.044% | 0.342% |
| RP 7 kg mix | 0.092% | 0.263% | 0.079% | 0.315% |
| 2. Chemical analysis of original mixes. | | $Na_2O$ | $K_2O$ | $Na_2O_e$ |
| All 3 kg mixes | | 0.077% | 0.046% | 0.123% |
| All 4 kg mixes | | 0.118% | 0.046% | 0.164% |
| All 7 kg mixes | | 0.241% | 0.046% | 0.287% |

3. Percentage difference between original concrete mixes and mixes after they have been immersed for 15 months in salt solution.

| | $Na_2O$ | $K_2O$ | $Na_2O_e$ | $Kg/m^3$ $Na_2O_e$ |
|---|---|---|---|---|
| DR 3 kg mix | +0.287 % | +0.141 % | +0.364 % | 8.86 |
| DR 7 kg mix | +0.089 % | +0.167 % | +0.183 % | 4.46 |
| HL 3 kg mix | +0.181 % | +0.024 % | +0.181 % | 4.41 |
| HL 7 kg mix | +0.031 % | +0.016 % | +0.026 % | 0.63 |
| MD 4 kg mix | +0.111 % | +0.068 % | +0.140 % | 3.41 |
| MD 7 kg mix | +0.072 % | -0.002 % | +0.055 % | 1.75 |
| RP 7 kg mix | +0.022 % | +0.033 % | +0.028 % | 0.68 |

4. Contribution of $Na_2O$ from the NaCl

| | $Na_2O$ |
|---|---|
| DR 3 kg mix | +0.281 % |
| DR 7 kg mix | +0.096 % |
| HL 3 kg mix | +0.274 % |
| HL 7 kg mix | +0.061 % |
| MD 4 kg mix | +0.171 % |
| MD 7 kg mix | +0.064 % |
| RP 7 kg mix | +0.080 % |

5. Difference in the various constituents between high and low initial alkali mixes after being immersed in salt solution for 15 months.

| Aggregate type | $Cl^-$ | $Na_2O$ | $K_2O$ | $Na_2O_e$ | Extra $Na_2O_e$ in mix |
|---|---|---|---|---|---|
| Dry Rigg siltstone | +0.211% | +0.198% | -0.026% | +0.181% | +4.4 kg/m$^3$ |
| Horrocksford Lst | +0.244% | +0.150% | +0.008% | +0.155% | +3.8 kg/m$^3$ |
| Maentwrog Grwke | +0.130% | +0.039% | +0.070% | +0.085% | +2.2 kg/m$^3$ |

TABLE 4.7 : Water soluble, acid soluble and total alkali contents of powdered samples of coarse aggregates analysed at the Building Research Establishment.

| | Water soluble (%) | | Acid soluble (%) | | TOTAL (%) | |
|---|---|---|---|---|---|---|
| | $Na_2O$ | $K_2O$ | $Na_2O$ | $K_2O$ | $Na_2O$ | $K_2O$ |
| Dry Rigg siltstone | 0.01 | 0.03 | 0.04 | 0.25 | 2.29 | 2.59 |
| Horrocksford Lst | 0.01 | 0.02 | 0.04 | 0.07 | 0.15 | 0.25 |
| Maentwrog Grywke | 0.02 | 0.02 | 0.11 | 0.24 | 2.66 | 0.95 |
| Trent Valley Gravel | 0.01 | 0.02 | 0.04 | 0.14 | 0.26 | 0.82 |

(The results obtained by standard BSI methods.)

# APPENDIX 5

TABLE 5.6: Chemical composition of extracted pore solutions shown in mmol / litre.

Dry Rigg siltstone.

| 1 DAY RESULTS. | $Na^+$ | $K^+$ | $OH^-$ |
|---|---|---|---|
| OPC Mix | | | |
| 3.0 kg/m$^3$ | 330.60 | 94.72 | 381.0 |
| 4.0 kg/m$^3$ | 439.35 | 87.04 | 490.0 |
| 5.0 kg/m$^3$ | 604.65 | 94.72 | 643.0 |
| 6.0 kg/m$^3$ | 713.40 | 87.04 | 752.0 |
| WB,Pfa Mix | | | |
| 3.0 kg/m$^3$ | 439.35 | 87.04 | 459.0 |
| 4.0 kg/m$^3$ | 522.00 | 74.24 | 556.0 |
| 5.0 kg/m$^3$ | 678.60 | 79.36 | 722.0 |
| 6.0 kg/m$^3$ | 843.90 | 79.36 | 855.0 |
| FF,Pfa Mix | | | |
| 3.0 kg/m$^3$ | 374.10 | 66.56 | 432.0 |
| 4.0 kg/m$^3$ | 495.90 | 66.56 | 533.0 |
| 5.0 kg/m$^3$ | 626.40 | 64.00 | 640.0 |
| 6.0 kg/m$^3$ | 769.95 | 71.68 | 781.0 |

| 7 DAY RESULTS. | $Na^+$ | $K^+$ | $OH^-$ |
|---|---|---|---|
| OPC Mix | | | |
| 3.0 kg/m$^3$ | 326.25 | 84.48 | 325.0 |
| 4.0 kg/m$^3$ | 439.35 | 92.80 | 441.0 |
| 5.0 kg/m$^3$ | 630.75 | 92.80 | 592.5 |
| 6.0 kg/m$^3$ | 717.75 | 92.80 | 695.0 |
| WB,Pfa Mix | | | |
| 3.0 kg/m$^3$ | 384.98 | 93.44 | 339.0 |
| 4.0 kg/m$^3$ | 569.85 | 81.92 | 464.0 |
| 5.0 kg/m$^3$ | 698.18 | 71.68 | 543.5 |
| 6.0 kg/m$^3$ | 817.80 | 79.36 | 722.5 |
| FF,Pfa Mix | | | |
| 3.0 kg/m$^3$ | 408.90 | 67.84 | 322.5 |
| 4.0 kg/m$^3$ | 539.40 | 66.56 | 433.5 |
| 5.0 kg/m$^3$ | 680.78 | 70.40 | 542.0 |
| 6.0 kg/m$^3$ | 802.58 | 67.84 | 650.0 |

| 28 DAY RESULTS. | $Na^+$ | $K^+$ | $OH^-$ |
|---|---|---|---|
| OPC Mix | | | |
| 3.0 kg/m$^3$ | 254.48 | 64.00 | 252.0 |
| 4.0 kg/m$^3$ | 356.70 | 54.40 | 326.0 |
| 5.0 kg/m$^3$ | 456.75 | 64.00 | 417.0 |
| 6.0 kg/m$^3$ | 543.75 | 67.84 | 484.0 |
| WB,Pfa Mix | | | |
| 3.0 kg/m$^3$ | 239.25 | 92.80 | 275.0 |
| 4.0 kg/m$^3$ | 337.13 | 88.32 | 342.0 |
| 5.0 kg/m$^3$ | 413.25 | 88.32 | 455.5 |
| 6.0 kg/m$^3$ | 530.70 | 72.96 | 499.0 |
| FF,Pfa Mix | | | |
| 3.0 kg/m$^3$ | 228.38 | 78.72 | 243.0 |
| 4.0 kg/m$^3$ | 315.38 | 84.48 | 337.0 |
| 5.0 kg/m$^3$ | 413.25 | 80.00 | 432.0 |
| 6.0 kg/m$^3$ | 435.00 | 80.00 | 434.0 |

| 183 DAY RESULTS. | $Na^+$ | $K^+$ | $OH^-$ |
|---|---|---|---|
| OPC Mix | | | |
| 3.0 kg/m$^3$ | 139.20 | 29.44 | 128.00 |
| 4.0 kg/m$^3$ | 154.43 | 23.68 | 147.00 |
| 5.0 kg/m$^3$ | 191.40 | 22.40 | 184.00 |
| 6.0 kg/m$^3$ | 247.95 | 22.40 | 218.00 |

| 365 DAY RESULTS. | $Na^+$ | $K^+$ | $OH^-$ |
|---|---|---|---|
| WB,Pfa Mix | | | |
| 3.0 kg/m$^3$ | 191.40 | 71.68 | 202.0 |
| 4.0 kg/m$^3$ | 224.03 | 65.92 | 226.0 |
| 5.0 kg/m$^3$ | 254.48 | 60.80 | 236.5 |
| 6.0 kg/m$^3$ | 252.30 | 48.00 | 229.5 |
| FF,Pfa Mix | | | |
| 3.0 kg/m$^3$ | 178.35 | 70.40 | 190.0 |
| 4.0 kg/m$^3$ | 206.63 | 60.16 | 177.0 |
| 5.0 kg/m$^3$ | 252.30 | 58.88 | 222.0 |
| 6.0 kg/m$^3$ | 297.98 | 61.44 | 234.0 |

Horrocksford limestone

| 365 DAY RESULTS. | $Na^+$ | $K^+$ | $OH^-$ |
|---|---|---|---|
| WB,Pfa Mix | | | |
| 3.0 kg/m$^3$ | 226.20 | 87.04 | 237.5 |
| 4.0 kg/m$^3$ | 274.05 | 108.80 | 286.0 |
| 5.0 kg/m$^3$ | 304.50 | 66.56 | 263.0 |
| 6.0 kg/m$^3$ | 380.63 | 71.68 | 320.5 |
| FF,Pfa Mix | | | |
| 3.0 kg/m$^3$ | 200.10 | 88.96 | 198.0 |
| 4.0 kg/m$^3$ | 281.66 | 87.68 | 245.0 |
| 5.0 kg/m$^3$ | 340.39 | 83.84 | 295.0 |
| 6.0 kg/m$^3$ | 345.83 | 68.48 | 277.0 |

# APPENDIX 6

Full petrographical analysis of concretes discussed in chapter 4.

## 1. Dry Rigg siltstone.

### 1.1.1 7 Kg/m$^3$ $Na_2O_e$ mix, Immersed in distilled water.

Degree of reaction (Scale 1 to 10) = 7

Extensive ASR with the features typical of the reaction in this aggregate all noted. These include; microcracks running along the long axis of coarse aggregate particles, divergent, bifurcating edge microcracks and pseudo-adhesion cracks running around the periphery of the aggregate particle, but still within the rock material these often containing desiccated ASR gel. The degree of reaction was less than that seen in the samples immersed in salt solution. The whole of the slide was affected by the reaction to the same extent. A little fibrous ettringite was observed in some paste microcracks, but it was not felt to represent a significant quantity. Its location was not expansive in form, but rather a late secondary infill product. ASR gel was observed in significant quantities, apparently developed as a single pulse or generation. The gel was generally found in voids, paste cracks and adhesion cracks on the limestone fine aggregate particles.

The cement paste was typical of all the first stage concrete prisms (Chapter 3) with the extensive impregnation of the region surrounding the paste cracks by the fluorescent araldite resin. The finer cement paste matrix material appears sound and unaffected by the reaction. Carbonation was only seen to a limited extent on the original external surfaces. Some evidence of ASR gel injection into the cement paste was also observed. The effects to the paste seen in the salt solution environments were not observed in this concrete.

### 1.1.2 3 Kg/m$^3$ $Na_2O_e$ mix, Immersed in distilled water.

Degree of reaction = 0

**No evidence of ASR was found in this slide**. Adhesion cracks found mainly on the fine aggregate particles, but a few on the coarse aggregate material were partly interconnected by a series of dry shrinkage paste microcracks. Patchy high porosity in the cement paste was observed around some voids and paste cracks. Large portlandite laths (200 x 400 $\mu$m) were found along with other debris to partially fill some voids. Ettringite was observed, but was not considered significant. The coarse aggregate was sound and uncracked. The fine aggregate was occasionally split by the fine paste cracks. The surface carbonation level was low. Coarse aggregate to paste bond was generally good.

### 1.2.1 7 Kg/m$^3$ $Na_2O_e$ Immersed in salt solution.

Degree of reaction = 8 to 9

Usual form of ASR in Dry Rigg siltstone observed, though on a more extensive scale. Two or even three pulses of ASR gel can be distinguished, 'Fresh' clear gel,

pinky / brown gel and possibly recrystallised material. **Massive volumes of ASR gel were present, with extensive injection of ASR gel into the cement paste surrounding paste microcracks.** Some coarse aggregate particles already heavily cracked appear to have been 'eaten out' by the reaction leaving large voids where areas previously rich in microcrystalline quartz should have been. Pyrite cubes (FeS) were seen in the coarse aggregate and appeared to be stable. Carbonation of original surfaces was confined to a depth of less than 1mm, though around some surface microcracks it continued to depths of 3 or 4 mm. In areas of the cement paste adjacent to paste microcracks and the outer surface of the concrete prism the paste appears darkened from the normal light brown / cream to a black / dark brown colour. This material also appears rather blurred and milky in appearance. In these areas of the cement paste, ASR gel could also be seen to have been injected into cement paste as had the fluorescent araldite resin. The area immediately adjacent to the paste microcracks was seen to have a high porosity now filled by this fluorescent resin.

### 1.2.2 3 Kg/m$^3$ $Na_2O_e$ Immersed in salt solution.

Degree of reaction = 10

**Most extensive alkali-silica reaction observed in any of the thin sections examined.** Wide, large open ASR induced microcracks running from areas of the coarse aggregate now 'eaten out' by the reaction. Large pseudo-adhesion cracks found running around the coarse aggregate particles. All the ASR microcracks connect up to form an extensive network. Normal three pronged divergent microcracking centred on the coarse aggregate were also frequently observed. Main volumes of ASR gel found in adhesion cracks on the edge of the coarse aggregate particles. Limited ettringite was observed in some paste microcracks. The cement paste was like all the other samples immersed in salt solution, heavily darken throughout, even in the central area. This may represent ASR gel injected into the paste from microcracks. Layered ASR gel was observed in some voids. ASR gel was most commonly found in paste microcracks. The carbonation was shallow, but greater than that seen in the samples immersed in distilled water. Development of microcracks directly from microcrystalline quartz band in the siltstone aggregate was often observed and may represent a recrystallised form of ASR gel in the aggregate.

### 1.3.1 7 Kg/m$^3$ $Na_2O_e$ Immersed for 1 month in salt solution then left dry for 1 month in air

Degree of reaction = 7 to 8.

**Effects of ASR found extensively and equally throughout this slide. Numerous paste cracks due to dry shrinkage were also observed.** As with all the other concrete prisms placed in a saline environment (see 4.5.1.2 / 4) an area of higher porosity was seen surrounding the paste microcracks which were now filled by fluorescent araldite resin. Surrounding this porous region was an area of extensive blackening / darkening of the cement paste and this was found next to patches of totally unaffected paste. All three forms of cement paste could be found in relatively close proximity. Evidence was seen of ASR gel recrystallised in paste microcracks and the transition of microquartz bands in the aggregate into fully developed microcracks in the cement paste containing clear ASR gel, all within the

space of 2 to 3 mm. Most ASR gel was, however, found in adhesion cracks on the coarse aggregate, voids, in paste cracks and in 'plug-like' deposit in microcracks, located at the coarse aggregate to cement paste interface. A little ASR gel could be identified in fine-edge fringe deposits to internal large microcracks in the coarse aggregate.

### 1.3.2 3 Kg/m$^3$ $Na_2O_e$ Immersed for 1 month in salt solution, then left dry for 1 month in air

Degree of reaction = 8 to 9

**Extensive ASR throughout the whole slide.** The reaction exhibited all the usual features seen with this aggregate type. The cement paste was darkened significantly in patches. The area of cement paste surrounding the ASR microcracks has a high porosity and therefore was filled by the fluorescent araldite resin. This localised porosity may be a result of the depletion of one of the cement paste phases, namely portlandite or Tricalcium aluminate. Some central areas of cement paste were unaffected by the injection of ASR gel. Carbonation may have reached a significant depth down some surface microcracks. This was confirmed by the later use of phenolphthalein. A small amount of a fibrous mineral was located in a number of the paste microcracks. This mineral did not appear to be ettringite and therefore it was postulated that it may represent Friedel salt's (calcium chloro-aluminate).

### 1.4.1 7 Kg/m$^3$ $Na_2O_e$ Prism half immersed in salt solution and half left above solution in moist air

Degree of reaction = 7 to 8 in dry area
8 to 9 in salt solution immersed area

**Alkali-silica reaction was found throughout the whole slide.** Almost all the siltstone coarse aggregate have evidence of reacting. However, the ASR microcracks in the area wetted by salt solution were larger and appear slightly more numerous. The ASR was also occurring to a greater extent, with respect to the volume of ASR gel and the size and frequency of microcracks in the region between the wetted and dry areas of the concrete prism. The paste shows heavy staining in the area surrounding the high porosity paste which itself surrounds the paste microcracks.

### 1.4.2 3 Kg/m$^3$ $Na_2O_e$ Prism half immersed in salt solution and half left above solution in moist air

Degree of reaction = 6 in dry area
7 to 8 in salt solution immersed area

In the wetted half of the prism the same darkening of the paste seen in other prisms immersed in salt solution was observed. Two pulses of ASR gel can be identified in the paste voids. The ASR was extensive throughout the slide, though it may be slightly less extensive in the central part of the dry half of the prism. There was some evidence of carbonated gel in microcracks connected to the outer surface of the dry upper prism. Dark staining was seen throughout though the thickness of the

layer surrounding the microcracks was noticeably less in the upper dry prism area. The main feature in this slide was the occurrence of salt crystals and Friedel's salt in a microcrack passing through a particle of aggregate near the edge of the prism. This microcrack reaches the original surface of the prism just above the wet / dry interface, hence the ability for the growth of the crystals in the void.

## 2 Horrocksford limestone

### 2.1.1 7 Kg/m$^3$ $Na_2O_e$ Immersed in distilled water

Degree of reaction = 6

The alkali-silica reaction takes the slightly unusual form described in section 3.5.2. In this slide the ASR was dominated by pseudo-adhesion cracks and microcracks running along the long axis of the reactive aggregate particles. Bifurcating and divergent microcracks centred on the coarse aggregate were rare, but still present. Injection of ASR gel into the cement paste was shown by a slight darkening of the paste surrounding the microcracks. Microcracks in and surrounding the limestone coarse aggregate were usually large, wide open and empty, whilst those in the cement paste were narrower and partially gel filled.

**The ASR gel volume larger than expected, maybe even greater than with the Dry Rigg siltstone**. Gel formation appears to have occurred in two pulses / generations. The source area of ASR reactivity appears to usually be patches of the limestone rich in chert, but occasionally microcrystalline quartz bands as was also seen within the Dry Rigg siltstone.

### 2.1.2 3 Kg/m$^3$ $Na_2O_e$ Immersed in distilled water

Degree of reaction = 1

**Evidence of alkali-silica reaction was observed but would not be considered significant.** Only one crack system would be considered to be due to primary ASR. ASR gel occurred but was very limited. A number of adhesion and dry shrinkage paste cracks were also observed. Cement paste of typical OPC appearance, with little if any staining / darkening noted.

### 2.2.1 7 Kg/m$^3$ $Na_2O_e$ Immersed in salt solution

Degree of reaction = 8

In some chert-rich patches of the limestone the ASR has been so severe that areas have been totally 'eaten away' by the reaction. The ASR developed was amongst the most severe observed. Some coarse aggregate particles contained up to 50 % chert, which was made up from fossiliferous siliceous spicules. These areas were the usual sites from which the microcracks develop. Extensive staining of the cement paste by injection of ASR gel and high porosity in cement paste surrounding the paste microcracks were also observed. Three different pulses / generations of the ASR gel were observed. No significant ettringite or Thaumasite deposits were seen.

### 2.2.2 3 Kg/m$^3$ $Na_2O_e$ Immersed in salt solution.

Degree of reaction = 7 to 8

**Extensive and typical expansive form of ASR in the Horrocksford limestone.** Ettringite crystals of non-expansive growth in some adhesion cracks surrounding the coarse aggregate. Possible depletion of a fine grained constituent of the cement paste in the area surrounding the paste microcracks. This substance maybe portlandite or Tricalcium aluminate, but the grain size was far too fine to be certain. Volume of ASR gel high and found in the usual locations. Possible Ettringite / ASR gel intergrowth were seen in some coarse aggregate adhesion cracks. The ASR gel in the coarse aggregate was clear and contains no other constituents. Gel found as plug-like deposits in the microcracks at the aggregate cement paste interface was often recrystallised possibly to an alkali silica mineral.

### 2.3.1 7 Kg/m$^3$ $Na_2O_e$ Immersed for 1 month in salt solution, then left dry for 1 month in air.

Degree of reaction = 8

Extensive ASR microcracking observed. Dry shrinkage paste microcracks observed associated with fluorescent resin impregnation of the porosity and paste staining. The dark patching and staining seen in the cement paste was more severe and extensive in this concrete, compared to that observed for the prism permanently immersed in salt solution. Three different paste colours can be seen together. Extensive surface carbonation of the paste to a depth of 2 to 3 mm often found associated with ASR gel, some of which itself appeared to be carbonated. Ettringite was observed in adhesion cracks on the coarse aggregate particles, but was not considered particularly extensive and did appear to have caused any of the observed distress seen in this concrete.

### 2.3.2 3 Kg/m$^3$ $Na_2O_e$ Immersed for 1 month in salt solution, then left dry for 1 month in air

Degree of reaction = 8 to 9

Reaction extensive throughout. Darkening / staining of the cement paste in most areas away from the paste microcracks. Area immediately adjacent to the paste cracks impregnated with fluorescent resin. Overall the cement paste exhibits a patchy coloured appearance. Carbonation was observed in the area next to the original surfaces of the prism and also down some surface paste cracks for a short distance.

### 2.4.1 7 Kg/m$^3$ $Na_2O_e$ Prism half immersed in salt solution and half left above solution in moist air

Degree of reaction = 6 in dry area.
7 in area immersed in salt solution.

Slightly less ASR was observed in the dry area. Chalcedonic quartz found in some

of the cherty limestone material and was potentially highly reactive material.

### 2.4.2 3 Kg/m$^3$ $Na_2O_e$ Prism half immersed in salt solution and half left above solution in moist air

Degree of reaction = 4 in dry area.
6 to 7 in area immersed in salt solution.

The same features of the cement paste, namely darkening / staining etc. occur in the lower salt solution immersed area of the prism, as has already been seen in the prism totally immersed in salt solution. Two pulses of ASR gel can be identified in voids, the central areas of the void gels were also often carbonated. Degree of ASR noticeably reduced in patches in the central area of the prism above the salt solution. The larger scale microcracks originating in the lower salt solution immersed area continue into the upper less obviously reacting dry area. As with all the other prisms placed in this environment, dark staining was seen to enter the concrete a short distance from the outer faces. This appears to be either the injection of ASR gel into the cement paste or some feature related to the impregnation of the concrete with salt solution. Iron pyrite cubes seen in the coarse aggregate were observed to be in a sound and unaltered state.

## 3 Maentwrog greywacke

### 3.1.1 7 Kg/m$^3$ $Na_2O_e$ Immersed in distilled water

Degree of reaction = 6

**The source of ASR was as before (chapter 3) considered to be the intergrain microcrystalline quartz.** ASR gel was more common than in the equivalent stage 1 samples. The finer grained greywacke material appeared less reactive than coarse. The overall extent of ASR appeared the same as in the sample immersed salt solution. No blackening of the cement paste or evidence of cement paste dry shrinkage was observed. Carbonation was limited to narrow band on original surfaces and a little way down some surface microcracks. The cement paste was a typical looking PC overall being well hydrated and in good sound condition. No ettringite observed.

### 3.1.2 4 Kg/m$^3$ $Na_2O_e$ Immersed in distilled water

Degree of reaction = 5

Evidence of extensive ASR typical of that observed for the earlier Maentwrog greywacke concretes. Cement paste shows local staining / darkening in the area immediately adjacent to the fluorescent resin impregnated paste, itself next to the paste microcracks. This feature may represent ASR gel pushed out of the cement paste in the area next to the paste cracks, by the more viscous impregnating resin used in the manufacture of the thin sections. It was possible that prior to impregnation with the araldite resin, these paste cracks were surrounded by a narrow band of cement paste impregnated with ASR gel. The volume of this ASR gel appears to be less than seen in the equivalent samples immersed in salt

solution.

### 3.2.1 7 Kg/m$^3$ $Na_2O_e$ Immersed in salt solution

Degree of reaction = 7

A number of long continuous microcracks centred on the greywacke aggregate, were seen to run over the whole slide. These microcracks form an overall network of interconnecting cracks. The reaction centres were located in coarse greywacke aggregate particles from which divergent microcracks were observed to develop. The origin of these microcracks appears to be the fine crystalline matrix between the larger quartz and feldspar clasts. This fine matrix material was made up of microcrystalline quartz, muscovite, sericite, chlorite and a number of other platey clay minerals. The number of microcracks observed was more numerous than seen in the prisms described in chapter 3 of this work. Pseudo-adhesion cracks were often seen running around the edges of the coarse aggregate particles. ASR gel appears to more common than in the prisms described in chapter 3. Gel was observed in a number of different forms, first as 'normal' clear gel, second as recrystallised gel which looks a lot like microquartz, this was often found in microcracks in the coarse aggregate. Finally ASR gel was seen as a series layers of differing colours (brown and orange), maybe representing different pulses / injections of gel. The cement paste contained a number of voids with large plates / laths of secondary portlandite growing into them.

### 3.2.2 4 Kg/m$^3$ $Na_2O_e$ Immersed in salt solution

Degree of reaction = 7

The alkali-silica reaction was apparent and quite extensive for this aggregate type. Cement paste heavily stained throughout by injection with the extensive amounts of ASR gel. Some of the coarse aggregate particles were also surrounded by this darkened stained cement paste due to the injection with ASR gel. Carbonation was limited to narrow surface areas on the paste microcracks and also the original outer surfaces of the prism. A brown crystalline substance was observed in some microcracks in the coarse aggregate and it was thought this may represent an impure ASR gel mixed with fine aggregate debris. In general, the ASR gel deposits were quite rare in the coarse aggregate. The reaction was found equally over the whole slide.

### 3.3.1 7 Kg/m$^3$ $Na_2O_e$ Immersed for 1 month in salt solution, then left dry for 1 month in air

Degree of reaction = 6

Very similar in many ways to the features observed in the prisms totally immersed in salt solution. The paste was dark throughout, indicating injection with large volumes of ASR gel. There were also numerous dry shrinkage paste cracks observed throughout the slide. A brown crystalline substance was observed in many microcracks in the coarse aggregate and it was thought this may represent an impure ASR gel containing aggregate debris. The reaction was found to an equal extent over the whole slide.

### 3.3.2 4 Kg/m$^3$ $Na_2O_e$ Immersed for 1 month in salt solution, then left dry for 1 month in air

Degree of reaction = 6 to 7

ASR extensive throughout the whole slide. Darkening of the cement paste occurs throughout the concrete. A fine grained greywacke of chert-like appearance was observed and this was seen to be highly reactive and the centre for a major microcrack network.

### 3.4.1 7 Kg/m$^3$ $Na_2O_e$ Prism half immersed in salt solution and half left above solution in moist air

Degree of reaction = 6 in wetted area
5 in dry area

Extensive ASR was seen and was identical to that observed in the other greywacke prisms immersed in salt solution. A fine mudstone (still greywacke type, but of finer grain size) was observed and was not seen to be involved in the reaction. This might imply, that the reactive particles in the matrix of the normal greywackes were of the coarser silt size and above. A number of microcracks were seen to run right through some of the larger strained quartz grains found in the greywacke, however, no evidence of involvement in the ASR was observed. The cement paste was seen to be darkened in patches in the area immersed in salt solution. The microcracks in this area were also surrounded by a area of darkened cement paste. The ASR gel in the coarse aggregate was often a brown crystalline material, whilst in the cement paste the gel was generally clear. Both types were observed in paste voids. No ettringite was observed. The reaction appears to be generally constant throughout the slide.

### 3.4.2 4 Kg/m$^3$ $Na_2O_e$ Prism half immersed in salt solution and half left above solution in moist air

Degree of reaction = 7 in wetted area
4 in dry area

The Maentwrog greywacke aggregates areas of greatest reactivity appear to be in sub-linear patches or vein-like deposits of microquartz and associated non reactive bands of calcite. In these microcrystalline quartz rich areas can be found many of the initial source site for the overall extensive divergent microcrack networks. The volume of ASR gel was greater in the wetted area. **ASR though still present, was less extensive in the central part of the dry area of the prism**. As seen in the section 2.4.2 sample previously, microcrack networks developed in the lower wetted area were frequently seen to traverse the boundary of the wetted area and continue for some length into the dry part of the prism. It was felt that the limited ASR seen in the upper area may be initiated by alkalis migrating up this microcrack network from below. These microcrack networks developed in the lower prism immersed in salt solution, could be a useful mechanism for the rapid migration of the extra alkalis derived from the salt solution into the upper dry region of the prism.

# 4 Trent Valley gravel

## 4.1 7 Kg/m$^3$ $Na_2O_e$ Immersed in distilled water

Degree of reaction = 4

The slide was typical of ASR developed in a chert-rich aggregate such as the Trent Valley gravel. The main cause of the limited ASR were a number of cherts which exhibit typical divergent expansive microcracking centred on them, which continues out into the cement paste on either side producing a complete network which passes from one side of the prism to the other. This concrete contained a number of metaquartzites which were also found to be lesser centres of ASR expansion. The microcracking associated with this aggregate type were generally in the form of a single straight microcrack that diminishes in size as it enters the rocks finer silica-rich matrix. In this area, it was just possible to see a spreading, branch-like divergence of the finer microcracks from the initial large one, these then disappear into the crypto and microcrystalline quartz that make the matrix of this rock. It was this material that was considered to be the reactive constituent causing the limited reaction observed to develop from within this rock type. The microcracks derived from the metaquartzites connect to the overall expansive microcrack network. Overall, the ASR appears extensive, but this may be just a result of there being a larger number of highly reactive cherts within this particular thin section. ASR gel was found mainly in the paste cracks, adhesion cracks and voids, though a little can be found in the coarse aggregate. The cement paste in this concrete was a light creamy brown typical of many OPC's. There was no patchy / blotchy appearance to it. There was only a little microcracking, but injection of the paste surrounding with ASR gel was still visible. Carbonation was very limited and generally confined to the original outer surface. A few surface dry shrinkage paste cracks were also noted.

## 4.2 7 Kg/m$^3$ $Na_2O_e$ Immersed in salt solution

Degree of reaction = 4

**The ASR present in this concrete was typical of that seen with Trent Valley gravels.** Chert being the main reactive constituent along with some metaquartzite. There was little evidence for ASR in the central area, but this just be as a result of there being no reactive particles there to initial the ASR microcracking. Surrounding the microcracks in the cement paste was an area of high porosity and fine calcitic material. Surrounding this porous area was a further area of darkened, stained paste. This staining was only apparent in the finer matrix material of the cement paste. Well away from these paste microcracks can be found areas of cement paste unaffected by this staining. The cement paste was also stained for a depth of up to 20 mm from the original prism surfaces.

## 4.3 7 Kg/m$^3$ $Na_2O_e$ Immersed for 1 month in salt solution, then left dry for 1 month in air

Degree of reaction = 5

**Cement paste was stained severely throughout the slide, only a few central 'islands' of unaffected paste remain.** The amount of paste staining was greater than seen in the prism permanently immersed in salt solution. Carbonation was frequently observed associated with voids and microcracks connected to the original surface of the prism. The cement paste contains numerous dry shrinkage cracks which also exhibit associated paste staining, which suggests the salt solution was gaining entry to the internal concrete via these and the other ASR related microcracks. A number of long, equal width adhesion cracks, now filled by ASR gel were seen and were indicative of plastic shrinkage of the paste at an early age. A large number of microcracks were due largely the dry shrinkage paste cracks.

## 4.4 7 Kg/m$^3$ $Na_2O_e$ Prism half immersed in salt solution and half left above solution in moist air

Degree of reaction = 2 in dry area
3 in area wetted by salt solution

Very few microcracks reached the outer surface of this prism. Evidence of ASR was very limited. An adhesion crack running parallel to the top surface surrounding a quartzite right at the top of the 'dry area' of the concrete was full of ASR gel. The source of this gel was not seen; however, due to splashing and movements of the prism, salt solution would have been present and maybe even concentrated in this region close to the original surface (see chemical analysis section 4.4.6). Main location for microcracks was in the wetted area. Only one definite source of ASR could be identified. Extensive staining of the paste surrounding microcracks in the area of the prism exposed to salt solution and for a short distance inwards from all the original surfaces of the prism.

---

# APPENDIX 7

TABLE 7.4: Electron microprobe analysis of ASR gels

**1.Dry Rigg siltstone 7 kg mix immersed in distilled water**

| Sample No. | $SiO_2$ | $Al_2O_3$ | FeO | MgO | CaO | $Na_2O$ | $K_2O$ | $SO_3$ | Cl | Total |
|---|---|---|---|---|---|---|---|---|---|---|
| PGU* 1 | 0.86 | 0.05 | 0.02 | 0.71 | 63.38 | 0.04 | 0.00 | 0.09 | 0.01 | 65.18 |
| PGC* 2 | 25.41 | 1.17 | 0.10 | 0.29 | 72.81 | 0.02 | 0.01 | 0.03 | 0.01 | 99.87 |
| PGR* 3 | 29.41 | 2.37 | 0.21 | 0.40 | 55.30 | 0.28 | 0.07 | 0.88 | 0.03 | 88.95 |
| PGC* 4 | 25.42 | 1.42 | 0.10 | 0.25 | 72.53 | 0.08 | 0.13 | 0.62 | 0.00 | 100.57 |
| PGC* 5 | 22.27 | 1.90 | 0.17 | 0.29 | 72.41 | 0.09 | 0.09 | 0.47 | 0.01 | 97.70 |
| PGR* 6 | 28.03 | 3.08 | 0.28 | 0.48 | 47.06 | 0.31 | 0.09 | 0.85 | 0.03 | 80.22 |
| PGR*7 | 21.21 | 1.43 | 0.19 | 0.28 | 39.79 | 0.12 | 0.07 | 0.74 | 0.02 | 63.85 |
| PGR* 8 | 32.66 | 1.96 | 0.16 | 0.29 | 30.99 | 0.84 | 0.38 | 0.11 | 0.07 | 67.46 |
| PGR* 9 | 40.29 | 2.41 | 0.29 | 0.45 | 39.87 | 0.71 | 0.37 | 0.15 | 0.01 | 84.55 |
| CP** 10 | 57.45 | 0.14 | 0.03 | 0.00 | 18.35 | 3.30 | 1.66 | 0.03 | 0.03 | 81.00 |
| CP** 11 | 56.36 | 0.13 | 0.01 | 0.01 | 17.50 | 2.46 | 1.56 | 0.03 | 0.02 | 78.09 |
| CP** 12 | 47.78 | 0.14 | 0.04 | 0.03 | 23.55 | 4.09 | 1.71 | 0.00 | 0.01 | 77.36 |
| CP** 13 | 46.47 | 0.14 | 0.03 | 0.03 | 23.72 | 3.29 | 1.71 | 0.03 | 0.00 | 75.43 |
| CP** 14 | 48.47 | 0.12 | 0.04 | 0.04 | 23.98 | 2.19 | 1.67 | 0.05 | 0.10 | 76.54 |
| CP** 15 | 48.40 | 0.20 | 0.05 | 0.05 | 25.28 | 3.72 | 1.67 | 0.03 | 0.00 | 79.40 |
| CP** 16 | 48.79 | 0.19 | 0.05 | 0.04 | 25.27 | 1.30 | 1.44 | 0.03 | 0.01 | 77.12 |
| CP** 17 | 49.88 | 0.19 | 0.04 | 0.05 | 25.30 | 3.85 | 1.81 | 0.03 | 0.00 | 81.17 |
| CI** 18 | 42.51 | 0.15 | 0.08 | 0.01 | 27.45 | 2.69 | 1.67 | 0.04 | 0.02 | 74.62 |
| PGR* 19 | 31.58 | 1.38 | 0.33 | 0.58 | 50.29 | 0.84 | 0.23 | 0.07 | 0.03 | 85.33 |
| PGC* 20 | 24.17 | 0.76 | 0.22 | 0.57 | 70.03 | 0.21 | 0.02 | 0.05 | 0.02 | 96.04 |
| PGR* 21 | 28.85 | 2.37 | 0.91 | 1.04 | 44.55 | 0.73 | 0.15 | 0.52 | 0.07 | 79.20 |
| PC** 22 | 15.73 | 1.24 | 0.24 | 0.22 | 30.94 | 1.03 | 0.13 | 0.23 | 0.04 | 49.79 |
| PGU* 23 | 7.86 | 0.72 | 0.13 | 0.29 | 42.20 | 0.56 | 0.11 | 0.17 | 0.02 | 52.06 |
| PC** 24 | 13.89 | 2.08 | 0.34 | 0.21 | 30.07 | 0.84 | 0.24 | 0.91 | 0.03 | 48.62 |
| PC** 25 | 13.23 | 2.85 | 0.23 | 0.24 | 32.18 | 0.80 | 0.13 | 1.53 | 0.02 | 51.22 |
| PC** 26 | 25.23 | 2.50 | 0.87 | 0.45 | 22.57 | 1.12 | 0.36 | 1.84 | 0.03 | 54.98 |
| PC** 27 | 20.98 | 4.01 | 0.22 | 0.21 | 31.26 | 0.99 | 1.39 | 1.32 | 0.01 | 60.39 |
| PC** 28 | 13.58 | 2.91 | 0.35 | 0.34 | 34.08 | 1.10 | 0.18 | 1.81 | 0.03 | 54.37 |
| PU** 29 | 11.34 | 5.13 | 0.28 | 0.25 | 47.33 | 0.80 | 0.13 | 1.71 | 0.01 | 66.98 |
| PGC* 30 | 22.87 | 1.37 | 0.13 | 0.27 | 73.57 | 0.03 | 0.11 | 0.31 | 0.01 | 98.68 |
| PGR* 31 | 22.13 | 3.74 | 0.33 | 0.40 | 56.46 | 0.42 | 0.04 | 0.64 | 0.03 | 84.20 |
| PGR* 32 | 17.31 | 5.60 | 0.37 | 0.37 | 47.81 | 0.17 | 0.14 | 1.26 | 0.02 | 73.06 |
| PGR* 33 | 27.36 | 1.69 | 0.31 | 0.30 | 47.64 | 0.33 | 0.10 | 1.86 | 0.02 | 79.61 |
| PGR* 34 | 26.65 | 2.02 | 0.17 | 0.42 | 61.53 | 0.21 | 0.50 | 0.98 | 0.01 | 92.03 |
| PGR* 35 | 25.39 | 1.89 | 0.23 | 0.42 | 55.72 | 0.17 | 0.05 | 0.94 | 0.01 | 84.82 |
| PGC* 36 | 22.07 | 1.77 | 0.18 | 0.29 | 73.10 | 0.03 | 0.05 | 0.43 | 0.02 | 97.94 |
| PGC* 37 | 22.31 | 2.11 | 0.12 | 0.27 | 71.94 | 0.02 | 0.06 | 0.28 | 0.01 | 97.11 |
| CI** 38 | 31.59 | 1.99 | 0.06 | 0.10 | 42.77 | 0.13 | 0.19 | 0.66 | 0.04 | 77.53 |
| CI** 39 | 30.77 | 1.74 | 0.12 | 0.05 | 43.52 | 0.14 | 0.05 | 0.81 | 0.04 | 77.25 |
| CI** 40 | 28.48 | 1.74 | 0.04 | 0.08 | 43.82 | 0.14 | 0.06 | 1.03 | 0.03 | 75.44 |
| CI** 41 | 28.70 | 2.42 | 0.06 | 0.15 | 42.43 | 0.28 | 0.12 | 0.78 | 0.04 | 74.97 |
| PU** 42 | 10.22 | 3.71 | 0.22 | 0.20 | 36.19 | 0.15 | 0.18 | 1.92 | 0.11 | 52.92 |
| CU** 43 | 40.62 | 1.05 | 0.09 | 0.04 | 39.22 | 1.06 | 0.52 | 0.05 | 0.01 | 82.66 |

| | | | | | | | | | | |
|---|---|---|---|---|---|---|---|---|---|---|
| CU** 44 | 23.46 | 0.75 | 0.24 | 0.48 | 46.81 | 0.53 | 0.28 | 0.05 | 0.00 | 72.60 |
| PGR* 45 | 33.38 | 1.65 | 0.22 | 0.13 | 48.75 | 0.29 | 0.13 | 0.47 | 0.04 | 85.08 |
| PGR* 46 | 30.32 | 1.74 | 0.35 | 0.33 | 50.98 | 0.22 | 0.12 | 0.71 | 0.03 | 84.82 |
| CP** 47 | 37.31 | 1.21 | 0.12 | 0.12 | 40.91 | 0.85 | 0.46 | 0.11 | 0.01 | 81.12 |
| PGC* 48 | 28.14 | 2.31 | 0.16 | 0.16 | 63.94 | 0.18 | 0.49 | 1.01 | 0.00 | 96.40 |
| PGC* 49 | 27.95 | 2.08 | 0.23 | 0.17 | 63.02 | 0.14 | 0.43 | 1.07 | 0.01 | 95.11 |
| PGR* 50 | 29.62 | 2.27 | 0.35 | 0.19 | 47.29 | 0.16 | 0.03 | 0.93 | 0.03 | 80.88 |
| PGU* 51 | 13.34 | 2.34 | 0.16 | 0.09 | 48.49 | 0.17 | 0.19 | 0.81 | 0.07 | 65.65 |
| PU** 52 | 19.35 | 6.67 | 0.36 | 0.37 | 38.57 | 0.82 | 0.23 | 2.55 | 0.06 | 68.97 |
| CA** 53 | 59.00 | 1.91 | 0.13 | 0.17 | 13.43 | 3.47 | 2.70 | 0.03 | 0.04 | 80.88 |
| CA** 54 | 53.64 | 0.74 | 0.14 | 0.02 | 12.39 | 4.61 | 2.37 | 0.04 | 0.08 | 74.03 |
| CA** 55 | 61.76 | 0.64 | 0.19 | 0.10 | 15.57 | 1.21 | 1.12 | 0.04 | 0.00 | 80.62 |
| CI** 56 | 52.90 | 1.92 | 0.20 | 0.33 | 16.50 | 1.54 | 2.07 | 0.08 | 0.01 | 75.55 |
| CI** 57 | 47.59 | 0.29 | 0.07 | 0.03 | 21.41 | 2.99 | 1.94 | 0.01 | 0.04 | 74.38 |
| CI** 58 | 46.16 | 0.50 | 0.09 | 0.02 | 32.19 | 0.43 | 0.78 | 0.01 | 0.01 | 80.19 |
| CP** 59 | 39.39 | 0.49 | 0.12 | 0.08 | 36.48 | 0.41 | 0.66 | 0.03 | 0.01 | 77.67 |
| CA** 60 | 21.43 | 3.42 | 3.42 | 0.74 | 18.58 | 0.36 | 1.13 | 0.57 | 0.14 | 49.78 |

| Continued: | $SiO_2$ | FeO | MgO | CaO | $Na_2O$ | $K_2O$ | $SO_3$ | Cl | Total | $Al_2O_3$ |
|---|---|---|---|---|---|---|---|---|---|---|
| ..... CA 56 | 23.13 | 2.56 | 1.15 | 18.32 | 0.61 | 1.26 | 0.61 | 0.08 | 52.49 | 4.78 |
| ..... CA 57 | 27.79 | 5.26 | 2.06 | 11.47 | 0.64 | 1.30 | 1.97 | 0.11 | 56.55 | 5.95 |
| ..... CA 60 | 23.46 | 7.99 | 1.26 | 7.32 | 0.68 | 1.40 | 0.73 | 0.08 | 49.76 | 6.85 |
| ..... CA 66 | 25.45 | 4.65 | 0.99 | 14.69 | 0.83 | 1.08 | 1.00 | 0.07 | 53.51 | 4.76 |
| ..... CA 67 | 54.45 | 6.96 | 7.12 | 0.82 | 0.36 | 4.04 | 0.02 | 0.02 | 91.15 | 17.35 |
| ..... CA 71 | 33.83 | 0.51 | 0.68 | 2.86 | 3.21 | 1.07 | 0.15 | 0.06 | 46.01 | 3.64 |
| ..... CA 73 | 37.87 | 4.16 | 3.70 | 3.66 | 1.56 | 0.31 | 0.27 | 0.08 | 55.68 | 4.06 |
| ..... CA 74 | 67.92 | 0.36 | 0.32 | 8.16 | 0.42 | 0.40 | 0.30 | 0.09 | 79.89 | 1.91 |
| ..... CA 75 | 56.18 | 0.43 | 0.38 | 12.41 | 0.26 | 0.18 | 0.11 | 0.04 | 70.65 | 0.66 |
| ..... CA 76 | 20.36 | 2.18 | 0.83 | 0.22 | 0.31 | 4.11 | 0.13 | 0.07 | 37.22 | 8.99 |
| .....CA 79 | 60.30 | 0.20 | 2.88 | 6.56 | 8.95 | 0.07 | 0.27 | 0.06 | 79.89 | 0.58 |
| ..... CA 80 | 27.73 | 0.14 | 0.23 | 8.16 | 0.41 | 0.25 | 0.12 | 0.08 | 38.21 | 1.08 |
| ..... CA 81 | 66.82 | 0.43 | 0.55 | 6.95 | 1.06 | 0.61 | 0.18 | 0.08 | 78.45 | 1.77 |
| ..... CA 82 | 68.00 | 0.59 | 1.04 | 5.75 | 2.43 | 0.43 | 0.48 | 0.07 | 80.66 | 1.86 |
| .....CA 85 | 48.95 | 2.92 | 1.52 | 5.26 | 0.93 | 2.60 | 0.40 | 0.05 | 70.41 | 7.78 |
| ..... CA 86 | 63.82 | 0.21 | 0.17 | 3.09 | 1.32 | 1.02 | 0.09 | 0.07 | 72.92 | 3.13 |
| ..... CA 87 | 21.65 | 1.59 | 2.54 | 13.39 | 1.66 | 0.52 | 0.69 | 0.07 | 46.00 | 3.88 |
| ..... CA 88 | 71.24 | 0.70 | 0.68 | 1.08 | 1.12 | 0.17 | 0.19 | 0.02 | 76.28 | 1.08 |
| ..... CA 89 | 25.35 | 0.60 | 1.36 | 12.50 | 2.80 | 0.41 | 0.44 | 0.12 | 45.75 | 2.17 |
| ..... CA 90 | 18.72 | 2.12 | 2.06 | 14.02 | 0.56 | 2.53 | 0.66 | 0.05 | 50.16 | 9.44 |
| ..... CA 91 | 57.26 | 0.96 | 1.31 | 4.36 | 4.66 | 0.41 | 0.52 | 0.04 | 73.63 | 4.11 |
| ..... CA 92 | 92.44 | 0.22 | 0.26 | 1.27 | 0.57 | 0.10 | 0.14 | 0.05 | 95.82 | 0.75 |
| .....CA 94 | 50.45 | 0.16 | 0.05 | 0.45 | 0.61 | 11.31 | 0.13 | 0.03 | 76.59 | 13.39 |
| ..... CA 95 | 47.44 | 0.46 | 1.96 | 6.04 | 3.35 | 0.96 | 0.47 | 0.08 | 64.83 | 4.07 |
| ..... CA 125 | 29.49 | 1.89 | 1.52 | 6.35 | 0.54 | 3.41 | 0.51 | 0.04 | 54.40 | 10.65 |
| ..... CA 126 | 23.75 | 0.11 | 0.26 | 42.33 | 1.49 | 0.49 | 0.36 | 0.02 | 69.76 | 0.96 |
| ..... CA 127 | 40.89 | 1.16 | 0.10 | 20.76 | 3.45 | 1.23 | 1.97 | 0.05 | 70.62 | 1.00 |
| ..... CA 128 | 43.89 | 0.02 | 0.00 | 12.98 | 3.18 | 1.28 | 0.21 | 0.26 | 61.95 | 0.13 |
| ..... CA 129 | 29.88 | 0.17 | 0.27 | 25.78 | 1.98 | 0.64 | 0.18 | 0.02 | 60.56 | 1.63 |
| ..... CA 132 | 18.21 | 1.59 | 1.21 | 13.53 | 1.16 | 1.14 | 1.16 | 0.04 | 42.38 | 4.33 |
| ..... CA 133 | 42.52 | 1.64 | 1.05 | 5.65 | 1.86 | 1.33 | 0.89 | 0.03 | 60.27 | 5.30 |
| ..... CA 135 | 68.48 | 1.71 | 2.49 | 2.78 | 5.86 | 1.92 | 0.13 | 0.03 | 96.98 | 13.57 |

..... CA 144 12.03 0.25 0.21 43.39 0.37 0.10 2.78 0.17 65.02 5.72
..... CA 145 47.29 7.27 0.93 3.89 1.47 0.37 15.13 0.09 78.46 2.03
..... CA 146 73.51 0.20 0.27 1.02 0.91 0.19 0.08 0.05 77.09 0.85
..... CA 147 47.13 0.65 1.26 3.13 2.16 0.63 0.12 0.05 57.02 1.90
..... CA 148 39.88 0.48 0.59 7.92 2.05 2.30 0.26 0.04 58.60 5.07
..... CA 149 41.35 0.60 2.15 7.27 4.72 0.25 0.17 0.05 58.13 1.58
..... CA 150 58.40 0.42 0.55 2.86 1.53 0.47 0.08 0.05 66.93 2.56
.....CA 153 42.44 0.75 2.08 8.84 5.66 0.55 0.34 0.06 62.49 1.77
..... CA 154 38.46 0.35 1.60 5.01 5.19 0.22 0.23 0.07 53.60 2.48
..... CA 155 57.51 0.77 1.65 5.46 3.59 0.31 0.21 0.05 71.31 1.75
..... CA 156 53.15 0.82 0.62 6.95 2.11 0.38 0.24 0.05 67.98 3.65
..... CA 157 31.08 0.51 1.17 21.10 3.26 0.40 0.19 0.05 60.13 2.37
..... CA 158 44.13 0.82 1.57 7.64 4.32 0.93 0.32 0.03 63.94 4.19
..... CA 170 56.82 0.49 1.27 4.96 4.58 0.98 0.31 0.03 71.73 2.28
..... CA 200 52.25 1.98 1.90 2.04 1.54 6.54 0.13 0.03 93.42 27.00
..... CA 201 51.20 1.98 1.08 0.77 1.91 7.55 0.01 0.01 95.14 30.64
..... CA 202 63.38 1.34 1.04 0.54 4.38 4.21 0.04 0.02 100.64 25.67
..... CA 208 68.09 1.68 2.03 0.08 8.38 2.00 0.01 0.01 102.03 19.73
..... CA 209 64.25 3.94 4.23 0.16 0.21 5.23 0.05 0.01 96.59 18.49
..... CA 210 68.91 1.60 2.14 0.84 0.30 4.88 0.07 0.02 94.15 15.38
..... CA 211 43.28 16.44 5.21 1.19 0.20 4.92 24.27 0.01 114.67 19.16
..... CA 212 72.64 0.61 0.51 0.88 6.39 2.95 0.05 0.03 102.46 18.39
..... CA 213 71.64 1.36 0.96 1.19 0.66 6.81 0.19 0.01 94.49 11.66
..... CA 214 25.72 13.12 2.56 21.53 0.36 1.53 20.21 0.02 92.62 7.57
..... CA 215 49.28 2.98 2.05 14.65 2.49 2.88 1.75 0.01 90.56 14.46
..... CA 216 56.36 4.43 3.91 0.96 5.39 4.24 0.19 0.01 97.57 22.07
..... CA 217 81.14 0.47 0.54 4.50 0.12 1.59 0.07 0.01 93.22 4.75
..... CA 218 40.31 1.46 2.04 2.40 4.10 2.69 0.07 0.04 66.38 13.25
..... CA 219 5.76 0.83 0.55 53.36 0.08 0.58 0.03 0.01 62.53 1.33
..... CA 220 56.39 0.40 0.26 4.20 0.84 10.06 0.05 0.01 87.46 15.24
..... CA 221 31.79 8.16 7.47 1.02 0.96 1.75 0.46 0.05 66.55 14.89
..... CA 222 25.76 1.56 1.54 8.85 0.85 1.97 0.25 0.06 49.21 8.36
..... CA 223 87.22 1.49 0.95 0.23 0.21 1.83 0.75 0.02 98.59 5.89
..... CA 224 36.53 1.40 0.80 1.45 0.85 1.86 1.98 0.06 51.02 6.06
..... CA 225 14.13 1.10 0.83 3.41 2.64 0.53 1.90 0.06 26.22 1.60
..... CA 226 58.73 8.47 4.26 1.38 0.47 3.89 0.09 0.02 94.41 17.10
..... CA 227 64.27 2.46 2.48 0.31 1.34 6.91 0.07 0.01 98.46 20.62
..... CA 228 53.19 3.59 3.86 0.04 0.22 6.98 0.03 0.01 94.77 26.84
..... CA 229 32.57 12.52 11.54 3.90 1.43 1.30 0.24 0.02 81.32 17.79
..... CA 230 35.72 11.72 10.16 0.60 0.25 2.92 0.08 0.02 81.44 19.93
..... CA 231 65.97 0.23 0.00 0.07 0.24 16.37 0.02 0.02 101.41 18.48
..... CA 232 55.34 3.27 3.97 0.72 1.22 6.01 0.06 0.01 95.77 25.16
..... CA 233 99.80 0.18 0.04 0.03 0.00 0.11 0.00 0.00 100.46 0.31
..... CA 234 73.82 8.41 3.90 0.15 0.27 1.65 0.05 0.01 97.83 9.56
.....CA 236 68.05 3.25 2.16 0.06 0.18 4.73 0.03 0.01 95.41 16.92
..... CA 237 57.31 5.81 4.50 0.60 0.21 5.69 0.39 0.01 96.26 21.74
..... CA 238 62.9 12.13 2.85 0.17 0.94 2.09 21.97 0.03 112.38 9.28
..... CA 239 25.39 26.45 13.12 0.07 0.03 0.02 0.03 0.00 87.76 22.64
..... CA 240 51.88 3.49 4.22 0.04 0.15 7.00 0.03 0.02 94. 93 28.10
..... CA 250 47.67 0.84 0.64 9.63 0.14 0.77 0.42 0.04 62.71 2.56
..... CA 251 52.32 0.02 0.02 17.49 0.73 0.29 0.39 0.03 71.45 0.16
..... CA 255 33.70 0.02 0.16 38.03 0.49 0.17 1.33 0.05 74.09 0.15

| | | | | | | | | | | | |
|---|---|---|---|---|---|---|---|---|---|---|---|
| ..... | CL | 22 | 0.02 | 0.02 | 0.19 | 58.99 | 0.01 | 0.01 | 0.00 | 0.01 | 59.25 0.00 |
| ..... | CL | 30 | 1.69 | 0.06 | 0.48 | 58.50 | 0.03 | 0.01 | 0.03 | 0.02 | 60.82 0.00 |
| ..... | CL | 31 | 34.36 | 0.01 | 0.02 | 42.33 | 0.41 | 0.08 | 0.49 | 0.42 | 79.87 1.73 |
| ..... | CL | 34 | 1.09 | 0.02 | 0.38 | 58.53 | 0.49 | 0.06 | 0.07 | 0.01 | 60.66 0.00 |
| ..... | CL | 45 | 50.81 | 0.04 | 0.00 | 28.18 | 0.75 | 0.85 | 0.01 | 0.00 | 80.75 0.10 |
| ..... | CL | 46 | 49.70 | 0.00 | 0.00 | 28.25 | 0.72 | 0.77 | 0.01 | 0.05 | 79.66 0.14 |
| ..... | CL | 65 | 21.69 | 0.23 | 0.06 | 4.92 | 1.20 | 0.52 | 0.10 | 0.07 | 29.01 0.23 |
| ..... | CL | 130 | 24.96 | 0.02 | 0.16 | 40.79 | 2.08 | 0.48 | 0.22 | 0.02 | 68.90 0.15 |
| ..... | CL | 131 | 33.34 | 0.01 | 0.02 | 27.47 | 2.91 | 0.79 | 0.92 | 0.04 | 65.85 0.34 |
| ..... | CL | 166 | 30.77 | 0.02 | 0.16 | 38.18 | 2.24 | 0.63 | 0.17 | 0.02 | 72.33 0.13 |
| ..... | CL | 168 | 18.06 | 0.02 | 0.05 | 48.83 | 1.33 | 0.35 | 0.06 | 0.04 | 68.86 0.11 |
| ..... | CP | 8 | 31.20 | 0.17 | 0.21 | 40.55 | 0.36 | 0.13 | 0.49 | 0.13 | 75.11 1.86 |
| ..... | CP | 15 | 55.14 | 4.26 | 2.73 | 1.32 | 0.42 | 6.44 | 0.03 | 0.01 | 90.51 20.16 |
| ..... | CPA | 27 | 36.51 | 3.46 | 1.77 | 2.15 | 0.39 | 6.39 | 0.18 | 0.05 | 69.23 18.32 |
| ..... | CPA | 28 | 49.38 | 1.60 | 0.38 | 6.32 | 0.15 | 0.30 | 0.62 | 0.05 | 60.51 1.72 |
| ..... | CPA | 29 | 20.76 | 3.47 | 1.04 | 17.16 | 0.57 | 0.98 | 0.95 | 0.05 | 49.17 4.18 |
| ..... | CPA | 32 | 33.18 | 0.07 | 0.03 | 41.25 | 0.36 | 0.12 | 0.50 | 0.38 | 77.61 1.72 |
| ..... | CPA | 33 | 33.29 | 0.03 | 0.04 | 40.36 | 0.37 | 0.13 | 0.47 | 0.70 | 77.28 1.89 |
| ..... | CPA | 35 | 46.13 | 0.21 | 0.13 | 37.61 | 0.95 | 0.37 | 0.02 | 0.16 | 86.58 1.00 |
| ..... | CPA | 40 | 11.76 | 0.43 | 0.96 | 36.08 | 0.69 | 0.30 | 1.63 | 0.06 | 54.92 3.01 |
| ..... | CPA | 41 | 33.53 | 0.02 | 0.03 | 42.85 | 0.35 | 0.05 | 0.59 | 0.50 | 79.72 1.79 |
| ..... | CPA | 42 | 14.91 | 0.10 | 0.40 | 31.14 | 0.69 | 0.20 | 1.04 | 0.11 | 50.08 1.49 |
| ..... | CP | 49 | 35.91 | 0.02 | 0.14 | 41.09 | 0.30 | 0.06 | 0.54 | 0.21 | 80.72 2.45 |
| ..... | CP | 51 | 0.03 | 0.04 | 0.27 | 59.84 | 0.03 | 0.01 | 0.03 | 0.02 | 60.28 0.01 |
| ..... | CP | 61 | 37.09 | 0.06 | 0.03 | 44.56 | 0.07 | 0.04 | 0.66 | 0.63 | 84.81 1.66 |
| ..... | CP | 62 | 34.38 | 0.02 | 0.08 | 43.44 | 0.60 | 0.13 | 0.40 | 0.12 | 81.31 2.14 |
| ..... | CP | 63 | 35.75 | 0.02 | 0.11 | 43.91 | 0.09 | 0.02 | 0.76 | 0.14 | 82.69 1.88 |
| ..... | CP | 64 | 33.72 | 0.06 | 0.18 | 43.75 | 0.28 | 0.10 | 0.86 | 0.08 | 81.17 2.13 |
| ..... | CP | 96 | 46.91 | 0.15 | 0.13 | 25.92 | 1.17 | 0.52 | 0.43 | 0.01 | 76.40 1.15 |
| ..... | CP | 97 | 34.54 | 0.10 | 0.01 | 28.70 | 1.67 | 0.70 | 0.21 | 0.01 | 68.47 2.53 |
| ..... | CP | 98 | 1.67 | 0.02 | 0.01 | 3.03 | 0.13 | 0.05 | 0.03 | 0.09 | 5.18 0.14 |
| ..... | CP | 99 | 24.67 | 0.07 | 0.01 | 24.36 | 1.16 | 0.62 | 0.23 | 0.04 | 53.03 1.87 |
| ..... | CP | 100 | 19.22 | 0.10 | 0.01 | 24.19 | 1.45 | 0.61 | 0.19 | 0.05 | 47.12 1.31 |
| ..... | CP | 101 | 0.84 | 0.06 | 0.03 | 2.89 | 0.17 | 0.07 | 0.06 | 0.09 | 4.43 0.22 |
| ..... | CP | 119 | 22.75 | 0.01 | 0.02 | 36.85 | 1.45 | 0.70 | 0.16 | 0.02 | 63.45 1.50 |
| ..... | CP | 120 | 6.35 | 0.00 | 0.01 | 15.43 | 0.51 | 0.13 | 0.05 | 0.07 | 22.93 0.38 |
| ..... | CP | 121 | 16.36 | 0.06 | 0.03 | 22.89 | 1.25 | 0.61 | 0.10 | 0.04 | 42.75 1.41 |
| ..... | CP | 122 | 23.77 | 0.03 | 0.02 | 28.59 | 0.44 | 0.16 | 0.23 | 0.03 | 54.83 1.55 |
| ..... | CP | 123 | 13.61 | 0.32 | 0.23 | 45.00 | 0.95 | 0.13 | 2.05 | 0.08 | 64.36 1.99 |
| ..... | CP | 124 | 18.57 | 0.15 | 0.32 | 40.39 | 0.83 | 0.21 | 0.72 | 0.05 | 63.06 1.82 |
| ..... | CP | 138 | 7.84 | 0.23 | 0.13 | 18.24 | 0.63 | 0.11 | 2.74 | 0.52 | 32.67 2.23 |
| ..... | CP | 139 | 28.15 | 0.33 | 0.31 | 35.76 | 0.46 | 0.19 | 0.31 | 0.06 | 67.87 2.31 |
| ..... | CP | 159 | 55.50 | 0.10 | 0.09 | 22.95 | 3.65 | 1.48 | 0.19 | 0.01 | 84.18 0.20 |
| ..... | CP | 160 | 33.76 | 0.05 | 0.06 | 27.69 | 5.21 | 0.77 | 0.36 | 0.01 | 69.00 1.09 |
| ..... | CP | 161 | 34.29 | 0.02 | 0.01 | 38.99 | 0.75 | 0.16 | 0.26 | 0.00 | 75.44 0.94 |
| ..... | CP | 162 | 33.42 | 0.02 | 0.02 | 38.90 | 1.42 | 0.18 | 0.76 | 0.04 | 76.15 1.38 |
| ..... | CP | 164 | 32.29 | 0.07 | 0.12 | 39.55 | 0.35 | 0.10 | 0.57 | 0.02 | 74.73 1.67 |
| ..... | CP | 165 | 38.15 | 0.15 | 0.19 | 35.02 | 1.53 | 0.53 | 0.53 | 0.02 | 77.16 1.04 |
| ..... | CP | 167 | 31.69 | 0.15 | 0.18 | 38.61 | 0.75 | 0.23 | 0.73 | 0.03 | 74.28 1.90 |
| ..... | CP | 169 | 31.86 | 0.03 | 0.00 | 37.85 | 0.40 | 0.13 | 0.59 | 0.05 | 72.12 1.20 |
| ..... | CP | 171 | 26.28 | 0.20 | 0.13 | 32.44 | 2.30 | 0.75 | 0.72 | 0.02 | 64.80 1.96 |
| ..... | CP | 172 | 29.62 | 0.81 | 0.86 | 38.03 | 0.53 | 0.28 | 0.72 | 0.03 | 73.86 2.97 |

| | | | | | | | | | | | |
|---|---|---|---|---|---|---|---|---|---|---|---|
| ..... CP | 173 | 34.98 | 0.01 | 0.02 | 38.16 | 0.16 | 0.07 | 0.55 | 0.00 | 75.24 | 1.26 |
| ..... CP | 174 | 33.07 | 0.05 | 0.03 | 38.43 | 0.23 | 0.09 | 0.69 | 0.02 | 74.30 | 1.69 |
| ..... CP* | 176 | 38.01 | 0.04 | 0.07 | 36.90 | 0.92 | 0.15 | 0.86 | 0.03 | 78.73 | 1.70 |
| ..... CP* | 177 | 32.26 | 0.04 | 0.05 | 31.48 | 0.56 | 0.18 | 0.73 | 0.02 | 66.61 | 1.29 |
| ..... CP* | 178 | 32.96 | 0.00 | 0.03 | 37.22 | 0.78 | 0.29 | 2.17 | 0.02 | 75.04 | 1.57 |
| ..... CP* | 179 | 31.72 | 0.01 | 0.02 | 38.47 | 1.04 | 0.15 | 0.59 | 0.03 | 73.54 | 1.51 |
| ..... CP | 257 | 28.96 | 0.40 | 0.95 | 43.76 | 0.42 | 0.09 | 1.15 | 0.10 | 77.60 | 1.79 |

## 2.Horrocksford limestone 7 kg mix immersed in distilled water

| Sample No. | $SiO_2$ | $Al_2O_3$ | FeO | MgO | CaO | $Na_2O$ | $K_2O$ | $SO_3$ | Cl | Total |
|---|---|---|---|---|---|---|---|---|---|---|
| .....CP** 1 | 35.00 | 1.27 | 0.01 | 0.00 | 40.21 | 0.53 | 0.21 | 0.32 | 0.05 | 76.61 |
| ..... CP** 2 | 35.91 | 0.98 | 0.02 | 0.01 | 39.47 | 0.41 | 0.36 | 0.31 | 0.05 | 77.54 |
| ..... CP** 3 | 16.82 | 0.42 | 0.01 | 0.17 | 45.40 | 0.30 | 0.12 | 0.30 | 0.09 | 63.64 |
| ..... CP** 4 | 38.52 | 1.33 | 0.04 | 0.00 | 39.76 | 0.67 | 0.62 | 0.17 | 0.05 | 81.15 |
| ..... CP** 5 | 18.40 | 1.47 | 0.03 | 0.06 | 25.76 | 0.34 | 0.14 | 0.29 | 0.09 | 46.57 |
| ..... PU** 6 | 15.60 | 1.68 | 0.08 | 0.14 | 53.98 | 0.23 | 0.06 | 0.91 | 0.06 | 72.76 |
| ..... CA** 7 | 41.15 | 0.50 | 0.00 | 0.00 | 36.57 | 1.03 | 0.74 | 0.09 | 0.05 | 80.15 |
| ..... A*** 8 | 0.96 | 0.00 | 0.02 | 0.27 | 63.69 | 0.11 | 0.07 | 0.08 | 0.01 | 65.21 |
| ..... CU** 9 | 18.79 | 1.60 | 0.22 | 0.20 | 37.03 | 0.30 | 0.12 | 0.77 | 0.06 | 59.09 |
| ..... PU** 10 | 12.92 | 1.39 | 0.11 | 0.24 | 42.54 | 0.32 | 0.05 | 0.50 | 0.06 | 58.14 |
| ..... PU** 11 | 29.90 | 0.41 | 0.02 | 0.00 | 33.38 | 0.58 | 0.46 | 0.20 | 0.08 | 65.05 |
| ..... PU** 12 | 23.74 | 2.09 | 0.09 | 0.17 | 41.99 | 0.48 | 0.12 | 1.35 | 0.05 | 70.07 |
| ..... PGU* 13 | 13.40 | 3.00 | 0.35 | 0.16 | 50.41 | 0.17 | 0.62 | 1.20 | 0.02 | 69.33 |
| ..... PU** 14 | 27.68 | 2.53 | 0.24 | 0.22 | 49.82 | 0.06 | 0.06 | 2.48 | 0.16 | 83.25 |
| ..... PU** 15 | 21.34 | 1.75 | 0.19 | 0.14 | 50.33 | 0.25 | 0.05 | 2.57 | 0.09 | 76.71 |
| ..... PU** 16 | 11.20 | 6.57 | 0.17 | 0.14 | 55.38 | 0.04 | 0.03 | 3.09 | 0.12 | 76.75 |
| ..... CI** 17 | 35.85 | 1.56 | 0.01 | 0.00 | 40.48 | 0.39 | 0.19 | 0.40 | 0.09 | 78.97 |
| ..... CI** 18 | 34.74 | 1.83 | 0.01 | 0.00 | 41.44 | 0.49 | 0.17 | 0.46 | 0.10 | 79.25 |
| ..... CU** 19 | 37.76 | 1.17 | 0.02 | 0.01 | 39.65 | 0.25 | 0.19 | 0.19 | 0.06 | 79.32 |
| ..... CU** 20 | 31.89 | 1.68 | 0.04 | 0.00 | 38.82 | 0.22 | 0.09 | 0.50 | 0.18 | 73.42 |
| ..... CP** 21 | 4.40 | 0.61 | 0.06 | 0.13 | 77.54 | 0.15 | 0.07 | 0.88 | 0.02 | 83.86 |
| ..... PU** 22 | 11.20 | 0.96 | 0.14 | 0.24 | 59.14 | 0.20 | 0.05 | 0.67 | 0.04 | 72.64 |
| ..... CA** 23 | 19.33 | 8.50 | 0.73 | 0.72 | 47.71 | 0.28 | 0.13 | 4.38 | 0.13 | 81.91 |
| ..... A*** 24 | 70.22 | 10.45 | 0.48 | 0.96 | 3.47 | 0.31 | 2.97 | 0.32 | 0.04 | 89.22 |
| ..... A*** 25 | 15.34 | 2.95 | 1.95 | 12.89 | 29.42 | 0.34 | 0.63 | 0.10 | 0.02 | 63.63 |
| ..... A*** 26 | 73.69 | 10.32 | 0.49 | 1.05 | 2.09 | 0.40 | 3.08 | 0.19 | 0.05 | 91.35 |
| ..... PGC* 27 | 29.98 | 2.27 | 0.11 | 0.12 | 64.36 | 0.15 | 0.31 | 1.24 | 0.01 | 98.83 |
| ..... PGR* 28 | 24.66 | 3.39 | 0.48 | 0.34 | 46.26 | 0.20 | 0.11 | 1.18 | 0.08 | 76.71 |
| ..... CP** 29 | 32.49 | 1.41 | 0.03 | 0.00 | 40.55 | 0.52 | 0.30 | 0.40 | 0.03 | 75.75 |
| ..... CP** 30 | 34.91 | 1.10 | 0.00 | 0.01 | 42.15 | 0.53 | 0.29 | 0.38 | 0.05 | 79.41 |
| ..... CP** 31 | 34.57 | 1.04 | 0.03 | 0.01 | 42.80 | 0.55 | 0.24 | 0.44 | 0.04 | 79.71 |
| ..... CP** 32 | 33.11 | 2.18 | 0.03 | 0.01 | 42.71 | 0.51 | 0.21 | 0.29 | 0.06 | 79.12 |
| ..... CP** 33 | 34.86 | 2.36 | 0.02 | 0.02 | 44.02 | 0.50 | 0.18 | 0.35 | 0.02 | 82.34 |
| ..... CA** 34 | 26.07 | 14.37 | 5.94 | 1.17 | 3.18 | 0.40 | 3.86 | 13.87 | 0.02 | 68.88 |
| ..... CA** 35 | 0.00 | 0.00 | 0.04 | 0.34 | 55.98 | 0.01 | 0.02 | 0.02 | 0.01 | 56.42 |
| ..... CA** 36 | 34.02 | 16.80 | 4.67 | 1.26 | 1.10 | 1.14 | 4.74 | 10.87 | 0.04 | 74.65 |
| ..... CA** 37 | 1.74 | 1.16 | 2.52 | 17.79 | 31.11 | 0.10 | 0.33 | 0.33 | 0.02 | 55.09 |
| ..... A*** 38 | 0.00 | 0.00 | 0.07 | 0.30 | 55.28 | 0.01 | 0.00 | 0.00 | 0.00 | 55.67 |

| | | | | | | | | | | |
|---|---|---|---|---|---|---|---|---|---|---|
| ..... A*** 39 | 96.75 | 0.08 | 0.01 | 0.00 | 0.13 | 0.08 | 0.02 | 0.01 | 0.04 | 97.14 |
| ..... A*** 40 | 27.25 | 0.01 | 0.01 | 0.41 | 39.22 | 0.02 | 0.01 | 0.04 | 0.00 | 66.99 |
| ..... A*** 41 | 1.98 | 0.03 | 0.05 | 0.66 | 72.36 | 0.04 | 0.00 | 0.02 | 0.02 | 75.18 |
| ..... A*** 42 | 0.54 | 0.00 | 0.00 | 0.40 | 58.43 | 0.01 | 0.02 | 0.02 | 0.04 | 59.48 |
| ..... CU** 43 | 25.01 | 0.10 | 0.01 | 0.01 | 19.79 | 0.92 | 0.66 | 0.02 | 0.04 | 46.57 |
| ..... CU** 44 | 39.99 | 1.20 | 0.03 | 0.08 | 36.88 | 0.78 | 0.80 | 0.08 | 0.03 | 79.88 |
| ..... CI** 45 | 38.62 | 1.17 | 0.11 | 0.08 | 36.63 | 0.55 | 0.79 | 0.12 | 0.05 | 78.12 |
| ..... PGR* 46 | 26.02 | 2.48 | 0.17 | 0.35 | 45.85 | 0.10 | 0.08 | 2.05 | 0.09 | 77.19 |
| ..... PGC* 47 | 29.03 | 5.08 | 0.63 | 0.26 | 62.44 | 0.18 | 0.51 | 0.66 | 0.01 | 98.78 |
| ..... PGC* 48 | 29.84 | 2.54 | 0.12 | 0.11 | 63.58 | 0.21 | 0.52 | 1.23 | 0.00 | 98.17 |
| ..... PU** 49 | 25.58 | 1.60 | 0.10 | 0.05 | 37.42 | 0.43 | 0.16 | 0.64 | 0.16 | 66.14 |
| ..... PC** 50 | 15.91 | 1.20 | 0.15 | 0.12 | 35.13 | 0.18 | 0.06 | 3.05 | 0.08 | 55.88 |
| ..... PC** 51 | 15.03 | 2.72 | 0.15 | 0.11 | 34.66 | 0.16 | 0.06 | 2.31 | 0.07 | 55.27 |
| ..... PC** 52 | 11.30 | 2.39 | 0.11 | 0.26 | 46.20 | 0.23 | 0.06 | 2.03 | 0.04 | 62.62 |
| ..... PC** 53 | 14.08 | 2.34 | 0.15 | 0.11 | 41.85 | 0.19 | 0.06 | 3.14 | 0.05 | 61.98 |
| ..... PU** 54 | 15.91 | 3.65 | 0.14 | 0.20 | 50.43 | 0.30 | 0.07 | 1.97 | 0.04 | 72.69 |

## 3. Anglesey granite 7 kg mix immersed in distilled water

| Sample No. | $SiO_2$ | $Al_2O_3$ | FeO | MgO | CaO | $Na_2O$ | $K_2O$ | $SO_3$ | Cl | Total |
|---|---|---|---|---|---|---|---|---|---|---|
| ..... PGC* 1 | 25.02 | 0.74 | 0.30 | 0.58 | 74.41 | 0.07 | 0.01 | 0.02 | 0.00 | 101.15 |
| ..... A*** 5 | 60.97 | 20.37 | 0.22 | 0.10 | 7.34 | 9.38 | 1.35 | 0.01 | 0.00 | 99.74 |
| ..... A*** 6 | 68.99 | 21.85 | 0.21 | 0.06 | 0.48 | 10.04 | 1.14 | 0.03 | 0.00 | 102.79 |
| ..... A*** 7 | 65.50 | 21.02 | 1.78 | 1.40 | 0.31 | 10.04 | 0.92 | 0.03 | 0.02 | 101.03 |
| ..... A*** 8 | 67.99 | 21.66 | 0.15 | 0.00 | 2.10 | 10.20 | 0.16 | 0.05 | 0.01 | 102.33 |
| ..... A*** 9 | 32.02 | 4.75 | 1.26 | 1.01 | 2.21 | 1.07 | 0.92 | 0.01 | 0.05 | 43.31 |
| ..... A*** 10 | 87.36 | 3.22 | 2.23 | 1.92 | 0.22 | 0.03 | 0.51 | 0.01 | 0.02 | 95.52 |
| ..... A*** 11 | 15.85 | 9.32 | 3.72 | 2.93 | 29.47 | 0.17 | 2.37 | 0.11 | 0.02 | 63.97 |
| ..... A*** 12 | 35.46 | 22.10 | 7.39 | 6.10 | 5.11 | 0.12 | 4.74 | 0.03 | 0.01 | 81.05 |
| ..... A*** 13 | 27.95 | 18.22 | 20.05 | 16.94 | 0.35 | 0.20 | 0.19 | 0.07 | 0.37 | 84.01 |
| ..... A*** 14 | 68.31 | 21.33 | 0.20 | 0.05 | 0.35 | 10.63 | 1.16 | 0.01 | 0.02 | 102.06 |
| ..... CA** 15 | 67.51 | 21.94 | 0.10 | 0.01 | 2.23 | 10.24 | 0.27 | 0.03 | 0.01 | 102.34 |
| ..... CA** 16 | 66.05 | 16.75 | 4.52 | 3.07 | 0.51 | 5.66 | 1.59 | 0.01 | 0.03 | 98.18 |
| ..... A*** 17 | 68.10 | 13.83 | 0.05 | 0.01 | 0.90 | 8.11 | 0.08 | 0.03 | 0.00 | 91.12 |
| ..... CI** 18 | 8.90 | 1.04 | 0.13 | 0.09 | 13.71 | 0.58 | 0.20 | 0.60 | 0.06 | 25.30 |
| ..... CP** 19 | 0.54 | 0.05 | 0.02 | 0.01 | 1.00 | 0.09 | 0.02 | 0.05 | 0.10 | 1.88 |
| ..... CP** 20 | 20.86 | 2.44 | 0.39 | 0.28 | 42.79 | 0.45 | 0.44 | 0.19 | 0.13 | 67.98 |
| ..... PU** 21 | 11.17 | 0.71 | 0.00 | 0.03 | 21.60 | 0.27 | 0.11 | 0.13 | 0.19 | 34.21 |
| ..... PU** 22 | 13.79 | 2.41 | 0.25 | 0.12 | 43.14 | 0.44 | 0.20 | 2.00 | 0.93 | 62.45 |
| ..... PU** 23 | 24.96 | 1.70 | 0.25 | 0.19 | 42.97 | 0.29 | 0.13 | 0.60 | 0.16 | 71.26 |
| ..... PGU* 24 | 12.10 | 5.04 | 0.15 | 0.10 | 51.48 | 0.20 | 0.13 | 2.53 | 0.29 | 72.03 |
| ..... CA** 25 | 1.40 | 0.25 | 0.81 | 0.65 | 58.43 | 0.07 | 0.02 | 0.01 | 0.01 | 61.65 |
| ..... CA** 26 | 64.62 | 0.10 | 0.36 | 0.28 | 18.68 | 0.14 | 0.02 | 0.02 | 0.01 | 84.22 |
| ..... CA** 27 | 68.02 | 19.60 | 0.76 | 0.28 | 0.07 | 11.19 | 0.05 | 0.00 | 0.00 | 99.98 |
| ..... CA** 28 | 47.45 | 17.74 | 8.52 | 5.86 | 0.16 | 6.69 | 0.20 | 0.10 | 0.02 | 86.74 |
| ..... A*** 29 | 11.29 | 2.30 | 0.46 | 0.24 | 1.33 | 1.75 | 0.77 | 0.03 | 0.10 | 18.28 |
| ..... A*** 30 | 44.57 | 24.51 | 9.21 | 7.49 | 0.04 | 1.55 | 4.99 | 0.02 | 0.00 | 92.40 |
| ..... CA** 31 | 67.33 | 21.61 | 0.29 | 0.01 | 2.24 | 10.25 | 0.21 | 0.02 | 0.01 | 101.93 |
| ..... CA** 32 | 68.09 | 21.41 | 0.15 | 0.00 | 2.17 | 10.47 | 0.09 | 0.01 | 0.01 | 102.41 |

| | | | | | | | | | | | |
|---|---|---|---|---|---|---|---|---|---|---|---|
| ..... CA** | 33 | 67.32 | 21.65 | 0.10 | 0.00 | 2.69 | 10.23 | 0.09 | 0.03 | 0.01 | 102.13 |
| ..... A*** | 34 | 46.30 | 26.91 | 3.96 | 1.58 | 0.34 | 0.39 | 9.24 | 0.03 | 0.00 | 88.76 |
| ..... A*** | 35 | 73.98 | 18.39 | 0.06 | 0.00 | 0.28 | 10.82 | 0.05 | 0.01 | 0.02 | 103.62 |
| ..... CP** | 36 | 71.31 | 19.69 | 0.01 | 0.00 | 0.36 | 11.81 | 0.06 | 0.03 | 0.00 | 103.28 |
| ..... PC** | 37 | 33.03 | 2.00 | 0.03 | 0.05 | 37.50 | 1.88 | 0.43 | 0.04 | 0.03 | 74.99 |
| ..... PGC* | 38 | 26.12 | 1.90 | 0.11 | 0.11 | 35.11 | 7.65 | 1.19 | 0.07 | 0.04 | 72.31 |
| ..... PGR* | 39 | 31.59 | 2.97 | 0.18 | 0.22 | 40.12 | 1.95 | 0.42 | 0.25 | 0.03 | 77.74 |
| ..... PC** | 40 | 28.86 | 3.08 | 0.24 | 0.35 | 30.02 | 6.50 | 0.93 | 0.11 | 0.04 | 70.13 |
| ..... PC** | 41 | 29.71 | 2.07 | 0.06 | 0.05 | 42.27 | 0.77 | 0.15 | 0.03 | 0.05 | 75.15 |
| ..... PC** | 42 | 25.13 | 1.82 | 0.24 | 0.62 | 36.59 | 1.13 | 0.22 | 0.13 | 0.04 | 65.92 |
| ..... PC** | 43 | 1.43 | 0.06 | 0.01 | 0.16 | 65.48 | 0.04 | 0.06 | 0.09 | 0.02 | 67.34 |
| ..... PU** | 44 | 0.14 | 0.01 | 0.02 | 0.12 | 62.05 | 0.09 | 0.07 | 0.01 | 0.01 | 62.53 |
| ..... PU** | 45 | 24.44 | 2.71 | 0.23 | 0.48 | 44.30 | 1.10 | 0.34 | 1.31 | 0.05 | 74.98 |
| ..... A*** | 46 | 85.13 | 0.92 | 0.25 | 0.09 | 0.06 | 0.11 | 0.47 | 0.00 | 0.02 | 87.07 |
| ..... CU** | 47 | 94.84 | 0.16 | 0.04 | 0.00 | 0.11 | 0.04 | 0.08 | 0.01 | 0.00 | 95.28 |
| ..... A*** | 48 | 97.84 | 0.07 | 0.03 | 0.00 | 0.01 | 0.00 | 0.03 | 0.01 | 0.02 | 98.02 |
| ..... A*** | 49 | 90.98 | 2.63 | 0.46 | 0.18 | 0.07 | 0.15 | 1.25 | 0.00 | 0.01 | 95.74 |
| ..... A*** | 50 | 5.33 | 28.00 | 2.38 | 1.49 | 0.13 | 1.48 | 8.38 | 0.01 | 0.01 | 95.18 |
| ..... CI** | 54 | 20.94 | 0.80 | 0.08 | 0.24 | 46.44 | 0.86 | 0.40 | 0.12 | 0.01 | 69.89 |
| ..... CP** | 55 | 28.89 | 2.29 | 0.33 | 0.57 | 43.41 | 0.91 | 0.20 | 0.20 | 0.27 | 76.82 |
| ..... CP** | 56 | 18.85 | 1.30 | 0.49 | 0.20 | 50.89 | 0.51 | 0.19 | 0.19 | 0.02 | 72.64 |
| ..... CP** | 57 | 16.19 | 1.53 | 0.08 | 0.12 | 50.65 | 0.69 | 0.16 | 0.72 | 0.02 | 70.17 |
| ..... CP** | 58 | 19.89 | 10.18 | 12.66 | 4.21 | 22.06 | 0.30 | 0.05 | 0.80 | 0.00 | 69.43 |
| ..... CP** | 59 | 29.45 | 2.17 | 0.17 | 0.14 | 42.40 | 0.51 | 0.10 | 0.26 | 0.15 | 75.34 |
| ..... PGU* | 60 | 25.68 | 2.58 | 0.22 | 0.12 | 47.56 | 0.38 | 0.06 | 1.89 | 0.03 | 78.53 |
| ..... PGU* | 61 | 13.08 | 1.93 | 0.15 | 0.13 | 53.66 | 0.35 | 0.15 | 1.45 | 0.09 | 71.00 |
| ..... PGU* | 62 | 3.15 | 0.34 | 0.03 | 0.38 | 65.71 | 0.11 | 0.03 | 0.31 | 0.00 | 70.07 |
| ..... PGU* | 63 | 43.47 | 24.69 | 2.34 | 0.83 | 9.83 | 0.27 | 6.69 | 0.45 | 0.03 | 88.61 |
| ..... CP** | 64 | 46.42 | 27.05 | 2.82 | 0.99 | 7.89 | 0.11 | 4.54 | 0.36 | 0.02 | 90.20 |
| ..... CP** | 65 | 12.45 | 0.99 | 0.20 | 0.14 | 43.32 | 0.50 | 0.13 | 0.82 | 0.05 | 58.61 |

**4.Dry Rigg siltstone 7 kg mix immersed in salt solution**

| Sample No. | $SiO_2$ | $Al_2O_3$ | FeO | MgO | CaO | $Na_2O$ | $K_2O$ | $SO_3$ | Cl | Total |
|---|---|---|---|---|---|---|---|---|---|---|
| ..... CA 1 | 70.23 | 3.91 | 0.08 | 0.09 | 0.72 | 3.41 | 0.25 | 0.00 | 0.00 | 81.93 |
| ..... CA 2 | 40.98 | 7.06 | 0.17 | 0.06 | 0.50 | 5.39 | 0.13 | 0.00 | 0.00 | 54.33 |
| ..... CA 3 | 27.78 | 18.48 | 10.47 | 15.12 | 0.01 | 0.02 | 0.00 | 0.00 | 0.00 | 72.08 |
| ..... CA 4 | 28.86 | 16.98 | 10.94 | 19.99 | 0.07 | 0.02 | 0.02 | 0.00 | 0.00 | 77.05 |
| CA 5 | 28.81 | 17.07 | 11.25 | 20.13 | 0.08 | 0.01 | 0.02 | 0.00 | 0.00 | 77.52 |
| ..... CA 6 | 70.23 | 0.16 | 0.64 | 0.38 | 12.37 | 2.83 | 0.53 | 0.24 | 0.09 | 87.49 |
| ..... CA 7 | 71.27 | 0.23 | 0.79 | 0.43 | 11.86 | 1.30 | 0.52 | 0.24 | 0.05 | 86.71 |
| ..... CA 8 | 72.84 | 0.22 | 0.91 | 0.52 | 10.92 | 2.58 | 0.63 | 0.28 | 0.11 | 89.01 |
| ..... CA 9 | 69.88 | 0.20 | 0.32 | 0.22 | 14.30 | 3.11 | 0.80 | 0.09 | 0.08 | 89.00 |
| ..... CA 10 | 59.14 | 20.58 | 7.54 | 5.79 | 0.23 | 3.97 | 1.30 | 0.01 | 0.03 | 98.61 |
| ..... CA 11 | 67.66 | 0.22 | 0.41 | 0.23 | 15.45 | 1.88 | 0.79 | 0.02 | 0.08 | 86.74 |
| ..... CA 12 | 56.45 | 0.24 | 0.38 | 0.12 | 14.14 | 0.86 | 0.60 | 0.03 | 0.13 | 72.97 |
| ..... CA 13 | 58.21 | 0.12 | 0.23 | 0.12 | 11.98 | 0.96 | 0.98 | 0.05 | 0.11 | 72.76 |
| ..... CA 14 | 66.51 | 0.18 | 0.08 | 0.04 | 16.79 | 6.71 | 1.03 | 0.01 | 0.06 | 91.41 |
| ..... CA 15 | 71.39 | 0.18 | 0.09 | 0.07 | 16.99 | 3.26 | 0.82 | 0.07 | 0.02 | 92.89 |

| | | | | | | | | | | | |
|---|---|---|---|---|---|---|---|---|---|---|---|
| ..... | CA | 16 | 58.97 | 0.28 | 0.04 | 0.03 | 15.89 | 9.79 | 1.30 | 0.04 | 0.04 | 86.39 |
| ..... | CP | 17 | 61.41 | 0.13 | 0.09 | 0.14 | 15.15 | 2.73 | 1.07 | 0.03 | 0.06 | 80.81 |
| ..... | CP | 18 | 55.53 | 0.14 | 0.05 | 0.05 | 13.54 | 7.74 | 1.87 | 0.02 | 0.04 | 78.99 |
| ..... | CP | 19 | 40.19 | 0.11 | 0.05 | 0.07 | 8.78 | 19.01 | 1.77 | 0.01 | 0.04 | 70.03 |
| ..... | CP | 20 | 47.08 | 0.11 | 0.05 | 0.05 | 9.65 | 1.93 | 0.27 | 0.03 | 0.36 | 59.54 |
| ..... | CP | 21 | 26.20 | 0.04 | 0.05 | 0.07 | 4.33 | 8.12 | 0.49 | 0.04 | 0.51 | 39.85 |
| ..... | CL | 22 | 64.67 | 0.14 | 0.09 | 0.15 | 12.83 | 5.78 | 1.30 | 0.07 | 0.06 | 85.11 |
| ..... | CL | 23 | 72.38 | 0.15 | 0.06 | 0.08 | 14.29 | 3.91 | 0.47 | 0.07 | 0.10 | 91.52 |
| ..... | CL | 24 | 70.46 | 0.16 | 0.11 | 0.20 | 13.35 | 4.68 | 0.94 | 0.03 | 0.10 | 90.03 |
| ..... | CL | 25 | 69.25 | 0.14 | 0.12 | 0.27 | 10.97 | 3.48 | 0.81 | 0.11 | 0.06 | 85.22 |
| ..... | CL | 26 | 71.97 | 0.14 | 0.10 | 0.20 | 11.40 | 4.12 | 0.90 | 0.01 | 0.07 | 88.91 |
| ..... | CL | 27 | 63.39 | 0.10 | 0.10 | 0.11 | 12.21 | 5.74 | 1.03 | 0.06 | 0.09 | 82.83 |
| ..... | CL | 28 | 67.45 | 0.15 | 0.14 | 0.07 | 12.19 | 6.48 | 0.88 | 0.05 | 0.06 | 87.48 |
| ..... | CA | 29 | 85.51 | 0.38 | 0.26 | 0.09 | 3.12 | 2.17 | 0.45 | 0.04 | 0.08 | 92.11 |
| ..... | A | 30 | 91.42 | 3.95 | 0.90 | 0.83 | 0.06 | 0.11 | 0.81 | 0.03 | 0.02 | 98.13 |
| ..... | CP | 31 | 50.31 | 0.16 | 0.17 | 0.16 | 17.04 | 11.92 | 1.42 | 0.03 | 0.02 | 81.22 |
| ..... | CP | 32 | 43.42 | 2.13 | 0.10 | 0.20 | 32.77 | 7.88 | 0.38 | 0.00 | 0.05 | 86.94 |
| ..... | CP | 33 | 57.58 | 0.10 | 0.04 | 0.02 | 15.84 | 2.48 | 0.80 | 0.09 | 0.03 | 76.99 |
| ..... | CP | 34 | 53.02 | 0.25 | 0.44 | 0.44 | 17.19 | 1.66 | 0.83 | 0.05 | 0.00 | 73.85 |
| ..... | CP | 35 | 53.00 | 0.19 | 0.24 | 0.21 | 18.92 | 15.54 | 1.65 | 0.04 | 0.01 | 89.82 |
| ..... | CP | 36 | 40.52 | 0.72 | 0.10 | 0.07 | 32.77 | 1.66 | 0.63 | 0.01 | 0.06 | 76.55 |
| ..... | CP | 37 | 25.13 | 12.19 | 1.57 | 0.70 | 38.70 | 1.06 | 0.23 | 1.42 | 0.05 | 81.05 |
| ..... | CP | 38 | 60.44 | 0.09 | 0.03 | 0.01 | 16.73 | 4.52 | 0.99 | 0.04 | 0.01 | 82.87 |
| ..... | CP | 39 | 67.38 | 0.11 | 0.02 | 0.01 | 18.18 | 2.99 | 1.17 | 0.03 | 0.01 | 89.89 |
| ..... | CP | 40 | 57.47 | 0.10 | 0.02 | 0.01 | 16.60 | 7.48 | 1.08 | 0.05 | 0.01 | 82.83 |
| ..... | CP | 41 | 64.02 | 0.10 | 0.04 | 0.01 | 16.70 | 2.54 | 1.17 | 0.01 | 0.02 | 84.62 |
| ..... | CP | 42 | 62.39 | 0.11 | 0.07 | 0.02 | 15.55 | 4.44 | 1.28 | 0.02 | 0.00 | 83.89 |
| ..... | CA | 43 | 56.26 | 0.19 | 0.42 | 0.33 | 15.48 | 5.64 | 1.21 | 0.06 | 0.03 | 79.64 |
| ..... | CA | 44 | 64.72 | 0.21 | 0.36 | 0.32 | 15.53 | 2.62 | 0.76 | 0.02 | 0.02 | 84.57 |
| ..... | CA | 45 | 67.04 | 0.14 | 0.19 | 0.17 | 14.90 | 4.28 | 1.11 | 0.05 | 0.03 | 87.89 |
| ..... | CA | 46 | 62.76 | 0.15 | 0.33 | 0.33 | 13.94 | 4.26 | 1.20 | 0.01 | 0.05 | 83.02 |
| ..... | CA | 47 | 56.05 | 0.16 | 0.41 | 0.38 | 13.41 | 4.32 | 1.94 | 0.07 | 0.03 | 76.76 |
| ..... | CA | 48 | 65.65 | 0.14 | 0.37 | 0.38 | 14.36 | 3.48 | 1.47 | 0.00 | 0.05 | 85.91 |
| ..... | CA | 49 | 59.73 | 0.13 | 0.40 | 0.32 | 12.88 | 4.81 | 1.37 | 0.07 | 0.05 | 79.75 |
| ..... | CA | 50 | 0.08 | 0.00 | 0.02 | 0.00 | 0.06 | 0.08 | 0.01 | 0.00 | 1.04 | 1.31 |
| ..... | CA | 51 | 60.45 | 0.11 | 0.35 | 0.32 | 12.82 | 3.79 | 0.76 | 0.07 | 0.13 | 78.80 |
| ..... | CA | 52 | 57.65 | 0.10 | 0.40 | 0.41 | 11.80 | 5.98 | 1.56 | 0.07 | 0.05 | 78.03 |
| ..... | CA | 53 | 68.22 | 0.11 | 0.49 | 0.46 | 12.62 | 4.34 | 1.16 | 0.03 | 0.06 | 87.49 |
| ..... | CA | 54 | 71.02 | 0.10 | 0.58 | 0.58 | 13.78 | 3.75 | 1.01 | 0.07 | 0.09 | 90.99 |
| ..... | CA | 55 | 55.91 | 0.17 | 0.59 | 0.60 | 12.72 | 2.31 | 0.61 | 0.04 | 0.07 | 73.02 |
| ..... | CP | 56 | 37.39 | 1.17 | 0.20 | 0.08 | 41.84 | 0.67 | 0.15 | 0.06 | 0.08 | 81.64 |
| ..... | CP | 57 | 37.46 | 1.27 | 0.17 | 0.09 | 42.02 | 0.73 | 0.15 | 0.10 | 0.10 | 82.12 |
| ..... | CP | 58 | 36.06 | 3.84 | 0.46 | 0.34 | 36.68 | 2.30 | 0.79 | 0.00 | 0.00 | 80.49 |
| ..... | CP | 59 | 34.21 | 0.88 | 0.25 | 0.27 | 38.46 | 1.64 | 0.19 | 0.05 | 0.04 | 75.98 |
| ..... | CP | 60 | 28.76 | 1.31 | 0.10 | 0.15 | 45.70 | 0.33 | 0.09 | 0.07 | 0.12 | 76.62 |
| ..... | CP | 61 | 31.31 | 1.53 | 0.20 | 0.07 | 42.05 | 0.29 | 0.08 | 0.15 | 0.13 | 75.81 |
| ..... | CP | 62 | 29.89 | 1.46 | 0.21 | 0.17 | 39.52 | 0.87 | 0.13 | 0.10 | 0.13 | 72.48 |
| ..... | CP | 63 | 27.79 | 0.87 | 0.02 | 0.02 | 35.82 | 1.76 | 0.24 | 0.11 | 0.18 | 66.81 |
| ..... | CP | 64 | 33.46 | 1.50 | 0.09 | 0.05 | 40.57 | 0.41 | 0.09 | 0.06 | 0.10 | 76.33 |
| ..... | CP | 65 | 33.24 | 1.69 | 0.04 | 0.02 | 38.29 | 0.14 | 0.04 | 0.17 | 0.07 | 73.71 |
| ..... | CP | 66 | 32.99 | 1.55 | 0.02 | 0.03 | 39.88 | 0.14 | 0.05 | 0.20 | 0.07 | 74.92 |
| ..... | CP | 67 | 4.22 | 0.15 | 0.01 | 0.26 | 66.25 | 0.02 | 0.02 | 0.03 | 0.02 | 70.98 |

| | | | | | | | | | | | |
|---|---|---|---|---|---|---|---|---|---|---|---|
| ..... CP | 68 | 27.36 | 5.50 | 0.18 | 0.14 | 42.50 | 0.11 | 0.11 | 0.14 | 0.12 | 76.18 |
| ..... CP | 69 | 33.85 | 1.61 | 0.06 | 0.03 | 42.52 | 0.38 | 0.09 | 0.10 | 0.11 | 78.75 |
| ..... CL | 70 | 35.44 | 1.45 | 0.03 | 0.01 | 42.87 | 0.36 | 0.08 | 0.05 | 0.14 | 80.43 |
| ..... CL | 71 | 34.81 | 1.86 | 0.02 | 0.02 | 42.83 | 0.40 | 0.08 | 0.04 | 0.14 | 80.21 |
| ..... CL | 72 | 49.12 | 0.97 | 0.03 | 0.04 | 27.73 | 6.63 | 0.68 | 0.01 | 0.42 | 85.64 |
| ..... CP | 73 | 54.07 | 0.13 | 0.08 | 0.07 | 20.31 | 14.24 | 1.21 | 0.38 | 0.10 | 90.59 |
| ..... CP | 74 | 34.11 | 0.06 | 0.13 | 0.06 | 7.65 | 2.22 | 0.45 | 0.08 | 0.56 | 45.32 |
| ..... CA | 75 | 63.89 | 0.25 | 0.11 | 0.07 | 15.30 | 2.30 | 0.89 | 0.07 | 0.03 | 82.91 |
| ..... CA | 76 | 65.11 | 0.15 | 0.15 | 0.18 | 14.49 | 1.67 | 0.73 | 0.06 | 0.08 | 82.62 |
| ..... CA | 77 | 45.51 | 0.12 | 0.06 | 0.05 | 22.86 | 9.90 | 1.47 | 0.01 | 0.06 | 80.06 |
| ..... CP | 78 | 28.39 | 1.05 | 0.00 | 0.01 | 36.17 | 1.17 | 0.13 | 0.17 | 0.57 | 67.67 |
| ..... PU | 79 | 32.92 | 1.60 | 0.05 | 0.02 | 40.63 | 1.60 | 0.15 | 0.33 | 0.49 | 77.80 |
| ..... PU | 80 | 33.13 | 1.42 | 0.05 | 0.02 | 40.05 | 1.83 | 0.21 | 0.26 | 0.46 | 77.44 |
| ..... PU | 81 | 33.78 | 1.48 | 0.01 | 0.01 | 39.07 | 2.16 | 0.14 | 0.16 | 0.60 | 77.41 |
| ..... PU | 82 | 54.86 | 0.09 | 0.00 | 0.01 | 27.94 | 3.07 | 1.51 | 0.02 | 0.02 | 87.53 |
| ..... CL | 83 | 59.42 | 0.08 | 0.08 | 0.18 | 15.77 | 1.64 | 1.10 | 0.01 | 0.05 | 78.34 |
| ..... CL | 84 | 51.76 | 0.21 | 0.11 | 0.13 | 24.12 | 1.33 | 0.74 | 0.00 | 0.04 | 78.44 |
| ..... CL | 85 | 64.11 | 0.12 | 0.07 | 0.11 | 14.36 | 3.06 | 1.33 | 0.03 | 0.02 | 83.21 |
| ..... CL | 86 | 14.11 | 0.04 | 0.00 | 0.00 | 2.49 | 1.73 | 0.34 | 0.02 | 0.76 | 19.49 |
| ..... CL | 87 | 1.98 | 0.01 | 0.02 | 0.00 | 0.41 | 0.70 | 0.05 | 0.01 | 0.73 | 3.93 |
| ..... CL | 88 | 1.36 | 0.01 | 0.03 | 0.00 | 0.41 | 0.61 | 0.06 | 0.02 | 0.81 | 3.30 |
| ..... CL | 89 | 34.51 | 0.10 | 0.04 | 0.14 | 41.40 | 3.46 | 1.12 | 0.03 | 0.02 | 80.84 |
| ..... CL | 90 | 46.26 | 1.70 | 0.17 | 0.20 | 32.35 | 2.54 | 0.71 | 0.02 | 0.13 | 84.08 |
| ..... CA | 91 | 1.92 | 0.03 | 0.08 | 0.00 | 0.73 | 1.56 | 0.10 | 0.01 | 0.82 | 5.25 |
| ..... CA | 92 | 68.57 | 0.19 | 0.68 | 0.59 | 12.54 | 3.24 | 0.65 | 0.04 | 0.04 | 86.54 |
| ..... CA | 93 | 62.09 | 0.16 | 0.63 | 0.57 | 11.55 | 3.13 | 1.14 | 0.01 | 0.03 | 79.31 |
| ..... CA | 94 | 61.06 | 6.17 | 1.11 | 1.25 | 6.22 | 2.02 | 2.16 | 0.04 | 0.02 | 80.06 |
| ..... CA | 95 | 63.67 | 2.49 | 1.75 | 2.01 | 9.50 | 1.17 | 0.52 | 0.09 | 0.03 | 81.24 |
| ..... CA | 96 | 62.19 | 0.87 | 0.68 | 0.42 | 9.91 | 2.21 | 0.91 | 0.02 | 0.13 | 77.34 |
| ..... ETT | 97 | 72.67 | 0.32 | 0.55 | 0.54 | 12.36 | 3.64 | 0.96 | 0.00 | 0.02 | 91.09 |
| ..... CA | 98 | 28.52 | 3.79 | 0.25 | 0.26 | 44.59 | 0.83 | 0.20 | 0.59 | 0.37 | 79.42 |
| ..... CP | 99 | 34.41 | 1.70 | 0.50 | 0.06 | 41.37 | 0.22 | 0.06 | 0.42 | 0.43 | 79.20 |
| ..... CP | 100 | 31.69 | 3.15 | 0.17 | 0.15 | 42.40 | 0.68 | 0.10 | 2.45 | 0.46 | 81.25 |
| ..... CP | 101 | 19.53 | 0.03 | 0.10 | 0.09 | 3.57 | 2.22 | 0.37 | 0.05 | 0.87 | 26.83 |
| ..... AGG | 102 | 34.24 | 0.07 | 0.67 | 0.21 | 6.00 | 4.07 | 0.70 | 0.14 | 0.47 | 46.56 |
| ..... AGG | 103 | 38.55 | 0.09 | 0.42 | 0.18 | 7.55 | 6.17 | 0.67 | 0.15 | 0.46 | 54.25 |
| ..... AGG | 104 | 52.68 | 0.09 | 0.66 | 0.36 | 8.93 | 7.00 | 0.78 | 0.22 | 0.27 | 71.00 |
| ..... AGG | 105 | 58.39 | 0.14 | 0.09 | 0.02 | 12.65 | 16.28 | 0.48 | 0.01 | 0.09 | 88.15 |
| ..... AGG | 106 | 10.74 | 0.05 | 0.02 | 0.39 | 55.95 | 0.99 | 0.06 | 0.01 | 0.01 | 68.23 |

**5.Dry Rigg siltstone 3 kg mix immersed in salt solution**

| Sample No. | $SiO_2$ | $Al_2O_3$ | FeO | MgO | CaO | $Na_2O$ | $K_2O$ | $SO_3$ | Cl | Total |
|---|---|---|---|---|---|---|---|---|---|---|
| .....CP 1 | 28.69 | 0.01 | 0.01 | 0.00 | 5.74 | 2.50 | 0.38 | 0.05 | 0.10 | 37.48 |
| ..... CP 2 | 41.10 | 0.00 | 0.02 | 0.01 | 4.85 | 4.87 | 0.55 | 0.09 | 0.04 | 51.52 |
| ..... CP 3 | 51.87 | 0.00 | 0.05 | 0.00 | 6.32 | 6.16 | 0.44 | 0.08 | 0.08 | 64.99 |
| ..... CP 4 | 33.54 | 0.00 | 0.02 | 0.01 | 4.26 | 7.37 | 0.43 | 0.04 | 0.04 | 45.70 |
| ..... CP 5 | 33.42 | 0.00 | 0.02 | 0.01 | 4.54 | 7.01 | 0.39 | 0.04 | 0.05 | 45.47 |
| ..... CP 6 | 0.47 | 0.00 | 0.02 | 0.00 | 0.10 | 0.03 | 0.00 | 0.00 | 0.01 | 0.65 |

| | | | | | | | | | | | |
|---|---|---|---|---|---|---|---|---|---|---|---|
| ..... | CP | 7 | 55.42 | 0.01 | 0.02 | 0.01 | 9.11 | 1.75 | 0.49 | 0.00 | 0.07 | 66.88 |
| ..... | CP | 8 | 21.01 | 0.16 | 0.00 | 0.00 | 12.96 | 1.34 | 0.09 | 0.25 | 0.44 | 36.25 |
| ..... | PU | 9 | 13.05 | 2.53 | 0.09 | 0.08 | 16.57 | 0.43 | 0.08 | 3.74 | 0.41 | 36.98 |
| ..... | CL | 10 | 53.09 | 0.17 | 0.03 | 0.00 | 19.24 | 7.34 | 0.61 | 0.10 | 0.59 | 81.19 |
| ..... | CL | 11 | 58.69 | 0.16 | 0.01 | 0.01 | 19.37 | 1.98 | 0.27 | 0.11 | 1.24 | 81.85 |
| ..... | CL | 12 | 55.75 | 0.14 | 0.02 | 0.00 | 18.63 | 1.22 | 0.27 | 0.08 | 1.05 | 77.18 |
| ..... | CL | 13 | 61.58 | 0.15 | 0.03 | 0.00 | 20.93 | 3.39 | 0.31 | 0.11 | 1.02 | 87.53 |
| ..... | ETT | 14 | 6.40 | 3.42 | 0.02 | 0.01 | 24.49 | 1.87 | 0.06 | 6.96 | 0.72 | 43.95 |
| ..... | ETT | 15 | 1.54 | 6.21 | 0.02 | 0.01 | 26.51 | 1.05 | 0.06 | 13.03 | 0.46 | 48.89 |
| ..... | CA | 16 | 34.00 | 1.24 | 0.00 | 0.01 | 37.97 | 2.94 | 0.14 | 0.12 | 0.96 | 77.38 |
| ..... | CA | 17 | 29.71 | 3.22 | 0.42 | 0.27 | 32.44 | 1.33 | 0.84 | 0.16 | 1.08 | 69.48 |
| ..... | CA | 18 | 34.15 | 1.17 | 0.02 | 0.00 | 37.06 | 2.50 | 0.17 | 0.22 | 1.36 | 76.66 |
| ..... | CA | 19 | 36.33 | 1.34 | 0.01 | 0.01 | 38.42 | 3.44 | 0.13 | 0.46 | 1.28 | 81.44 |
| ..... | CA | 20 | 63.25 | 0.12 | 0.05 | 0.02 | 16.41 | 2.04 | 0.75 | 0.18 | 0.19 | 83.00 |
| ..... | CA | 21 | 55.96 | 0.26 | 0.13 | 0.04 | 14.95 | 3.99 | 0.76 | 0.34 | 0.39 | 76.81 |
| ..... | CA | 22 | 61.66 | 0.17 | 0.15 | 0.02 | 16.43 | 2.11 | 0.73 | 0.19 | 0.39 | 81.84 |
| ..... | CA | 23 | 56.74 | 0.33 | 0.10 | 0.02 | 14.82 | 5.35 | 1.30 | 0.22 | 0.35 | 79.22 |
| ..... | CA | 24 | 61.40 | 0.23 | 0.08 | 0.01 | 16.17 | 2.94 | 0.95 | 0.23 | 0.39 | 82.39 |
| ..... | CP | 25 | 33.34 | 0.03 | 0.00 | 0.02 | 7.71 | 15.45 | 1.00 | 0.05 | 0.08 | 57.69 |
| ..... | CP | 26 | 64.11 | 0.06 | 0.03 | 0.01 | 15.28 | 3.76 | 0.84 | 0.06 | 0.17 | 84.32 |
| ..... | CP | 27 | 36.91 | 0.05 | 0.02 | 0.01 | 9.61 | 7.26 | 0.76 | 0.03 | 0.18 | 54.82 |
| ..... | CP | 28 | 59.78 | 0.05 | 0.02 | 0.00 | 14.98 | 2.86 | 0.88 | 0.06 | 0.23 | 78.87 |
| ..... | CP | 29 | 47.39 | 0.05 | 0.00 | 0.00 | 13.45 | 2.46 | 0.94 | 0.03 | 0.19 | 64.50 |
| ..... | CP | 30 | 57.76 | 0.07 | 0.02 | 0.00 | 15.17 | 3.20 | 0.80 | 0.00 | 0.20 | 77.22 |
| ..... | CP | 31 | 63.70 | 0.09 | 0.03 | 0.00 | 18.21 | 1.63 | 0.92 | 0.06 | 0.21 | 84.85 |
| ..... | CP | 32 | 47.56 | 0.04 | 0.02 | 0.00 | 14.46 | 1.61 | 0.39 | 0.04 | 0.31 | 64.44 |
| ..... | CP | 33 | 47.89 | 0.26 | 0.03 | 0.01 | 18.46 | 12.67 | 0.69 | 0.10 | 0.41 | 80.53 |
| ..... | CP | 34 | 8.46 | 0.15 | 0.01 | 0.00 | 11.00 | 0.97 | 0.16 | 0.00 | 1.08 | 21.84 |
| ..... | CP | 35 | 33.52 | 0.54 | 0.04 | 0.00 | 19.64 | 2.64 | 0.25 | 0.26 | 0.94 | 57.83 |
| ..... | CP | 36 | 21.37 | 0.39 | 0.01 | 0.00 | 26.10 | 2.44 | 0.16 | 0.06 | 1.70 | 52.24 |
| | CP | 37 | 42.81 | 0.06 | 0.03 | 0.00 | 21.40 | 10.93 | 0.96 | 0.07 | 0.52 | 76.79 |
| ..... | CP | 38 | 47.19 | 0.21 | 0.07 | 0.00 | 27.94 | 8.01 | 0.44 | 0.18 | 1.43 | 85.48 |
| ..... | CP | 39 | 51.27 | 0.20 | 0.05 | 0.01 | 30.54 | 2.89 | 0.36 | 0.11 | 1.67 | 87.10 |
| ..... | CP | 40 | 65.21 | 0.09 | 0.02 | 0.01 | 13.09 | 11.27 | 1.09 | 0.08 | 0.17 | 91.03 |
| ..... | CP | 41 | 62.74 | 0.08 | 0.05 | 0.00 | 13.50 | 9.18 | 1.06 | 0.11 | 0.24 | 86.97 |
| ..... | CP | 42 | 56.66 | 0.19 | 0.07 | 0.00 | 22.20 | 12.09 | 0.75 | 0.07 | 0.56 | 92.59 |
| ..... | CP | 43 | 56.00 | 0.09 | 0.06 | 0.00 | 28.79 | 6.59 | 0.99 | 0.01 | 0.27 | 92.79 |
| ..... | CP | 44 | 53.20 | 0.11 | 0.06 | 0.01 | 27.42 | 3.07 | 0.86 | 0.03 | 0.34 | 85.09 |
| ..... | CP | 45 | 54.32 | 0.09 | 0.05 | 0.00 | 28.00 | 2.08 | 0.52 | 0.05 | 0.37 | 85.48 |
| ..... | CP | 46 | 55.46 | 0.11 | 0.03 | 0.01 | 27.14 | 5.23 | 1.00 | 0.05 | 0.28 | 89.30 |
| ..... | CA | 47 | 60.92 | 0.23 | 0.20 | 0.07 | 12.18 | 4.57 | 1.37 | 0.25 | 0.18 | 79.97 |
| ..... | CA | 48 | 69.50 | 0.13 | 0.11 | 0.02 | 13.72 | 3.68 | 0.81 | 0.04 | 0.17 | 88.17 |
| ..... | CA | 49 | 48.92 | 0.12 | 0.10 | 0.02 | 12.14 | 2.30 | 0.88 | 0.13 | 0.31 | 64.93 |
| ..... | CA | 50 | 66.92 | 0.24 | 0.21 | 0.06 | 14.96 | 2.25 | 0.88 | 0.07 | 0.33 | 85.92 |
| ..... | CA | 51 | 59.08 | 0.12 | 0.05 | 0.02 | 17.14 | 4.42 | 1.14 | 0.05 | 0.26 | 82.27 |
| ..... | CA | 52 | 56.55 | 0.68 | 0.03 | 0.02 | 23.58 | 1.83 | 0.50 | 0.02 | 0.24 | 83.45 |
| ..... | CA | 53 | 53.65 | 0.14 | 0.12 | 0.01 | 13.57 | 11.64 | 1.02 | 0.01 | 0.10 | 80.27 |
| ..... | CP | 54 | 57.68 | 0.32 | 0.02 | 0.00 | 19.43 | 7.17 | 0.77 | 0.06 | 0.45 | 85.90 |
| ..... | CP | 55 | 53.94 | 0.14 | 0.01 | 0.00 | 14.87 | 9.40 | 1.65 | 0.04 | 0.20 | 80.26 |
| ..... | PU | 56 | 30.11 | 2.02 | 0.33 | 0.24 | 40.92 | 0.73 | 0.23 | 0.51 | 0.57 | 75.66 |
| ..... | PU | 57 | 35.81 | 1.80 | 0.01 | 0.01 | 40.00 | 0.33 | 0.09 | 0.35 | 0.92 | 79.33 |
| ..... | CA | 58 | 66.07 | 4.76 | 0.25 | 0.06 | 16.83 | 2.73 | 0.53 | 0.02 | 0.57 | 91.81 |

| | | | | | | | | | | | |
|---|---|---|---|---|---|---|---|---|---|---|---|
| ..... | CA | 59 | 77.22 | 0.23 | 0.18 | 0.04 | 8.97 | 1.01 | 0.42 | 0.03 | 0.10 | 88.22 |
| ..... | CA | 60 | 76.26 | 0.25 | 0.17 | 0.01 | 7.15 | 1.57 | 0.51 | 0.02 | 0.09 | 86.05 |
| ..... | CA | 61 | 65.62 | 0.21 | 0.13 | 0.03 | 12.90 | 7.12 | 1.00 | 0.05 | 0.11 | 87.17 |
| ..... | CL | 62 | 7.29 | 0.03 | 0.00 | 0.01 | 1.95 | 2.47 | 0.19 | 0.15 | 0.65 | 12.74 |
| ..... | CL | 63 | 65.01 | 0.10 | 0.02 | 0.02 | 16.52 | 1.64 | 0.49 | 0.03 | 0.16 | 83.99 |
| ..... | CL | 64 | 32.78 | 0.03 | 0.01 | 0.01 | 8.53 | 1.76 | 0.65 | 0.15 | 1.81 | 45.74 |
| ..... | CL | 65 | 28.23 | 0.04 | 0.01 | 0.01 | 7.98 | 1.08 | 0.53 | 0.09 | 0.51 | 38.48 |
| ..... | CL | 66 | 60.99 | 0.11 | 0.03 | 0.01 | 14.78 | 1.49 | 0.66 | 0.11 | 0.21 | 78.41 |
| ..... | CL | 67 | 20.12 | 1.07 | 2.09 | 21.60 | 30.07 | 0.91 | 0.32 | 0.09 | 0.11 | 76.40 |
| ..... | CA | 68 | 57.76 | 0.11 | 0.09 | 0.03 | 14.52 | 1.64 | 0.62 | 0.04 | 0.46 | 75.28 |
| ..... | CA | 69 | 59.37 | 0.10 | 0.08 | 0.04 | 15.48 | 2.53 | 0.56 | 0.05 | 0.35 | 78.56 |
| ..... | CA | 70 | 61.35 | 0.19 | 0.13 | 0.14 | 14.94 | 1.41 | 0.69 | 0.06 | 0.19 | 79.12 |
| ..... | CA | 71 | 36.34 | 0.70 | 0.02 | 0.00 | 38.53 | 1.31 | 0.14 | 0.17 | 0.97 | 78.19 |
| ..... | CA | 72 | 23.22 | 0.38 | 0.03 | 0.00 | 27.87 | 1.41 | 0.16 | 0.02 | 1.20 | 54.30 |
| ..... | CA | 73 | 39.50 | 1.35 | 0.01 | 0.03 | 41.08 | 1.06 | 0.12 | 0.23 | 2.92 | 86.29 |
| ..... | CA | 74 | 43.08 | 0.14 | 0.18 | 0.01 | 11.96 | 1.42 | 0.73 | 0.09 | 0.33 | 57.93 |
| ..... | CA | 75 | 66.50 | 0.79 | 0.10 | 0.00 | 13.10 | 2.78 | 0.49 | 0.03 | 0.48 | 84.29 |
| ..... | CA | 76 | 41.26 | 0.05 | 0.05 | 0.00 | 9.01 | 1.35 | 0.51 | 0.05 | 0.43 | 52.71 |
| ..... | CA | 77 | 68.56 | 0.19 | 0.14 | 0.02 | 13.88 | 1.95 | 0.69 | 0.02 | 0.39 | 85.85 |
| ..... | CA | 78 | 42.56 | 0.05 | 0.01 | 0.00 | 23.94 | 5.95 | 0.51 | 0.04 | 1.55 | 74.60 |
| ..... | CP | 79 | 44.03 | 0.02 | 0.02 | 0.00 | 25.90 | 4.03 | 0.39 | 0.01 | 1.77 | 76.18 |
| ..... | CP | 80 | 44.64 | 0.02 | 0.03 | 0.00 | 25.06 | 1.77 | 0.36 | 0.03 | 2.12 | 74.03 |
| ..... | CP | 81 | 51.57 | 0.07 | 0.05 | 0.00 | 20.90 | 3.93 | 0.60 | 0.03 | 1.66 | 78.81 |
| ..... | CP | 82 | 17.52 | 0.37 | 0.09 | 0.00 | 22.53 | 1.99 | 0.33 | 0.20 | 0.94 | 43.98 |
| ..... | CP | 83 | 22.95 | 0.07 | 0.02 | 0.00 | 26.24 | 1.11 | 0.22 | 0.08 | 0.90 | 51.60 |
| ..... | CL | 84 | 31.09 | 1.04 | 0.02 | 0.01 | 36.27 | 1.62 | 0.36 | 0.21 | 0.36 | 70.97 |
| ..... | CL | 85 | 33.41 | 1.41 | 0.02 | 0.03 | 39.02 | 0.72 | 0.12 | 0.39 | 1.48 | 76.60 |
| ..... | CP | 86 | 14.82 | 0.64 | 0.05 | 0.05 | 29.76 | 2.04 | 0.24 | 0.17 | 1.39 | 49.17 |